NOVEL WITTIG REACTIONS AND ORGANOCATALYTIC METHODOLOGIES

NOVEL WITTIG AND ORGANOCATALYTIC METHODS FOR THE SYNTHESIS OF CHEMOTHERAPEUTIC COMPOUNDS

By ALEXANDER J. NIELSEN, B.Sc.

A Thesis Submitted to the School of Graduate Studies in Partial Fulfilment of the Requirements for the Degree Doctor of Philosophy

McMaster University DOCTOR OF PHILOSOPHY (2019) Hamilton, Ontario (Chemical Biology)

TITLE: Novel Wittig and Organocatalytic Methodologies for the Synthesis of Chemotherapeutic Compounds. AUTHOR: Alexander J. Nielsen, H. BSc. (McMaster University). SUPERVISOR: Professor James McNulty. NUMBER OF PAGES: xv; 424.

Lay Abstract

The Wittig reaction is one of the best ways to make alkenes, a type of reactive bond between two carbon atoms. A new Wittig reaction was developed and used in the preparation and discovery of potent inhibitors of aromatase, an enzyme responsible for the proliferation of many breast cancers. As well, another Wittig methodology was created for the straightforward synthesis of an otherwise difficult to prepare class of alkenes. In turn, these types of alkenes were used in a novel preparation of cyclobutanes, a chemical structure that is difficult to make but can impart useful properties to drugs and materials. Finally, a Wittig reaction previously reported by the McNulty group was used as part of a chemical synthesis of *trans*-dihydronarciclasine, a rare natural product isolated from daffodils. *Trans*-dihydronarciclasine was discovered to have antiviral activity and is one of the most potent inhibitors of the Zika virus discovered to date.

Abstract

This thesis is primarily focused on the development of Wittig methodologies and the applications of the product alkenes in organocatalysis and drug discovery. Herein is described an aqueous Wittig methodology for the synthesis of α-methylstilbenes and their use in the preparation of novel triazole stilbene inhibitors of aromatase, a clinically validated target for the treatment of estrogen receptor positive breast cancer. As well, a one-step, stereoselective synthesis of alkenyl phenols was developed. The method provides easy access to a variety of compounds that contain this synthetically and biologically important functionality, including natural product phenolic stilbenes. In turn, alkenyl phenols were used as a key component in a novel organocatalytic methodology for the synthesis of cyclobutanes in good yields and high enantioselectivity. Notably, this is one of relatively few asymmetric, catalytic methods for cyclobutane synthesis. Preliminary biological activity of some of these cyclobutane derivatives is reported, including promising anti-cancer activity. Finally, a ten-step total synthesis of the Amaryllidaceae alkaloid (+)-*trans*-dihydronarciclasine was completed. The synthesis features an organocatalytic Michael-aldol cascade on a cinnamaldehyde derivative, which was prepared using a Wittig methodology previous reported by the McNulty group. Importantly, this compound was found to be one of the most potent anti-Zika compounds reported to date. Future work should focus on improving the potency and selectivity of the various aforementioned chemotherapeutics, with concurrent efforts to build upon the novel methodologies discussed herein.

Acknowledgements

First and foremost, I would like to thank my supervisor Dr. James McNulty, whose passion for organic chemistry and natural products is contagious. The guidance, support, and opportunities you consistently provided have shaped me as a scientist and a chemical biologist. Also, thank you for turning a blind eye to my occasionally less than pristine bench space and fumehood.

Thank you as well to my committee members, Dr. Paul Harrison and Dr. Philip Britz-McKibbin, whose feedback and suggestions were always helpful. I am especially grateful to Dr. Harrison, who supported me in my first experience as an instructor for a university course.

Furthermore, I would like to acknowledge all my colleagues who have come and gone from the McNulty Group. Although too numerous to list, your input in group meetings and advice in the lab was always appreciated. Special thanks to Dave McLeod for our many chemistry chats and coffee trips, and for being an excellent example of a chemist. As well, Carla Brown was my comrade in commiseration for most of my degree; our friendship was forged during many long days in the lab and tempered in longer nights at the Phoenix. Special thanks to the undergrads I had the opportunity to mentor, especially Wen-Jing Lin, Tiffany Kong, Lewis Jones and Julia Mason.

I would be remiss if I didn't thank all the friends I made in the department, especially those I worked with in the MCGSS and MRCIS or played with on the Mother Liquors. Some of my fondest (and vaguest) memories come from the many Halloween parties, Mystery Road Trips, and other social events. As well, somewhere along this graduate school process, Alison Stewart and Samantha Slikboer have become my life-long friends and confidants.

I am forever grateful to my family for their constant love and support, as well as for asking the often unsolicited but always warranted question, "When are you going to finish?". A special thanks to my parents who never seemed overly concerned about having a son in his late 20s who was still in school. Thanks as well to Daisy the dog for all the cuddles, although you made it that much harder to get out of bed in the morning. Finally, a heartfelt thanks to my fiancée Anna, who was by my side the whole time, celebrating my achievements, providing motivation when I needed it, and yelling "Get out of bed!" when I snuggled too long with Daisy. Anna, I couldn't have done it without you.

Table of Contents

List of Figures

List of Tables

List of Schemes

List of Abbreviations and Symbols

[α]	Specific rotation (expressed without units; the implicit units are deg mL g^{-1} dm^{-1})	*e.e* or *ee*	Enantiomeric excess
ACN	Acetonitrile	EI	Electron impact ionization
Ac	Acetyl	Elec	Electrophile
Ac₂O	Acetic anhydride	eq	Molar equivalent
AI	Aromatase inhibitor	ER	Estrogen receptor
Ar	Aryl	ESI	Electrospray ionization
atm	Atmosphere (unit of pressure)	Et	Ethyl
aq	Aqueous	EtOAc	Ethyl acetate
BBN	Banwell-modified Bischler-Napieralski reaction	EtOH	Ethanol
		EWG	Electron withdrawing group
Bn	Benzyl	ΔG	Gibb's free energy
BOC	*Tert*-butoxycarbonyl (COO*t*Bu)	H	Hour
BPO	Benzoyl peroxide	het	Heterocycle
br	Broad	HFF	Human foreskin fibroblasts
Bu	Butyl	hiPSC	Human induced pluripotent stem cell
BQ	Benzoquinone		
Bz	Benzoyl	HIV	Human Immunodeficiency Virus
CCDC	Cambridge Crystallographic Data Centre	HMBC	Heteronuclear multiple bond correlation (NMR)
CC_{50}	Cytotoxicity concentration 50%	HOMO	Highest occupied molecular orbital
CMV	Cytomegalovirus	HRMS	High resolution mass spectrometry
CPA	Chiral phosphoric acid	HSQC	Heteronuclear single quantum correlation (NMR)
CYP450	Cytochrome P450		
COSY	Homonuclear correlation spectroscopy	hν	Light
		Hz	Hertz
δ	Chemical shift in ppm	IC_{50}	Median inhibitory concentration
d	Doublet (NMR)		
DBF	Dibenzylfluorescein	iPrOH	Isopropyl alcohol
DCM	Dichloromethane	IR	Infrared
DEPT	Distortionless Enhancement by Polarization Transfer	*J*	Coupling constant (NMR)
		KOtBu	Potassium *tert*-butoxide
DIPEA	Diisopropylethylamine	λ	Wavelength
DMAP	4-dimethylaminopyridine	L	Litre
DMF	Dimethylformamide	LDA	Lithium diisopropylamide
DMSO	Dimethylsulfoxide	LUMO	Lowest unoccupied molecular orbital
DNA	Deoxyribonucleic acid		
d.r. or *dr*	Diastereomeric ratio	*m*	Meta
E	Entgegen (opposite, trans)	m	milli
EC_{50}	Effective concentration 50%	M	Molarity

m	Multiplet (NMR)	TBAF	Bu_4NF
m-CPBA	*m*-chloroperbenzoic acid	TBS	*Tert*-butyldimethylsilyl
Me	Methyl	TD_{50}	Median toxic dose
MeOH	Solvent	TEA	Triethylamine
mER	Membrane estrogen receptor	Tf	Trifluoromethanesulfonyl
Min	Minute	THF	Tetrahydrofuran
MOC	Methoxycarbonyl (-COOMe)	TI	Therapeutic index
mol	Mole	Tr	Trityl; triphenylmethyl
mp	Melting point	TMS	Trimethylsilyl
mRNA	Messenger ribonucleic acid	μ	Micro
MS	Mass spectrometry	UV	Ultraviolet
MsCl	Methanesulfonyl chloride	*Z*	Zusammen (together, cis)
n	nano	ZIKV	Zika virus
n-BuLi	*n*-butyllithium		
NBS	*N*-bromosuccinimide		
NIAID	National Institute of Allergy and Infectious Diseases		
NMO	*N*-methylmorpholine *N*-oxide		
NMR	Nuclear magnetic resonance		
NPC	Neural progenitor cell		
Nu	Nucleophile		
o	Ortho		
p	Para		
P	Pentet (NMR)		
PET	Photoinduced electron transfer		
Ph	Phenyl		
PhMe	Toluene		
PPTS	Pyridinium *p*-toluenesulfonate		
Pr	Propyl		
Py	pyridine		
q	Quartet (NMR)		
QM	Quinone methide		
R_f	Retention factor		
RNA	Ribonucleic acid		
rt	Room temperature		
SI	Selectivity Index		
s	Singlet (NMR)		
SAR	Structure activity relationship		
SERM	Selective estrogen receptor modulator		
SMRI	Stanley Medical Research Institute		
SOMO	Singly occupied molecular orbital		
t	Triplet (NMR)		

Declaration of Academic Achievement

All chemistry in this thesis was performed by A. J. Nielsen unless noted otherwise. Compounds in Chapter 3 were prepared collaboratively by A. J. Nielsen and Wen Jing Lin, a thesis student under his supervision. The total synthesis of *trans*-dihydronarciclasine reported in Chapter 5 was completed collaboratively by A. J. Nielsen, Dr. Omkar Revu, and Dr. Carlos Zepeda-Velázquez.

All biological assays were performed by collaborators at McMaster University or abroad. The aromatase assays performed on the triazole stilbenes discussed in Chapter 2 were completed by Sergio Ráez-Villanueva under the supervision of Dr. Alison Holloway at McMaster University. Anti-HSV testing on the alkenyl phenol derivatives discussed in Chapter 3 was conducted under the supervision of Dr. Leonardo D'Aiuto and Dr. Vishwajit Nimgaonkar at the University of Pittsburgh. The anti-viral screening on the cyclobutane derivatives discussed in Chapter 4 were performed at the National Institute of Allergy and Infectious Diseases in Baltimore, Maryland. Anti-cancer screening for the cyclobutane derivatives were performed at the Ontario Institute for Cancer Research in Toronto, Ontario. Anti-Zika testing on *trans*-dihydronarciclasine was performed by Dr. Lorraine Jones-Brando at Johns Hopkins University.

The academic achievements discussed in this thesis consist of:

-A review of polyphenolic natural product inhibitors of aromatase, as published in *Med. Res. Rev.*, 2018, *Early View* (reproduced in its entirety in Chapter 2.2)

-The development of a novel synthesis of α-methylstilbenes and their use in the synthesis of potent aromatase inhibitors, as published in *Bioorg. Med. Chem. Lett.*, 2019, *29*, 1395-1398 (reproduced in its entirety in Chapter 2.3)

-The development of a protecting group free synthesis of alkenyl phenols. The exploration of some of these compounds as anti-HSV agents was reported in *Antiviral Res.*, 2017, *142*, 136-140, and is discussed in Chapter 3.3

-The development of an asymmetric organocatalytic synthesis of cyclobutane derivatives and their preliminary anti-viral and anti-cancer activities, as published in *Chem. Eur. J.*, 2016, *22*, 9111-9115 (reproduced in its entirety in Chapter 4.4); awarded the 2016 McMaster Chemical Biology Impact award for this work

-The asymmetric, organocatalytic total synthesis of *trans*-dihydronarciclasine, and the discovery of its potent anti-Zika activity, as published in *ChemistrySelect*, 2016, *1*, 5895-5899 (reproduced in its entirety in Chapter 5.4)

1 Recent Developments and Applications of the Wittig Reaction

1.1 A brief overview of the Wittig reaction

Carbonyl olefinations are among the most strategic C-C bond forming reactions in organic synthesis as they are typically high yielding and offer excellent positional, regio- and stereoselectivity.[1] Their reliability has made their use ubiquitous in total synthesis as well as in pharmaceutical and industrial processes.[2-4] These reactions often feature the addition of an α-functionalised carbanion to an aldehyde or ketone to give an alkene product, but reactions using metal carbene complexes are also well known. Examples include the Horner-Wadsworth-Emmons, Julia-Lythgoe, Peterson, Tebbe and Petasis olefinations, but the Wittig reaction is the most widely studied and it has played an important role in this thesis.[5-11]

First described in 1953, the Wittig reaction involves the generation of a phosphorous ylide via deprotonation of a phosphonium salt, which subsequently reacts with a carbonyl or carbonyl equivalent to give the corresponding alkene and phosphine oxide (Figure 1.1).[11] The Wittig reaction can give both (*E*) and (*Z*) alkenes and the ratio of these products is affected by several variables, the most significant of which are the electronic nature of the ylidic carbanion, the presence of lithium salts, and the non-participating substituents on the phosphorous, *i.e.* if the phosphonium salt is derived from a trialkyl vs. a triaryl phosphine (*vide infra*, Section 1.2).
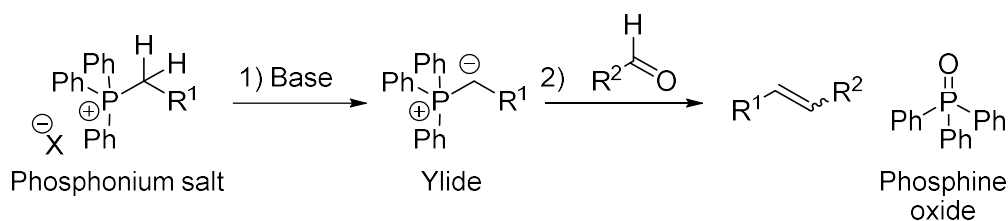
FIGURE 1.1 The quintessential Wittig reaction. Deprotonation of a phosphonium salt generates a phosphorous ylide, which subsequently reacts with a carbonyl to give an alkene and a phosphine oxide.
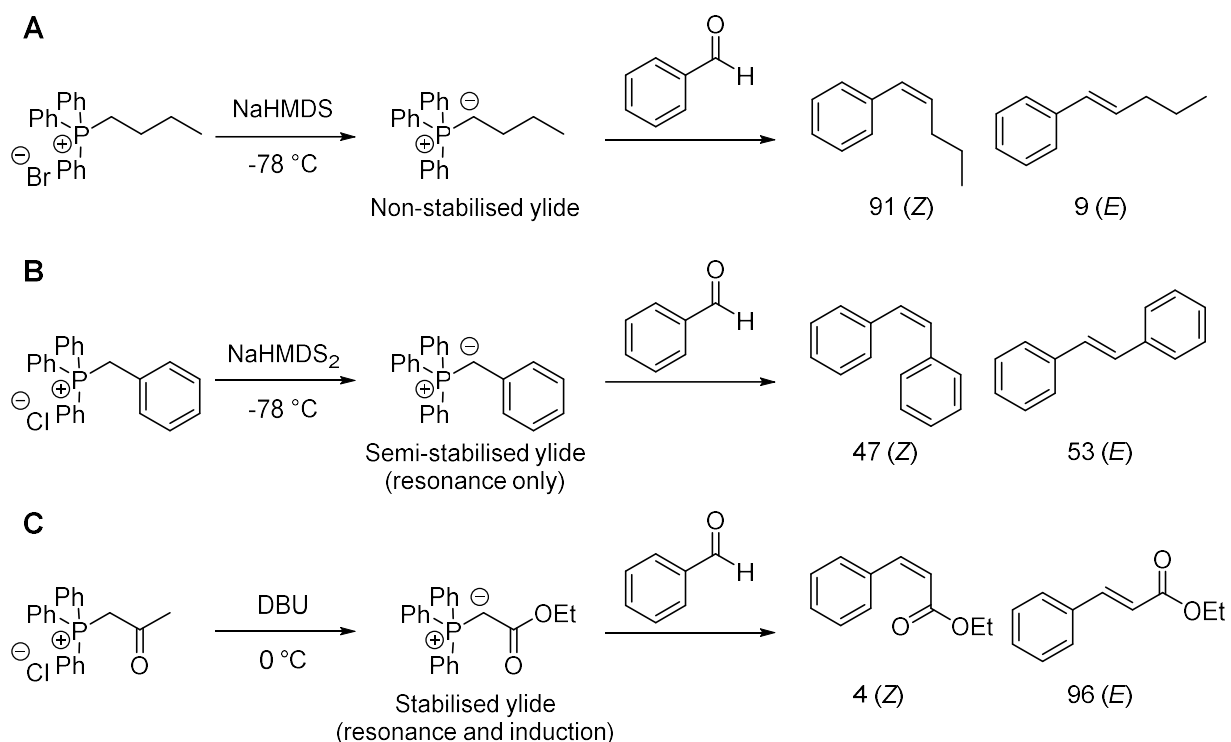
FIGURE 1.2 Examples of the effect of ylide stabilisation on (*E*):(*Z*) ratios. Non-stabilised ylides are highly (*Z*) selective in the absence of lithium salts (A). Semi-stabilised ylides typically give mixtures of (*E*) and (*Z*) isomers (B). Ylides with an anion that is stabilized by an electron withdrawing group are usually (*E*) selective (C).

Historically, most research on the Wittig reaction has been on triphenylphosphine derived phosphonium salts and Wittig reactions have been characterised based on how well the corresponding carbanion of the ylide is stabilised electronically.[12] Non-stabilised ylides typically have an alkyl group as the side chain, and under lithium salt free conditions these ylides offer very high (*Z*) selectivity (Figure 1.2, A).[13-16] Ylides that are stabilised by resonance with neighbouring vinyl or aryl groups are categorised as semi-stabilised and typically lack stereoselectivity, giving mixtures of (*E*) and (*Z*) isomers (Figure 1.2, B).[17-20] Stabilised ylides feature anions that are functionalized with electron withdrawing groups (EWG) and tend to provide olefins with high *E* selectivity (Figure 1.2, C).[17] The high degree of stereocontrol offered by stabilised and non-stabilised ylides has led to their use in many total syntheses, while semi-stable ylides are somewhat less useful due to their poorer selectivity.

A

erythro
kinetic

B

threo
thermodynamic
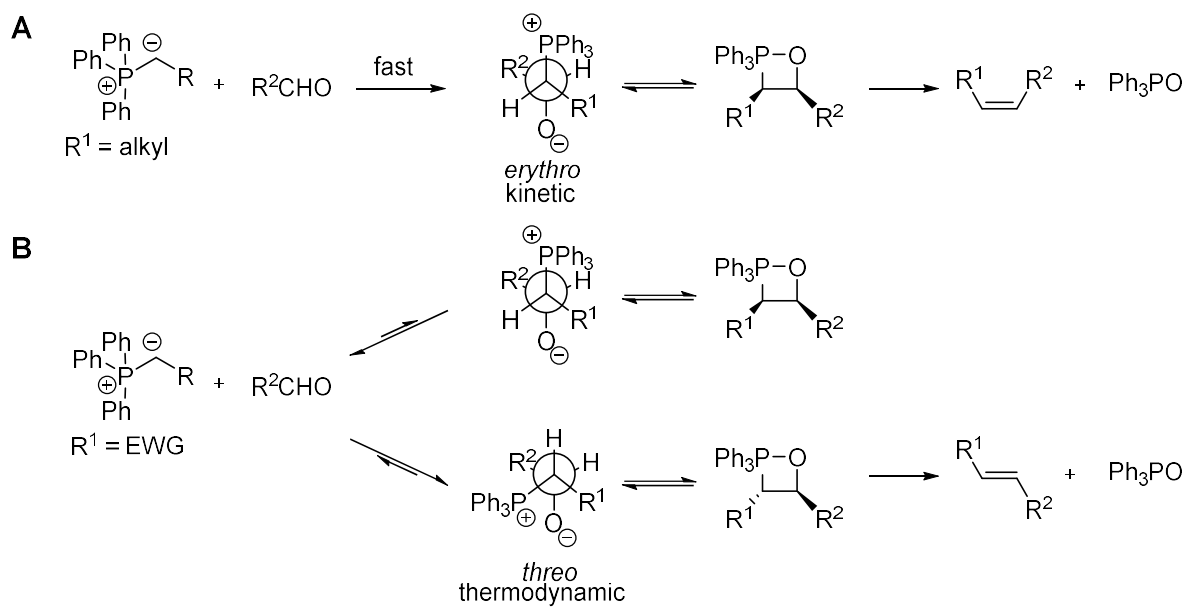
FIGURE 1.3 Proposed betaine mechanism of the Wittig reaction. Non-stabilised ylides react rapidly with aldehydes, leading to the kinetic *erythro* betaine (A). Conversely, addition of stabilised ylides to aldehydes is slow and reversion facile, thereby allowing equilibration to the thermodynamic *threo* betaine (B).

A substantial amount of research has been dedicated towards elucidating the exact mechanism of the Wittig reaction in order to improve its utility and stereochemical predictability. All proposed mechanisms of the Wittig reaction feature the formation of an oxaphosphetane ring that undergoes a stereospecific cycloreversion to give the product alkene and phosphine oxide. However, the mechanism by which the oxaphosphetane is formed has been the object of significant study and debate. For decades, it was widely accepted that the Wittig reaction proceeds via a betaine intermediate, produced by the nucleophilic attack of the ylide on the carbonyl (Figure 1.3).[21-25]

Differences in (*E*):(*Z*) selectivity were rationalized based on differences in the rate of formation and decomposition of two stereoisomeric betaines due to the electronic nature of the ylide.[26,27] For example, the addition of non-stabilised ylides to the carbonyl would be rapid and lead to the kinetic *erythro* betaine, and reversion to ylide and carbonyl components would be unfavorable (Figure 1.3, A). The betaine would then convert into the *cis*-oxaphosphetane prior to undergoing a

cycloreversion to the corresponding (*Z*) alkene and phosphine oxide. Thus, non-stabilised ylides would react under kinetic control based on the initial attack of ylide to carbonyl. Conversely, addition to the carbonyl would be slow and reversible for stabilised ylides, allowing equilibration to the thermodynamically more stable *threo* betaine and corresponding *trans*-oxaphosphetane, the decomposition of which gives an (*E*) alkene (Figure 1.3, B).

A betaine mechanism is supported by the fact that deprotonation of non-stabilised ylides with phenyllithium at low temperature leads to the formation of betaine-LiBr precipitates that decompose to the corresponding alkene and phosphine oxide upon warming or give β-hydroxy phosphonium salts if treated with anhydrous HBr.[24,27,28] As well, deprotonation of β-hydroxy phosphonium salts leads directly to betaines that subsequently form alkene and phosphine oxide products. However, these only show that phosphorous betaines can form alkene and phosphine oxide products, but do not prove that betaines are true intermediates in the Wittig reaction, especially in the absence of lithium salts. Furthermore, betaine intermediates are not observable by ^{31}P NMR under lithium salt-free conditions, unlike oxaphosphetanes which are clearly present, and betaines are higher in energy compared to both reactants and oxaphosphetanes.[14,17,29]

Substantial research, primarily conducted by Vedejs and his coworkers, with more recent computational work by Aggarwal, Harvey and co-workers, has been used to inform the modern Wittig mechanism, wherein the phosphorous ylide undergoes a [2+2] cycloaddition with the carbonyl to directly produce the oxaphosphetane intermediate.[29-38] Under lithium salt-free conditions, it has been shown that oxaphosphetane formation is irreversible and that equilibration does not occur, with limited exceptions. Thus, the stereochemistry of the alkene is determined during the initial cycloaddition and Wittig reactions are under kinetic control regardless of the electronic nature of the ylide.

Non-Stabilised   **Stabilised**
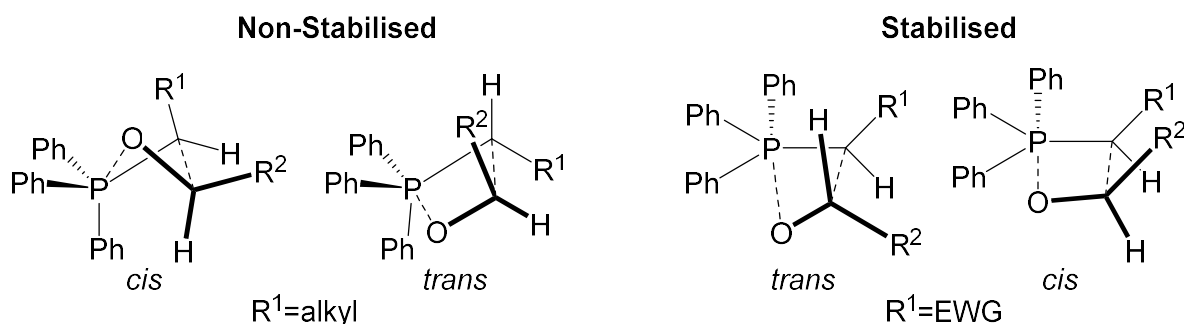
FIGURE 1.4 Cycloaddition mechanism of the Wittig reaction. Non-stabilised ylides react via an early transition state where the phosphorous has significant tetrahedral character. The *cis* transition state minimizes 1,2- and 1,3-interactions. Stabilised ylides proceed via a late transition state where the phosphorous is essentially trigonal bipyramidal, and the *trans* transition state avoids 1,2-interactions.

The addition of non-stabilised ylides to carbonyls is an exothermic process that proceeds via an early transition state where the phosphorous still has substantial tetrahedral character (Figure 1.4). Puckering in the *cis* transition state helps to minimize 1,2-interactions between ylidic and carbonyl substituents as well as 1,3-interactions between the one of the phosphorous substituents and the carbonyl that are present in the *trans* transition state.[38] Subsequent pseudorotation generates the planar *cis*-oxaphosphetane, and kinetic data suggests that oxaphosphetane decomposition is the rate limiting step.[35] Conversely, the addition of stabilised ylides to carbonyls is a rate-limiting, endothermic process where the phosphorous has significant trigonal bipyramidal character, consistent with a late transition state. The transition state leading to the *cis* oxaphosphetane is nearly planar and oxaphosphetane-like, but it has significant 1,2-interactions due to almost eclipsing ylidic and carbonyl side chains. The *trans* transition state is puckered which mitigates the 1,2-interactions and allows for favorable dipole-dipole interactions between the carbonyl and ylidic electron withdrawing group.[37-38] Semi-stabilised ylides proceed via a pathway that is intermediate between the early transition states of non-stabilised and the late transition states of stabilised ylides, typically resulting in poor selectivity for either *cis* or *trans* oxaphosphetane and hence poor (*E*):(*Z*) selectivity.
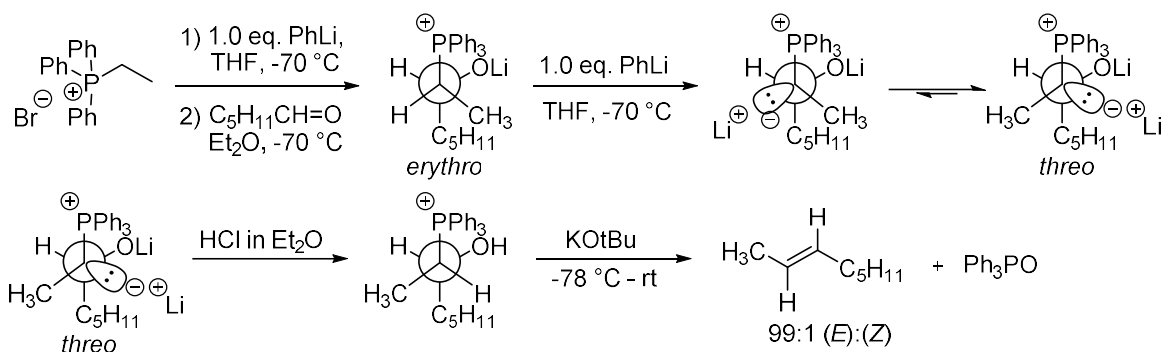
FIGURE 1.5 Schlosser modification of the Wittig reaction. The presence of lithium salts allows the formation of lithiated *erythro*-betaines which readily convert to less sterically hindered *threo*-betaines. Reprotonation at low temperature leads to corresponding (*E*) olefin.

In reactions where lithium salts are present it is challenging to demonstrate a single predictive mechanism, but they generally lead to an enrichment of the (*E*) isomer for non-stabilised ylides. Solvent choice (e.g. coordinating vs. non-coordinating), lithium salt concentration, and the presence of even trace amounts of acidic protons or water can have pronounced effects on the stereochemical outcome of Wittig reactions with lithium present.[12,13,16,27,39,40] Results from positive cross-over experiments demonstrate that lithium salts may facilitate oxaphosphetane reversal when aromatic aldehydes are used, potentially allowing equilibration to the thermodynamically more stable *trans*-oxaphosphetane and subsequent (*E*) olefin.[41] However, this process is not general, as several studies have demonstrated that oxaphosphetanes derived from aliphatic aldehydes do not undergo reversion in the presence of lithium salts, even though they readily open to give betaine-lithium salt adducts.[29,33,35]

Lithium salts can also facilitate the base catalyzed epimerization of betaines and β-hydroxy ylides.[42,43] This is demonstrated by the well-known Schlosser modification of the Wittig reaction (Figure 1.5).[44,45] In this variation, excess lithium salts present in the reaction of non-stabilised phosphorous ylides with aldehydes force the formation of lithium-betaine adducts. The addition of another equivalent of lithium base causes epimerization to the more stable lithiated *threo*-betaine. Reprotonation with anhydrous HCl and gradual warming leads to the (*E*) alkene with excellent

stereoselectivity. Ultimately, lithium affects the Wittig reaction in several ways and more than one mechanism may be operable depending on the precise reaction conditions.

Despite the synthetic utility of the classical Wittig reaction, it suffers from several drawbacks. For example, high (*E*) and (*Z*) selectivity can be obtained from the lithium salt-free reactions of stabilised and non-stabilised ylides, respectively, but semi-stabilised ylides often provide mixtures of isomers that can be synthetically useless for subsequent transformations. As well, the reaction is typically performed under anhydrous conditions using pyrophoric bases at cryogenic temperatures, all of which can be undesirable from a practical synthetic standpoint, especially if sensitive or acidic functional groups are present. Furthermore, most Wittig syntheses use triphenylphosphonium salts, resulting in a stoichiometric amount of triphenylphosphine oxide that can be notoriously difficult to remove using standard chromatographic or crystallization techniques. Various adaptations to the Wittig reaction address many of these concerns and some major advances are discussed below.

1.2 Advantages of using trialkylphosphines in Wittig chemistry

Triphenylphosphine derived ylides are the most common phosphorous species employed in the Wittig reaction. However, ylides derived from trialkyl phosphines are also used and offer several advantages in both reaction handling and stereochemical outcome. Direct access to (*E*) olefins from non-stabilised or semi-stabilised triphenylphosphoranes is not tenable using standard Wittig conditions and instead requires the use of the procedurally more involved Schlosser modification. However, replacing the phenyl substituents on a triphenylphosphorane with short-chain alkyl substituents (e.g. ethyl, propyl), results in an enrichment of the (*E*) isomer.[33,46] This is rationalized through decreased 1,3-interactions between the phosphorous substituent and the carbonyl in the early transition state leading to the *trans*-oxaphosphetane. Thus, non-stabilised and semi-stabilised ylides can have exceptional (*E*) selectivity in the Wittig reaction when derived from trialkylphosphines.

Besides offering improved (*E*) selectivity, trialkylphosphine derived phosphonium salts can also enable easier purification of alkenes produced via Wittig reaction. Wittig reactions employing triphenylphosphonium salts frequently require chromatographic purification of the desired alkene, even when the reaction proceeds "spot-to-spot". This is because the triphenylphosphine oxide by-product is difficult to remove via aqueous-organic partitioning, and chromatography can be difficult as it tends to streak through columns. Phenol and carboxylic acid functionalized triarylphosphines, as well as PEG supported phosphonium salts, have been prepared in order to significantly improve the solubility of the corresponding phosphine oxide in aqueous base. Unfortunately, these phosphines are not readily available and Wittig reactions employing the related phosphonium salts demonstrated poor stereocontrol and reactivity.[47,48] Conversely, short-chain trialkylphosphine oxides are completely water soluble, and alkenes produced by Wittig reactions using trialkylphosphine derived phosphonium salts can be purified simply by washing the organic phase with water prior to concentration.[46]

It should be noted that the use of trialkylphosphine derived phosphonium salts introduce the possibility of multiple sites for deprotonation, potentially enabling the formation of several olefinic products (Figure 1.6 A). Fortunately, complete regioselectivity in deprotonation can be achieved in the cases of salts whose corresponding ylide would be classified as stabilised or semi-stabilised. This is easily explained as the substituent protons should have a lower pKa than the protons on the phosphorous side chains. However, selective deprotonation for the generation of non-stabilized ylides is challenging. Recent work by the McNulty group has shown that the presence of pendant acetal groups can direct deprotonation, likely via a chelation-controlled pathway (Figure 1.6 B).[49-51] When the acetal oxygens are two carbons away from the phosphorous, total regioselectivity is observed and the desired alkene is the only isolable product, but increasing the distance of the oxygen directing groups results in less selective deprotonation and mixtures of alkene products.

A

B
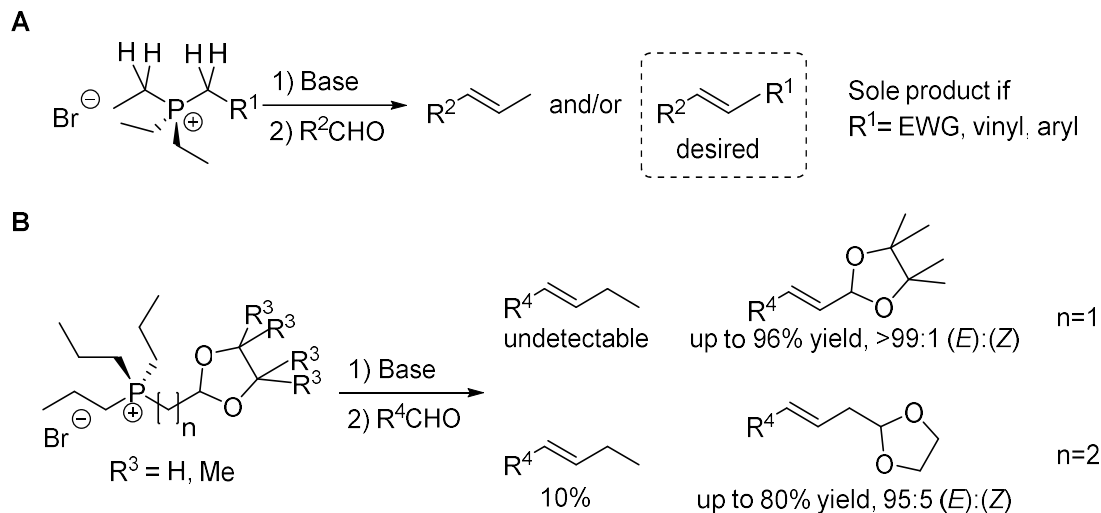
FIGURE 1.6 Deprotonation of trialkylphosphine derived phosphonium salts. Total selectivity in deprotonation can be obtained in the case of stabilised or semi-stabilised ylides (A). Selectivity is also possible for non-stabilised ylides if there is a pendant acetal directing group but is otherwise difficult (B).

An additional consideration for using trialkyl vs. triphenylphosphine in the Wittig reaction is that it improves the overall greenness of the reaction. While it is difficult to argue that the Wittig is a green methodology due to the stoichiometric production of phosphine oxide by-product, trialkylphosphines offer improved atom economy compared to triphenylphosphine. As well, the ability to purify the alkene without the use of column chromatography can significantly reduce the solvent burden for a given synthesis. Approximately 15% of anthropogenic greenhouse gasses come from the use of organic solvents in the chemical industry, and any opportunity to reduce solvent usage should be lauded.[52] While the greenness of the Wittig reaction may not be a top priority for a bench chemist, the synthetic advantages associated with using trialkylphosphine-derived phosphonium salts, e.g. ease of isolation and improved stereochemical purity, are surely appreciated.

1.3 Aqueous and organocatalytic Wittig methodologies

The classic Wittig reaction typically uses strong base (e.g. LDA, NaH, *n*-BuLi), cryogenic temperatures, inert atmosphere and dry solvent. These conditions are not only operationally difficult, they can also be dangerous for inexperienced chemists or when performed on large scales. Furthermore, using strong bases frequently requires the protection of sensitive functional groups and acidic protons, potentially adding unwanted steps to a synthesis. As well, there has been a significant push in recent years to replace organic reaction solvents with water to lessen the cost and environmental impact of synthetic chemistry.[53]

Besides environmental and economic benefits, water can also greatly increase the rate and selectivity of a reaction when it is used as solvent.[54,55] This is largely explained by the hydrophobic effect, where non-polar molecules are forced to aggregate in order to alleviate the high entropic cost of solvation. This increases the effective concentration of the semi-soluble reactants and allows novel modes of activation at the aggregate-water interface, such as transition state stabilisation via hydrogen bonding and micellar catalysis.[56-59]

The application of phase transfer catalysis to the Wittig reaction has been well studied, allowing the use of aqueous inorganic bases (e.g. $NaOH_{(aq)}$, $K_2CO_{3\ (aq)}$) as biphasic mixtures with traditional organic solvents.[60,61] This addresses one of the main drawbacks of the Wittig reaction, namely the use of strong bases. Notably, in many reactions the phosphonium salts act as the phase transfer catalyst, and other catalysts are unnecessary.[62] Unfortunately, (*E*):(*Z*) ratios are typically poor and highly solvent dependent, and the concentration and choice of base must be carefully controlled to minimize competitive aldol and Cannizzaro reactions.[63-65]

Exclusively aqueous Wittig reactions have only recently been developed, despite early evidence that functionalized styrenes could be obtained using benzyltriphenylphopshonium salts and formaldehyde in aqueous base.[66,67] Concurrent work by Bergdahl *et al* and Wu *et al.* in the mid-2000s
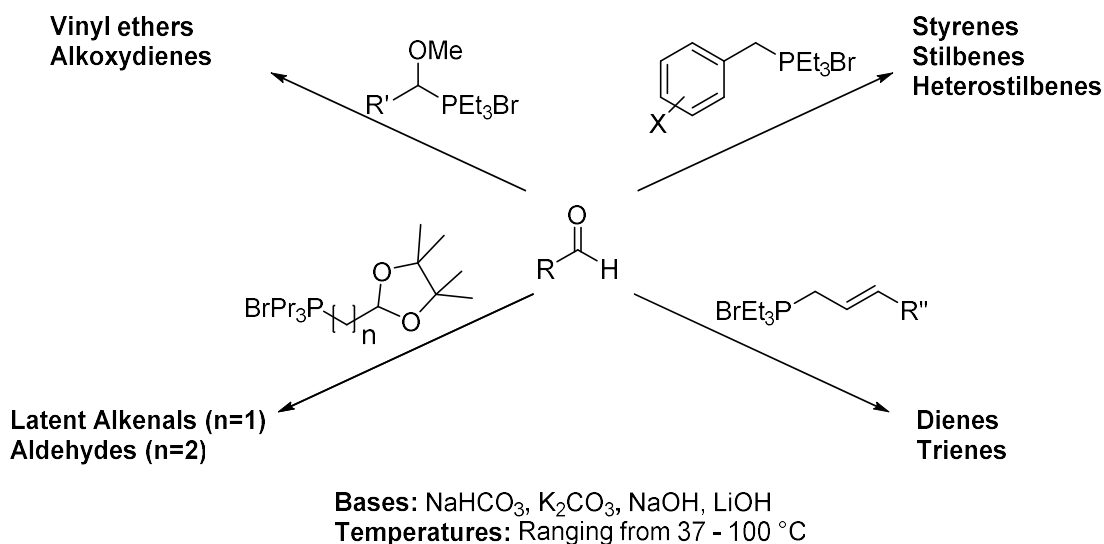
FIGURE 1.7 Structures accessible via aqueous Wittig chemistry. A wide variety of functionalized olefins can be accessed in good yields and high E selectivity from trialkylphosphonium salts using aqueous Wittig chemistry.

explored the reactions of stabilised ylides in water, rationalizing that aqueous Wittig reactions with these water-insensitive ylides could benefit from the hydrophobic effect.[68-71] Indeed, it was found that α,β-unsaturated esters and ketones could be prepared with high (E) selectivity from the reactions of various aromatic and aliphatic aldehydes with the corresponding triphenylphosphoranylides at either room temperature or reflux. Acrylonitriles were also prepared, albeit with lower (E):(Z) selectivity.[70] Notably, the reactions proceed faster and are higher yielding in water than in all organic solvents except methanol, even though the reactants are mostly insoluble in aqueous media.

Perhaps the largest advance in Wittig chemistry in the last decade has come from the combination of aqueous Wittig chemistry and trialkylphosphine derived phosphonium salts. Research from the McNulty group has demonstrated that trialkylphosphine derived stabilised, semi-stabilised, and non-stabilised salts can be used in aqueous Wittig reactions to produce a variety of synthetically valuable alkenes including styrenes, dienes, trienes, α,β-unsaturated carbonyls or their protected surrogates, stilbenes and heterostilbenes (Figure 1.7).[46,49,50,71-79] These methods address many of the

common complaints regarding the Wittig reaction, namely difficult access to (*E*) olefins, the use of strong bases, low temperature, and organic solvent in both the reaction and purification of the product. These reactions proceed in water with bases as mild as sodium bicarbonate and the products precipitate or oil out of solution. In most cases, purification is as simple as washing the product with water, as any residual salts and the trialkylphosphine oxide are readily soluble in water. Furthermore, the reactions are highly selective for the *E* olefin due to the use of trialkyl phosphines (*vide supra*).

Work by the McNulty group has pushed the mildness of the Wittig reaction even further with the development of aqueous organocatalytic Wittig methodologies. Inspired by previous reports that N-sulfonylimines act as carbonyl surrogates in the Wittig reaction, McNulty and McLeod demonstrated that the amine could be used in catalytic quantities to form an iminium species *in situ*.[80] Thus, the Wittig reaction can be performed under incredibly mild conditions, requiring only aqueous NaHCO₃ (1.0 eq.), 0.1 equivalents of weakly basic or non-basic amines or tosylamide, and stirring at 50 °C. The reaction was proven to be organocatalytic, as the background reactions were very slow in the absence of amine.

This organocatalytic methodology was then adapted to demonstrate the first biological Wittig reaction, wherein a phosphonium salt and aldehyde were separately administered to the roots and leaves of secondary amine-rich *C. sepium* or *P. sativum*, resulting in the formation of a UV active reporter stilbene that was visible in the intercellular fluid of the stem and leaf tissure.[81] The reaction was also biorthogonal, as the salt demonstrated no reactivity towards naturally occurring aldoses such as D-glucose.[82] Thus, the Wittig reaction has been developed to the point that it can be performed selectively under mild physiological conditions, a quality that may enable the future development of biological probes or related applications through biorthogonal chemistry.

1.4 Applications of Wittig chemistry to organocatalysis

The use of the Wittig reaction and the classical synthetic applications of its product alkenes are well known, even at an undergraduate level. As well, alkenes are frequently substrates for various coupling reactions and asymmetric transformations, with obvious examples including epoxidations and diol formation, hydrogenation, cyclopropanations, normal and inverse-electron demand cycloadditions, Heck cross-coupling, and ring opening, closing and cross-metathesis.[83,84] More recently the Wittig reaction has proven its usefulness in the burgeoning field of organocatalysis.

The term "organocatalysis" was first coined by MacMillan in 2001 following seminal and almost concurrent work by his group and the Barbas group on secondary-amine catalyzed Diels-Alder and Aldol reactions, respectively.[85,86] In the years following this discovery, intense research by numerous research groups around the world helped establish organocatalysis as a paradigm shift for organic chemistry.[87-91] Organocatalysis now encompasses a wide variety of transformations and is used to describe any process that is facilitated by the use of a non-metallic, organic catalyst. Major organocatalyst classes include chiral primary and secondary amines, N-heterocyclic carbene, chiral phosphines, asymmetric proton sources and H-bonding catalysts such as thioureas and squaramides.[92-98] Equally varied are the number of activation methods which include HOMO or LUMO activation, umpoled-carbonyl/acyl anion generation, and SOMO/photoredox catalysis.[87,95,99-102]

Importantly, the Wittig reaction can be used to make many of the substrates used in organocatalytic reactions. For example, both non-conjugated and α,β-unsaturated carbonyls are ubiquitous substrates in organocatalysis, as they can be activated by each of the aforementioned catalyst classes (Figure 1.8). Where not commercially available, these are readily prepared via Wittig homologations of the corresponding aldehydes (*vide supra*). Other compounds that can be prepared by the Wittig reaction and are useful in organocatalysis include styrenes, dienes, vinyl ethers, allenes,
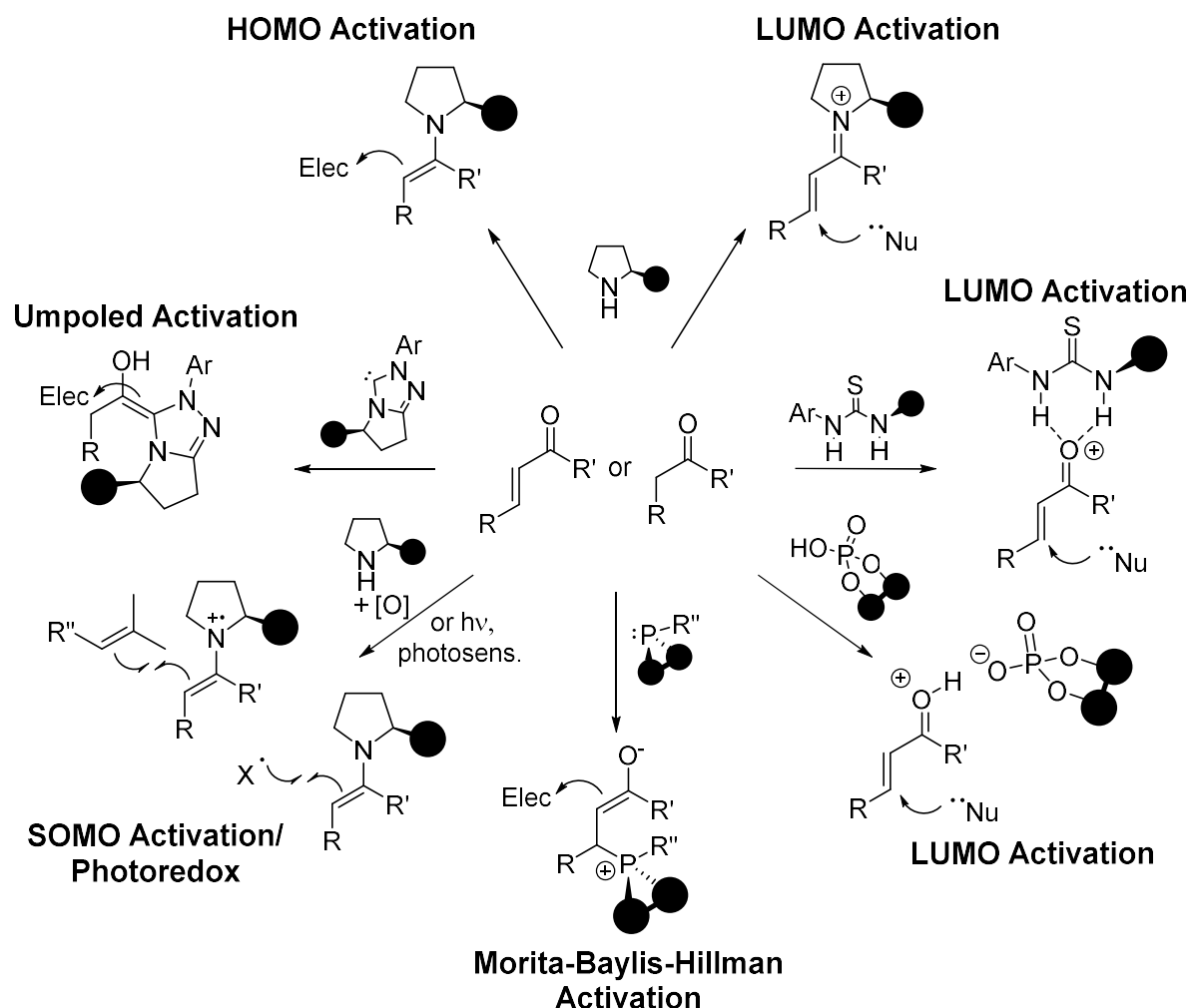
FIGURE 1.8 Common activation pathways in organocatalysis. Conjugated and non-conjugated carbonyls are frequent substrates in organocatalysis as they can be activated by many different catalyst classes. Although left unspecified, both nucleophiles (Nu:) and electrophiles (Elec) could be products of the Wittig reaction.

and various electron-poor alkenes.[87-103] Perhaps it is more a testament to the expansive range of chemistry that can be performed on or by carbon-carbon double bonds, but the Wittig reaction has maintained its utility in organic synthesis because it can provide access to a wide range of alkenes that are substrates for novel asymmetric transformations.

1.5 Conclusions

In the decades following its discovery, the Wittig reaction has been established as one of the most reliable ways to form carbon-carbon double bonds, a fact that earned Georg Wittig the Nobel Prize for Chemistry in 1979. Despite this, the mechanism of the reaction has been hotly debated for many decades and outdated mechanisms are still routinely taught in the classroom. Mechanistic misunderstandings notwithstanding, the conditions under which the reaction is known to be operable have grown significantly since the turn of the century. Classic Wittig methods are typically performed at low temperature, using dry solvent and strong bases. However, it is now known that the Wittig reaction can be performed in water with simple inorganic bases, and even organocatalytically in living systems. As well, the Wittig reaction has remained a laboratory staple as the number of applications for its product alkenes has steadily grown, especially in the fields of asymmetric metal catalysis and organocatalysis. Most importantly, the Wittig reaction plays a key role in this thesis, where it is used in the syntheses of novel anti-cancer and anti-viral compounds.

1.6 References

1) T. Laue, A. Plagens. *Named Organic Reactions 2nd Ed.* **2005**, John Wiley & Sons, 293.

2) H. Pommer, P. C. Thieme. *Top. Curr. Chem : Wittig Chem.* **1983**, *109*, Springer, Berlin, Heidelberg.

3) T. Takeda. *Modern Carbonyl Olefination: Methods and Applications.* **2006**, Wiley-VCH: Weinheim.

4) K. C. Nicolaou, M. W. Härter, J. L. Gunzner, A. Nadin. *Liebegs Ann.* **1997**, *7*, 1283.

5) L. Horner, H. M. R. Hoffmann, H. G. Wippel. *Ber.* **1958**, *91*, 61.

6) L. Horner, H. M. R. Hoffmann, H. G. Wippel, G. Klahre. *Ber.* **1959**, *92*, 2499.

7) W. S. Wadsworth Jr., W. D. Emmons. *J. Am. Chem. Soc.* **1961**, *83*, 1733.

8) M. Julia, J-M. Paris, *Tetrahedron Lett.* **1973**, *14*, 4833.

9) P. J. Kocienski, B. Lythgoe, S. Ruston. *J. Chem. Soc., Perkin Trans.* **1978**, *1*, 829.

10) D. J. Peterson. *J. Org. Chem.* **1968**, *33*, 780.

11) G. Wittig, G. Geissler. *Liebigs Ann. Chem.* **1953**, *580*. 44.

12) L. D. Bergelson, M. M. Shemyakin. *Tetrahedron*, **1963**, *19*, 149.

13) M. Schlosser. *Top. Stereochem.,* ed. E. L. Eliel & N. L. Allinger, Wiley, New York, New York, **1970**, vol. 5.

14) E. Vedejs, K. A. J. Snoble. *J. Am. Chem. Soc.* **1973**, *95*, 5778-5780.

15) M. Schlosser, B. Schaub, J. Oliveira-Neto, S. Jeganathan. *Chimia* **1986**, *40*, 246-247.

16) A. B. Reitz, S. O. Nortey, A. D. Jordan, M. S. Mutter, B. E. Maryanoff. *J. Org. Chem.* **1986**, *51*, 3302-3308.

17) E. Vedejs, M. J. Peterson. *Top. Stereochem.*, ed. E. L. Eliel & S. H. Wilen, **1994**, vol. 21 Wiley, New York, New York.

18) E. G. McKenna. *Tetrahedron Lett.* **1988**, *29*, 485.

19) H. Yamataka, K. Nagareda, K. Ando, T. Hanafusa. *J. Org. Chem.* **1992**, *57*, 2865.

20) W. J. Ward Jr., W. E. McEwan. *J. Org. Chem.* **1990**, *55*, 493.

21) G. Wittig, H-D. Weigmann, M. Schlosser, *Chem. Ber.* **1961**, *94*, 676.

22) S. Trippett. *Q. Rev. Chem. Soc.* **1963**, *17*, 406.

23) G. Wittig, A. Haag. *Chem. Ber.* **1963**, *96*, 1535.

24) M. E. Jones, S. Trippett. *J. Chem. Soc. C.* **1966**, 1090.

25) A. Johnson. *Organic Chemistry*, **1966**, *7*, 132.

26) H. O. House, G. H. Rasmusson. *J. Org. Chem.* **1961**, *26*, 4278.

27) M. Schlosser, K. F. Christmann. *Liebigs Ann. Chem.* **1967**, *708*, 1.

28) G. Wittig, U. Schöllkopf. *Chem. Ber.* **1954**, *87*, 1318.

29) E. Vedejs, G. P. Meier, K. A. J. Snoble. *J. Am. Chem. Soc.* **1981**, *103*, 2823.

30) P. A. Bryne, D. G. Gilheany. *J. Am. Chem. Soc.* **2012**, *134*, 9225.

31) E. Vedejs, T. Fleck, S. Hara. *J. Org. Chem.* **1987**, *52*, 4637.

32) E. Vedejs, C. F. Marth. *Tetrahedron Lett.* **1987**, *28*, 3445.

33) E. Vedejs, C. F. Marth, R. Ruggeri. *J. Am. Chem. Soc.* **1988**, *110*, 3940.

34) E. Vedejs, C. F. Marth. *J. Am. Chem. Soc.* **1988**, *110*, 3948.

35) E. Vedejs, C. F. Marth. *J. Am. Chem. Soc.* **1989**, *111*, 1519.

36) E. Vedejs, T. Fleck. *J. Am. Chem. Soc.* **1989**, *111*, 5861.

37) R Robiette, J. Richardson, V. K. Aggarwal, J. N. Harvey. *J. Am. Chem. Soc.* **2005**, *127*, 13468.

38) R. Robiette, J. Richardson, V. K. Aggarwal, J. N. Harvey. *J. Am. Chem. Soc.* **2006**, *128*, 2394.

39) D. L. Hooper, S. Garagan. *J. Org. Chem.* **1994**, *59*, 1126.

40) B. E. Maryanoff, A. B. Reitz. *Chem. Rev.* **1989**, *89*, 863.

41) M. Schlosser, K. F. Christmann. *Angew. Chem. Int. Ed. Engl.* **1965**, *4*, 689.

42) R. J. Anderson, C. A. Henrick. *J. Am. Chem. Soc.* **1975***, 97*, 4327.

43) H. J. Bestmann. *Pure Appl. Chem.* **1979**, *51*, 515.

44) M. Schlosser, K. F. Christmann. *Angew. Chem. Int. Ed. Engl.* **1966**, *5*, 126.

45) M. Schlosser, K. F. Christmann, A. Piskala, A. *Chem. Ber.* **1970**, *103*, 2814.

46) J. McNulty, D. McLeod, P. Das, C. Zepeda-Velázquez. *Phosphorous, Sulfur, and Silicon* **2015**, *190*, 619.

47) M. G. Russel, S. Warren. *J. Chem. Soc. Perkin Trans. 1* **2000**, 505.

48) F. Sieber, P. Wentworth Jr., J. D. Toker, A. D. Wentworth, W. A. Metz, N. N. Reed, K. D. Janda. *J. Org. Chem.* **1999**, *64*, 5188.

49) J. McNulty, C. Zepeda-Velázquez, D. McLeod. *Green Chem.* **2013**, *13*, 3146.

50) D. McLeod, J. McNulty. *Roy. Soc. Open. Sci.* **2016**, *3*, 160374.

51) A. Narayanappa, D. Hurem, J. McNulty. *Synlett.* **2017**, *28*, 2961.

52) J. F. Jenck, F. Agterberg, M. J. Droescher. *Green Chem.* **2004**, *6*, 544.

53) J. M. DeSimone. *Science* **2002**, *297*, 799.

54) S. Otto, J. B. F. N. Engberts. *Org. Biomol. Chem.* **2003**, *1*, 2809.

55) S. Narayan *et al. Angew. Chem. Int. Ed.* **2005**, *44*, 3275.

56) R. Breslow. *Acc. Chem. Res.* **1991**, *24*, 159.

57) R. Breslow, K. Groves, M. U. Mayer. *Pure Appl. Chem.* **1998**, *70*, 1933.

58) L. F. Scatena, M. G. Brown, G. L. Richmond. *Science.* **2001***, 292*, 908.

59) R. Breslow. *Acc. Chem. Res.* **2004**, *37*, 471.

60) Y. Al Jasem, R. El-Esawi, T. Thiemann. *J. Chem. Res.* **2014**, *38*, 453.

61) W. P. Weber, G. W. Gokel. *React. Structure: Concepts in Org. Synth. Vol 4: Phase Transfer Catal. Org. Synth.* **2012**, Springer Science and Business Media.

62) C. M. Starks. *J. Am. Chem. Soc.* **1971**, *93*, 195.

63) W. Tagaki, I. Inoue, Y. Yano, T. Okonogi. *Tetrahedron Lett.* **1974**, *30*, 2587.

64) Y. Le Bigot, M. Delmas, A. Gaset. *Synth. Commun.* **1982**, *12*, 107.

65) J-J. Hwang, R-L. Lin, R-L. Shieh, J-J. Jwo. *J. Mol. Catal. A: Chem.* **1999**, *142*, 125.

66) M. Butcher, R. J. Mathews, S. Middleton. *Aus. J. Chem.* **1973**, *26*, 2067.

67) R. Broos, M. Anteunis. *Synth. Commun.* **1976**, *6*, 53.

68) J. Dambacher, W. Zhao, A. El-Batta, R. Anness, C. Jiang, M. Bergdahl. *Tetrahedron Lett.* **2005**, *46*, 4473.

69) A. El-Batta, C. Jiang, W. Zhao, R. Anness, A. L. Cooksy, M. Bergdahl. *J. Org. Chem.* **2007**, *72*, 5244.

70) J. Wu, D. Zhang, S. Wei. *Synth. Commun.* **2005**, *35*, 1213.

71) J. Wu, C. Yue. *Synth. Commun.* **2006**, *36*, 2939.

72) J. McNulty, D. McLeod. *Tet. Lett.* **2013**, *54*, 6303.

73) J. McNulty, D. McLeod. *Tet. Lett.* **2011**, *52*, 5467.

74) P. Das, D. McLeod, J. McNulty. *Tet. Lett.* **2011**, *52*, 199.

75) P. Das, J. McNulty. *Eur. J. Org. Chem.* **2010**, 3587.

76) P. Das, J. McNulty. *Tet. Lett.* **2010**, *51*, 3199.

77) J. McNulty, P. Das, D. McLeod. *Chem. Eur. J.* **2010**, *16*, 6756.

78) J. McNulty, P. Das. *Tet. Lett.* **2009**, *50*, 5737.

79) J. McNulty, P. Das. *Eur. J. Org. Chem.* **2009**, 4031.

80) J. McNulty, D. McLeod. *Chem. Eur. J.* **2011**, *17*, 8794.

81) D. McLeod, J. McNulty. *Eur. J. Org. Chem.* **2012**, 6127.

82) E. M. Sletten, C. R. Bertozzi. *Angew. Chem. Int. Ed.* **2009**, *48*, 6974.

83) E. N. Jacobsen, A. Pfaltz, H. Yamamoto. *Comprehensive Asymmetric Catalysis: Supplement 1 and 2.* **2004**. *Springer-Verlag Berlin Heidelburg.*

84) M. B. Smith, J. March. *March's Advanced Organic Chemistry: Reactions, Mechanisms and Structure.* **2007**, 6ᵗʰ Ed. John Wiley and Sons, Inc., Hoboken, New Jersey.

85) K. A. Ahrendt, C. J. Borths, D. W. C. MacMillan. *J. Am. Chem. Soc.* **2000**, *122*, 4243.

86) B. List, R. A. Lerner, C. F. Barbas III. *J. Am. Chem. Soc.* **2000**, *122*, 2395.

87) D. W. C. MacMillan. *Nature* **2008**, *455*, 304.

88) A. Dondoni, A. Massi. *Angew. Chem. Int. Ed.* **2008**, *47*, 4638.

89) W. Notz, F. Tanaka, C. F. Barbas III. *Acc. Chem. Res.* **2004**, *37*, 580.

90) S. Bertelsen, K. A. Jørgensen. *Chem. Soc. Rev.* **2008**, *38*, 2178.

91) P. I. Dalko. *Enantioselective Organocatalysis: Reaction and Experimental Procedures.* **2007**, Wiley-VCH Verlag GmbH and Co. KGaA, Weinheim.

92) L-W. Xu, J. Luo, Y. Lu. *Chem Commun.* **2009**, *0*, 1807.

93) X. Yu, W. Wang. *Org. Biomol. Chem.* **2008**, *6*, 2037.

94) M. Tsakos, C. G. Kokotos. *Tetrahedron* **2013**, *69*, 10199.

95) D. M. Flanigan, F. Romanov-Michailidis, N. A. White, T. Rovis. *Chem. Rev.* **2015**, *115*, 9307.

96) Y. Wei, M. Shi. *Acc. Chem. Res.* **2010**, *43*, 1005.

97) J. L. Methot, W. R. Roush. *Adv. Synth. Catal.* **2004**, *346*, 1035.

98) D. Kampen, C. M. Reisinger, B. List. *Top. Curr. Chem.*, ed. B. List. Springer, Berlin, Heidelberg, **2010**, vol. 291.

99) D. A. Nicewicz, D. W. C. MacMillan. *Science* **2008**, *322*, 77.

100) T. D. Beeson, A. Mastracchio, J-B. Hong, K. Ashton, D. W. C. MacMillan. *Science.* **2007**, *316*, 582.

101) A. Erkkilä, I. Majander, P. M. Pihko. *Chem. Rev.* **2008**, *107*, 5416.

102) S. Mukherjee, J. W. Yang, S. Hoffmann, B. List. *Chem. Rev.* **2007**, *107*, 5471.

103) Berkessel, A., Gröger, H. *Asymmetric Organocatalysis: From Biomimetic Concepts to Applications in Asymmetric Synthesis.* 2005, Wiley-VCH: Weinheim.

2 Wittig Derived Inhibitors of Human Aromatase

2.1 Estrogen-receptor positive breast cancer, its prevalence and treatment

Breast cancer accounts for 30% of all new cancer diagnoses in women and almost 15% of all female cancer deaths.[1,2] As well, approximately 70% of breast cancer in post-menopausal women can be attributed to overexpression of the nuclear estrogen receptors (ERs) in breast tissue, with the resultant cancer being called ER positive. Estrogen acts as a growth hormone for many tissues including the breast, and its binding to the overexpressed ERs leads to mammary cell proliferation and tumorigenesis. Unfortunately, the rate of ER positive breast cancer has been increasing although this is partially offset by declining rates of hormone receptor negative breast cancers.

Despite the growing prevalence of ER positive breast cancer, breast cancer death rates have decreased by 39% from 1989 to 2014, largely due to improvements in early detection and treatment of the disease.[1,2] Modern chemotherapeutic treatment of ER positive breast cancer typically involves the administration of selective estrogen receptor modulators, e.g. tamoxifen, which compete with estrogen binding to the ERs, and aromatase inhibitors (AIs).[3] Aromatase catalyzes the rate limiting step in the conversion of androgens to estrogens, thus AIs such as anastrozole and letrozole reduce the amount of estrogen present in the body.

Although the co-administration of SERMs and AIs is proven to significantly reduce breast cancer mortality, many patients discontinue their treatment regimen due to the significant side effects they experience.[4,5] As well, long term estrogen deprivation can lead to resistance and cancer relapse.[6] Thus, there is a pressing need for the development of new AIs. Fortunately, many natural products exhibit anti-aromatase activity and have been used as promising leads for the design of novel AIs. Recently, A. J. Nielsen and J. McNulty authored a review on the anti-aromatase activity of the main classes of polyphenolic natural products and the synthetic derivatives derived therefrom, published in

Med. Res. Rev., 2018, *Early View*, and it is reproduced below (Chapter 2.2). Immediately following the review is a paper on the design and synthesis of stilbene-derived aromatase inhibitors, as published in *Bioorg. Med. Chem. Lett.*, 2019, *29*, 1395-1398 (Chapter 2.3). For the latter work, A. J. Nielsen developed the method and performed all the synthesis, Sergio Raez-Villanueva ran the assays for anti-aromatase activity, and the manuscript was written by A. J. Nielsen and J. McNulty. Chapters 2.2 and 2.3 are reproduced with permission; figures were formatted to be in sequence with the rest of the chapter.

2.2 Polyphenolic natural products and natural product–inspired steroidal mimics as aromatase inhibitors

The discovery of biologically active polyphenolic natural products, including chalcones, stilbenes, flavanones, and isoflavones as steroidal mimics has proven to be a subject of considerable importance in medicine. Some of these natural compounds have been shown to modulate key human metabolic processes via steroidal hormone receptors, or to inhibit crucial enzymes involved in the biosynthesis of steroidal hormones themselves. Isoflavone polyphenolics such as genistein are well known for this "phytoestrogenic" biological activity. This review focuses on the ability of select polyphenolics and their synthetic derivatives to function as steroidal mimics in the inhibition of the enzyme aromatase, thereby lowering production of endogenous estrogen growth hormones. The discovery of potent, natural product–based aromatase inhibitors (AIs) as hit compounds has led to the introduction of steroidal-based irreversible inhibitors, such as exemestane and reversible AIs such as anastrozole and letrozole, now standard therapy in the treatment of estrogen receptor–positive breast cancer and other hormone related indications. Pursuit of this strategy over the last few decades has been largely successful although complications and challenges remain. This review highlights the aromatase activity of natural stilbenes, chalcones, and flavanones and synthetically inspired versions thereof and draws attention to new and under-investigated areas within each class worthy of pursuit.

2.2.1 – From Selective Estrogen Receptor Modulation to Aromatase Inhibition

Cancer remains the second leading cause of death in the United Sates, accounting for approximately 25% of all fatalities, statistically only slightly lower than the figures for heart disease.[1] Breast cancer remains the most frequently diagnosed cancer amongst women and while the incidence rate increased about 30% between 1975 and 2002, recent statistics show that the incidence rate has now dropped somewhat and has levelled off since 2002. Nonetheless, breast cancer still accounted for over 250 000 newly diagnosed cases in 2017 in the United States alone, representing 30% of all diagnosed cancers. More encouraging is the statistically significant increases in the 5-year survival rates that have been documented over the last few decades.[1] The overall death rate for female breast cancer has dropped 38% between 1989 and 2014. This success has been attributed to various factors including smoking cessation, educational awareness, and most importantly, early detection and treatment.

Approximately 70% to 80% of all postmenopausal breast cancer patients have hormone-dependent, nuclear estrogen receptor (ER)-positive breast cancer.[2] Estrogen is produced largely in the ovary and to a lesser extent in adipose tissue, as well as in the placenta during pregnancy. Along with related metabolites, estrogen functions as a growth hormone for numerous tissues through selective action at membrane-bound estrogen receptors (mERs) and the intracellular nuclear ERs (ERα and ERβ). While the hormonal treatment of breast cancer dates from the classic surgical interventions of Beatson in 1895,[3] modern pharmacological treatments have focused first on selective blockage of ERs[4] and more recently on the reduction in the production of endogenous estrogen through inhibition of the enzyme aromatase.[5] The use of receptor blockers or selective estrogen receptor modulators (SERMs) dates from the late 1960s and early 1970s when positive clinical outcomes were reported with the use of antiestrogenic agents such as tamoxifen (**1**) (Figure 2.1).[6] Tamoxifen was originally developed at ICI Pharmaceuticals as ICI-46474 as a potential birth control agent and was finally

Tamoxifen (**1**)   Raloxifene (**2**)
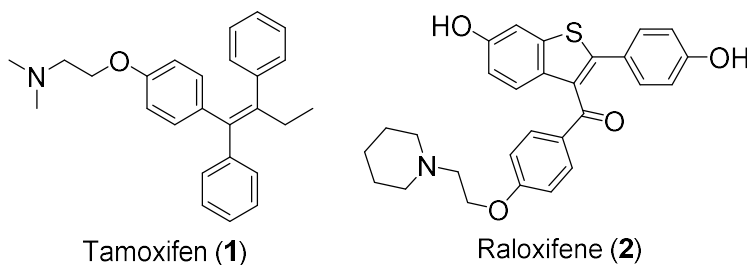
FIGURE 2.1 Chemical structures of clinically used selective estrogen receptor modulators tamoxifen (**1**) and raloxifene (**2**).

introduced for the treatment of breast cancer in 1977. A second SERM drug raloxifene (**2**) (Figure 2.1) was found to be ineffective in the treatment of breast cancer, but has found use as a breast cancer chemopreventive agent in high-risk individuals since 2007.[7]

Despite the encouraging results with tamoxifen, not all patients with ER‑positive breast cancer respond to it and drug resistance (relapse) is common.[8] In addition, significant side effects have been reported including thromboembolism and an increased risk in the development of endometrial cancer. The development of AIs[5] has been a more recent focus within the pharmaceutical industry.[9] Aromatase (cytochrome P450 19A1) is responsible for the final rate-limiting step in the conversion of androgens such as androstenedione (**3**) or testosterone (**4**) to estrogens such as estrone (**5**) or estradiol (**6**) through a multistep process (Figure 2.2). It has also been established that estrone (**5**) and estradiol (**6**) interconvert biosynthetically in postmenopausal women.[10] Overall, AIs act by lowering the production of endogenous estrogen rather than selectively modulating ERs.

While some details of the conversion of androgens to estrogens by aromatase remain unknown, the key steps of the process have been largely worked out.[11] The C19-methyl group of the androgen substrate binds within a lipophilic pocket to the iron-center of the enzyme, where it is oxidized stepwise through the intermediacy of a primary alcohol, aldehyde (hydrate), and carboxylic acid, allowing for subsequent oxidative-deformylation (loss of formic acid), involving cleavage of the C10–C19 carbon–carbon bond, to yield the aromatic A ring of estrogen.
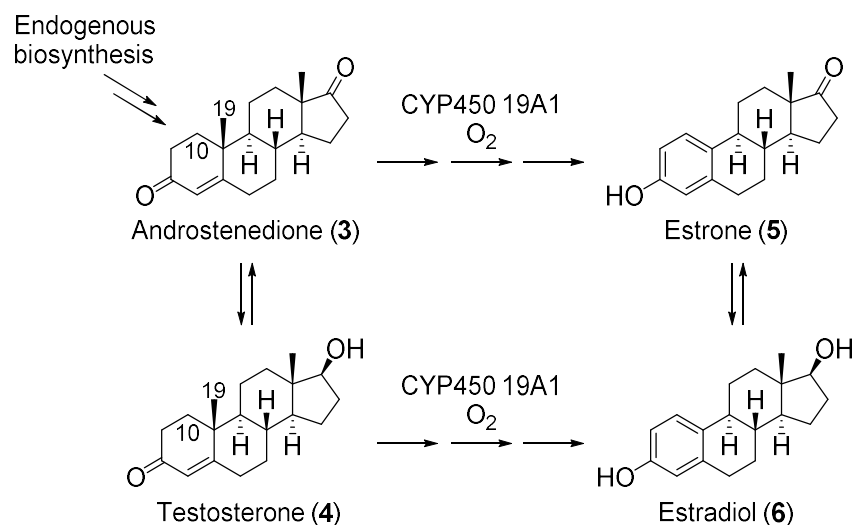
FIGURE 2.2 Key biosynthetic pathways involved in the conversion of the endogenous androgens androstenedione (**3**) and testosterone (**4**) to the estrogens estrone (**5**) and estradiol (**6**) by the cytochrome P450 enzyme CYP450 19A1, otherwise known as aromatase.

Since the mid-1990s, three clinically used AIs have been introduced for the treatment of ER-positive breast cancer: the steroidal irreversible inhibitor exemestane (**7**) and the nonsteroidal reversible inhibitors anastrozole (**8**) and letrozole (**9**) (Figure 2.3).[12] From a general structural viewpoint, synthetic AIs frequently contain a lipophilic core as a mimic of the steroidal framework, hydrogen-bond acceptors as bioisosteres of the substrate carbonyls, and a key donor substituent that reversibly binds to the heme-containing core of the enzyme. For example, anastrozole and letrozole are potent, reversible AIs that feature two nitrile groups as carbonyl mimics and a 1,2,4-triazole group
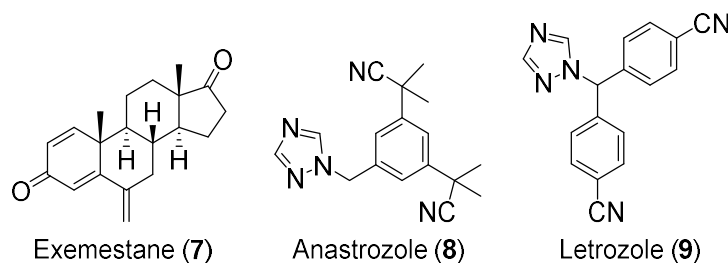
FIGURE 2.3 Chemical structures of clinically used aromatase inhibitors exemestane (**7**) anastrozole (**8**) and letrozole (**9**).

that chelates the heme of aromatase, and their use alone or as adjuvant to initial treatment with tamoxifen or raloxifene is now the standard-of-care in remission and long-term chemotherapeutic management of ER-positive breast cancer.[4,5]

2.2.2 – Natural Products as Steroidal Mimics

Natural products of the phenylpropanoid pathway are known to function as steroidal mimics or phytoestrogens, e.g., the structural similarities of the isoflavone genistein and 17-β-estradiol are well known.[23] The secondary metabolic pathway leading to the phenylpropanoid class of secondary metabolites is totally distinct from steroidal biosynthesis. Steroidal biosynthesis derives from a branch of terpenoid biosynthesis proceeding via dimerization of farnesyl diphosphate to squalene, squalene epoxide, and further modification of the tetracyclic triterpenoid core leading to steroids such as cholesterol and androstenedione. In contrast, phenylpropanoids follow a mixed biosynthetic path involving an amino acid-triketide incorporation and is outlined in Figure 2.4. The process is initiated from the amino acids phenylalanine (**10a**) or tyrosine (**10b**), which, following deamination with phenylalanine ammonia lyase, proceeds via the coenzyme-A (CoASH) conjugated cinnamyl starter unit (**11**). The biosynthesis involves incorporation of three acetate units through Claisen condensations with malonyl-coenzyme A, leading to the intermediate **12**. This triketide unit may cyclize in various conformationally restricted pathways leading to the major classes of polyphenolic natural products. Conversion of intermediate **12** with the enzyme stilbene synthase[13] involves an intramolecular aldol process followed by decarboxylation leading to the key stilbenoid natural product resveratrol (**13**), which has been the subject of many biological evaluations and claims.[14] Further modifications such as oxidation, methylation, glycosylation, dimerization, prenylation, and combinations of these lead to the expansive class of stilbenoid derived natural products.[15]
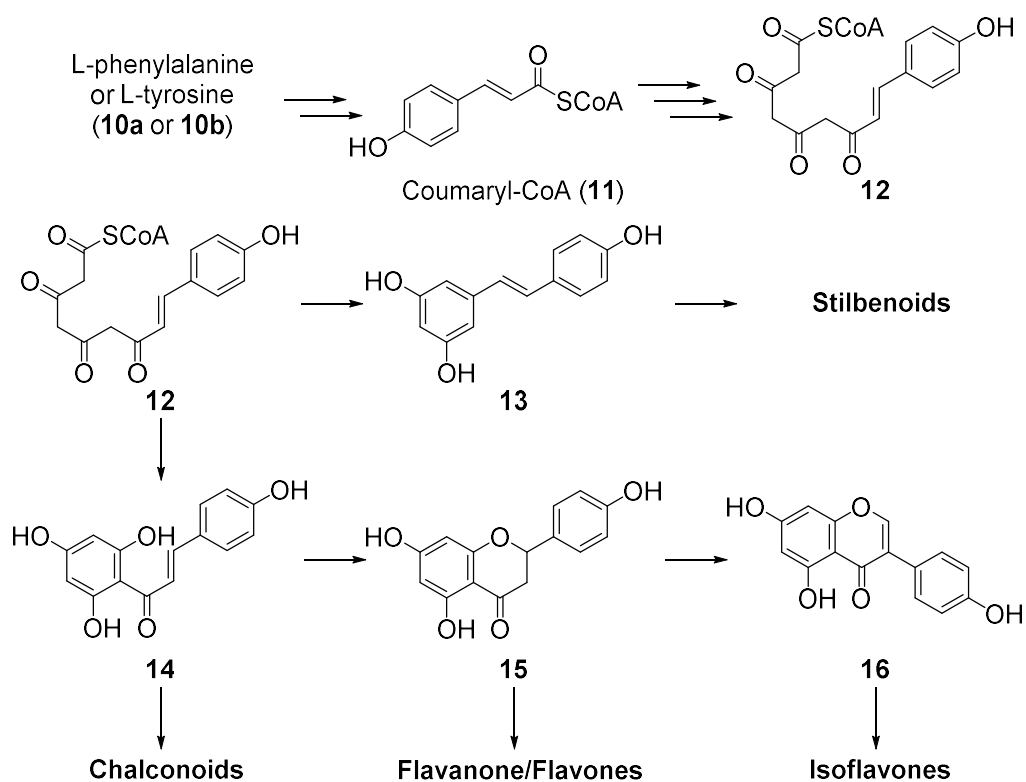
FIGURE 2.4 Central secondary metabolic pathways involved in the biosynthesis of aromatic amino acid-polyketide derived polyphenolic natural products including stilbenoids, chalconoids, flavonoids and isoflavanoids.

Conversion of intermediate **12** with the enzyme chalcone synthase[16] involves an intramolecular Claisen process leading to chalcone (**14**), from which similar modifications leads to chalconoid natural products. Cyclization of intermediate 14 through an intramolecular oxy-Michael reaction carried out by the enzyme chalcone isomerase leads to the flavanone intermediate **15**, usually as the (2S)-stereoisomer naringenin (**15**).[17] Oxidation of naringenin with the enzyme flavone synthase[18] leads to formation of a large class of aromatic flavanone natural products that includes the anthocyanidins, while oxidation with isoflavonoid synthase proceeds through a 1,2-aryl migration leading to the isoflavone class of natural products, such as genistein (**16**).[19]

While most of the enzymes and natural products derived from the aforementioned pathways are of plant-specific origin[20] this exclusivity has been challenged.[21] Nonetheless, the majority are regarded as plant-derived secondary metabolites.[22,23] The structural diversity of compounds produced through these expansive pathways is impressive. For example, the structures of over 8500 flavonoid natural products alone have been described.[24] The chemical biology displayed by these metabolites is equally fascinating, in particular the role of plant-derived polyphenols as phytoalexins,[25] and the study of their role in modulating plant-fungal interactions[26,27] is a highly active area of what may be called molecular-level evolutionary biology. One of the key elements involved in these interactions is the ability of certain of the polyphenols to function as steroidal mimics. The term "phytoestrogen" aptly describes the role of such polyphenolic compounds that are thus able to interact with signaling pathways typically modulated through endogenous steroidal signal transduction.

The most well known of these natural phytoestrogen steroidal mimics is the isoflavone genistein (**16**) shown in Figure 2.5.[23] The estradiol receptor is a target for genistein due to the similar steric positioning of the key hydroxyl groups and the lipophilic nature of the core in **16**. Genistein mimics estradiol and initiates signal transduction through interaction with the ER. This results in partial agonist activity, activating transcription factors and biosynthesis of the epidermal growth factor receptor.[28,29]
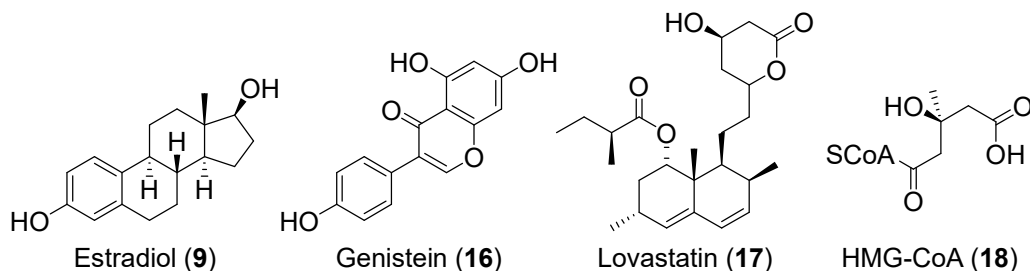

FIGURE 2.5 Structure of the phytoestrogen genistein (**16**) and its relation to the endogenous hormone estradiol (**9**) (top) and the fungal-derived polyketide lovastatin (**17**) and the enzyme substrate HMG-CoA (**18**).

The ability of a natural polyketide produced through an unrelated pathway to modulate a key biochemical event via mimicry of an endogenous steroidal mediator of said event represents a fascinating adaptation and is not restricted to the endocrine pharmacological receptors. Natural fungal–derived polyketides such as lovastatin (**17**)[30] are capable of modulating steroid biosynthesis through inhibition of the enzyme hydroxymethylglutaryl coenzyme A (**18**) (HMGCoA) reductase, acting as a transition-state mimic.[31] This enzyme catalyzes the rate-limiting step involved in the biosynthesis of cholesterol and is the key target of the block-buster statin-type cholesterol lowering drugs (Zocor, Lipitor, etc.). These examples serve to illustrate that natural products produced through distinct pathways can modulate the two classic targets of small-molecule pharmacological intervention: the enzymes by which they are biosynthesized and the pharmacological receptors upon which they act. The role of the major structural types of the polyphenolics (stilbenes, chalcones, and flavonoids/isoflavonoids) and synthetic derivatives thereof in modulating estrogenic effects has been the focus of a significant amount of research over the past several decades. This review focuses on small-molecule derivatives of these polyphenols as novel AIs and pharmacological candidates for the treatment of breast cancer.

2.2.3 – Stilbenes and Stilbenoids as AIs

Stilbenes and stilbenoids are one of the most studied classes of natural products. Naturally occurring stilbenes such as resveratrol (**13**), piceatannol (**19**), pterostilbene (**20**), combretastatin A4 (**21**), and synthetic stilbene DMU-212 (**22**) are potent antioxidants that have been reported to possess potential anti-inflammatory, cardioprotective, neuroprotective, antiobesity, antiangiogenic, antiproliferative, and cancer chemopreventive effects (Figure 2.6).[32–37]
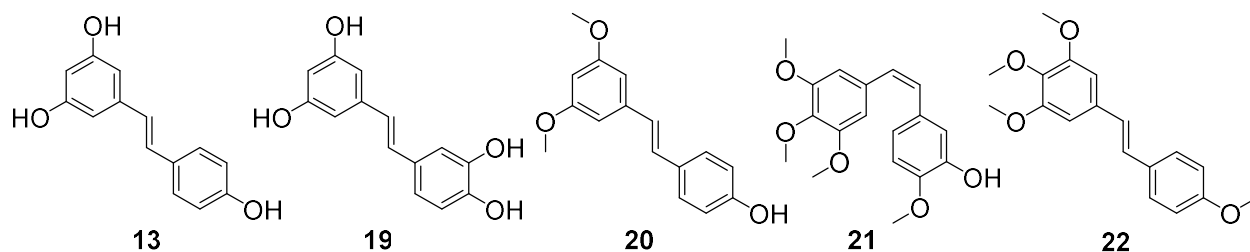
FIGURE 2.6 Structures of common natural and synthetic stilbenes.

Resveratrol in particular has been the focus of numerous studies due to its prevalence in red wines and grapes, and its proposal as the explanation for the popular "French paradox."[38] In spite of the myriad studies touting their efficacy, resveratrol and other natural stilbenes are poor drug candidates due to their low potency, lack of tissue and target specificity, rapid metabolism, and low-serum concentrations.[39] Their lack of specificity also makes their overall biological effect difficult to predict. For example, resveratrol is reported to be an ER agonist and promote the proliferation of estrogen-dependent T47D, KPL-1, and MCF-7 breast cancer cell lines.[32,40] However, it causes apoptosis of both ER positive and hormone independent cell lines at higher concentrations even in the presence of linoleic acid, a breast cancer cell promoter.[32] As well, consumption of resveratrol was reported to increase or decrease breast cancer risk, depending on the dietary source of the compound.[41]

While resveratrol and related stilbenes are poor drug candidates, their structural similarity to the natural substrates of aromatase has prompted the exploration of synthetic stilbene analogues for the treatment of ER-dependent breast cancer. Simple exploration of substitution on the A and B rings of resveratrol has allowed for the development of more potent and selective AIs. For example, Sun et al[42] identified that 4-aminostilbene (**23**) was a potential lead compound with an IC$_{50}$ of 20 μM, four

23
22 µM

24
0.67 µM

**25**
0.90 µM

26
0.98 µM

27
0.76 µM

28
0.59 µM
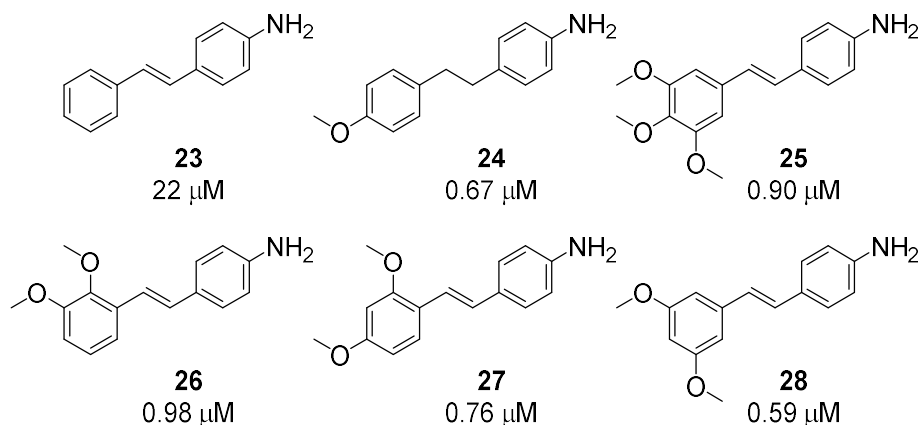
FIGURE 2.7 Aminostilbene inhibitors of aromatase with sub-micromolar IC_{50} values.

times more potent than resveratrol (IC_{50} = 80 µM) (Figure 2.7). A library of 44 substituted stilbene analogues were tested against aromatase in vitro, the majority of which were prepared using a Heck cross coupling between substituted styrenes and aryl iodides as the key synthetic step.[42]

This resulted in the discovery of five additional stilbenes with submicromolar IC_{50} (**24** to **28**). The results demonstrated that replacing the amino group with acetyl, aminomethyl, halogen, nitrile, or nitro groups led to a loss of activity, and changing its position in the ring resulted in a reduction of activity. Substitution of methoxy groups in the B ring was also explored, and the aminostilbene analogue of pterostilbene (**28**) was the most potent stilbene tested (IC_{50} = 0.59 µM).

Follow-up screening of 92 resveratrol analogues by Kondratyuk et al[39] sought to identify compounds with improved specificity, and the analogues were tested against a wide variety of

29
2.8 µM

30
0.68 µM

**31**
3.9 µM

32
3.2 µM
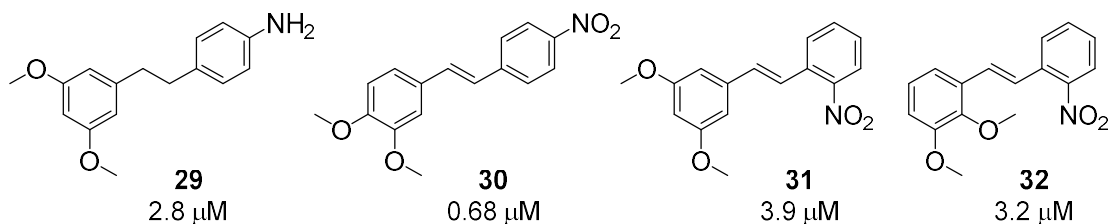
FIGURE 2.8 Selective and potent inhibitors of aromatase featuring a simple stilbene scaffold.

resveratrol's known biological targets (Figure 2.8). Seven compounds were discovered to be selective for aromatase, four of which feature a simple stilbene core (**29** to **32**). Compound **29** was also identified by Sun et al,[42] but compounds **30** to **32** suggest that the effect of nitro group substitution may not be fully understood.
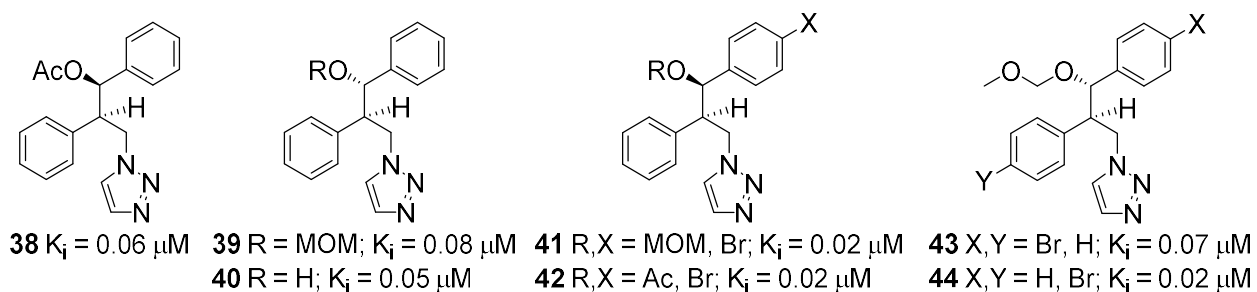
The addition of an imidazole core appended to the resveratrol skeleton has also been identified as a successful strategy in developing potent and selective AIs. This is due to the ability of these groups to chelate the heme of aromatase, a strategy already validated by anastrozole and letrozole. Molecular modeling of **28** by Sun et al[42] lead to the design and synthesis of imidazole-containing nanomolar AIs **33** and **34**, via a classical Wittig reaction with synthetic intermediate **35** (Figure 2.9). Notably, **35** and its amine homolog **36** were also potent inhibitors of aromatase. We posit that, in addition to possible chelation to the heme group, keto-enol tautomerization in situ may allow **35** and **36** to more closely mimic a stilbene core. The selectivity study by Kondratyuk et al demonstrated that **33**, **35**, and **36** were selective for aromatase, as was the alcohol analogue of ketone **36** (**37**), albeit with somewhat less potency.[39]

Concurrent studies by our group identified potent and selective stilbene-inspired inhibitors of aromatase featuring an 1,2,3-triazole moiety (Figure 2.10).[43] The inhibitors were prepared in several
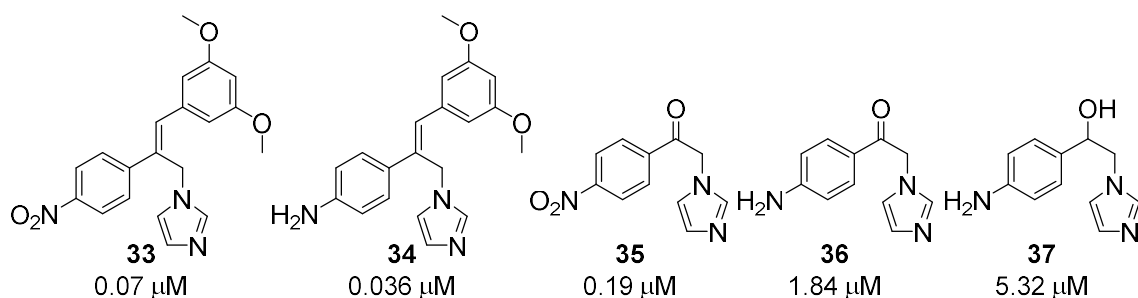
FIGURE 2.9 Inhibitors of aromatase featuring a heme-chelating imidazole moiety. Stilbene **33** and synthetic precursors and analogues **35**-**37** displayed high selectivity for aromatase.

38 K_i = 0.06 μM **39** R = MOM; K_i = 0.08 μM **41** R,X = MOM, Br; K_i = 0.02 μM **43** X,Y = Br, H; K_i = 0.07 μM
40 R = H; K_i = 0.05 μM **42** R,X = Ac, Br; K_i = 0.02 μM **44** X,Y = H, Br; K_i = 0.02 μM

FIGURE 2.10 Potent and selective aldol derived inhibitors of aromatase featuring a 1,2,3-triazole moiety.

steps from the product of the aldol reaction between methyl phenylacetate and benzaldehyde, with both syn and anti aldol adducts capable of strongly binding to aromatase. The compounds were also screened against human cytochromes 3A4, 1A1, and 2D6, which are involved in xenobiotic metabolism and are frequently affected by AIs. Notably, out of the three most potent compounds (**38** to **40**), **38** and **39** were totally selective for aromatase and **40** only weakly inhibited CYP2A6 (pKi = 3.15).
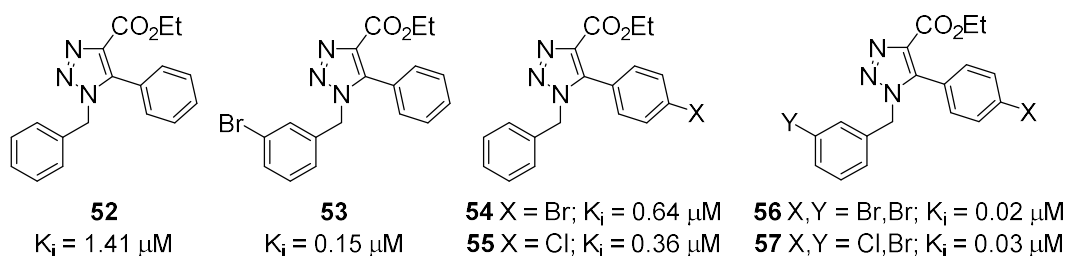
Subsequent research in our group explored the effect of halide substitution on the phenyl rings of these 1,2,3-triazole based AIs (Figure 2.10).[44] Notably, the incorporation of an aryl halide resulted in an increase in activity, with all tested compounds demonstrating submicromolar K_i and the four most potent compounds (**41** to **44**) exhibiting K_i ranging from 20 to 70 nM. A molecular docking study confirmed the ability of the triazole to bind to the heme group and suggested that the halide substituents act as ketone bioisosteres, possibly explaining the modest increase in potency over previous compounds **38** to **40**.[44]

Other than the incorporation of auxiliary heme-chelating functional groups, replacing the central alkene of resveratrol with various aromatic heterocycles has been explored as a strategy to improve their anticancer activity. For example, this strategy was used to improve the antitumor properties of combretastatin A4 (**21**).[45–47] A series of 5H-furan-2-ones were prepared by Sanderson et
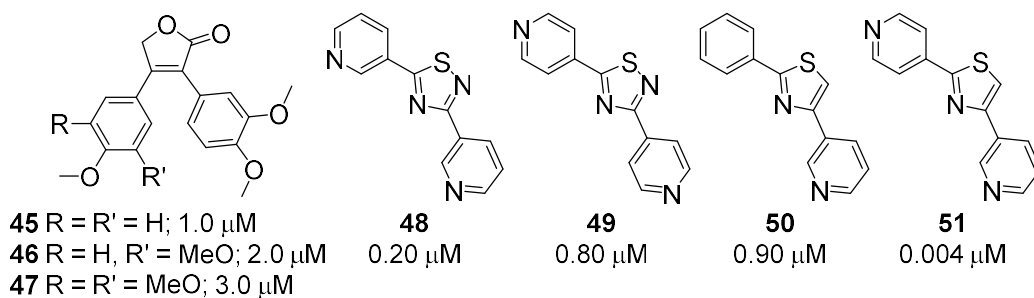
FIGURE 2.11 Stilbene-inspired inhibitors of aromatase with lactone, thiazole and thiadiazole cores.

al,[48] and three were found to be competitive AIs in H295R human adrenocortical cells (**45** to **47**) (Figure 2.11). The most potent derivative (**45**) had an IC_{50} of 1.0 µM, and additional substitution at R or R' resulted in a loss of activity.[48] Replacement of the resveratrol alkene nucleus was also explored by Mayhoub et al[49] to find compounds that were selective for either aromatase inhibition, nuclear factor kB inhibition or induction of detoxifying enzyme QR1 (Figure 2.11). A series of 1,2,4-thiadiazoles were synthesized using a tricomponent condensation reaction, and it was found that derivatives with phenyl substituents were inactive against aromatase but bis-pyridyl substituted derivatives **48** and **49** were 0.2 and 0.8 µM inhibitors. As well, **48** showed total selectivity for aromatase vs the other resveratrol targets tested. Docking studies demonstrated that one of the pyridine rings of **48** likely chelated the heme of aromatase, while the other was involved in hydrogen bonding in the active site. Synthetic challenges to making differentially substituted thiadiazoles prompted the switch to substituted thiazoles, and a series of thiazoles based on structure **48** that would improve hydrogen bonding in the active site were synthesized via classic condensation chemistry.[50] It was discovered that changing the thiadiazole to a simpler thiazole ring was not deleterious, and that the position of the pyridine nitrogens had a profound effect on activity, with **51** having an IC_{50} of 4 nM. In general, substitutions on either pyridyl ring in **51** resulted in less potent compounds.

52
$K_i = 1.41 \ \mu M$

53
$K_i = 0.15 \ \mu M$

54 X = Br; $K_i = 0.64 \ \mu M$
55 X = Cl; $K_i = 0.36 \ \mu M$

56 X,Y = Br,Br; $K_i = 0.02 \ \mu M$
57 X,Y = Cl,Br; $K_i = 0.03 \ \mu M$

FIGURE 2.12 Stilbene-inspired inhibitors of aromatase featuring a heme-chelating 1,2,3-triazole core.

Synthetic efforts in our group also explored the replacement of the alkene core of natural stilbenes with a heteroaromatic core.[51] Continuing our exploration of stilbene-inspired inhibitors with a triazole moiety, a series of 1,2,3-triazoles were synthesized via a novel thermal click reaction between Wittig-derived β-methoxycinnamates and benzyl azides (Figure 2.12). A small library of novel triazoles were synthesized, and the most potent (**52** to **57**) were found to bind to aromatase with a K_i between 0.02 and 1.4 µM. Notably, we believe these compounds are interacting with the heme of aromatase via the triazole core as opposed to a pyridine side–group, as in the compounds designed by Mayhoub et al.[49] As well, the data support our hypothesis for halides functioning as carbonyl bioisosteres, as the addition of halogens on either aromatic ring caused a significant increase in activity, and substitution on both aromatic rings (**56** and **57**) resulted in a 50- to 70-fold increase in activity as compared with the unsubstituted **52**. Other substituents (e.g., methyl and methylenedioxy) did not result in as significant of improvements.

Despite a relative lack of literature specifically demonstrating the antiaromatase activity of stilbene natural products, many synthetic stilbenoids have been developed as potent AIs. As well, a major issue with the druggability of natural stilbenes such as resveratrol is their biochemical promiscuity, leading to pleitropic effects in vivo. Work by the Cushman, McNulty, and other groups have identified distinct compounds that display enhanced target selectivity. As such, we think it may

be appropriate to evaluate the most potent compounds developed to date (e.g. **51**) in mouse or animal models of breast cancer to evaluate the clinical efficacy of these stilbene-inspired inhibitors.

2.2.4 – Chalcones and Chalconoids as AIs

Chalcones, exemplified by the central biosynthetic product **14** (Figure 2.4), which is also known as naringenin chalcone, appear to be much less investigated for aromatase inhibitory activity, although their general role as phenolic antioxidants is well known. The anticancer activity of chalcone natural products unrelated to aromatase activity has also been reported.[52] The presence of an electrophilic Michael acceptor intrinsic to the chalcone core is considered a negative element in pharmaceutical design, a factor which may have hampered their development.[53] Nonetheless, moderate aromatase activity has been documented for simple chalcones[54] and initial structure-activity studies reported. More potent activity was demonstrated by prenylated[55] chalcones and more recently dimeric dihydrochalcones[56] have been reported to have moderate activity.

The investigation of aromatase activity of a range of polyphenolic natural products was first reported by Le Bail et al.[54] Of the 12 synthetic chalcones investigated (Figure 2.13), most proved to be weak or showed no activity to aromatase. Naringenin chalcone (**14**) itself was found to be most potent exhibiting an IC$_{50}$ of 2.6 μM, while most interestingly the α,β-dihydro analog **58** exhibited no activity. This result strongly implicates the requirement of the electrophilic Michael acceptor for
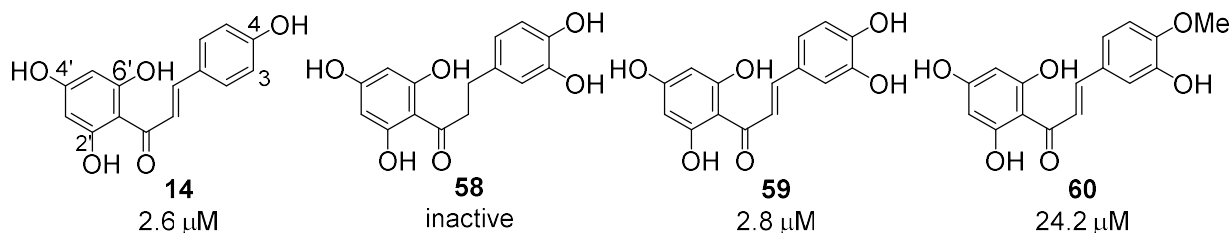
FIGURE 2.13 Structure of synthetic chalcones and chalconoids and their selective aromatase activities.

aromatase activity, although it is likely that the structural rigidity of **14**, or conversely rotational flexibility of **58**, may also be contributing factors. It is not known if **14** acts as a reversible inhibitor of the enzyme. The 3-hydroxy analogue of naringin chalcone (**59**) also proved active with an IC_{50} of 2.8 µM, indicating that substitution at C3 is tolerated. Finally, these authors showed that the free 4-hydroxyl group is very important as the 4-methyl ether derivative (**60**) proved nearly 10-fold less potent. The presence of at least two hydroxyl groups at the 2', 4' and/or 6' positions also appears to be critical on the chalcone core, although a clear substitution pattern correlating to potent activity is not evident. The most potent compounds contain the 2',4',6'-trihydroxyaryl polyketide extension and the overall overlap with estradiol is apparent, again implying the importance of structural rigidity.

Shortly after this study was reported, Lee et al[55] described the aromatase activity of a wide range of natural polyphenolics including the unusual 3'-prenylated ferulate ester (**61**) and coumarate ester (**62**) and the likely biosynthetic intermediate (**63**) (Figure 2.14). The compounds were isolated
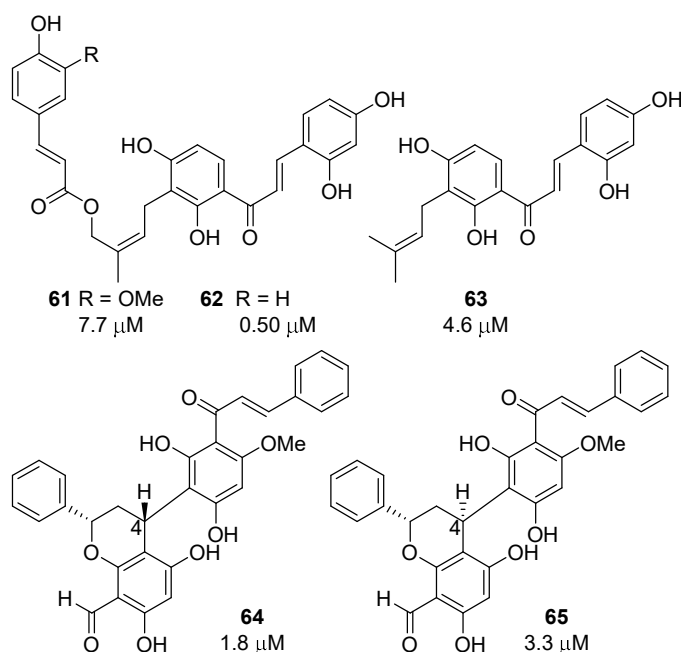
FIGURE 2.14 Structure of chalcones and chalconoids and their selective aromatase activities.

from a deciduous tree of the Moraceae (mulberry) family. While compounds **61** and **63** showed moderate aromatase activities of 7.1 and 4.6 µM, respectively, compound **62** proved potent at 0.5 µM and is thus far the most potent chalcone analogue reported. No further compounds of this structural type have been reported making relation to the aromatase pharmacophore of **14** impossible. A lipophilic substituent at the 3'-position is clearly well tolerated and the core chalcone resembles the active derivatives **14** and **59**, and also estradiol. The role of the 3'-substituent in binding within the active site is unclear. The fact that the potent molecule **62** is 10-fold more active than **61** indicates that these chalcone derivatives may in-fact inhibit aromatase through a completely different binding mode via the ferulate and coumarate substituents.
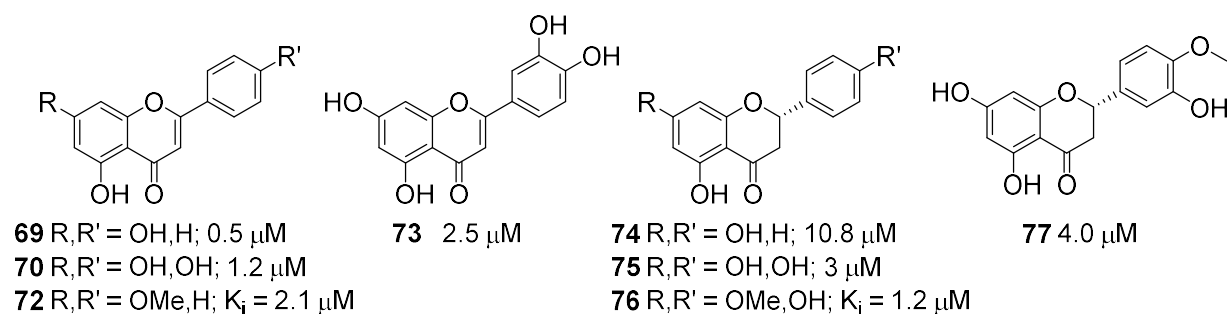
More recently, Bajgai et al[56] reported the occurrence two natural 3'-substituted chalcones derivative **64** and its C4-epimer **65** from a plant of the Annonaceae family. Structurally, these natural products are chalcone-flavanone dimers, epimeric at C4 and implicating arylation of the chalcone with a 4-hydroxyl catechin isomer. This is an example of a rarely observed carbon–carbon bond connection within natural polyphenolics.[57] Compounds **64** and **65** were reported to exhibit moderate aromatase activities of 1.8 and 3.3 µM, respectively. From a structure-activity viewpoint, it is noted that both derivatives lack the presence of a C4-hydroxyl unit on the aromatic amino acid–derived unit and have a methoxy substituent at C6'. The presence of a large substituent at C3' and lack of a free C6'-hydroxyl group are features shared with natural compounds **61**, **62**, and **63**. As the presence of the C4-hydroxyl group was shown to be required for potency in the simple chalcones (such as **14**), the limited structure-activity relationships (SAR) available so far with compounds **61** to **65** indicate that a completely different mode of binding is likely for these derivatives.

Considering a general aromatase pharmacophore contained within the chalcone natural products, we note that only the fully conjugated chalcones, preferably with a strongly electron donating

4-hydroxy group, exhibit good aromatase activity (Figure 2.13). Given the nature of the active site,[29] a logical hypothesis would involve the conjugated ketone carbonyl binding as a Lewis-base donor coordinating to the heme group of aromatase. The electronic effects and rigidity of the chalcone mimic the androgen steroidal core with the chalcone carbonyl donor, occupying the position of the C19-methyl group of the natural steroidal substrates. The natural products **61** to **65** (Figure 2.14) contain the peripheral rigid chalcone and are functionalized with a lipophilic and/or bulky substituent. The active site of aromatase contains a large pocket distal to the heme group in the core, into which the lipophilic side chains of these inhibitors **61** to **65** may interact. Given the availability of X-ray structural information and knowledge of the binding characteristics of AIs,[29] the synthesis of a wider range of designed chalcones with vaulted, lipophilic, phenolic substituents at C3' is indicated as a fruitful avenue of further research.

2.2.5 – Flavonoids as AIs

As a class, flavonoids are the most common polyphenolic natural products produced by plant species, and they are frequently consumed as part of a healthy diet. As well, they are the most extensively explored class of natural products in terms of activity as AIs. Indeed, the first proof of natural products acting as AIs was provided by Kellis and Vickery,[58] when they demonstrated the ability of several natural flavonoids and alpha-benzoflavone **66** to inhibit aromatase in human placental and ovarian microsomes (Figure 2.15). Notably, they reported that **66** and chrysin **69** both induced spectral changes indicative of the heme iron changing from a low-spin to a high-spin state. This is explained by competitive displacement of the native androstenedione substrate and coordination of the C4 carbonyl to the heme iron.
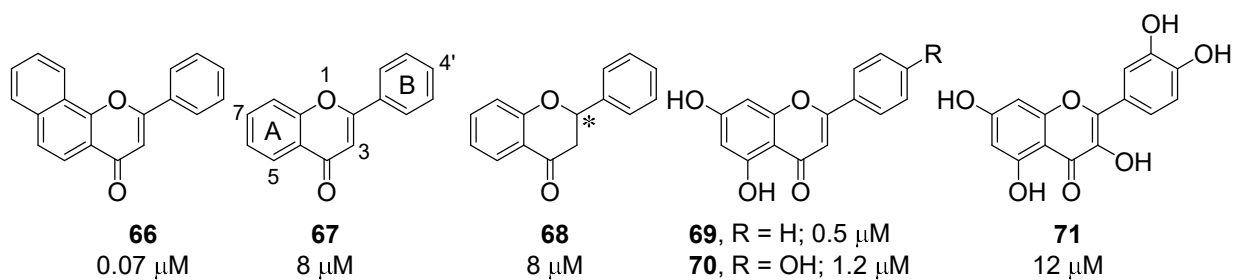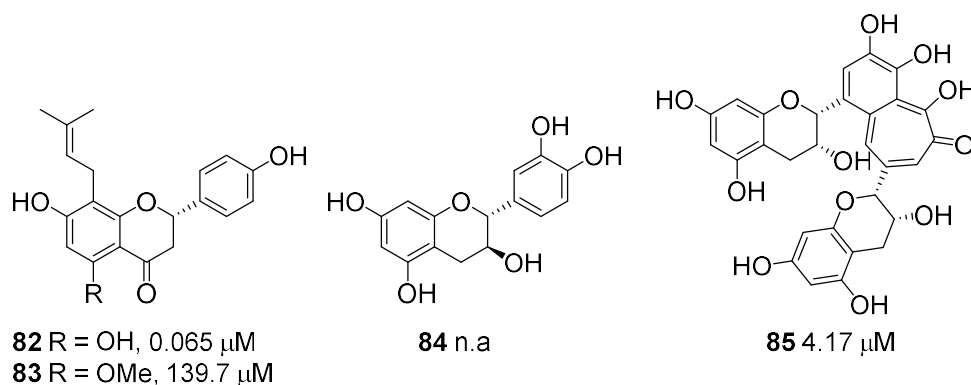
FIGURE 2.15 Flavonoids initially identified by Kellis and Vickery as inhibitors of aromatase.

69 R,R' = OH,H; 0.5 μM
70 R,R' = OH,OH; 1.2 μM
72 R,R' = OMe,H; K$_i$ = 2.1 μM

73   2.5 μM

74 R,R' = OH,H; 10.8 μM
75 R,R' = OH,OH; 3 μM
76 R,R' = OMe,OH; K$_i$ = 1.2 μM

77 4.0 μM

FIGURE 2.16 Select flavone and flavanone inhibitors of aromatase.

Since 1984 there have been dozens of reports on the antiaromatase activity of various flavonoid compounds, and these results have been summarized in several previous reviews.[59–64] In general, it has been found that flavones (e.g., chrysin **69**,[58] apigenin **70**,[58] tectochrysin **72**,[65] and luteolin **73**[66]) (Figure 2.16) are more potent inhibitors than flavanones (e.g., pinocembrin **74**,[67] naringenin **75**,[66] sakuranetin **76**,[65] and hesperitin **77**),[66] and both are more potent than flavonols like quercetin (**71**),[58] galangin (**78**),[68] and kaempferol (**79**)[69] (Figure 2.17). Despite their structural similarity to estrogen and their ability to bind to ERs, isoflavones such as **16** and biochanin A (**80**) are typically poor AIs.[59,62] Nevertheless, one of the most potent known flavonoid inhibitors of aromatase is rotenone (**81**), a prenylated isoflavone derivative.[59] Based on its complexity, it is possible that **81** binds to the active site of aromatase via a different method than other flavonoids (Figure 2.18).
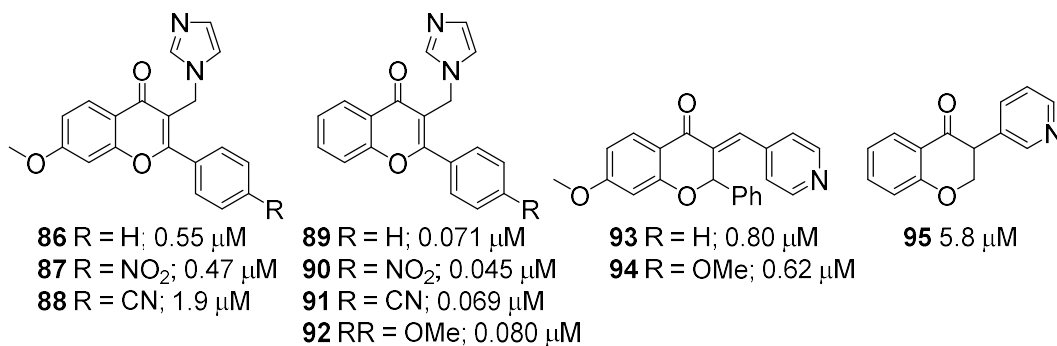
78 R = H, 12 μM
79 R = OH, K$_i$ = 27 μM

16 R = OH, n/a
80 R = OMe, 10.2 μM

81 0.30 μM
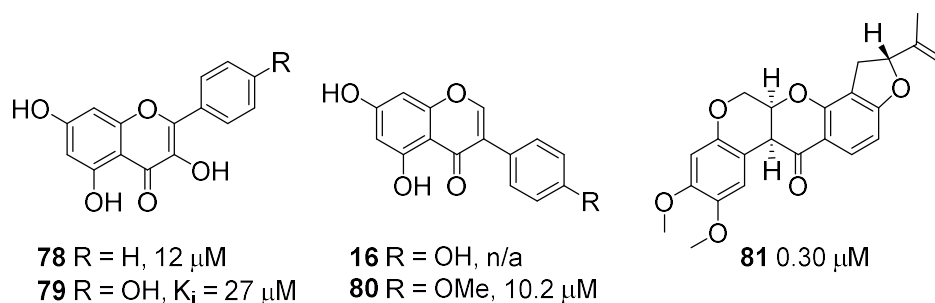
FIGURE 2.17 Select flavonol and isoflavone aromatase inhibitors.

82 R = OH, 0.065 μM
83 R = OMe, 139.7 μM

84 n.a

85 4.17 μM

FIGURE 2.18 Flavonoids with differential activity towards aromatase based on their ability to chelate the heme of aromatase.

These differences in activity between different flavonoid natural product classes have been explained by several computational studies, which demonstrate that coordination by the C4 carbonyl to the heme of aromatase is a key interaction, and that steric hindrance of the carbonyl (e.g., by the C3 hydroxyl or C3 phenyl group of flavonols and isoflavones, respectively) can significantly reduce the inhibitory activity of the flavonoid.[29,70–72] An example of the importance of heme chelation can be seen in the difference between 8-prenylnaringenin (**82**) and isoxanthohumol (**83**), isoflavones present in hops (*Humulus lupus*) and beer, which differ only in the substituent at C5 but display dichotomous activity toward aromatase.[73,74] The presence of the methoxy at C5 in **82** may act as a steric shield, blocking the interaction between the carbonyl and heme group. The importance of

86 R = H; 0.55 μM
87 R = NO$_2$; 0.47 μM
88 R = CN; 1.9 μM

89 R = H; 0.071 μM
90 R = NO$_2$; 0.045 μM
91 R = CN; 0.069 μM
92 RR = OMe; 0.080 μM

93 R = H; 0.80 μM
94 R = OMe; 0.62 μM

95 5.8 μM

FIGURE 2.19 Potent synthetic flavonoid AIs substituted with aromatic heterocycles at C3.

binding to the heme group is further demonstrated by the general lack of antiaromatase activity demonstrated by flavan-3-ols such as catechin (**84**), which lack the chelating C4 carbonyl.[75,76] Interestingly, theaflavins (e.g., **85**) are produced by the enzymatic oxidation of catechins and are potent inhibitors of aromatase, possibly due to heme coordination by the tropolone pseudocarbonyl.

Considering the wealth of knowledge surrounding the interaction between natural flavonoid and aromatase, significant effort has gone into developing AIs that incorporate heme-chelating heterocycles appended to a flavonoid scaffold. In general, these heterocycles are appended to C2 or C3 of the flavonoid skeleton, or directly replace the C4 carbonyl. Substitution at C3 was first explored by Recanatini et al[77] in 2001, where it was discovered that adding an imidazole ring to C3 of 7-methoxyflavone via a methylene linker resulted in a submicromolar inhibitor of aromatase (**86**) (Figure 2.19). Interestingly, exchanging the imidazole group for a 1,3,4-triazol-1-yl moiety resulted in a compound that was completely inactive (not shown). Later work by Gobbi et al[78] explored the effect of substitution in the A and B rings of **86** (**87** to **92**), resulting in a 45 nM lead compound (**90**). In general, it was discovered that substitution at 4' on the B ring was better tolerated than substitution on the A ring, and that electron withdrawing groups at this position led to more potent inhibitors.

Incorporating a pyridine ring at C3 is also tolerated, as evidenced by compounds **93** to **95**. Pouget et al[64] showed that a linking a pyridine-4-yl at C3 via an E alkene led to potent inhibitors (**93**

96 R,R' = OBn,H; 0.21 μM
97 R,R' = OH,OMe; 0.22 μM
98 R,R' = biphenylmethoxy,H
0.079 μM

99 R = allyl; n/a
100 R = benzyl; n/a

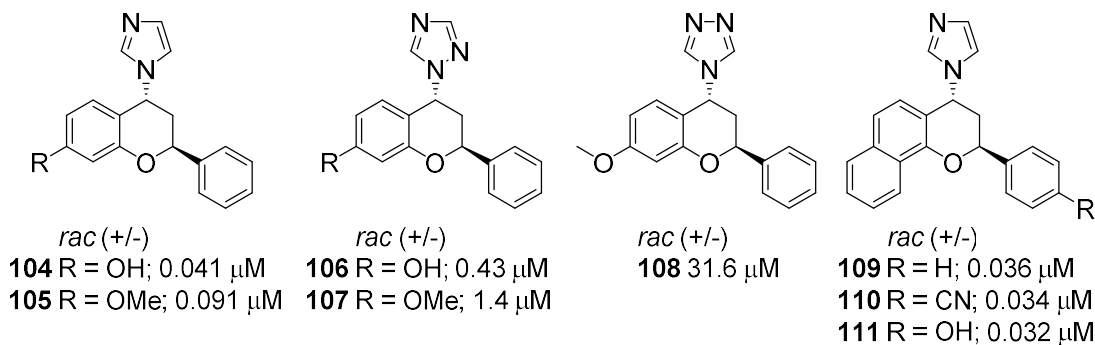**101** R = OMe; 0.77 μM
102 R = OBn; 0.52 μM

103 18 μM
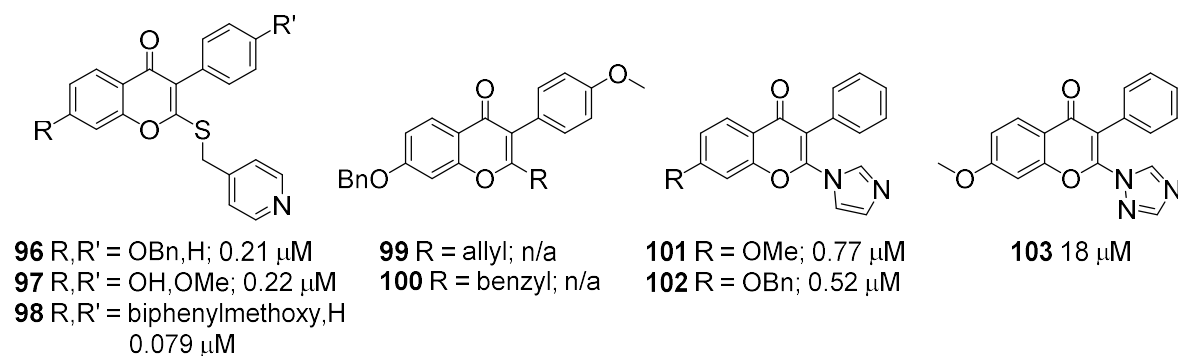
FIGURE 2.20 Potent synthetic flavonoid AIs substituted with aromatic heterocycles at C2.

and **94**). The authors were unable to fully purify the Z isomers of **93** and **94** but reported that the mixtures enriched with the Z isomer were three to four times less potent. As well, work by Bonfield et al[80] found that a synthetic isoflavanone with the B ring replaced by a pyridine-3-yl group (**95**) was a low-micromolar inhibitor aromatase, which is a substantial improvement over natural isoflavanoids that are typically inactive.[80]

Substitution of various heterocycles at C2 has been explored by the Brueggemeier group. In 2004, Kim et al[81] demonstrated appending a pyridin-4-yl group to C2 via a flexible thiomethylene group generated potent inhibitors of aromatase (**96** and **97**) (Figure 2.20). The pyridine was critical for the antiaromatase activity as replacement of the groups at C2 with allyl or benzyl groups resulted in a total loss in activity (**99** and **100**). Later work by Hackett et al[82] explored the effect of replacing the pyridine moiety with imidazole and 1,2,4-triazole groups (**101** to **103**). The imidazole derivatives were potent inhibitors, albeit less than the previous pyridyl derivatives, but substituting with a triazole significantly reduced activity. This result was rationalized using density functional theory (DFT), which demonstrated that the HOMO of the imidazole derivative places more electron density on the nitrogen heterocycle than the HOMO of the triazole derivative. The increased electron density corresponds with an improved ability to bond to the iron of the heme group, and a corresponding

increase in potency. Further optimization has been performed on the 3-pyridine substituted derivatives, and it has been found that the addition of an even larger hydrophobic group off C7 can increase activity significantly (**98**).[83] We posit that this improvement in activity can be explained by the hydrophobic group accessing the large binding pocket distal to the aromatase active site. It is also worth noting that all these derivatives are significantly more active than the generally inactive isoflavonoid natural products by which they were inspired.

There have been several publications that explore substituting the C4 carbonyl with a more potent heme-chelating heterocycle (Figure 2.21). Flavanoid derivatives with an imidazole group at C4 were found to be potent inhibitors of aromatase, with IC_{50}s of 41 and 91 nM (**104** and **105**).[84] Interestingly, the imidazole derivatives were one order of magnitude more potent than the corresponding 1*H*-triazole derivatives (**106** and **107**), and two orders of magnitude more potent than the 4*H*-triazole derivatives (**108**).[85] As well, it was found that a free hydroxy at C7 was more active than a methoxy at the same position. The results from Kellis and Vickery[58] that benzoflavone is a more potent inhibitor of aromatase than flavanone was used as an inspiration for the synthesis of benzoflavone derivatives **109** to **111**, which demonstrated a slight improvement of the activity of **104** and **105**.[86]

rac (+/-)
104 R = OH; 0.041 μM
105 R = OMe; 0.091 μM

rac (+/-)
106 R = OH; 0.43 μM
107 R = OMe; 1.4 μM

rac (+/-)
108 31.6 μM

rac (+/-)
109 R = H; 0.036 μM
110 R = CN; 0.034 μM
111 R = OH; 0.032 μM

FIGURE 2.21 Potent synthetic flavonoid AIs substituted with aromatic heterocycles at C4.

Besides providing a privileged scaffold for the development of novel AIs, natural flavonoids exhibit other biological activities that may be exploited for the treatment of breast cancer. For example, a diverse set of flavonoids including apigenin, quercetin, genistein, biochanin A, and luteolin have been found to downregulate the expression of aromatase in either human granulosa-luteal cells or MCF-7 cells.[66,87,88] Conversely, hesperitin increases aromatase messenger RNA levels in MCF-7 cells but was also found to prevent letrozole-induced bone loss in mouse models of breast cancer.[66,89] The ability to reduce aromatase expression, or mitigate the negative side effects of current AIs, may offer alternate or complementary strategies for the treatment of ER-positive breast cancer and could provide future avenue of research for synthetic flavonoid derivatives.

2.2.6 – Conclusion

There is a pressing need for new AIs. While currently used as standard treatment, the inhibitors anastrozole and letrozole suffer from significant side effects, including hot flashes, weight gain, and insomnia.[90] As well, up to 50% of women using AIs experience significant muscle and joint pain, resulting in 20% discontinuing AI therapy despite its proven ability to significantly reduce the long-term risk of death from breast cancer.[91]

The goal of this review was to highlight the promising antiaromatase activity demonstrated by a variety of natural polyphenolic compounds and the synthetic inhibitors derived therefrom. However, we also want to emphasize the fact that while unmodified natural products can provide inspiration as potential lead compounds, they are generally unsuitable as drug candidates. As well, many polyphenolic natural products have been reported to either possess no activity toward aromatase or to be micromolar inhibitors of aromatase, depending on the specific assay used. An excellent example, but by no means the only example, is provided by genistein (**16**). It has been reported to induce aromatase and negate the effect of fadrozole in breast adipose fibroblasts in vitro[92] and promote

proliferation of estrogen-dependent human breast cancer MCF-7 cells both in vivo and in vitro.[93] Conversely, it was found to have no effect on aromatase activity in human preadipocytes,[94] adrenocortical carcinoma cells,[59] and human placental microsomes,[95] but was found to inhibit aromatase (IC_{50} = 3.6 µM) in healthy mammary fibroblasts.[96]

A lack of standardization in assays, combined with the promiscuous biological activity of polyphenolic natural products, makes it difficult to determine the true extent of activity of the compounds tested. For example, compounds that are inactive in microsomal assays may be active in cell-based assays after undergoing metabolism to an active intermediate, and vice versa. Conversely, a promising lead may be ignored if the compound is inactive in the specific cell line tested, despite the fact that the antiaromatase ability of these compounds is frequently tissue-specific. A compounding issue is the fact that single cell-type assays do not adequately mimic the dynamic environment present in breast cancer tumors. As well, many of the compounds discussed above suffer from poor oral bioavailability. Perhaps tellingly, Saarinen et al[68] found no evidence of in vivo activity of aromatase-inhibiting flavonoids after oral administration to rats at doses substantially higher than what normally occurs in human diets.[68]

Natural product polyphenolics evolved as mediators of molecular-level interactions in their native environment, and we may confidently assume, not as human pharmaceuticals. No class of polyphenolic better describes this issue than the curcuminoids, isolated from *Curcuma longa* (turmeric), the source of the common household spice turmeric. Many publications describe important biological activities attributed to curcuminoids; however, only much later was the poor gut absorption and very low plasma concentration of these metabolites investigated.[97] Gut penetration and plasma concentration, i.e., pharmacokinetic assays, should be considered early in any investigation considering the translation of natural product biological activity to modulate orally deliverable pharmacodynamic activity, such as aromatase activity.

Despite the challenges, natural polyphenolics have proved themselves extremely valuable in providing active hit compounds in the discovery of potent AIs. Lead synthetic AIs, based upon such polyphenolic core structures, often possess significantly more potent aromatase inhibitory activity and can be designed to optimize the human pharmacokinetic and pharmacodynamic properties for oral delivery. Clearly this overall strategy, originating with tamoxifen, is working. Future work must focus on the development of potent and selective AIs with fewer side effects than current treatments. The discovery of new phytoestrogens will continue to provide an excellent starting point for this endeavor. Promising results have been obtained by incorporating or appending heme-chelating heterocycles to promising stilbene and flavonoid scaffolds, and potent chalcones highlight the existence of a large hydrophobic binding pocket in the target, largely unexplored, that may lead to more potent and selective leads. These results, with due attention paid to the pharmacokinetic requirements not considered in the discovery of the native polyphenols, assure a continued supply of structurally novel leads as potential clinical candidates in this important field.

References

1. Siegel RL, Miller KD, Jemel, A. Cancer Statistics 2017. CA *Cancer J Clin* 2017; 67: 7-30.

2. Ingle JN. Pharmacogenomics of endocrine therapy in breast cancer. *J Hum Genet.* 2013; 58(6): 306-312.

3. Beatson GT. On the treatment of inoperable cases of carcinoma of the mamma: Suggestions for a new method of treatment, with illustrative cases. *The Lancet.* 1896; 2: 104–107.

4. Smith GL. The Long and short of tamoxifen therapy: A review of the ATLAS trial. *J Adv Pract Oncol.* 2014; 5(1): 57-60.

5. Schneider R, Barakat A; Pippen J, Osbourne C. Aromatase inhibitors in the treatment of breast cancer in post-menopausal female patients: An update. *Breast Cancer Targ Ther.* 2011; 3(5): 113-125.

6. Cole MP, Jones CT, Todd ID. A new anti-oestrogenic agent in late breast cancer. An early clinical appraisal of ICI46474. *Brit J Canc.* 1971; 25(2): 270-275.

7. Maximov PY, Lee TM, Jordan VC. The Discovery and Development of Selective Estrogen Receptor Modulators (SERMs) for Clinical Practice. *Curr Clin Pharmacol.* 2013; 8(2): 135-155.

8. Johnston SRD, Dowsett M. Aromatase inhibitors for breast cancer: Lessons from the laboratory. *Nat Rev Canc.* 2003; 3: 821-831.

9. McFadyen MCE, Melvin WT, Murray GI. Cytochrome P450: Novel options for cancer therapeutics. *Molec. Canc. Ther.* 2004; 3(3): 363-371.

10. Reed MJ, Beranek PA, Ghilchik MW, James VH. Conversion of estrone to estradiol and estradiol to estrone in postmenopausal women. *Obstet Gynecol.* 1985; 66(3): 361-5.

11. Yoshimoto FK, Guengerich FP. Mechanism of the third oxidative step in the conversion of androgens to estrogens by cytochrome P450 19A1 steroid aromatase. *J Am Chem Soc.* 2014; 136: 151016-15025.

12. LI JJ. Aromatase inhibitors for breast cancer: Exemestane (Aromasin), Anastrozole (Arimidex) and Letrozole (Femara). *The Art of Drug Synthesis.* 2007, John Wiley & Sons, Inc; pp 31-38.

13. Schröder J , Schröder G . Stilbene and chalcone synthases: related enzymes with key functions in plant-specific pathways. Z fur Naturfors C, *J Biosci.* 1990; 45(1-2): 1-8.

14. Berman, AY, Motechin RA, Wiesenfeld MY, Holz MK. The therapeutic potential of resveratrol: a review of clinical trials. *NPJ Precis Oncol.* 2017; 35.

15. Wang XF, Yao CS. Naturally active oligostilbenes. *J Asian Nat Prod Res.* 2016; 18(4): 376-407.

16. Ferrer JL , Jez JM , Bowman ME , Dixon RA , Noel JP Structure of chalcone synthase and the molecular basis of plant polyketide biosynthesis. *Nature Struct Biol.* 1999, 6(8):775-784.

17. Jez JM, Noel JP. Reaction mechanism of chalcone isomerase. *J Biol Chem.* 2002; 277(2): 1361-1369.

18. Lukacin R, Wellman F, Britsch L, Martens S, Matern U. Flavanol synthase from *Citrus unshiu* is a bifunctional dioxygenase. *Phytochem.* 2003; 62: 287-292.

19. Jung W, Yu O, Lau SM, O'Keefe DP, Odell J, Fader G, McGonigle B. Identification and expression of isoflavone synthase, the key enzyme for biosynthesis of isoflavones in legumes. *Nat Biotechnol.* 2000 18(2):208-12.

20. Jez JM, Bowman ME, Dixon RA, Noel JP. Structure and mechanism of the evolutionary unique plant enzyme chalcone isomerase. *Nat Struct Biol.* 2000; 7(9): 786-791.

21. Gensheimer, M, Mushegian, A. Chalcone isomerase family and fold: No longer unique to plants. *Prot Sci.* 2004; 13: 540-54.

22. Kaufman PB, Cseke LJ, Warber S, Duke JA, Brielmann HL. *Natural Products from Plants*, 199, CRC Press, Boca Raton, FL.

23. Gutzeit HO, Ludwig-Muller J. *Plant Natural Products: Synthesis, Biological Functions and Practical Applications*, 2014, Wiley-Blackwell, Darmstadt, Germany.

24. Andersen OM, Markham KR, *Flavonoids: Chemistry, Biochemistry and Applications*, 2006, Taylor & Francis, Boca Raton, FL.

25. Harborne JB. The comparative biochemistry of phytoalexin induction in plants. *Biochem Syst & Ecol.* 1999; 27: 335-367.

26. Grayer J, Kokbun T. Plant-fungal interactions: the search for phytoalexins and other antifungal compounds from higher plants 2001; *Phytochem.* 56; 253-263.

27. Graye RJ, Harborne JB. A survey of antifungal compounds from higher plants. *Phytochem.* 1994; 37: 19-42.

28. Prossnitz ER, Barton M. The G-protein-coupled estrogen receptor GPER in health and disease. *Nat Rev Endocrinol.* 2011; 7: 715-726.

29. Chen S, Kao YC, Laughton CA. Binding characteristics of aromatase inhibitors and phytoestrogens to human aromatase. *J Ster Biochem & Molec Biol.* 1997; 61: 1078-115.

30. Alberts AW. Discovery, biochemistry and biology of lovastatin. *Am J Cardiol.* 1988; 62(15): J10-J15.

31. Roitelman J, Olender EH, Bar-Nun S, Dunn WA Jr, Simoni RD. Immunological evidence for eight spans in the membrane domain of 3-hydroxy-3-methylglutaryl coenzyme A reductase: implications for enzyme degradation in the endoplasmic reticulum. *J Cell Biol.* 1992; 117(5): 959-73.

32. Nakagawa H, Kiyozuka Y, Uemura Y, Senzaki H, Shikata N, Hioki K, Tsubura A. Resveratrol inhibits human cancer cell growth and may mitigate the effect of linoleic acid, a potent breast cancer cell stimulator. *J Cancer Res Clin Oncol.* 2001; 127: 258-264.

33. Baur JA, Sinclair DA. Therapeutic potential of resveratrol: the *in vivo* evidence. Nature Rev Drug Disc 2006; 5: 493-506.

34. Potter GA, Patterson LH, Wanogho E, Perry PJ, Butler PC, Ijaz T, Ruparelia KC, Lamb JH, Farmer PB, Stanley LA, Burke MD. The cancer preventative agent resveratrol is converted to the anticancer agent piceatannol by the cytochrome P450 enzyme CYP1B1. *Brit J Cancer.* 2002; 86: 774-778.

35. Rimando AM, Cuendet M, Desmarchelier C, Mehta RG, Pezzuto JM, Duke SO. Cancer Chemopreventive and Antioxidant Activities of Pterostilbene, a Naturally Occurring Analogue of Resveratrol. *J of Agricultural Food Chem.* 2002; 50: 3453-3457.

36. Schneider Y, Chabert P, Stutzmann J, Coelho D, Fougerousse A, Gossé F, Launay J-F, Brouillard R, Raul F. Resveratrol Analog (Z)-3,5,4'-trimethoxystilbene is a Potent Anti-Mitotic Drug Inhibiting Tubulin Polymerization. *Int J Cancer.* 2003; 107: 189-196.

37. Tron GC, Pirali T, Sorba G, Pagliai F, Busacca S, Genazzani AA. Medicinal Chemistry of Combretastatin A4: Present and Future Directions. *J Med Chem.* 2006; 49: 3033-3044.

38. Kopp P. Resveratrol, a phytoestrogen found in red wine. A possible explanation for the conundrum of the 'French paradox'?. *Eur J Endocrinol.* 1998; 138: 619-620.

39. Kondratyuk, TP, Park E-J, Marler LE, Ahn S, Yuan Y, Choi Y, Yu R, van Breemen RB, Sun B, Hoshino J, Cushman M, Jermihov KC, Mesecar AD, Grubbs CJ, Pezzuto JM. Resveratrol derivatives as promising chemopreventive agents with improved potency and selectivity. *Mol Nutr Food Res.* 2011; 55: 1249-1265.

40. Gehm BD, McAndrews JM, Chien P-Y, Jameson JL. Resveratrol, a polyphenolic compound found in grapes and wine, is an agonist for the estrogen receptor. *Proc Natl Acad Sci.* 1997; 94:14138-14143.

41. Levi F, Pasche C, Lucchini F, Ghidoni R, Ferraroni M, La Vecchia C. Resveratrol and breast cancer risk. *Eur J Cancer Prev.* 2005; 14: 139-142.

42. Sun B, Hoshino J, Jermihov K, Marler L, Pezzuto JM, Mesecar AD, Cushman M. Design, synthesis, and biological evaluation of resveratrol analogues as aromatase and quinone reductase 2 inhibitors for chemoprevention of cancer. *Bioorg & Med Chem.* 2010; 18: 5352-5366.

43. McNulty J, Nair JJ, Vurgun N, DiFrancesco BR, Brown CE, Tsoi B, Crankshaw DJ, Holloway AC. Discovery of a novel class of aldol-derived 1,2,3-triazoles: Potent and selective inhibitors of human cytochrome P450 19A1 (aromatase). *Bioorg & Med Chem Lett.* 2012; 22: 718-722.

44. McNulty J, Nielsen AJ, Brown CE, DiFrancesco B, Vurgun N, Nair JJ, Crankshaw DJ, Holloway AC. Investigation or aryl halides as ketone bioisosteres: Refinement of potent and selective inhibitors of human cytochrome P450 19A1 (aromatase). *Bioorg & Med Chem Lett.* 2013; 23: 6060-6063.

45. Simoni D, Grisolia G, Giannini G, Roberti M, Rondanin R, Piccagli L, Baruchello R, Rossi M, Romagnoli R, Invidiata FP, Grimaudo S, Jung MK, Hamel E, Gebbia N, Crosta L, Abbadessa V, Di Cristina A, Dusonchet L, Meli M, Tolomeo M. Heterocyclic and Phenyl Double-Bond-Locked Combretastatin Analogues Possessing Potent Apoptosis-Inducing Activity in HL60 and in MDR Cell Lines. *J Med Chem.* 2005; 48: 723–736.

46. Romagnoli R, Baraldi PG, Cruz-Lopez O, Cara CL, Carrion MD, Brancale A, Hamel E, Chen L, Bortolozzi R, Basso G, Viola GJ. Synthesis and Antitumor Activity of 1,5-Disubstituted 1,2,4-Triazoles as Cis-Restricted Combretastatin Analogues. *Med Chem*. 2010; 53: 4248–4258.

47. Schobert R, Biersack B, Dietrich A, Effenberger K, Knauer S, Mueller TJ. 4-(3-Halo/amino-4,5-dimethoxyphenyl)-5-aryloxazoles and -N-methylimidazoles That Are Cytotoxic against Combretastatin A Resistant Tumor Cells and Vascular Disrupting in a Cisplatin Resistant Germ Cell Tumor Model. *Med Chem*. 2010; 53: 6595–6602.

48. Sanderson T, Renaud M, Scholten D, Nijmeijer S, van den Berg M, Cowell S, Guns E, Nelson C, Mutarapat T, Ruchirawat S. Effects of lactone derivatives on aromatase (CYP19) activity in H295R human adrenocortical and (anti)androgenicity in transfected LNCaP human prostate cancer cells. *Eur J Pharmacol*. 2008; 593: 92-98.

49. Mayhoub AS, Marler L, Kondratyuk TP, Park E-J, Pezzuto JM, Cushman M. Optimizing thiadiazole analogues of resveratrol versus three chemopreventive targets. *Bioorg & Med Chem*. 2012; 20: 510-520.

50. Mayhoub AS, Marler L, Kondratyuk TP, Park E-J, Pezzuto JM, Cushman M. Optimization of the aromatase inhibitory activities of pyridylthiazole analogues of resveratrol. *Bioorg & Med Chem*. 2012; 20: 2427-2434.

51. McNulty J, Keskar K, Crankshaw DJ, Holloway AC. Discovery of a new class of cinnamyl triazole as potent and selective inhibitors of aromatase (cytochrome P450 19A1). *Bioorg & Med Chem Lett*. 2014; 24: 4586-4589.

52. Modzelewska A, Pettit C, Achanta G, Davison NE, Huang P, Khan SR. Anticancer Activities of Novel Chalcone and Bis-chalcone Derivatives. *Bioorg Med Chem*. 2006; 14: 3491-3494.

53. Blagg J. Structure-Activity Relationships for In vitro and In vivo Toxicity. *Ann Rep Med Chem*. 2006; 41: 353-368.

54. Le Bail JC, Pouget C, Fagnere C, Basly JP, Chulia AJ, Babrioux G. Chalcones are Potent Inhibitors of Aromatase and 17β-hydroxysteroid Dehydrogenase Activities. *Life Sci*. 2001; 68: 751-761.

55. Lee D, Bhat KPL, Fong HHS, Farnsworth NR, Pezzuto JM, Kinghorn AD. Aromatase inhibitors from *Broussonetia papyrifera*. *J Nat Prod*. 2001; 64:1286–1293

56. Bajgai SP, Prachyawarakorn V, Mahidol C, Ruchirawat S, Kittakoop P. Hybrid Flavan-chalcones, Aromatase and Lipoxygenase Inhibitors from *Desmos cochinchinensis*. *Phytochem*. 2011; 72: 2062-2067.

57. Deng JZ, Starck SR, Li S, Hecht SM. (+)-Myristinins A and D from *Knema elegans*, which Inhibit DNA Polymerase β and Cleave DNA. *J Nat Prod*. 2005; 68: 1625-1628.

58. Kellis JT Jr., Vickery LE. Inhibition of human estrogen synthetase (aromatase) by flavones. *Science*. 1984; 225: 1032-1034.

59. Sanderson JT, Hordijk J, Denison MS, Springsteel MF, Nantz MH, van den Berg M. Induction and inhibition of aromatase (CYP19) activity by natural and synthetic flavonoid compounds in H295R human adrenocortical carcinoma cells. *Toxicol Sci.* 2004; 82: 70-79.

60. Balunas MJ, Su B, Brueggemeier RW, Kinghorn AD. Natural Products as Aromatase Inhibitors. *Anticancer Agents Med Chem.* 2008; 8: 646-682.

61. Cabrera M, Simoens M, Falchi G, Lavaggi ML, Piro OE, Castellano EE, Vidal A, Azqueta A, Monge A, de Ceráin, AL, Sagrera G, Seoane G, Cerecetto H, González M. Synthetic chalcones, flavanones, and flavones as antitumoral agents: Biological evaluation and structure–activity relationships. *Bioorg & Med Chem.* 2007; 15: 3356-3367.

62. Jeong H-J, Shin YG, Kim I-H, Pezzuto JM. Inhibition of Aromatase Activity by Flavonoids. *Arch Pharm Res.* 1999; 22: 309-312.

63. Adam LS, Chen S. Phytochemicals for breast cancer prevention by targeting aromatase. *Frontiers in Biosci.* 2009; 14: 3846-3863.

64. Pouget C, Fagnere C, Basly J-P, Besson A-E, Champavier Y, Habrioux G, Chulia A-J. Synthesis and Aromatase Inhibitory Activity of Flavanones. *Pharma Res.* 2002; 19: 286-291.

65. McNulty J, Nair JJ, Bollareddy E, Keskar K, Thorat A, Crankshaw DJ, Holloway AC, Khan G, Wright GD, Ejim L. Isolation of flavonoids from the heartwood and resin of *Prunus avium* and some preliminary biological investigations. *Phytochem.* 2009; 70: 2040-2046.

66. Li F, Ye L, Lin S-M, Leung LK. Dietary flavones and flavonones display differential effects on aromatase (CYP19) transcription in the breast cancer cells MCF-7. *Mol and Cell Endocrin.* 2011; 344: 51-58.

67. Zhao J, Dasmahapatra AK, Khan SI, Khan IA. Anti-aromatase activity of the constituents from damiana (Turnera diffusa). *J Ethnopharm.* 2008; 120: 387-393.

68. Saarinen N, Joshi SC, Ahotupa M, Li X, Ammala J, Makela S, Santii R. No evidence for the in vivo activity of aromatase-inhibiting flavonoids. *J Steroid Biochem Mol Biol.* 2001; 78: 231-239.

69. Wang C, Mäkelä T, Hase T, Adlercreutz H, Kurzer MS. Lignans and Flavonoids Inhibit Aromatase Enzyme in Human Preadipocytes. *J Steroid Biochem Mol Biol.* 1994; 3-4: 205-212.

70. Kao Y-C, Zhou C, Sherman M, Laughton CA, Chen S. Molecular Basis of the Inhibition of Human Aromatase (Estrogen Synthetase) by Flavone and Isoflavone Phytoestrogens: A Site-directed Mutagenesis Study. *Environ. Health Perspect.* 1998; 106: 86 – 91.

71. Mojaddami A, Sakhteman A, Fereidoonnezhad M, Faghih Z, Najdian A, Khabnadideh S, Sadeghpour H, Rezaei Z. Binding mode of triazole derivatives as aromatase inhibitors based on docking, protein ligand interaction fingerprinting, and molecular dynamics simulation studies. *Res Pharm Sci.* 2017; 12: 21-30.

72. Neves MAC, Dinis TCP, Colombo G, Sá e Melo ML. DOI: Combining Computational and Biochemical Studies for a Rationale on the Anti-Aromatase Activity of Natural Polyphenols. *Chem Med Chem.* 2007; 2: 1750-1762.

73. Monteiro R, Becker H, Azevedo I, Calhau C. Effect of Hop (Humulus lupulus L.) Flavonoids on Aromatase (Estrogen Synthase) Activity. *J Agric Food Chem.* 2006; 54: 2938-2943.

74. Monteiro R, Faria A, Azevedo I, Calhau C. Modulation of breast cancer cell survival by aromatase inhibiting hop (Humulus lupulus L.) flavonoids. *J Steroid Biochem Mol Biol.* 2007; 105: 124-130.

75. Way T-D, Lee H-H, Kao M-C, Lin J-K. Black tea polyphenol theaflavins inhibit aromatase activity and attenuate tamoxifen resistance in HER2/neu-transfected human breast cancer cells through tyrosine kinase suppression. *Eur J Cancer.* 2004; 40: 2165-2174.

76. Satoh K, Sakamoto Y, Ogata A, Nagai F, Mikuriya H, Numazawa M, Yamada K, Aoki N. Inhibition of aromatase activity by green tea extract catechins and their endocrinological effects of oral administration in rats. *Food Chem Toxicol.* 2002; 40: 925-933.

77. Racanatini M, Bisi A, Cavalli A, Belluti F, Gobbi S, Rampa A, Valenti P, Palzer M, Palusczak A, Hartmann RW. A New Class of Nonsteroidal Aromatase Inhibitors: Design and Synthesis of Chromone and Xanthone Derivatives and Inhibition of the P450 Enzymes Aromatase and 17α-Hydroxylase/C17,20-Lyase. *J Med Chem.* 2001; 44: 672-680.

78. Gobbi S, Cavalli A, Rampa A, Belluti F, Piazzi L, Paluszcak A, Hartmann RW, Recanatini M, Bisi A. Lead Optimization Providing a Series of Flavone Derivatives as Potent Nonsteroidal Inhibitors of the Cytochrome P450 Aromatase Enzyme. *J Med Chem.* 2006; 49: 4777-4780.

79. Pouget C, Fagnere C, Basly J-P, Habrioux G, Chulia A-J. New Aromatase Inhibitors. Synthesis and Inhibitory Activity of Pyridinyl-Substituted Flavanone Derivatives. *Bioorg Med Chem Lett.* 2002; 12: 1059-1061.

80. Bonfield K, Amato E, Bankemper T, Agard H, Steller J, Keeler JM, Roy D, McCallum A, Paula S, Ma L. Development of a new class of aromatase inhibitors: Design, synthesis and inhibitory activity of 3-phenylchroman-4-one (isoflavanone) derivatives. *Bioorg Med Chem.* 2012; 20: 2603-2613.

81. Kim Y-W, Hackett JC, Brueggemeier, RW. Synthesis and Aromatase Inhibitory Activity of Novel Pyridine-Containing Isoflavones. *J Med Chem.* 2004; 47(16): 4032-4040.

82. Hackett JC, Kim Y-W, Su B, Brueggemeier, RW. Synthesis and characterization of azole isoflavone inhibitors of aromatase. *Bioorg Med Chem.* 2005; 13: 4063-4070.

83. Su B, Hackett JC, Díaz-Cruz ES, Kim Y-W, Brueggemeier, RW. Lead optimization of 7-benzyloxy 2-(4'-pyridylmethyl)thio isoflavone aromatase inhibitors. *Bioorg Med Chem.* 2005; 13: 6571-6577.

84. Pouget C, Fagnère C, Basly J-P, Habrioux G, Chulia AJ. Design, Synthesis and Evaluation of 4-Imidazolylflavans as New Leads for Aromatase Inhibition. *Bioorg Med Chem Lett.* 2002; 12: 2859-2861.

85. Yahiaoui S, Pouget C, Fagnère C, Champavier Y, Habrioux G, Chulia AJ. *Bioorg Med Chem Lett.* 2004; 14: 5215-5218.

86. Yahiaoui S, Pouget C, Buxeraud J, Chulia AJ, Fagnère C. Lead optimization of 4-imidazolylflavans: New promising aromatase inhibitors. *Eur J Med Chem.* 2011; 46: 2541-2545.

87. Rice S, Mason HD, Whitehead, SA. Phytoestrogens and their low dose combinations inhibit mRNA expression and activity of aromatase in human granulosa-luteal cells. *J Steroid Biochem and Mol Biol.* 2006; 101:216-225.

88. Wang Y, Gho WM, Chan FL, Chen S, Leung LK. The red clover (Trifolium pratense) isoflavone biochanin A inhibits aromatase activity and expression. *Brit J Nutr.* 2008; 99: 303-310.

89. Li F, Chow S, Cheung W-H, Chan FL, Chen S, Leung LK. The citrus flavonone hesperetin prevents letrozole-induced bone loss in a mouse model of breast cancer. *J Nutr Biochem.* 2013; 24: 1112-1116.

90. Garreau JR, Delamelena T, Walts D, Karamlou K, Johnson N. Side effects of aromatase inhibitors versus tamoxifen: the patients' perspective. *Am J Surg.* 2006; 192: 496-498.

91 Niravath P. Aromatase inhibitor-induced arthralgia: a review. *Annals Oncol.* 2013; 24: 1443-1449.

92. van Duursen MBM, Nijmeijer SM, de Morree ES, de Jong PC, van den Berg M. Genistein induces breast cancer-associated aromatase and stimulates estrogen-dependent tumor cell growth in *in vitro* breast cancer model. *Toxicol.* 2011; 289: 67-73.

93. Hsieh C-Y, Santell RC, Haslam SZ, Helferich WG. Estrogenic Effects of Genistein on the Growth of Estrogen Receptor-positive Human Breast Cancer (MCF-7) Cells *in Vitro* and *in Vivo. Cancer Res.* 1998; 58: 3833-3838.

94. Campbell DR, Kurzer MS. Flavonoid inhibition of aromatase enzyme activity in human preadipocytes. *J Steroid Biochem Mol Biol.* 1993; 46: 381-388.

95. Le Bail JC, Laroche T, Marre-Fournier F, Habrioux G. Aromatase and 17β-hydroxysteroid dehydrogenase inhibition by flavonoids. *Cancer Lett.* 1998; 133: 101-106.

96. Van Meeuwen JA, Korthagen N, de Jong PC, Piersma AH, van den Berg M. (Anti)estrogenic effects of phytochemicals on human primary mammary fibroblasts, MCF-7 cells and their co-culture. *Toxicol Applied Pharmacol.* 2007; 221: 372-383.

97. Anand P, Kunnumakkara AB, Newman RA, Aggarwal BB. Bioavailability of Curcumin: Problems and Promises. *Molec Pharmaceut.* 2007; 4(6): 807-818.

2.3 Synthesis of α-methylstilbenes using an aqueous Wittig methodology and application toward the development of potent human aromatase inhibitors

Breast cancer remains the most frequently diagnosed cancer in women with 250,000 diagnosed cases in the US (2017), comprising 30% of all new cancer diagnoses and 15% of cancer fatalities.[1] While the incidence rate increased about 30% between 1975 and 2002, recent statistics show it has plateaued since 2002. More encouraging is the significant increase in the 5-year survival rates that have been documented over the last few decades.[1] The death rate in female breast cancer dropped 39% between 1989 and 2014. This success has been attributed to various factors including smoking cessation, educational awareness, and most importantly, early detection and treatment. Chemotherapeutic intervention for estrogen receptor (ER) positive breast cancer is largely based on mitigating the proliferative effect of estrogen on breast tissue via the administration of selective estrogen receptor modulators (SERMs) and/or aromatase inhibitors (AIs).[2] SERMs such as tamoxifen (**1**) compete with endogenous estrogens for binding to the ERs, while blockbuster AIs such as anastrozole (Astra-Zeneca) (**2a**) and letrozole (Novartis) (**2b**) reduce overall estrogen levels through inhibition of aromatase (cytochrome P450-19A1), the enzyme responsible for the rate limiting step in estrogen biosynthesis.

While long-term AI therapy is significantly associated with reduced cancer recurrence and mortality, patients often experience significant side effects and may discontinue treatment.[3] In addition, long term estrogen deprivation can lead to resistance to treatment and cancer re-occurrence. New treatment protocols using AIs in combination with kinase inhibitors such as abemaciclib (Lilly) and ribociclib (Novartis/Astex) have recently been introduced. Despite the development of promising natural product-inspired leads by several academic research groups,[4] the clinical development of new aromatase inhibitors has been minimal since the approval of **2a** and **2b** in the mid-late 1990s. Thus, there is a pressing need for the development of new AIs.
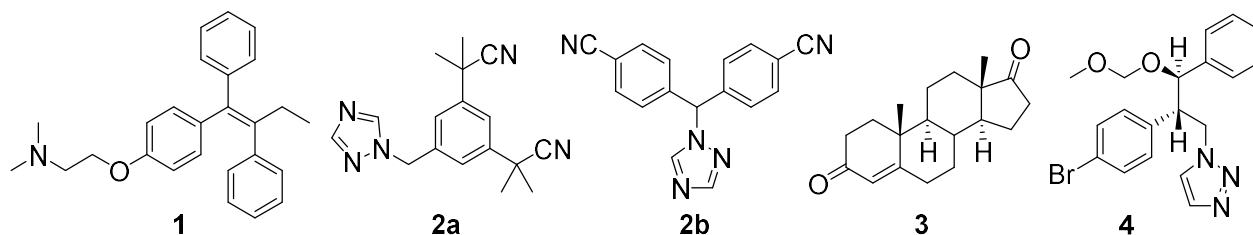
FIGURE 2.22. SERMs (**1**) and AIs (**2**) used clinically for the treatment of ER-dependent breast cancer. Androstenedione (**3**) and a dihydro-stilbene type AI (**4**) previously reported by our group.

Previous work in our group resulted in the discovery of potent and selective AIs based on a conformationally flexible dihydrostilbene scaffold (**4**).[5] Preliminary data showed compounds such as **4** to be more potent than their corresponding non-halogenated analogues, allowing us to develop the hypothesis that the aryl halide groups may function as ketone bioisosteres, overlapping with the ketone functional groups of the natural substrates, such as androstenedione (**3**). Inhibitors such as **4** are conformationally flexible with several central rotatable bonds, and we considered that analogues with greater structural rigidity might better mimic the core of the native steroidal substrates or SERMs such as tamoxifen and could result in more potent AIs. This led us to consider the (*E*)- and (*Z*)- unsaturated triazole stilbenes **5** and **6** (Scheme 2.1), which could be accessed in several steps from α-methylstilbene derivatives (**7**). In this paper we discuss a facile synthesis of structurally rigid α-methylstilbenes, their conversion to potent aromatase inhibitors and further insights into the role of aryl halides as ketone bioisosteres.
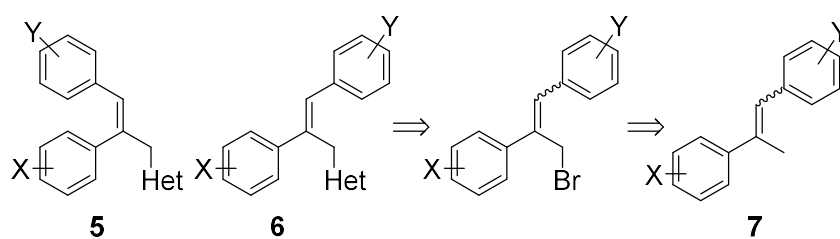
SCHEME 2.1. Proposed heterocycle (Het) substituted stilbene AIs **5** and **6** are accessible via allylic bromination and substitution on α-methylstilbenes such as **7**.
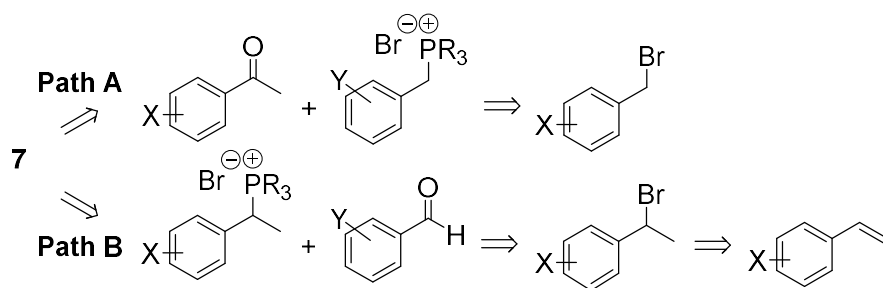
SCHEME 2.2. Retrosynthetic analysis of **7** reveals two obvious synthetic routes. Path A, involving olefination of less reactive acetophenones is difficult whereas Path B, involving olefination of aromatic aldehydes proved to be a highly efficient route to these novel AIs.

Our group has extensive experience in the development and application of non-classical aqueous Wittig reactions using short-chain trialkylphosphines (PEt_3 and PPr_3), and we imagined that the desired α-methylstilbene derivatives could be prepared by such a methodology.[6] We first considered the reaction of benzyl ylides with ketones, however this proved to be inefficient (Scheme 2.2, Path A).[6g] Switching the reaction partners, we decided to investigate the reaction of aldehydes with α-methylbenzyl phosphonium salts. While significantly less common, such phosphonium salts could be accessed from the reaction of a phosphine with α-methylbenzyl bromides (**8**) which, in turn, could be obtained from the hydrobromination of substituted styrenes (Scheme 2.2, Path B).

Substituted styrenes were readily synthesized from formalin using a previously reported aqueous Wittig methodology.[6e] To achieve selective hydrobromination on these styrenes, we were attracted to a literature method employing phosphorus tribromide and a silica gel catalyst, a process that appears to have attracted little attention.[7] While typical conditions for styrene hydrobromination require the use of dry HBr gas, the PBr_3/SiO_2 method proved highly efficient (Table 2.1) and proceeded with complete regiocontrol. The reactions are performed in open air at ambient temperature and are typically finished within 45 minutes. As well, the reactions proceed cleanly despite the potential for cation-induced styrene polymerization. In all cases, the crude reaction mixture could be filtered, concentrated and the α-methylbenzyl bromide used without further purification.

TABLE 2.1 Synthesis of α-methylbenzyl bromides and substitution with tripropylphosphine
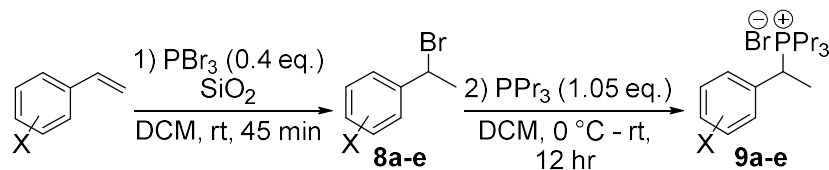
Entry	X =	Step 1 Yield[a]	Step 2 Yield[a]
1	H	8a (98%)	9a (98%)
2	4-Cl	8b (94%)	9b (91%)
3	4-Br	8c (93%)	9c (98%)
4	4-I	8d (95%)	9d (93%)
5	3-Br	8e (94%)	9e (93%)

a) isolated yields.

Initially, the reaction between (1-bromoethyl)benzene and triphenylphosphine was explored as a model reaction for the synthesis of the desired α-methylbenzyl phosphonium salts. Previous work states that the desired phosphonium salt can be isolated in 88% yield by refluxing the above reagents in toluene for an extended period of time.[8] Following this same procedure, we were only able to isolate the triphenylphosphonium salt in 66% yield. Significant elimination and styrene formation was noted by ^{1}H NMR. Due to the poor yield using triphenylphosphine, the alternative methodology using the more nucleophilic tripropylphosphine was developed. Satisfyingly, the addition of a slight excess of tripropylphosphine to the benzyl bromides **8a-e** at 0 °C with warming to room temperature cleanly yielded the desired phosphonium salts **9a-e** in excellent yields (Table 2.1). The reactions were completed after stirring overnight and no detectable reformation of styrenes was noted. As well, the pure salts could be isolated by simply evaporating the solvent and rinsing the resulting solid with ether or ethyl acetate. Importantly, the entire process for preparing these salts (i.e. styrene synthesis, hydrobromination, and substitution) could be performed in a 24-hour period, making the methodology much faster than the synthesis of analogous salts using triphenylphosphine.

TABLE 2.2 Synthesis of α-methylstilbenes via aqueous Wittig reaction
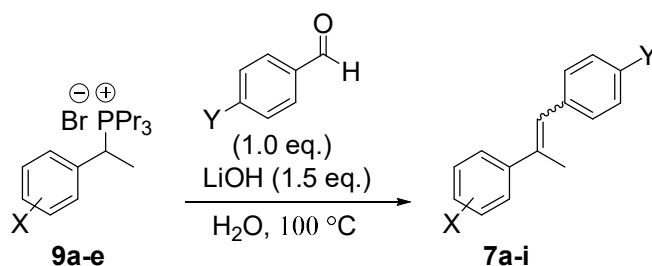
Entry	Salt	Y =	Yield[b]	(E):(Z)[c]
1	9a	H	7a (97%)	2.9 : 1
2[a]	9a	H	7a (80%)	3.0 : 1
3	9a	Cl	7b (88%)	3.7 : 1
4	9a	Br	7c (91%)	3.0 : 1
5	9b	H	7d (93%)	2.3 : 1
6	9b	Cl	7e (85%)	1.9 : 1
7	9c	H	7f (95%)	2.1 : 1
8	9c	Br	7g (86%)	4.5 : 1
9	9d	H	7h (90%)	2.3 : 1
10	9e	H	7i (92%)	2.5 :1

a) Performed at 70 °C. b) Isolated yield. c) Determined by ^{1}H NMR.

We next pursued the reaction of the above salts **9a-e** with substituted benzaldehydes under aqueous Wittig conditions. Initial attempts using the unsubstituted tripropylphosphonium salt **9a** and benzaldehyde with aqueous lithium hydroxide at 100 °C overnight gave the desired α-methylstilbene in 97% yield (3:1 *E:Z*). The reaction proceeds more slowly at lower temperatures, with an 80% yield obtained after heating overnight at 70 °C. Similar yields and (*E*):(*Z*) ratios (~2.3:1) were obtained using all salts prepared (Table 2.2).

To compare our aqueous Wittig method to more classical conditions, a reaction was performed with the unsubstituted α-methylbenzyl tripropylphosphonium salt and benzaldehyde using *n*-BuLi in THF at -78 °C with warming to room temperature. The yield proved to be substantially lower (32%) and the (*E*):(*Z*) (3.2:1) ratio was not significantly better. Moreover, the product required purification using column chromatography. A major benefit of the aqueous methodology is that the
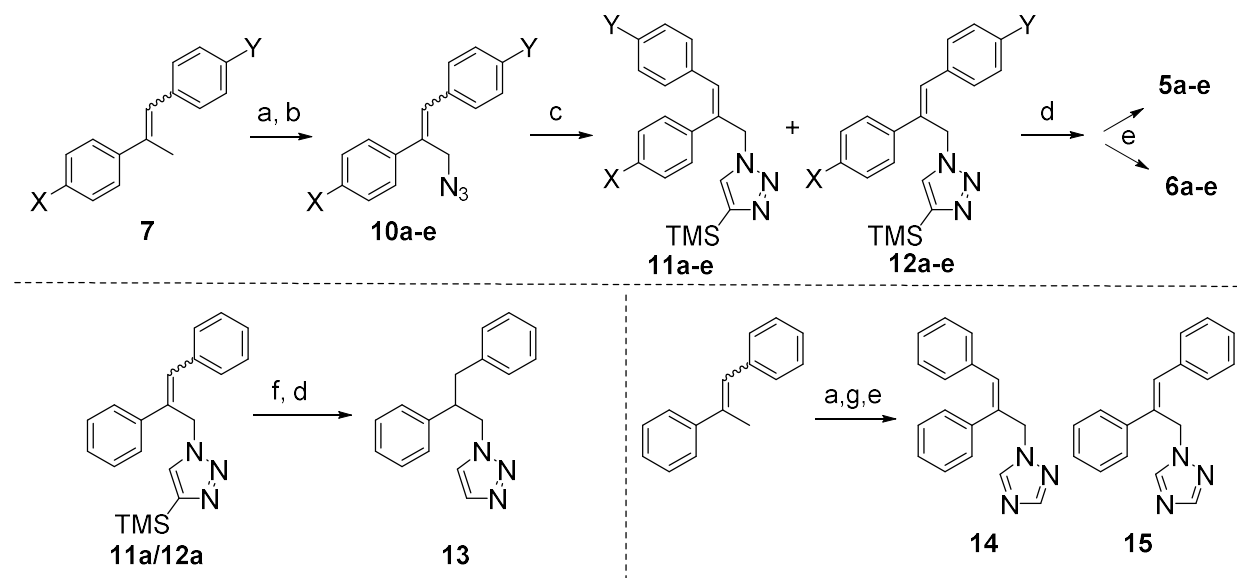
SCHEME 2.3 Synthesis of stilbene derived AIs. Reagents and conditions: (a) NBS, BPO, benzene, 70 °C, 4h; (b) NaN₃, ACN, rt, 12 h; (c) TMS-acetylene, CuI, THF, 50 °C, 12h; (d) TBAF, THF, 50 °C, 12h; (e) Separation over silica gel; (f) Raney Ni, MeOH, rt, 12h. (g) NaH, 1,2,4-triazole, THF, 0 °C – rt, 36h.

product precipitates from solution and is readily isolated via filtration and washing with water, as all salts and the phosphine oxide side-product are water soluble.

Having developed a high yielding synthesis of these α-methylstilbenes, we explored a short synthesis of 1,2,3-triazole stilbenes **5(a-e)** and **6(a-e)**, as well as the hydrogenated derivative **13** and 1,2,4-triazole derivatives **14** and **15** (Scheme 2.3)**.** Briefly, the α-methylstilbenes **7** were converted to allyl azides **10** via radical bromination using N-bromosuccinimide and benzoyl peroxide as a radical initiator, followed by substitution with sodium azide; the two step yields were typically between 70-80%. The azides were then used to synthesize the TMS-protected triazoles **11** and **12** via a copper catalyzed Huisgen dipolar cycloaddition with TMS-acetylene in 60-80% yield.[9] The (*E*) and (*Z*) isomers **11** and **12** were separable using silica gel chromatography, but thermally isomerized during the subsequent deprotection of the triazole group using tetra-*n*-butylammonium fluoride (TBAF), which gave deprotected isomers **5** and **6** in combined yields of 75-92%. The final products were also separable using silica gel chromatography. The hydrogenated derivative **13** was prepared in 80% two-

step yield via the reaction of compounds **11a/12a** with Raney nickel, followed by deprotection with

TBAF. Compounds **14** and **15** and were readily prepared from the reaction of 1,2,4-triazole with the

allyl bromide derived from **7a**.

The collection of compounds was next screened for AI activity against recombinant human

aromatase via kinetic monitoring of the conversion of dibenzylfluorescein (DBF) substrate to

fluorescein. Fluorometric measurement of emission was made at 535 nm after excitation at 485 nm

utilizing ketoconazole as a positive control following a literature protocol.[5]

The results of this assay demonstrated that newly synthesized triazoles **5**, **6**, **14** and **15** are all

nanomolar inhibitors of human recombinant aromatase *in vitro*. Several structure-activity-relations

(SARs) were immediately discernible upon examination of the data. First, halogenated analogues were

consistently more potent than their non-halogenated derivatives, consistent with the ketone-

bioisostere hypothesis. Secondly, there is a clear trend when comparing the geometric isomers **5** and

6, as the (*Z*)-compounds **6** proved consistently more potent than their (*E*)-counterparts **5**, possibly

TABLE 2.3 Inhibitory activity of select α-methylstilbene derivatives on recombinant human aromatase. Values are the means of three separate experiments.

Entry	Compound	X =	Y =	K_i (µM)
1	5a	H	H	0.180
2	5b	Cl	H	0.081
3	5c	Cl	Cl	0.097
4	5d	Br	H	0.125
5	5e	Br	Br	0.45
6	6a	H	H	0.100
7	6b	Cl	H	0.057
8	6c	Cl	Cl	**0.008**
9	6d	Br	H	0.074
10	6e	Br	Br	0.024
11	13	H	H	0.290
12	14	-	-	0.079
13	15	-	-	0.032
14	4*	-	-	0.020

*inhibitory activity on human aromatase previously reported[5a]

reflecting the better steroidal overlap of the (Z)-analogues. Third, comparison of derivatives **6a**, **6b** and **6c** directly (Table 2.3, entries 6-8) showed a clear synergistic effect with double halogenation resulting in the most potent activity. This result is fully consistent with the ketone bioisostere hypothesis (i.e. in relation to androstenedione). Fourth, aryl chloride analogues were consistently more potent than the corresponding aryl bromides, for example, comparing **6b/6c** with **6d/6e**, indicating the carbon-chlorine bond to be a better ketone mimic (sterically and electronically) than the carbon-bromine bond. Finally, conformational rigidity improves activity, as the hydrogenated product **13** was less active than either corresponding isomer, **5a** and **6a**. The 1,2,4-triazole derivatives **14** and **15** were also 2-3 times more potent than their related 1,2,3-triazole derivatives **5a** and **6a**, presenting an interesting avenue for further investigation. When comparing these new compounds with previously developed inhibitors such as **4**, it is clear that hydrogen bonding acceptor groups in the core of the inhibitors (such as methoxymethyl) are not required for potent anti-aromatase activity.

Overall, this structure-activity study has identified compound **6c** as a potent aromatase inhibitor with a K_i of 8 nM. This compound is a structurally rigid stilbene featuring synergistic *para*-chloro substitution on each phenyl ring. Compound **6c** is the most potent analogue discovered thus far in the series. All SAR data are in agreement with previous studies from our group, suggesting that aryl chlorides act as bioisosteres for the keto-groups of the native aromatase substrate, androstenedione **3**.[5]

In conclusion, a novel, high yielding aqueous Wittig methodology for the synthesis of α-methylstilbenes has been developed. We have shown that α-methylbenzyl phosphonium salts can be readily prepared chemoselectively (no elimination) using tripropylphosphine and α-methylbenzyl bromides obtained in high yields from the hydrobromination of substituted styrenes. The entire process can be completed in a 24-hour period, in high yields and purity without the use of column chromatography. Finally, we have used our ready access to α-methylstilbenes as a starting point for

the synthesis of novel, highly-potent inhibitors of aromatase. Future work will focus on expanding the

scope of the Wittig methodology using α-methylbenzyl phosphonium salts and exploring additional

stilbene derivatives as potential aromatase inhibitors.

References

1) (a) Siegel, R. L; Miller, K. D.; Jemal, A. *CA Cancer J. Clin.* **2017**, 67, 7-30. (b) C. E. DeSantis et al., *CA Cancer J. Clin.* **2017**, 67, 439-448.

2) Chlebowski, R. T. *Clin. Breast Cancer*, **2013**, 13, 159-166.

3) (a) Shapiro, C. L.; Recht, A. *N. Engl. J. Med.* **2001**, 344, 1997-2008. (b) Binkley, J. M.; Harris, S. R.; Levangie, P. K.; Pearl, M.; Guglielmino, J.; Kraus, V.; Rowden, D. *Cancer*, **2012**, 118, 2207-2216. (c) Johnston, S. R. D.; Dowsett, M. *Nat. Rev. Cancer*, **2003**, 3, 821-831.

4) (a) Nielsen, A. J.; McNulty, J. *Med. Res. Rev.* **2018**, 1-20, DOI: 10.1002/med.21536. (b) Kondratyuk, T. P.; Park, E-J.; Marler, L. E.; Ahn, S.; Yuan, Y.; Choi, Y.; Yu, R.; van Breemen, R. B.; Sun, B.; Hoshino, J.; Cushman, M.; Jermihov, K. C.; Mesecar, A. D.; Grubbs, C. J.; Pezzuto, J. M. *Mol. Nutr. Food Res.*, **2011**, 55, 1249-1265. (c) Sun, B.; Hoshino, J.; Jermihov, K.; Marler, M.; Pezzuto, J. M.; Mesecar, A. D.; Cushman, M. *Bioorg. Med. Chem.* **2010**, 18, 5352-5366. (d) Mayhoub A. S.; Marler, L.; Kondratyuk, T. P.; Park, E-J.; Pezzuto, J. M.; Cushman, M. *Bioorg. Med. Chem.* **2012**, 20, 510-520. (e) Mayhoub A. S.; Marler, L.; Kondratyuk, T. P.; Park, E-J.; Pezzuto, J. M.; Cushman, M. *Bioorg. Med. Chem.* **2012**, 20, 2427-2434. (f) Bonfield, K.; Amato, E.; Bankemper, T.; Agard, H.; Steller, J.; Keeler, J. M.; Roy, D.; McCallum, A.; Paula, S.; Ma, L. *Bioor. Med. Chem.* **2012**, 20, 2603-2613. (g) Su, B.; Hackett, J. C.; Díaz-Cruz, E. S.; Kim, Y-W.; Brueggemeier, R. W. *Bioorg. Med. Chem.* **2005**, 13, 6571-6577. (h) Yahiaoui, S.; Pouget, C.; Buxeraud, J.; Chulia, A. J.; Fagnère, C. *Eur. J. Med. Chem.* **2011**, 46, 2541-2545. (i) Ghosh, D.; Lo, J.; Egbuta, C. *J. Med. Chem.* **2016**, 59, 5131-5148.

5) (a) McNulty, J.; Nielsen, A. J.; Brown, C. E.; DiFrancesco, B. R.; Vurgun, N.; Nair, J. J.; Crankshaw, D.; Holloway, A. *Bioorg. & Med. Chem. Lett.* **2013**, 23, 6060-6063 (b) McNulty, J.; Nair, J. J.; Vurgun, N.; DiFrancesco, B.; Brown, C.; Holloway, A.; Crankshaw, D.; Tsoi, B. *Bioorg. & Med. Chem. Lett.* **2012**, 22, 718-722. (c) McNulty, J.; Keskar, K.; Crankshaw, D. J.; Holloway, A. C. *Bioorg. & Med. Chem. Lett.* **2014**, 24, 4586-4589.

6) (a) Wittig, G.; Geissler, G. *Liebigs Ann.* **1953**, 44–57 (b) McNulty, J.; Zepeda-Velázquez, C.; McLeod, D. *Green Chem.* **2013**, 15, 3146-3149 (c) McNulty, J.; McLeod, D. *Tetrahedron Lett.* **2011**, *52*, 5467-5470 (d) McNulty, J.; McLeod, D. *Tetrahedron Lett.* **2013**, 54, 6303-6306 (e) Das, P.; McLeod, D.; McNulty, J. *Tetrahedron Lett.* **2011**, *52,* 199-201 (f) Das, P.; McNulty, J. *Eur. J. Org. Chem.* **2010**, 3587-3591 (g) McNulty, J.; Das, P.; McLeod, D. *Chem. Eur. J.* **2010**, 16, 6756-6760 (h) McNulty, J.; Das, P. *Tetrahedron Lett.* **2009**, 50, 5737-5740 (i) McNulty, J.; Mcleod, D. *Chem. Eur. J.* **2011**, 17, 8794-8798. (j) McNulty, J.; Das, P. *Eur. J. Org. Chem.* **2009**, 4031-4035.

7) Sanseverino, A. M.; de Mattos, M. C. S. *J. Braz. Chem. Soc.* **2001**, 12, 685-687.

8) Hüggenberg, W.; Seper, A.; Oppel, I. M.; Dyker, G. *Eur. J. Org. Chem.* **2010**, 35, 6786-6797.

9) (a) Rostovtsev, V. V.; Green, L. G.; Fokin, V. V.; Sharpless, K. B. *Angew. Chem. Int. Ed.* **2002**, 41, 2596-2599. The reaction may also be catalyzed by homogeneous silver (I) complexes, see: (b) McNulty, J.; Keskar, K.; Vemula, R. *Chem. Eur. J.* **2011**, 17, 14727-14730. (c) McNulty, J.; Keskar, K. *Eur. J. Org. Chem.* **2012**, 5462-5470.

2.4 Conclusions and future work

The synthesis and discovery of novel stilbenoid AIs with potent *in vitro* activity is a promising first step in the development of new breast cancer chemotherapeutics. The McNulty group is currently in the process of making derivatives that probe the replacement of the 1,2,3-triazole core with different heterocycles. The results discussed in Chapter 2.3 indicate that 1,2,4-triazoles may be even more potent than the corresponding 1,2,3-triazoles and can be prepared in fewer steps. Pyrazole and imidazole derivatives should also be readily accessible using the same alkylative strategy used in the preparation of the 1,2,4-triaole derivatives and are worth exploration.

Besides elucidating the SAR around heterocycle substitution, future work should explore whether these compounds recapitulate their activity in cell-based assays. Proliferation assays using ER-positive human breast cancer cell lines such as MCF-7, BT-474 and T-47D are a common and widely used method for determining the efficacy of AIs.[7,8,9,10,11] As well, recent work has developed MCF-7 cells that are resistant to commercial AIs such as anastrozole and letrozole. If the aforementioned compounds demonstrate activity in these resistant cell lines, that may represent a significant advantage of these compounds over existing breast cancer chemotherapeutics.[11,12] These cell lines are also tumorigenic in mice and frequently used to produce cell-derived xenografts for use in mouse models of breast cancer.[10] If the compounds show promise in cell based assays, testing them in such mouse models may be warranted.

Other future work should explore the selectivity these compounds display for aromatase versus other CYP450 enzymes; the lack of selectivity demonstrated by older generations of AIs resulted in increased drug-drug interactions and negative side effects.[13,14] Regardless of any future experiments, the development and discovery of novel stilbenoid AIs highlights the fact that natural products are still an excellent inspiration for modern efforts in drug-discovery.

2.5 Experimental

This experimental is provided as published in *Bioorg. Med. Chem. Lett.*, 2019, *29*, 1395-1398.

All reactions were performed in sealed glass vials or round-bottom flasks without prior drying or use of inert atmosphere. It was unnecessary to distill the dichloromethane prior to use in the styrene hydrobrominations. ^{1}H and ^{13}C spectra were recorded on Bruker AV 600 or 700 MHz spectrometers in CDCl$_3$ or CD$_2$Cl$_2$. THF and benzene were distilled over sodium with a benzophenone indicator. Reactions were monitored using thin layer chromatography (TLC) using Macherey-Nagel silica gel 60 F$_{254}$ TLC aluminum plates and visualized with UV fluorescence and staining with 2,4-dinitrophenylhydrazine or vanillin stains. Bulk solvent removal was performed by rotary evaporation under reduced pressure. For reactions with solvent volumes under 3 mL, the solvent was evaporated under a stream of nitrogen. Column chromatographic purification was performed using Silicycle silica gel (40–63 µM, 230-400 mesh) with technical grade solvents. Yields are reported for spectroscopically pure compounds, unless stated otherwise. Coupling constants are recorded in Hz and chemical shifts are reported in ppm downfield of TMS. ^{31}P NMR was recorded on Bruker AV 200 or 600 MHz spectrometers in CDCl$_3$ and chemical shifts are reported downfield from an external standard of 85% H$_3$PO$_4$ in H$_2$O. The (*E*) to (*Z*) ratios of the alpha-methyl stilbenes were determined based on the chemical shift and relative integration of the methyl peaks in the ^{1}H NMR. HRMS (ESI$^+$) was performed on a Waters Micromass Q-ToF Ultima Global. EI HRMS was performed on a Micromass GCT. All reagents were purchased from Sigma Aldrich or Cytec Solvay Group and used without purification.

For the synthesis of substituted styrenes, refer to Das, P.; McLeod, D.; McNulty, J. *Tetrahedron Lett.* **2011**, *52*, 199-201.

The following styrene hydrobromination procedure is based on Sanseverino, A. M.; de Mattos, M. C. S. *J. Braz. Chem. Soc.* **2001**, 12, 685-687.

General Procedure for Styrene Hydrobromination

Into a round-bottom flask containing a magnetic stirring bar was added styrene (1.0 eq.), SiO_2 gel (230-400 mesh; 0.5 g/mmol styrene) and DCM (2.5 mL/mmol styrene). The mixture was stirred vigorously, and 0.4 eq. PBr_3 (0.4 M in DCM) was added in one portion, resulting in a deep orange or red solution. The reaction was stirred for 30-60 minutes and monitored by TLC. When the reaction appeared complete by TLC, 10% $NaHCO_3$ was added dropwise to the reaction until the solution became colourless or light yellow, and no further evolution of CO_2 was noted. The resulting slurry was filtered through a Celite plug and eluted with DCM. The resulting organic solution was evaporated to dryness to afford the hydrobromination product **8a**.
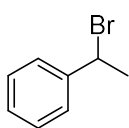
8a (1-bromoethyl)benzene: 98% yield. Clear colourless oil. ^{1}H NMR (600 MHz, $CDCl_3$) δ 7.45 (d, J = 7.7 Hz, 2H), 7.36 (t, J = 7.6 Hz, 2H), 7.30 (t, J = 7.3 Hz, 1H), 5.23 (q, J = 6.9 Hz, 1H), 2.06 (d, J = 6.9 Hz, 3H). All data are in agreement with the literature.
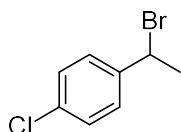
8b 1-chloro-4-(1-bromoethyl)benzene: 94% yield. Clear colourless oil. ^{1}H NMR (600 MHz, $CDCl_3$) δ 7.37 (d, J = 8.5 Hz, 2H), 7.31 (d, J = 8.5 Hz, 2H), 5.17 (q, J = 6.9 Hz, 1H), 2.03 (d, J = 6.9 Hz, 3H). ^{13}C NMR (151 MHz, $CDCl_3$) δ 141.9, 134.2, 129.0, 128.3, 48.3, 26.9. EI HRMS calculated for C_8H_8ClBr (M)[+]: 217.9498 found 217.9494.
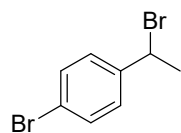
8c 1-bromo-4-(1-bromoethyl)benzene: 93% yield. Clear light-yellow oil. ^{1}H NMR (600 MHz, $CDCl_3$) δ 7.46 (d, J = 8.5 Hz, 2H), 7.32 (d, J = 8.5 Hz, 2H), 5.15 (q, J = 6.9 Hz, 1H), 2.02 (d, J = 6.9 Hz, 3H). ^{13}C NMR (151 MHz, $CDCl_3$) δ 142.4, 132.0, 128.6, 122.3, 48.3, 26.8. EI HRMS calculated for $C_8H_8Br_2$ (M)[+]: 261.8993 found 261.8997.
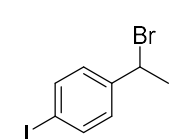
8d 1-iodo-4-(1-bromoethyl)benzene: 95% yield. White waxy solid. ^{1}H NMR (600 MHz, CDCl$_3$) δ: ^{1}H NMR (600 MHz, CDCl$_3$) δ 7.67 (d, J = 8.4 Hz, 2H), 7.18 (d, J = 8.4 Hz, 2H), 5.13 (q, J = 6.9 Hz, 1H), 2.01 (d, J = 6.9 Hz, 3H); ^{13}C NMR (151 MHz, CDCl$_3$) δ 143.1, 138.0, 128.8, 94.0, 48.4, 26.8. EI HRMS calculated for C$_8$H$_8$IBr (M)$^+$: 309.8854 found: 309.8843.
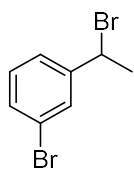
8e 1-bromo-3-(1-bromoethyl)benzene: 94% yield. Clear colourless oil. ^{1}H NMR (600 MHz, CDCl$_3$) δ 7.58 (t, J = 1.8 Hz, 1H), 7.42 (ddd, J = 7.9, 1.9, 1.0 Hz, 1H), 7.38 – 7.35 (m, 1H), 7.22 (t, J = 7.9 Hz, 1H), 5.12 (q, J = 6.9 Hz, 1H), 2.02 (d, J = 6.9 Hz, 3H). ^{13}C NMR (151 MHz, CDCl$_3$) δ 145.5, 131.6, 130.4, 130.1, 125.7, 122.7, 47.9, 26.8. EI HRMS calculated for C$_8$H$_8$Br$_2$ (M)$^+$: 261.8993 found 261.8995.

General procedure for secondary phosphonium salt preparation:

(1-bromoethyl)benzene **8a** (2.0 M in DCM, 1.0 eq.) was added to a round-bottom flask containing a magnetic stirring bar. The flask was sealed and cooled to 0°C. Then, tripropylphosphine (1.05 eq.) was added dropwise to the mixture. The reaction was allowed to stir overnight with gradual warming to room temperature. Then, solvent was removed under vacuum and the resulting solid was washed with either diethyl ether or ethyl acetate to remove any trace tripropylphosphine, yielding the desired phosphonium salt **9a**.
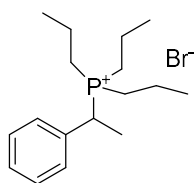
9a (1-phenylethyl)tripropylphosphonium bromide: 98% yield. White solid. ^{1}H NMR (600 MHz, CDCl$_3$) δ 7.46 – 7.49 (2H, m), 7.39 (t, J = 7.6 Hz, 2H), 7.32 – 7.37 (1H, m), 4.79 (dq, $J_{31P,1H}$ = 15.0, $J_{1H,1H}$ = 7.5 Hz, 1H), 2.28 – 2.42 (6H, m), 1.74 (dd, $J_{31P,1H}$ = 17.3, $J_{1H,1H}$ = 7.5 Hz, 3H), 1.42 – 1.60 (6H, m), 1.07 (td, $J_{1H,1H}$ = 7.2, $J_{31P,1H}$ = 1.8 Hz, 9H). ^{13}C NMR (151 MHz, CDCl$_3$) δ 134.5 (d, $J_{31P,13C}$ = 5.8 Hz), 129.6, 129.0, 128.9 (d, $J_{31P,13C}$ = 4.6 Hz), 33.4

(d, $J_{31P,13C}$ = 42.0 Hz), 20.4 (d, $J_{31P,13C}$ = 44.5 Hz), 16.2 (d, $J_{31P,13C}$ = 4.4 Hz), 15.9 (d, $J_{31P,13C}$ = 15.9 Hz), 15.0. ^{31}P NMR (80 MHz, CDCl$_3$) δ: 34.6. ESI HRMS calculated for C$_{17}$H$_{30}$P (M − Br$^-$)$^+$: 265.2085 found: 265.2092. Exact Mass: 265.2080.
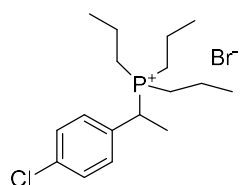
9b (1-(4-chlorophenyl)ethyl)tripropylphosphonium bromide: 91% yield. White solid. ^{1}H NMR (600 MHz, CDCl$_3$) δ 7.52 (d, J = 8.2 Hz, 2H), 7.39 (d, J = 8.2 Hz, 2H), 5.11 (dq, $J_{31P,1H}$ = 15.0, $J_{1H,1H}$ = 7.4 Hz, 1H), 2.39 − 2.30 (m, 6H), 1.72 (dd, $J_{31P,1H}$ = 17.2, $J_{1H,1H}$ = 7.4 Hz, 3H), 1.63 − 1.46 (m, 6H), 1.10 (td, $J_{1H,1H}$ = 7.2, $J_{31P,1H}$ = 1.6 Hz, 9H). ^{13}C NMR (151 MHz, CDCl$_3$) δ 135.2 (d, $J_{31P,13C}$ = 3.8 Hz), 133.2 (d, $J_{31P,13C}$ = 6.0 Hz), 130.4 (d, $J_{31P,13C}$ = 4.8 Hz), 129.8 (d, $J_{31P,13C}$ = 2.0 Hz), 32.7 (d, $J_{31P,13C}$ = 42.1 Hz), 20.4 (d, $J_{31P,13C}$ = 44.4 Hz), 16.3 (d, $J_{31P,13C}$ = 4.7 Hz), 15.9 (d, $J_{31P,13C}$ = 15.8 Hz), 15.1. ^{31}P NMR (80 MHz, CDCl$_3$) δ 34.3. ESI HRMS calculated for C$_{17}$H$_{29}$ClP (M − Br$^-$)$^+$: 299.1695 found 299.1683.
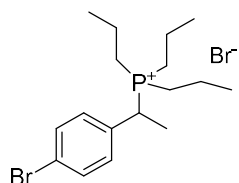
9c (1-(4-bromophenyl)ethyl)tripropylphosphonium bromide: 98% yield. ^{1}H NMR (600 MHz, CDCl$_3$) δ 7.53 (d, J = 8.2 Hz, 2H), 7.46 (dd, $J_{1H,1H}$ = 8.6 Hz, $J_{31P,1H}$ = 2.2 Hz, 2H), 5.06 (dq, $J_{31P,1H}$ = 15.0 Hz, $J_{1H,1H}$ = 7.4 Hz, 1H), 2.40 − 2.29 (m, 6H), 1.71 (dd, $J_{31P,1H}$ = 17.2 Hz, $J_{1H,1H}$ = 7.4 Hz, 3H), 1.63 − 1.45 (m, 6H), 1.08 (td, $J_{1H,1H}$ = 7.2 Hz, $J_{31P,1H}$ = 1.7 Hz, 9H). ^{13}C NMR (151 MHz, CDCl$_3$) δ 133.8 (d, $J_{31P,13C}$ = 6.0 Hz), 132.7 (d, $J_{31P,13C}$ = 1.8 Hz), 130.7 (d, $J_{31P,13C}$ = 4.8 Hz), 123.2 (d, $J_{31P,13C}$ = 4.1 Hz), 32.7 (d, $J_{31P,13C}$ = 42.3 Hz), 20.4 (d, $J_{31P,13C}$ = 44.4 Hz), 16.3 (d, $J_{31P,13C}$ = 4.7 Hz), 15.9 (d, $J_{31P,13C}$ = 15.9 Hz), 15.0. ^{31}P NMR (80 MHz, CDCl$_3$) δ 34.2. White solid. ESI HRMS calculated for C$_{17}$H$_{29}$BrP (M − Br$^-$)$^+$: 343.1190 found 343.1201.
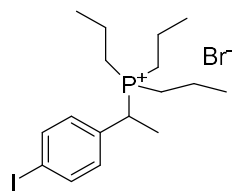
9d (1-(4-iodophenyl)ethyl)tripropylphosphonium bromide: 93% yield. White solid. ^{1}H NMR (600 MHz, CDCl$_3$) δ 7.74 (d, J = 8.1 Hz, 2H), 7.32 (dd, $J_{1H,1H}$ = 8.4, $J_{31P,1H}$ = 2.0 Hz, 2H), 5.12 – 5.04 (m, 1H), 2.39 – 2.31 (m, 6H), 1.71 (dd, $J_{31P,1H}$ = 17.2, $J_{1H,1H}$ = 7.4 Hz, 3H), 1.62 – 1.46 (m, 6H), 1.10 (td, $J_{1H,1H}$ = 7.2, $J_{31P,1H}$ = 1.6 Hz, 9H). ^{13}C NMR (151 MHz, CDCl$_3$) δ 138.7 (d, $J_{31P,13C}$ = 1.9 Hz), 134.4 (d, $J_{31P,13C}$ = 6.1 Hz), 130.8 (d, $J_{31P,13C}$ = 4.8 Hz), 94.9 (d, $J_{31P,13C}$ = 4.3 Hz), 32.9 (d, $J_{31P,13C}$ = 42.1 Hz), 20.5 (d, $J_{31P,13C}$ = 44.4 Hz), 16.4 (d, J = 4.8 Hz), 16.0 (d, $J_{31P,13C}$ = 15.9 Hz), 14.9. ^{31}P NMR (80 MHz, CDCl$_3$) δ: 34.1. ESI HRMS calculated for C$_{17}$H$_{29}$PI (M – Br$^-$)$^+$: 391.1058 found 391.1052.
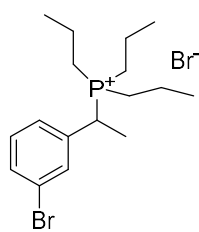
9e (1-(3-bromophenyl)ethyl)tripropylphosphonium bromide: 93% yield. White powdery solid. ^{1}H NMR (600 MHz, CDCl$_3$) δ 7.65 (d, J = 7.6 Hz, 1H), 7.54 – 7.48 (m, 2H), 7.31 (t, J = 7.8 Hz, 1H), 5.06 (dq, $J_{31P,1H}$ = 14.9, $J_{1H,1H}$ = 7.4 Hz, 1H), 2.43 – 2.30 (m, 6H), 1.73 (dd, $J_{31P,1H}$ = 17.1, $J_{1H,1H}$ = 7.4 Hz, 3H), 1.63 – 1.46 (m, 6H), 1.11 (td, $J_{1H,1H}$ = 7.2, $J_{31P,1H}$ = 1.8 Hz, 9H). ^{13}C NMR (151 MHz, CDCl$_3$) δ 137.1 (d, $J_{31P,13C}$ = 5.8 Hz), 132.3, 131.3, 131.1 (d, $J_{31P,13C}$ = 4.5 Hz), 128.4 (d, $J_{31P,13C}$ = 5.0 Hz), 123.5 (d, $J_{31P,13C}$ = 3.2 Hz), 33.1 (d, $J_{31P,13C}$ = 41.9 Hz), 20.4 (d, $J_{31P,13C}$ = 44.3 Hz), 16.3 (d, $J_{31P,13C}$ = 4.8 Hz), 15.9 (d, $J_{31P,13C}$ = 15.9 Hz), 15.0. ^{31}P NMR (243 MHz, CDCl$_3$) δ 34.3. C$_{17}$H$_{29}$BrP (M – Br$^-$)$^+$: 343.1190 found 343.1191.

General procedure for the synthesis of α-methylstilbenes:

Benzaldehyde (1.0 Eq), (1-phenylethyl)tripropylphosphonium bromide **9a** (1.0 eq.) and lithium hydroxide (1.5 eq.) were combined in H$_2$O (reactions performed at 1.25-2.5 M, depending on salt solubility) and sealed in a flask containing a magnetic stirring bar. The mixture was heated to 100 °C overnight with vigorous stirring and then cooled to room temperature, resulting in the precipitation of the stilbene product. The mixture was filtered off and washed with water to remove any

tripropylphosphine oxide, yielding the pure stilbene **7a** as a mixture of (*E*):(*Z*) isomers. In many cases, the major (*E*)-stilbene could be selectively recrystallized from the (*E*):(*Z*) mixture using absolute ethanol.
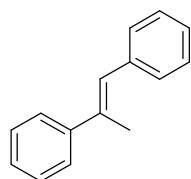
7a prop-1-ene-1,2-diyldibenzene: 97% yield. White waxy solid. 2.9:1 (*E*):(*Z*) mixture (determined by ^{1}H NMR). Pure (*E*) isomer obtained by recrystallization from absolute ethanol. (*E*) isomer: ^{1}H NMR (600 MHz, CDCl$_3$) δ 7.54 – 7.52 (m, 1H), 7.41 – 7.36 (m, 2H), 7.29 (t, *J* = 7.3 Hz, 1H), 7.27 – 7.24 (m, 1H), 6.85 (d, *J* = 1.0 Hz, 1H), 2.29 (d, *J* = 1.3 Hz, 1H). ^{13}C NMR (151 MHz, CDCl$_3$) δ 144.1, 138.5, 137.6, 129.3, 128.5, 128.3, 127.9, 127.3, 126.6, 126.2, 17.6. EI HRMS calculated for C$_{15}$H$_{14}$ (M)$^+$: 194.1096 found: 194.1096.
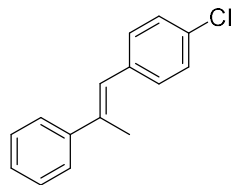
7b (*E*)-1-chloro-4-(2-phenylprop-1-en-1-yl)benzene. 88% yield. White solid. 3.7:1 (*E*):(*Z*) mixture (determined by ^{1}H NMR). Pure (*E*) isomer obtained by recrystallization from absolute ethanol. (*E*) isomer: ^{1}H NMR (600 MHz, CDCl$_3$) δ 7.51 (d, *J* = 8.1 Hz, 2H), 7.38 (t, *J* = 7.6 Hz, 2H), 7.34 (d, *J* = 8.4 Hz, 2H), 7.32 - 7.27 (3H, m), 6.77 (s, 1H), 2.26 (s, 3H). ^{13}C NMR (151 MHz, CDCl$_3$) δ 143.8, 138.3, 136.9, 132.3, 130.6, 128.5, 128.5, 127.5, 126.6, 126.1, 17.6. EI HRMS calculated for C$_{15}$H$_{13}$Cl (M)$^+$: 228.0706 found 228.0709.
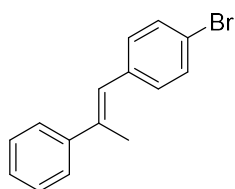
7c (E)-1-bromo-4-(2-phenylprop-1-en-1-yl)benzene. 91% yield. White solid. 3.0:1 (*E*):(*Z*) mixture (determined by ^{1}H NMR). Pure (*E*) isomer obtained by recrystallization from absolute ethanol. (*E*) isomer: ^{1}H NMR (600 MHz, CDCl$_3$) δ 7.50 (t, *J* = 8.8 Hz, 4H), 7.38 (t, *J* = 7.6 Hz, 2H), 7.30 (t, *J* = 7.3 Hz, 1H), 7.23 (d, *J* = 8.3 Hz, 2H), 6.75 (s, 1H), 2.26 (s, 3H). ^{13}C NMR (151 MHz, CDCl$_3$) δ 143.8, 138.4, 137.4, 131.4, 130.9, 128.5, 127.6, 126.6, 126.1, 120.5, 17.7. EI HRMS calculated for C$_{15}$H$_{13}$Br (M)$^+$: 272.0201 found: 272.0190.
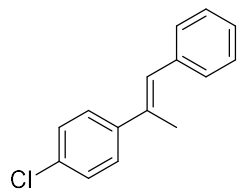
7d 1-chloro-4-(1-phenylprop-1-en-2-yl)benzene: 93% yield. White solid. 2.3:1 (*E*):(*Z*) mixture (determined by ^{1}H NMR). Pure (*E*) isomer obtained by recrystallization from absolute ethanol. (*E*) isomer: ^{1}H NMR (600 MHz, CDCl$_3$) δ 7.47 – 7.44 (m, 2H), 7.40 – 7.32 (m, 6H), 7.27 – 7.24 (m, 1H), 6.82 (s, 1H), 2.26 (d, *J* = 1.3 Hz, 3H). ^{13}C NMR (151 MHz, CDCl$_3$) δ 142.5, 138.2, 136.4, 133.1, 129.3, 128.6, 128.4, 128.3, 127.4, 126.8, 17.5. EI HRMS calculated for C$_{15}$H$_{13}$Cl (M)$^+$: 228.0706 found: 228.0699.
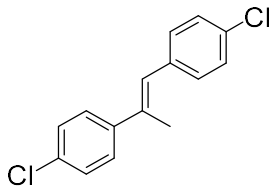
7e 4,4'-(prop-1-ene-1,2-diyl)bis(chlorobenzene). 85% yield. White solid. 1.2:1 (*E*):(*Z*) mixture (determined by ^{1}H NMR). Pure (*E*) isomer obtained by recrystallization from absolute ethanol. (*E*) isomer: ^{1}H NMR (600 MHz, CDCl$_3$) δ 7.43 (d, *J* = 8.6 Hz, 1H), 7.36 – 7.32 (m, 2H), 7.27 (d, *J* = 8.4 Hz, 1H), 6.75 (s, 1H), 2.23 (d, *J* = 1.2 Hz, 1H). ^{13}C NMR (151 MHz, CDCl$_3$) δ 142.2, 137.1, 136.6, 133.3, 132.6, 130.5, 128.6, 128.6, 127.4, 127.0, 17.6. EI HRMS calculated for C$_{15}$H$_{12}$Cl$_2$ (M)$^+$: 262.0316 found 262.0316.
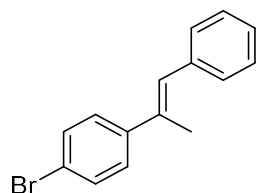
7f 1-bromo-4-(1-phenylprop-1-en-2-yl)benzene: 95% yield. White solid. 2.1:1 (*E*):(*Z*) mixture (determined by ^{1}H NMR). Pure (*E*) isomer obtained by recrystallization from absolute ethanol. (*E*) isomer: ^{1}H NMR (600 MHz, CDCl$_3$) δ 7.50 – 7.47 (m, 2H), 7.41 – 7.33 (m, 6H), 7.28 – 7.24 (m, 1H), 6.82 (s, 1H), 2.25 (d, *J* = 1.3 Hz, 3H). ^{13}C NMR (151 MHz, CDCl$_3$) δ 143.0, 138.1, 136.4, 131.5, 129.3, 128.4, 128.3, 127.8, 126.8, 121.2, 17.5. EI HRMS calculated for C$_{15}$H$_{13}$Br (M)$^+$: 272.0201 found: 272.0195.
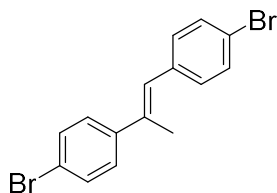
7g 4,4'-(prop-1-ene-1,2-diyl)bis(bromobenzene). 86% yield. White solid. 4.5:1 (*E*):(*Z*) ratio (determined by ^{1}H NMR). Pure (*E*) isomer obtained by recrystallization from absolute ethanol. (*E*) isomer: ^{1}H NMR (600 MHz,

CDCl₃) δ 7.50 (d, J = 8.2 Hz, 2H), 7.49 (d, J = 8.6 Hz, 2H), 7.37 (d, J = 8.6 Hz, 2H), 7.21 (d, J = 8.2 Hz, 2H), 6.73 (s, 1H), 2.22 (d, J = 1.1 Hz, 3H). ^{13}C NMR (151 MHz, CDCl₃) δ 142.6, 137.3, 137.0, 131.6, 131.5, 130.9, 127.8, 127.1, 121.5, 120.7, 17.5. EI HRMS calculated for $C_{15}H_{12}Br_2$ (M)$^+$: 349.9306 found 349.9300.
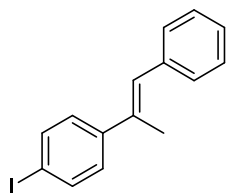
7h 1-iodo-4-(1-phenylprop-1-en-2-yl)benzene: Reaction performed as 1.25 M in water. 90% yield. White solid. 2.3:1 (E):(Z) mixture (determined by ^{1}H NMR). Pure (E) isomer obtained by recrystallization from absolute ethanol. (E) isomer: ^{1}H NMR (600 MHz, CDCl₃) δ 7.69 (d, J = 8.6 Hz, 2zH), 7.41 – 7.33 (m, 4H), 7.28 - 7.24 (m, 3H), 6.83 (s, 1H), 2.25 (d, J = 1.2 Hz, 3H). ^{13}C NMR (151 MHz, CDCl₃) δ 143.6, 138.1, 137.5, 136.5, 129.3, 128.4, 128.1, 126.9, 92.7, 17.4. EI HRMS calculated for $C_{15}H_{13}I$ (M)$^+$: 320.0062 found: 320.0063.
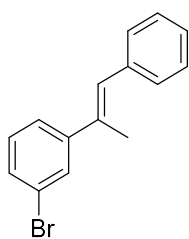
7i 1-bromo-3-(1-phenylprop-1-en-2-yl)benzene: 92% yield. White solid. 2.5:1 (E):(Z) mixture (determined by ^{1}H NMR). Pure (E) isomer obtained by recrystallization from absolute ethanol. (E) isomer: ^{1}H NMR (600 MHz, CDCl₃) δ 7.67 (s, 1H), 7.45 (d, J = 7.8 Hz, 1H), 7.42 (d, J = 8.0 Hz, 1H), 7.40 - 7.34 7.38 (m, 4H), 7.29 - 7.22 (m, 2H), 2.26 (s, 3H). ^{13}C NMR (151 MHz, CDCl₃) δ 146.3, 138.0, 136.2, 130.2, 130.0, 129.3, 128.9, 128.4, 126.9, 124.8, 122.7, 17.6. EI HRMS calculated for $C_{15}H_{13}Br$ (M)$^+$: 272.0201 found 272.0195.

Representative two-step procedure for synthesis of allyl azides 10a-e

α-methylstilbene (1.60 mmol, 1.00 eq.) **7a** was dissolved in 15 mL of benzene in a round bottom flask charged with a stirbar. Then N-bromosuccinimide (1.80 mmol, 1.1 eq.) and benzoyl peroxide (0.017 mmol, 0.01 eq.) were added to the solution. Next, the reaction was stirred at 70 °C for 5 hours until TLC (100% hexanes) indicated complete conversion of the starting material. The reaction was allowed

to cool to room temperature prior to quenching with sodium thiosulfate and concentration *in vacuo*. The crude oil was then filtered through a plug of silica, eluting with 100% hexanes. Concentration of the eluent gives the intermediate allyl bromide[(3-bromoprop-1-ene-1,2-diyl)dibenzene] as a yellow oil in 86% yield as a 1:2 (*E*):(*Z*) mixture (by ^{1}H NMR), which can be stored in the freezer but was typically immediately used in the next step. The allyl bromide (1.40 mmol, 1.00 eq.) was dissolved in 4 mL of acetonitrile in a round bottom flask, to which was added sodium azide (4.20 mmol, 3.00 eq.). The flask was sealed and the mixture was allowed to stir at room temperature overnight, or until TLC demonstrated completed consumption of the starting material. The acetonitrile was removed *in vacuo*, and the resulting slurry was partitioned between ethyl acetate and water. The aqueous phase was extracted with ethyl acetate (3 x 10 mL) and the combined organic layers were dried over sodium sulfate and concentrated to give azide **10a** in 93% yield as a clear, light yellow oil. Note: the intermediate bromides and azides **10** are distinguishable both by Rf (TLC: neat hexanes or 3% EtOAc in hexanes), as well as the fact that the azides invariably stain yellow with vanillin stain and heating (bromide spot is unaffected).
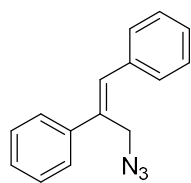
10a (3-azidoprop-1-ene-1,2-diyl)dibenzene. 80% two-step yield. Light yellow oil. Inseparable 1:2 (*E*):(*Z*) mixture (determined by ^{1}H NMR). (*Z*) isomer: ^{1}H NMR (600 MHz, CDCl$_3$) δ: 7.59 – 7.55 (m, 2H), 7.45 – 7.12 (m, 8H), 4.41 (s, 2H). ^{13}C NMR: peaks from (*E*):(*Z*) isomers are not reliably distinguishable. EI HRMS calculated for C$_{15}$H$_{13}$N$_3$ (M)$^+$: 235.1109 found 235.1114.
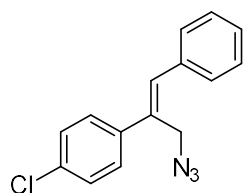
10b 1-(3-azido-1-phenylprop-1-en-2-yl)-4-chlorobenzene. Light yellow oil. 69% two-step yield. Inseparable 2:3 (*E*):(*Z*) mixture (determined by ^{1}H NMR). (*Z*) Isomer: ^{1}H NMR (700 MHz, CDCl$_3$) δ 7.50 (dd, *J* = 8.5, 1.9 Hz, 2H), 7.43 (t, *J*

= 7.4 Hz, 2H), 7.40 (dd, J = 8.5, 1.8 Hz, 2H), 7.37 – 7.33 (m, 3H), 7.12 (s, 1H), 4.38 (d, J = 1.3 Hz, 2H). ^{13}C NMR: peaks from (E):(Z) isomers are not reliably distinguishable. EI HRMS calculated for $C_{15}H_{12}ClN_3$ (M)$^+$: 269.0720 found 269.0719.
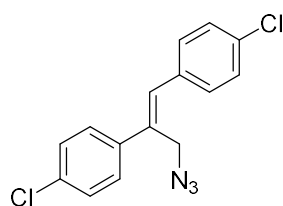
10c 4,4'-(3-azidoprop-1-ene-1,2-diyl)bis(chlorobenzene). 68% yield two-step yield. Light yellow oil. Inseparable 4:5 (E):(Z) mixture (determined by ^{1}H NMR). (Z) Isomer: ^{1}H NMR (700 MHz, CDCl$_3$) δ 7.48 (d, J = 8.7 Hz, 2H), 7.42 - 7.38 (m, 4H), 7.28 (d, J = 8.2 Hz, 2H), 7.04 (s, 1H), 4.34 (s, 2H). ^{13}C NMR: peaks from (E):(Z) isomers are not reliably distinguishable. EI HRMS calculated for $C_{15}H_{11}Cl_2N_3$ (M)$^+$: 303.0330 found 303.0330.
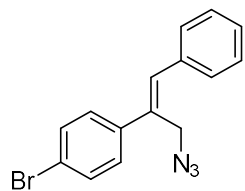
10d 1-(3-azido-1-phenylprop-1-en-2-yl)-4-bromobenzene. 76% two-step yield. Light yellow oil. Inseparable 2:3 (E):(Z) mixture (determined by ^{1}H NMR). (Z) Isomer: ^{1}H NMR (700 MHz, CDCl$_3$) δ 7.55 (d, J = 8.6 Hz, 2H), 7.11 - 7.45 (8H, Ar), 4.37 (s, 2H). ^{13}C NMR: peaks from (E):(Z) isomers are not reliably distinguishable. EI HRMS calculated for $C_{15}H_{12}BrN_3$ (M)$^+$: 313.0215 found 313.0222.
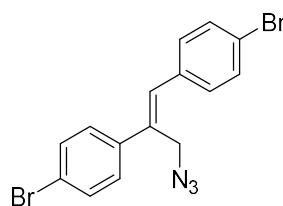
10e 4,4'-(3-azidoprop-1-ene-1,2-diyl)bis(chlorobenzene). 71% two-step yield. Off-white resin. Inseparable 1:2 (E):(Z) mixture (determined by ^{1}H NMR). (Z) Isomer: ^{1}H NMR (700 MHz, CDCl$_3$) δ 7.57 – 7.53 (m, 4H), 7.41 (d, J = 8.7 Hz, 2H), 7.21 (d, J = 8.3 Hz, 2H), 7.01 (s, 1H), 4.32 (s, 2H). ^{13}C NMR: peaks from (E):(Z) isomers are not reliably distinguishable. EI HRMS calculated for $C_{15}H_{11}Br_2N_3$ (M)$^+$: 390.9320 found 390.9308.

Representative synthesis of protected triazoles 11/12 a-e

10a (0.023 g, 0.10 mmol, 1.0 Eq) (1:2 E/Z) was dissolved in 0.25 mL THF and placed in a round bottom flask charged with a stir bar. Then CuI (1.9 mg, 0.01 mmol, 0.1 eq.), 2,6-lutidine (4.6 µL, 0.04 mmol, 0.4 eq.), acetic acid (2.3 µL, 0.04 mmol, 0.4 eq.) and TMS-acetylene (0.055 mL, 0.4 mmol, 4 Eq) was added the flask. The mixture was allowed to stir for 24 hours at 50 °C. TLC (20% EtOAc in hexanes) demonstrated the disappearance of starting material and the appearance of two product spots. The THF was removed *in vacuo* and the crude mixture was purified via silica gel chromatography (0-25% EtOAc in hexanes). 12.7 mg of the (E) isomer (**11a**) and to 12.4 mg of the (Z) isomer (**12a**) were isolated and characterized separately for a total yield of 80%.
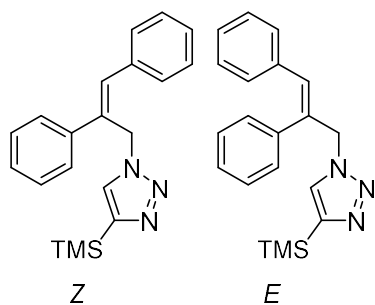
11/12 a 1-(2,3-diphenylallyl)-1H-1,2,3-triazole. 80% combined yield. White solids. **11a (E)**: ^{1}H NMR (600 MHz, CDCl$_3$) δ 7.39 (s, 1H), 7.29 – 7.27 (m, 3H), 7.14 – 7.11 (m, 3H), 7.08 – 7.06 (m, 2H), 6.99 – 6.96 (m, 2H), 6.58 (s, 1H), 5.36 (d, J = 0.7 Hz, 2H), 0.29 (s, 9H). ^{13}C NMR (151 MHz, CDCl$_3$) δ 146.7, 137.6, 136.1, 135.6, 130.9, 129.5, 129.1, 128.7, 128.2, 128.2, 127.7, 57.7, -1.0. ESI HRMS calculated for C$_{20}$H$_{24}$N$_3$Si (M+H)$^+$: 334.1740 found: 334.1739. **12a (Z)**: ^{1}H NMR (600 MHz, CDCl$_3$) δ 7.45 – 7.43 (m, 2H), 7.42 – 7.39 (m, 4H), 7.37 – 7.32 (m, 3H), 7.32 – 7.28 (m, 1H), 7.28 (s, 1H), 7.20 (s, 1H), 5.62 (s, 2H), 0.23 (s, 9H). ^{13}C NMR (151 MHz, CDCl$_3$) δ 146.4, 139.6, 136.2, 134.5, 134.3, 129.0, 129.0, 128.9, 128.8, 128.4, 128.2, 126.5, 49.1, -1.0. ESI HRMS calculated for C$_{20}$H$_{24}$N$_3$Si (M+H)$^+$: 334.1740 found: 334.1742.

Z   E
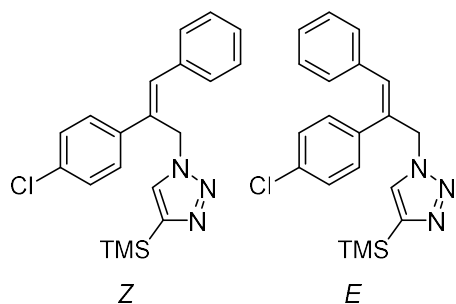
11/12 b 1-(2-(4-chlorophenyl)-3-phenylallyl)-4-(trimethylsilyl)-1H-1,2,3-triazole. 75% combined yield. White solids. **11b (*E*)**: ^{1}H NMR (600 MHz, CDCl$_3$) δ 7.41 (s, 1H), 7.24 (d, *J* = 8.4 Hz, 2H), 7.17 – 7.13 (m, 3H), 6.96-7.01 (m, 4H), 6.61 (s, 1H), 5.33 (s, 2H), 0.28 (s, 9H). ^{13}C NMR (151 MHz, CDCl$_3$) δ 147.2, 136.1, 135.4, 135.1, 134.2, 131.7, 130.3, 129.6, 129.4, 129.3, 128.5, 128.0, 57.4, -0.9. ESI HRMS calculated for C$_{20}$H$_{23}$ClN$_3$Si (M+H)$^+$: 368.1344 found 368.1351. **12b (*Z*)**: ^{1}H NMR (600 MHz, CDCl$_3$) δ 7.44 – 7.38 (m, 5H), 7.37 – 7.34 (m, 2H), 7.31 (d, *J* = 8.5 Hz, 2H), 7.26 (s, 1H), 7.18 (s, 1H), 5.58 (s, 2H), 0.24 (s, 9H). ^{13}C NMR (151 MHz, CDCl$_3$) δ 146.8, 137.9, 136.0, 134.6, 134.6, 134.3, 133.6, 129.1, 129.0, 128.9, 128.6, 128.3, 127.8, 48.8, -1.0. ESI HRMS calculated for C$_{20}$H$_{23}$ClN$_3$Si (M+H)$^+$: 368.1344 found 368.1336.

Z   E
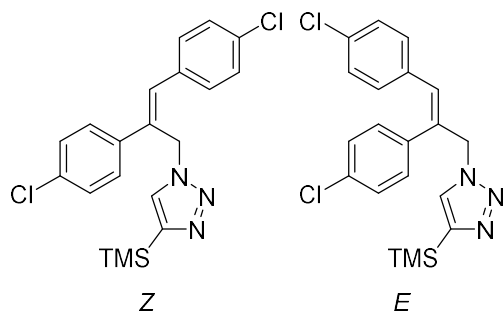
11/12 c 1-(2,3-bis(4-chlorophenyl)allyl)-4-(trimethylsilyl)-1H-1,2,3-triazole. 70% combined yield. White solids. **11c (*E*)**: ^{1}H NMR (600 MHz, CDCl$_3$) δ 7.39 (s, 1H), 7.25 (d, *J* = 8.3 Hz, 2H), 7.11 (d, *J* = 8.5 Hz, 2H), 6.98 (d, *J* = 8.4 Hz, 2H), 6.89 (d, *J* = 8.4 Hz, 2H), 6.53 (s, 1H), 5.32 (s, 2H), 0.28 (s, 9H). ^{13}C NMR (151 MHz, CDCl$_3$) δ 147.1, 135.8, 135.6, 134.4, 133.8, 133.7, 130.7, 130.1, 130.1, 129.5, 129.3, 128.6, 57.1, -1.0. ESI HRMS calculated for C$_{20}$H$_{22}$Cl$_2$N$_3$Si (M+H)$^+$: 402.0955 found 402.0952. **12c (*Z*)**: ^{1}H NMR (600 MHz, CDCl$_3$) δ 7.41 – 7.35 (m, 4H), 7.35 (d, *J* = 8.5 Hz, 2H), 7.31 (d, *J* = 8.5 Hz, 2H), 7.24 (s, 1H), 7.07 (s, 1H), 5.52 (s, 2H), 0.24 (s, 9H). ^{13}C NMR (151 MHz, CDCl$_3$) δ 146.9, 137.8, 134.5, 134.4, 134.3, 133.3, 130.3, 129.2, 129.2, 128.7, 127.9, 48.8, -1.0. ESI HRMS calculated for C$_{20}$H$_{22}$Cl$_2$N$_3$Si (M+H)$^+$: 402.0955 found 402.0945.

Z   E
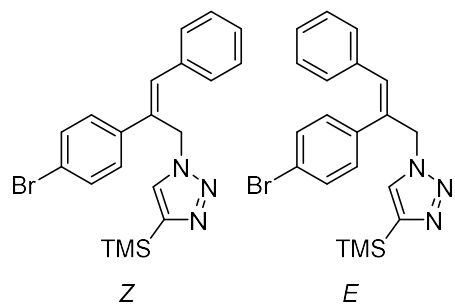
11/12 d 1-(2-(4-bromophenyl)-3-phenylallyl)-4-(trimethylsilyl)-1H-1,2,3-triazole. 73% combined yield. White solids. **11d (E)**: ^{1}H NMR (600 MHz, CDCl$_3$) δ 7.41 (s, 1H), 7.39 (d, J = 8.4 Hz, 2H), 7.16 – 7.13 (m, 3H), 7.00 – 6.97 (m, 2H), 6.93 (d, J = 8.4 Hz, 2H), 6.62 (s, 1H), 5.33 (s, 2H), 0.29 (s, 9H). ^{13}C NMR (151 MHz, CDCl$_3$) δ 147.1, 136.4, 135.3, 134.9, 132.3, 131.6, 130.5, 129.5, 129.3, 128.4, 128.0, 122.3, 57.3, -1.0. ESI HRMS calculated for C$_{20}$H$_{23}$BrN$_3$Si (M+H)$^+$: 412.0839 found 412.0836. **12d (Z)**: ^{1}H NMR (600 MHz, CDCl$_3$) δ 7.46 (d, J = 8.5 Hz, 2H), 7.42 – 7.39 (m, 4H), 7.37 - 7.33 (m, 1H), 7.31 (d, J = 8.5 Hz, 2H), 7.26 (s, 1H), 7.18 (s, 1H), 5.57 (s, 2H), 0.24 (s, 9H). ^{13}C NMR (151 MHz, CDCl$_3$) δ 146.8, 138.4, 135.9, 134.6, 133.7, 132.1, 129.0, 128.8, 128.6, 128.4, 128.1, 122.4, 48.7, -1.0. ESI HRMS calculated for C$_{20}$H$_{23}$BrN$_3$Si (M+H)$^+$: 412.0839 found 412.0835.

Z   E
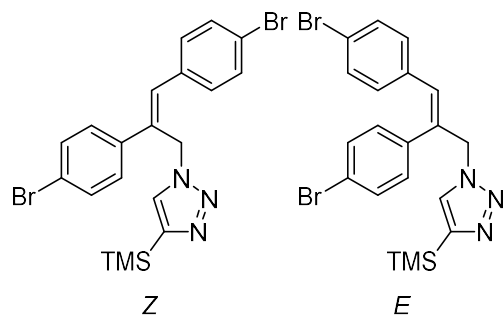
11/12 e 1-(2,3-bis(4-bromophenyl)allyl)-4-(trimethylsilyl)-1H-1,2,3-triazole. 60% combined yield. White solids. **11e (E)**: ^{1}H NMR (600 MHz, CDCl$_3$) δ 7.41 (d, J = 8.4 Hz, 2H), 7.39 (s, 1H), 7.27 (d, J = 8.4 Hz, 2H), 6.91 (d, J = 8.4 Hz, 2H), 6.83 (d, J = 8.4 Hz, 2H), 6.50 (s, 1H), 5.31 (s, 2H), 0.28 (s, 9H). ^{13}C NMR (151 MHz, CDCl$_3$) δ 147.2, 136.0, 135.9, 134.2, 132.5, 131.6, 131.0, 130.3, 130.1, 129.3, 122.6, 122.0, 57.0, -1.0. ESI HRMS calculated for C$_{20}$H$_{22}$Br$_2$N$_3$Si (M+H)$^+$: 489.9944 found 489.9939. **12e (Z)**: ^{1}H NMR (600 MHz, CDCl$_3$) δ 7.54 (d, J = 8.3 Hz, 2H), 7.47 (d, J = 8.5 Hz, 2H), 7.31 (d, J = 8.2 Hz, 2H), 7.28 (d, J = 8.5 Hz, 2H), 7.24 (s, 1H), 7.05 (s, 1H), 5.51 (s, 2H), 0.24 (s, 9H). ^{13}C NMR (151 MHz, CDCl$_3$) δ 146.9, 138.3, 134.8, 134.5, 133.3, 132.2, 132.1, 130.5, 128.7, 128.2, 122.7, 122.5, 48.7, -1.0. ESI HRMS calculated for C$_{20}$H$_{22}$Br$_2$N$_3$Si (M+H)$^+$: 489.9944 found 489.9941.

Representative synthesis of deprotected triazoles 5/6 a-e

Deprotection of triazoles **11** or **12** could be performed separately but typically resulted in partial (*E*):(*Z*) isomerization, thus necessitating the chromatographic separation of resultant triazoles **5** and **6**. Therefore, the protected triazoles **11** and **12** were typically combined and deprotected together, using the following method: In a round bottom flask, an approximately 1:1 mixture of **11/12** (78 mg, 0.23 mmol, 1 Eq) was dissolved in 0.8 mL THF. Then, 1 M tetrabutylammonium fluoride in THF was added (0.69 mL, 0.69 mmol, 3 Eq), and the reaction mixture was heated at 45-50°C for 18 hours. The crude mixture was concentrated *in vacuo*, and the resulting residue was purified via silica gel chromatography (0-80% EtOAc in hexanes). The desired fractions for the separate (*E*) and (*Z*) isomers were collected and concentrated *in vacuo* to yield 33 mg of the (*E*) isomer **(5)** and 23 mg of the (*Z*) isomer **(6)**, both as off-white powdery solids, for a total yield of 90%.
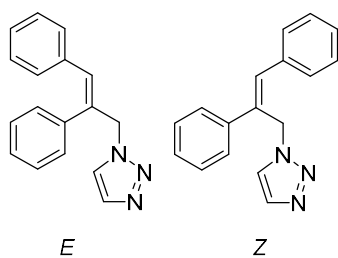
5/6a 1-(2,3-diphenylallyl)-1H-1,2,3-triazole. White solids. 90% combined yield. **5a (*E*)**: ^{1}H NMR (600 MHz, CDCl$_3$) δ 7.64 (s, 1H), 7.45 (s, 1H), 7.29 – 7.26 (m, 3H), 7.14 – 7.11 (m, 3H), 7.10 – 7.07 (m, 2H), 7.00 – 6.97 (m, 2H), 6.65 (s, 1H), 5.38 (d, J = 0.8 Hz, 2H). ^{13}C NMR (151 MHz, CDCl$_3$) δ 137.3, 135.8, 135.5, 134.0, 131.3, 129.5, 129.1, 128.7, 128.2, 127.7, 123.7, 58.2. ESI HRMS calculated for C$_{17}$H$_{16}$N$_3$ (M+H)$^+$:262.1344, found: 262.1353. **6a (*Z*)**: ^{1}H NMR (600 MHz, CDCl$_3$) δ 7.57 (d, J = 0.7 Hz, 1H), 7.46 – 7.39 (m, 5H), 7.37 – 7.32 (m, 4H), 7.31 – 7.28 (m, 1H), 7.22 (s, 1H), 5.63 (s, 2H). ^{13}C NMR (151 MHz, CDCl$_3$) δ 139.3, 136.1, 134.5, 134.3, 133.9, 129.0, 128.8, 128.5, 128.2, 126.5, 123.3, 49.3. HRMS calculated for C$_{17}$H$_{16}$N$_3$ (M+H)$^+$: 262.1344, found: 262.1341.
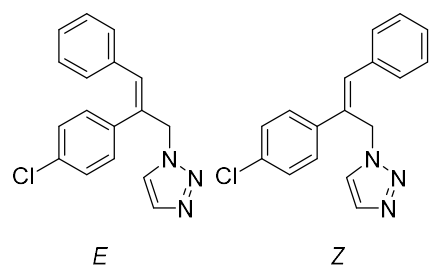
5/6b   1-(2-(4-chlorophenyl)-3-phenylallyl)-1H-1,2,3-triazole. White solids. 81% combined yield. **5b (Z)**: ^{1}H NMR (700 MHz, CD$_2$Cl$_2$) δ 7.61 (s, 1H), 7.52 (s, 1H), 7.25 (d, J = 8.4 Hz, 2H), 7.17 – 7.14 (m, 3H), 7.04 – 6.99 (m, 4H), 6.72 (s, 1H), 5.35 (s, 2H). ^{13}C NMR (176 MHz, CD$_2$Cl$_2$) δ 136.2, 135.7, 135.3, 134.2, 132.1, 130.6, 129.7, 129.48, 128.6, 128.1, 58.1. ESI HRMS calculated for C$_{17}$H$_{14}$ClN$_3$Na (M+Na)$^+$: 318.0768 found 318.0769. **6b (E)**: ^{1}H NMR (600 MHz, CD$_2$Cl$_2$) δ 7.54 (s, 1H), 7.45 – 7.42 (m, 4H), 7.42 – 7.38 (m, 3H), 7.38 – 7.34 (m, 1H), 7.32 (d, J = 8.6 Hz, 2H), 7.21 (s, 1H), 5.60 (s, 2H). ^{13}C NMR (176 MHz, CD$_2$Cl$_2$) δ 138.2, 136.3, 134.9, 134.3, 133.9, 133.9, 129.2, 129.2, 129.1, 128.5, 128.2, 123.7, 49.4. ESI HRMS calculated for C$_{17}$H$_{15}$ClN$_3$ (M+H)$^+$: 296.0949 found 296.0948.
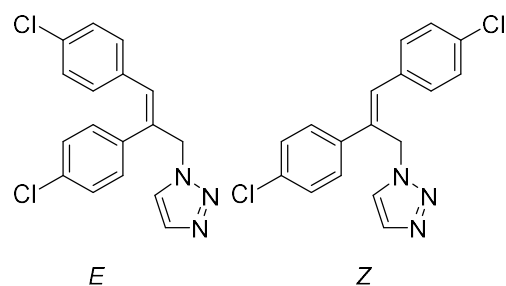
5/6c   (2,3-bis(4-chlorophenyl)allyl)-1H-1,2,3-triazole. White solids. 77% combined yield. **5c (E)**: ^{1}H NMR (600 MHz, CD$_2$Cl$_2$) δ 7.61 (s, 1H), 7.50 (s, 1H), 7.26 (d, J = 8.3 Hz, 2H), 7.13 (d, J = 8.5 Hz, 2H), 7.01 (d, J = 8.4 Hz, 2H), 6.94 (d, J = 8.5 Hz, 2H), 6.65 (s, 1H), 5.34 (s, 2H). ^{13}C NMR (176 MHz, CD$_2$Cl$_2$) δ 136.2, 135.8, 134.5, 134.3, 134.2, 133.8, 131.0, 130.7, 130.5, 129.6, 128.7, 124.1, 57.9. ESI HRMS calculated for C$_{17}$H$_{14}$Cl$_2$N$_3$ (M+H)$^+$: 330.0559 found 330.0558. **6c (Z)**: ^{1}H NMR (600 MHz, CD$_2$Cl$_2$) δ 7.54 (s, 1H), 7.43 – 7.36 (m, 7H), 7.32 (d, J = 8.7 Hz, 2H), 7.12 (s, 1H), 5.55 (s, 2H). ^{13}C NMR (151 MHz, CD$_2$Cl$_2$) δ 138.0, 134.8, 134.7, 134.5, 134.4, 134.0, 133.6, 130.6, 129.4, 129.3, 128.3, 123.8, 49.3. ESI HRMS calculated for C$_{17}$H$_{14}$Cl$_2$N$_3$ (M+H)$^+$: 330.0559 found 330.0557.
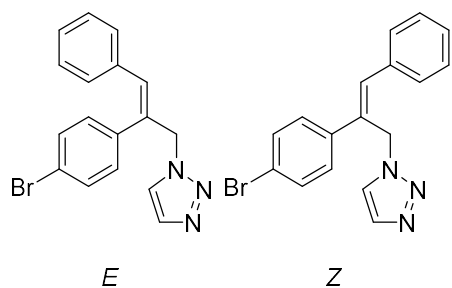
5/6d 1-(2-(4-bromophenyl)-3-phenylallyl)-1H-1,2,3-triazole. White solids. 79% combined yield. **5d (*E*)**: ^{1}H NMR (700 MHz, CDCl$_3$) δ 7.66 (s, 1H), 7.45 (s, 1H), 7.39 (d, *J* = 8.3 Hz, 2H), 7.18 – 7.15 (m, 3H), 7.00 – 6.97 (m, 2H), 6.94 (d, *J* = 8.3 Hz, 2H), 6.70 (s, 1H), 5.35 (s, 2H). ^{13}C NMR (176 MHz, CDCl$_3$) δ 136.1, 135.2, 134.6, 134.2, 132.4, 132.1, 130.4, 129.5, 128.4, 128.1, 123.6, 122.4, 57.9. ESI HRMS calculated for C$_{17}$H$_{14}$BrN$_3$Na (M+Na)[+]: 362.0263 found 362.0255. **6d (Z)**: ^{1}H NMR (700 MHz, CD$_2$Cl$_2$) δ 7.54 (d, *J* = 0.7 Hz, 1H), 7.48 (d, *J* = 8.6 Hz, 2H), 7.44 – 7.42 (m, 4H), 7.39 (d, *J* = 0.7 Hz, 1H), 7.38 – 7.35 (m, 1H), 7.34 (d, *J* = 8.6 Hz, 2H), 7.21 (s, 1H), 5.59 (s, 2H). ^{13}C NMR (176 MHz, CD$_2$Cl$_2$) δ 138.6, 136.3, 135.0, 134.0, 134.0, 132.3, 132.2, 129.2, 129.1, 128.5, 123.7, 122.5, 49.3. ESI HRMS calculated for C$_{17}$H$_{15}$BrN$_3$ (M+H)[+]: 340.0444 found 340.0446.
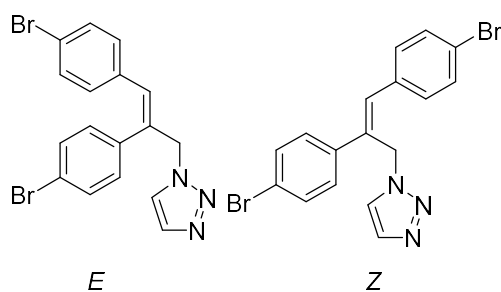
5/6e 1-(2,3-bis(4-bromophenyl)allyl)-1H-1,2,3-triazole. White solids. 75% combined yield. **5e (*E*)**: ^{1}H NMR (600 MHz, CDCl$_3$) δ 7.66 (s, 1H), 7.44 (s, 1H), 7.40 (d, *J* = 8.4 Hz, 2H), 7.27 (d, *J* = 8.5 Hz, 2H), 6.92 (d, *J* = 8.4 Hz, 2H), 6.83 (d, *J* = 8.5 Hz, 2H), 6.58 (s, 1H), 5.33 (s, 2H). ^{13}C NMR (151 MHz, CDCl$_3$) δ 135.7, 135.6, 134.2, 134.1, 132.5, 131.6, 130.9, 130.6, 130.3, 123.8, 122.8, 122.1, 57.7. ESI HRMS calculated for C$_{17}$H$_{13}$Br$_2$N$_3$ (M+H)[+]: 417.9549 found 417.9550. **6e (Z)**: ^{1}H NMR (600 MHz, CDCl$_3$) δ 7.59 (s, 1H), 7.55 (d, *J* = 8.4 Hz, 2H), 7.46 (d, *J* = 8.4 Hz, 2H), 7.32 (s, 1H), 7.31 (d, *J* = 8.5 Hz, 2H), 7.29 – 7.27 (m, 2H), 7.07 (s, 1H), 5.54 (s, 2H). ^{13}C NMR (151 MHz, CDCl$_3$) δ 138.0, 134.7, 134.3, 134.1, 133.5, 132.2, 132.2, 130.5, 128.2, 123.4, 122.8, 122.6, 49.1. ESI HRMS calculated for C$_{17}$H$_{13}$Br$_2$N$_3$ (M+H)[+]: 417.9549 found 417.9544.

Synthesis of hydrogenated triazole stilbene 13

A 1:1 (*E*):(*Z*) mixture of **11/12 a** (0.060 g, 0.180 mmol, 1 Eq) was dissolved in 0.75 mL of MeOH and placed in a vial charged with a stirbar. The mixture was sonicated for 5 minutes to allow for the stilbene to completely dissolve. Then, 0.25 mL of Raney Nickel (1:1 in water) was added to the mixture. The reaction vessel was sealed and the heterogeneous mixture was allowed to stir vigorously for 24 hours. The mixture was filtered through celite, the celite was washed with 10 mL of THF, and the combined organic fractions were collected and concentrated *in vacuo* to yield 56 mg of a waxy cream coloured solid (93%). The hydrogenated product (0.030 g, 0.089 mmol, 1 Eq) was dissolved in 0.3 mL of THF and added to a vial. Then, 0.27 mL of tetrabutylammonium fluoride (1 M in THF, 0.27 mM, 3 Eq) was added and the vial was sealed. The mixture was heated with stirring for 24 hours at 45 °C. The reaction was quenched with saturated ammonium chloride solution, and the mixture was extracted three times with dichloromethane (3 x mL). The combined organic layers were dried over sodium sulfate and concentrated *in vacuo*. The resulting yellow oil was purified via silica gel chromatography (0-50% EtOAc in hexanes) yielding 20 mg of a white amorphous solid (86% yield; 80% over two steps from **11/12 a**).
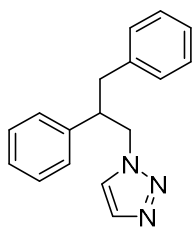
13 1-(2,3-diphenylpropyl)-1H-1,2,3-triazole. White solid. ^{1}H NMR (600 MHz, CDCl$_3$) δ 7.50 (s, 1H), 7.26 – 7.20 (m, 5H), 7.17 (t, *J* = 7.3 Hz, 1H), 7.09 (d, *J* = 7.0 Hz, 2H), 7.03 (d, *J* = 7.0 Hz, 2H), 6.99 (s, 1H), 4.71 (dd, *J* = 13.7, 5.8 Hz, 1H), 4.49 (dd, *J* = 13.7, 8.7 Hz, 1H), 3.54 – 3.47 (m, 1H), 3.04 (dd, *J* = 13.6, 7.4 Hz, 1H), 3.00 (dd, *J* = 13.6, 7.3 Hz, 1H). ^{13}C NMR (151 MHz, CDCl$_3$) δ 140.6, 138.7, 133.3, 129.2, 128.9, 128.6, 127.8, 127.5, 126.6, 124.1, 55.0, 48.7, 39.8. ESI HRMS calculated for C$_{17}$H$_{18}$N$_3$ (M+H)[+]: 264.1501 found: 264.1508.

Synthesis of hydrogenated 1,2,4-triazole stilbenes 14 and 15

To a small vial with a stir bar was added NaH (0.008 g, 0.33 mmol, 2.0 Eq; previously washed with hexanes) and 0.3 mL THF. Then, 1,2,4-triazole (0.023 g, 0.33 mmol, 2.0 Eq) was added in small portions, resulting in the immediate formation of hydrogen gas. The mixture was allowed to stir at room temperature for 20 minutes before the addition of 1-bromo-2,3-diphenylpropene (prepared from **9a** using NBS as described above; 0.045 g, 0.165 mmol, 1.0 Eq.) in 0.3 mL THF. The reaction was stirred at room temperature for 2.5 days. The reaction was quenched with the addition of 2 mL water and 1 mL EtOAc. The organic layer was collected, and the aqueous layer was extracted with EtOAc (3 x 2mL). The combined organic layers were washed with brine (2 mL) and dried over sodium sulphate before concentration *in vacuo*. The crude residue was purified using silica gel chromatography (20-80% EtOAc in hexanes) and the desired fractions were concentrated to give 8 mg of **14** and **16** mg of **15** for a combined yield of 56%.

E   *Z*
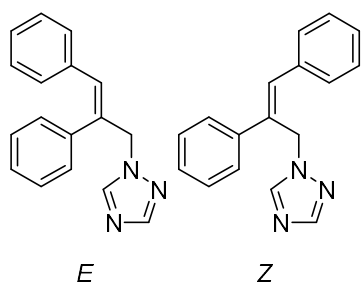
14/15 1-(2,3-diphenylallyl)-1H-1,2,4-triazole. White solids. 56% combined yield. **14 (*E*)**: ^{1}H NMR (600 MHz, CD$_2$Cl$_2$) δ 7.90 (s, 1H), 7.85 (s, 1H), 7.30 – 7.27 (m, 3H), 7.14 – 7.10 (m, 3H), 7.06 (dd, J = 6.5, 2.9 Hz, 2H), 7.00 - 6.97 (m, 2H), 6.65 (s, 1H), 5.13 (s, 2H). ^{13}C NMR (151 MHz, CD$_2$Cl$_2$) δ 152.2, 143.9, 138.0, 136.7, 136.1, 131.1, 129.7, 129.3, 128.9, 128.4, 128.3, 127.8, 58.1. ESI HRMS calculated for C$_{17}$H$_{16}$N$_3$ (M+H)$^+$: 262.1339 found 262.1345. **15 (*Z*)** ^{1}H NMR (600 MHz, CD$_2$Cl$_2$) δ 7.89 (s, 1H), 7.83 (s, 1H), 7.48 – 7.40 (m, 6H), 7.38 – 7.29 (m, 4H), 7.19 (s, 1H), 5.38 (s, 2H). ^{13}C NMR (151 MHz, CD$_2$Cl$_2$) δ 152.1, 143.5, 139.9, 136.7, 134.9, 134.5, 129.2, 129.1, 128.6, 128.3, 126.8, 49.3. ESI HRMS calculated for C$_{17}$H$_{16}$N$_3$ (M+H)$^+$: 262.1339 found 262.1339.

Aromatase Assay

The velocity of biotransformation of fluorogenic substrates by cytochrome P450 19A1 was determined by fluorescence intensity assays. Reactions were carried out at 37 °C in black, 96-well plates (Costar) in a final volume of 200 µL containing (final concentrations): potassium phosphate buffer pH 7.4 (0.15 M), NADP (330 µM), glucose-6-phosphate (830 µM), $MgCl_2$ (845 µM), glucose-6-phosphate dehydrogenase (70–75 mU/well), the substrate DBF (0.248 µM), and test compounds in DMSO (1%), and were started by the addition of the CYP19 enzyme (0.364 pmol/well). To compensate for solvent effects on enzyme activities, 1% DMSO was present in all control wells. The incubation time after the addition of CYP19 was of 1 h and then the reaction was stopped by adding 75 µL of 2 M NaOH to each well. The plate was incubated for an additional 2 h at 37 °C to improve the signal-to-noise ratio of the assay (Stresser *et al.*, *Anal. Biochem.*, **2000**, *284*, 427-430). In all cases, the duration of the incubation and the enzyme concentration were in the linear range of metabolite formation. Fluorescence was measured using a Biotek Synergy H4 Hybrid Reader at an excitation wavelength of 485 nm and an emission wavelength of 535 nm. Fluorescein (5 pmol/well) was used as the standard and ketoconazole (99 µM) was used as a fully inhibited enzyme blank.

2.6 References

1) R. L. Siegel, K. D. Miller, A. Jemal, *CA. Cancer J. Clin.* **2017**, *67*, 7.

2) C. E. DeSantis, J. Ma, A. Goding Sauer, L. A. Newman, A. Jemal, *CA. Cancer J. Clin.* **2017**, *67*, 439.

3) R. T. Chlebowski, *Clin. Breast Cancer* **2013**, *13*, 159.

4) C. L. Shapiro, A. Recht, *N. Engl. J. Med.* **2001**, *344*, 1997.

5) J. M. Binkley, S. R. Harris, P. K. Levangie, M. Pearl, J. Guglielmino, V. Kraus, D. Rowden, *Cancer* **2012**, *118*, 2207.

6) S. R. D. Johnston, M. Dowsett, *Nat. Rev. Cancer* **2003**, *3*, 821.

7) E. Y. Lasfargues, W. G. Coutinho, E. S. Redfield, *JNCI J. Natl. Cancer Inst.* **1978**, *61*, 967.

8) H. D. Soule, J. Vazquez, A. Long, S. Albert, M. Brennan, *JNCI J. Natl. Cancer Inst.* **1973**, *51*, 1409.

9) I. Keydar, L. Chen, S. Karby, F. R. Weiss, J. Delarea, M. Radu, S. Chaitcik, H. J. Brenner, *Eur. J. Cancer* **1979**, *15*, 659.

10) I. Holen, V. Speirs, B. Morrissey, K. Blyth, *Dis. Model. Mech.* **2017**, *10*, 359.

11) E. E. Sweeney, R. E. McDaniel, P. Y. Maximov, P. Fan, V. C. Jordan, *Horm. Mol. Biol. Clin. Investig.* **2012**, *9*, 143.

12) S. Hole, A. M. Pedersen, S. K. Hansen, J. Lundqvist, C. W. Yde, A. E. Lykkesfeldt, *Int. J. Oncol.* **2015**, *46*, 1481.

13) M. Dowsett, *Endocr. Relat. Cancer* **1999**, *6*, 181.

14) C. J. Fabian, *Int. J. Clin. Pract.* **2007**, *61*, 2051.

3 Wittig Synthesis and Applications of Alkenyl Phenols

3.1 Alkenyl phenols are common motifs in synthetic and biosynthetic processes

Alkenyl phenols are a common motif in many classes of natural products including curcuminoids, stilbenes, lignans, and polyketides.[1–5] The diverse array of natural products containing alkenyl phenols demonstrate a range of biological effects including anti-inflammatory, anti-viral, anti-proliferative, anti-oxidant and radical scavenging capabilities. The innate reactivity of alkenyl phenols also makes them common precursors for more complex natural products. For example, homolignols such as coniferyl and coumaryl alcohol are the biosynthetic precursors of lignan natural products and the structural biopolymer lignin.[6–9] As well, stilbene natural products often co-occur with oligostilbenoids.[2,10] In both cases, structurally complex natural products are produced via oxidative couplings enabled by the alkenyl phenol functionality.

An important property of alkenyl phenols is their propensity to form quinone methides (QMs). QMs are reactive Michael acceptors that are transiently formed and consumed in many biological processes, such as the sclerotization of insect cuticles and eumelanin biosynthesis.[11–13] They react with biologically relevant nucleophiles including DNA, and their *in vivo* formation is likely responsible for the cytotoxic activity of many phenolic chemotherapeutics.[14,15] In nature, alkenyl phenols are usually converted to QMs via oxidative processes, but they also readily form QMs under acidic conditions via addition of a proton to the electron rich alkene (Figure 3.1). As such, alkenyl phenols can be considered the enol tautomer of QMs with a strongly pH dependent equilibrium.
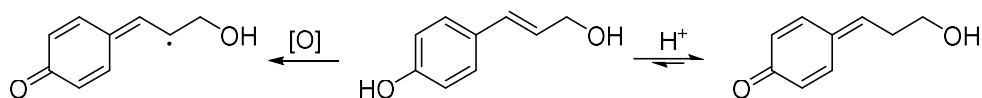
FIGURE 3.1 Alkenyl phenols readily generate QMs under both oxidative and acidic conditions.

Despite their ubiquity in biosynthesis, QMs were relatively unexplored by synthetic chemists for decades as they were considered too reactive and short-lived for practical use; a 2002 review on *o*-QMs deemed them "outside the synthetic mainstream."[16] Since then, QMs have been the subject of extensive research, appearing in numerous methodologies and total syntheses.[17–32] By 2014, a review deemed them "tamed" and "domesticated".[33] Unsurprisingly, alkenyl phenols are a common entry point to QMs under both oxidative and acidic conditions.

The oxidative dimerization of alkenyl phenols has been used in several biomimetic syntheses of natural products. For example, the dimerization of isoeugenol by hypervalent iodine was used to prepare dehydrodiisoeugenol, also known as licarin A, in 35% yield as the key intermediate in the synthesis of benzofuranoid neolignans from *Myristica fragrans* (Figure 3.2, A).[34] Interestingly, the conversion of isoeugenol to licarin A using $FeCl_3$ was reported as early as 1933 and gives the product in similar yield.[35,36] Other benzofuranoids have been prepared from alkenyl phenols using stoichiometric oxidants such as ceric ammonium nitrate or silver oxide.[37,38] Conceptually similar syntheses of resveratrol dimers and tetramers have been achieved using $FeCp_2PF_6$ with protected resveratrol derivatives (Figure 3.2, B).[39,40]
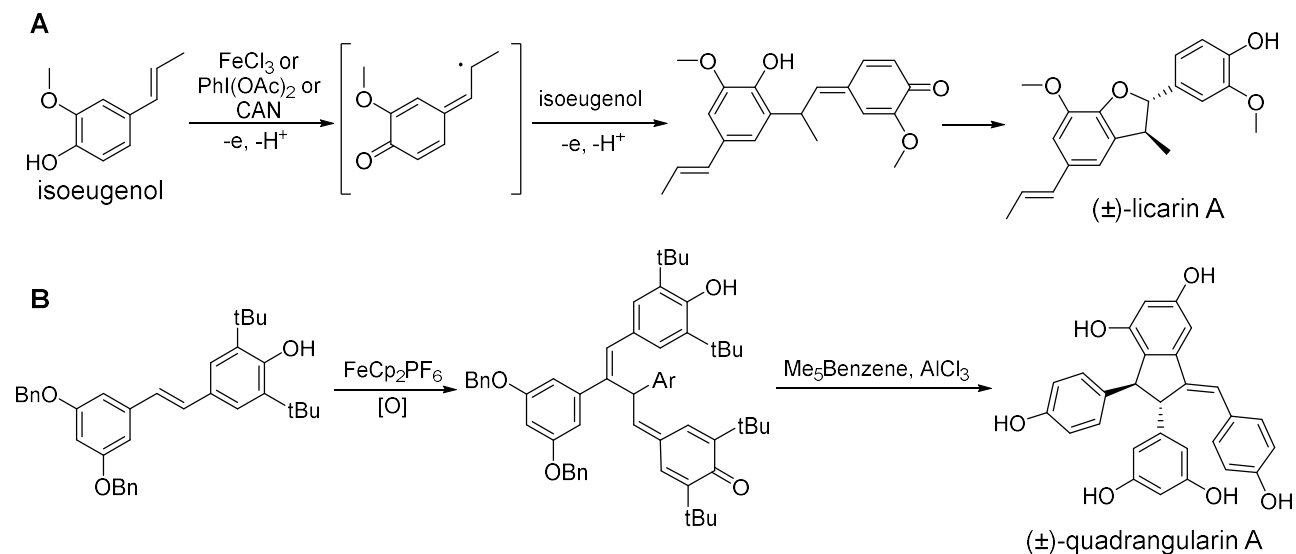
FIGURE 3.2 Some biomimetic syntheses of natural products via oxidation of alkenyl phenols.

A body of work has shown that Pd(II) salts effectively catalyze the formation of *o*-QMs from

o-alkenyl phenols under oxidative conditions.[41] Interestingly, the synthetic utility of this approach was

first demonstrated in Chapman *et al.*'s elegant one-step synthesis of carpanone in 46% yield from l-

propenyl-4,5-methylenedioxyphenol using stoichiometric PdCl$_2$ (Fig 3.3, A).[42] However, the generality

of the reaction was unproven until the work by the Sigman group over three decades later. In their

initial work, Pd(MeCN)$_2$Cl$_2$ was used to oxidatively dimethoxylate alkenyl phenols, with methanol

acting as both solvent and nucleophile.[43] Significantly, no reaction occurred when the formation of a

quinone methide was prevented, for example by methylating the phenol. Later works expanded the

scope of these methods to include intramolecular cyclizations with pendant alcohols or amines and

replace the alcoholic nucleophiles with electron rich heterocycles (Figure 3.3, B).[44–47]
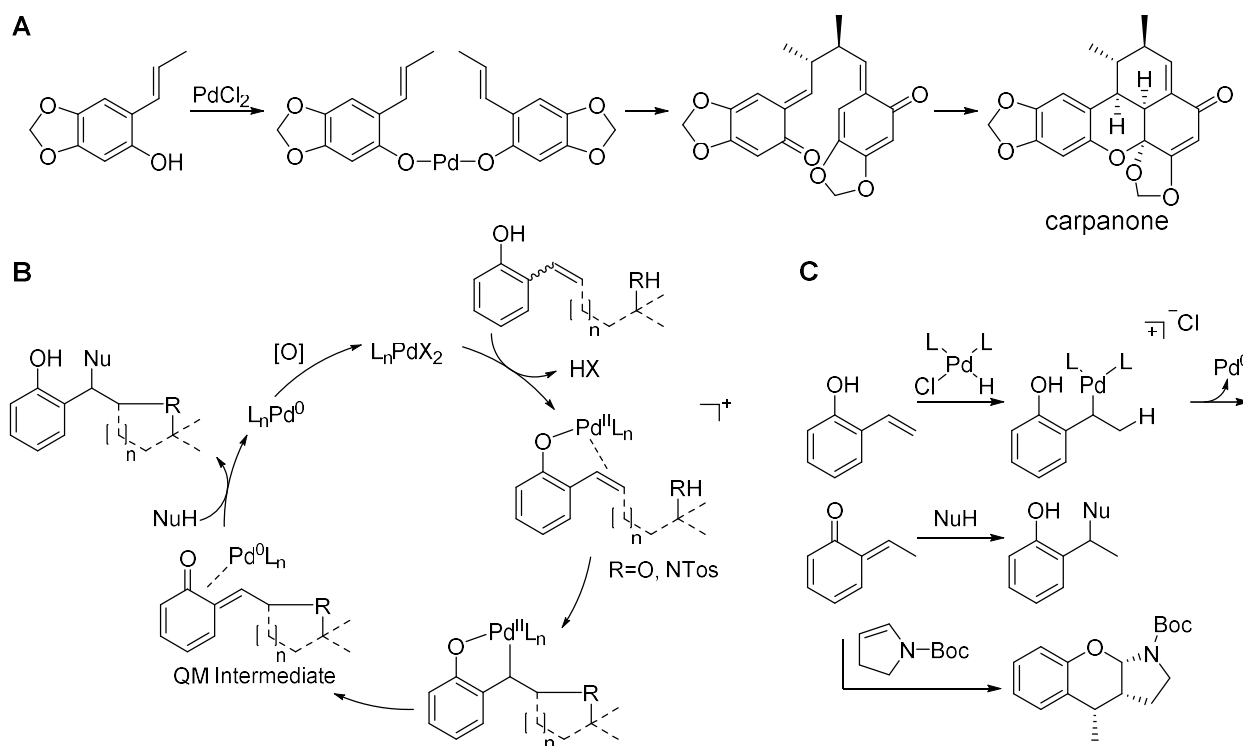
FIGURE 3.3 Generation of *o*-quinone methides from *o*-alkenyl phenols using Pd(II). Although this concept was first shown in Chapman *et al.*'s synthesis of carpanone (A), general methods for palladium catalyzed difunctionalization (B) and hydrofunctionalization (C) of *o*-alkenyl phenols weren't developed until work by the Sigman group decades later.

The Sigman group also found that *in situ* generation of a palladium hydride species, for example by the β-hydride elimination of 1-chlorobutane, allowed for Markovnikov addition of various nucleophiles across the double bond in an overall oxidatively neutral process (Figure 3.3, C).[48–50] As well, several inverse electron demand Diels-Alder reactions were developed, wherein electron rich enol ethers were used to trap the QM intermediates. Importantly, the use of chiral ligands such as (*S*)-*i*Pr-Quinox allowed the above processes to be performed with substantial enantiocontrol.[44–47,51]

More recently, alkenyl phenols have emerged as useful substrates for generating QMs under organocatalytic conditions. For example, both *p*- and *o*-alkenyl phenols have been used as 2π components in asymmetric inverse electron demand Diels-Alder (Povarov) cyclizations (Figure 3.4).[52–55] The formation of a reactive iminium species is catalyzed by a chiral phosphoric acid (CPA) and allows attack by the alkenyl phenol with concurrent formation of a QM. A subsequent intramolecular Friedel-Crafts alkylation on the reactive QM generates the piperidine core. The CPA is thought to coordinate to both iminium and phenol group, and high enantioselectivity was possible for both *o*-
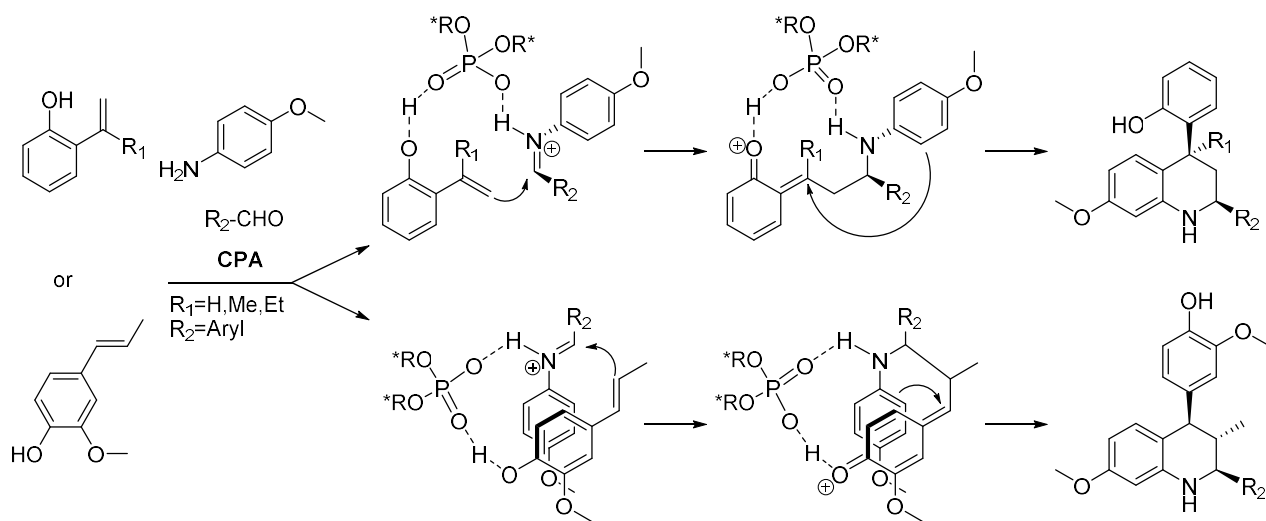
FIGURE 3.4 Participation of alkenyl phenols in CPA catalyzed Povarov cyclizations. Both *o* and *p*-alkenylphenols have been used to trap iminium species formed by CPAs *in situ*, resulting in asymmetric inverse electron demand Diels-Alder reactions.
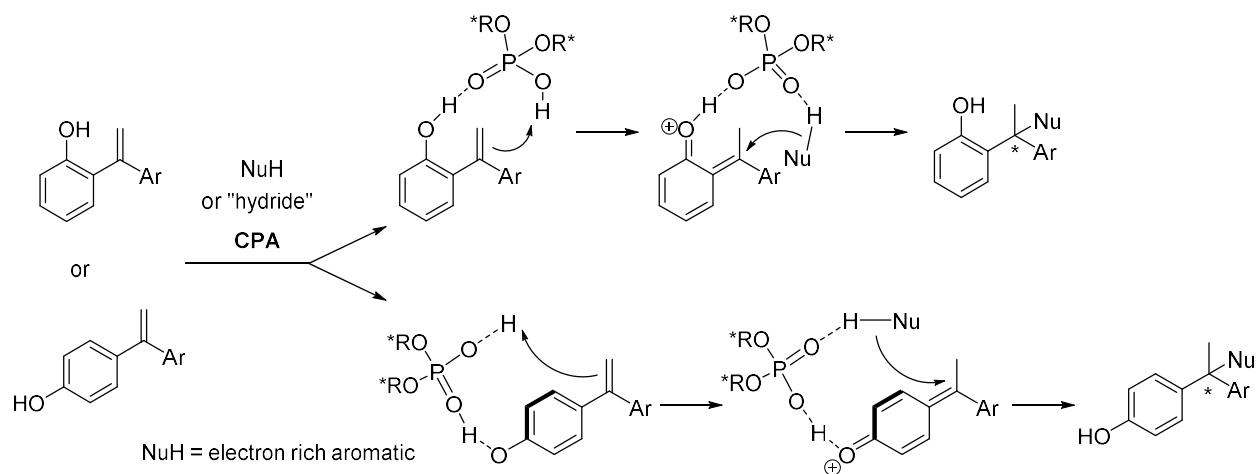
FIGURE 3.5 CPA catalyzed hydrofunctionalization of alkenyl phenols. Both *o* and *p*-alkenylphenols have been converted to QMs by CPAs *in situ*, with subsequent trapping of the QM intermediate by electron rich aromatics or hydride provided by a Hantzsch ester.

and *p*-alkenyl phenols. A mechanism invoking a quinone methide is supported by the fact that methylating the substrate phenol leads to no or trace product formation, since the analogous methyl ether can not be converted to a quinone methide.

In other reports, phosphoric acid catalysts have been used to directly protonate/tautomerize alkenyl phenols, with high enantioselectivity possible with the use of CPAs.[31,56–59] The resultant QM's could be reacted with various nucleophiles, with electron rich aromatics being the most common (Figure 3.5). The asymmetric reduction of the QM intermediates using Hantzsch ester has also been reported. Interestingly, in one of the control experiments wherein a benzylic alcohol was used instead of the alkene moiety, the *e.e.* was significantly reduced despite proceeding through a similar proposed mechanism.[58] This highlights the synthetic advantages alkenyl phenols can provide in the development of asymmetric synthetic methods.

Despite their growing recognition as synthetically useful substrates, there are relatively few ways to prepare alkenyl phenols without the use of protecting groups. The innate reactivity of many alkenyl phenols makes them incompatible under a range of synthetic conditions. For example, early

attempts to prepare *p*-vinylphenol noted that it readily polymerized in air even at 0 °C, and that this process was promoted by even trace amounts of acid.[60,61] As well, in methods using protecting groups, the substrate and product sensitivity can also result in low yields in otherwise straightforward deprotections. Nevertheless, a handful of relatively simple alkenyl phenols can be prepared from commercially available starting materials. For example, propenylphenols are readily obtained by the thermal isomerization of allyl phenols with KO*t*Bu, or using various transition metals under inert atmosphere.[62] As well, a simple entry to homolignols or vinylphenols is provided by the respective hydride reduction or decarboxylation of the corresponding cinnamic acids.[63–67] Unfortunately, these methods are often limited to commercially available or naturally abundant substrates and do not provide general access to the alkenyl phenol functionality.

Phenolic stilbenes can be prepared by transition metal catalyzed cross-couplings, in particular the palladium catalyzed Mizoroki-Heck reaction between styrenes and halogenated phenols or between vinyl phenols and aryl halides. Unfortunately, yields on the cross coupling tend to be low (30-60%) and require harsh conditions, e.g. heating in triethanolamine at 100 °C for 24 hours.[68,69] The difficulties associated with accessing phenolic stilbenes is highlighted in a recent paper focusing on the synthesis of resveratrol via Mizoroki-Heck reaction; even after extensive optimization, resveratrol was only obtained in 77% yield when accounting for necessary deprotection of the phenols.[70] As well, methods that use vinyl phenols typically prepare them using low-yielding Wittig reactions (*vide infra*), and there are relatively few cases that provide access to *o*-hydroxystilbenes[69,71] Rhodium (III) catalyzed cross-couplings provide better access to *o*-alkenyl phenols; a 2013 report details the C-H activations of directing group protected phenols and their coupling with various conjugated olefins, and a 2014 paper describes the coupling of *o*-hydroxystyrenes with aryl boronic acids. [72,73] However, the same methods cannot be used to provide *m* and *p*-alkenyl phenols. Thus, transition metal catalyzed cross-couplings also fail to provide general access to alkenyl phenols.

It is worth noting that synthetically useful alkenyl phenols and phenolic stilbenes are also difficult to access using the Wittig reaction, despite its pre-eminence in olefin synthesis. Numerous phenolic aldehydes are readily available and would seem an obvious substrate for Wittig olefinations leading to alkenyl phenols. However, the basic conditions of the Wittig reaction results in deprotonation of the phenol and electronic deactivation of the aldehyde to attack by the ylide. This can be partially overcome by using large excesses of unhindered ylides. Vinyl phenols, substrates for the Mizoroki-Heck reactions used to produce phenolic stilbenes, are often prepared in yields around 60-70% from the respective aldehydes via Wittig reactions with 2.5 – 3.0 equivalents of methyltriphenylphosphonium iodide.[68,69] More complicated alkenyl phenols are not typically prepared using the Wittig reaction because issues with atom economy and yield are compounded by poor (E):(Z) selectivity.[74] Many syntheses of phenolic stilbenes are known wherein the phenols are protected prior to the Wittig and deprotected after, but yields in the deprotection step are often disappointing.[71,75–77]

Given the ubiquity of alkenyl phenols in natural products, their growing use in asymmetric synthesis, and the difficulty in directly accessing these compounds, the McNulty group decided to develop a highly stereoselective, protecting group free Wittig methodology for their synthesis. This work is described below, and a manuscript is in preparation. A. J. Nielsen developed the method and synthesized compounds with the assistance of W. J. Lin, who was a thesis student under his supervision, and D. McLeod offered expertise on phosphonium salt preparation and insight to reaction optimization.

3.2 One-pot, protecting group free synthesis of hydroxy stilbenes and alkenyl phenols

Previous successes by the McNulty group in the development of Wittig methodologies using trialykylphosphine-derived ylides, inspired the exploration of a protecting group free synthesis of alkenyl phenols using a Wittig protocol. There are two obvious disconnections for accessing the desired compounds. The first involves the reaction of relatively common phosphonium salts with phenolic aldehydes (Scheme 3.1, Route A). However, the phenolic groups present on the aldehydes will be deprotonated under the basic conditions of the Wittig reaction, electronically deactivating the aldehyde groups from attack by the phosphorous ylide. Although there are Wittig reactions reported on phenolic aldehydes, they typically use sterically unhindered non-stabilized ylides (e.g. methyl or ethyltriphenylphosphorane) in excess to obtain the product alkenes in acceptable yields, and (*E*):(*Z*) selectivity is poor.[74]

The second disconnection involves the preparation of phosphonium salts **1** featuring free phenol groups and exploring their reactions with various aldehydes (Scheme 3.1, Route B). The use of trialkylphosphine instead of triphenylphosphine derived salts should confer high (*E*) selectivity and simplify purification, and the resulting phosphine oxide would be readily water soluble. Unclear in this route is whether the ylides of these phosphonium salts would be readily generated; at least two equivalents of base would be necessary, the first being consumed via deprotonation of the phenol. Indeed, in a previous Wittig synthesis of hydroxystilbenes using protected phosphonium salts similar
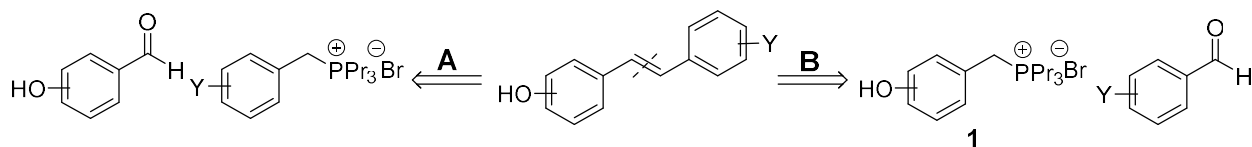
SCHEME 3.1 Retrosynthetic analysis of alkenyl phenols and hydroxystilbenes. There are two obvious disconnections using the Wittig reaction; Route A involves the use of common phosphonium salts on phenolic aldehydes, while Route B uses unusual phosphonium salts **1** with a free phenol and variably functionalized aldehydes.
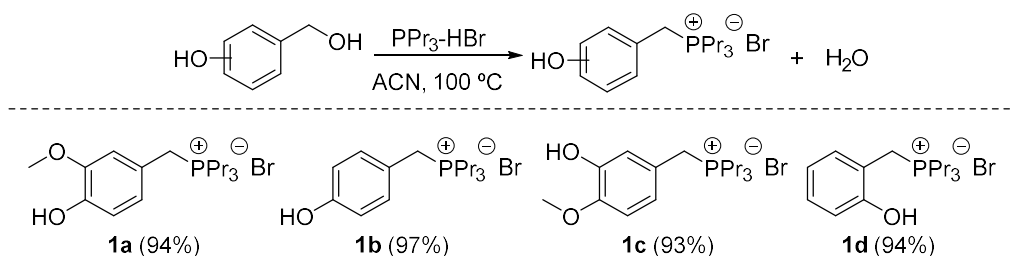
SCHEME 3.2 Synthesis of phenolic phosphonium salts **1**. The salts were obtained in excellent yields directly from commercially available hydroxybenzyl alcohols by heating with tripropylphosphine-HBr.

to **1**, it was argued that it would not be possible to generate the ylide from salts with free phenols in the *ortho* or *para* position since resonance from the corresponding phenolate anions would deactivate the benzylic position to deprotonation.[75] As well, there was concern about the possibility of these salts decomposing under basic conditions via elimination of the phosphine and formation of a quinone methide. Nevertheless, the known issues associated with Route A prompted exploration of Route B.

It was found that phosphonium salts **1** with substitution of a phenol at either the *o*, *m*, or *p* position were readily prepared using a method previously reported by the McNulty group in the synthesis of pterostilbene.[78] Simply heating a concentrated mixture of readily available hydroxybenzyl alcohols and tripropyl phosphine-HBr overnight in acetonitrile gave the salts **1** in effectively quantitative yields (Scheme 3.2). In all cases, pure product could be obtained by removing the solvent *in vacuo* followed by trituration with a small amount of diethyl ether or ethyl acetate. Of note, the reaction producing salt **1d** proceeded slower and seemed to retain more water than the other reactions, possibly because water can be trapped by hydrogen bonding between the phenol and benzyl alcohol or phosphonium groups.

A thorough search of the literature proved concerns about the decomposition of salts **1** under basic conditions to be unwarranted. The preparation of salt **1a** in 57% yield was previously reported by Moiseev *et al.*, who generated QMs via the thermal dehydration of *o*- and *p*-hydroxybenzyl alcohols and trapped them with various trialkylphosphines, giving phosphobetaines (Figure 3.6).[79]
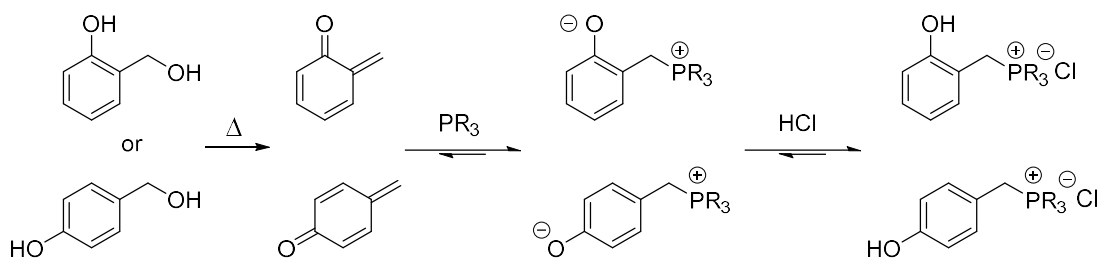
FIGURE 3.6 Thermal generation of phosphobetaines from hydroxybenzyl alcohols. Previous work by Moiseev *et al.* demonstrates that the decomposition of phosphobetaines to phosphines and QMs is unfavorable.[79]

Subsequent treatment with HCl produced the phosphonium salts in yields ranging from 56-96%. Thus, the equilibrium of free phosphine and QM versus phosphobetaine clearly favors the latter even at elevated temperatures, and deprotonation of salts **1** should not result in the formation of substantial amounts of free phosphine. It is worth noting that this method cannot be used to generate *m*-hydroxy substituted phosphonium salts, since the corresponding benzyl alcohols do not eliminate to form QMs, and the new method of preparing salts **1** is both higher yielding and more general.

Having prepared phenolic phosphonium salts **1a-d** and being convinced of their stability under basic conditions, their use in Wittig reactions using various aromatic aldehydes was explored. Gratifyingly, it was found that using two equivalents of strong base allowed for the double deprotonation of the salts at 0 °C, in direct contrast to previous expectations. The addition of an aromatic aldehyde to these unusual anionic ylides gave the desired phenolic stilbene products **2** in yields consistently around 65-80% and very high (99:1) (*E*):(*Z*) ratio (Table 3.1). Importantly, this reaction worked on salts with phenolic substitution in any position on the aromatic ring. The lowest yield was observed when using 4-nitrobenzaldehyde, as the product stilbene decomposed rapidly decomposed during silica gel chromatography (Table 3.1, Entry 7). Of note, this method allows for a protecting group-free synthesis of the natural product pterostilbene **2i**.

TABLE 3.1 Protecting group free synthesis of phenolic stilbenes **2**

Entry	Salt	Benzaldehyde (Y=)	Product	Yield[a]	(E):(Z)[b]
1	1a	H	2a	71	99:1
2	1a	4-Cl	2b	63	99:1
3	1a	4-Br	2c	75	99:1
4[c]	1a	4-Br	2c	67	99:1
5[d]	1a	4-Br	2c	38	n.d
6	1a	3,4-methylenedioxy	2d	70	99:1
7	1a	4-NO$_2$	2e	25	99:1
8	1b	H	2f	64	99:1
9	1b	4-Cl	2g	64	99:1
10[e]	1b	4-Cl	2g	40	99:1
11	1b	4-Br	2h	75	99:1
12	1b	3,5-dimethoxy	2i	63	99:1
13	1c	4-Br	2j	68	99:1
14	1d	H	2k	79	99:1
15	1d	4-Cl	2l	67	99:1

[a] Isolated yield of spectroscopically pure product. [b] Determined by integration in ^{1}H NMR. [c] NaH used instead of BuLi. [d] Deprotonation performed at -78 °C; crude yield reported. [e] 2.0 equivalents of LiBr were added.

For these reactions *n*-BuLi was chosen for its ready availability and operational ease of use, but other suitably strong bases such as NaH also worked, giving the desired product albeit in slightly lower yield (Table 3.1, Entry 4). Although the reaction worked with a variety of benzaldehydes with excellent stereoselectivity, attempts were made to improve the yield of stilbenes **2**. Performing the reaction -78 °C resulted in a much lower yield of stilbene product (Table 3.1, Entry 5), leading to the consideration that the salts may not be completely deprotonated under these conditions. It was thought that the addition of Lewis acidic lithium bromide might coordinate the phenolate anion, allowing for a more facile deprotonation of the benzylic carbon. Instead, the addition of LiBr also resulted in a much lower yield (Table 3.1, Entry 10) possibly due to ionic screening of the ylide.

Although unable to improve the yield of these reactions, it is worth noting that this one-pot, protecting group-free method is higher yielding and more stereoselective than previously reported methods employing a Wittig reaction followed by deprotection.[71,75,76]

Further work explored the Wittig reaction of phosphonium salts **1** with aliphatic and conjugated aldehydes to give alkenyl phenols **3** and phenolic dienes **4** (Table 3.2). When the reactions were performed at 0 °C, (*E*):(*Z*) ratios were lower than when the same reactions were performed at -78 °C (Table 3.2, Entries 4 and 5, 9 and 10). As well, yields were generally lower than the reactions with aromatic aldehydes, but this is readily explained. An enolizable aldehyde has an approximate pKa of 17 and benzyltriphenylphopshonium bromide has a pKa of 17.4 in DMSO.[80] However, the pKa of the benzylic hydrogens for salts **1** are likely much higher than this because of their conjugation to an

TABLE 3.2 Protecting group free synthesis alkenyl phenols **3** and dienyl phenols **4**

Entry	Salt	Aldehyde (R=)	Temp. (°C)	Product	Yield[a]	(*E*):(*Z*)[b]
1	**1a**	Propanal (-C$_2$H$_5$)	-78	**3a**	58	95:5
2	**1a**	Pentanal (-C$_4$H$_9$)	-78	**3b**	57	95:5
3	**1b**	Propanal (-C$_2$H$_5$)	-78	**3c**	61	95:5
4	**1b**	Pentanal (-C$_4$H$_9$)	-78	**3d**	51	98:2
5	**1b**	Pentanal (-C$_4$H$_9$)	0	**3d**	46	85:15
6	**1d**	Pentanal (C$_4$H$_9$)	-78	**3e**	22	95:5
7	**1a**	(*E*)-hexenal (-HC=CHC$_3$H$_7$)	-78	**4a**	58	95:5
8	**1a**	(*E*)-cinnamaldehyde (-HC=CHC$_6$H$_6$)	0	**4b**	68	99:1
9	**1b**	(*E*)-hexenal (-HC=CHC$_3$H$_7$)	0	**4c**	46	95:5
10	**1b**	(*E*)-hexenal (-HC=CHC$_3$H$_7$)	-78	**4c**	38	98:2

[a] Isolated yield of spectroscopically pure product. [b] Determined by integration in ^{1}H NMR. Dienes are reported as the (*E*):(*Z*) ratio of the newly formed double bond.

electron-rich phenolate anion. This outcome is compounded by the fact that trialkylphosphonium salts are more basic than their triphenyl counterparts due to higher electron density around the phosphorus. The relatively high basicity of the anionic ylides generated from **1** may cause simple acid-base processes to dominate at room temperature, resulting in the formation enolates and enabling non-productive side reactions. This hypothesis is further supported by the fact that cinnamaldehyde, which contains no enolizable protons, gives the desired diphenyl diene in acceptable yields even when performed at 0 °C (Table 3.2, Entry 8). Overall, alkenyl phenols and phenolic dienes of varying chain length could be obtained in yields generally in the range of 40-70% and with (*E*):(*Z*) selectivity at or above 95:5 under optimal conditions.

This work also granted a much better appreciation for the inherent reactivity of some of these electron rich alkenes. While the phenolic stilbenes **2** and diphenyl diene **4b** were stable for months if stored dry, alkenyl phenols **3** decompose within the span of several days at room temperature if not carefully stored under nitrogen. Even storing the samples in the freezer did not prevent degradation if they were sealed under air. An NMR spectrum was taken of alkenyl phenol **3d** after being stored at room temperature for one month revealing only trace amounts of **3d** remaining. From the crude mixture, peaks corresponding to 4-hydroxybenzaldehyde were clearly present, suggesting an ozonolysis-like mechanism of decomposition. The sensitivity of these substrates to air may also play a role in the somewhat lower yields of reactions producing alkenyl phenols **3** and dienes **4**, as rigorous exclusion of air is difficult during standard organic workup and chromatography; if performed on larger scales, vacuum distillation of **3** and **4** may be more appropriate.

Overall, a protecting group-free methodology capable of accessing a variety of conjugated phenols with very high stereoselectivity was developed, and biological and synthetic applications of these products were eagerly explored. The most developed synthetic application is the topic of Chapter 4, wherein alkenyl phenols are used in a novel organocatalytic [2+2] cycloaddition. For biological

applications, stilbenes **2** were deemed to be more suitable candidates as they demonstrated higher stability under biologically relevant conditions. Their potential as anti-viral agents was explored and is discussed in detail in Chapter 3.3.

3.3 Evaluation of hydroxystilbenes for anti-HSV activity in three cell lines

Approximately 60-80% of all people globally have been infected with HSV-1, which results in a life-long latent infection in the dorsal root ganglion with recurrent episodes of active lytic infection.[81,82] The active lytic phase of viral replication is typically associated with the occurrence of open sores on the mucosa and general malaise, but active infections may also occur in the brain, leading to a condition known as herpes simplex encephalitis (HSE).[83,84] HSE is uncommon in immunocompetent individuals, but is much more common in immunocompromised individuals, such as infants and the elderly. HSE is fatal in 70% of cases if left untreated and treatment with high-dose antivirals (e.g. acyclovir) only reduces mortality to 30%, with half of survivors experiencing serious long-term neurological sequelae. Fetal exposures to HSV frequently prove fatal, and neural progenitor cells are highly susceptible to HSV infection.[85–88] Finally, there is growing evidence of etiological links between early HSV-1 infection and later development of diseases associated with cognitive impairment, such as schizophrenia.[89,90]

There are no known vaccines or cures for HSV-1. Acyclovir is frequently and successfully used to suppress the lytic stage of viral infection in mucosal tissues but does not affect the latent infection in the dorsal root ganglion. As well, it is toxic to the kidneys and brain, and the high doses required to treat active infections in the brain can result in renal failure.[91,92] Furthermore, acyclovir administration improves survival rates in neonatal HSE but does not reduce the risk of substantially impaired neurological development.[85,87] Viral resistance to acyclovir treatment is also a growing

concern, particularly in the immunocompromised population, where the rate of resistance is 30 times that of the immunocompetent population.[93,94]

For the most of the duration of this thesis, the McNulty research group had a collaboration with the Stanley Medical Research Institute (SMRI) with a focus on discovering treatments for latent infections in the brain. For the reasons discussed above, there has been substantial effort to discover novel therapeutics that can better treat active HSV infections in the brain and possibly cure the latent viral infection. Many HSV assays are based in non-neural cell lines that may not be accurate predictors of antiviral effect in neural cells. Researchers at the SMRI developed anti-HSV assays in neural progenitor cells (NPCs) and differentiated neurons derived from human induced pluripotent stem cells (hiPSCs) and tested a library of compounds developed by the McNulty group, comparing the assay results in neural tissues with the results from testing in an epithelial cell line (Vero).[95,96] In brief, the three different cell lines were infected with an HSV-1 strain engineered to express enhanced green fluorescent protein and treated with the drugs at 10 or 50 µM after two hours, with fluorescence being measured after 24 hours in NPCs and Vero cells or 48 hours in hiPSC neurons. Acyclovir was used as a positive control. The assay results were published by D'Aiuto *et al.* in the journal *Antiviral Research* with several coauthor contributors from the McNulty group, including the author of this thesis.[96]

Included in the library of compounds tested were a number of the hydroxystilbenes generated using the previously discussed Wittig methodology as well as resveratrol, which can be prepared by the demethylation of **2i** via literature procedure using BBr_3.[97] It was anticipated that these compounds might demonstrate anti-HSV activity, as the antiviral activity of select natural product stilbenes has been widely reported.[98–103] In particular, the effects of resveratrol on HSV infections in several non-neural cell lines have shown it to inhibit viral transcription, protein and DNA synthesis and lead to a rapid albeit transient generation of reactive oxygen species that further inhibit viral replication.[104–106] Topical applications can also reduce the development of herpetic lesions in mouse models.[107,108]
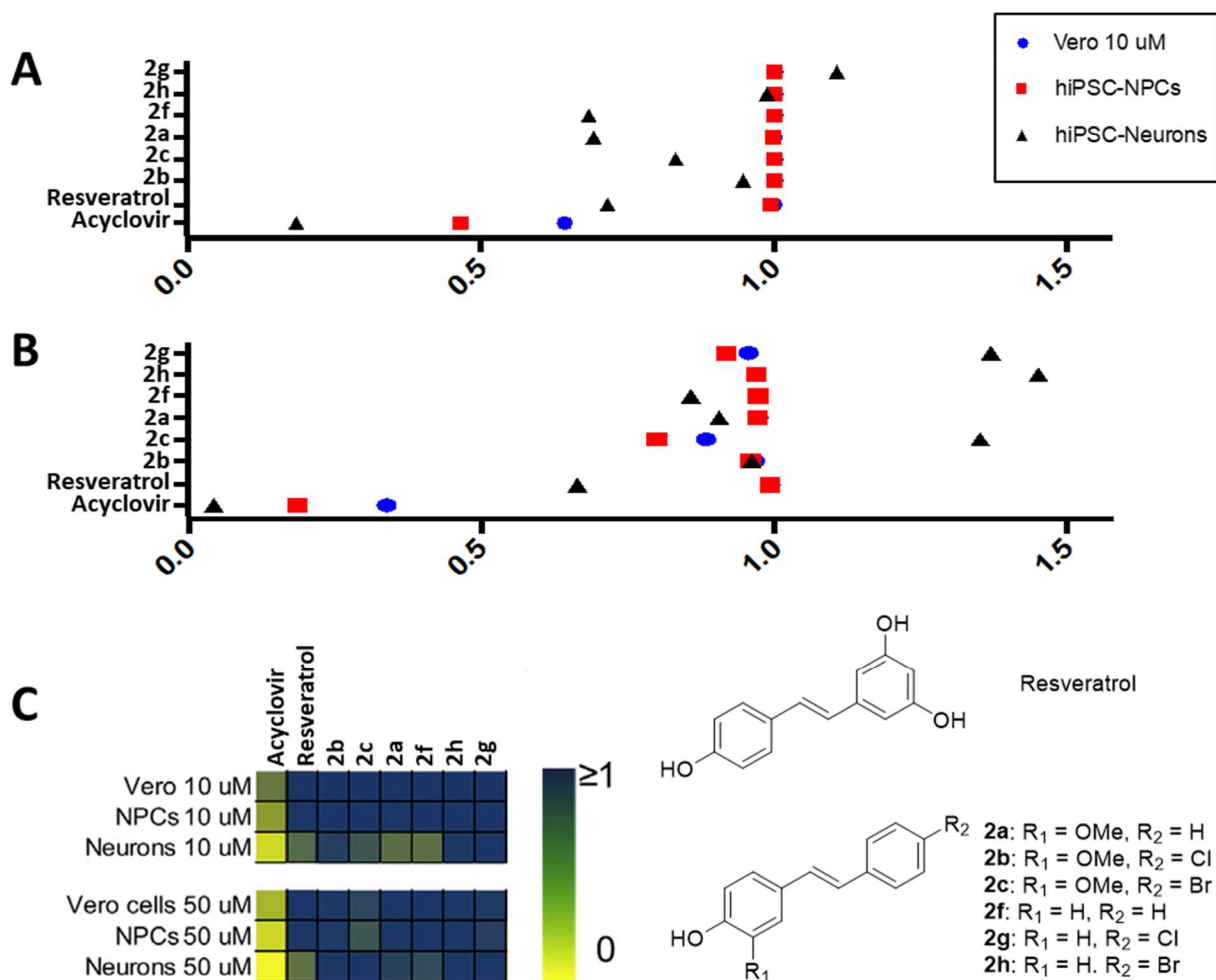
FIGURE 3.7 Effect on HSV-1 viral replication by hydroxystilbenes in three different cell lines. Seven stilbenes were tested in two neural and one epithelial cell line at both 10 μM (A) and 50 μM (B) for effects on HSV proliferation, correlated to the expression of EGFP. X-axis is the relative fluorescence of the treated cells versus an untreated negative control; values near unity imply no effect. Results are summarized in a heatmap (C). Acyclovir is a positive control. Modified from D'Aiuto *et al.*[96]

Interestingly, the assay results did not corroborate those of previous studies which indicated possible antiviral activity of resveratrol and related stilbenes (Figure 3.7, A-C). At both concentrations tested, none of the compounds reduced viral replication by more than 25% in either Vero or NPC lines. While several stilbenes including resveratrol seemed to moderately inhibit it HSV at 10 μM in the neuronal cell line, most of these compounds either had lesser antiviral effect or actually increased viral replication at 50 μM. The antiviral effect of resveratrol increased slightly at 50 μM but still failed to inhibit viral replication to a 50% benchmark.

These findings were surprising, especially for resveratrol which had no effect in Vero and NPC cell lines despite previous studies that reported an anti-HSV effect in the Vero line.[104–106] However, it is known that natural product-like hydroxystilbenes are generally bad drug candidates as they usually have low aqueous solubility, poor target specificity, low potency, are rapidly metabolized, and display pleitropic effects *in vivo*.[109–112] Any or all of these factors may explain the apparently nonsensical stimulation of viral replication at high concentration despite very slight inhibition at low concentration. Indeed, it was never expected that these compounds would be suitable for clinical use. Instead, it was hoped that these results would confirm and expand upon the results of previous studies, providing preliminary SAR and a starting point for the creation of more drug-like molecules. Given the results obtained from these assays, antiviral applications for the alkenyl phenols or stilbenes produced using the previously discussed Wittig methodology are not being pursued.

3.4 Conclusions and future work

A straightforward synthesis of alkenyl phenols, a sensitive but synthetically useful function group, has been developed. Due to disappointing antiviral activities displayed by some of the derivatives prepared using this method, further exploration of biological applications is a low priority. Instead, the exploration of synthetic applications for these alkenyl phenols should be a more fruitful avenue of research. Indeed, some of the derivatives prepared using this method were advantageously used in a novel organocatalytic [2+2] cycloaddition, which is the topic of the following chapter. Current efforts in the McNulty lab are focused on the development of other cyclizations using alkenyl phenols as substrates. The ready formation of reactive quinone methides from alkenyl phenols under both oxidative and acidic conditions is sure to be exploited in future methodologies.

3.5 Experimental

General

All reactions were carried out under nitrogen atmosphere in oven-dried flasks, unless otherwise stated. All fine chemicals were obtained from Sigma Aldrich and used without further purification, except tripropylphosphine which was provided by Solvay Cytec Group. Tetrahydrofuran was distilled over sodium/benzophenone under nitrogen atmosphere. Reactions were monitored using thin layer chromatography (TLC) using Macherey-Nagel silica gel 60 F_{254} TLC aluminum plates and visualized with UV fluorescence and staining with 2,4-dinitrophenylhydrazine or vanillin stains. Bulk solvent removal was performed by rotary evaporation under reduced pressure. For reactions with solvent volumes under 3 mL, the solvent was evaporated under a stream of nitrogen. Column chromatographic purification was performed using Silicycle silica gel (40–63 µM, 230-400 mesh) with technical grade solvents. Yields are reported for spectroscopically pure compounds, unless stated otherwise.

Data Analyses

HRMS (EI) were performed with a Waters GCT and HRMS (ESI) were performed on a Waters QToF Global Ultima spectrometer. ^{1}H and ^{13}C NMR spectra were recorded on a Bruker AV 600 spectrometer in with TMS as internal standard, chemical shifts (δ) are reported in ppm downfield of TMS and coupling constants (J) are expressed in Hz. ^{1}H-decoupled ^{31}P NMR are reported downfield from an external standard of 85% H_3PO_4 in H_2O. (*E*):(*Z*) ratios were determined from the relative integration in the ^{1}H NMR spectra. Melting points are uncorrected.

Preparation of Tripropylphosphine hydrobromide:

Tripropylphosphine (9.60 mL, 48 mmol, 1 eq.) was added to an oven-dried round bottom flask under nitrogen along with a magnetic stir bar. After cooling to 0 °C, aqueous hydrobromic acid (48% w/v, 5.42 mL, 48 mmol, 1 eq.) was added dropwise and the reaction was stirred overnight with gradual warming to room temperature. The mixture was then extracted with dichloromethane (3 x 5 mL) and the combined organic layers were dried over magnesium sulphate and concentrated under reduced pressure to give the desired product. 93% yield (10.7g), fine white powder. ^{1}H NMR (600 MHz, CDCl$_3$) δ 7.60 – 6.73 (hept d, J = 485.9, 5.6 Hz, 1H), 2.37 – 2.30 (m, 6H), 1.66 – 1.57 (m, 6H), 0.98 (td, J = 7.3, 0.9 Hz, 9H); ^{13}C NMR (151 MHz, CDCl$_3$) δ 19.1 (d, J = 46.4 Hz), 16.6 (d, J = 4.5 Hz), 15.1 (d, J = 15.6 Hz); ^{31}P NMR (243 MHz, CDCl$_3$) δ 8.6. All data are in accordance with the literature.[1]

General experimental procedure for the synthesis of benzyl phosphonium salts 1:

Tripropylphosphine hydrobromide (1.0 eq.), benzyl alcohol (1.0 eq.) and acetonitrile (0.1 mL/mmol) were added to an oven-dried vial and sealed under nitrogen. The sealed vials were then heated at 100 °C overnight. The resulting precipitate was washed with diethyl ether or ethyl acetate and then dried under high vacuum to obtain the pure product.

1a (4-hydroxy-3-methoxybenzyl)tripropylphosphonium bromide. 94% yield (1.27 g), white solid. ^{1}H NMR (600 MHz, MeOD$_4$) δ 6.93 (t, J = 2.2 Hz, 1H), 6.84 (d, J = 8.1 Hz, 1H), 6.76 (dt, J = 8.1, 2.5 Hz, 1H), 4.84 (s, 1H), 3.88 (s, 3H), 3.67 (d, J = 14.2 Hz, 2H), 2.21 – 2.13 (m, 6H), 1.65 – 1.55 (m, 6H), 1.10 (td, J = 7.3, 1.7 Hz, 9H); ^{13}C NMR (151 MHz, MeOD$_4$) δ 149.7, 148.2, 123.7 (d, J = 5.5 Hz), 120.2 (d, J = 8.8 Hz), 117.1, 114.4 (d, J = 4.6 Hz), 56.7, 26.8 (d, J = 45.6 Hz), 21.3 (d, J = 47.4 Hz), 16.3 (d, J = 4.4 Hz), 15.8 (d, J = 16.4 Hz); ^{31}P NMR (243 MHz, MeOD$_4$) δ 30.9. M.P. = 199-200 °C (recrystallized from ACN). All data are in agreement with the literature.[2]
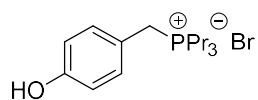
1b (4-hydroxybenzyl)tripropylphosphonium bromide. 97% yield (2.70 g), fine white powder. ^{1}H NMR (600 MHz, MeOD$_4$) δ 7.18 (d, J = 8.4 Hz, 2H), 6.85 (d, J = 8.2 Hz, 2H), 4.83 (s, 1H), 3.68 (d, J = 14.2 Hz, 2H), 2.20 – 2.12 (m, 6H), 1.63 – 1.54 (m, 6H), 1.09 (t, J = 7.2 Hz, 9H); ^{13}C NMR (151 MHz, MeOD$_4$) δ 159.0, 132.2 (d, J = 5.0 Hz), 119.7 (d, J = 8.8 Hz), 117.3, 26.5 (d, J = 45.6 Hz), 21.3 (d, J = 47.2 Hz), 16.3 (d, J = 4.7 Hz), 15.8 (d, J = 16.2 Hz); ^{31}P NMR (243 MHz, MeOD$_4$) δ 30.8. All data are in agreement with the literature.[1]
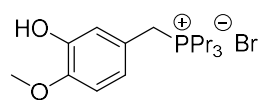
1c (3-hydroxy-4-methoxybenzyl)tripropylphosphonium bromide. 93% yield, white/light yellow powder. ^{1}H NMR (600 MHz, MeOD$_4$) δ 6.97 (d, J = 8.8 Hz, 1H), 6.79 – 6.76 (m, 2H), 4.83 (s, 1H), 3.86 (s, 3H), 3.65 (d, J = 14.4 Hz, 2H), 2.20 – 2.12 (m, 6H), 1.65 – 1.55 (m, 6H), 1.10 (td, J = 7.3, 1.7 Hz, 9H); ^{13}C NMR (151 MHz, MeOD$_4$) δ 149.4, 148.5, 122.3 (d, J = 5.5 Hz), 121.8 (d, J = 8.8 Hz), 117.7 (d, J = 4.5 Hz), 113.4, 56.5, 26.6 (d, J = 45.6 Hz), 21.3 (d, J = 47.1 Hz), 16.3 (d, J = 4.4 Hz), 15.8 (d, J = 16.4 Hz); ^{31}P NMR (243 MHz, MeOD$_4$) δ 31.0. ESI HRMS calculated for C$_{17}$H$_{30}$O$_2$P$^+$ (M-Br⁻) 297.1978, found 297.1988.
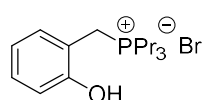
1d (2-hydroxybenzyl)tripropylphosphonium bromide. 94% yield (0.66 g), white solid. ^{1}H NMR (600 MHz, MeOD$_4$) δ 7.26 – 7.20 (m, 2H), 6.93 – 6.87 (m, 2H), 4.85 (s, 1H), 3.66 (d, J = 14.6 Hz, 2H), 2.20 – 2.14 (m, 6H), 1.65 – 1.56 (m, 6H), 1.09 (td, J = 7.3, 1.7 Hz, 9H); ^{13}C NMR (151 MHz, MeOD$_4$) δ 156.9 (d, J = 4.6 Hz), 132.7 (d, J = 5.1 Hz), 131.1 (d, J = 1.8 Hz), 121.3, 116.5, 116.3 (d, J = 8.7 Hz), 22.2 (d, J = 46.9 Hz), 21.9 (d, J = 46.2 Hz), 16.3 (d, J = 4.5 Hz), 15.8 (d, J = 16.7 Hz); ^{31}P NMR (243 MHz, MeOD$_4$) δ 32.0. ESI HRMS calculated for C$_{16}$H$_{28}$OP$^+$ (M-Br⁻) 267.1872, found 267.1885. M.P. = 123-124 °C (recrystallized from ACN).

General experimental procedure for the synthesis of *E*-stilbene derivatives 2:

Benzyl phosphonium salt **1** (1.3 eq.) was dissolved in dry THF (1.2 mL/mmol) in an oven-dried two-necked round bottom flask along with a magnetic stir bar. The flask was purged and sealed under nitrogen to maintain an anhydrous and oxygen free environment. After cooling to 0 °C, *n*-butyl lithium (1.6 M in hexanes, 2.6 eq.) was added dropwise and the reaction was stirred for 40 minutes before the dropwise addition of functionalized benzaldehyde (1.0 eq.) in dry THF (0.8 mL/mmol). The solution was maintained at 0 °C for 30 minutes prior to warming to room temperature, and the reaction was stirred until complete consumption of the aldehyde was observed by TLC (typically overnight). Then, the reaction was quenched via dropwise addition of 0.1 N HCl. The crude reaction mixture was then extracted with ethyl acetate (3 x 5 mL for ½ mmol scale), and the combined organic extracts were dried over magnesium sulphate, filtered, and concentrated under reduced pressure. The crude product was purified by silica gel column chromatography to yield the (*E*)-stilbene **2**.
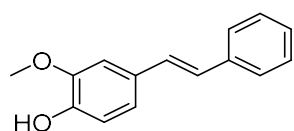
2a (*E*)-2-methoxy-4-styrylphenol. 71% yield (62 mg), colourless crystalline plates, 99:1 (*E*):(*Z*). ^{1}H NMR (600 MHz, CDCl$_3$) δ 7.49 (d, *J* = 7.3 Hz, 2H), 7.35 (t, *J* = 7.7 Hz, 2H), 7.24 (t, *J* = 7.4 Hz, 1H), 7.07 – 7.01 (m, 3H), 6.96 (d, *J* = 16.3 Hz, 1H), 6.91 (d, *J* = 8.1 Hz, 1H), 5.65 (s, 1H), 3.96 (s, 3H); ^{13}C NMR (151 MHz, CDCl$_3$) δ 146.8, 145.7, 137.7, 130.2, 128.8, 127.4, 126.7, 126.4, 120.6, 114.7, 108.4, 56.1; ESI HRMS calculated for C$_{15}$H$_{13}$O$_2$ (M-H$^+$)$^-$ 225.0916, found 225.0922. M.P. = 123-125 °C (recrystallized from EtOH).
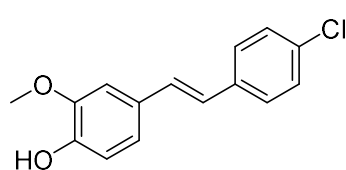
2b (*E*)-4-(4-chlorostyryl)-2-methoxyphenol. 63% yield (63 mg), off-white crystalline solid, 99:1 (*E*):(*Z*). ^{1}H NMR (600 MHz, CDCl$_3$) δ 7.41 (d, *J* = 8.5 Hz, 2H), 7.31 (d, *J* = 8.5 Hz, 2H), 7.05 – 6.97 (m, 3H), 6.93 – 6.87 (m, 2H), 5.70 (s, 1H), 3.95 (s, 3H); ^{13}C NMR (151 MHz, CDCl$_3$) δ 146.9, 145.9, 136.2, 132.9,

129.8, 129.4, 128.9, 127.5, 125.3, 120.7, 114.7, 108.4, 56.1; ESI HRMS calculated for $C_{15}H_{12}O_2{}^{35}Cl$ (M-H$^+$)$^-$ 259.0526, found 259.0526. M.P. = 116-117 °C (recrystallized from EtOH)
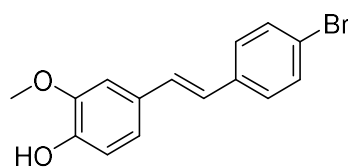
2c (*E*)-4-(4-bromostyryl)-2-methoxyphenol 75% yield (88 mg), yellow crystalline solid, 99:1 (*E*):(*Z*). ^{1}H NMR (600 MHz, CDCl$_3$) δ 7.46 (d, *J* = 8.5 Hz, 2H), 7.34 (d, *J* = 8.5 Hz, 2H), 7.06 – 6.99 (m, 3H), 6.92 (d, *J* = 8.7 Hz, 1H), 6.87 (d, *J* = 16.3 Hz, 1H), 5.71 (s, 1H), 3.95 (s, 3H); ^{13}C NMR (151 MHz, CDCl$_3$) δ 146.9, 145.9, 136.6, 131.8, 129.7, 129.5, 127.8, 125.3, 120.9, 120.7, 114.7, 108.4, 56.0; ESI HRMS calculated for $C_{15}H_{12}O_2{}^{79}Br$ (M-H$^+$)$^-$ 303.0021, found 303.0021.
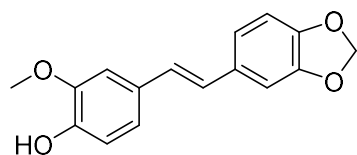
2d (*E*)-4-(2-(benzo[d][1,3]dioxol-5-yl)vinyl)-2-methoxyphenol. 70% yield (72 mg), tan crystalline solid, 99:1 (*E*):(*Z*). ^{1}H NMR (600 MHz, CDCl$_3$) δ 7.04 (d, *J* = 1.7 Hz, 1H), 7.02 – 6.98 (m, 2H), 6.93 – 6.89 (m, 2H), 6.87 (s, 2H), 6.79 (d, *J* = 8.0 Hz, 1H), 5.97 (s, 2H), 5.63 (s, 1H), 3.95 (s, 3H); ^{13}C NMR (151 MHz, CDCl$_3$) δ 148.3, 147.2, 146.8, 145.5, 132.3, 130.2, 127.1, 126.4, 121.2, 120.4, 114.7, 108.6, 108.2, 105.5, 101.2, 56.1; ESI HRMS calculated for $C_{16}H_{13}O_4$ (M-H$^+$)$^-$ 269.0814, found 269.0822. M.P. = 149-150 °C (recrystallized from EtOH).
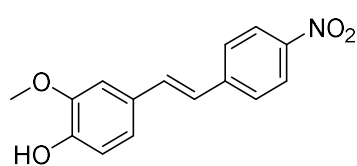
2e (*E*)-2-methoxy-4-(4-nitrostyryl)phenol. 25% yield (25 mg), orange crystalline solid, 99:1 (*E*):(*Z*). ^{1}H NMR (600 MHz, CDCl$_3$) δ 8.21 (d, *J* = 8.8 Hz, 2H), 7.60 (d, *J* = 8.8 Hz, 2H), 7.20 (d, *J* = 16.2 Hz, 1H), 7.10 – 7.06 (m, 2H), 6.99 (d, *J* = 16.3 Hz, 1H), 6.94 (d, *J* = 8.1 Hz, 1H), 5.77 (s, 1H), 3.97 (s, 3H); ^{13}C NMR (151 MHz, CDCl$_3$) δ 147.0, 146.8, 146.6, 144.3, 133.5, 129.0, 126.6, 124.3, 124.2, 121.6, 114.9, 108.7, 56.1; ESI HRMS calculated for $C_{15}H_{12}NO_4$ (M-H$^+$)$^-$ 270.0766, found 270.0768. M.P. = 166-167 °C (recrystallized from EtOH).
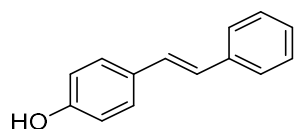
2f (*E*)-4-styrylphenol. 64% yield (48 mg), colourless crystalline solid, 99:1 (*E*):(*Z*). ^{1}H NMR (600 MHz, Acetone-d_6) δ 8.47 (s, 1H), 7.54 (d, *J* = 7.3 Hz, 2H), 7.46 (d, *J* = 8.4 Hz, 2H), 7.34 (t, *J* = 7.8 Hz, 2H), 7.22 (t, *J* = 7.4 Hz, 1H), 7.17 (d, *J* = 16.4 Hz, 1H), 7.05 (d, *J* = 16.4 Hz, 1H), 6.87 (d, *J* = 8.6 Hz, 2H); ^{13}C NMR (151 MHz, Acetone-d_6) δ 158.2, 138.8, 130.0, 129.4, 129.3, 128.7, 127.8, 127.0, 126.5, 116.4; ESI HRMS calculated for $C_{14}H_{11}O$ (M-H$^+$)$^-$ 195.0810, found 195.0805.
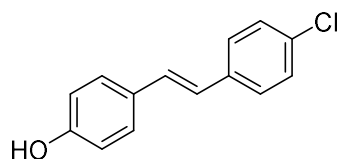
2g (*E*)-4-(4-chlorostyryl)phenol. 64% yield (57 mg), white crystalline solid, 99:1 (*E*):(*Z*). ^{1}H NMR (600 MHz, CDCl$_3$) δ 7.40 (m, 4H), 7.31 (d, *J* = 8.5 Hz, 2H), 7.02 (d, *J* = 16.2 Hz, 1H), 6.91 (d, *J* = 16.3 Hz, 1H), 6.83 (d, *J* = 8.5 Hz, 2H), 4.80 (s, 1H); ^{13}C NMR (151 MHz, CDCl$_3$) δ 155.5, 136.3, 132.9, 130.2, 128.9, 128.9, 128.1, 127.5, 125.5, 115.8; ESI HRMS calculated for $C_{14}H_{10}O^{35}Cl$ (M-H$^+$)$^-$ 229.0420, found 229.0427. M.P. = 177-178 (EtOH). M.P. = 177-178 °C (recrystallized from EtOH).
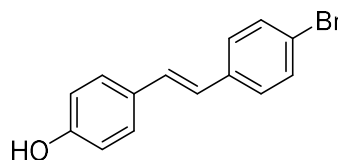
2h (*E*)-4-(4-chlorostyryl)phenol. Yield 73% (77 mg), white crystalline solid, 99:1 (*E*):(*Z*). ^{1}H NMR (600 MHz, Acetone-d_6) δ 8.52 (s, 1H), 7.50 (m, 4H), 7.46 (d, *J* = 8.6 Hz, 2H), 7.20 (d, *J* = 16.3 Hz, 1H), 7.02 (d, *J* = 16.4 Hz, 1H), 6.86 (d, *J* = 8.6 Hz, 2H); ^{13}C NMR (151 MHz, Acetone-d_6) δ 158.5, 138.2, 132.5, 130.4, 129.7, 128.9, 128.8, 125.1, 120.8, 116.5; ESI HRMS calculated for $C_{14}H_{10}O^{79}Br$ (M-H$^+$)$^-$ 272.9915, found 272.9910. M.P. = 186-187 °C (recrystallized from EtOH).
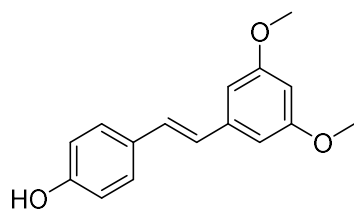
2i (*E*)-4-(3,5-dimethoxystyryl)phenol. 63% yield (31 mg), white crystalline solid, 99:1 (*E*):(*Z*). ^{1}H NMR (600 MHz, CDCl$_3$) δ 7.40 (d, *J* = 8.5 Hz, 2H), 7.03 (d, *J* = 16.2 Hz, 1H), 6.90 (d, *J* = 16.2 Hz, 1H), 6.83 (d, *J* = 8.6 Hz, 2H), 6.66 (d, *J* = 2.3 Hz, 2H), 6.39 (t, *J* = 2.3 Hz, 1H), 3.84 (s, 6H). All data are in agreement with literature.[1]
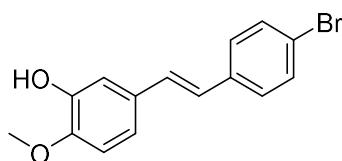
2j (*E*)-5-(4-bromostyryl)-2-methoxyphenol. 68% yield (35 mg), white crystalline solid, 99:1 (*E*):(*Z*). ^{1}H NMR (600 MHz, CDCl$_3$) δ 7.46 (d, *J* = 8.4 Hz, 2H), 7.34 (d, *J* = 8.5 Hz, 2H), 7.14 (d, *J* = 2.1 Hz, 1H), 7.02 – 6.96 (m, 2H), 6.88 (d, *J* = 16.3 Hz, 1H), 6.83 (d, *J* = 8.3 Hz, 1H), 5.62 (s, 1H), 3.91 (s, 3H); ^{13}C NMR (151 MHz, CDCl$_3$) δ 146.7, 146.0, 136.6, 131.8, 130.9, 129.1, 127.9, 126.0, 121.0, 119.6, 111.9, 110.8, 56.1; ESI HRMS calculated for $C_{15}H_{12}O_2{}^{79}Br$ (M-H$^+$)$^-$ 303.0021, found 303.0031. M.P = 166-167 °C (recrystallized from EtOH)
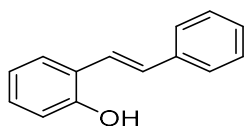
2k (*E*)-2-styrylphenol. 79% yield (60 mg), white powder, 99:1 (*E*):(*Z*). ^{1}H NMR (600 MHz, CD$_2$Cl$_2$) δ 7.57 – 7.53 (m, 3H), 7.41 – 7.34 (m, 3H), 7.26 (t, *J* = 7.4 Hz, 1H), 7.18 – 7.12 (m, 2H), 6.96 (t, *J* = 7.5 Hz, 1H), 6.82 (d, *J* = 8.0 Hz, 1H), 5.12 (s, 1H); ^{13}C NMR (151 MHz, CD$_2$Cl$_2$) δ 153.5, 138.0, 130.2, 129.1, 129.0, 128.0, 127.5, 126.8, 124.9, 123.3, 121.5, 116.3; ESI HRMS calculated for $C_{14}H_{11}O$ (M-H$^+$)$^-$ 195.0810, found 195.0814.
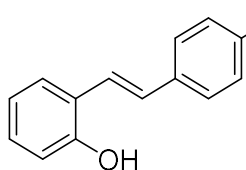
2l (*E*)-2-(4-chlorostyryl)phenol. 67% yield (60 mg), white powder, 99:1 (*E*):(*Z*). ^{1}H NMR (600 MHz, CDCl$_3$) δ 7.52 (d, *J* = 7.7 Hz, 1H), 7.45 (d, *J* = 8.4 Hz, 2H), 7.35 (d, *J* = 16.4 Hz, 1H), 7.32 (d, *J* = 8.5 Hz, 2H), 7.16 (td, *J* = 7.7, 1.6 Hz, 1H), 7.08 (d, *J* = 16.4 Hz, 1H), 6.96 (t, *J* = 7.5 Hz, 1H), 6.80 (d, *J* = 8.0 Hz, 1H), 4.96 (s, 1H); ^{13}C NMR (151 MHz, CDCl$_3$) δ 153.1, 136.3, 133.2, 129.0, 128.9, 128.8, 127.8, 127.4, 124.5, 123.8, 121.4, 116.1; ESI HRMS calculated for $C_{14}H_{10}O^{35}Cl$ (M-H$^+$)$^-$ 229.0420, found 229.0409.

General experimental procedure for the synthesis of (*E*)-alkenyl phenols 3 and dienes 4:

Benzyl phosphonium salt **1** (1.3 eq.) was dissolved in dry THF (1.2 mL/mmol) in an oven-dried two-necked round bottom flask along with a magnetic stir bar. The flask was connected to a nitrogen line, purged and sealed under nitrogen. After cooling to 0 °C, *n*-butyl lithium (1.6 M in hexanes, 2.6 eq.) was added dropwise and the reaction stirred for 40 minutes. Then, the mixture was either cooled to -78 °C prior to the dropwise addition of aldehyde in dry THF (0.8 mL/mmol) or the aldehyde solution was added at 0 °C. The reaction stirred for 30 minutes before gradual warming to room temperature. The reactions stirred until complete consumption of the aldehyde by TLC (typically overnight), and then quenched by the dropwise addition of 0.1 N HCl. The crude reaction mixture was then extracted with ethyl acetate (3 x 5 mL), and the combined organic extracts were dried over magnesium sulphate, filtered, and concentrated under reduced pressure. The crude product was purified by silica gel column chromatography (10 % ethyl acetate in hexane) to yield the (*E*)-alkene. All reactions proceeded at -78 °C unless otherwise stated.
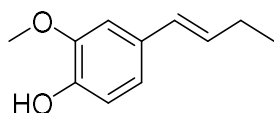
3a (*E*)-4-(but-1-en-1-yl)-2-methoxyphenol. 58% yield (40 mg), 95:5 (*E*):(*Z*), viscous dark-yellow oil. ^{1}H NMR (600 MHz, CDCl$_3$) δ 6.89 – 6.84 (m, 3H), 6.30 (d, *J* = 15.8 Hz, 1H), 6.11 (dt, *J* = 15.8, 6.5 Hz, 1H), 5.55 (s, 1H), 3.90 (s, 3H), 2.28 – 2.10 (m, 2H), 1.09 (t, *J* = 7.5 Hz, 3H); ^{13}C NMR (151 MHz, CDCl$_3$) δ 146.7, 144.9, 130.7, 130.6, 128.7, 119.6, 114.5, 108.0, 56.0, 26.1, 13.9; ESI HRMS calculated for C$_{11}$H$_{13}$O$_2$ (M-H$^+$)$^-$ 177.0916, found 177.0909.
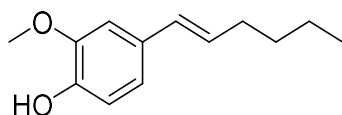
3b (*E*)-4-(hex-1-en-1-yl)-2-methoxyphenol. 57% yield (45 mg), 95:5 (*E*):(*Z*), viscous yellow oil. ^{1}H NMR (600 MHz, CDCl$_3$) δ 6.89 – 6.84 (m, 3H), 6.31 (d, *J* = 15.8 Hz, 1H), 6.07 (dt, *J* = 15.8, 6.9 Hz, 1H), 5.59 (s, 1H), 3.90 (s, 3H), 2.20 (qd, *J* = 7.1, 1.5 Hz, 2H), 1.48 – 1.42 (m, 2H), 1.38 (m, 2H), 0.93 (t, *J* = 7.3 Hz, 3H); ^{13}C NMR (151 MHz,

CDCl$_3$) δ 146.7, 144.9, 130.8, 129.6, 129.1, 119.5, 114.5, 108.0, 56.0, 32.8, 31.8, 22.4, 14.1; ESI HRMS

calculated for C$_{13}$H$_{17}$O$_2$ (M-H$^+$)$^-$ 205.1229, found 205.1227.
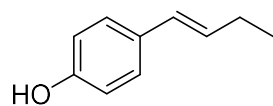
3c (*E*)-4-(but-1-en-1-yl)phenol. 61% yield (92 mg), 95:5 (*E*):(*Z*), white powder. ^{1}H NMR (600 MHz, CDCl$_3$) δ 7.23 (d, *J* = 8.6 Hz, 2H), 6.76 (d, *J* = 8.6 Hz, 2H), 6.31 (d, *J* = 15.8 Hz, 1H), 6.12 (dt, *J* = 15.8, 6.5 Hz, 1H), 4.64 (s, 1H), 2.23 – 2.17 (m, 2H), 1.08 (t, *J* = 7.5 Hz, 3H); ^{13}C NMR (151 MHz, CDCl$_3$) δ 154.6, 131.2, 130.8, 128.2, 127.3, 115.5, 26.2, 13.9; ESI HRMS calculated for C$_{10}$H$_{11}$O (M-H$^+$)$^-$ 147.0810, found 147.0818.
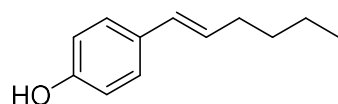
3d (*E*)-4-(hex-1-en-1-yl)phenol. 51% yield (35 mg), 98:2 (*E*):(*Z*), white/light yellow solid. ^{1}H NMR (600 MHz, CDCl$_3$) δ 7.23 (d, *J* = 8.5 Hz, 2H), 6.76 (d, *J* = 8.6 Hz, 2H), 6.31 (d, *J* = 15.8 Hz, 1H), 6.08 (dt, *J* = 15.7, 6.9 Hz, 1H), 4.82 (s, 1H), 2.18 (qd, *J* = 7.1, 1.5 Hz, 2H), 1.48 – 1.41 (m, 2H), 1.41 – 1.33 (m, 2H), 0.92 (t, *J* = 7.3 Hz, 3H); ^{13}C NMR (151 MHz, CDCl$_3$) δ 154.6, 131.2, 129.3, 129.1, 127.3, 115.5, 32.8, 31.8, 22.4, 14.1; ESI HRMS calculated for C$_{12}$H$_{15}$O (M-H$^+$)$^-$ 175.1123, found 175.1114.
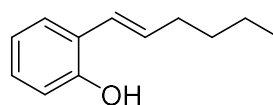
3e (*E*)-2-(hex-1-en-1-yl)phenol. 22% yield (15 mg), 95:5 (*E*):(*Z*). ^{1}H NMR (600 MHz, CDCl$_3$) δ 7.32 (dd, *J* = 7.7, 1.4 Hz, 1H), 7.09 (td, *J* = 7.8, 1.6 Hz, 1H), 6.89 (td, *J* = 7.6, 0.7 Hz, 1H), 6.79 (dd, *J* = 8.0, 1.0 Hz, 1H), 6.57 (d, *J* = 15.9 Hz, 1H), 6.20 (dt, *J* = 15.9, 6.9 Hz, 1H), 5.10 (s, 1H), 2.27 – 2.23 (m, 2H), 1.50 – 1.45 (m, 2H), 1.39 - 1.36 (m, 2H), 0.94 (t, *J* = 7.3 Hz, 3H). ^{13}C NMR (151 MHz, CDCl$_3$) δ 152.6, 133.9, 128.1, 127.5, 125.2, 124.1, 121.0, 115.8, 33.3, 31.7, 22.4, 14.1. ESI HRMS calculated for C$_{12}$H$_{15}$O (M-H$^+$)$^-$ 175.1123, found 175.1116.
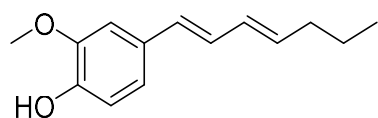
4a 4-((1*E*,3*E*)-hepta-1,3-dien-1-yl)-2-methoxyphenol. 58% yield (48 mg), 98:2 (*E*):(*Z*), orange solid. ^{1}H NMR (600 MHz, Acetone-*d$_6$*) δ 7.61 (s, 1H), 7.07 (d, *J* = 1.8 Hz, 1H), 6.87 (dd, *J* = 8.1, 2.0 Hz, 1H), 6.77 (d, *J* = 8.1 Hz, 1H), 6.70 (dd,

J = 15.6, 10.4 Hz, 1H), 6.40 (d, J = 15.6 Hz, 1H), 6.19 (dd, J = 15.1, 10.4 Hz, 1H), 5.76 (dt, J = 14.7,

7.1 Hz, 1H), 3.86 (s, 3H), 2.10 (q, J = 7.4 Hz, 2H), 1.43 (h, J = 7.4 Hz, 2H), 0.91 (t, J = 7.4 Hz, 3H);

^{13}C NMR (151 MHz, Acetone-d_6) δ 148.5, 147.2, 134.4, 132.1, 131.2, 130.7, 127.7, 120.7, 115.9, 109.7,

56.2, 35.6, 23.3, 13.9; ESI HRMS calculated for $C_{14}H_{17}O_2$ (M-H$^+$)$^-$ 217.1229, found 217.1225.
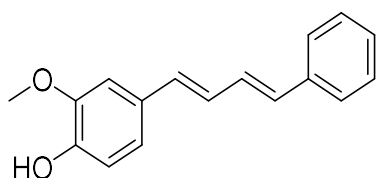
4b 2-methoxy-4-((1E,3E)-4-phenylbuta-1,3-dien-1-yl)phenol. 68%

yield (66 mg), 99:1 (E):(Z), pale yellow powder. ^{1}H NMR (600 MHz,

CDCl$_3$) δ 7.43 (d, J = 7.4 Hz, 2H), 7.33 (t, J = 7.7 Hz, 2H), 7.22 (t, J

= 7.3 Hz, 1H), 6.98 – 6.91 (m, 3H), 6.89 (d, J = 8.1 Hz, 1H), 6.82 (dd, J = 15.2, 10.7 Hz, 1H), 6.66 –

6.58 (m, 2H), 5.65 (s, 1H), 3.94 (s, 3H); ^{13}C NMR (151 MHz, CDCl$_3$) δ 146.8, 145.7, 137.7, 133.0,

131.9, 130.2, 129.5, 128.8, 127.5, 127.3, 126.4, 120.6, 114.7, 108.2, 56.0; ESI HRMS calculated for

$C_{17}H_{15}O_2$ (M-H$^+$)$^-$ 251.1072, found 251.1071. Reaction proceeded at 0 °C.
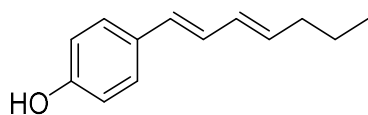
4c 4-((1E,3E)-hepta-1,3-dien-1-yl)phenol. 46% yield (33 mg), 95:5

(E):(Z), pale-yellow solid. ^{1}H NMR (600 MHz, Acetone-d_6) δ 8.38 (s,

1H), 7.28 (d, J = 8.6 Hz, 2H), 6.79 (d, J = 8.7 Hz, 2H), 6.66 (dd, J = 15.7, 10.4 Hz, 1H), 6.40 (d, J =

15.7 Hz, 1H), 6.19 (dd, J = 15.1, 10.4 Hz, 1H), 5.75 (dt, J = 14.7, 7.1 Hz, 1H), 2.12 – 2.07 (m, 2H),

1.43 (h, J = 7.4 Hz, 2H), 0.91 (t, J = 7.4 Hz, 3H); ^{13}C NMR (151 MHz, Acetone-d_6) δ 157.8, 134.3,

132.1, 130.9, 130.3, 128.3, 127.5, 116.3, 35.6, 23.3, 14.0; ESI HRMS calculated for $C_{13}H_{15}O$ (M-H$^+$)$^-$

187.1123, found 187.1114.

Experimental References

1) J. McNulty, D. McLeod, *Tetrahedron Lett.* **2013**, *54*, 6303.

2) D. V. Moiseev, B. O. Patrick, B. R. James, *Inorg. Chem.* **2009**, *48*, 239.

3.6 References

1) H. Lv, G. She, *Nat. Prod. Commun.* **2010**, *5*, 1687.

2) K. Xiao, H.-J. Zhang, L.-J. Xuan, J. Zhang, Y.-M. Xu, D.-L. Bai, *Stud. Nat. Prod. Chem.* **2008**, *34*, 453.

3) J.-F. Sun, X. Lin, X.-F. Zhou, J. Wan, T. Zhang, B. Yang, X.-W. Yang, Z. Tu, Y. Liu, *J. Antibiot. (Tokyo).* **2014**, *67*, 451.

4) J. L. Occolowitz, *Anal. Chem.* **1964**, *36*, 2177.

5) J.-Y. Pan, S.-L. Chen, M.-H. Yang, J. Wu, J. Sinkkonen, K. Zou, *Nat. Prod. Rep.* **2009**, *26*, 1251.

6) L. B. Davin, N. G. Lewis, *Plant Physiol.* **2000**, *123*, 453.

7) T. Umezawa, *Phytochem. Rev.* **2003**, *2*, 371.

8) S. Suzuki, T. Umezawa, *J. Wood Sci.* **2007**, *53*, 273.

9) J. Barros, H. Serk, I. Granlund, E. Pesquet, *Ann. Bot.* **2015**, *115*, 1053.

10) T. Shen, X.-N. Wang, H.-X. Lou, *Nat. Prod. Rep.* **2009**, *26*, 916.

11) D. C. Thompson, J. A. Thompson, M. Sugumaran, P. Moldéus, *Chem. Biol. Interact.* **1993**, *86*, 129.

12) S. Saul, M. Sugumaran, *FEBS Lett.* **1988**, *237*, 155.

13) M. Sugumaran, V. Semensi, J. S. Buckner, *J. Biol. Chem.* **1991**, *266*, 6073.

14) P. Wang, Y. Song, L. Zhang, H. He, X. Zhou, *Curr. Med. Chem.* **2005**, *12*, 2893.

15) J. L. Bolton, *Curr. Org. Chem.* **2014**, *18*, 61.

16) R. W. Van De Water, T. R. R. Pettus, *Tetrahedron* **2002**, *58*, 5367.

17) M. M. Toteva, *Adv. Phys. Org. Chem.* **2011**, *45*, 39.

18) *Quinone methides*, ed. by Steven Edward. Rokita, John Wiley & Sons, Inc, Hoboken, New Jersey, **2009**.

19) L. Caruana, M. Fochi, L. Bernardi, *Molecules* **2015**, *20*, 11733.

20) N. J. Willis, C. D. Bray, *Chem. Eur. J.* **2012**, *18*, 9160.

21) K. Zielke, M. Waser, *Org. Lett.* **2018**, *20*, 768.

22) L. Roiser, M. Waser, *Org. Lett.* **2017**, *19*, 2338.

23) C. Jarava-Barrera, A. Parra, A. López, F. Cruz-Acosta, D. Collado-Sanz, D. J. Cárdenas, M. Tortosa, *ACS Catal.* **2016**, *6*, 442.

24) A. López, A. Parra, C. Jarava-Barrera, M. Tortosa, *Chem. Commun. (Camb).* **2015**, *51*, 17684.

25)   A. Parra, M. Tortosa, *ChemCatChem* **2015**, *7*, 1524.

26)   Z. Wang, J. Sun, *Org. Lett.* **2017**, *19*, 2334.

27)   X. Wu, L. Xue, D. Li, S. Jia, J. Ao, J. Deng, H. Yan, *Angew. Chemie - Int. Ed.* **2017**, *56*, 13722.

28)   Z. Wang, J. Sun, *Synthesis (Stuttg).* **2015**, *47*, 3629.

29)   A. A. Jaworski, K. A. Scheidt, *J. Org. Chem.* **2016**, *81*, 10145.

30)   T. H. Jepsen, S. B. Thomas, Y. Lin, C. I. Stathakis, I. de Miguel, S. A. Snyder, *Angew. Chem. Int. Ed. Engl.* **2014**, *53*, 6747.

31)   Z. Wang, Y. F. Wong, J. Sun, *Angew. Chemie Int. Ed.* **2015**, *54*, 13711.

32)   L. Caruana, M. Mondatori, V. Corti, S. Morales, A. Mazzanti, M. Fochi, L. Bernardi, *Chem. - A Eur. J.* **2015**, *21*, 6037.

33)   W.-J. Bai, J. G. David, Z.-G. Feng, M. G. Weaver, K.-L. Wu, T. R. R. Pettus, *Acc. Chem. Res.* **2014**, *47*, 3655.

34)   László Juhász, A. László Kürti, S. Antus, *J. Nat. Prod* **2000**, *63*, 866.

35)   H. Erdtman, *Biochem. Z.* **1933**, *258*, 179.

36)   B. Leopold, *Acta Chem. Scand.* **1950**, *4*, 1523.

37)   P.-Y. Chen, Y.-H. Wu, M.-H. Hsu, T.-P. Wang, E.-C. Wang, *Tetrahedron* **2013**, *69*, 653.

38)   L. Pieters, S. Van Dyck, M. Gao, R. Bai, E. Hamel, A. Vlietinck, G. Lemière, *J. Med. Chem* **1999**, *42*, 5475.

39)   B. S. Matsuura, M. H. Keylor, B. Li, Y. Lin, S. Allison, D. A. Pratt, C. R. J. Stephenson, *Angew. Chem. Int. Ed. Engl.* **2015**, *54*, 3754.

40)   M. H. Keylor, B. S. Matsuura, M. Griesser, J.-P. R. Chauvin, R. A. Harding, M. S. Kirillova, X. Zhu, O. J. Fischer, D. A. Pratt, C. R. J. Stephenson, *Science (80-.).* **2016**, *354*, 1260.

41)   T. P. Pathak, M. S. Sigman, *J. Org. Chem.* **2011**, *76*, 9210.

42)   O. L. Chapman, M. R. Engel, J. P. Springer, J. C. Clardy, *J. Am. Chem. Soc.* **1971**, *93*, 6696.

43)   M. J. Schultz, M. S. Sigman, *J. Am. Chem. Soc.* **2006**, *128*, 1460.

44)   R. Jana, T. P. Pathak, K. H. Jensen, M. S. Sigman, *Org. Lett.* **2012**, *14*, 4074.

45)   T. P. Pathak, K. M. Gligorich, B. E. Welm, M. S. Sigman, *J. Am. Chem. Soc.* **2010**, *132*, 7870.

46)   K. H. Jensen, J. D. Webb, M. S. Sigman, *J. Am. Chem. Soc.* **2010**, *132*, 17471.

47)   K. H. Jensen, T. P. Pathak, Y. Zhang, M. S. Sigman, *J. Am. Chem. Soc.* **2009**, *131*, 17074.

48)   T. P. Pathak, M. S. Sigman, *Org. Lett.* **2011**, *13*, 2774.

49)   Y. Zhang, M. S. Sigman, *Org. Lett.* **2006**, *8*, 5557.

50)   K. M. Gligorich, M. J. Schultz, M. S. Sigman, *J. Am. Chem. Soc.* **2006**, *128*, 2794.

51)   Y. Zhang, M. S. Sigman, *J. Am. Chem. Soc.* **2007**, *129*, 3076.

52)   F. Shi, G.-J. Xing, R.-Y. Zhu, W. Tan, S. Tu, *Org. Lett.* **2013**, *15*, 128.

53)   F. Shi, G.-J. Xing, Z.-L. Tao, S.-W. Luo, S.-J. Tu, L.-Z. Gong, *J. Org. Chem.* **2012**, *77*, 6970.

54)   M. Fochi, L. Caruana, L. Bernardi, *Synthesis (Stuttg).* **2013**, *46*, 135.

55)   L. He, M. Bekkaye, P. Retailleau, G. Masson, *Org. Lett.* **2012**, *14*, 3158.

56)   W. Dai, H. Lu, X.-L. Jiang, T.-T. Gao, F. Shi, *Tetrahedron: Asymmetry* **2015**, *26*, 109.

57)   M.-L. Li, D.-F. Chen, S.-W. Luo, X. Wu, *Tetrahedron: Asymmetry* **2015**, *26*, 219.

58)   Z. Wang, F. Ai, Z. Wang, W. Zhao, G. Zhu, Z. Lin, J. Sun, *J. Am. Chem. Soc.* **2015**, *137*, 383.

59)   I. Fleischer, J. Pospech, *RSC Adv.* **2015**, *5*, 493.

60)   R. C. Sovish, *J. Org. Chem.* **1959**, *24*, 1345.

61)   B. B. Corson, W. J. Heintzelman, L. H. Schwartzman, H. E. Tiefenthal, R. J. Lokken, J. E. Nickels, G. R. Atwood, F. J. Pavlik, *J. Org. Chem.* **1958**, *23*, 544.

62)   M. Hassam, A. Taher, G. E. Arnott, I. R. Green, W. A. L. van Otterlo, *Chem. Rev.* **2015**, *115*, 5462.

63)   P. Terpinc, T. Polak, N. Šegatin, A. Hanzlowsky, N. P. Ulrih, H. Abramovič, *Food Chem.* **2011**, *128*, 62.

64)   V. Aldabalde, M. L. Derrudi, D. Gamenara, F. Geymonat, P. Saenz-Méndez, M. Risso, G. Seoane, *Open J. Phys. Chem.* **2011**, *01*, 85.

65)   R. Bernini, E. Mincione, M. Barontini, G. Provenzano, L. Setti, *Tetrahedron* **2007**, *63*, 9663.

66)   J. P. N. Rosazza, Z. Huang, L. Dostal, T. Volm, B. Rousseau, *J. Ind. Microbiol.* **1995**, *15*, 457.

67)   S. Quideau, J. Ralph, *J. Agric. Food Chem.* **1992**, *40*, 1108.

68)   R. Csuk, S. Albert, B. Siewert, S. Schwarz, *Eur. J. Med. Chem.* **2012**, *54*, 669.

69)   S. Albert, R. Horbach, H. B. Deising, B. Siewert, R. Csuk, *Bioorg. Med. Chem.* **2011**, *19*, 5155.

70)   A. V. Martínez, J. I. García, J. A. Mayoral, *Tetrahedron* **2017**, *73*, 5581.

71)   M. Chalal, D. Vervandier-Fasseur, P. Meunier, H. Cattey, J.-C. Hierso, *Tetrahedron* **2012**, *68*, 3899.

72)   Y. Shen, G. Liu, Z. Zhou, X. Lu, *Org. Lett.* **2013**, *15*, 3366.

73)   Y. Zhang, M. Shen, S. Cui, T. Hou, *Bioorg. Med. Chem. Lett.* **2014**, *24*, 5470.

74)   Y. Le Bigot, M. Delmas, A. Gaset, *Tetrahedron Lett.* **1983**, *24*, 193.

75)   L. Lonsky, W. Lonsky, K. Kratzl, I. Falkehag, *Monatshefte fur Chemie* **1976**, *107*, 685.

76)   E. Reimann, *Tetrahedron Lett.* **1970**, *11*, 4051.

77)   F. Lara-Ochoa, L. C. Sandoval-Minero, G. Espinosa-Pérez, *Tetrahedron Lett.* **2015**, *56*, 5977.

78) J. McNulty, D. McLeod, *Tetrahedron Lett.* **2013**, *54*, 6303.

79) D. V. Moiseev, B. O. Patrick, B. R. James, *Inorg. Chem.* **2009**, *48*, 239.

80) X.-M. Zhang, F. G. Bordwell, *J. Am. Chem. Soc* **1994**, *116*, 968.

81) J. S. Smith, N. J. Robinson, *J. Infect. Dis.* **2002**, *186*, S3.

82) A. L. Cunningham, R. J. Diefenbach, M. Miranda-Saksena, L. Bosnjak, M. Kim, C. Jones, M. W. Douglas, *J. Infect. Dis.* **2006**, *194*, S11.

83) R. J. Whitley, J. W. Gnann, *Lancet* **2002**, *359*, 507.

84) R. J. Whitley, *Antiviral Res.* **2006**, *71*, 141.

85) M.-L. Engman, I. Adolfsson, I. Lewensohn-Fuchs, M. Forsgren, M. Mosskin, G. Malm, *Pediatr. Neurol.* **2008**, *38*, 398.

86) A. J. Chucair-Elliott, C. Conrady, M. Zheng, C. M. Kroll, T. E. Lane, D. J. J. Carr, *Glia* **2014**, *62*, 1418.

87) J. A. Carter, B. G. R. Neville, C. R. J. C. Newton, *Brain Res. Rev.* **2003**, *43*, 57.

88) R. Y. Kropp, T. Wong, L. Cormier, A. Ringrose, S. Burton, J. E. Embree, M. Steben, *Pediatrics* **2006**, *117*, 1955.

89) R. Yolken, *Herpes* **2004**, *11 Suppl 2*, 83A.

90) K. M. Prasad, A. M. M. Watson, F. B. Dickerson, R. H. Yolken, V. L. Nimgaonkar, *Schizophr. Bull.* **2012**, *38*, 1137.

91) M. H. Sawyer, D. E. Webb, J. E. Balow, S. E. Straus, *Am. J. Med.* **1988**, *84*, 1067.

92) W. E. Haefeli, R. A. Z. Schoenenberger, P. Weiss, R. F. Ritz, *Am. J. Med.* **1993**, *94*, 212.

93) E. Frobert, S. Burrel, S. Ducastelle-Lepretre, G. Billaud, F. Ader, J.-S. Casalegno, V. Nave, D. Boutolleau, M. Michallet, B. Lina, F. Morfin, *Antiviral Res.* **2014**, *111*, 36.

94) S. Burrel, C. Aime, L. Hermet, Z. Ait-Arkoub, H. Agut, D. Boutolleau, *Antiviral Res.* **2013**, *100*, 365.

95) L. D'Aiuto, Y. Zhi, D. Kumar Das, M. R. Wilcox, J. W. Johnson, L. McClain, M. L. MacDonald, R. Di Maio, M. E. Schurdak, P. Piazza, L. Viggiano, R. Sweet, P. R. Kinchington, A. G. Bhattacharjee, R. Yolken, V. L. Nimgaonka, *Organogenesis* **2014**, *10*, 365.

96) L. D'Aiuto, K. Williamson, P. Dimitrion, J. McNulty, C. E. Brown, C. B. Dokuburra, A. J. Nielsen, W. J. Lin, P. Piazza, M. E. Schurdak, J. Wood, R. H. Yolken, P. R. Kinchington, D. C. Bloom, V. L. Nimgaonkar, *Antiviral Res.* **2017**, *142*, 136.

97) U. Shadakshari, S. Rele, S. K. Nayak, S. Chattopadhyay, *Indian J. Chem.* **2004**, *34B*, 1934.

98) Y. Abba, H. Hassim, H. Hamzah, M. M. Noordin, *Adv. Virol.* **2015**, *2015*, 1.

99) T. Shen, X.-N. Wang, H.-X. Lou, *Nat. Prod. Rep.* **2009**, *26*, 916.

100) D. L. Evers, X. Wang, S.-M. Huong, D. Y. Huang, E.-S. Huang, *Antiviral Res.* **2004**, *63*, 85.

101) A. De Leo, G. Arena, E. Lacanna, G. Oliviero, F. Colavita, E. Mattia, *Antiviral Res.* **2012**, *96*, 196.

102) I. Galindo, B. Hernáez, J. Berná, J. Fenoll, J. L. Cenis, J. M. Escribano, C. Alonso, *Antiviral Res.* **2011**, *91*, 57.

103) M. Campagna, C. Rivas, *Biochem. Soc. Trans.* **2010**, *38*, 50.

104) S. A. Faith, T. J. Sweet, E. Bailey, T. Booth, J. J. Docherty, *Antiviral Res.* **2006**, *72*, 242.

105) X. Chen, H. Qiao, T. Liu, Z. Yang, L. Xu, Y. Xu, H. M. Ge, R.-X. Tan, E. Li, *Antiviral Res.* **2012**, *95*, 30.

106) J. J. Docherty, M. H. Ming Fu, B. S. Stiffler, R. J. Limperos, C. M. Pokabla, A. L. DeLucia, *Antiviral Res.* **1999**, *43*, 135.

107) J. J. Docherty, M. M. Fu, J. M. Hah, T. J. Sweet, S. A. Faith, T. Booth, *Antiviral Res.* **2005**, *67*, 155.

108) J. J. Docherty, J. S. Smith, M. M. Fu, T. Stoner, T. Booth, *Antiviral Res.* **2004**, *61*, 19.

109) B. Calamini, K. Ratia, M. G. Malkowski, M. Cuendet, J. M. Pezzuto, B. D. Santarsiero, A. D. Mesecar, *Biochem. J* **2010**, *429*, 273.

110) R. Pangeni, J. K. Sahni, J. Ali, S. Sharma, S. Baboota, *Expert Opin. Drug Deliv.* **2014**, *11*, 1285.

111) A. R. Neves, M. Lúcio, J. L. C. Lima, S. Reis, *Curr. Med. Chem.* **2012**, *19*, 1663.

112) T. P. Kondratyuk, E.-J. Park, L. E. Marler, S. Ahn, Y. Yuan, Y. Choi, R. Yu, R. B. Van Breemen, J. Hoshino, M. Cushman, K. C. Jermihov, A. D. Mesecar, C. J. Grubbs, J. M. Pezzuto, *Mol. Nutr. Food. Res.* **2011**, *55*, 1249.

4 Development of an Organocatalytic [2+2] Cycloaddition

4.1 Cyclobutanes are valuable synthetic targets

The first synthesis of a cyclobutane was reported by Perkin in 1887, who prepared several "tetramethylene carboxylates" using an alkylative methodology wherein diethyl malonate was treated with 1,3-dibromopropane under basic conditions.[1] Other early discoveries on cyclobutanes were a by-product of natural product research, particularly on cocaine and related alkaloids.[2-5] One of the first reported natural products containing a cyclobutane core was truxilline, a dimer of cinnamylmethecgonine (Figure 4.1). Truxilline hydrolyses to give the cyclobutane α-truxillic acid, itself a natural product formed by the photochemical dimerization of cinnamic acid. As such, one of the first deliberate total syntheses of a cyclobutane natural product occurred when Riiber discovered that cinnamylidene malonic acid dimerizes in light and the resulting cyclobutane undergoes oxidative cleavage to give truxillic acid.[6,7] This discovery led to the exploration of a more direct synthesis, which was accomplished by exposing a flat sheet of cinnamic acid to direct sunlight for 50 h.[8]
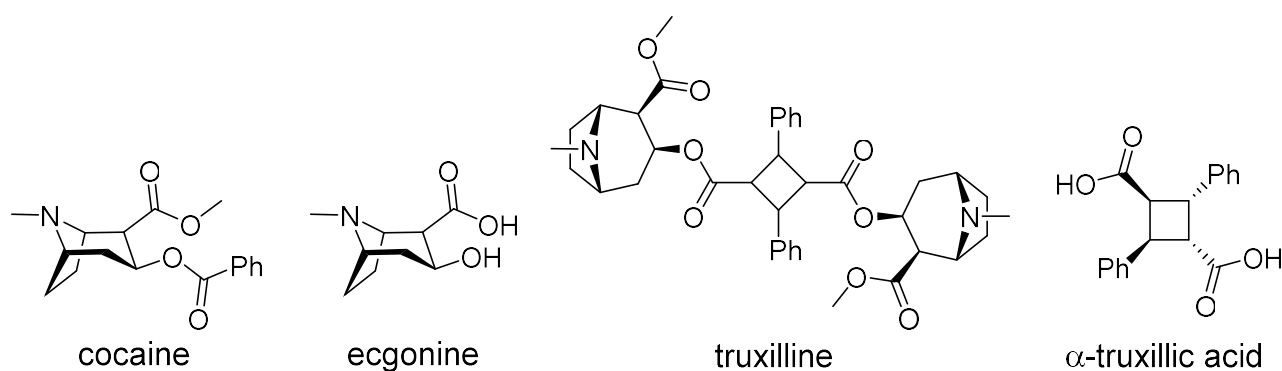
FIGURE 4.1 Research on the Coca alkaloids led to the discovery of the first natural cyclobutanes. Early research into cocaine and related natural products found truxilline, one of the first identified natural products with a cyclobutane core.

Since the discovery of truxilline, the number of cyclobutane containing natural products has grown significantly.[9,10] Many of these natural products are reported to have anti-cancer, anti-viral and other medically relevant biological activity. As well, cyclobutanes are increasingly recognized as a useful motif in drugs. The intrinsic strain in the cyclobutane allows for the creation of stereochemically complex, albeit structurally rigid molecules, which can be beneficial when designing new drugs; four-membered rings can also impart unique pharmacokinetic and physicochemical properties.[11-13] In general, cyclobutanes offer the opportunity to probe novel chemical spaces, which is a major emphasis of modern drug discovery and design.

Besides their ubiquity in biologically active compounds and natural products, cyclobutanes are valuable synthetic intermediates. The high degree of ring strain (23-26 kcal mol^{-1}) is comparable to the ring strain of cyclopropanes and allows for selective cleavage of cyclobutane C-C bonds. This inherent reactivity has been used in many ring opening reactions and ring expansion reactions to generate five-to nine-membered rings, and these strategies have been used in a number of natural product total syntheses.[14-16]

4.2 Brief review of [2+2] cycloadditions for cyclobutane synthesis

Perkin used an alkylative methodology to prepare the first synthetic cyclobutanes in 1887, but photochemical [2+2] cyclodimerization reactions emerged as the most prominent method for preparing cyclobutanes over the next 70 years (Figure 4.2, A). The direct thermal cycloaddition of two unactivated alkenes is symmetry forbidden, but irradiation with UV light leads to an excited state which undergoes a symmetry allowed concerted [2+2] cycloaddition. Some of the earliest examples of photochemical cyclobutane syntheses include the photodimerization of cinnamic acid and the intramolecular cycloaddition of carvone to carvone-camphor in strong "Italian sunlight" (Figure 4.2, B and C).[8,17,18] For the next several decades, research focused on similar photodimerizations and
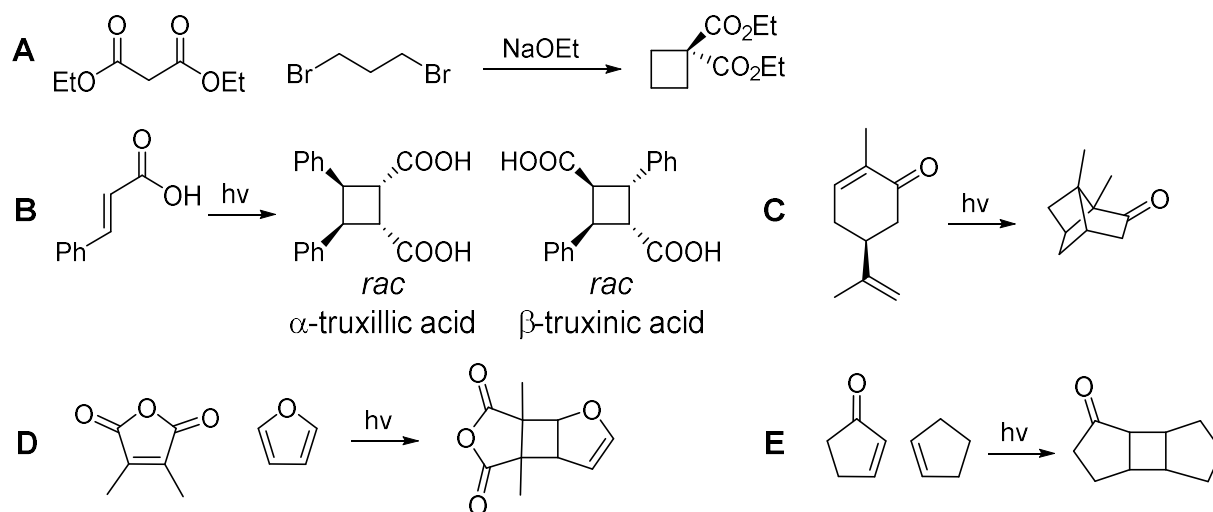
FIGURE 4.2 Classic alkylative and photochemical cyclobutane syntheses. Although the first cyclobutane was prepared using an alkylative strategy (A), most early syntheses were photochemical (B and C). Non-symmetrical photocycloadditions (D and E) were not developed until the 1960s.

photocycloadditions. Mixed intermolecular [2+2] cycloadditions weren't developed until the 1960s when it was realized that combining two different alkenes together could allow for relatively selective intermolecular reactions, provided one alkene was used in a large excess (e.g. as the solvent) and one is easier to excite with lower λ_{max}. Relevant examples include the [2+2] photocycloadditions of dimethylmaleic anhydride in furan[19] and cyclopentenone in cyclopentene (Figure 4.2, D and E).[20]

Despite their ubiquity in classical cyclobutane syntheses, photochemical [2+2] reactions suffer from several limitations. For example, the required excited states can be difficult to generate using common sources of radiation, particularly if the alkene is not conjugated, and can be prohibitively short-lived. Photochemical cycloadditions can also have poor regio- and chemoselectivity due to the high reactivity of the active intermediates. Another issue with classic photochemical approaches to cyclobutanes is a general lack of stereocontrol and tunability. For example, the dimerization of *trans*-cinnamic acid only generates racemic α-truxillic and β-truxinic acid, and the ratio of these products varies if the reaction is performed in the solid or liquid phase and changes depending on the crystal structure of the starting material.[21]

There have been many advances in photochemical [2+2] cycloadditions which help improve reactivity, selectivity and yield.[22] The use of transition metal catalysts, particularly Cu(I) salts, allows for excitation of the alkene at longer wavelengths via metal-to-ligand and/or ligand-to-metal charge transfer.[23-25] Other advances include the development of novel organic and inorganic sensitizers that has led to visible light catalysis, and the development of photoinduced electron transfer (PET) or photoredox catalysis.[22,26] Photoredox catalysis is a powerful strategy for cyclobutane synthesis and offers a mechanistic departure from traditional photochemical reactions. It uses catalysts that are redox active and exhibit long-lived excited states after absorbing a photon, thereby allowing electron abstraction or electron donation to an alkene. The resultant radical cations or radical anions then undergo a [2+2] addition with other alkenes. These reactions typically display excellent diastereoselectivity and use catalysts such as polypyridyl ruthenium and iridium species, pyrylium salts and specific organic dyes.[22]

Despite these improvements, a recent review focusing on the last 20 years of photochemical [2+2] reactions demonstrates that most methods are either racemic or rely on chiral auxiliaries, chiral reaction matrices or substrate control to obtain cyclobutanes in high *e.e.*[22,27-31] Methods using chiral catalysts in photochemical cycloadditions are much less common, partially due to the fact that the interaction between catalysts and compounds in photoexcited states is minimal, and the high-energy intermediates can readily participate in non-catalyzed background reactions. Nevertheless, exceptions exist. For example, [2+2] reactions involving enones are amenable to Lewis acid catalysis, where coordination by the catalyst causes a bathochromic shift of the $\pi \rightarrow \pi^*$ absorption band, and the absorption coefficient near the new absorption maxima can be hundreds of times that of the uncomplexed substrate at the same wavelength. Thus, carefully selecting the radiation wavelength to correspond to the complexed $\pi \rightarrow \pi^*$ absorption band, combined with the use of a chiral Lewis acid catalyst, allows for asymmetric [2+2] photocycloadditions. This methodology has been used in
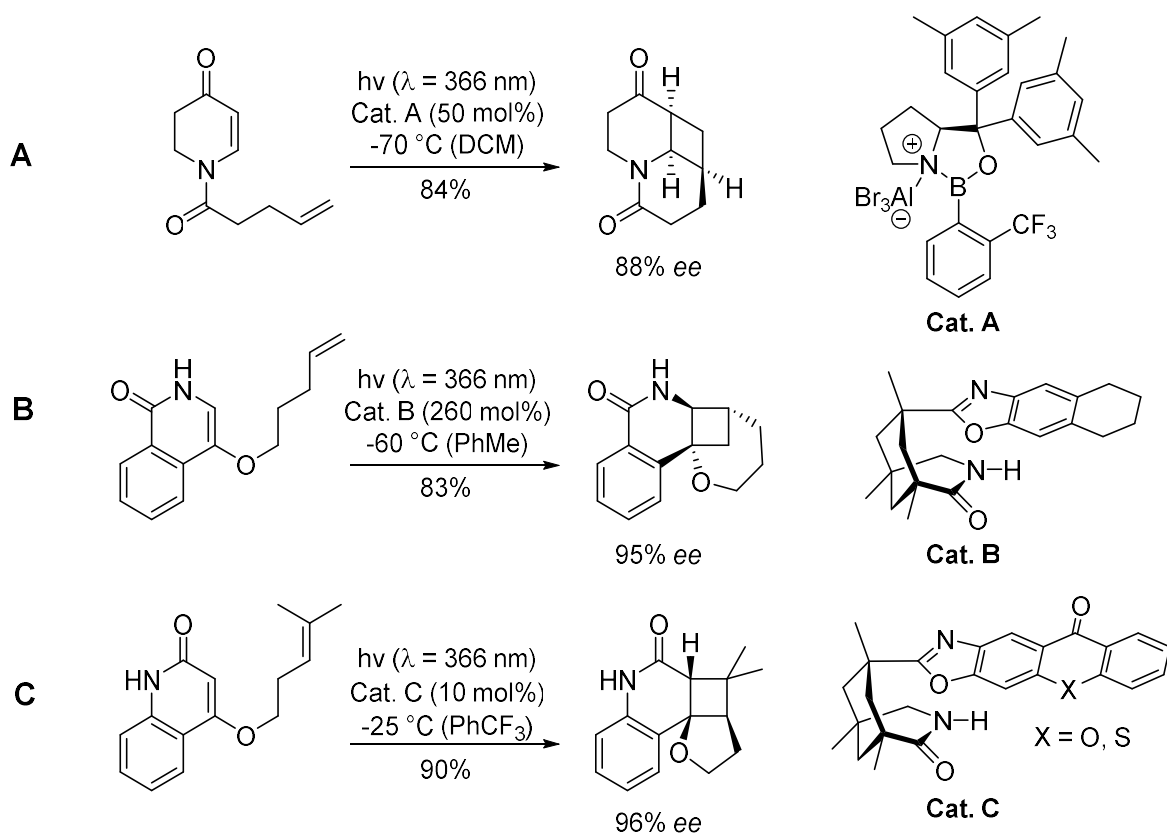
FIGURE 4.3 Representative catalytic asymmetric methods for photochemical [2+2] reactions. The previous two decades have seen the development of chiral Lewis acid (A), hydrogen bonding (B), and photosensitizer-based strategies for asymmetric [2+2] photocycloadditions.

predominantly intramolecular [2+2] cycloadditions on coumarins, substituted enones and dihydropyridones using a chiral oxazaborolidine-AlBr$_3$ catalyst, but very recent work led to optimization of the catalyst for an intermolecular reaction using cyclohexenone.[32-36] Unfortunately, all these methods require high catalyst loading (50%) to obtain good *e.e* (Figure 4.3, A).

Other examples of asymmetric photocyclizations use chiral hydrogen bonding catalysts based on a 3-azabicyclo[3.3.1]nonan-2-one skeleton that facilitate enantioselective intra- and intermolecular [2+2] photocycloadditions in quinolones, isoquinolones, 5,6-dihydropyridones and pyridones and work by selectively blocking one face of the substrate (Figure 4.3, B).[37-45] However, these methods use exceptionally high catalyst loading (ca. 250 mol%) to obtain good *e.e.*, although a conceptually similar

methodology has been reported for intramolecular [2+2] photocycloadditions on coumarins using chiral thiourea catalysts with more reasonable loadings (1-10%).[46,47]

Another strategy for chiral photochemical reactions involves the use of chiral photosensitizers. While asymmetric induction with chiral photosensitizers has been known since the 1960s, early work resulted in little success for obtaining synthetically useful levels of enantioenrichment.[34,48,49] In 2003, intramolecular [2+2] reactions on pyridones using a chiral photosensitizer were reported, but only 20% *e.e.* was obtained despite a 50 mol% catalyst loading.[50] More recently, chiral xanthone and thioxanthone photosensitizers based on a 3-azabicyclo[3.3.1]nonan-2-one skeleton were reported to catalyze intramolecular [2+2] cyclizations of quinolones and pyridones and work at lower catalyst loadings (5-10%) but require fluorinated solvents (e.g. PhCF$_3$ and hexafluoro-*meta*-xylene) (Figure 4.3, C).[51-55]

In general, the substrates employed in asymmetric photochemical [2+2] cycloadditions reactions are limited, universally requiring cyclic α,β-unsaturated carbonyls, and frequently only working well for intramolecular cyclizations (Figure 4.3). Thus, broadening substrate scope and improving catalyst loadings are worthwhile areas of future research in catalytic asymmetric photochemical [2+2] reactions.

While photochemical [2+2] cycloadditions are the most well-known route to cyclobutanes, non-photochemical routes have also been extensively explored.[56] Unlike photochemical [2+2] cycloadditions, concerted thermal [2+2] reactions are symmetry forbidden. However, they can proceed in a stepwise manner through charged intermediates and typically occur between an electron rich, nucleophilic double bond and an electron poor, electrophilic double bond. Diradical processes are also possible for thermal [2+2] cycloadditions, particularly those involving allenes.[57] Since the orbital symmetry limitations of photochemical [2+2] cycloadditions are avoided in the stepwise mechanism, thermal cycloadditions can offer more stereochemical control and tunability.
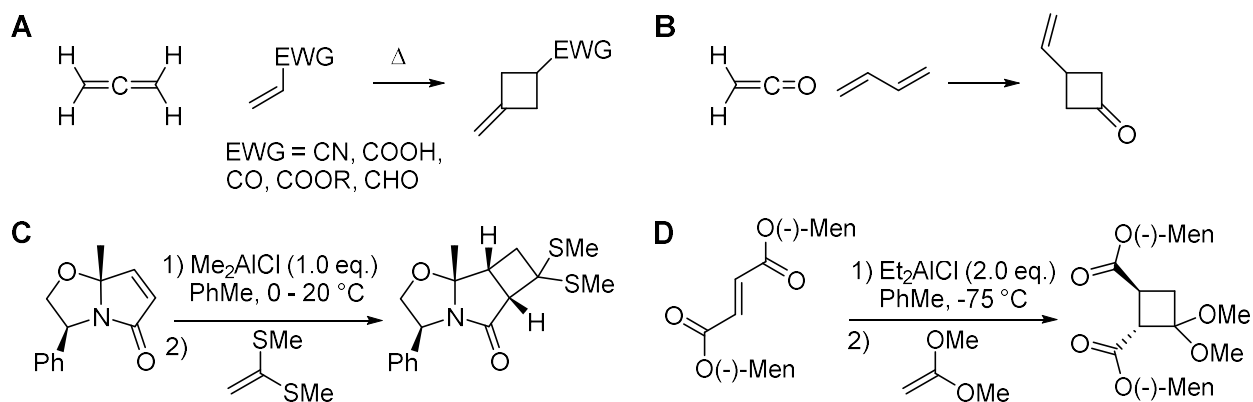
FIGURE 4.4 Representative thermal and non-photochemical Lewis acid catalyzed [2+2] reactions. Many early cyclobutane syntheses exploited the unique electronic character of allenes (A) and ketenes (B). More recently, Lewis acid catalysis has been identified as a fruitful avenue for the development of asymmetric [2+2] cycloadditions, although initial works relied on induction of asymmetry through chiral auxiliaries.

Early thermal cyclobutane syntheses frequently exploited the unique electronic nature of cumulenes like and allenes and ketenes. Some historically relevant thermal [2+2] cycloadditions include the dimerization of allene to give 1,2-dimethylene cyclobutanes,[58-60] the reaction of allenes with maleic anhydride and other alkenes conjugated to an electron withdrawing group,[61-63] the autodimerization of ketenes to give cyclobutane-1,3-diones,[64] and the reaction of ketenes with dienes to give cyclobutanones (Figure 4.4, A and B).[65-67] [2+2] reactions with allenes and ketenes remain one of the most popular ways to create four membered rings in total synthesis.[57, 68-70]

Like photochemical [2+2] reactions, most thermal [2+2] cycloadditions were racemic or depended on substrate control to induce chirality. In a 1984 review, asymmetric thermal syntheses of cyclobutanes consisted predominantly of the reactions of chiral allenes with various alkenes and ketenes.[71] However, developments in chiral auxiliary chemistry, combined with Lewis acid catalysis, led to new methods for chiral cyclobutane synthesis. Thermal [2+2] cycloadditions are highly amenable to Lewis or Bronsted acid catalysts which work by further polarizing double bonds and stabilising the charged reaction intermediates.[15,56] Early examples included the reaction of chiral

oxazolidone-fused lactam with ketene dithioacetal using dimethylaluminum chloride as a catalyst, which gives chiral cyclobutanopyrrolidinones after a two-step cleavage of the oxazolidinone auxiliary,[72] and the reaction of dimenthylfumarate with 1,1-dimethoxy ethene using diethylaluminum chloride to give a cyclobutanone that was used in the synthesis of antiviral and DNA polymerase inhibiting lubocavir (Figure 4.4, C and D).[73]

The use of chiral Lewis acids, as opposed to chiral auxiliaries, has also emerged as a strategy for the catalysis of asymmetric thermal [2+2] reactions. The first enantioselective cycloaddition using a chiral catalyst was reported in 1989 by Narasaka and Hayashi and featured the reaction of ketene dithioacetals with various oxazolidine enamides using titanium-TADDOLate as a catalyst, with subsequent studies exploring the use of thioalkenes, thioalkynes, and enamines as 2π donors (Figure 4.5, A).[74-77] Other examples include the titanium-TADDOLate catalyzed reaction of p-benzoquinones
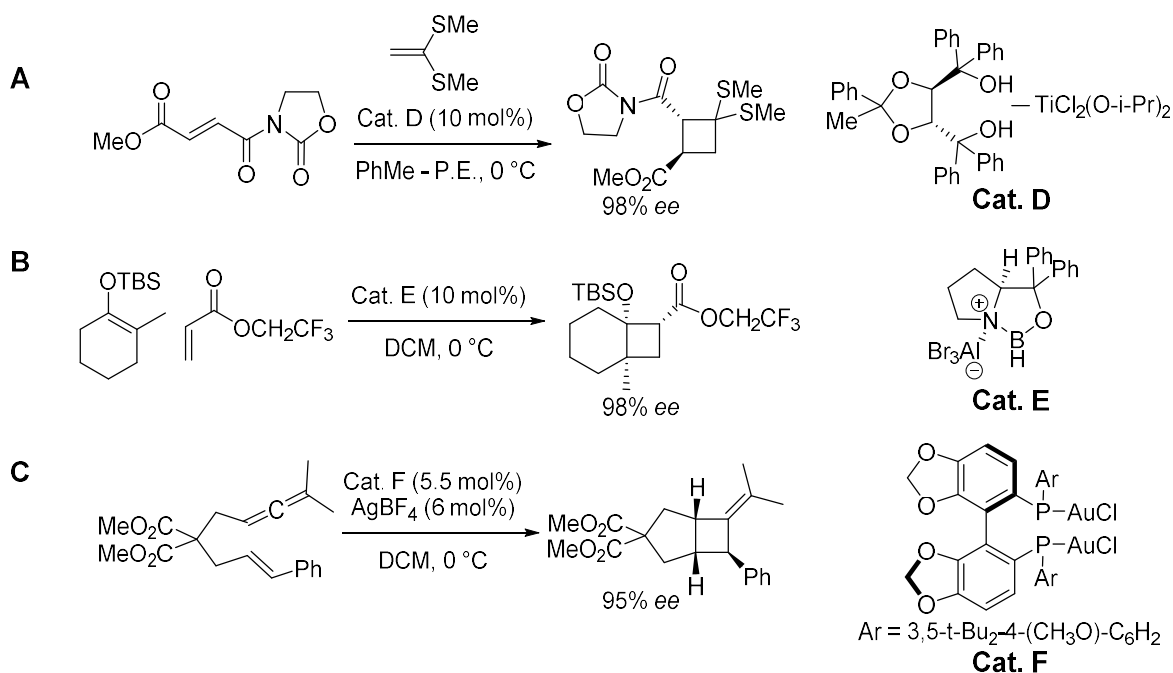
FIGURE 4.5 Representative asymmetric [2+2] cycloadditions using chiral Lewis acid catalysts. The use of chiral Lewis acid catalysts in thermal [2+2] cycloadditions is recognized as one of the best ways to construct chiral cyclobutanes, offering access to more diverse structures than are available through related photochemical reactions. The catalysts used in such reactions are also more diverse and include chiral titanium (A), aluminum (B) and gold (C) species.

and electron-rich styrenyl systems,[78,79] and the [2+2] cycloaddition of cyclic silylenol ethers and benzyloxyacroleins catalyzed by an oxazaborolidine-aluminium bromide complex (Figure 4.5, B).[80] The use of π-philic chiral cationic gold catalysts for the [2+2] reaction of allenes with various electron rich alkenes has also become a useful method for cyclobutane synthesis in the last decade, first demonstrated by Toste *et al.* in 2007 for the intramolecular cyclization of allenenes (Figure 4.5, C).[81-83]

The number of chiral catalytic approaches to thermal [2+2] cycloadditions continues to grow, and in general offer significant synthetic advantages over related photochemical reactions. However, when compared to the number of strategies for the synthesis of larger carbocycles, it is obvious that there is still significant need for new cyclobutane syntheses. Fortunately, developments in newer fields of asymmetric synthesis, for example organocatalysis, have begun to offer novel methods for accessing chiral cyclobutanes.

4.3 Organocatalytic [2+2] cycloadditions

Since MacMillan's seminal work describing the first organocatalytic Diels-Alder reaction in 2001, the number of reported organocatalytic cycloadditions has blossomed. However, in the decade following, during the "Golden Age" of organocatalysis, there was only one report of an organocatalytic [2+2] cycloaddition, wherein a chiral triamine (Cat. G) was used to catalyze the reaction between acyloxyacroleins and relatively unactivated alkenes (Figure 4.6).[84] Despite the slow start in discovering
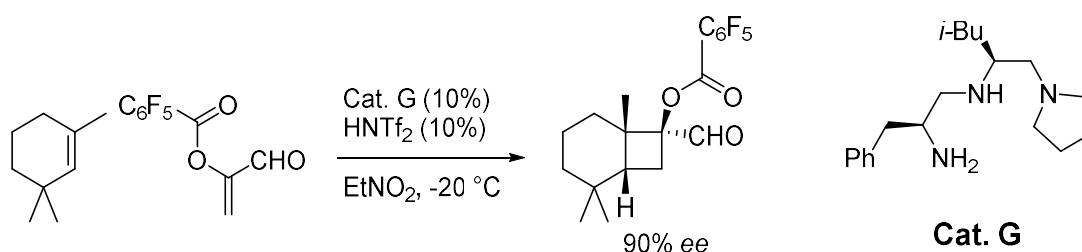
FIGURE 4.6 First organocatalytic [2+2] cycloaddition. The use of a peptide inspired primary amine catalyst based on Phe-Ile-Pro enabled the asymmetric [2+2] reaction between acyloxyacroleins and alkenes, giving cyclobutanes in up to 90% *ee*.
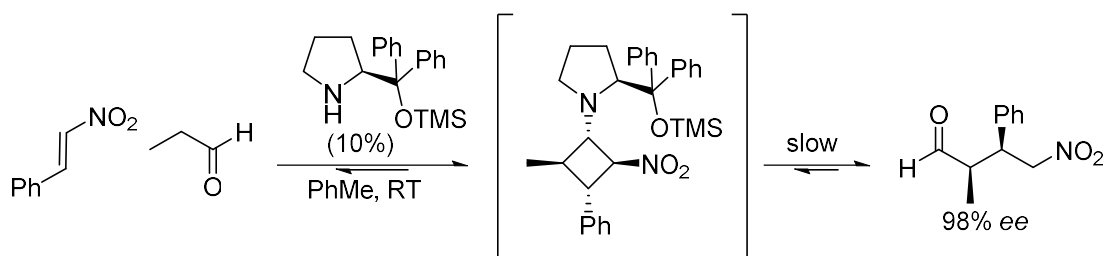
FIGURE 4.7 Cyclobutanes form readily under organocatalytic conditions. The organocatalytic Michael addition of aldehydes to nitrostyrenes proceed via a semi-stable cyclobutane intermediate.

organocatalytic cyclobutane syntheses, it has been known since the early 1960s that enamines undergo [2+2] cycloadditions with α,β-unsaturated carbonyls, such as methyl propiolate.[85] As well, it was previously determined that enamines participate in chiral Lewis acid catalyzed [2+2] cycloadditions (*vide supra*).

In 2011, several mechanistic studies demonstrated that the organocatalytic Michael addition of aldehydes to nitroalkenes using the Jørgensen-Hiyashi diarylsilaprolinol catalyst (Cat. H) proceeds through a semi-stable cyclobutane intermediate, and that the cyclobutane adduct corresponds to the resting state of the catalyst *in situ* (Figure 4.7).[86-88] Inspired by these results, Vicario *et al.* designed a methodology wherein enolizable α,β-unsaturated aldehydes underwent a [2+2] cycloaddition to nitroolefins (Figure 4.8, A).[89] Their method employed dual catalysis: Cat. H was used to form a dienamine from the enal, and a hydrogen bonding thiourea catalyst (Cat. I) was added to coordinate the nitro group and further activate the olefin to attack. Simultaneously, the Jørgensen group developed a similar methodology, but used a bifunctional catalyst (Cat. J) containing a secondary amine for activation of the enal and a pendant squaramide for hydrogen bonding to the nitroolefin (Figure 4.8, B).[90] Later, Qi *et al* developed a similar methodology for the addition of enolizable enals to methyleneindolinones using a Jørgensen-type catalyst (Cat. K) to give cyclobuta-spirooxindoles (Figure 4.8, C).[91] Notably, in the above dienamine-based methodologies, addition consistently occurred at the 3,4-position despite the possibility for 1,2-activation and terminal [4+2] reactions.
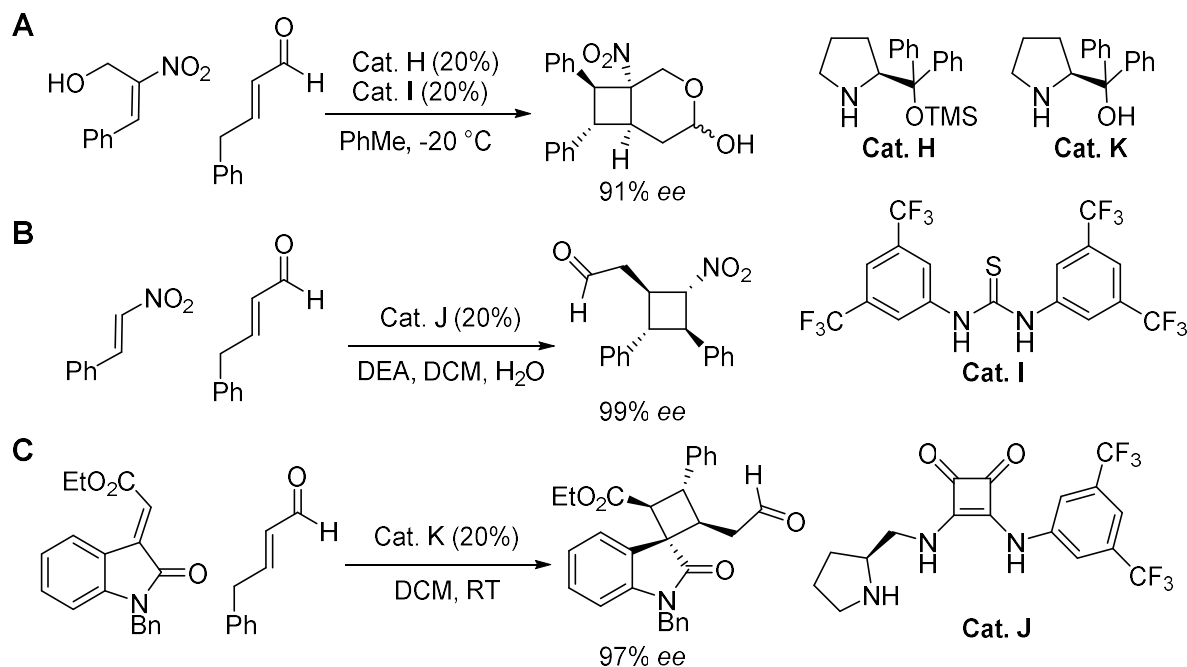
FIGURE 4.8 Organocatalytic [2+2] cycloadditions via dienamine formation. Organocatalytic [2+2] reactions have been developed for the addition of dieneamines to a variety of electron poor alkenes, including nitroolefins (A and B) and methyleneindolinones (C).

Most of the asymmetric organocatalytic [2+2] methodologies developed to date proceed via dienamine formation and addition to an electron poor alkene. An exception to this was demonstrated by Xu *et al.* who developed a [2+2] cycloaddition between non-enolizable α,β-unsaturated aldehydes and vinyl-pyrroles that proceeded via iminium activation of the enals with Cat. H (Figure 4.9).[92] This result is unique, as several studies demonstrate that using structurally related 2- and 3-vinylindoles in organocatalytic reactions give exclusively [4+2] adducts.[93-97]
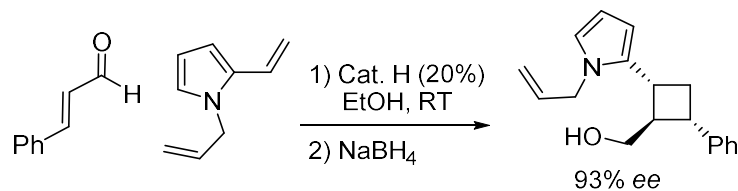
FIGURE 4.9 Organocatalytic [2+2] cycloaddition via iminium formation. Organocatalytic [2+2] cycloadditions can also proceed via iminium formation and attack by an electron rich olefin.

Despite interest in developing asymmetric [2+2] cycloadditions via Lewis acid catalyzed, photochemical, organocatalytic and other methods, the number of methods reported to date pales in comparison to the number of asymmetric [3+2], [4+2] and related cycloadditions. As such, there is still a need for the development of novel strategies for the preparation of chiral cyclobutanes. In order to expand the scope of cyclobutane synthesis and further the McNulty group's interest in organocatalysis, a novel method for the preparation of homochiral cyclobutanes from phenylpropanoid derivatives was developed. This work was published in *Chem. Eur. J.*, 2016, *22*, 9111-9115 and is reproduced below with permission; figures were formatted to be in sequence with the rest of the chapter. A. J. Nielsen developed the method and performed all syntheses. H. A. Jenkins performed the X-ray crystallography to determine absolute configuration, and the manuscript was written by A. J. Nielsen and J. McNulty.

4.4 Asymmetric Organocatalytic Stepwise [2+2] Entry to Tetrasubstituted Heterodimeric and Homochiral Cyclobutanes

The synthesis of cyclobutane derivatives has risen in prominence over the last few years in view of an increased recognition of their importance within bioactive natural products, with well over 200 derivatives now known.[1] In addition, cyclobutanes are often used as synthetically useful, strained intermediates. Classical alkylation and photochemical routes to achiral cyclobutanes including solid-state photochemistry[2] have been supplemented[3] with novel methods involving step-wise, thermal [2+2]-cycloaddition reactions mediated by transition metals,[4] organocatalysis,[5] and one-electron oxidants.[6] In addition to expanding the scope of alkene participants, these methods often allow for regio-controlled cycloaddition leading to non-symmetrical dimers and/or asymmetric entries to chiral cyclobutane derivatives.

Although many dimeric and pseudo-dimeric (non-symmetrical) naturally occurring cyclobutanes appear to be derived from the dimerization of cinnamyl, coumaryl, or extended diene amides, the precise enzyme responsible ("[2+2]-ase"),[7a] and hence mechanism of the biological dimerization is unknown. Nonetheless, for non-meso examples, such cyclobutanes may be homo-chiral, indicating the involvement of an enzymatic biosynthesis rather than a strictly abiotic photochemical or oxidative dimerization process. In addition, these cinnamic acid derivatives are known to dimerize through either ahead-to-head or ahead-to-tail alignment leading to regioisomeric cyclobutanes. Examples of head-to-head coupled cyclobutanes include piperarborenine D (Figure 4.10)[7a] and the iridoid argenteoside A,[7b] whereas head-to-tail derivatives are exemplified by dipiperamide A,[7c] nigramide P,[7d] dipiperamide E,[7e] and argenteoside B,[7b] among many others.[7] The argenteosides have recently been identified as potent inhibitors of heat shock protein 90 (Hsp90), a high-value therapeutic target, whereas dipiperamides A and B have potent activity against cytochrome P450 (CYP) 3A4.
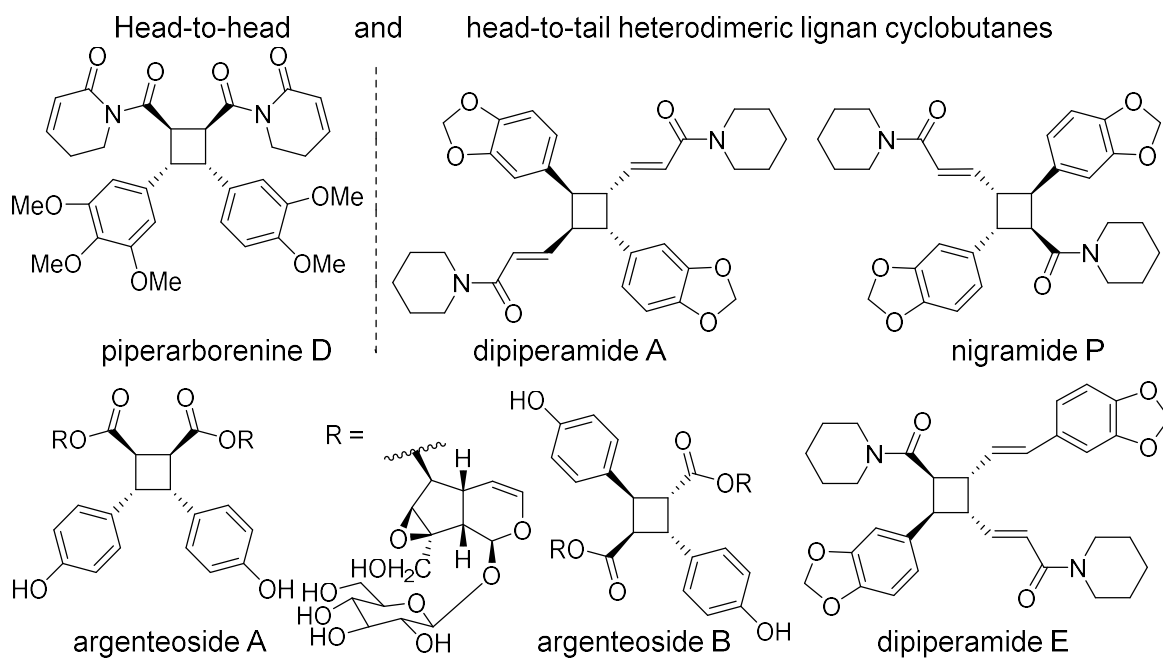
FIGURE 4.10 Structures of selected biologically active natural product cyclobutane-containing lignan-dimers including head-to-head (left) and head-to-tail (right) coupled derivatives.
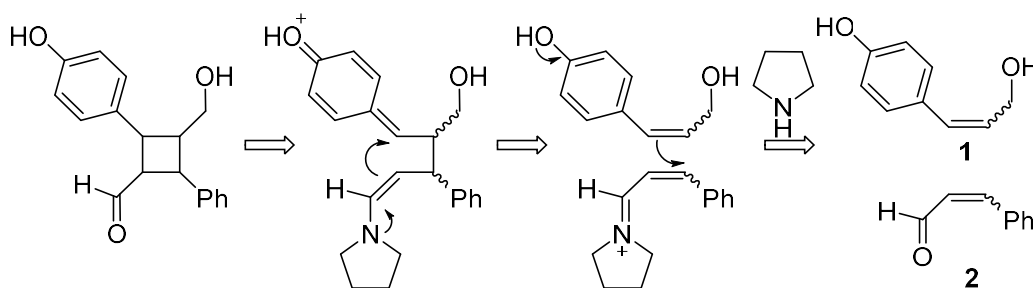
SCHEME 4.1 Retrosynthetic analysis of a heterodimeric cyclobutane derivative potentially available from dimerization of a cinnamaldehyde derivative **2** and cinnamyl alcohol **1** precursors.

Despite the number of approaches developed to access chiral cyclobutanes,[3] no process has been reported that permits direct asymmetric heterodimerization of two different cinnamyl-derived sub-units. The closest examples reported to date involve remote dienamine-mediated couplings of 3-vinyloxindoles,[5a] nitroolefins,[5c] and vinylpyrroles.[5f] The development of a direct asymmetric heterodimerization process would be of great utility given the valuable biological activities reported for these and other related non-symmetrical dimers, such as sceptrin,[8] and lignans that could be accessed through cyclobutane fragmentation.[2a] In this communication, we report the first examples of organocatalytic heterodimerization of two different cinnamyl-derived olefins in a regioselective and highly enantioselective fashion to yield tetra-substituted cyclobutanes.

A retrosynthetic analysis detailing the potential iminium-ion mediated cascade to access cyclobutanes is shown in Scheme 4.1. It was postulated that heterodimerization might be achieved through reaction of a cinnamaldehyde derivative with a cinnamyl alcohol as indicated. Activation of the olefin of cinnamyl alcohol **1** with a 4-hydroxyl group, for example, would direct the stepwise cycloaddition onto the iminium ion derived from **2** in a regioselective fashion. It should be noted that, although organocatalytic Friedel–Crafts reactions of phenols,[9] vinylogous electron-rich anilines,[10] and pyrroles[5f] onto Michael acceptors are known, in no case have two phenylpropanoid sub-units been converted to cyclobutanes through such a method.

TABLE 4.1 Catalyst and solvent screening for the organocatalytic [2+2] cycloaddition[a]

3a: R = H
3b: R = COOH
3c: R = (Ph, Ph, OH)
3d: R = (Ph, Ph, OTMS)
3e: R = (Ar, Ar, OTMS) Ar = 3,5-(CF$_3$)$_2$C$_6$H$_3$

Entry	Catalyst (x mol%)	Solvent	Time	Yield[b]	ee[c] (%)
1	**3a** (20)	THF	48 h	14	--
2	**3a** (20)	DMSO	48 h	26	--
3	**3a** (20)	DCM	48 h	30	--
4	**3a** (20)	Toluene	48 h	31	--
5	**3a** (20)	iPrOH	48 h	46	--
6	**3a** (20)	EtOH	48 h	53	--
7	**3a** (20)	MeOH	48 h	80	--
8	**3b** (20)	MeOH	48 h	n.r	--
9	**3c** (10)	MeOH	4 d	Trace	n.d
10	**3e** (10)	MeOH	4 d	Trace	n.d
11	**3d** (10)	MeOH	5 d	77	82
12[d]	**3d** (10)	MeOH	5 d	78	97

[a] Unless otherwise noted, reactions were performed on with **1a** (0.66 mmol), **2a** (1.00 mmol) with catalyst in 1.33 mL of solvent. Reactions using catalysts **3b**-**e** were performed on half scale. [b] Isolated % yield of the cyclobutane aldehyde. [c] Enantiomeric excess (*ee*) was determined on the reduced cyclobutanol employing chiral HPLC analysis. [d] Reaction performed at 8 °C without stirring. n.r. = no reaction. n.d. = not determined.

We began this investigation with attempts to engage isoeugenol **1a** in reaction with cinnamaldehyde **2a** in the presence of the achiral secondary amine pyrrolidine **3a** at room temperature in THF (Table 4.1, entry 1). We identified that a [2+2]-cycloadduct was being formed slowly, and isolated *rac*-**4a** in 14% yield. A solvent screen (Table 4.1, entries 1–7) demonstrated a strong preference for polar protic solvents, with methanol being identified as the ideal solvent in a process that provided the cyclobutane *rac*-**4a** as a single diastereomer in 80% isolated yield. We next explored asymmetric induction using l-proline **3b** and several versions of the common diarylsilylprolinol (Jørgensen-type)

catalysts (**3c–e**). Interestingly, no product was detected using l-proline (Table 4.1, entry 8) and only trace amounts of the cyclobutane were detected using the free diphenylprolinol **3c** or the second generation Jørgensen catalyst **3e**, even on extended reaction times (Table 1, entries 9 and 10).

Nonetheless, to our delight, the (2*S*)-diarylsilylprolinol catalyst **3d** proved to be highly efficient, giving the desired product in 77% isolated yield and with 82% *ee* (Table 4.1, entry 11). The enantioselectivity of the reaction was also significantly improved by cooling to 8 °C (refrigerator) for the duration of the reaction. This process yielded essentially a single enantiomer without any decrease in the isolated yield (Table 4.1, entry 12). The *ee* of the cyclobutane **4a** was determined using chiral HPLC analysis of the alcohol **5a** in direct comparison to *rac*-**5a** prepared using pyrrolidine as catalyst.

The structure of the isolated cyclobutane **4a** was initially deduced through 1- and 2-D ^{1}H NMR analysis, through which the stereochemistry appeared to be all-trans. We hoped to confirm this result as well as to ascertain the absolute stereochemistry of the reaction mediated by secondary amine **3d** through X-ray analysis of a suitable derivative. The reaction of isoeugenol **1a** was repeated using 4-bromocinnamaldehyde, and the resulting cycloadduct **4c** converted to its crystalline semicarbazone **6** (Figure 4.11). Single-crystal X-ray diffraction analysis confirmed the structure, the crystals proved to be homochiral, and the absolute stereochemistry **6** was defined as shown (Figure 4.11).
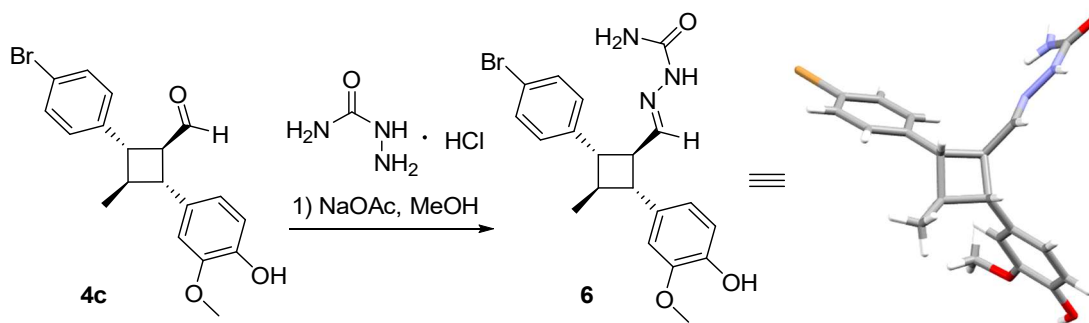
FIGURE 4.11 Structure and absolute stereochemistry of the cyclobutane adduct from the [2+2] cycloaddition of 4-bromocinnamaldehyde and isoeugenol as determined via the semicarbazone (CCDC 1456076; see ref. [14]).

While optimizing the conditions for the asymmetric catalysis, we discovered that the [2+2] cycloaddition is in fact thermally reversible and subject to an interesting dynamic kinetic resolution. When purified racemic **4a** was stirred with catalyst **3d** in methanol at room temperature for several days, partial reformation of starting materials was noted. Re-isolation and analysis of **4a** showed enantioenrichment of the product in favor of the opposite enantiomer ent-**4a** (23% *ee*), produced using catalyst **3d**. This result is readily explained by the process of microscopic reversibility, with catalyst **3d** favoring the lower energy retro-cycloaddition pathway available. The cycloaddition is therefore forward-driven under kinetic conditions by enthalpic considerations (formation of two sigma bonds) but reversible thermodynamically at higher temperatures. The cyclobutane aldehyde **4a** can readily be isolated and handled under normal conditions but should be prevented from re-establishing an iminium ion mediated cycloreversion.

The scope of the reaction was next investigated using isoeugenol **1a** in reaction with a variety of aromatic α,β-unsaturated aldehydes **2** (Table 4.2, A). The desired alkenals were readily prepared using our recently described two-carbon homologation reagent.[11] To avoid cycloreversion, the aldehydes were immediately reduced after the cycloaddition reaction was complete. The cyclobutane adducts were obtained in good yields (66–80%) and very high *ee* values (91–98%) with either electron donating or electron withdrawing substituents on the alkenal **2**, which was also successful with *ortho*, *meta*, or *para* substituents.

We next explored the reaction of cinnamaldehyde **2a** with several different electron rich alkenes to probe the donor requirements of the reaction (Table 4.2, B). Whereas isoeugenol **1a** was used successfully in many examples, its corresponding methyl ether methylisoeugenol **1b** did not produce a cycloadduct, demonstrating that a free phenol is required for the donor to enter into the organocatalytic [2+2] cascade. Most importantly, in view of access to the natural cinnamyl-derived cyclobutanes, the reaction of cinnamaldehyde proved highly successful with coniferyl alcohol **1c**,

TABLE 4.2 Scope and selectivity of the organocatalytic [2+2] cycloaddition reaction (isolated yield, ee).

A) Reaction of 1a with acceptor α,β-unsaturated aldehydes.

5a (78%, 98% ee)	**5b** (78%, 98% ee)	**5c** (80%, 98% ee)	**5d** (66%, 95% ee)	**5e** (74%, 96% ee)	**5f** (66%, 91% ee)
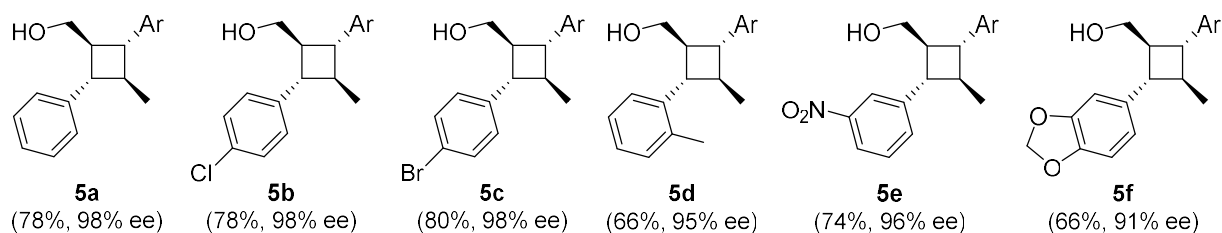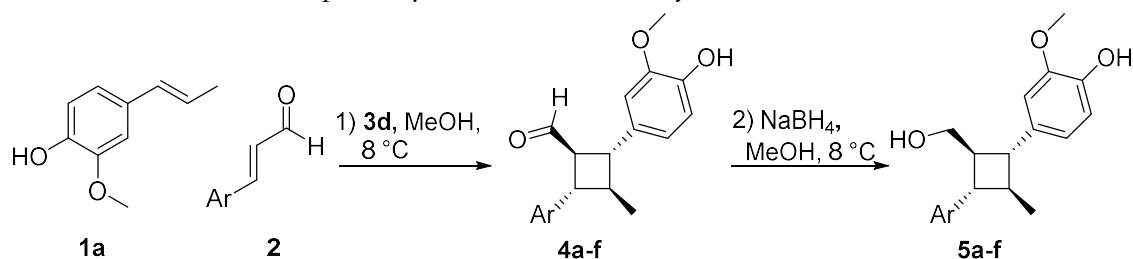
Ar = 4-hydroxy-3-methoxyphenyl

B) Reaction of cinnamaldehyde with other donor alkenes.
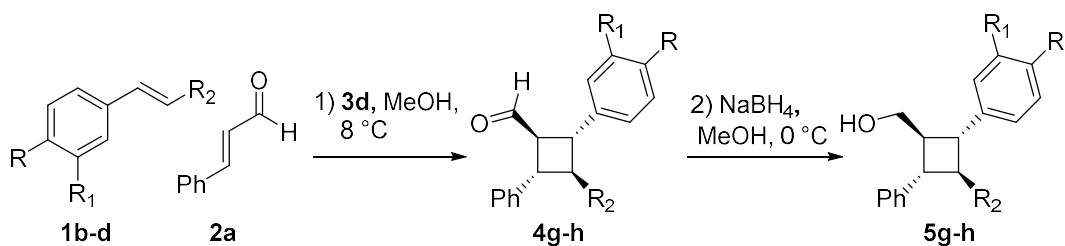
1b: R = R$_1$ = OMe, R$_2$ = Me **1c**: R = OH, R$_1$ = OMe, R$_2$ = CH$_2$OH **1d**: R = OH, R$_1$ = H, R$_2$ = CH$_2$CH$_3$

n.r   **4g** (77%, 99% ee)   **5h** (45%, 97% ee)
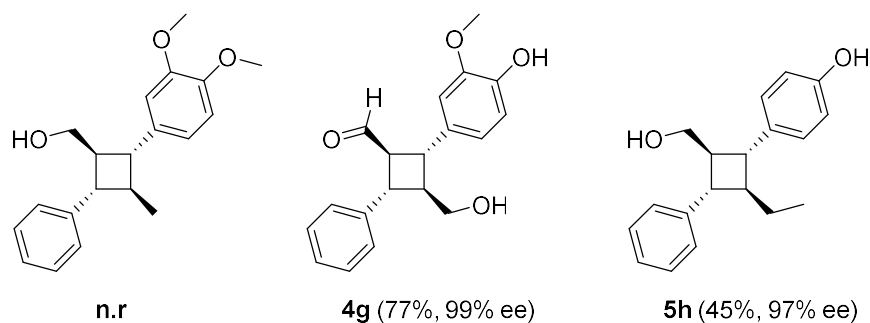
Unless otherwise noted, reactions were performed on with **1** (0.33 mmol), **2** (0.50 mmol) with catalyst **3d** (0.1 eq.) in 0.66 mL of MeOH, over 5 days at 8 °C. Yields are reported of the cyclobutane aldehyde. ee was determined using the reduced cyclobutanes using HPLC analysis. **4g** was benzoylated prior to reduction to avoid production of a meso diol. n.r = no reaction.

giving rise to the cyclobutane **4g** in 77% isolated yield as essentially a single enantiomer. Hence, the method allows for the catalytic asymmetric head-to-tail dimerization of a cinnamaldehyde derivative with a cinnamyl alcohol permitting access to heterodimeric cyclobutane carboxaldehydes (*vide infra*). The reaction was also successful employing (*E*)-1-(4'-hydroxyphenyl)-1-butene **1d**, yielding the corresponding cycloadduct **5h** (after reduction). Overall, the results show that a conjugated free-phenolic substituent is required to activate the electron-rich donor olefin for successful engagement in the reaction, and that the reaction works well with a wide variety of cinnamaldehyde derivatives **2**.

A selection of transformations was developed to investigate applications while retaining chirality on the heterodimeric cyclobutane **4g** (Scheme 4.2). Direct reduction of **4g** would lead to a meso-triol (not shown), however **4g** could be converted to the bis-benzoate **7**, allowing reduction of the aldehyde to yield the cyclobutamethanol **8**. Chiral HPLC analysis of **8** demonstrated that homochirality was maintained through this tightrope of reactions (Scheme 4.2, ii and iii).
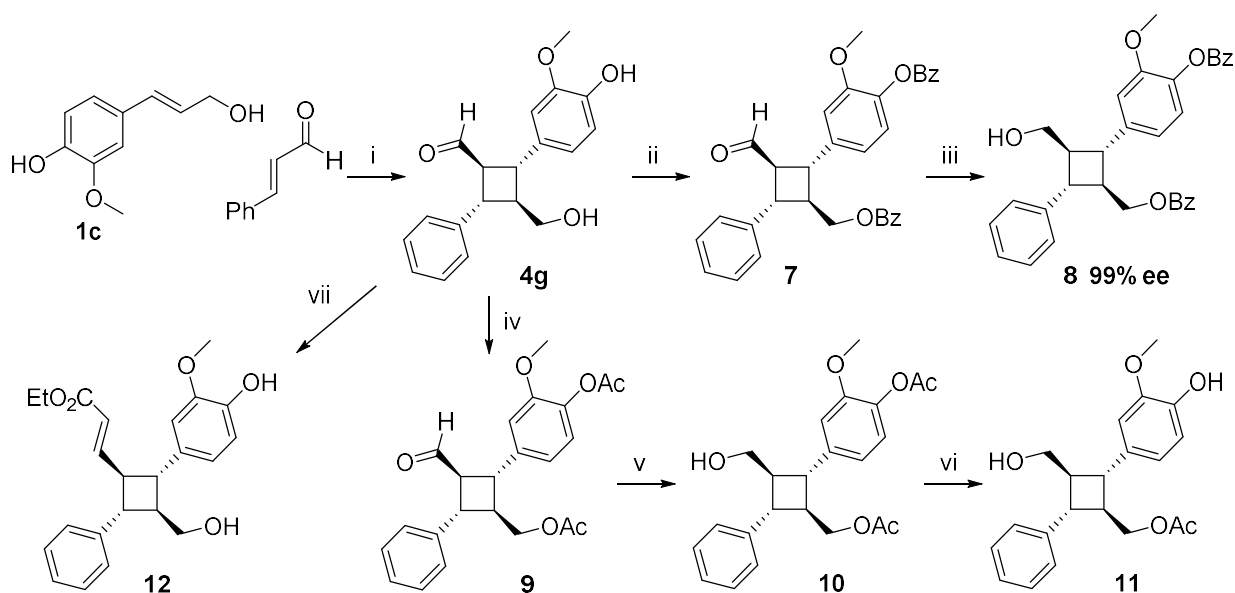
SCHEME 4.2 Selective manipulations of **4g**. i: 3d (0.1 eq), MeOH, 8 °C, **5d**, 77%. ii: Benzoyl chloride (2.2 eq), 4-dimethylaminopyridine (0.1 eq), diisopropylethylamine, CH$_2$Cl$_2$, 58%. iii: NaBH$_4$ (1.0 eq), EtOH, 95%. iv: acetyl chloride (2.2 eq), 4-dimethylaminopyridine (0.1 eq), diisopropylethylamine, CH$_2$Cl$_2$, 50%. v: NaBH$_4$ (1.0 eq), MeOH, 20 min, 90%. vi: NaBH$_4$ (5 eq), MeOH, 8 h (90%). vii: (ethoxycarbonylmethyl)triisobutylphosphonium bromide (3.0 eq), KOtBu (3.0 eq), THF, 0 °C – rt, 1 h, 75%.

In addition, rac-**4a** was readily converted to the diacetate **9**, reduction of which led quickly to the diacetoxy alcohol **10**. We also discovered that reaction of **9** or **10** with excess sodium borohydride led to the reductive cleavage of the ortho-methoxy acetate, most likely through a chelation-assisted pathway. This reaction yields the free phenol derivative **11**, an intermediate that appears suitable for one-electron oxidative fragmentation reactions.[2a] Finally, reaction of *rac*-**4g** with the ylide derived from (ethoxycarbonylmethyl)triisobutylphosphonium bromide, gave the two-carbon extended ester **12**, analogous to natural products such as nigramide P (Figure 4.10).

It is important to note that the two-step sequence of i followed by vii (Scheme 4.2) opens a controlled access to vinyl-cyclobutanes, avoiding possible [4+2]-type adducts[7d] that often co-occur with the natural cyclobutanes.
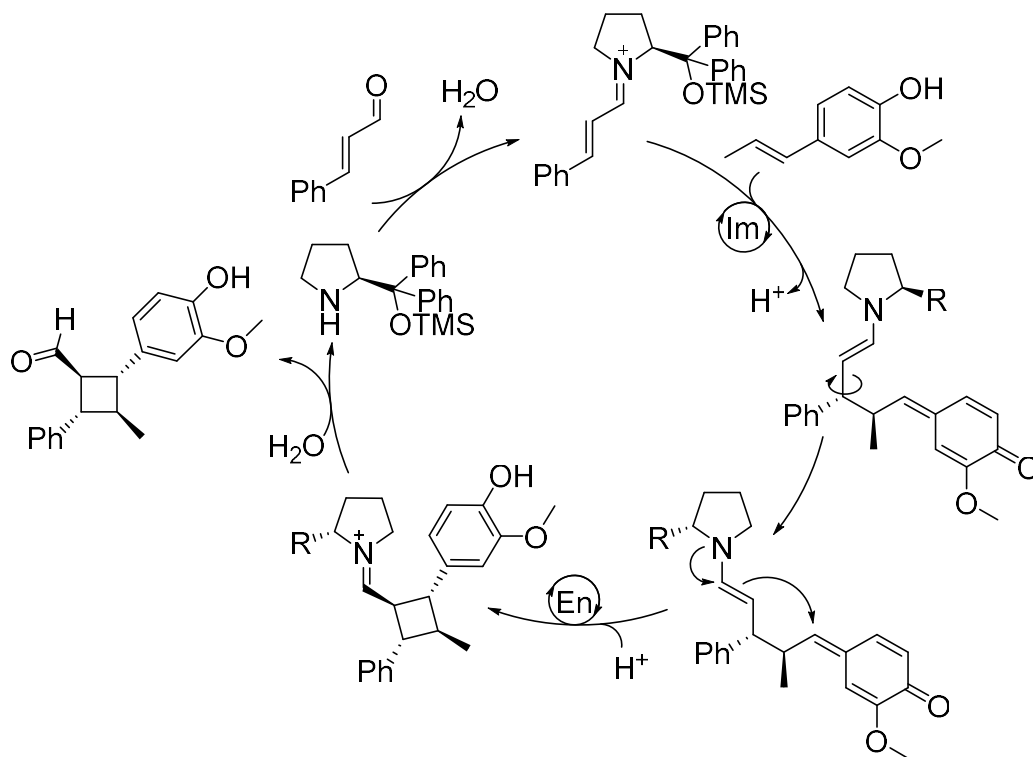
FIGURE 4.12 Proposed catalytic cycle and absolute stereochemical configuration of cyclobutane derivatives.
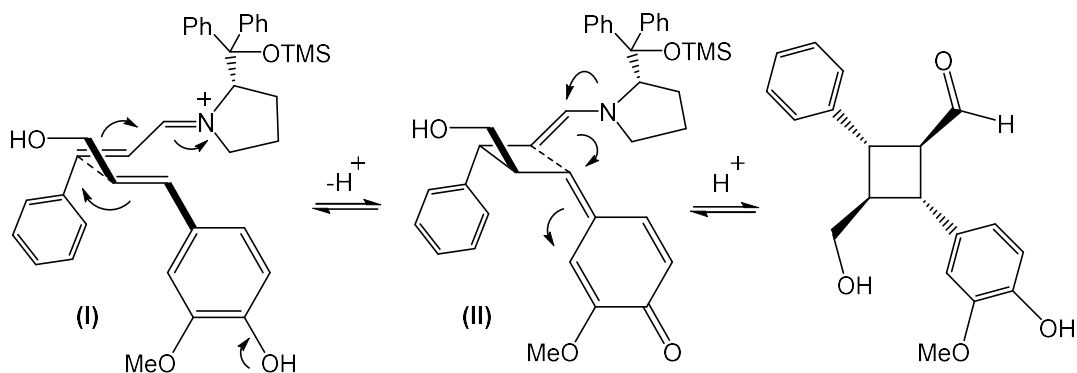
FIGURE 4.13 Transition-state assembly using catalyst **3d** leading to the product of absolute stereochemistry shown in Figure 4.11.

From a mechanistic perspective, we were able to successfully conduct the stepwise [2+2]-reaction of **1a** with **2a** using pyrrolidine **3a** catalysis either in the dark or in the presence of 5 mol% 4-tertbutylcatechol indicating that neither photochemical nor oxidative processes are involved. In conjunction with the very high *ee* values observed, the evidence indicates that the reaction proceeds through a stepwise formal [2+2] using tandem iminium-enamine catalysis (Figure 4.12).

The stereochemistry of the reaction is rationalized through the transition-state assembly depicted in Figure 4.13 using catalyst **3d**. The donor substituent (most likely the phenoxide anion) attacks the least hindered *Si*-face of the iminium ion (Figure 4.13, (I)) with the diarylprolinol substituent placed distal allowing an overall *anti*-periplanar HOMO–LUMO alignment for the first step of the cascade. The model shows that a strong possibility exists for stabilising face or edge-on π–π secondary orbital interactions in this assembly. The enamine (II) now closes the cyclobutane ring by adding on to the *p*-quinomethide intermediate, with iminium hydrolysis completing the cascade.

In conclusion, we report the discovery of novel organocatalytic methodology for the asymmetric synthesis of highly functionalized chiral cyclobutanes in a regiospecific manner from α,β-unsaturated aldehydes and alkenylphenols. The process yields heterodimeric head-to-tail coupled cyclobutanes in good yield and with excellent enantioselectivity.

A selection of transformations on the cyclobutane carboxaldehyde **4g** have been developed to showcase the potential of this method to access chiral synthetic intermediates and adducts suitable for fragmentation reactions or conversion to natural product-containing cyclobutanes and analogues. Finally, the ease with which these strained tetrasubstituted cyclobutanes are formed under iminium-ion catalysis opens another consideration regarding the nature of the [2+2]-ase,[7a] which could lead to such natural products under non-oxidative and non-photoinduced conditions. As novel methods for the synthesis of cyclobutanes are actively sought,[3] the present discovery highlights a widening gap in comparison to classic approaches to "tetramethylene" carboxylates[12] and cyclobutane itself,[13] in terms of reaction yield, regio-control, and now one-step asymmetric entry to these intermediates. Our group is actively exploring umpoled variations of the chemistry to access head-to-head dimers as well as applications in total synthesis.

Acknowledgments

Notes and References

1) V. M. Dembitsky, *J. Nat. Med.* 2007, *62*, 1–33.

2) a) A. K. F. Albertson, J.-P. Lumb, *Angew. Chem. Int. Ed.* 2015, *54*, 2204 –2208; *Angew. Chem.* 2015, *127*, 2232–2236; b) M. A. Ischay, M. E. Anzovino, J. Du, T. P. Yoon, *J. Am. Chem. Soc.* 2008, *130*, 12886–12887; c) M. D. Cohen, G. M. J. Schmidt, *J. Chem. Soc.* 1964, 2000–2013.

3) For a recent, comprehensive mini-review, see: Y. Xu, M. L. Coner, M. K. Brown, *Angew. Chem. Int. Ed.* 2015, *54*, 11918–11928; *Angew. Chem.* 2015, *127*, 12086–12097.

4) a) J. M. Hoyt, V. A. Schmidt, A. M. Tondreau, P. J. Chirik, *Science* 2015, *349*, 960–963; b) Y.-J. Chen, T.-J. Hu, C.-G. Feng, G.-Q. Lin, *Chem. Commun.* 2015, *51*, 8773–8776; c) Y. Wang, Z. Zheng, L. Zhang, *Angew. Chem. Int. Ed.* 2014, *53*, 9572–9576; *Angew. Chem.* 2014, 126, 9726–9730.

5) a) L.-W. Qi, Y. Yang, Y.-Y. Gui, Y. Zhang, F. Chen, F. Tian, L. Peng, L.-X. Wang, *Org. Lett.* 2014, *16*, 6436–6439; b) N. Vallavoju, S. Selvakumar, S. Jockusch, M. P. Sibi, J. Sivaguru, *Angew. Chem. Int. Ed.* 2014, *53*, 5604–5608; *Angew. Chem.* 2014, *126*, 5710–5714; c) L. Albrecht, G. Dickmeiss, F. C. Acosta, C. Rodriguez-Escrich, R. L. Davis, K. A. Jørgensen, *J. Am. Chem. Soc.* 2012, *134*, 2543–2546. For two recent reviews, see: d) H. Jiang, L. Albrecht, K. A. Jørgensen, *Chem. Sci.* 2013, *4*, 2287–2300; e) I. D. Jurberg, I. Chatterjee, R. Tannert, P. Melchiorre, *Chem. Commun.* 2013, *49*, 4869–4883; f) G.-J. Duan, J.-B. Ling, W.-P. Wang, Y.-C. Luo, P.-F. Xu, *Chem. Commun.* 2013, *49*, 4625–4627.

6) I. Colomer, R. C. Barcelos, T. J. Donohoe, *Angew. Chem. Int. Ed.* 2016, *55*, 4748–4752; *Angew. Chem.* 2016, *128*, 4826–4830; b) M. Riener, D. A. Nicewicz, *Chem. Sci.* 2013, *4*, 2625–2629.

7) a) W. R. Gutekunst, P. S. Baran, *J. Am. Chem. Soc.* 2011, *133*, 19076–19079; b) F. D. Piaz, A. Vassallo, A. Temraz, R. Cotugno, M. A. Belisario, G. Bifulco, M. G. Chini, C. Pisano, N. De Tommasi, A. Braca, *J. Med. Chem.* 2013, *56*, 1583–1595; c) M. Takahashi, M. Ichikawa, S. Aoyagi, C. Kibayashi, *Tetrahedron Lett.* 2005, *46*, 57–59; d) K. Wei, W. Li, K. Koike, Y. Chen, T. Nikaido, *J. Org. Chem.* 2005, *70*, 1164–1176; e) S. Tsukamoto, K. Tomise, K. Miyakawa, B.-C. Cha, T. Abe, T. Hamada, H. Hirota, T. Ohta, *Bioorg. Med. Chem.* 2002, *10*, 2981–2985; f) S. Tsukamoto, B.-C. Cha, T. Ohta, *Tetrahedron* 2002, *58*, 1667–1671; g) R. Muharini, Z. Liu, W. Lin, P. Proksch, *Tetrahedron Lett.* 2015, *56*, 2521–2525.

8) Z. Ma, X. Wang, X. Wang, R. A. Rodriguez, C. E. Moore, S. Gao, X. Tan, Y. Ma, A. L. Rheingold, P. S. Baran, C. Chen, *Science* 2014, *346*, 219–224.

9) S. Bai, X. Liu, Z. Wang, W. Cao, L. Lin, X. Feng, *Adv. Synth. Catal.* 2012, *354*, 2096–2100.

10) A. R. Philipps, L. Fritze, N. Erdmann, D. Enders, *Synthesis* 2015, *47*, 2377–2384.

11) a) J. McNulty, C. Zepeda-Velazquez, D. McLeod, *Green Chem.* 2013, *15*, 3146–3149; b) J. McNulty, C. Zepeda-Velazquez, *Angew. Chem. Int. Ed.* 2014, *53*, 8450–8454; *Angew. Chem.* 2014, *126*, 8590–8594; c) J. McNulty, D. McLeod, H. A. Jenkins, *Eur. J. Org. Chem.* 2016, 688–692.

12) W. H. Perkin Jun., *J. Chem. Soc.* 1887, *51*, 1–28.

13) R. M. Willstätter, J. Bruce, *Ber. Dtsch. Chem. Ges.* 1907, *40*, 3979–3999.

15) CCDC 1456076 contains the supplementary crystallographic data for this paper. These data can be obtained free of charge from The Cambridge Crystallographic Data Centre.

4.5 Preliminary biological activity of cyclobutane derivatives and future work

As part of the McNulty group's collaboration with the Stanley Medical Research Institute, several of the racemic cyclobutane (**5a**, **5b**, **5f**) derivatives described above were screened against a wide range of viruses through the National Institute of Allergy and Infectious Diseases (NIAID). In general, the compounds showed only moderate activity and poor selectivity (most potent activities shown in Table 4.3). Where not inactive, the anti-viral activities were confounded by similar levels of toxicity to the host cell line. Thus, reduction in viral replication was more likely due to cell death as opposed to any real antiviral effect of the compounds. The highest selectivity was seen for the Tacaribe virus, but the Selectivity Index (SI = CC_{50}/EC_{50}) was still quite low.
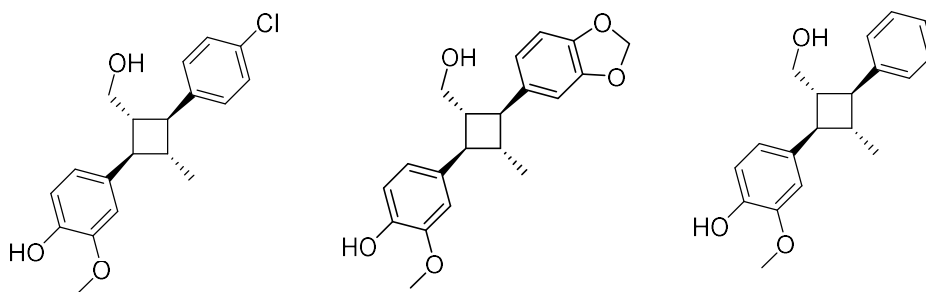
Virus (Cell line)	EC_{50}	CC_{50}	SI	EC_{50}	CC_{50}	SI	EC_{50}	CC_{50}	SI
Coxsackie Virus (Vero)	3.2	3.5	1.1	■	>10	<1	■	>10	<1
Hep C (Huh 7)	■	11.6	<1	■	>20	<1	■	>20	<1
Murine CMV (HFF)	17.2	23.4	1.36	■	54.2	<1	■	72.1	<1
Rift Valley Fever (Vero)	3.2	3.2	1	4.6	6.8	1.5	>10	>10	<1
Tacaribe Virus (Vero)	1	2.8	2.8	1.2	4.6	3.8	1.4	5.2	3.7
Ven. Equine Enceph. (Vero)	■	3.1	<1	■	7.1	<1	■	>10	<1

TABLE 4.3 Racemic cyclobutanes tested for antiviral activity in an NIAID screen. EC_{50} – compound concentration that reduces viral replication by 50%; CC_{50} – compound concentration that reduces cell viability by 50%. SI = CC_{50}/EC_{50}) All concentrations are in µM. Black box – no anti-viral effect.

While host cell toxicity reduces the utility of these compounds as antiviral agents, it was thought that this cytotoxicity might grant them anticancer properties. The McNulty Group sent a small library of compounds, including a sample of racemic cyclobutane **4a**, to be screened for activity against four different leukemia cell lines at the Ontario Institute for Cancer Research (OICR). The OICR screen demonstrated that **4a** possesses low micromolar IC_{50} values against human β-cell non-Hodgkin lymphoma (Karpas-422 and Toledo) and leukemia (K-562 and MV4-11) cell lines (Table 4.4). These initial results may warrant further exploration. Screening additional racemic cyclobutane aldehydes (**4**) and alcohols (**5**) would likely reveal even more potent anti-cancer compounds. Any hits from the racemates could be further optimized by screening each enantiomer separately, as one enantiomer may be significantly more active than the other. Thus, future work on this project could focus on further elaborating the cytotoxic properties of the novel cyclobutane derivatives accessed via organocatalytic [2+2] cycloaddition.
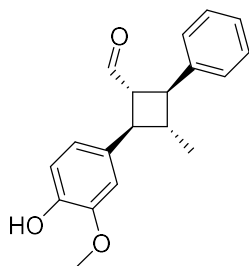
Cell line (cell type)	IC_{50} (µM)
Toledo (β lymphocyte)	14.7
Karpas-422 (β lymphocyte)	8.3
K-562 (lymphoblast)	5.3
MV4-11 (lymphoblast)	1.9

TABLE 4.4 Activity of racemic cyclobutane derivative **4a** against several cancer cell lines. IC_{50} – compound concentration that reduces cell proliferation by 50%.

4.6 Conclusions

The asymmetric [2+2] reaction described in this thesis represents one of very few organocatalytic methodologies for cyclobutane synthesis. As well, it builds upon the Wittig methodology discussed in Chapter 3 by demonstrating the synthetic utility of alkenyl phenols in asymmetric synthesis. This method is notable for its use of cheap and readily available catalysts, high diastereo- and enantioselectivity, and the ability to create four contiguous stereocenters in a single step. The cyclobutanes prepared using this method are also readily derivatized, containing several reactive functional groups upon which more complicated structures could be built. This fact should help any future work that is aimed at elucidating and improving the promising anti-cancer activity displayed by these compounds. Overall, this chapter best highlights the intersection of organocatalysis and the Wittig reaction, the two cornerstones of this thesis.

4.7 Experimental

This experimental is provided as published in *Chem. Eur. J.*, 2016, *22*, 9111-9115.

All reactions were carried out under nitrogen atmosphere in oven-dried flasks, unless otherwise stated. All fine chemicals were obtained from Sigma Aldrich. Tetrahydrofuran, toluene and N,N-diisopropylethylamine were distilled over sodium/benzophenone under nitrogen atmosphere. Methanol was distilled over magnesium turnings under nitrogen atmosphere. Dichloromethane was distilled over calcium hydride under nitrogen atmosphere. Reactions were monitored using thin layer chromatography (TLC) using Macherey-Nagel silica gel 60 F_{254} TLC aluminum plates and visualized with UV fluorescence and staining with 2,4-dinitrophenylhydrazine or vanillin stains. Bulk solvent removal was performed by rotary evaporation under reduced pressure. For reactions with solvent volumes under 3 mL, the solvent was evaporated under a stream of nitrogen. Column chromatographic purification was performed using Silicycle silica gel (40–63 µM, 230-400 mesh) with technical grade solvents. Yields are reported for spectroscopically pure compounds, unless stated otherwise.

Data Analyses

HRMS (EI) were performed with a Waters GCT and HRMS (ESI) were performed on a Waters QToF Global Ultima spectrometer. ^{1}H and ^{13}C NMR spectra were recorded on a Bruker AV 600 spectrometer in CDCl$_3$ with TMS as internal standard, chemical shifts (δ) are reported in ppm downfield of TMS and coupling constants (J) are expressed in Hz. Enantiomeric ratios were determined using an Agilent 1220 Infinity HPLC with manual injection and a variable wavelength detector, using a Chiralcel OD-H column; wavelength = 250 nm, flow rate 1.0 mL/min n-hexane/iPrOH (80:20) as mobile phase. Optical rotations were measured using a Perkin-Elmer 241 MC polarimeter. X-ray crystallographic analysis was performed by Dr. Hilary A. Jenkins at the McMaster Analytical X-Ray (MAX) Diffraction Facility.

Preparation of Starting Materials
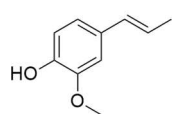
1a (*E*)-2-methoxy-4-(prop-1-en-1-yl)phenol (isoeugenol) was prepared following a procedure reported by Curti *et al*:[1] Eugenol (1.00 g, 6.10 mmol, 1.0 eq.) was dissolved in MeOH (40 mL) and the solution thoroughly degassed. Then, $PdCl_2$ (0.054 g, 0.31 mmol, 0.05 eq) was added and the solution was stirred vigorously under nitrogen atmosphere. After 24 h, NMR analysis of the crude mixture demonstrated essentially complete isomerization of the double bond. The mixture was then filtered over celite, concentrated under reduced pressure and the resulting oil flash chromatographed over silica gel (0-20% EtOAc/hexanes). The desired fractions were concentrated under reduced pressure to give the desired product in 90% yield as light-yellow oil that crystallizes upon refrigeration. ^{1}H NMR (600 MHz, $CDCl_3$) δ 6.86 – 6.80 (m, 3H), 6.31 (dq, *J* = 15.7, 1.7 Hz, 1H), 6.06 (dq, *J* = 15.7, 6.6 Hz, 1H), 5.52 (s, 1H, Ar-OH), 3.88 (s, 3H), 1.84 (dd, *J* = 6.6, 1.7 Hz, 3H). All data are in accordance with the literature.[1]
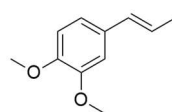
1b (*E*)-1,2-dimethoxy-4-(prop-1-en-1-yl)benzene (methylisoeugenol): Isoeugenol (0.238 g, 1.45 mmol, 1.0 eq.) and KOH (0.115 g, 2.03 mmol, 1.4 eq.) were combined in 3.0 mL DMSO and stirred for 1 hour at room temperature. Then, MeI (0.135 mL, 2.17 mmol 1.5 eq.) was added and the reaction was stirred overnight, after which complete consumption of the starting material was noted by TLC. The reaction was then quenched with 0.4 mL trimethylamine and stirred for a further 30 min. Then, 3.0 mL water was added, and the mixture was extracted with Et_2O (3 x 10 mL). The combined organic layers were dried over $MgSO_4$ and concentrated *in vacuo* to give the desired product in 98% yield as a yellow oil with no further purification necessary. ^{1}H NMR (600 MHz, $CDCl_3$) δ 6.91 – 6.82 (m, 2H), 6.79 (d, *J* = 8.2 Hz, 1H), 6.33 (dd, *J* = 15.7, 1.3 Hz, 1H), 6.10 (dq, *J* = 15.6, 6.6 Hz, 1H), 3.88 (s, 3H), 3.86 (s, 3H), 1.86 (dd, *J* = 6.6, 1.3 Hz, 3H). All data are in accordance with the literature.[2]
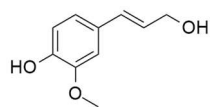
1c (*E*)-4-(3-hydroxyprop-1-en-1-yl)-2-methoxyphenol (coniferyl alcohol) was prepared following a procedure reported by Quideau and Ralph.[3] Ethyl ferulate (1.07 g, 4.77 mmol, 1.0 eq.) was dissolved in toluene (50 mL) and cooled to 0 °C in an ice-water bath. Then, diisobutylaluminum hydride (20 mL of 1.0 M solution in toluene, 4.2 eq.) was added dropwise to the mixture over 10 minutes. The reaction was allowed to stir for another hour and was then quenched with the slow addition of 5 mL EtOH. The mixture was partially concentrated under reduced pressure and mild warming (35 – 40 °C) in a rotary evaporator. Then water (25 mL) was added, resulting in the formation of a gelatinous precipitate that was filtered off and washed extensively with EtOAc (4 x 75 mL). The aqueous layer was discarded, and the combined organic extracts were dried over sodium sulphate and concentrated under reduced pressure to give the desired product in 92% yield as a white solid, which was stored at 8 °C. ^{1}H NMR (600 MHz, CDCl$_3$) δ 6.93 – 6.85 (m, 3H), 6.54 (dt, *J* = 15.8, 1.4 Hz, 1H), 6.22 (dt, *J* = 15.8, 6.0 Hz, 1H), 5.63 (s, 1H, Ar-OH), 4.30 (td, *J* = 6.0, 1.4 Hz, 2H), 3.91 (s, 3H). All data are in accordance with the literature.[3]
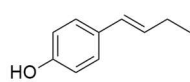
1d (*E*)-4-(but-1-en-1-yl)phenol) was prepared using a novel Wittig methodology that will be published shortly. Data are as follows: ^{1}H NMR (600 MHz, CDCl$_3$) δ 7.23 (d, *J* = 8.6 Hz, 2H), 6.76 (d, *J* = 8.6 Hz, 2H), 6.31 (d, *J* = 15.9 Hz, 1H, Ar-OH), 6.11 (dt, *J* = 15.9, 6.5 Hz, 1H), 4.72 (s, 1H), 2.24 – 2.18 (m, 2H), 1.07 (t, *J* = 7.5 Hz, 3H). ^{13}C NMR (151 MHz, CDCl$_3$) δ 154.6, 131.2, 130.8, 128.2, 127.3, 115.5, 26.2, 13.9. HMRS (ES$^-$) calc. for C$_{10}$H$_{11}$O [M-H]$^-$ 147.0810; found 147.0818.

α,β-unsaturated aldehydes (**2**) were prepared using the aqueous Wittig methodology developed by our group.[4] Yields and spectroscopic data were in agreement with the literature. 3-nitrocinnamaldehyde was not previously made using our aqueous methodology, but was prepared from (2,2-diethoxyethyl)tripropylphosphonium bromide and 3-nitrobenzaldehyde using an anhydrous Wittig methodology previously reported by our group.[5]
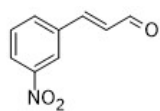
(*E*)-3-nitrocinnamaldehyde. 80% yield, tan solid. ^{1}H NMR (600 MHz, CDCl$_3$) δ 9.78 (d, *J* = 7.4 Hz, 1H), 8.42 (t, *J* = 1.9 Hz, 1H), 8.30 (ddd, *J* = 8.2, 2.2, 0.9 Hz, 1H), 7.89 (d, *J* = 7.7 Hz, 1H), 7.65 (t, *J* = 8.0 Hz, 1H), 7.54 (d, *J* = 16.1 Hz, 1H), 6.82 (dd, *J* = 16.1, 7.4 Hz, 1H). ^{13}C NMR (151 MHz, CDCl$_3$) δ 192.9, 149.1, 135.9, 133.7, 131.0, 130.4, 125.5, 123.2. HMRS (ES[-]) calc. for C$_9$H$_6$NO$_3$ [M-H][-] 176.0348; found 176.0340.

Preparation of Cyclobutanes via Organocatalytic Cascade Reaction
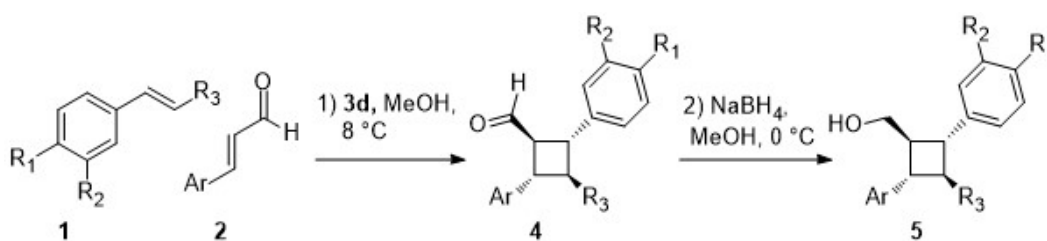
General conditions: To a solution of cinnamaldehyde **2** (0.50 mmol, 1.5 eq.) in MeOH (0.33 mL) was added catalyst **3d** (0.033 mmol, 0.1 eq) at 8 °C. Then, a solution of alkene **1** (0.33 mmol, 1.0 eq.) in MeOH (0.33 mL) was added, and the reaction mixture held at 8 °C for 5 days without stirring. Then, the reaction mixture was concentrated under a stream of nitrogen and the resulting crude oil purified using silica gel chromatography. Purity of the cyclobutane aldehyde was determined using ^{1}H NMR.

Most derivatives were stable at room temperature, but some derivatives could undergo decomposition if left in solution. As such, the aldehydes were immediately reduced using $NaBH_4$ (1.0 eq) in MeOH (5 ml/mmol aldehyde) at 0 °C. After 15 minutes, the reactions were quenched with 1 M HCl. The resulting mixtures were then extracted with DCM, concentrated under a stream of nitrogen or using rotary evaporation and the resulting resin was purified directly using silica gel chromatography. The resulting cyclobutane alcohols are stable at room temperature and were used to determine *ee* and optical rotation.
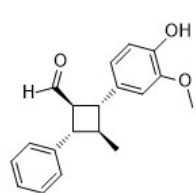
4a (1R,2R,3S,4S)-2-(4-hydroxy-3-methoxyphenyl)-3-methyl-4-phenylcyclobutane carbaldehyde. Yield: 78%, yellow oil. Chromatography: 0 – 25% EtOAc/hexanes. ^{1}H NMR (600 MHz, CDCl$_3$) δ 9.87 (d, *J* = 2.0 Hz, 1H), 7.35 (t, *J* = 7.6 Hz, 2H), 7.29 – 7.24 (m, 3H), 6.90 (d, *J* = 8.1 Hz, 1H), 6.80 (dd, *J* = 8.1, 1.8 Hz, 1H), 6.75 (s, 1H), 5.54 (s, 1H, Ar-OH), 3.90 (s, 3H), 3.28 (td, *J* = 9.5, 2.0 Hz, 1H), 3.21 (t, *J* = 9.4 Hz, 1H), 3.15 (t, *J* = 9.4 Hz, 1H), 2.56 (tq, *J* = 9.4, 6.5 Hz 1H), 1.30 (d, *J* = 6.5 Hz, 3H). ^{13}C NMR (151 MHz, CDCl$_3$) δ 201.5, 146.7, 144.7, 142.0, 133.9, 128.8, 127.0, 126.9, 119.5, 114.6, 109.7, 58.1, 56.1, 46.0, 45.9, 43.0, 19.5. HMRS (ES$^+$) calc. for C$_{19}$H$_{21}$O$_3$ [M+H]$^+$ 297.1491; found 297.1493.
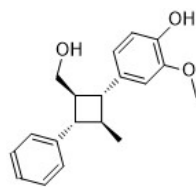
5a 4-((1R,2R,3S,4S)-2-(hydroxymethyl)-4-methyl-3-phenylcyclobutyl)-2-methoxy phenol. Yield: 95% from 4a, yellow oil. Chromatography: 20 – 40% EtOAc/hexanes. [α]$_D$ = +4.1 (c 1.73, CHCl$_3$, 97.5% ee). ^{1}H NMR (600 MHz, CDCl$_3$) δ 7.38 – 7.29 (m, 4H), 7.25 – 7.22 (m, 1H), 6.89 (d, *J* = 7.9 Hz, 1H), 6.83 – 6.80 (m, 2H), 5.57 (s, 1H, Ar-OH), 3.90 (s, 3H), 3.80 (br s, 2H), 2.76 (t, *J* = 9.4 Hz, 1H), 2.71 (t, *J* = 9.4 Hz, 1H), 2.59 – 2.53 (m, 1H), 2.32 (tq, *J* = 9.4, 6.5 Hz, 1H), 1.36 (s, 1H, OH), 1.25 (d, *J* = 6.5 Hz, 3H). ^{13}C NMR (151 MHz, CDCl$_3$) δ 146.6, 144.3, 143.4, 135.4, 128.6, 127.1, 126.4, 119.7, 114.5, 109.8, 65.1, 56.0, 49.5,

47.7, 47.5, 43.8, 19.5. HMRS (ES$^-$) calc. for $C_{19}H_{21}O_3$ [M-H]$^-$ 297.1496; found 297.1483. HPLC (e.e. determination): RT_{major} = 9.0 min, RT_{minor} = 11.1 min, OD-H column, iPrOH/Hexane (20:80) as a mobile phase; flow rate 1.00 ml/min, sample: 0.1 mg / ml dissolved in the mobile phase.
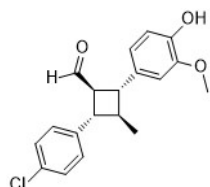
4b (1R,2S,3S,4R)-2-(4-chlorophenyl)-4-(4-hydroxy-3-methoxyphenyl)-3-methyl cyclobutane carbaldehyde. Yield: 78%, yellow oil. Chromatography: 0 – 25% EtOAc/hexanes. ^{1}H NMR (600 MHz, CDCl$_3$) δ 9.85 (d, J = 1.9 Hz, 1H), 7.31 (d, J = 8.4 Hz, 2H), 7.20 (d, J = 8.4 Hz, 2H), 6.90 (d, J = 8.1 Hz, 1H), 6.79 (dd, J = 8.1, 1.8 Hz, 1H), 6.73 (d, J = 1.8 Hz, 1H), 5.58 (s, 1H, Ar-OH), 3.90 (s, 3H), 3.22 (td, J = 9.3, 1.8 Hz, 1H), 3.18 (t, J = 9.3 Hz, 1H), 3.13 (t, J = 9.3 Hz, 1H), 2.50 (tq, J = 9.3, 6.5 Hz, 1H), 1.29 (d, J = 6.5 Hz, 3H). ^{13}C NMR (151 MHz, CDCl$_3$) δ 201.2, 146.7, 144.8, 140.4, 133.6, 132.7, 128.9, 128.3, 119.4, 114.7, 109.6, 58.0, 56.1, 46.2, 45.0, 43.0, 19.4. HRMS (EI) calc. for $C_{19}H_{19}O_3Cl$ [M]$^+$ 330.1023; found 330.1020.
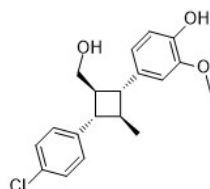
5b 4-((1R,2R,3S,4S)-3-(4-chlorophenyl)-2-(hydroxymethyl)-4-methylcyclobutyl)-2-methoxyphenol. Yield: 94% from 4b, clear colourless oil. Chromatography: 20 – 40% EtOAc/hexanes. [α]$_D$ = +3.2 (c 1.92, CHCl$_3$, 98% ee). ^{1}H NMR (600 MHz, CDCl$_3$) δ 7.30 (d, J = 8.4 Hz, 2H), 7.23 (d, J = 8.4 Hz, 2H), 6.88 (d, J = 8.0 Hz, 1H), 6.80 (dd, J = 8.1, 1.8 Hz, 1H), 6.78 (d, J = 1.8 Hz, 1H), 5.56 (s, 1H, Ar-OH), 3.90 (s, 3H), 3.80 – 3.76 (m, 2H), 2.73 (t, J = 9.4 Hz, 1H), 2.70 (t, J = 9.4 Hz, 1H), 2.54 – 2.46 (m, 1H), 2.26 (tq, J = 9.4, 6.5 Hz, 1H), 1.38 (s, 1H, OH), 1.23 (d, J = 6.5 Hz, 2H). ^{13}C NMR (151 MHz, CDCl$_3$) δ 146.6, 144.3, 141.9, 135.1, 132.1, 128.7, 128.5, 119.6, 114.5, 109.8, 64.9, 56.0, 49.6, 47.6, 47.0, 43.9, 19.4. HMRS (ES$^+$) calc. for $C_{19}H_{22}O_3Cl$ [M+H]$^+$ 333.1257; found 333.1265. HPLC (e.e. determination): RT_{major} = 8.5 min, RT_{minor} = 10.7 min, OD-H column, iPrOH/Hexane (20:80) as a mobile phase; flow rate 1.00 ml/min, sample: 0.1 mg / ml dissolved in the mobile phase.
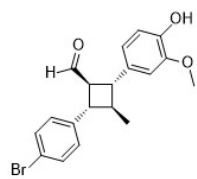
4c (1R,2S,3S,4R)-2-(4-bromophenyl)-4-(4-hydroxy-3-methoxyphenyl)-3-methyl cyclobutane carbaldehyde. Yield: 80%, light yellow oil. Chromatography: 0 – 25% EtOAc/hexanes. ^{1}H NMR (600 MHz, CDCl$_3$) δ 9.85 (d, J = 1.9 Hz, 1H), 7.46 (d, J = 8.3 Hz, 2H), 7.15 (d, J = 8.3 Hz, 2H), 6.90 (d, J = 8.1 Hz, 1H), 6.79 (dd, J = 8.1, 1.8 Hz, 1H), 6.73 (d, J = 1.8 Hz, 1H), 5.60 (s, 1H, Ar-OH), 3.90 (s, 3H), 3.22 (td, J = 9.4, 1.9 Hz, 1H), 3.19 – 3.11 (m, 2H), 2.50 (tq, J = 9.4, 6.5 Hz, 1H), 1.29 (d, J = 6.5 Hz, 3H). ^{13}C NMR (151 MHz, CDCl$_3$) δ 201.2, 146.7, 144.8, 140.9, 133.5, 131.9, 128.7, 120.7, 119.4, 114.7, 109.6, 58.0, 56.1, 46.2, 45.1, 43.0, 19.4. HMRS (ES$^-$) calc. for C$_{19}$H$_{18}$O$_3$Br [M-H]$^-$ 373.0439; found 373.0435.
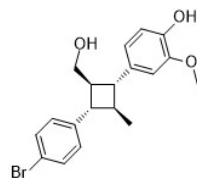
5c 4-((1R,2R,3S,4S)-3-(4-bromophenyl)-2-(hydroxymethyl)-4-methylcyclobutyl)-2-methoxyphenol. Yield: 95% from 4c, light yellow oil. Chromatography: 20 – 40% EtOAc/hexanes. [α]$_D$ = +4.0 (c 1.48, CHCl$_3$, 98% ee). ^{1}H NMR (600 MHz, CDCl$_3$) δ 7.45 (d, J = 8.4 Hz, 2H), 7.18 (d, J = 8.4 Hz, 2H), 6.88 (d, J = 8.0 Hz, 1H), 6.81 – 6.76 (m, 2H), 5.53 (s, 1H, Ar-OH), 3.90 (s, 3H), 3.78 (d, J = 5.2 Hz, 2H), 2.72 (t, J = 9.6 Hz, 1H), 2.70 (t, J = 9.6 Hz, 1H), 2.49 (tt, J = 9.6, 5.2 Hz, 1H), 2.26 (tq, J = 9.6, 6.5 Hz, 1H), 1.37 (s, 1H, OH), 1.23 (d, J = 6.5 Hz, 3H). ^{13}C NMR (151 MHz, CDCl$_3$) δ 146.6, 144.4, 142.4, 135.1, 131.7, 128.9, 120.2, 119.6, 114.5, 109.8, 64.9, 56.1, 49.5, 47.6, 47.0, 43.8, 19.4. HMRS (ES$^+$) calc. for C$_{19}$H$_{22}$O$_3$Br [M+H]$^+$ 377.0752; found 377.0746. HPLC (e.e. determination): RT$_{major}$ = 9.1 min, RT$_{minor}$ = 12.0 min, OD-H column, iPrOH/Hexane (20:80) as a mobile phase; flow rate 1.00 ml/min, sample: 0.1 mg / ml dissolved in the mobile phase.
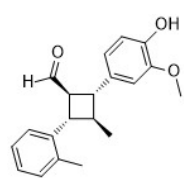
4d (1S,2R,3R,4S)-2-(4-hydroxy-3-methoxyphenyl)-3-methyl-4-(o-tolyl) cyclobutane carbaldehyde. Yield: 66%, light yellow oil. Chromatography: 0 – 20% EtOAc/hexanes. ^{1}H NMR (600 MHz, CDCl$_3$) δ 9.85 (d, J = 2.4 Hz, 1H), 7.40 (d, J =

7.7 Hz, 1H), 7.27 – 7.24 (m, 1H), 7.19 – 7.15 (m, 2H), 6.91 (d, J = 8.1 Hz, 1H), 6.83 (dd, J = 8.1, 1.7

Hz, 1H), 6.76 (d, J = 1.9 Hz, 1H), 5.56 (s, 1H, Ar-OH), 3.91 (s, 3H), 3.41 (t, J = 9.4 Hz, 1H), 3.28 (td,

J = 9.4, 2.4 Hz, 1H), 3.17 (t, J = 9.4 Hz, 1H), 2.64 (tq, J = 9.4, 6.5 Hz, 1H), 2.35 (s, 3H), 1.27 (d, J =

6.5 Hz, 3H). ^{13}C NMR (151 MHz, CDCl$_3$) δ 201.5, 146.7, 144.7, 139.6, 136.3, 134.0, 130.6, 126.9,

126.5, 126.2, 119.5, 114.6, 109.8, 58.6, 56.1, 45.7, 43.1, 42.5, 20.4, 19.6. HMRS (ES$^-$) calc. for C$_{20}$H$_{21}$O$_3$

[M-H]$^-$ 309.1491; found 309.1499.
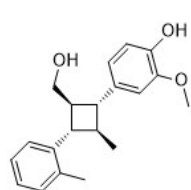
5d 4-((1R,2S,3S,4R)-2-(hydroxymethyl)-4-methyl-3-(o-tolyl)cyclobutyl)-2-methoxy phenol. Yield: 93% from 4d, light yellow oil. Chromatography: 15 – 30% EtOAc/hexanes. [α]$_D$ = +4.7 (c 1.25, CHCl$_3$, 95% ee). ^{1}H NMR (600 MHz, CDCl$_3$)

δ 7.41 (d, J = 7.6 Hz, 1H), 7.24 (dd, J = 10.8, 4.1 Hz, 1H), 7.17 (d, J = 6.7 Hz, 1H), 7.13 (td, J = 7.4,

1.2 Hz, 1H), 6.90 (d, J = 8.0 Hz, 1H), 6.87 – 6.81 (m, 2H), 5.53 (s, 1H, Ar-OH), 3.92 (s, 3H), 3.77 -

3.70 (m, 2H), 3.03 (t, J = 9.4 Hz, 1H), 2.73 (t, J = 9.4 Hz, 1H), 2.57 (tt, J = 9.4, 5.0 Hz, 1H), 2.41 (s,

3H), 2.38 – 2.30 (m, 1H), 1.24 (t, J = 5.7 Hz, 1H, OH), 1.21 (d, J = 6.5 Hz, 3H). ^{13}C NMR (151 MHz,

CDCl$_3$) δ 146.6, 144.3, 141.1, 136.3, 135.5, 130.3, 126.4, 126.4, 126.2, 119.7, 114.5, 109.9, 64.7, 56.1,

50.1, 47.3, 44.5, 43.3, 20.2, 19.6. HMRS (ES$^-$) calc. for C$_{20}$H$_{23}$O$_3$ [M-H]$^-$ 311.1647; found 311.1638.

HPLC (e.e. determination): RT$_{major}$ = 8.8 min, RT$_{minor}$ = 10.3 min, OD-H column, iPrOH/Hexane

(20:80) as a mobile phase; flow rate 1.00 ml/min, sample: 0.1 mg / ml dissolved in the mobile phase.
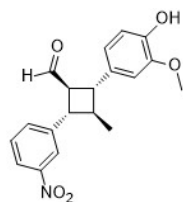
4e (1R,2R,3S,4S)-2-(4-hydroxy-3-methoxyphenyl)-3-methyl-4-(3-nitrophenyl) cyclobutane carbaldehyde. Yield: 74%, yellow oil. Chromatography: 0 – 50% Et$_2$O/hexanes. ^{1}H NMR (600 MHz, CDCl$_3$) δ 9.88 (d, J = 1.7 Hz, 1H), 8.16 – 8.10

(m, 2H), 7.60 (d, J = 7.7 Hz, 1H), 7.54 – 7.49 (m, 1H), 6.91 (d, J = 8.1 Hz, 1H), 6.81 (dd, J = 8.1, 1.9

Hz, 1H), 6.75 (d, J = 1.9 Hz, 1H), 5.57 (s, 1H, Ar-OH), 3.92 (s, 3H), 3.34 (t, J = 9.4 Hz, 1H), 3.29 (td,

J = 9.4, 1.7 Hz, 1H), 3.16 (t, J = 9.3 Hz, 1H), 2.58 (tq, J = 9.3, 6.5 Hz, 1H), 1.33 (d, J = 6.5 Hz, 3H).

^{13}C NMR (151 MHz, CDCl$_3$) δ 200.7, 148.7, 146.8, 145.0, 144.1, 133.4, 133.1, 129.8, 122.1, 121.7,

119.4, 114.8, 109.6, 57.8, 56.1, 46.7, 44.6, 43.0, 19.4. HMRS (ES$^-$) calc. for C$_{19}$H$_{18}$NO$_5$ [M-H]$^-$ 340.1185;

found 340.1195.
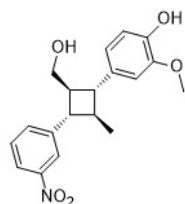
5e 4-((1R,2R,3S,4S)-2-(hydroxymethyl)-4-methyl-3-(3-nitrophenyl)cyclobutyl)-2-methoxyphenol. Yield: 92% from 4e, yellow oil. Chromatography: 50 – 80% Et$_2$O/hexanes. [α]$_D$ = -2.5 (c 0.85, CHCl$_3$, 96% ee). ^{1}H NMR (600 MHz, CDCl$_3$) δ

8.17 (t, J = 1.9 Hz, 1H), 8.08 (ddd, J = 8.1, 2.2, 0.9 Hz, 1H), 7.64 (d, J = 7.6 Hz, 1H), 7.49 (t, J = 7.9

Hz, 1H), 6.89 (d, J = 8.0 Hz, 1H), 6.79 (dt, J = 4.3, 1.8 Hz, 2H), 5.53 (s, 1H, Ar-OH), 3.92 (s, 3H),

3.86 – 3.78 (m, 2H), 2.91 (t, J = 9.4 Hz, 1H), 2.77 (t, J = 9.4 Hz, 1H), 2.57 (tt, J = 9.4, 5.3 Hz 1H),

2.38 – 2.30 (m, 1H), 1.39 (t, J = 5.1 Hz, 1H, OH), 1.28 (d, J = 6.5 Hz, 3H). ^{13}C NMR (151 MHz,

CDCl$_3$) δ 148.6, 146.7, 145.7, 144.5, 134.7, 133.5, 129.5, 122.0, 121.5, 119.6, 114.6, 109.7, 64.5, 56.1,

49.5, 47.4, 47.2, 43.8, 19.4. HMRS (ES$^-$) calc. for C$_{19}$H$_{20}$NO$_5$ [M-H]$^-$ 342.1341; found 342.1344. HPLC

(e.e. determination): RT$_{major}$ = 11.2 min, RT$_{minor}$ = 13.6 min, OD-H column, iPrOH/Hexane (20:80)

as a mobile phase; flow rate 1.00 ml/min, sample: 0.1 mg / ml dissolved in the mobile phase.
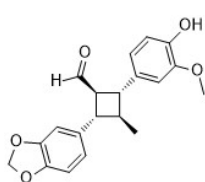
4f (1S,2S,3R,4R)-2-(benzo[d][1,3]dioxol-5-yl)-4-(4-hydroxy-3-methoxyphenyl)-3-methylcyclobutane carbaldehyde. Yield: 66%, yellow oil. Chromatography: 10 – 30% EtOAc/hexanes. ^{1}H NMR (600 MHz, CDCl$_3$) δ 9.84 (d, J = 2.1 Hz, 1H), 6.89

(d, J = 8.1 Hz, 1H), 6.79 – 6.76 (m, 3H), 6.74 – 6.71 (m, 2H), 5.95 (s, 2H), 5.57 (s, 1H, Ar-OH), 3.90

(s, 3H), 3.19 (td, J = 9.5, 2.1 Hz, 1H), 3.10 (td, J = 9.4, 4.1 Hz, 2H), 2.47 (tq, J = 9.4, 6.4, 1H), 1.26 (d,

J = 6.4 Hz, 3H). ^{13}C NMR (151 MHz, CDCl$_3$) δ 201.5, 148.1, 146.7, 146.6, 144.7, 135.9, 133.8, 120.00,

119.4, 114.6, 109.7, 108.5, 107.4, 101.2, 58.5, 56.1, 45.9, 45.8, 43.3, 19.4. HRMS (ES$^+$) calc. for C$_{20}$H$_{21}$O$_5$ [M+H]$^+$ 341.1389; found 341.1390.
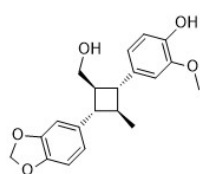
5f 4-((1R,2S,3S,4R)-3-(benzo[d][1,3]dioxol-5-yl)-2-(hydroxymethyl)-4-methyl cyclobutyl)-2-methoxy phenol. Yield: 93% from 4f, yellow oil. Chromatography: 20 – 40% EtOAc/hexanes. [α]$_D$ = -0.8 (c 1.14, CHCl$_3$, 91% ee). ^{1}H NMR (600 MHz, CDCl$_3$) δ 6.88 (d, J = 8.0 Hz, 1H), 6.82 – 6.73 (m, 5H), 5.94 (s, 2H), 5.50 (s, 1H, Ar-OH), 3.91 (s, 3H), 3.77 (d, J = 5.0 Hz, 2H), 2.66 (td, J = 9.3, 5.3 Hz, 2H), 2.47 (tt, J = 9.3, 5.0 Hz, 1H), 2.23 (tq, J = 9.3, 6.5 Hz, 1H), 1.25 (s, 1H, OH), 1.21 (d, J = 6.5 Hz, 3H). ^{13}C NMR (151 MHz, CDCl$_3$) δ 148.0, 146.6, 146.2, 144.3, 137.4, 135.3, 120.0, 119.7, 114.5, 109.8, 108.4, 107.6, 101.0, 65.1, 56.1, 50.0, 47.6, 47.5, 44.2, 19.3. HMRS (ES$^+$) calc. for C$_{20}$H$_{22}$O$_5$Na [M+Na]$^+$ 365.1365; found 365.1370. HPLC (e.e. determination): RT$_{major}$ = 13.0 min, RT$_{minor}$ = 14.7 min, OD-H column, iPrOH/Hexane (20:80) as a mobile phase; flow rate 1.00 ml/min, sample: 0.1 mg / ml dissolved in the mobile phase.
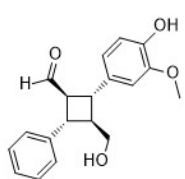
4g (1R,2R,3S,4S)-2-(4-hydroxy-3-methoxyphenyl)-3-(hydroxymethyl)-4-phenyl cyclobutane carbaldehyde. Yield: 77% yield, white foamy solid. Chromatography: 0 – 4% MeOH/DCM. ^{1}H NMR (600 MHz, CDCl$_3$) δ 9.89 (d, J = 2.0 Hz, 1H), 7.37 – 7.31 (m, 4H), 7.28 – 7.25 (m, 1H), 6.89 (d, J = 8.0 Hz, 1H), 6.83 (dd, J = 8.2, 1.8 Hz, 1H), 6.81 (d, J = 1.9 Hz, 1H), 5.61 (s, 1H, Ar-OH), 3.89 (s, 3H), 3.85 (d, J = 5.0 Hz, 2H), 3.56 (t, J = 9.5 Hz, 1H), 3.51 (t, J = 9.5 Hz, 1H), 3.31 (td, J = 9.5, 2.0 Hz, 1H), 2.79 (tt, J = 9.6, 5.0 Hz, 1H). ^{13}C NMR (151 MHz, CDCl$_3$) δ 201.3, 146.7, 144.8, 141.7, 133.8, 128.9, 127.1, 127.1, 119.5, 114.6, 109.9, 64.1, 57.7, 56.1, 48.8, 40.3, 40.0. HMRS (ES$^-$) calc. for C$_{19}$H$_{19}$O$_4$ [M-H]$^-$ 311.1283; found 311.1295.
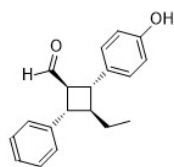
4h   (1R,2R,3S,4S)-3-ethyl-2-(4-hydroxyphenyl)-4-phenylcyclobutanecarbaldehyde.

Yield: 45%, light yellow oil. Chromatography: 0 – 20% EtOAc/hexanes. ^{1}H NMR

(600 MHz, CDCl$_3$) δ 9.83 (d, J = 1.4 Hz, 1H), 7.36 – 7.29 (m, 4H), 7.26 – 7.23 (m,

1H), 7.19 (d, J = 8.5 Hz, 2H), 6.81 (d, J = 8.6 Hz, 2H), 4.79 (s, 1H, Ar-OH), 3.28 - 3.23 (m, 1H), 3.23

– 3.17 (m, 2H), 2.59 – 2.50 (m, 1H), 1.72 - 1.65 (m, 2H), 0.80 (t, J = 7.5 Hz, 3H). ^{13}C NMR (151 MHz,

CDCl$_3$) δ 201.5, 154.5, 142.5, 134.8, 128.8, 128.4, 127.2, 126.9, 115.6, 58.5, 49.0, 44.2, 43.9, 28.3, 11.5.

HMRS (ES⁻) calc. for C$_{19}$H$_{19}$O$_2$ [M-H]⁻ 279.1385; found 279.1397.
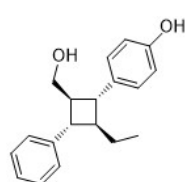
5h   4-((1R,2S,3S,4R)-2-ethyl-4-(hydroxymethyl)-3-phenylcyclobutyl)phenol.   Yield:

95% from 4h, clear colourless oil. Chromatography: 15 – 30% EtOAc/hexanes [α]$_D$

= -3.3 (c 0.77, CHCl$_3$, 97% ee). ^{1}H NMR (600 MHz, CDCl$_3$) δ 7.36 – 7.29 (m, 4H),

7.25 – 7.21 (m, 1H), 7.19 (d, J = 8.4 Hz, 2H), 6.78 (d, J = 8.4 Hz, 2H), 5.00 (s, 1H, Ar-OH), 3.76 (t, J

= 5.3 Hz, 2H), 2.80 (t, J = 9.3 Hz, 1H), 2.76 (t, J = 9.3 Hz, 1H), 2.47 (tt, J = 9.3, 5.3 Hz, 1H), 2.33 (tt,

J = 9.3, 6.9 Hz, 1H), 1.64 (dq, J = 6.9, 7.4 Hz, 2H), 1.32 (t, J = 5.3 Hz, 1H, OH), 0.76 (t, J = 7.4 Hz,

3H). HMRS (ES⁻) calc. for C$_{19}$H$_{21}$O$_2$ [M-H]⁻ 281.1542; found 281.1537. HPLC (e.e. determination):

RT$_{major}$ = 5.9 min, RT$_{minor}$ = 8.3 min, OD-H column, iPrOH/Hexane (20:80) as a mobile phase; flow

rate 1.00 ml/min, sample: 0.2 mg / ml dissolved in the mobile phase.

4g Derivatization
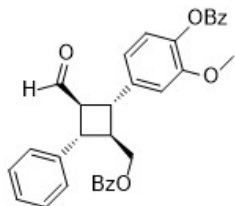
To avoid the formation of a meso-diol, **4g** was first protected as the bis-benzoate

7 prior to reduction. Other derivatives were prepared using *rac*-4g to explore

applications of these compounds.

7

To a solution of **4g** (0.020 g, 0.064 mmol, 1.0 eq.) in DCM (0.32 mL) was added benzoyl chloride (0.020 g, 0.14 mmol, 2.2 eq.), DIPEA (0.1 mL) and 4-(dimethylamino)pyridine (0.0008 g, 0.006 mmol, 0.1 eq). The reaction was stirred at room temperature for 8 hours before quenching with 1.0 mL of water. The mixture was then extracted with EtOAc (3 x 1 mL), dried over Na_2SO_4 and evaporated to dryness. The crude resin was then purified using silica gel chromatography (0 – 25% EtOAc/hexanes) to give **7** as a white solid in 58% yield.

7 ((1S,2R,3R,4S)-2-(4-(benzoyloxy)-3-methoxyphenyl)-3-formyl-4-phenylcyclobutyl)methyl benzoate. Yield: 58% from 4g, white solid. Chromatography: 0 – 25% EtOAc/hexanes. ^{1}H NMR (600 MHz, CDCl$_3$) δ 9.95 (d, J = 1.6 Hz, 1H), 8.22 (dd, J = 8.3, 1.2 Hz, 2H), 7.90 (dd, J = 8.3, 1.2 Hz, 2H), 7.64 (t, J = 7.5 Hz, 1H), 7.55 (t, J = 7.4 Hz, 1H), 7.51 (t, J = 7.8 Hz, 2H), 7.42 (t, J = 7.8 Hz, 2H), 7.38 – 7.33 (m, 4H), 7.30 – 7.26 (m, 1H), 7.14 (d, J = 8.1 Hz, 1H), 6.99 (dd, J = 8.1, 1.8 Hz, 1H), 6.94 (d, J = 1.9 Hz, 1H), 4.61 – 4.53 (m, 2H), 3.77 (s, 3H), 3.67 (t, J = 9.7 Hz, 1H), 3.64 (t, J = 9.7 Hz, 1H), 3.47 (td, J = 9.5 1.6 Hz, 1H), 3.09 (tt, J = 9.5, 5.5 Hz 1H). ^{13}C NMR (151 MHz, CDCl$_3$) δ 200.6, 166.6, 164.9, 151.6, 141.0, 140.2, 139.2, 133.7, 133.3, 130.5, 130.0, 129.8, 129.5, 129.0, 128.7, 128.6, 127.4, 127.1, 123.3, 118.9, 111.6, 66.0, 57.3, 56.1, 45.8, 41.3, 41.1. HMRS (ES$^+$) calc. for $C_{33}H_{28}O_6Na$ [M+Na]$^+$ 543.1784; found 543.1789.
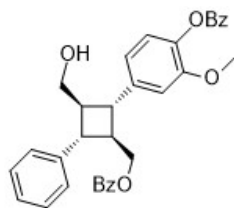
8

To a solution of **7** (0.012 g, 0.023 mmol, 1.0 eq.) in absolute ethanol (0.2 mL) was added NaBH$_4$ (0.0008 g, 0.0023 mmol, 1.0 eq.) at 0 °C. The reaction was allowed to warm to room temperature and stirred for 20 minutes. The reaction was then quenched with 1 M HCl (1 drop) and 0.3 mL H$_2$O. The reaction mixture was then extracted with EtOAc (0.3 x 3 mL) and the combined organic layers were concentrated under a stream of nitrogen. The resulting resin was purified using silica gel chromatography (0 – 25% EtOAc/hexanes), giving **8** as a colourless oil in 95% yield.

8 ((1S,2S,3R,4R)-2-(4-(benzoyloxy)-3-methoxyphenyl)-3-(hydroxymethyl)-4-phenylcyclobutyl) methyl benzoate. Yield: 94% from 7, colourless oil. Chromatography: 0 – 25% EtOAc/hexanes. $[\alpha]_D$ = 8.3 (c 0.69, CHCl$_3$, 99% ee). ^{1}H NMR (600 MHz, CDCl$_3$) δ 8.22 (dd, J = 8.3, 1.2 Hz, 2H), 7.88 (dd, J = 8.3, 1.2 Hz, 2H), 7.65 – 7.62 (m, 1H), 7.56 – 7.50 (m, 3H), 7.40 (t, J = 7.8 Hz, 2H), 7.38 – 7.33 (m, 4H), 7.26 – 7.23 (m, 1H), 7.12 (d, J = 8.0 Hz, 1H), 7.02 – 6.98 (m, 2H), 4.57 – 4.51 (m, 2H), 3.87 (d, J = 4.9 Hz, 2H), 3.77 (s, 3H), 3.26 (t, J = 9.5 Hz, 1H), 3.24 (t, J = 9.5 Hz, 1H), 2.88 (tt, J = 9.4, 5.7 Hz, 1H), 2.74 (tt, J = 9.5, 4.9 Hz, 1H). ^{13}C NMR (151 MHz, CDCl$_3$) δ 166.7, 165.0, 151.4, 142.4, 141.7, 138.7, 133.6, 133.1, 130.5, 130.2, 129.7, 129.6, 128.8, 128.7, 128.5, 127.3, 126.8, 123.0, 119.2, 111.9, 66.5, 64.3, 56.1, 49.4, 46.6, 42.6, 42.2. HMRS (ES$^+$) calc. for C$_{33}$H$_{34}$NO$_6$ [M+NH$_4$]$^+$ 540.2386; found 540.2382. HPLC (e.e. determination): RT$_{major}$ = 6.9 min, RT$_{minor}$ = 12.6 min, OD-H column, iPrOH/Hexane (40:60) as a mobile phase; flow rate 1.00 ml/min, sample: 0.25 mg/ml dissolved in the mobile phase.
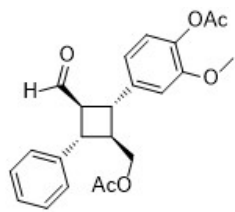
9

To a solution of **4g** (0.020 g, 0.064 mmol, 1.0 eq.) in DCM (0.32 mL) was added acetyl chloride (0.011 g, 0.14 mmol, 2.2 eq.), DIPEA (0.1 mL) and 4-(dimethylamino)pyridine (0.0008 g, 0.006 mmol, 0.1 eq). The reaction was stirred at room temperature for 2 hours before quenching with 1.0 mL of water. The mixture was then extracted with EtOAc (3 x 1 mL), dried over Na_2SO_4 and evaporated to dryness. The crude resin was then purified using silica gel chromatography (0-25% EtOAc/hexanes), giving **9** as a clear colourless oil in 50% yield.

9 ((1S,2R,3R,4S)-2-(4-acetoxy-3-methoxyphenyl)-3-formyl-4-phenylcyclobutyl)methyl acetate. Yield: 50% from **4g**, clear colourless oil. Chromatography: 0 - 25% EtOAc/hexanes. ^{1}H NMR (600 MHz, CDCl$_3$) δ 9.90 (d, J = 1.6 Hz, 1H), 7.36 (t, J = 7.6 Hz, 2H), 7.30 – 7.26 (m, 3H), 7.01 (d, J = 8.6 Hz, 1H), 6.89 – 6.87 (m, 2H), 4.33 – 4.27 (m, 2H), 3.84 (s, 3H), 3.53 (t, J = 9.5 Hz, 1H), 3.50 (t, J = 9.5 Hz, 1H), 3.36 (td, J = 9.5, 1.6 Hz, 1H), 2.92 (tt, J = 9.6, 5.5 Hz, 1H), 2.31 (s, 3H), 1.98 (s, 3H). ^{13}C NMR (151 MHz, CDCl$_3$) δ 200.6, 171.1, 169.3, 151.3, 140.9, 140.2, 138.8, 129.0, 127.3, 127.0, 123.1, 118.8, 111.4, 65.3, 57.2, 56.1, 45.4, 41.2, 40.7, 20.9, 20.8. HMRS (ES$^+$) calc. for $C_{23}H_{24}O_6Na$ [M+Na]$^+$ 419.1471; found 419.1464.

10 and **11**
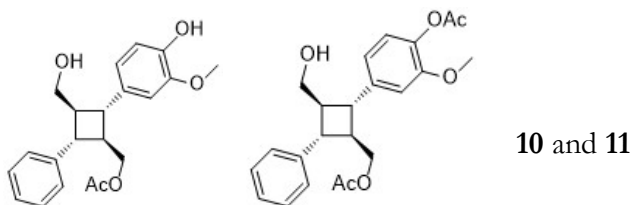
To a solution of **9** (0.010 g, 0.025 mmol, 1.0 eq.) in MeOH (0.25 mL) was added NaBH₄ (0.001 g, 0.025 mmol, 1.0 eq.) at 0 °C. The reaction was allowed to warm to room temperature with stirring over 20 minutes and was then quenched with 1 M HCl and water (0.25 mL). The reaction mixture was extracted with EtOAc (3 x 0.5 mL), and the combined organic layers were dried over sodium sulphate and concentrated under a stream of nitrogen to give a colourless resin in 90% yield. ¹H NMR of the resin demonstrated products **10** and **11** in a 5:1 molar ratio, respectively. Major product: ¹H NMR (600 MHz, CDCl₃) δ 7.35 – 7.29 (m, 4H), 7.25 – 7.22 (m, 1H), 6.99 (d, *J* = 8.1 Hz, 1H), 6.93 (d, *J* = 1.8 Hz, 1H), 6.90 (dd, *J* = 8.2, 1.8 Hz, 1H), 4.31 – 4.24 (m, 2H), 3.84 (s, 3H), 3.82 (t, *J* = 5.3 Hz, 2H), 3.10 (t, *J* = 9.4, 1H), 3.09 (t, *J* = 9.4, 1H), 2.72 (tt, *J* = 9.5, 5.7 Hz, 1H), 2.64 (tt, *J* = 9.5, 5.0 Hz, 1H), 2.31 (s, 3H), 1.95 (s, 3H). To the 5:1 mixture of **10** and **11** (0.008 g, 0.02 mmol, 1.0 eq.) in methanol (0.25 mL) was added NaBH₄ (0.004 g, 0.1 mmol, 5 eq.). The reaction was allowed to stir for 8 hours at room temperature and was then quenched with 1M HCl and water (0.25 mL). The reaction mixture was then extracted with EtOAc (3 x 0.5 mL) and the combined organic layers were dried over sodium sulphate and concentrated under a stream of nitrogen to give **11** as a colourless oil in 90% yield. NMR demonstrated the product to be essentially pure, with no further purification required.

11   ((1S,2S,3R,4R)-2-(4-hydroxy-3-methoxyphenyl)-3-(hydroxymethyl)-4-phenylcyclobutyl)methyl acetate. Yield: 90% from **10**, clear colourless oil. ¹H NMR (600 MHz, CDCl₃) δ 7.35 - 7.29 (m, 4H), 7.25 – 7.22 (m, 1H), 6.88 (d, *J* = 8.2 Hz, 1H), 6.85 - 6.81 (m, 2H), 5.51 (s, 1H), 4.27 (d, *J* = 5.7 Hz, 2H), 3.91 (s, 3H), 3.82 (d, *J* = 5.1 Hz, 1H), 3.06 (t, *J* = 9.4 Hz, 1H), 3.01 (t, *J* = 9.4 Hz, 1H), 2.68 (tt, *J* = 9.4, 5.7 Hz, 1H), 2.61 (tt, *J* = 9.4, 5.1 Hz, 1H), 1.94 (s, 3H). ¹³C NMR (151 MHz, CDCl₃) δ 171.2,

146.6, 144.5, 142.6, 134.6, 128.7, 127.2, 126.7, 119.7, 114.5, 109.9, 66.0, 64.6, 56.1, 49.5, 46.5, 42.5, 42.3, 21.0. HMRS (ES$^+$) calc. for $C_{21}H_{28}NO_5$ [M+NH$_4$]$^+$ 374.1967; found 374.1967.
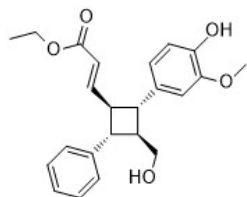
12

To a solution of (2-ethoxy-2-oxoethyl)triisobutylphosphonium bromide (0.046 g, 0.013 mmol, 3.0 eq.) in THF (0.3 mL) was added potassium *tert*-butoxide (0.014 g, 0.013 mmol, 3.0 eq.) at room temperature. The mixture was allowed to stir for 20 minutes and was then cooled to 0 °C prior to the addition of **4g** (0.013 g, 0.042 mmol, 1.0 eq.) in THF (0.15 mL). The mixture was allowed to warm to room temperature and stirred for 1 hour. Then, the reaction was quenched with 0.2 mL saturated NH$_4$Cl and 0.2 mL H$_2$O and extracted with diethyl ether (3 x 0.5 mL). The combined ether layers were dried over MgSO$_4$ and concentrated to give a light-yellow resin that was purified using silica gel chromatography (1:99 MeOH:DCM) to give the desired product in 75% yield.

12 (*E*)-ethyl 3-((1R,2S,3S,4R)-2-(4-hydroxy-3-methoxyphenyl)-3-(hydroxymethyl)-4-phenylcyclobutyl)acrylate. ^{1}H NMR (600 MHz, CDCl$_3$) δ 7.34 (t, J = 7.5 Hz, 2H), 7.29 (d, J = 7.2 Hz, 2H), 7.24 (t, J = 7.3 Hz, 1H), 7.13 (dd, J = 15.6, 7.2 Hz, 1H), 6.88 (d, J = 8.1 Hz, 1H), 6.81 (dd, J = 8.1, 1.8 Hz, 1H), 6.78 (d, J = 1.9 Hz, 1H), 5.84 (dd, J = 15.6, 1.2 Hz, 1H), 5.53 (s, 1H), 4.17 (q, J = 7.1 Hz, 2H), 3.89 (s, 3H), 3.84 (d, J = 5.0 Hz, 2H), 3.20 (t, J = 9.4 Hz, 1H), 3.14 (t, J = 9.4 Hz, 1H), 3.09 – 3.03 (m, 1H), 2.68 (tt, J = 9.6, 5.0 Hz, 1H), 1.27 (t, J = 7.1 Hz, 3H). ^{13}C NMR (151 MHz, CDCl$_3$) δ 166.7, 149.2, 146.7, 144.7, 142.1, 134.0, 128.8, 127.0, 126.9, 121.4, 119.7, 114.6, 109.8, 64.3, 60.5, 56.1, 50.1, 49.5, 45.3, 44.8, 14.4. HMRS (ES$^+$) calc. for $C_{23}H_{26}O_5Na$ [M+Na]$^+$ 405.1678; found 405.1679.

CCDC 1456076
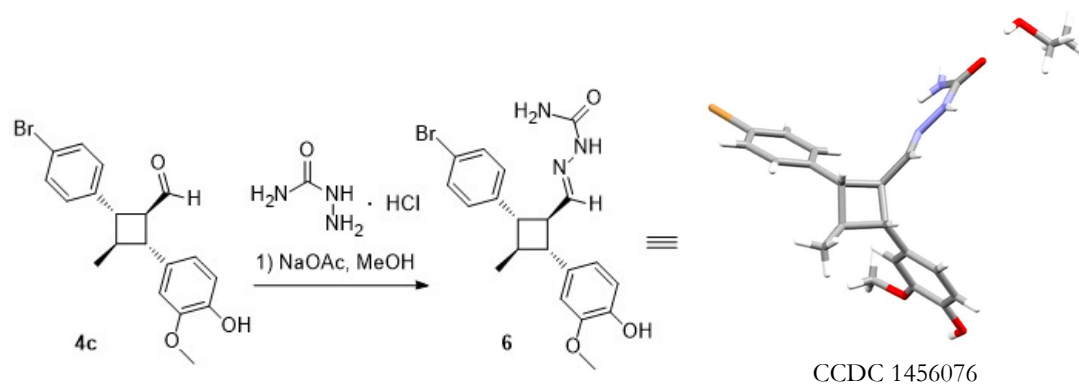
Determination of Absolute Stereochemistry of Cyclobutane Derivatives

To a solution of **4c** (0.0180 g, 0.048 mmol, 1.0 eq.) in MeOH (0.25 mL) was added semicarbazide hydrochloride (0.0059 g, 0.053 mmol, 1.1 eq.) and sodium acetate (0.0043 g, 0.053 mmol, 1.1 eq). The solution was stirred at room temperature for 30 minutes. Then, water was added (0.5 mL), immediately resulting in the formation of a white precipitate. The mixture was centrifuged briefly and the supernatant was discarded. The precipitate was washed again with water (0.3 mL x 2), giving a white solid in 90% yield. The white solid was then slowly recrystallized from hot EtOH (95%) giving clear colourless crystals of the desired semicarbazone adduct **6**. X-Ray crystallographic analysis was used to determine the absolute stereochemistry of the cyclobutane product, and significant hydrogen bonding to ethanol was also observed in the crystal structure.

Table S1. Crystal data and structure refinement for **6**.

Identification code	an3_final_a
Empirical formula	C22 H28 Br N3 O4
Formula weight	478.38
Temperature	173(2) K

Wavelength	1.54178 Å	
Crystal system	Monoclinic	
Space group	$P2_1$	
Unit cell dimensions	a = 10.2716(2) Å	α= 90°.
	b = 8.4623(2) Å	β= 103.3230(10)°.
	c = 13.4925(3) Å	γ = 90°.
Volume	1141.22(4) Å^3	
Z	2	
Density (calculated)	1.392 Mg/m^3	
Absorption coefficient	2.722 mm^{-1}	
F(000)	496	
Crystal size	0.465 x 0.145 x 0.038 mm^3	
Theta range for data collection	3.366 to 72.548°.	
Index ranges	-12<=h<=12, -9<=k<=9, -16<=l<=16	
Reflections collected	12874	
Independent reflections	3916 [R(int) = 0.0289]	
Completeness to theta = 67.679°	99.1 %	
Absorption correction	Numerical	
Max. and min. transmission	0.8427 and 0.4344	
Refinement method	Full-matrix least-squares on F^2	
Data / restraints / parameters	3916 / 1 / 286	
Goodness-of-fit on F^2	1.057	
Final R indices [I>2sigma(I)]	R1 = 0.0256, wR2 = 0.0689	

R indices (all data)   R1 = 0.0261, wR2 = 0.0698

Absolute structure parameter   0.019(7)

Extinction coefficient   n/a

Largest diff. peak and hole   0.462 and -0.256 e.Å^{-3}

Experimental References

1) C. Curti, F. Zanardi, L. Battistini, A. Sartori, G. Rassu, L. Pinna, and G. Casiraghi, *J. Org. Chem.*, **2006**, *71*, 8552.

2) J. C. Roberts and J. A Pincock, *J. Org. Chem.*, **2006**, *71*, 1480.

3) S. Quideau and J. Ralph, *J. Agric. Food Chem.*, **1992**, *40*, 1108.

4) J. McNulty, C. Zepeda-Velázquez, and D. McLeod, *Green Chem.*, **2013**, *15*, 3146.

5) J. McNulty and C. Zepeda-Velázquez. *Angew. Chemie Int. Ed.*, **2014**, *53*, 8450.

4.8 References

1) W. H. Perkin Jun., *J. Chem. Soc.* **1887**, *51*, 1.

2) R. Stockman, *Brit. Med. J.* **1889**, *1* (1480), 1043.

3) C. Liebermann and O. Bergami, *Ber. Dtsch. Chem. Gesel.* **1889**, *22*, 782.

4) C. Liebermann, *Ber. Dtsch. Chem. Gesel.* **1889**, *22*, 124.

5) C. Liebermann, *Ber. Dtsch. Chem. Gesel.* **1889**, *22*, 130.

6) C. N. Riiber. *Ber. Dtsch. Chem. Gesel.* **1902**, *35*, 2411.

7) C. Liebermann, *Ber. Dtsch. Chem. Gesel.* **1895**, *28*, 1438.

8) C. N. Riiber, *Ber. Dtsch. Chem. Gesel.* **1902**, *35*, 2908.

9) V. M. Dembitsky, *J. Nat. Med.* **2007**, *62*, 1.

10) Y-Y. Fan, X-H. Gao, J-M. Yue, *Sci. China Chem.* **2016**, *59*, 1126.

11) E. M. Carreira and T. C Fessard, *Chem. Rev.* **2014**, *114*, 8257.

12) C. M. Marson, *Chem. Soc. Rev.* **2011**, *40*, 5514.

13) K. A. Brameld, B. Kuhn, D. C. Reuter, M. Stahl. *J. Chem. Inf. Model.* **2008**, *48*, 1.

14) F. Secci, A. Frongia, P. P. Piras, *Molecules.* **2013**, *18*, 15541.

15) E. Lee-Ruff and G. Mladenova, *Chem. Rev.* **2003**, *103*, 1449.

16) J. C. Namyslo and D. E. Kaufmann, *Chem. Rev.* **2003**, *103*, 1485.

17) G. Ciamician and P. Silber, *Ber. Dtsch. Chem. Gesel.* **1908**, *41*, 1928.

18) G. Büchi and I. M. Goldman, *J. Am. Chem Soc.* **1957**, 79, 4741.

19) G. O. Schenk, W. Hartmann, S-P. Mannsfeld, W. Metzner, C. H. Krauch, *Chem. Ber.* **1962**, *95*, 1642.

20) P. E. Eaton, *J. Am. Chem. Soc.* **1962**, *84*, 2454.

21) H. I. Bernstein and W. C. Quimby. *J. Am. Chem. Soc.* **1943**, *65*, 1845.

22) S Poplata, A. Tröster,Y-Q. Zou, T. Bach, *Chem. Rev.* **2016**, *116*, 9748.

23) S. Ghosh, In CRC Handbook of Photochemistry and Photobiology, 2nd ed.; Eds: W. M. Horspool, F. Lenci; CRC Press: Boca Raton, **2004**; pp 18-1.

24) K. Langer, J. Mattay. In CRC Handbook of Photochemistry and Photobiology; Eds: W. M. Horspool, P-S. Song; CRC Press: Boca Raton, **1995**; pp 84.

25) R. G. Salomon, *Tetrahedron* **1983**, *39*, 485.

26) C. K. Prier, D. A. Rankic, D. W. C. MacMillan, *Chem. Rev.* **2013**, *113*, 5322.

27) K. Tanaka and T. Fujiwara, *Org. Lett.* **2005**, *7*, 1501.

28) K. Tanaka *et al.*, *Tetrahedron* **2000**, *56*, 6853.

29) J. Bernstein and B. S. Green, *J. Am. Chem. Soc.* **1980**, *102*, 323.

30) D. Haag, H-D. Scharf *J. Org. Chem.* **1996**, *61*, 6127.

31) A. I. Meyers and S. A. Fleming, *J. Am. Chem. Soc,* **1986***, 108*, 306.

32) R. Brimioulle, T. Bach, *Science* **2013**, *342*, 840.

33) R. Brimioulle, A. Bauer, T. Bach, *J. Am. Chem. Soc.* **2015**, *137*, 5170.

34) R. Brimioulle, D. Lenhart, M. M. Maturi, T. Bach, *Angew. Chem., Int. Ed.* **2015**, *54*, 3872.

35) R. Brimioulle, T. Bach, *Angew. Chem., Int. Ed.* **2014**, *53*, 12921.

36) S. Poplata and T. Bach, *J. Am. Chem. Soc.* **2018**, *140*, 3228.

37) H. Guo, E. Herdtweck, T. Bach. *Angew. Chem., Int. Ed.* **2010**, *49*, 7782.

38) R. Brimioulle, H. Guo, T. Bach. *Chem. Eur. J.* **2012**, *18*, 7552.

39) K. A. Austin, E. Herdtweck, T. Bach, *Angew. Chem., Int. Ed.* **2011**, *50*, 8416.

40) S. C. Coote, A. Pöthig, T. Bach, *Chem. Eur. J.* **2015**, *21*, 6906.

41) S. C. Coote, T. Bach, *J. Am. Chem. Soc.* **2013**, *135*, 14948.

42) D. Albrecht, B. Basler, T. Bach, *J. Org. Chem.* **2008**, *73*, 2345.

43) P. Selig and T. Bach, *J. Org. Chem.* **2006**, *71*, 5662.

44) T. Bach and H. Bergmann, *J. Am. Chem. Soc.* **2000**, *122*, 11525.

45) F. Mayr, C. Wiegand, T. Bach, *Chem. Comm.* **2014**, *50*, 3353.

46) N. Vallavoju *et al.*, *Angew. Chem., Int. Ed.* **2014**, *53*, 5604.

47) N. Vallavoju *et al.*, *Adv. Synth. Catal.* **2014**, *356*, 2763.

48) G. S. Hammond and R. S. Cole, *J. Am. Chem. Soc.* **1965**, *87*, 3256.

49) C. Ouannès, R. Beugelmans, G. Roussi, *J. Am. Chem. Soc.* **1973**, *95*, 8472.

50) D. F. Cauble, V. Lynch, M. J. Krische, *J. Org. Chem.* **2003**, *68*, 15.

51) C. Müller, A. Bauer, T. Bach, *Angew. Chem. Int. Ed.* **2009**, *48*, 6640.

52) R. Alonso and T. Bach, *Angew. Chem. Int. Ed.* **2014**, *53*, 4368.

53) M. M. Maturi *et al.*, *Chem. Eur. J.* **2013**, *19*, 7461.

54) C. Müller *et al.*, *J. Am. Chem. Soc.* **2011**, *133*, 16689.

55) M. M. Maturi and T. Bach, *Angew. Chem. Int. Ed.* **2014**, *53*, 7661.

56) Y. Xu, M. L. Conner, M. K. Brown, *Angew. Chem. Int. Ed.* **2015**, *54*, 11918.

57) B. Alcaide, P. Almendros, C. Aragoncillo, *Chem. Soc. Rev.* **2010**, *39*, 783.

58) S. V. Lebedev, *Zhur. Russ. Fiz-Khim. Obshch.* **1911**, *43*, 820.

59) S. V. Lebedev and B. K. Merezhkovskii, *Zhur. Russ. Fiz-Khim. Obshch.* **1925**, *45*, 1913.

60) A. T. Blomquist and J. A. Verdol, *J. Am. Chem. Soc.* **1956**, *78*, 109.

61) K. Alder and O. Ackermann, *Chem. Ber.* **1957**, *90*, 1697.

62) H. N. Cripps, J. K. Williams, W. H. Sharkey, *J. Am. Chem. Soc.* **1958**, *80*, 751.

63) H. N. Cripps, J. K. Williams, W. H. Sharkey, *J. Am. Chem. Soc.* **1959**, *81*, 2723.

64) E. R. Buchman and H. L. Herzog, *J. Org. Chem.* **1951**, *16*, 99.

65) H. Staudinger and E. Suter, *Ber.* **1920**, *53*, 1092.

66) H. Staudinger, *Helv. Chim. Acta* **1924**, *7*, 19.

67) E. Vogel and K. Muller, *Just. Lieb. Annalen Chem.* **1958**, *615*, 29.

68) A. D. Allen and T. T. Tidwell, *Chem. Rev.* **2013**, *113*, 7287.

69) S. Ma, *Chem. Rev.* **2005**, *105*, 2829.

70) D. H. Paull, A. Weatherwax, T. Lectka, *Tetrahedron* **2009**, *65*, 6771.

71) L. A. Paquette. In Asymmetric Synthesis Volume 3; Eds: J. Morrison; Academic Press: **1984**; pp 483.

72) A. I. Myers, M. A. Tschantz, G. P. Brengel, *J. Org. Chem.* **1995**, *60*, 4359.

73) S. Ahmad, *Tet. Lett.* **1991**, *32*, 6997.

74) Y. Hayashi and K. Narasaka, *Chem. Lett.* **1989**, *18*, 793.

75) K. Narasaka, Y. Hayashi, H. Shimadzu, S. Niihata, *J. Am. Chem. Soc.* **1992**, *114*, 8869.

76) K. Narasaka, K. Hayashi, Y. Hayashi, *Tetrahedon* **1994**, *50*, 4529.

77) Y. Hayashi, K. Otaka, N. Saito, K. Narasaka. *Bull. Chem. Soc. Jpn.* **1991**, *64*, 2122.

78) T. A. Engler, M. A. Letavic, J. P. Reddy. *J. Am. Chem. Soc.* **1991**, *113*, 5068.

79) T. A. Engler, M. A. Letavic, R. Iyengar, K. O. LaTessa, *J. Org. Chem.* **1999**, *64*, 2391.

80) E. Canales and E. J. Corey, *J. Am. Chem. Soc.* **2007**, *129*, 12686.

81) M. R. Luzung, P. Mauleon, F. D. Toste. *J. Am. Chem. Soc.* **2007**, *129*, 12402.

82) S. Suárez-Pantiga, C. Hernández-Diaz, E. Rubio, J. M. González. *Angew. Chem. Int. Ed.* **2013**, *51*, 11552.

83) F. Lopez and J. L Mascareñas. *Beilstein J. Org. Chem.* **2013**, *9*, 2250.

84) K. Ishihara and K. Nakano. *J. Am. Chem. Soc.* **2007**, *129*, 8930.

85) K. C. Brannock, R. D. Burpitt, V. W. Goodlett, J. G. Thweatt. *J. Org. Chem.* **1964**, *29*, 818.

86) J. Burési, A. Armstrong, D. G. Blackmond. *J. Am. Chem. Soc.* **2011**, *133*, 8822.

87) K. Patora-Komisarska *et al.*, *Helvetica*, **2011**, *94*, 719.

88) J. Burési, A. Armstrong, D. G. Blackmond. *J. Am. Chem. Soc.* **2012**, *134*, 6741.

89) G. Talavera, E. Reyes, J. L. Vicario, L. Carillo. *Angew. Chem.* **2012**, *124*, 4180.

90) L. Albrecht *et al. J. Am. Chem. Soc.* **2012**, *134*, 2543.

91) L-W. Qi *et al. Org. Lett.* **2014**, *16*, 6436.

92) G-J. Duan *et al. Chem. Commun.* **2013**, *49*, 4625.

93) G. Bergonzini *et al. Chem. Commun.* **2010**, *46*, 327.

94) C. Gioia, L. Bernardi, A. Ricci. *Synthesis.* **2010**, *1*, 161.

95) C. Zheng *et al. Chem. Eur. J.* **2010**, *16*, 5853.

96) L-J. Huang, J. Weng, S. Wang, G. Lu. *Adv. Syn. Catal.* **2015**, *357*, 993.

97) E. Rossi, G. Abbiati, V. Pirovano. *Eur. J. Org. Chem.* **2017**, *31*, 4512.

5 Amaryllidaceae Alkaloid Total Synthesis and Biological Activity

5.1 Anti-cancer and anti-viral activity of the Amaryllidaceae alkaloids

The Amaryllidaceae are a cosmopolitan family of flowering plants that typically grow from underground bulbs, encompassing approximately 75 genera and 1100 species, and they produce a diverse array of alkaloid natural products.[1–4] The first reported Amaryllidaceae alkaloid was lycorine, isolated from N. *pseudonarcissus* by Gerrard in 1877.[5] Since then, over 500 different alkaloids have been reported, covering 11 major structural classes (Figure 5.1).[1] These natural products display a wide range of promising biological activities including antidiabetic, antiviral, anticancer, anti-inflammatory, antioxidant, and cholinesterase inhibiting activities. These activities have prompted many total syntheses and the exploration of synthetic derivatives by medicinal chemists. The potential of the Amaryllidaceae alkaloids as chemotherapeutics is well demonstrated by galanthamine, currently approved for the treatment of moderate memory impairment in Alzheimer's disease and dementia.[6]
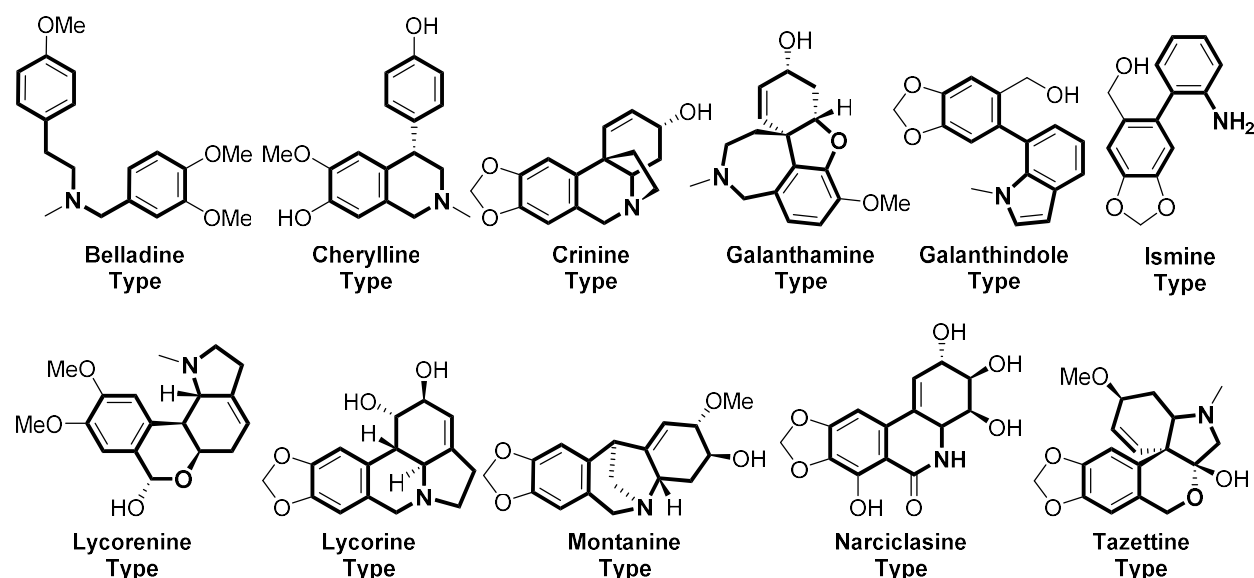
FIGURE 5.1 The major Amaryllidaceae alkaloid classes (generic skeletons shown in bold) and their eponymous natural products.
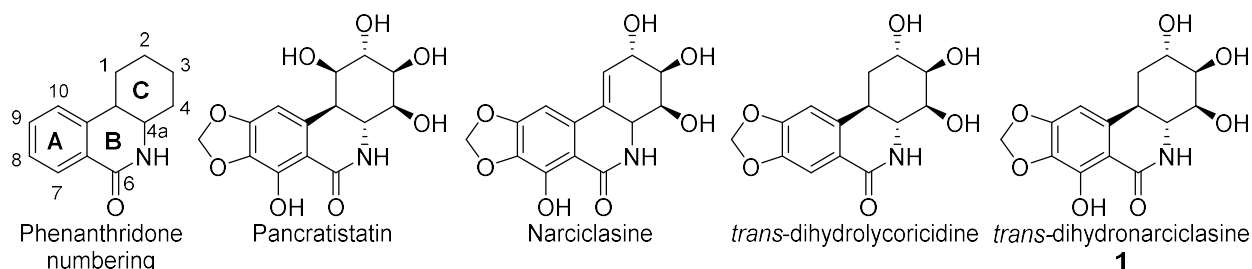
FIGURE 5.2 Amaryllidaceae alkaloids based on the narciclasine phenanthridone core.

The McNulty group and collaborators have dedicated a substantial amount of work exploring the biological activity and synthesis of the Amaryllidaceae alkaloids, with an emphasis on the narciclasine class which features a phenanthridone core (Figure 5.2).[7,8,17–25,9–16] Pancratistatin and narciclasine are the most well-known members of this class and are known to reduce cancer cell proliferation by various mechanisms.[26] Narciclasine targets the 60S subunit of ribosomes and hence protein biosynthesis, as well as GTPase elongation factors eEF1A and RhoA which impairs cytoskeleton organization.[27–29] Unfortunately, it also inhibits human cytochrome P450 3A4, and has demonstrated limited efficacy in mouse tumour models of cancer.[7,24,27] Pancratistatin selectively induces apoptosis in cancer cells and is known to target complex II and III of the mitochondria and has proven efficacious in mouse models using human tissue xenografts for several different cancers.[9,10,26,30] Substantial synthetic efforts have led to the refinement and discovery of the minimum pancratistatin pharmacophore, proving the C2, C3, and C4 hydroxyls as well as the *trans* B/C ring junction to be critical.[17] This pharmacophore is well represented by *trans*-dihydrolycoricidine and *trans*-dihydronarciclasine **1**. Elimination of the C ring double bond reduces the ability of these compounds to inhibit CYP450 3A4, thus increasing their potential as human chemotherapeutics.[7]

Amaryllidaceae alkaloids from the narciclasine class were reported by Gabrielsen *et al.* in 1992 to possess potent activity against several flaviviruses including Japanese encephalitis, yellow fever and dengue viruses *in vitro*.[31] However, further research into this antiviral activity was limited, possibly due

to a strong focus on their anticancer effects. The McNulty group's collaboration with the Stanley Medical Research Institute prompted the exploration of the anti-HSV-1 activity of these compounds. To that end, an organocatalytic total synthesis of *trans*-dihydrolycoricidine was completed, and the compound proved to be more effective than acyclovir in reducing HSV-1 replication in iPSC neurons.[32,33] Not only did it inhibit the lytic infection, it significantly reduced reactivation of latent HSV-1 infections, and proved even more effective against the lytic phase of the closely related varicella zoster virus. Additional work has shown that *trans*-dihydrolycoricidine is effective in acyclovir resistant strains of HSV-1 and completely inhibits viral gene transcription.[34]

In Gabrielsen *et al.*'s initial report, *trans*-dihydronarciclasine **1** consistently demonstrated the most potent anti-flaviviral activity compared to the other Amaryllidaceae alkaloids tested.[31] Given the promising anti-HSV results obtained with *trans*-dihydrolycoricidine, the McNulty group and their collaborators at the SMRI were eager to test **1** against other flaviviruses. Unfortunately, **1** has a very low natural abundance making isolation from plant material impractical.[35] Although semi-synthesis via hydrogenation of narciclasine is known, facial selectivity in the hydrogenation can be poor; c*is*-dihydronarciclasine is substantially less potent as an antiviral and very difficult to separate from the desired *trans*-dihydronarciclasine.[31,36] This left total synthesis as the best method for obtaining **1**.

Several racemic and asymmetric total syntheses of **1** have been reported and are reviewed below (Chapters 5.2 and 5.3). Although meritorious efforts, most of the syntheses are quite lengthy and low yielding. Thus, a total synthesis of **1** based on the same strategy used by the McNulty group to prepare *trans*-dihydrolycoricidine was developed and is the subject of Chapter 5.4. While ultimately successful, substantial work was necessary to overcome problems with a late stage-oxidation, discussed in more detail in Chapter 5.5.

5.2 Racemic total syntheses of *trans*-dihydronarciclasine

The first total synthesis of *trans*-dihydronarciclasine was reported by the Cho group in 2007.[37] Their synthesis begins with the thermal Diels-Alder reaction between 3,5-dibromopyrone and an electron-rich styrene, produced by the Wittig methylenation of 5-methoxypiperonal (Scheme 5.1).[38] Previous work by Cho had demonstrated that dibromopyrones are highly *endo* selective participants in Diels-Alder reactions.[39] This fact was well-demonstrated in the first step of their synthesis, which gave the desired cycloadduct in effectively quantitative yield and 98:2 *endo:exo* ratio. Subsequent debromination and acid catalyzed methanolysis of this cycloadduct gives the carbon skeleton of (±)-**1** in only three steps. Alkene *syn*-hydroxylation on the less hindered face was achieved using catalytic osmium tetroxide and 4-methylmorpholine-*N*-oxide (NMO), mild conditions that have been successfully used in the syntheses of several other Amaryllidaceae alkaloids.[40–42]

Having successfully installed all three alcohol groups in the correct relative stereochemistry, the methyl ester was cleaved with lithium hydroxide. Treatment with diphenylphosphoryl azide and triethylamine in refluxing toluene causes a Curtius rearrangement, and the isocyanate intermediate was
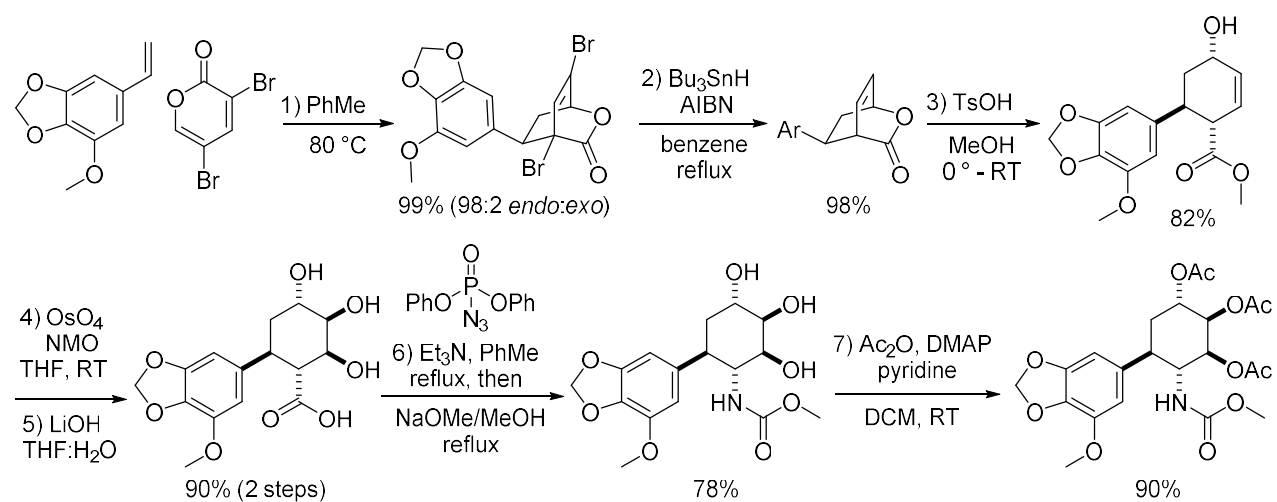
SCHEME 5.1 Cho *et al.*'s synthesis of (±)-**1** is based on a high yielding and highly *endo*-selective Diels-Alder reaction, providing the basic carbon skeleton of **1** in three steps.
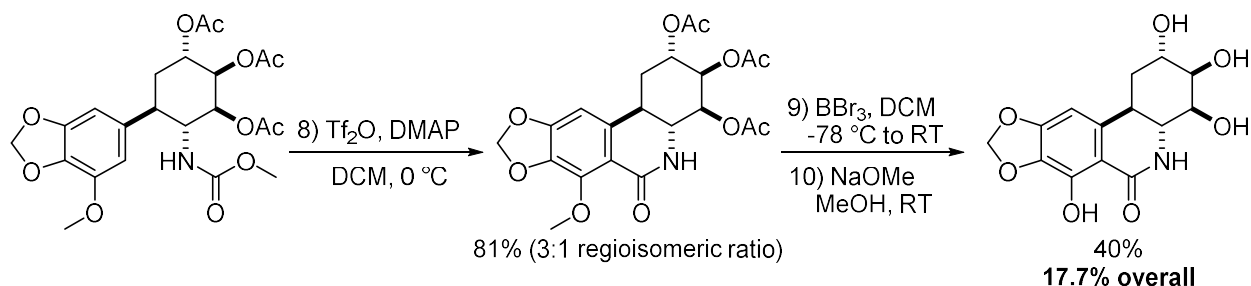
SCHEME 5.2 Cho *et al.*'s total synthesis of (±)-**1** was completed using a Banwell modified Bischler-Napieralski reaction followed by global deprotection.

trapped with sodium methoxide to form a methoxycarbamate at C4a.[43] Peracetylation of the hydroxy groups was performed prior to the construction of the B ring, which was accomplished by a Banwell modified Bischler-Napieralski (BBN) reaction (Scheme 5.2).[44] The synthesis was completed by deprotecting the phenol with boron tribromide and basic cleavage of the acetate protecting groups, giving (±)-**1** in 15.8% yield over ten steps from the starting styrene. Most of the steps in the synthesis are very high yielding, except for the BBN reaction which gives a mixture of regioisomers and the phenol deprotection. Nevertheless, the last three steps of the synthesis, namely the BBN followed demethylation and basic ester cleavage, appear in many other total syntheses of **1**.

Shortly after their first total synthesis, the Cho group published a total synthesis of (±)-**1** designed to eliminate the need for the BBN reaction, which gave an inseparable mixture of regioisomers and was one of the lowest yielding steps in their synthesis.[45] Their overall strategy was similar, but used a carboxylate substituted styrene in the initial Diels-Alder reaction (Scheme 5.3).
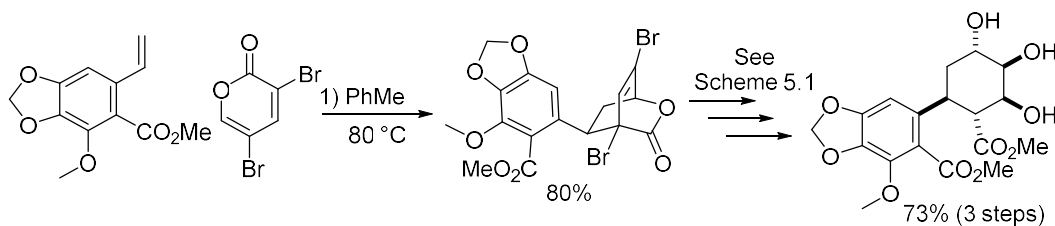
SCHEME 5.3 Cho *et al.*'s second synthesis (±)-**1** used a carboxylate substituted styrene.
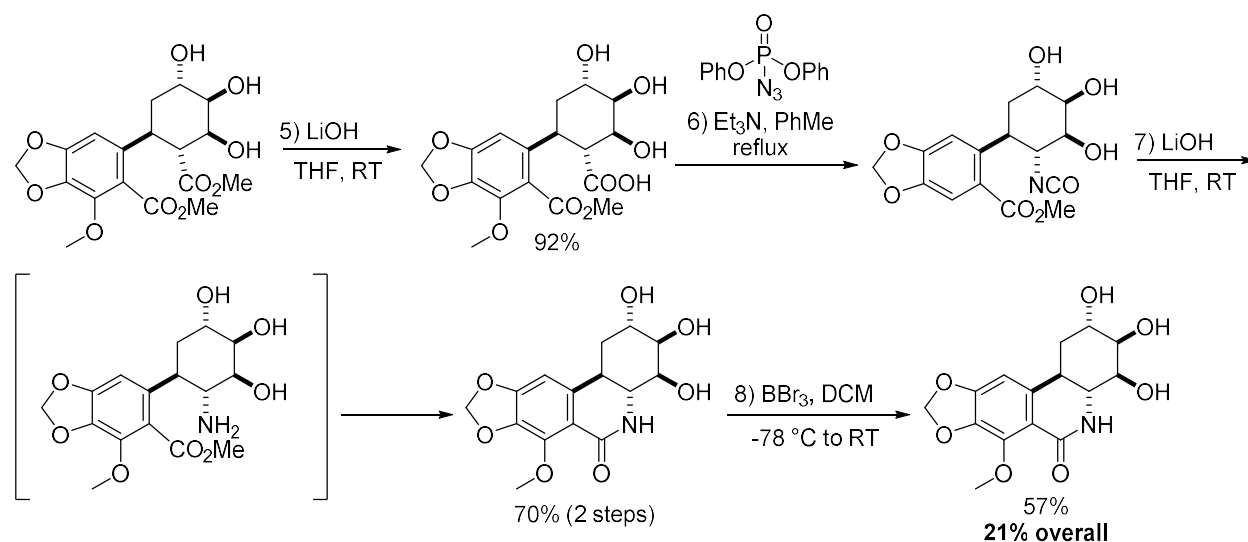
SCHEME 5.4 Cho *et al.*'s second synthesis of (±)-**1** prepared the B ring via the conversion of the C4a carboxylate to an amine, resulting in spontaneous intramolecular amide formation.

The Diels-Alder adduct was carried through the previously described steps to give a triol with methyl esters substituted at C4a and C6a. Selective cleavage of the methyl ester at 4a was performed, enabling a Curtius rearrangement with diphenylphosphoryl azide to generate an isocyanate intermediate, as reported in their first synthesis (Scheme 5.4).[37] However, instead of treating the isocyanate with methanolic sodium methoxide, it was hydrolyzed to a free amine which spontaneously reacted with the C6a methyl ester, forming the B ring in two steps and 70% yield. After demethylation using boron tribromide, (±)-**1** was obtained in only 8 steps and 21% overall yield, without requiring the installation of protecting groups. However, it should be noted that the dienophile styrene used in the Diels-Alder reaction took seven steps to prepare from readily available starting materials, thus hindering the overall efficiency of the synthesis.

The most recent racemic total synthesis of **1** was reported by the Kádas group in 2016 and begins with the Michael addition of nitromethane to the phenylbutenone derived from methoxypiperonal (Scheme 5.5).[46] A tandem Claisen Henry reaction onto ethyl formate formed the C ring of **1** in 19.5% yield from methoxypiperonal. Protection of the ketone, followed by hydrogenation
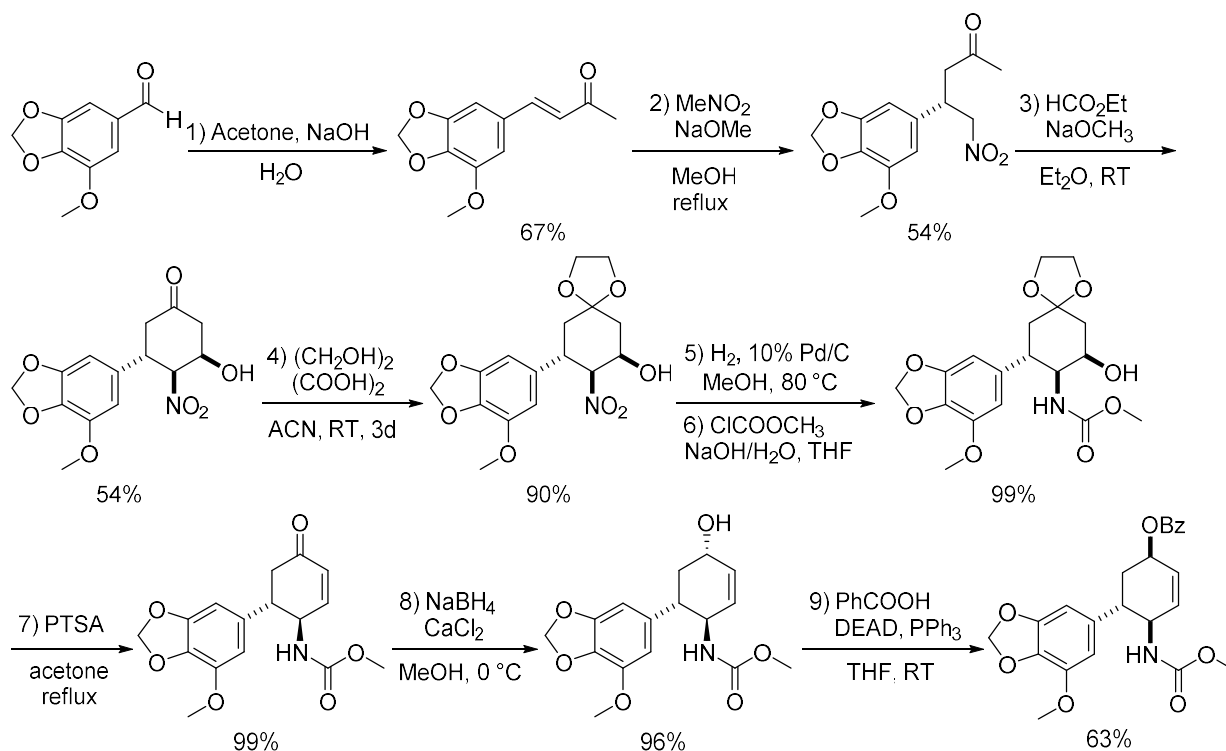
SCHEME 5.5 The total synthesis of (±)-**1** by the Kádas group used a Michael reaction of nitromethane onto a butenone derivative, followed by a tandem Claisen Henry reaction on ethyl formate to construct the C ring.

of the C4a nitro group and treatment with methyl chloroformate gave the MOC protected amine in 88% yield over three steps. Simultaneous elimination of the C4 hydroxyl and deprotection of the C2 carbonyl was achieved with total regioselectivity and in 99% yield by refluxing with PTSA in acetone. Hydride reduction of the carbonyl gave the wrong relative stereochemistry, necessitating an inversion via Mitsunobu esterification with benzoic acid.[47] Oxidation with osmium tetroxide followed by acetylation and a BBN reaction are all reported to proceed in quantitative yield (Scheme 5.6). Interestingly, the BBN was reported to produce a methoxyphenanthridine product with total regioselectivity, even though poor regioselectivity is a well known issue in other total syntheses of related Amaryllidaceae alkaloids.[37,41,42,48–51] Phenanthridines are known products of the BBN reaction but hydrolysis during workup is often unavoidable and the amide product is far more common. The reasons for this unusual result cannot be determined as no experimental details were provided.
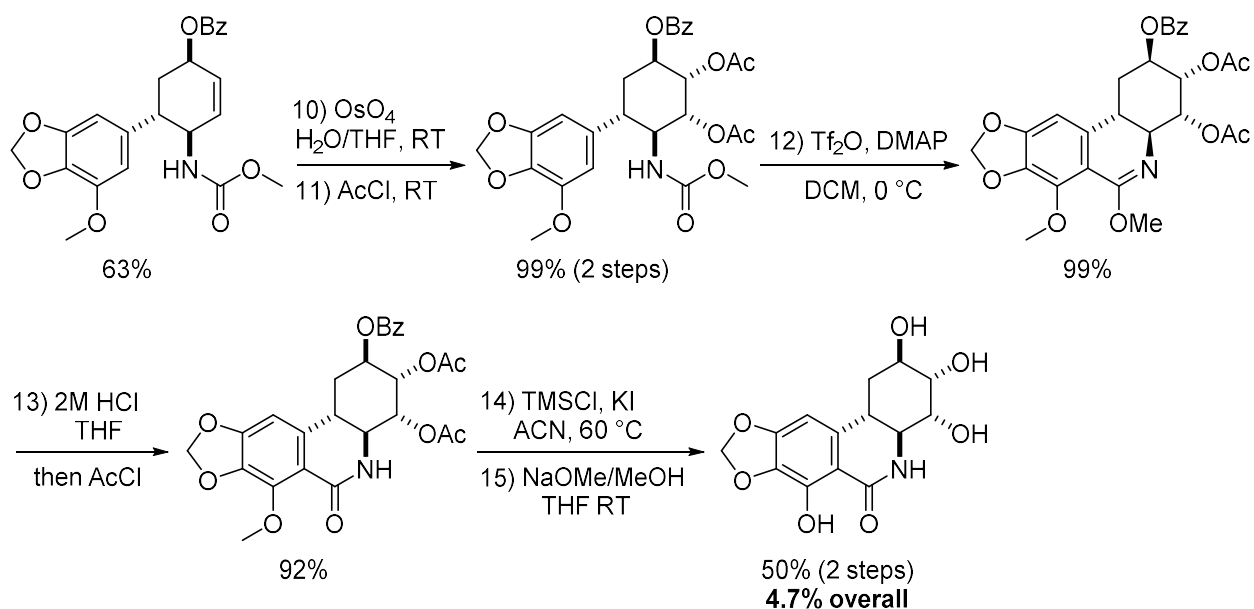
SCHEME 5.6 The Kádas group's total synthesis of (±)-**1** was completed after a number of remarkably high yielding transformations.

Demethylation using TMSCl and potassium iodide, followed by basic ester hydrolysis afforded (±)-**1** in 4.7% overall yield. A series of exceptionally high yielding steps, including an entirely regioselective BBN reaction, are inconsistent with the literature yields of similar reactions on closely related substrates. As well, inspection of the ^{13}C NMR data suggests that noise was assigned and reported as peaks in more than one instance. These facts, combined with the lack of a provided experimental procedure, raise substantial concerns about the reproducibility of the synthesis, especially for the steps following the formation of the C ring. Even so, this synthesis required more steps and was also lower yielding than the previously discussed syntheses of (±)-**1**.

5.3 Asymmetric syntheses of *trans*-dihydronarciclasine

Prior to the work by the McNulty group, there were three asymmetric total syntheses of (+)-**1** reported in the literature, and a synthesis of (-)-**1** appeared shortly thereafter. The first total synthesis of (+)-**1** was completed by Jana and Studer in 2008 and begins with the preparation of a bromoanisole derivative in three steps from *o*-vanillin (Scheme 5.7).[49,50] Br-Li exchange and transmetalation with copper enabled a cross coupling with an iron-complexed cyclohexadienyl cation to prepare a racemic cyclohexadiene after oxidative decomplexation with ceric ammonium nitrate.[52,53] This effectively builds the carbon backbone of both A and C rings in 85% yield over two steps. Next, a copper catalyzed regiodivergent Diels-Alder reaction between the diene and 2-nitrosopyridine was performed using Walphos as a chiral ligand.[54] Previously reported by their group, this reaction converts each enantiomer of a racemic diene into separable regioisomeric cycloadducts.[55] Although capable of high enantioselectivity, a limitation of the reaction is that it cannot produce the desired product in more than 50% yield. N-O bond cleavage using molybdenum hexacarbonyl and sodium borohydride prepares the C ring with correct stereochemistry for the substituents at C2 and C4a.
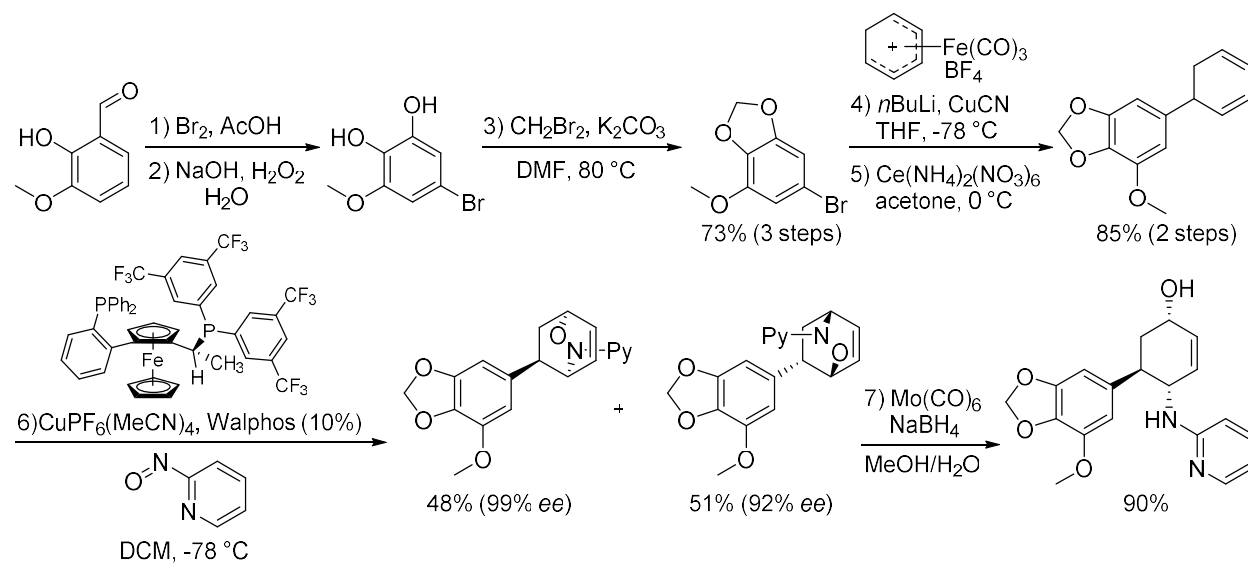
SCHEME 5.7 Jana and Studer's total synthesis of (+)-**1** had an enantioselective regiodivergent Diels-Alder reaction as the key asymmetry inducing step.
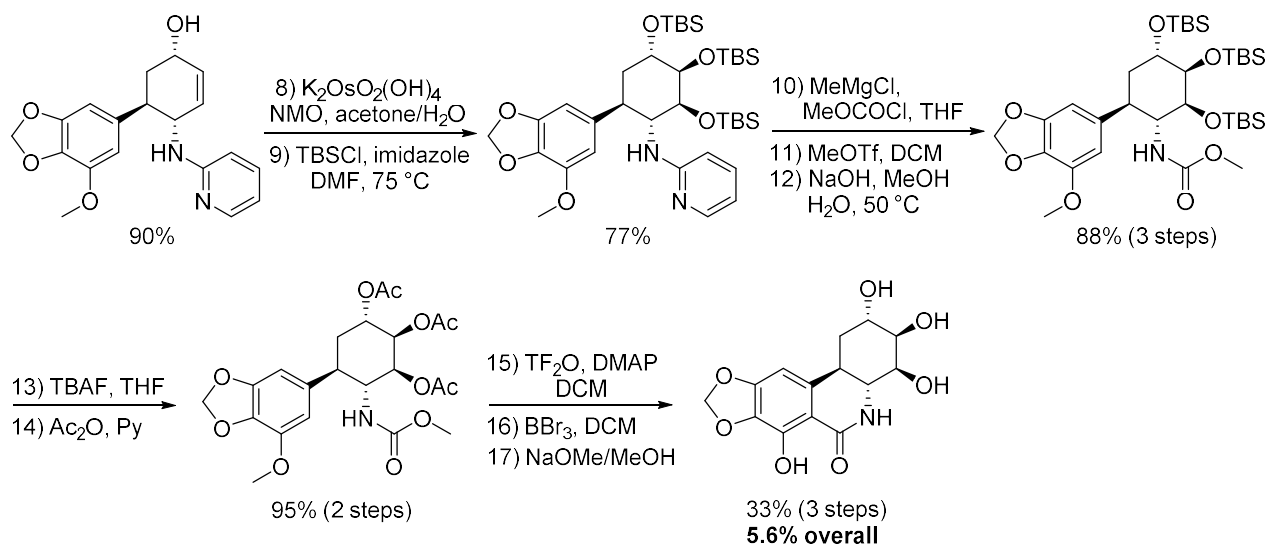
SCHEME 5.8 Jana and Studer's total synthesis of (+)-**1** employed a *syn* dihydroxylation, followed by several protecting group manipulations and was completed using the common strategy of BBN reaction followed by demethylation and ester cleavage.

Installation of the C3 and C4 hydroxyl groups was accomplished by facially selective *syn* dihydroxylation with potassium osmate (Scheme 5.8). Global TBS protection of the alcohol groups followed by formation of a MOC carbamate on the C4a nitrogen allowed for sequential methylation and basic hydrolysis of the pyridine ring. Exchange of the TBS protecting groups for acetate esters was performed prior to the BBN reaction, and completion of the synthesis was achieved after phenol demethylation and acetate cleavage. Although remarkable for being the first total synthesis of (+)-**1** and highlighting a novel and highly stereoselective Diels-Alder reaction, the synthesis suffers from late stage protecting group manipulations and uses costly ligands and transition metal complexes. Overall, the synthesis was completed in 5.6% yield over 17 linear steps.

The next total syntheses of (+)-**1** were both completed in 2012, with Hwang *et al.*'s work preceding the Tomioka group's by mere months. In the Hwang synthesis, asymmetry is instilled by using a chiral vinyl stannane in a Stille cross coupling on the same bromoanisole derivative used in Jana and Studer's total synthesis (Scheme 5.9).[48,49] The stannane can be prepared in large quantities
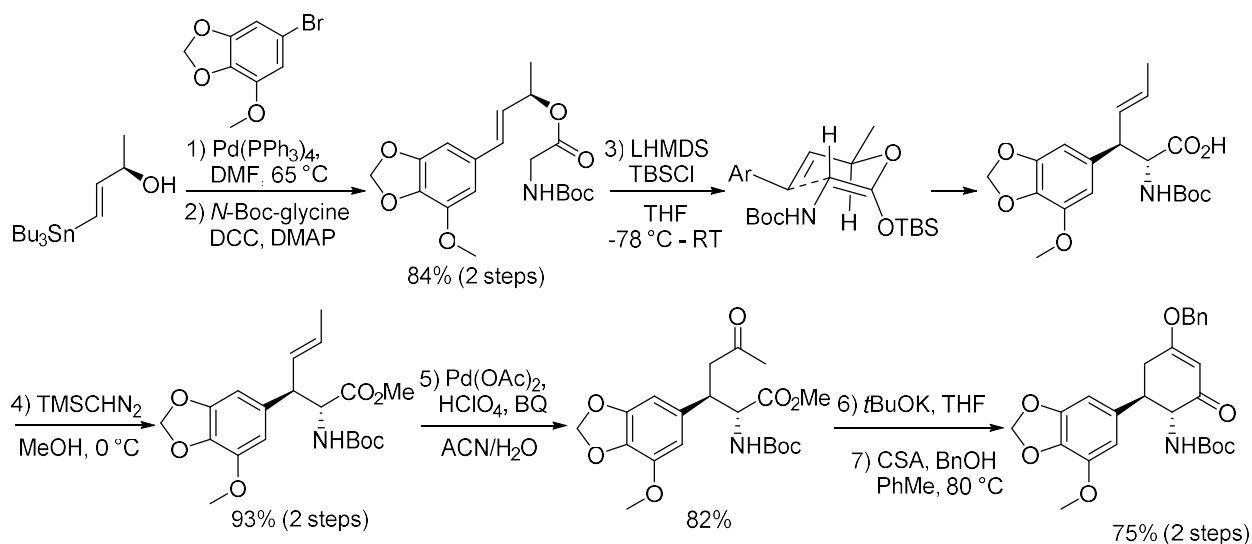
SCHEME 5.9 Hwang *et al.*'s total synthesis of (+)-**1** instilled asymmetry via the use of a chiral vinylstannane in an initial Stille cross coupling and prepared the C ring backbone of (+)-**1** in six steps.

in two steps by the palladium catalyzed hydrostannylation of butyne-3-ol followed by chiral enzymatic resolution.[56] After the Stille cross coupling, the allylic alcohol was coupled with *N*-BOC-glycine. Next, an ester-enolate Claisen rearrangement was performed by treating this amino acid ester with LiHMDS in the presence of TBS-Cl, and total diastereoselectivity was enforced by the equatorial position of the BOC group in the transition state.[57,58] Methylation using TMS-azidomethane, followed by a regioselective Wacker oxidation with perchloric acid and benzoquinone (BQ) enabled an intramolecular Claisen reaction to form the C ring of (+)-**1**.[59,60]

A series of manipulations were performed to functionalize the C ring, starting with the formation of an electron rich benzyl enol ether and stereospecific hydride reduction at C4 (Scheme 5.10). Epoxide formation and opening to install the C3 and C4 *trans* hydroxyl groups proved challenging and was unsuccessful using *m*-CPBA in DCM or vanadium acetylacetonate with *t*-butylhydroperoxide. Carefully buffered *m*-CPBA in methanol allowed tandem epoxide formation and methanolysis. Hydrogenative removal of the benzyl ether unmasked the C2 carbonyl which was reduced using L-selectride as a bulky hydride source.
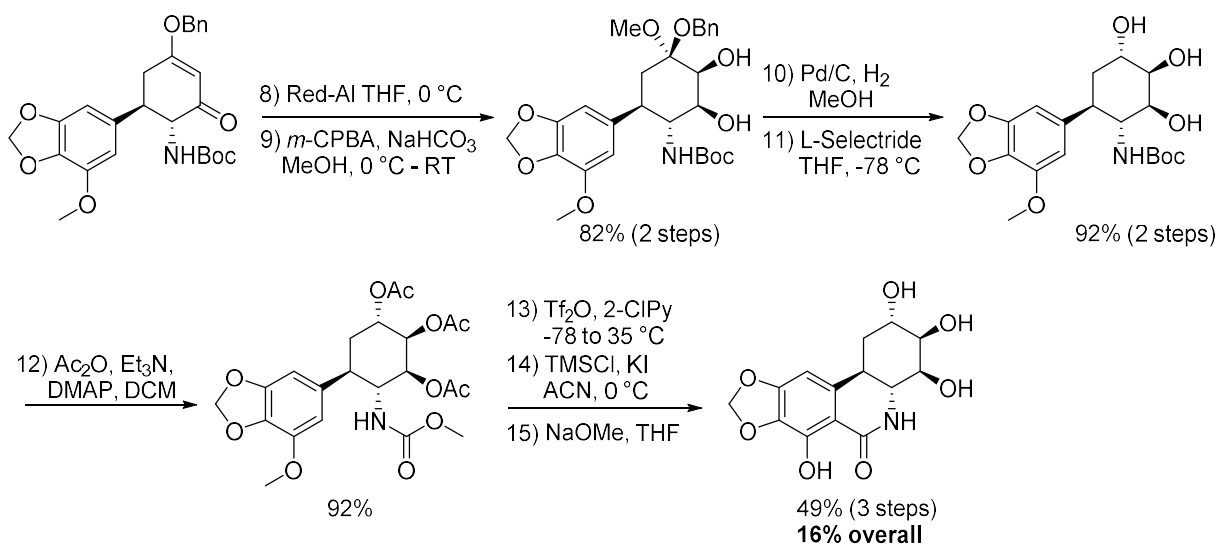
SCHEME 5.10 Hwang *et al.*'s synthesis of (+)-**1** required a series of reactions to prepare the C ring hydroxyl groups and then formed the B ring using a BBN reaction.

The completion of the synthesis was achieved using the same essential steps used in most other total syntheses of **1**, namely protection of the C ring alcohols, formation of the B ring via BBN reaction, removal of the phenolic methyl ether and cleavage of the acetate esters. Thus, the synthesis was completed in 15 linear steps and 16% overall yield from the Stille cross coupling. However, the yield would be less if the preparation of the starting bromoanisole derivative is considered. Even so, this remains the highest yielding total synthesis of (+)-**1** reported to-date.

Shortly after Hwang *et al.*'s total synthesis, the Tomioka group published a synthesis based on the asymmetric Michael addition of an aryl organolithium to an α,β-unsaturated ester using a C2-symmetric chiral ligand (Scheme 5.11).[61] Similar asymmetric conjugate additions have been extensively explored by the Tomioka group.[62–66] The product of the conjugate addition was obtained in good yield and enantioselectivity but has the wrong stereochemistry at C2. This was remedied by basic epimerization using potassium *t*-butoxide in a refluxing dioxane water mixture, conditions that also caused hydrolysis of the *t*-butyl ester. A Curtius rearrangement with diphenylphosphoryl azide was used to generate an isocyanate intermediate, which was then treated with TMSCl and *t*-butanol to
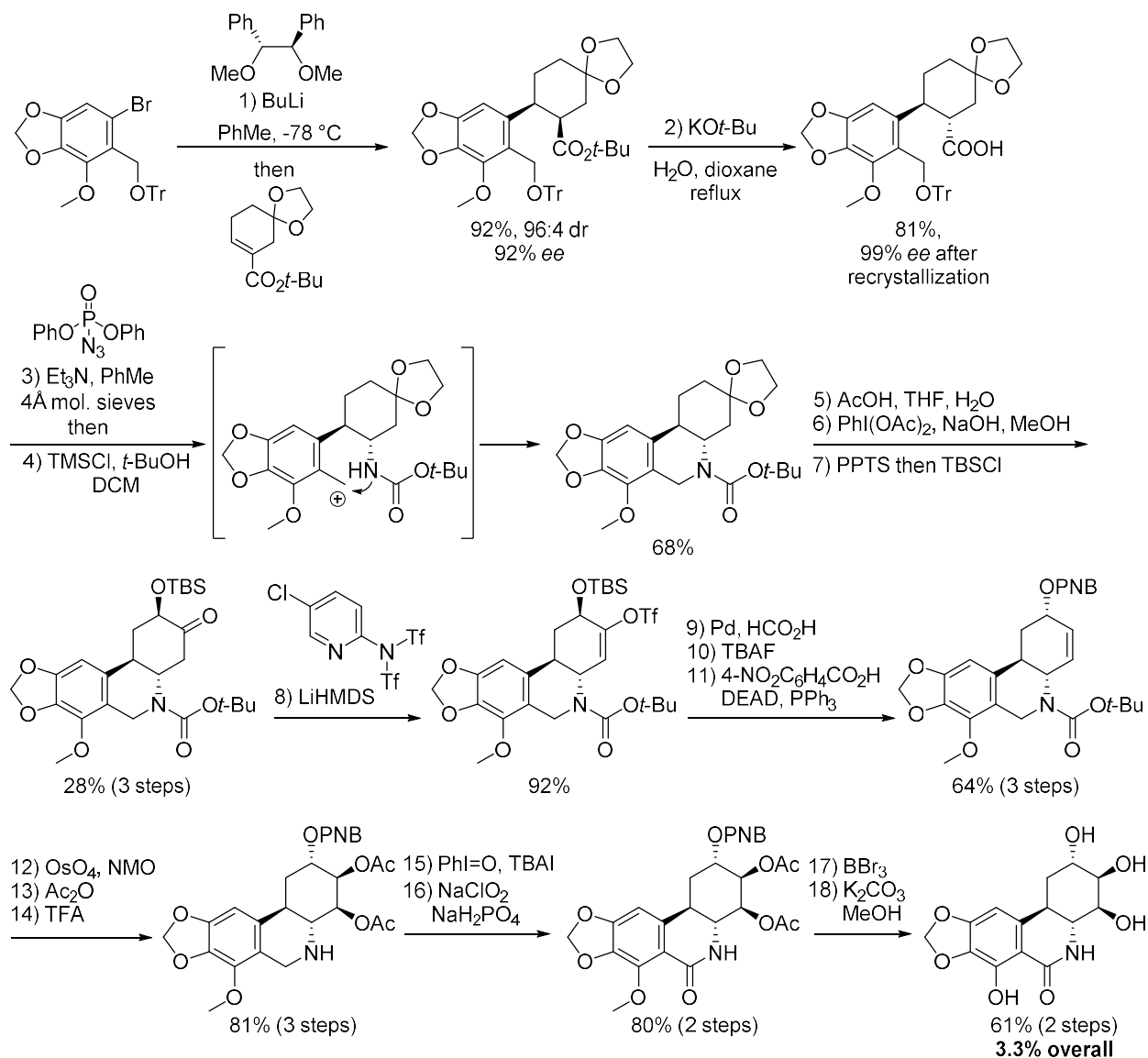
SCHEME 5.11 The synthesis of (+)-**1** by the Tomioka group used a chiral ligand to promote the asymmetric Michael addition of an aryllithium to an unsaturated ester. The carbon skeleton of both B and C rings was constructed within the first four steps, and the remainder of the synthesis focuses on the oxidative installation of the C ring hydroxyl groups and the B ring carbonyl.

obtain a BOC protected amine. Interestingly, the acidic conditions generated by the *in situ* hydrolysis of TMSCl also resulted in the protonolysis of the tritylated benzyl alcohol, generating a stable carbocation that was trapped by the contemporaneously installed amine. This fortuitous result allowed for the construction of the phenanthridone carbon skeleton in 51% yield over four steps.

Although the B and C rings were prepared in only four steps, another 14 steps were required to complete the synthesis (Scheme 5.11). Acetal cleavage at C3 using acetic acid, followed by a regioselective oxidation α to the carbonyl with PhI(OAc)$_2$ was used to install the C2 hydroxyl, albeit with the wrong stereochemistry. This intermediate was then protected as a TBS ether and the C3 carbonyl was converted to a vinyl triflate with Comin's reagent prior to hydrogenolysis with palladium using formic acid as the hydrogen source.[67] Deprotection of the C2 hydroxyl was followed by its inversion via Mitsunobu reaction with 4-nitrobenzoic acid. *Syn* dihydroxylation of the alkene and subsequent acetate protection yields a fully functionalized C ring.

Completion of the B ring was achieved by sequential oxidation of C6, first to the imine after BOC deprotection and then to the required amide. Ester cleavage and phenol demethylation complete the synthesis, for an overall yield of 3.3% over 18 linear steps. Although not discussed, the exact order and choice of oxidants required careful optimization to avoid oxidative decomposition of the electron rich A ring. This fact also necessitated multiple protecting group manipulations, making this the lengthiest synthesis of (+)-**1** even without considering the steps required to prepare the starting materials. Overall, the synthesis highlights a novel way to quickly access the phenanthridone skeleton but is less suitable for the synthesis of (+)-**1** in appreciable quantities.

After the synthesis of (+)-**1** by the McNulty group (*vide infra*, Chapter 5.4) a synthesis of (-)-**1** was published by the Kádas group using essentially the same synthetic strategy as reported in their racemic synthesis.[68] The main difference takes place in the initial Michael addition of nitromethane to the butanone derivative (Scheme 5.12), where use of a chiral cinchona derived primary amine catalyst allows the reaction to be performed under much milder conditions and with substantial enantioselectivity.[69] Unfortunately, many of the same issues associated with their racemic synthesis reappear in the asymmetric synthesis. As well as exceptionally high yields in the latter half of the synthesis, the spectra in the supporting information are direct copies from the racemic synthesis and
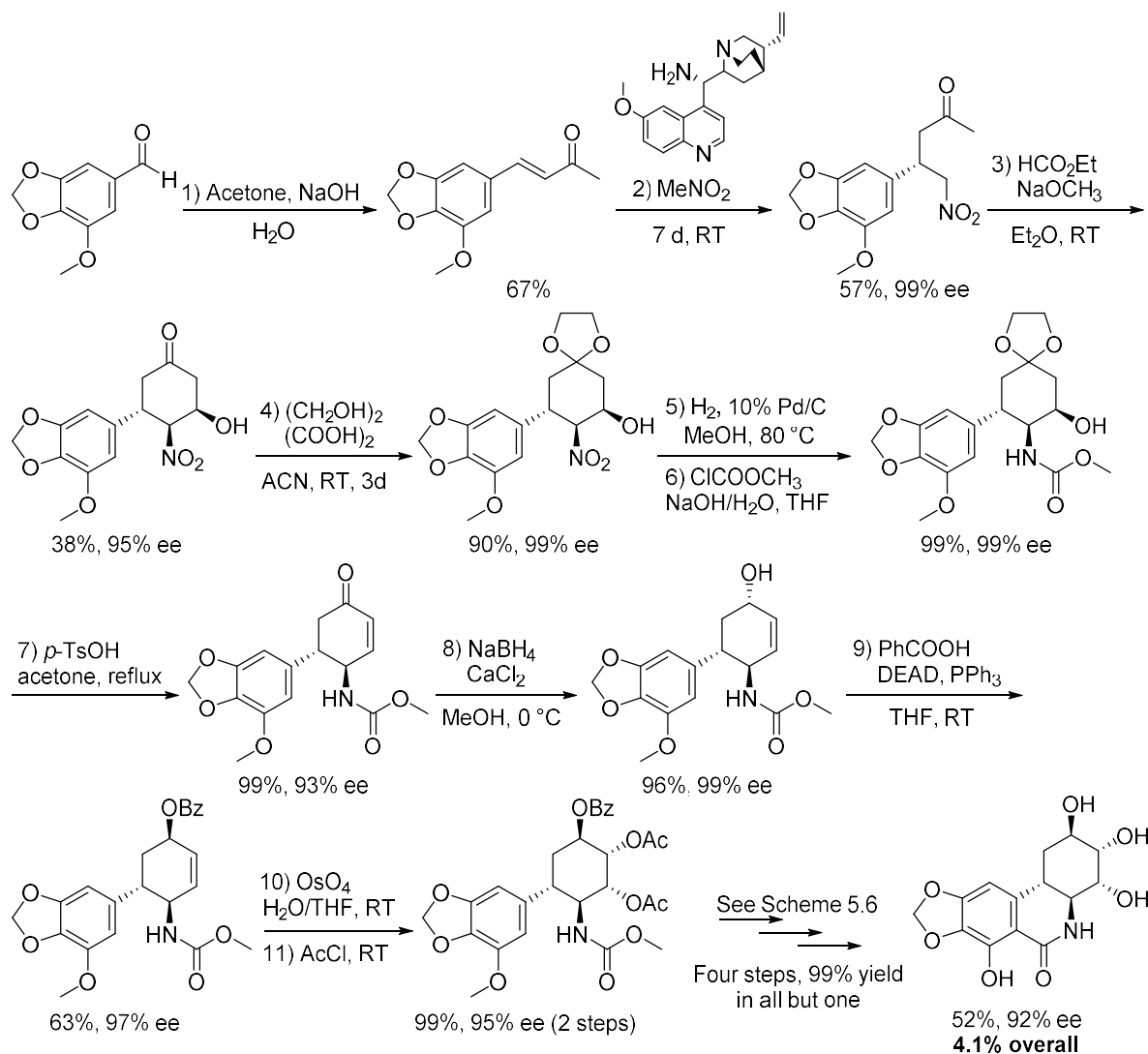
SCHEME 5.12 The Kádas group reported the total synthesis of (-)-**1** using an almost identical strategy as reported for their synthesis of the racemic natural product.

noise is reported as desired peaks.[46,68] Furthermore, the reported *e.e.* varies throughout the synthesis for non-obvious and unexplained reasons, dropping from 99% *e.e.* in several intermediates to 92% *e.e* in the final product. Despite these issues, their report technically constitutes the first total synthesis of (-)-**1**, although it is worth noting that simply using the antipode of the catalyst used in the McNulty group's synthesis (*vide infra*) would readily and reproducibly provide the non-natural enantiomer of *trans*-dihydronarciclasine.

Given the promising biological activity of (+)-**1** and other Amaryllidaceae alkaloids, the McNulty group was interested in exploring its anti-viral activity with their collaborators at the SMRI. Although there are several asymmetric total syntheses for **1,** they are either too lengthy or expensive to be viable sources of **1** in quantities necessary for biological testing. Thus, a total synthesis of compound **1** based on the organocatalytic methodology used by the McNulty group for the preparation of *trans*-dihydrolycoricidine was pursued.[32] These efforts and the potent anti-Zika activity of **1** were published in *ChemistrySelect*, 2016, *1*, 5895-5899, which is reproduced in Chapter 5.4 with permission. Figures and schemes were modified to be in sequence with the rest of the chapter. The synthesis was completed collaboratively by the author of this thesis and Dr.s Omkar Revu and Carlos Zepeda-Velázquez; anti-Zika assays were performed by Dr. Lorraine Jones-Brando.

5.4 Total Synthesis of the Natural Product (+)-trans-Dihydronarciclasine via an Asymmetric Organocatalytic [3+3]-Cycloaddition and discovery of its potent anti-Zika Virus (ZIKV) Activity

Amaryllidaceae plants[1–2] continue to be a valuable source of compounds that exhibit potent anticancer, antiviral and other biological properties. As a class, the compounds feature complex, densely functionalized and synthetically challenging[3] aminocyclitol cores.[4] The narciclasine sub-class[1d] of the Amaryllidaceae alkaloids (Figure 5.3), exemplified by *trans*-dihydronarciclasine **1**, *trans*-dihydrolycoricidine **2**, narciclasine **3**, the 7-deoxy analogue (lycoricidine) **4**, pancratistatin **5** and 7-deoxy analogue **6** have attracted particular interest due to their anticancer and antiviral activity.[2]

The antiviral activity of specific lycorane-type compounds against both RNA[5a] and DNA viral pathogens[5b] has been previously described. In particular, the antiviral activity demonstrated against flaviviruses such as Japanese encephalitis, yellow fever and Dengue[5a] is of prime importance given the recent outbreak of the genetically related Zika flavivirus (ZIKV).

While very few structure-activity antiviral studies have been performed with synthetic lycorane derivatives,[5] Gabrielsen and co-workers demonstrated that natural (+)-*trans*-dihydronarciclasine **1** was the most effective anti-flaviviral analogue exhibiting IC_{50} values of <0.003 - 0.015 mg/mL.[5a] The specificity of the lycorane antiviral pharmacophore was also of considerable note among 23 alkaloids
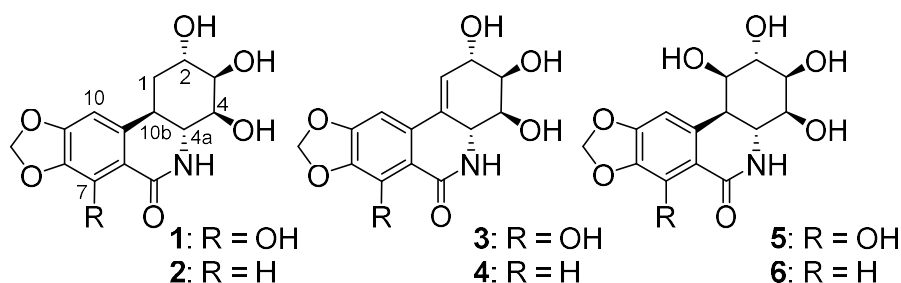
FIGURE 5.3. Structure of the anti-flaviviral natural product trans-dihydronarciclasine **1** and related natural derivatives **2–6**.

investigated. Slight modifications to **1** such as incorporation of a cis-fused B/C-ring junction, or presence of deoxy or epimeric alcohols in the cyclohexane portion, resulted in compounds with significantly reduced, or no antiviral activity.[5a] To our knowledge, no antiviral activity of the lycorane sub-class of Amaryllidaceae alkaloids has been reported to date with regards to ZIKV. The efficacy of **1** towards these other flaviviruses, as well as the need for new therapeutics and discovery of biological targets specific to ZIKV led us to hypothesize compound **1** as a high-value candidate for the discovery of a lead inhibitor of ZIKV infection.

Natural (+)-*trans*-dihydronarciclasine **1** has been the subject of three prior asymmetric syntheses,[6a–c] three racemic syntheses,[6d–f] and the compound has also been the subject of semisynthesis via selective hydrogenation of narciclasine **3**.[2d, 6h] We were inspired by recent enantioselective organocatalytic approaches toward six member carbocycles[7a] to develop a stepwise [3+3]-type Michael-aldol sequence,[7b–g] involving an α-nitrogen-substituted acetone moiety reacting with an unsaturated aldehyde, as a rapid entry to the Amaryllidaceae core. Such an approach proved successful in our recent synthesis of alkaloid **2**, which provided access to the natural product and structural analogues that permitted investigation of the antiviral activity against herpes viruses.[5b, 8]

A retrosynthetic analysis of trans-dihydronarciclasine is outlined in Scheme 5.13. We expected that compound **1** would be derived from the methoxycarbonyl-substituted protected amino-triol A, which would be produced from the cyclohexene B via epoxidation and 2,3-diaxial diol formation. The critical synthesis of the cyclohexane C would hinge upon the organocatalytic regiocontrolled syn-stereoselective Michael-aldol addition of azidoacetone onto the cinnamaldehyde derivative D, prepared from commercially available 5-methoxypiperonal. In this communication we report a successful asymmetric synthesis of compound **1** following this route and the discovery of its potent anti-ZIKV activity.
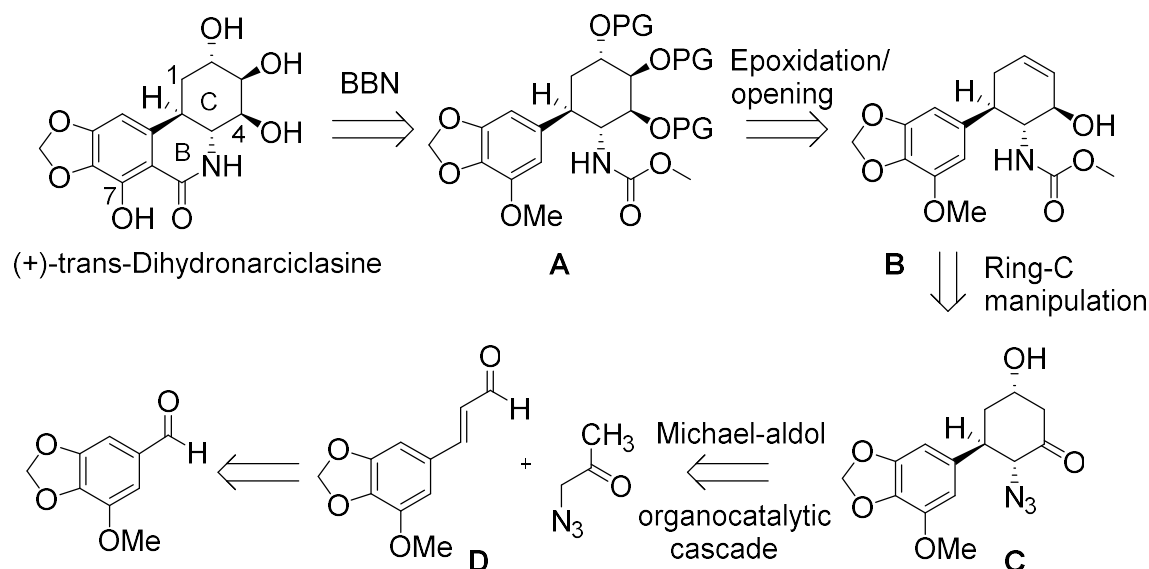
SCHEME 5.13. Retrosynthetic analysis of (+)-trans-dihydronarciclasine. BBN=Banwell modified Bischler-Napieralski reaction, PG=protecting group.

Commercially available 5-methoxypiperonal was subject to a two-carbon aldehyde to alkenal homologation using a diethylacetal-functionalized Wittig reagent[9] yielding the cinnamaldehyde derivative **7** in 82% yield (Scheme 5.14). The crucial iminium ion-mediated [3+3]-Michael-aldol sequence[5a, 8] of **7** with azidoacetone **8** proved highly effective using the Jørgensen (*R*)-diphenylsilaprolinol secondary amine catalyst in combination with the tertiary amine quinidine, providing the cycloadduct **9** in 58% isolated yield and >99% enantiomeric excess (e.e.). The mirror-image reaction employing (*S*)-diphenylsilaprolinol in the presence of quinidine gave **ent-9** also in 99% e.e. The enantiomers of **9** were cleanly baseline resolved using chiral HPLC on a AS-RH column (see supporting information). Hydrogenation of the azido functional group of **9** in the presence of dimethyldicarbonate gave the Moc-protected cyclohexanone **10** in 74% overall yield from **9**. Dehydration of **10** gave the enone **11**, the carbonyl of which was subsequently reduced to the equatorial alcohol **12** in 82% yield using lithium tri-*tert*-butoxyaluminium hydride.
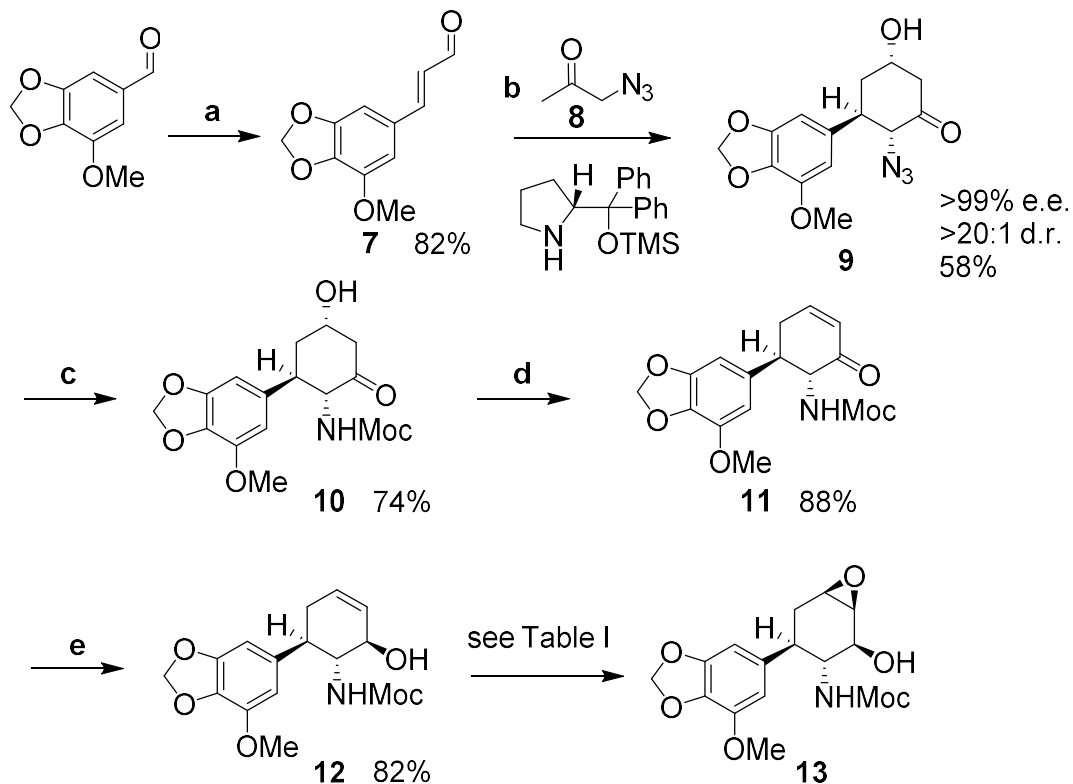
SCHEME 5.14. a) tripropyl (2,2-diethoxyethyl)-phosphonium bromide, NaH, THF, 82%; b) (R)-α,α-diphenyl-2-pyrrolidinemethanol trimethylsilyl ether, quinidine, CH₂Cl₂, rt, 48 h, 58%, >99% e.e., >20:1 dr.; c) H₂, 10% Pd/C, dimethyl dicarbonate, MeOH, rt, 10 h, 74%; d) DIPEA, MsCl, CH₂Cl₂, 3 h, 88%; e) Li(tBuO)₃AlH, THF, 0 °C to rt, 1 h, 82%.

Cyclohexene epoxidation followed by base mediated ring opening is a standard synthetic protocol in accessing 1,2-diaxial cyclohexanediols and the process has been employed in various circumstances towards the synthesis of lycorane derivatives, including the 2,3-diol subunit.[2m, 5b, 8] Epoxidation of the highly electron-rich methoxy-methylenedioxyaryl-substituted cyclohexene **12** proved to be extremely challenging. The reaction proceeded very slowly under standard conditions[2m] using *m*-CPBA in dichloromethane, or in carefully buffered media[10] (Table 5.1, entries 1 and 2). The β-epoxide was obtained in a maximum yield of 5 %, contrasting sharply to the analogous reaction on the cyclohexene lacking the allylic hydroxyl (ring-c) and aryl methoxy substituents (93% isolated yield).[2m] When more forcing conditions were applied, a major side product and several minor side

TABLE 5.1. Epoxidation attempts of cyclohexene derivative **12**. [A]isolated product, [B]No Reaction. *m*-CPBA=*meta*-chloroperoxybenzoic acid.
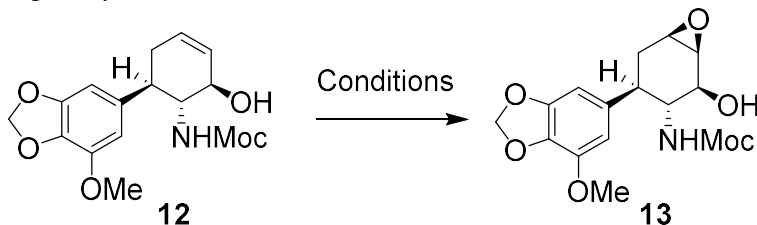
Entry	Conditions	Yield 13[A]
1	m-CPBA (1.5 eq.), NaHCO$_3$ (2.0 eq.), CH$_2$Cl$_2$, -20 °C to rt, 12 h	<5%
2	m-CPBA (2.0 eq.), Na$_2$HPO$_4$ (3.0 eq.), CH$_2$Cl$_2$, rt, 12 h	NR[B]
3	PhI(OAc)$_2$ (1 eq.), LiBr (20 mol%), AcOH, 95%, 16 h	Decomposition
4	Oxone (3.0 eq.), K$_2$CO$_3$ (13.3 eq.), Bu$_4$NHSO$_4$ (4 mol%), Acetone (30 eq.) CH$_3$CN:CH$_2$(OMe)$_2$ (2:1), EDTA, 12 h	<5%
5	VO(acac)$_2$ (5 mol%), ^{t}BuOOH (4.0 eq.), benzene, 4 h	40% of 11 was isolated
6	Ti(O^{i}Pr)$_4$ (1.0 eq.), ^{t}BuOOH (2.0 eq.), DIPT (1.0 eq.), CH$_2$Cl$_2$, -20 °C to rt, 5 h	25% of 11 was isolated
7	m-CPBA (2.0 eq.), NaHCO$_3$ (3.0 eq.), nitrobenzene (1:1), rt, 24 h	15%
8	m-CPBA (2.0 eq.), NaHCO$_3$ (3.0 eq.), benzene-dioxane (1:1), rt, 24 h	38% 55% (brsm)

products were observed to form along with the desired epoxide. The epoxidation of cyclohexene **12** was investigated using a range of alternative reagents, a selection of which is shown in Table 5.1. Attempted epoxidation via bromohydrin intermediates (entry 3),[11] oxone under Shi-type epoxidation conditions (entry 4),[12] Vanadium reagents (entry 5)[13] or under Sharpless conditions (entry 6)[14] all proved futile, but these studies revealed the chemoselective nature of the problem. The major side product from **12** (entries 5 and 6) was identified as the ketone **11** (Scheme 2) produced via oxidation of the allylic alcohol. Minor side products have not been unambiguously identified, but they contain a methylenedioxy sub-unit and lack the methoxy group, indicating that cleavage and/or oxidation of the electron rich aromatic ring is problematic. It has been shown that conformationally biased axial-allylic cyclohexenols readily form epoxides, while equatorial-allylic alcohols (similar to **12**) rapidly yield
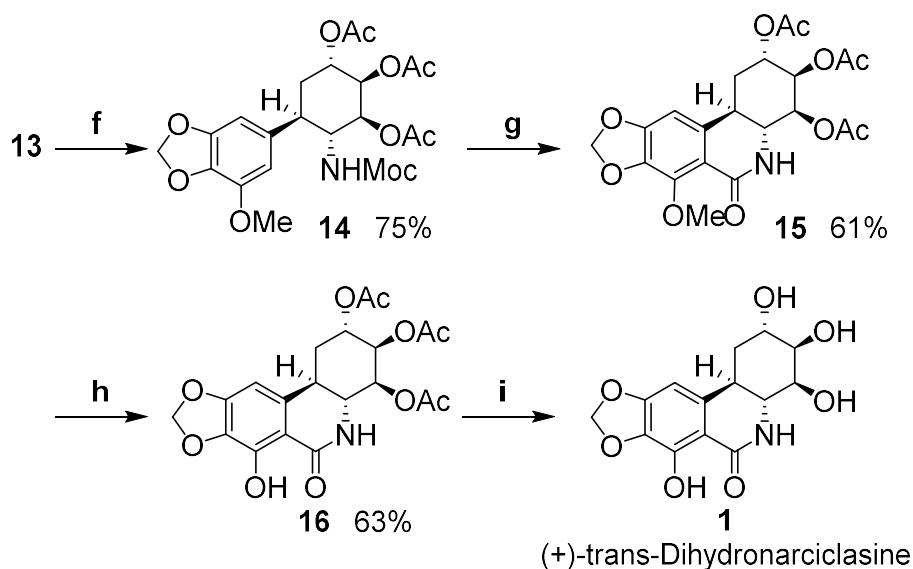
SCHEME 5.15. f) i) NaOBz, H_2O, 100 °C, 18 h; then ii) Ac_2O, Pyridine, CH_2Cl_2, 12 h, 75% (for 2 steps); g) Tf_2O, DMAP, CH_2Cl_2, 0 °C to rt, 16 h, 61%; h) TMSCl, KI, CH_3CN, 1 h, 60 °C, 63% (or) BBr_3, CH_2Cl_2, -78 °C to rt, 1 h, 57%; i) NaOMe, MeOH, 0 °C to rt, 95%.

enones,[13] and indeed up to 40% of the enone **11** could be isolated (entry 5) as the major side-product of the epoxidation. Given that the only success was seen using *m*-CPBA, we returned to screening its use in alternative solvents such as nitrobenzene, which met with some success (entry 7). Finally use of a benzene/dioxane mixture, as described by Woodward and co-workers in their classic synthesis of reserpine,[15] allowed for isolation of the β-epoxide **13** in 38% yield, and 55% yield based on recoverable starting cyclohexene.

With access to the epoxide secured, we turned our attention to completion of the synthesis of the *trans*-dihydronarciclasine **1**, as outlined in Scheme 5.15. Epoxide opening with aqueous sodium benzoate and immediate protection gave the triacetate **14** without incident. The phenanthridone ring was closed using Banwell's modification of the Bischler-Napieralski reaction,[16] giving the tetracycle **15**. Cleavage of the C7-methyl ether was conducted chemoselectively to give the triacetoxy phenol **16**, and removal of the three acetate protecting group under basic conditions completed the total synthesis of **1** in 95% yield from **16**.

Synthetic **1** as prepared above displayed NMR (^{1}H and ^{13}C) data consistent with published values (see the Supporting Information) for the natural product[2a] and optical rotation,[2a, 6] was fully in accord with that of the dextrorotatory enantiomer of **1** ($[\alpha]^{20}_D$ 1=+4.58 (c=0.20, THF), lit[6a] $[\alpha]_D$=+4.78 (c=0.27, THF), in agreement with our earlier observations on the absolute stereocontrol of the critical [3+3]-organocatalytic cascade leading to analogues of **9**.[5b, 8] Overall, *trans*-dihydronarciclasine was obtained in 9 chemical steps from azidoacetone **8** and 5-methoxy-3,4-methylenedioxycinnamaldehyde derivative **7**, with an overall yield of 4.7%

Returning to our hypothesis of potential anti-ZIKV activity of compound **1** based on the reported antiflaviviral- activity,[5a] we next interrogated synthetic (+)-*trans*-dihydronarciclasine **1** along with natural products **3**, and **5** for in vitro anti-ZIKV activity as well as for cytotoxicity against the host cells. This was accomplished using an assay based on the virus's ability to cause a cytopathic effect (CPE; measured in median Tissue Culture Infective Dose, TCID$_{50}$) in viable host cells. The detailed method can be found in the Supporting Information. Briefly, African green monkey kidney cells (Vero C1008; ATCC) growing in 96 well tissue culture plates were exposed to a range of compound concentrations. Cells were then inoculated with either 300 TCID$_{50}$ ZIKV strain MR766 suspended in cell growth medium (CGM) or with CGM alone. After 5 days of incubation at 37 °C / 5% CO_2, the cell viability reagent CellTiter 96® Aqueous One Solution (Promega Corp, WI, USA) was added to all wells; colour reactions were read in a Filtermax F5 microplate reader (Molecular Devices, CA, USA). Median and 90% viral inhibitory concentrations (IC$_{50}$, IC$_{90}$ respectively) and the median cytotoxic dose (TD$_{50}$) was calculated using Calcusyn software (Biosoft, Cambridge, UK). The therapeutic index (TI), a measure of virus specific activity, was calculated for each compound. Results (Table 5.2) show that all three of the Amaryllidaceae compounds exhibit anti-ZIKV activity and cytotoxicity comparable to the natural purified isolates reported against related flaviviruses.[5a] Both *trans*-dihydronarciclasine **1** and narciclasine **3** displayed potent activity (corresponding to 0.03

TABLE 5.2. In vitro anti-Zika virus (ZIKV) Strain MR766 activity.

Cpd	IC$_{50}$ µM[a]	IC$_{90}$ µM[b]	TD$_{50}$ µM[c]	TI[d]
1	0.1	0.5	0.7	7
3	0.1	0.6	0.4	4
5	0.3	3.1	1.1	4

Data compiled from 3 independent experiments. [a] Concentration that inhibits 50% of viral CPE [b] Concentration that inhibits 90% of viral CPE [c] Concentration that inhibits or kills 50% of host cells [d] Therapeutic index, a measure of selectivity. TI=TD$_{50}$/IC$_{50}$

mg/mL), pancratistatin **5** proved to be less potent and compound **1** demonstrated the highest selectivity (TI=7). Compound **1** is as active as the most potent hits that have been identified from two random high-throughput screening assays that interrogated 774[17b] FDA approved drugs and a library of 6,096[17c] compounds consisting of approved drugs, clinical trial drug candidates and other pharmacologically active compounds. Synthetic compound **1** validates our targeted hypothesis of anti ZIKV activity, as evidenced by its ability to inhibit the growth of Zika virus at nanomolar concentrations.

In conclusion, we have developed a 10-step total synthesis of the antiviral natural product (+)-*trans*-dihydronarciclasine **1** from readily available 5-methoxypiperonal. The synthesis extends the scope of regiospecific organocatalytic addition of azidoacetone onto highly functionalized Michael acceptors leading to densely functionalized, homo-chiral azidocyclitol intermediates. The synthesis proceeds through the penultimate triacetoxy protected phenol **16**, an intermediate that should permit synthesis of a heterobifunctional compound with a recruiting ligand connected via a linker onto C7, allowing pulldown assays for antiviral and target identification. In addition, compound **1** exhibits the highest calculated LogP value amongst the three derivatives, indicating that conjugation of lipophilic chains at the C7 phenol could prove a valuable strategy to further optimize selectivity. The discovery of small molecule inhibitors of ZIKV replication[17a–c] and host-cell entry[17d] is an exceedingly active area of research in view of the Zika outbreak and its now demonstrated link to neurodevelopmental

impairment.[17e] The discovery of multiple drugs and targets operative against ZIKV has been identified as critical to the development of an effective therapeutic agent targeting this pandemic.[17a] Preparation of a series of analogues of compound **1** with the intention of increasing the selectivity, followed by the assessment of their in vitro and in vivo antiviral activity against several strains of ZIKV as well as biochemical studies described to identify a target and mechanism of action for this antiviral activity are in progress.

Acknowledgements

References

[1] For general reviews on the chemistry and biology of Amaryllidaceae constituents see: a) J. Bastida, S. Berkov, L. Torras, N. B. Pigni, J. , P. de Andrade, V. Martinez, C. Codina, F. Viladomat, in *Receent Advances in Pharmaceutical Sciences* (Ed. D. Munoz-Torrero), Transworld Research Network, 2011, pp 65–100; b) A. Evidente, A. S. Kireev, A. R. Jenkins, A. E. Romero, W. F. A. Steelant, S. van Slambrouck, A. Kornienko, *Planta Med.* 2009, *75*, 501–507; c) S. F. Martin, in *The Alkaloids*, Vol. 30, (Ed: A. Brossi), Academic Press, New York, 1987, pp 251–376; d) Z. Jin, *Nat. Prod. Rep.* 2013, *30*, 849–868; e) W. C. Wildman, in *The Alkaloids*, Vol. 11, (Ed: R. H. F. Manske), Academic Press, New York, 1968, pp 307–405; f) J. W. Cook, J. D. Loudon, in *The Alkaloids*, Vol. 2, (Eds: R. H. F. Manske, and H. L. Holmes), Academic Press, New York, 1952, pp 331–352.

[2] Original isolation of *trans*-dihydronarciclasine from *Zephyranthes candida* (Amaryllidaceae) see: a) G. R. Pettit, G. M. Cragg, S. B. Singh, J. A. Duke, D. L. Doubek, *J. Nat. Prod.* 1990, *53*, 176–178. For biological investigations on *trans*-dihydronarciclasine and analogues see: b) G. R. Pettit, V. Gaddamidi, G. M. Cragg, D. L. Herald, Y. Sagawa, *J. Chem. Soc. Chem. Commun.* 1984, 1693–1694; c) G. R. Pettit, V. Gaddamidi, D. L. Herald, S. B. Singh, G. M. Cragg, J. M. Schmidt, F. E. Boettner, M. Williams, Y. Sagawa, *J. Nat. Prod.* 1986, *49*, 995–1002; d) G. R. Pettit, S. Ducki, S. A. Eastham, N. Melody, *J. Nat. Prod.* 2009, *72*, 1279–1282; e) G. R. Pettit, Pettit, G. R. III R. A. Backhaus, M. R. Boyd, A. W. Meerow, *J. Nat. Prod.* 1993, *56*, 1682–1687; f) A. McLachlan, N. Kekre, J. McNulty, S. Pandey, *Apoptosis* 2005, *10*, 619–630; g) N. Kekre, C. Griffin, J. McNulty, S. Pandey, *Cancer Chemother. Pharmacol.* 2005, *10*, 619–630; h) S. Pandey, N. Kekre, J. Naderi, J. McNulty, *Artifi. Cells, Blood. Sub. & Biotech.* 2005, *33*, 279–295; i) P. Siedlakowski, A. McLachlan-Burgess, C. Griffin, S. Tirumalai, J. McNulty, S. Pandey, *Canc. Biol.& Therap.* 2008, *7*, 376–384; j) L. Ingrassia, F. Lefranc, J. Dewelle, L. Pottier, V. Mathieu, S. Spiegl-Kreinecker, S. Sauvage, M. El Yazidi, M. Dehoux, W. Berger, E. van Quaquebeke, R. Kiss, *J.*

Med. Chem. 2009, *52*, 1100–1114; k) F. Lefranc, S. Sauvage, G. Van Goietsnoven, V. Megalizzi, D. Lamoral-Theys, O. Debeir, S. Spiegl-Kreinecker, W. Berger, V. Mathieu, C. Decaestecker, R. Kiss, *Mol. Cancer Therap.* 2009, *8*, 1739–1750; l) J. McNulty, R. Mo, *Chem. Commun.* 1998, 933–935; m) J. McNulty, J. Mao, R. Gibe, R. Mo, S. Wolf, G. R. Pettit, D. L. Herald, M. R. Boyd, *Bioorg. Med. Chem. Lett.* 2001, *11*, 169–172; n) U. Rinner, H. L. Hillebrenner, D. R. Adams, T. Hudlicky, G. R. Pettit, *Bioorg. Med. Chem. Lett.* 2004, *14*, 2911–2914; o) J. McNulty, V. Larichev, S. Pandey, *Bioorg. Med. Chem. Lett.* 2005, *15*, 5315–5318; p) J. McNulty, J. J. Nair, C. Griffin, S. Pandey, *J. Nat. Prod.* 2008, *71*, 357–363.

[3] For reviews and select synthetic studies on Amaryllidaceae constituents see: a) M. Ghavre, J. Froese, M. Pour, T. Hudlicky, *Angew. Chem. Int. Ed.* 2016, *55*, 5642–5691; b) M. G. Banwell, N. Y. Gao, B. D. Schwartz, L. V. White, *Topp. Curr. Chem.* 2012, *309*, 163–202; c) M. Manpadi, A. Kornienko, *Org. Prep. Proc. Int.* 2008, *40*, 107–161; d) Y. Chapleur, F. Chretien, S. Ibn-Ahmed, M. Khaldi, *Curr. Org. Synth.* 2006, *3*, 169–185; e) U. Rinner, T. Hudlicky, *Synlett.* 2005, 365–387.

[4] J. A. Griffen, J. C. White, G. Kociok-Kohn, M. D. Lloyd, A. Wells, T. C. Arnot, S. E. Lewis, *Tetrahedron* 2013, *69*, 5989–5997.

[5] a) B. Gabrielsen, T. P. Monath, J. W. Huggins, D. F. Kefauver, G. R. Pettit, G. Groszek, M. Hollingshead, J. J. Kirsi, W. M. Shannon, E. M. Schubert, J. DaRe, B. Ugarkar, M. Ussery, M. J. Phelan, *J. Nat. Prod.* 1992, *55*, 1569–1581; b) J. McNulty, L. D'Aiuto, Y. Zhi, L. McClain, C. Zepeda-Velázquez, S. Ler, H. A. Jenkins, M. B. Yee, P. Piazza, R. H. Yolken, P. R. Kinchington, V. L. Nimgaonkar, *ACS Med. Chem. Lett.* 2016, *7*, 46–50.

[6] For previous enantioselective syntheses of natural (+)-trans-dihydronarciclasine see: a) C. K. Jana, A. Studer, *Chem. Eur. J.* 2008, *14*, 6326–6328; b) S. Hwang, D. Kim, S. Kim, *Chem. Eur. J.* 2012, *18*, 9977–9982; c) K. Yamada, Y. Mogi, M. Mohamed, K. Takasu, K. Tomioka, *Org. Lett.* 2012, *14*, 5868–5871. For racemic syntheses of trans-dihydronarciclasine see: d) I.-J. Shin, E.-S. Choi, C.-G. Cho, *Angew. Chem.* 2007, *119*, 2353–2355; *Angew. Chem. Int. Ed.* 2007, *46*, 2303–2305; e) Y.-S. Cho, C.-G. Cho, *Tetrahedron* 2008, *64*, 2172–2177; f) G. Varró, L. Hegedus, A. Simon, I. Kádas, *Tetrahedron Lett.* 2016, *57*, 1544–1546. For syntheses of *trans*-dihydronarciclasine through natural product relays see ref. 2d and h) J. McNulty, A. Thorat, N. Vergun, J. J. Nair, E. Makaji, D. J. Crankshaw, A. C. Holloway, S. Pandey, *J. Nat. Prod.* 2011, *74*, 106–108.

[7] a) S. Goudedranche, W. Raimondi, X. Bugaut, T. Constantieux, D. Bonne, *Synthesis* 2013, *45*, 1909–1930; b) C. Grondal, M. Jeanty, D. Enders, *Nat. Chem.* 2010, *2*, 167–178; c) Ł. Albrecht, H. Jiang, K. A. Jørgensen, *Angew. Chem. Int. Ed.* 2011, *50*, 8492–8509; d) H. Pellissier, *Adv. Synth. Catal.* 2012, *354*, 237–294; e) A. Carlone, M. Marigo, C. North, A. Landa, K. A. Jørgensen, *Chem. Comm.* 2006, 4928–4930; f) J. Alemán, V. Marcos, L. Marzo, J. L. G. Ruano, *Eur. J. Org. Chem.* 2010, 4482–4491; g) S. Duce, M. Jorge, I. Alonso, J. L. G. Ruano, M. B. Cid, *Org. Biomol. Chem.* 2011, *9*, 8253–8260.

[8] J. McNulty, C. Zepeda-Velázquez, *Angew. Chem. Int. Ed.* 2014, *53*, 8450–8454.

[9] J. McNulty, C. Zepeda-Velázquez, D. McLeod, Green Chem. 2013, *15*, 3146–3149.

[10] R. Angelaud, O. Babot, T. Charvat, Y. Landais, *J. Org. Chem.* 1999, *64*, 9613–9624.

[11] L. Emmanuvel, T. M. A. Shaikh, A. Sudalai, *Org. Lett.* 2005, *7*, 5071–5074.

[12] M. Frohn, Z_X. Wang, Y Shi, *J. Org. Chem.* 1998, *63*, 6425–6426.

[13] R. B. Dehnel, G. H. Whitman, *J. Chem. Soc. Perkin Trans 1.* 1979, 953–955.

[14] T. Katsuki, K. B. Sharpless, *J. Am. Chem. Soc.* 1980, *102*, 5974–5976.

[15] R. B. Woodward, F. E. Bader, H. Bickbl, A. J. Frey, R. W. Kibrstea, *Tetrahedron* 1958, *2*, 1–57.

[16] a) M. G. Banwell, C. J. Cowden, R. W. Gable, *J. Chem. Soc. Perkin Trans 1*. 1994, 3515–3518; b) M. G. Banwell, B. D. Bissett, S. Busato, C. J. Cowden, D. C. R. Hockless, J. W. Holman, R. W. Read, A. W. Wu, *J. Chem. Soc. Chem. Commun*. 1995, 2551–2553.

 [17] a) E. Kincaid, *Nature Medicine* 2016, *22*, 824–825; b) N. J. Barrows, R. K. Campos, S. T. Powell, K. R. Prasanth, G. Schott-Lerner, R. Soto-Acosta, G. Galarza-Munoz, E. L. McGrath, R. Urrabanz-Garza, J. Gao, P. Wu, R. Menon, G. Saade, I. Fernandez-Salas, S. L. Rossi, N. Vasilakis, A. Routh, S. S. Bradrick, M. A. Garcia-Blanco, *Cell Host & Microbe* 2016, *20*, 259–270; c) M. Xu, E. M. Lee, Z. Wen, Y. Cheng, W.-K. Huang, X. Qian, J. Tcw, J. Kouznetsova, S. C. Ogden, C. Hammack, F. Jacob, H. N. Nguyen, M. Itkin, C. Hanna, P. Shinn, C. Allen, S. G. Michael, A. Simeonov, W. Huang, K. M. Christian, A. Goate, K. J. Brennand, R. Huang, M. Xia, G.-L. Ming, W. Zheng, H. Song, H. Tang, *Nature Medicine* 2016, (doi: 10.1038/nm.4184); d) B. M. Carneiro, M. N. Batista, A. C. S. Braga, M. L. Nogueira, P. Rahal, *Virology* 2016, *496*, 215–218; e) M. Onorati, Z. Li, F. Liu, A. M. M. Sousa, N. Nakagawa, M. Li, M. T. Dell-Anno, F. O. Gulden, S. Pochareddy, A. T. N. Tebbenkamp, W. Han, M. Pleitkos, T. Gao, Y. Zhu, C. Bichsel, L. Varela, K. Szigeti-Buck, S. Lisgo, Y. Zhang, A. Testen, X.-B. Gao, J. Mlakar, M. Popovic, M. Flamand, S. M. Strittmatter, L. K. Kaczmarek, E. S. Anton, T. L. Horvath, B. D. Lindenbach, N. Sestan, *Cell Reports* 2016, (doi 10.1016/j.celrep.2016.08.038); f) J. Zmurko, R. E. Marques, D. Schols, E. Verbeken,S. J. F. Kaptein, J. Neyts, *PLOS Negl. Trop. Dis.* 2016, (doi: 10.1371/journal.pntd.0004695).

5.5 Additional discussion of the late-stage epoxidation and future work

As discussed in Chapter 5.4, formation of the C2-C3 epoxide from intermediate **12** proved to be the most challenging aspect of the total synthesis of **1**. Whereas treatment of the allylic alcohol intermediate corresponding to **12** with *m*-CPBA smoothly gave the desired epoxide in the previously reported synthesis of closely related *trans*-dihydrolycoricidine, all but the most careful conditions led to decomposition in the current case (Scheme 5.16).[32] Although these results were frustrating, they are not unexpected; many syntheses of related Amaryllidaceae alkaloids report similar chemoselectivity issues when trying to manipulate the densely functionalized C ring through oxidation.[41,42,48,61] The discrepancy in reactivity between the previous synthesis and the current effort is readily explained by the increased electron density of the A ring in **12** due to the C7 methoxy, which increases its susceptibility to oxidative degradation. NMR of the crude reaction mixtures after epoxidation attempts demonstrated loss of the C7 methoxy, and a logical assumption is that oxidative demethylation of intermediate **12** may lead to either quinol or quinone products (Scheme 5.16).
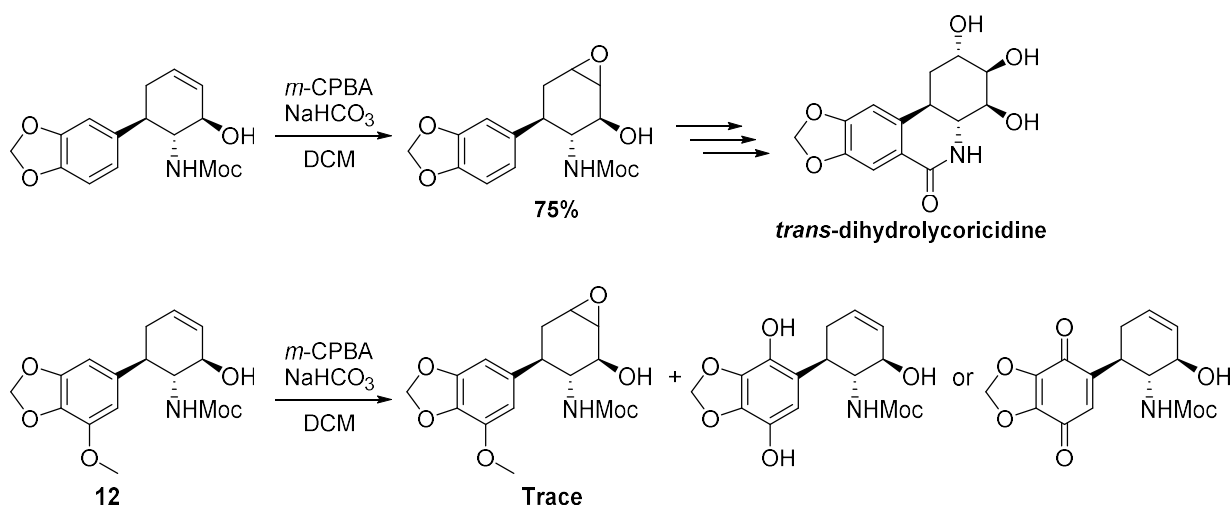
SCHEME 5.16 Epoxidation of the C2-C3 olefin proceeded smoothly using *m*-CPBA in the previously reported synthesis of *trans*-dihydrolycoricidine, but the same conditions result in oxidative degradation of the A ring when performed on more electron rich **12**.
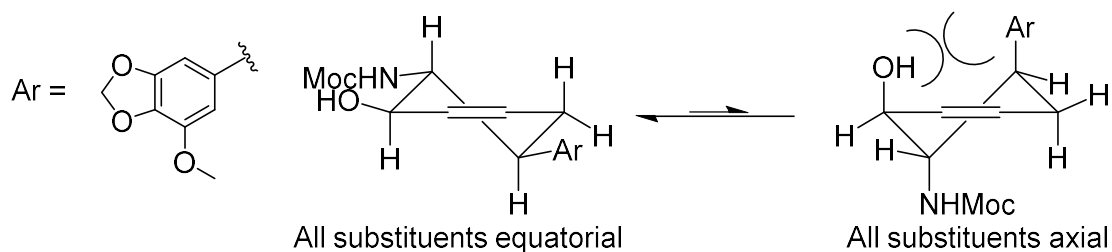
FIGURE 5.4 Conformational analysis of **12** demonstrates the equatorial position of the C4 alcohol, preventing chelation directed epoxidation with metal catalysts.

After many failed attempts using *m*-CPBA, other common epoxidation conditions were explored as presented in Table 5.1 and proved similarly disappointing. In both metal catalyzed epoxidation reactions tested, reoxidation to the enone **11** was the primary result (Table 5.1, entries 5 and 6). Conformational analysis of **12** demonstrates that it is strongly biased to place the C3 alcohol in an equatorial position (Figure 5.4). An axial C3 alcohol requires all other substituents to be in an axial position and introduces a repulsive 1,3-diaxial interaction between the alcohol and the aryl ring. However, titanium and vanadium catalyzed oxidation of allylic alcohols require chelation to an axial alcohol to direct epoxidation on the alkene, or else alcohol oxidation predominates.[70–73] Given the conformational bias of **12** and the mechanistic behavior of metal catalyzed epoxidations on allylic alcohols, the exploration of similar epoxidations is not recommended in any future efforts to improve the total synthesis of **1**.

Attempted epoxidations using dioxiranes generated *in situ* from acetone also failed to give appreciable quantities of the desired product (Table 5.1, entry 4). Although epoxidations using dioxiranes usually proceed under mild conditions, it is known that the rate of decomposition of the dioxirane competes with epoxide formation and that rates of reaction are more sensitive to substrate bulkiness than epoxidations with *m*-CPBA.[74–78] However, using trifluoroacetone instead of acetone results in a more reactive dioxirane, leading to faster reaction rates and higher yield, and may be worth attempting in any future syntheses of **1** using the synthetic route discussed in Chapter 5.4.[79]
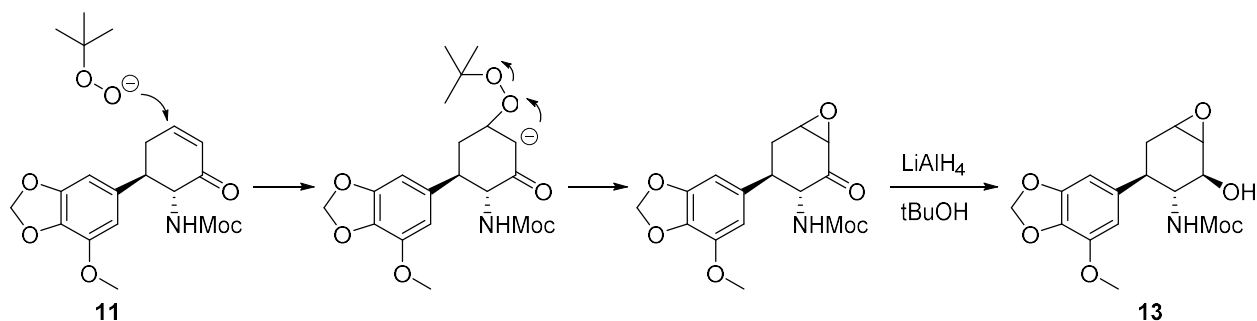
SCHEME 5.17 Nucleophilic epoxidations on **11** may be more chemoselective and provide better access to the C2-C3 diol functionality.

A narrow set of conditions was found that allowed the completion of the synthesis of **1**, but retrospective analysis suggests other solutions that might mitigate the issues associated with the late stage epoxidation. Decomposition of the A ring at a comparative rate to epoxidation should be considered the primary issue requiring redress; steric biases may prevent the use of metal catalyzed reactions, but the fact that the epoxidation using *m*-CPBA proceeds smoothly in the case of *trans*-dihydrolycoricidine indicates that electronic differences in the A ring are the biggest factors contributing to overall low yields. Future work can address this by avoiding the use of electrophilic oxidants or altering the synthesis so that the A ring is less electron-rich when the epoxidation is performed.

Instead of using electrophilic oxidants on allylic alcohol intermediate **12**, the use of nucleophilic oxidants on enone **11** might offer a chemoselective route to the desired functionality (Scheme 5.17). For example, the Michael addition of *tert*-butylhydroperoxide to **11** under basic conditions should generate a C2-C3 epoxide.[80] Hydride reduction of the C4 carbonyl would then serve as a relay into the original synthesis. The epoxidation of enone **11** using peroxides under basic conditions may also be amenable to organocatalysis. Carbonyl coordination by various organocatalyst classes, including H-bonding thioureas and chiral amines, is a proven method for catalyzing the epoxidation of enones, allowing both faster reaction rates and milder conditions.[81–83]
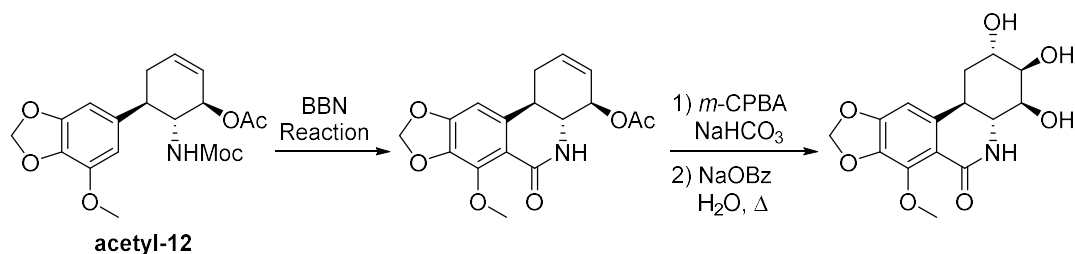
SCHEME 5.18 Performing the BBN reaction earlier in the synthesis may reduce the oxidative decomposition of the A ring during epoxidation.

Another alternative would be to perform the BBN reaction prior to epoxidation, as the electron withdrawing B ring carbonyl would make the A ring less electron rich and thus less prone to oxidation. For example, acetylation of **12** followed by the BBN should allow for epoxidation of the C2-C3 alkene using *m*-CPBA with alleviated concerns of A ring decomposition (Scheme 5.18). An added benefit of this suggested route is that it may make the synthesis more efficient by performing the BBN reaction at an earlier stage, reducing the amount of material that is carried through the synthesis only to be lost in a late stage low-yielding step.

Ultimately, there are likely many alternative methods that would allow for effective functionalization of the A ring without significantly deviating from the synthesis of **1**, as described in Chapter 5.4. As well, the above recommendations were made with the full understanding that any changes to a synthesis can have unpredictable results. However, the yields obtained for the epoxidation in the current synthesis present a significant challenge for future efforts that should be focused on refinement of the anti-ZIKV pharmacophore or on the preparation of quantities of **1** necessary for testing in animal models of the virus. Given the remarkably potent anti-ZIKV demonstrated by **1** and the lack of effective treatments for the virus, any optimization of the total synthesis should be considered a high priority for future work.

5.6 Conclusions

An asymmetric total synthesis of (+)-*trans*-dihydronarciclasine was accomplished, further demonstrating the synthetic utility of the formal organocatalytic [3+3] cycloaddition developed by the McNulty group, especially for the creation of densely functionalized aminocyclitol cores. Besides providing a useful route to a rare natural product, the present work also adds to the growing number of biological applications exhibited by the Amaryllidaceae alkaloids. In particular, *trans*-dihydronarciclasine was found to possess extremely potent anti-Zika activity. The synthesis and exploration of additional derivatives is highly warranted but may be hindered by the problematic late stage oxidation used in the current synthetic route, and future work should focus on developing routes that can mitigate this issue. Regardless of any shortcomings, the present synthesis of *trans*-dihydronarciclasine remains the shortest reported to date.

5.7 Experimental

This experimental is provided as published in *ChemistrySelect*, 2016, *1*, 5895-5899.

Solvents and reagents: All chemicals and solvents were purchased from Acros, Aldrich, J.T. Baker, Caledon, Solvay-Cytec Industries and Fluka and used as received with the following exceptions: deuterated solvents were obtained from ACP Chemicals, Toronto, Canada; tetrahydrofuran (THF), diethyl ether (Et$_2$O), and toluene were distilled from sodium/benzophenone under an atmosphere of dry nitrogen; dichloromethane (CH$_2$Cl$_2$) was distilled from calcium hydride under an atmosphere of dry nitrogen; methanol (MeOH) was distilled from magnesium turnings under an atmosphere of dry nitrogen; triethylamine (NEt$_3$), *N,N*-diisopropylethylamine (Hünig's) and pyridine were distilled from potassium hydroxide under an atmosphere of dry nitrogen; solid sodium hydride (NaH) was obtained by filtration and washing with *n*-hexanes.

Reaction handling: All non-aqueous reactions were performed in flame dried round bottom flasks or in non-flame dried amber 1-dram vials. Reactions were magnetically stirred and monitored by thin-layer chromatography (TLC) unless otherwise noted. TLC was performed on Macherey-Nagel silica gel 60 F254 TLC aluminum plates and visualized with UV fluorescence quenching and/or potassium permanganate (KMnO$_4$) or 2,4-dinitrophenylhydrazine or *p*-anisaldehyde stains.[1] Concentrations under reduced pressure were performed by rotary evaporation at 40 °C at the appropriate pressure, unless otherwise noted. Column chromatographic purification was performed as flash column chromatography with 0.3–0.5 bar pressure using Silicycle silica gel (40–63, 60 Å) or EcoChrom silica gel (12–26, 60 Å).[2] Distilled technical grade solvents were employed. The yields given refer to chromatographically purified and spectroscopically pure compounds, unless stated otherwise.

Melting points: Melting points were measured on a melting point apparatus using open glass capillaries and are uncorrected, the measurements were performed on material crystallized from the stated chromatographic solvent, unless stated otherwise.

NMR spectroscopy: ^{1}H, ^{13}C{1H}, DEPTq, COSY, HSQC and HMBC NMR spectra were obtained on Bruker DRX-500, AV-600 and AV-700 spectrometers. All ^{1}H NMR spectra were referenced relative to SiMe$_4$ through a resonance of the employed deuterated solvent or proteo impurity of the solvent; chloroform (7.26 ppm), acetone (2.05 ppm), DMSO (3.33 ppm) and methanol (3.31 ppm) for ^{1}H NMR; chloroform (77.00 ppm), acetone (29.84 ppm), DMSO (39.52 ppm) and methanol (49.00 ppm) for ^{13}C NMR. All NMR spectra were obtained at RT (*ca.* 22 °C) unless otherwise specified. The data is reported as (s = singlet, d = doublet, t = triplet, m = multiplet or unresolved, br = broad signal, coupling constant(s) in Hz, integration). ^{13}C NMR spectra were recorded with complete [1]H-decoupling. Service measurements were performed by the NMR service team of the Nuclear Magnetic Resonance (NMR) Facility at McMaster University by Dr. Bob Berno, Dr. Dan Sorensen and Dr. Hilary A. Jenkins.

Mass spectrometry: Mass spectrometric analyses were performed as high resolution ESI measurements on a Waters/Micromass QTof Global Ultima (quadrupole time-of-flight mass spectrometer) or high resolution EI in a Waters/Micromass GCT (time-of-flight mass spectrometer) instrument by the mass spectrometry service of the McMaster Regional Centre for Mass Spectrometry (MRCMS) at McMaster University by Sujan Fernando, Tadek Olech and Leah Allan under the supervision of Dr. M. Kirk Green.

Enantiomeric ratios: Were determined using a Waters 2695 Alliance HPLC system with a 996 detector or an Agilent 1220 Infinity HPLC manual injection with a variable wavelength detector, using

a Daicel Chiralpak® AS-RH column (150 x 4.6 mm, 5μ), Water/ACN (70:30) as a mobile phase; flow rate 0.75 ml/min, column temperature 20 °C, λ236, sample 0.2 mg/ml dissolved in the mobile phase.

Optical rotations: Optical rotations were measured with a Perkin-Elmer 241 MC polarimeter.

Fourier Transform Infrared Spectroscopy (FTIR): were performed at the Combustion Analysis and Optical Spectroscopy (CAOS) facility using a Thermo, Nicolet 6700 FTIR.

Anti Zika virus Assessment

Cells and virus

Vero C1008 cells (ATCC CRL-1586) were used for growing and titering stocks of virus as well as for host cells in the antiviral assays. Cells were grown in Eagles Minimum Essential Medium (EMEM) supplemented with 10% fetal bovine serum (FBS). Cells were used between passage numbers 21 and 41.

Zika virus strain MR766 (ATCC VR-1838), isolated from a rhesus monkey in Uganda in 1947, was used for all antiviral experiments reported here.

Antiviral / Cytotoxicity Assay

We employed a simple assay that interrogates both antiviral and cytopathic properties of test compounds. The antiviral portion of the assay is predicated upon the virus's ability to damage or kill the host cells, i.e., the viral cytopathic effect (CPE). Specifically, Vero C1008 host cells were plated in Corning 96 well half area plates 24 hours prior to the assay at 5.5×10^3 cells per well in ZKV cell growth medium (ZKV CGM; Dulbecco's Modified Eagle Medium without phenol red supplemented with 3% FBS). 20 mM stocks of experimental compounds were made in DMSO and stored at -25 °C. On the day of the assay working solutions (1 mM or 32 μM) of compounds were made by dilution of stock in ZKV CGM. Fifty microliters of compound working solution was added to each well in the

first column of cells and then compounds were serially diluted across the plate by dilutions of 0.5 $\log_{10}$. Two different concentration ranges were tested: 320 µM – 0.032 µM and 10 µM – 0.001 µM. The last column was left without anycompound and served as virus control (VC, 6 of 8 wells per column) or cell control (CC, 2 of 8 wells). Directly following, 300 median Tissue Culture Infective Dose ($TCID_{50}$) of Zika MR766 were added to 6 of 8 wells in each column; comparable volume of ZKV CGM was added to the remaining 2 of 8 wells per column. Plates were incubated at 37 °C / 5% CO_2 for 5 days at which time the reagent for colourimetric determination of cell viability / cell number, CellTiter 96® AQ_{ueous} One Solution (Promega Corp), was added to each well and allowed to react for 4 h at 37 °C / 5% CO2. Absorbance (490 – 650 nm) in wells was measured on a Filtermax F5 microplate reader (Molecular Devices) using SoftMax Pro 6.5 software.

Calculation of median inhibitory concentration (IC_{50}), 90% inhibitory concentration (IC_{90}), and median cytotoxic dose (TD_{50}).

CellTiter 96® AQ_{ueous} One Solution contains a tetrazolium compound that is bioreduced by the mitochondria in viable cells into a soluble, coloured formazan product. Thereby the amount of absorbance in wells is directly proportional to the number of viable cells in the well. To calculate the antiviral IC_{50}, the amount of absorbance in wells containing compound, Zika virus and cells was compared to that in wells containing only Zika virus and cells using the formula ($A_{490-650}$ Cpd x - $A_{490-650}$ VC) / A490-650 CC) for each concentration of compound. The resulting dose-effect fractions were used to calculate the IC_{50} and IC_{90} using Calcusyn software (Biosoft). Likewise, the amount of absorbance in wells containing drugs and cells was compared to that in wells containing cells alone for each concentration and then the TD_{50} was calculated by Calcusyn. Finally, for determination of selectivity of a compound, a therapeutic index (TI) was calculated by the formula TI = TD_{50}/ IC_{50}.

Experimental Procedures
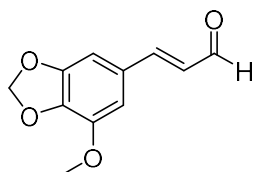
(2*E*)-3-(7-Methoxy-1,3-benzodioxol-5-yl)-2-propenal 7. 5-Methoxypiperonal (2.0 g, 11.1 mmol) and tri-*n*-propyl-(2,2-diethoxyethyl)-phosphonium bromide (5.15 g, 14.4 mmol, 1.3 eq.) were dissolved in anhydrous THF (20 mL). Sodium hydride (1.33 g, 33.3 mmol, 3.0 eq., 60% dispersed in mineral oil) was added slowly, maintaining the temperature below 30 °C, and the suspension was stirred for 24 h at RT. The THF was evaporated and water (15 mL) was added to the crude, which was extracted with CH_2Cl_2 (3 × 15 mL). The extracts were combined and washed again with water (2 × 15 mL). The organic layer was concentrated *in vacuo* to afford a mixture of the acetal and aldehyde as red oil. After 20 mL of 1 M HCl were added an off-white precipitate appeared. Then the suspension was stirred for 1 h at RT. After extracted with CH_2Cl_2 (3 × 15 mL) a flash chromatography (eluent CH_2Cl_2/MeOH 100:0 to 98:2) was performed giving 1.88 g of **7** as a yellow solid.[3]

Yield: 82%; **TLC**: *Rf* = 0.22 (CH_2Cl_2; UV / DNP); **M.P.**: 149-151 °C (material solidified from CH_2Cl_2) [lit.[4] 133 °C (EtOH)]; **IR** (neat, cm^{-1}): ν 2980, 2804, 2727, 1682, 1666, 1509, 1474, 1451, 1435, 1331, 1141, 1095, 968, 814; **^{1}H NMR** (600 MHz, CDCl$_3$): δ 9.65 (d, *J* = 7.7 Hz, 1H), 7.35 (d, *J* = 15.8 Hz, 1H), 6.78 (d, *J* = 1.3 Hz, 1H), 6.75 (d, *J* = 1.2 Hz, 1H), 6.57 (dd, *J* = 15.8, 7.7 Hz, 1H), 6.05 (s, 2H), 3.94 (s, 3H); **^{13}C NMR** (151 MHz, CDCl$_3$): δ 193.4, 152.5, 149.6, 143.8, 138.2, 128.8, 127.3, 109.7, 102.2, 101.8, 56.7; **HRMS** (ESI): calculated for $C_{11}H_{11}O_4$ [(M + H]$^+$): 207.0657, found: 207.0652.
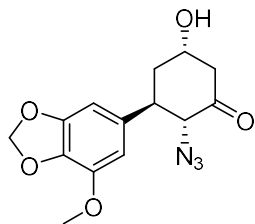
(2R,3R,5S)-2-Azido-3-(7-methoxy-1,3-benzodioxol-5-yl)-5-hydroxycyclohexanone   **9**.   A

solution of (2E)-3-(7-methoxy-1,3-benzodioxol-5-yl)-2-propenal **7** (1.35 g, 6.53 mmol, 1.05 eq.) and

(R)-(+)-α,α-diphenyl-2-pyrrolidinemethanol trimethylsilyl ether (0.202 g, 0.62 mmol, 0.10 eq.) in

CH_2Cl_2 (13.5 mL) was stirred for 10 min, after which it was cooled to -20 °C. 1-Azidopropan-2-one **8**

(0.616 g, 6.22 mmol) was added dropwise during 10 min. The red solution was stirred for 20 min at

RT and quinidine (0.202 g, 0.62 mmol, 0.10 eq.) was added in one portion. The reaction was stirred at

RT for 48 h, after which HPLC showed full conversion. The CH_2Cl_2 was carefully evaporated (30 °C,

32 mbar) yielding a red oil that was purified by flash chromatography (eluent CH_2Cl_2/MeOH 100:0 to

98:2, required two columns, 100 g of silica was used per column) giving 1.102 g as an yellow solid [first

column 1.005 g (53.0%) pure compound, second column {impure fractions from first column} 0.097

g].

Yield: 58%; **TLC**: Rf = 0.43 (CH_2Cl_2 / MeOH; 95:5; UV); **M.P.**: 149-151 °C (material solidified from

CH_2Cl_2:MeOH, 98:2); **[α]$^{23}_D$** = +90 (c = 0.19, MeOH, l = 1 dm); **IR** (neat, cm^{-1}): ν 3473, 2917, 2104,

1725, 1634, 1513, 1452, 1434, 1093, 1043, 927; **^{1}H NMR** (600 MHz, CDCl$_3$): δ 6.48 (d, J = 1.1 Hz,

1H), 6.44 (d, J = 1.0 Hz, 1H), 5.98 (s, 2H), 4.60 – 4.54 (m, 1H), 4.02 (d, J = 12.0 Hz, 1H), 3.92 (s, 3H),

3.39 (td, J = 12.3, 3.9 Hz, 1H), 2.74 (m, 2H), 2.21 (dd, J = 14.4, 2.4 Hz, 1H), 2.16 – 2.09 (m, 1H); **^{13}C**

NMR (151 MHz, CDCl$_3$): δ 202.8, 149.3, 143.7, 135.1, 134.6, 107.6, 101.6, 100.7, 71.5, 67.7, 56.8, 48.1,

44.8, 39.4; **HRMS** (ESI): exact mass calculated for $C_{14}H_{16}NO_5$ [(M − N$_2$ + H)$^+$], 278.1028; found

278.1027; **ee.**: τmajor = 11.2 min, τminor = 9.5 min (>99% *ee*), AS-RH column (150 x 4.6 mm, 5μ),

H_2O/MeCN (70:30) as a mobile phase; flow rate 0.750 mL/min, column temperature 20 °C, λ236,

sample 0.2 mg / mL dissolved in the mobile phase. **dr**.: 96:4, τmajor = 8.47 min, ZORBAX SB-C18 column (150 x 4.6 mm, 5μ), H_2O/MeCN (70:30 to 35:65, 30 min) as a mobile phase; flow rate 1.0 mL/min, column temperature 20 °C, λ236, sample 0.01 mg / mL dissolved in the mobile phase.

Note: *The purity of 1-Azidopropan-2-one should be confirmed prior to being used in the reaction.*

Caution! *For relatively fast reactions, the rate of addition of the azido compound should be slow enough so that it reacts rapidly and no significant unreacted excess is allowed to build up. The reaction mixture should be stirred efficiently while the azido compound is being added, and cooling should generally be provided.*
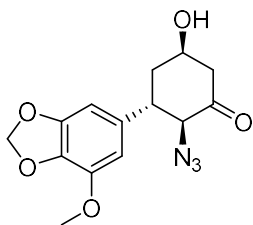
(2*S*,3*S*,5*R*)-2-Azido-3-(7-Methoxy-1,3-benzodioxol-5-yl)-5-hydroxycyclohexanone ent-**9**.

M.P.: 147-150 °C (material solidified from CH_2Cl_2:MeOH, 98:2); $[\alpha]^{23}_D$ = -58 (*c* = 0.43, MeOH, *l* = 1 dm); **ee**.: τmajor = 9.5min, τminor = 11.1 min (97% *ee*), AS-RH column (150 x 4.6 mm, 5μ), H_2O/MeCN (70:30) as a mobile phase; flow rate 0.750 mL/min, column temperature 20 °C, λ236, sample 0.2 mg /mL dissolved in the mobile phase.
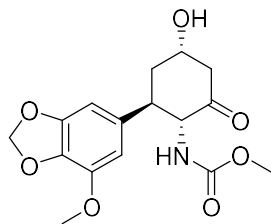
N-[(1R,4R,6R)-6-(7-Methoxy-1,3-benzodioxol-5-yl)-4-hydroxy-2-oxocyclohexyl]-carbamic acid methyl ester 10. In a stainless-steel hydrogenation vessel **9** (0.405 g, 1.33 mmol), dimethyl dicarbonate (0.535 g, 3.99 mmol, 3.0 eq.) and 10 % Pd/C (0.106 g, 0.100 mmol, 0.075 eq.) were suspended in methanol (40.5 mL). The vessel was sealed and subjected to 50 psi of hydrogen gas with vigorous stirring for 10 h, after which TLC (CH_2Cl_2/MeOH 95:5) showed full conversion. The suspension was filtered through a Celite® pad and carefully evaporated (20 °C, 0.1 mbar). The translucent yellow oil was purified by flash chromatography (eluent CH_2Cl_2/MeOH 100:0 to 95:5, 50 g of silica were used) giving the product as a translucent oil (0.332 g).

Yield: 74%; **TLC**: Rf = 0.28 (CH_2Cl_2 / MeOH; 95:5; UV); **[α]$^{23}_D$** = -5.9 (c = 1.98, MeOH, l = 1 dm); **IR** (neat, cm^{-1}): ν 3385, 2943, 2901, 1729, 1706, 1634, 1513, 1452, 1434, 1194, 1090, 1044, 928, 735; **^{1}H NMR** (600 MHz, CDCl$_3$): δ 6.46 (d, J = 0.8 Hz, 1H), 6.43 (s, 1H), 5.93 (d, J = 1.0 Hz, 2H), 5.18 (d, J = 8.9 Hz, 1H), 4.55 (m, 2H), 3.87 (s, 3H), 3.53 (s, 3H), 3.20 (td, J = 12.0, 3.8 Hz, 1H), 2.82 (d, J = 12.5 Hz, 1H), 2.68 (dd, J = 14.0, 2.2 Hz, 1H), 2.64 (s, 1H), 2.22 – 2.11 (m, 2H); **^{13}C NMR** (151 MHz, CDCl$_3$): δ 205.7, 157.0, 148.9, 143.4, 135.3, 134.1, 107.2, 101.4, 101.4, 68.0, 63.4, 56.6, 52.2, 48.2, 45.5, 40.5; **HRMS** (ESI): exact mass calculated for $C_{16}H_{20}NO_7$ [(M + H)$^+$], 338.1240 found 338.1248.
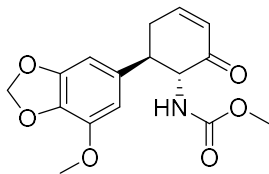
N-[(1R,6R)-6-(7-Methoxy-1,3-benzodioxol-5-yl)-2-oxo-3-cyclohexen-1-yl] - carbamic acid methyl ester 11. In a 50 mL RBF, **10** (0.317 g, 0.94 mmol) was dissolved in CH_2Cl_2 (16 mL) under nitrogen and cooled in an ice bath. Methanesulfonyl chloride (0.094 mL, 1.22 mmol, 1.30 eq.) was added in one portion, and then dry Hünig's base (0.491 mL, 2.83 mmol, 3.0 eq.) was added dropwise over a period of 10 min. The resulting solution was stirred for 3 h at RT, then poured into water (8 mL) and the layers separated. The organic phase was washed with 0.1 M HCl (8 mL) then brine (8 mL) and dried over Na_2SO_4. Concentration under reduced pressure followed by column chromatography on silica (CH_2Cl_2 / MeOH; 100:0 to 98:2) gave the product as a translucent oil. The product was triturated with MeOH to obtain a white solid (0.264 g).

Yield: 88%; TLC: Rf = 0.20 (CH2Cl2 / MeOH; 98:2; UV); **M.P.**: 186-188 °C (material solidified from MeOH); $[a]^{25}_D$ = +15.0 (c = 0.68, MeOH, l = 1 dm); **IR** (neat, cm-1): ν 3328, 2947, 1717, 1686, 1634, 1513, 1451, 1435, 1315, 1136, 1092, 1062, 927; **¹H NMR** (600 MHz, CDCl₃): δ 6.98 (dt, J = 9.9, 4.0 Hz, 1H), 6.46 (s, 1H), 6.45 (s, 1H), 6.17 (d, J = 10.1 Hz, 1H), 5.96 (s, 2H), 4.80 (brd, J = 5.3 Hz, 1H), 4.71 – 4.52 (m, 1H), 3.89 (s, 3H), 3.59 (s, 3H), 3.19 (m, 1H), 2.76 – 2.62 (m, 2H); **¹³C NMR** (151 MHz, CDCl₃): δ 196.3, 157.1, 148.9, 148.5, 143.5, 134.8, 134.3, 128.6, 107.1, 101.6, 101.5, 60.7, 56.6, 52.3, 47.9, 36.0; **HRMS** (ESI): exact mass calculated for $C_{16}H_{18}NO_6$ [(M + H)⁺], 320.1134; found 320.1129.
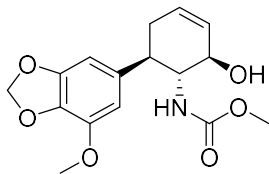
N-[(1R,2R,6R)-6-(7-Methoxy-1,3-benzodioxol-5-yl)-2-hydroxy-3-cyclohexen-1-yl]-carbamic acid methyl ester 12. To a solution of LiAlH$_4$ (0.058 g, 1.53 mmol, 3.0 eq.) in THF (8 mL) at 0 °C, *t*-BuOH (0.476 mL, 4.85 mmol, 9.5 eq.) was added dropwise and the resulting mixture was stirred at RT for 30 min. The suspension was cooled to 0 °C and added to **11** (0.163 g, 0.51 mmol). After 2 h of stirring TLC showed full conversion (CH$_2$Cl$_2$/MeOH 95:5, quenched before spotted), saturated aqueous NH$_4$Cl was added to quench the reaction. The product was extracted with EtOAc (3 x 15 mL) and the combined organic layer was washed with brine (10 mL) and dried over Na$_2$SO$_4$. The solvent was removed under reduced pressure (50 °C, 32 mbar) and the residue was purified by column chromatography (CH$_2$Cl$_2$ / MeOH; 100:0 to 95:5) to afford the product (0.135 g) as a light brown solid. Storage temperature: 0 °C.

Yield: 82%; **M.P.**: 116-118 °C (material solidified from CH$_2$Cl$_2$); **TLC**: *Rf* = 0.41 (CH$_2$Cl$_2$ / MeOH; 95:5; UV); **[α]^{24}D** = -62 (*c* = 0.3, MeOH, *l* = 1 dm); **IR** (neat, cm-1): ν 3386, 2915, 1701, 1633, 1512, 1451, 1433, 1313, 1242, 1091, 1045, 926; **^{1}H NMR** (600 MHz, CDCl$_3$): δ 6.38 (d, *J* = 1.3 Hz, 1H), 6.36 (d, *J* = 1.1 Hz), 5.92 (s, 2H), 5.75 (ddd, *J* = 10.0, 4.5, 2.1 Hz, 1H), 5.68 (d, *J* = 10.2 Hz, 1H), 4.75 (d, *J* = 3.5 Hz, 1H), 4.28 (s, 1H), 3.86 (s, 3H), 3.74 (dt, *J* = 11.9, 7.5 Hz, 1H), 3.54 (s, 3H), 2.80 (td, *J* = 11.4, 5.5 Hz, 1H), 2.33 (dt, *J* = 18.0, 5.0 Hz, 1H), 2.30 – 2.22 (m, 1H); **^{13}C NMR** (151 MHz, CDCl$_3$): δ 158.3, 149.1, 143.6, 135.7, 134.1, 129.4, 126.8, 107.1, 101.4, 101.3, 73.7, 58.6, 56.5, 52.3, 44.8, 35.1; **HRMS** (ESI): exact mass calculated for C$_{16}$H$_{19}$NO$_6$Na [(M + Na)$^+$], 344.1108; found 344.1110.
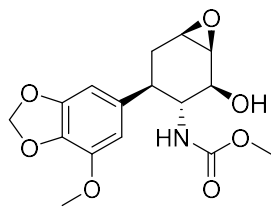
methyl ((1S,2S,3R,4R,6R)-2-hydroxy-4-(7-methoxybenzo [1,3]dioxol- 5-yl)-7-oxabicyclo [4.1.0]heptan-3-yl)carbamate 13. In a dry 10 mL RBF, **12** (0.010 g, 0.03 mmol) was dissolved in benzene-dioxane (1 mL, 1:1) along with NaHCO$_3$ (0.008 g, 0.09 mmol, 3.0 eq.) and *m*-CPBA (0.011 g, 0.06 mmol, 2.0 eq.) at RT. The resulting solution was stirred vigorously for 12 h at RT. Then solvent was evaporated in *vacuo* at 20 °C to obtain crude solid, which was dissolved in CH$_2$Cl$_2$ and washed with sat. NaHCO$_3$ solution (5 mL) and was extracted with CH$_2$Cl$_2$ (2 × 5 mL). The combined organic layers were washed with brine (5 mL) then dried with anhydrous Na$_2$SO$_4$. The solvent was removed under reduced pressure (50 °C, 32 mbar) and the residue was purified by column chromatography (CH$_2$Cl$_2$ / MeOH; 100:0 to 95:5) to afford the product **13** (0.004 g) as a light brown viscous liquid along with starting material **12** (0.003 g).

Yield: 55% (brsm); **TLC**: Rf = 0.22 (CH2Cl2 / MeOH; 95:5; UV); **[α]^{20}$_D$** = -6.4 (*c* = 0.25, CHCl$_3$, l = 1 dm); **^{1}H NMR** (600 MHz, CDCl$_3$): δ 6.36 (d, J = 1.2 Hz, 1H), 6.34 (s, 1H), 5.97 (brs, 2H), 4.49 (brs, 1H), 4.07 (bs, 1H), 3.90 (s, 3H), 3.84 – 3.75 (m, 1H), 3.58 (s, 3H), 3.51 (dd, J = 3.7, 1.4 Hz, 1H), 3.37 (t, J = 4.5 Hz, 1H), 2.69 (brs, 1H), 2.30 (ddd, J = 15.9, 6.5, 5.2 Hz, 1H), 2.11 (dd, J = 15.8, 12.0 Hz, 1H); **^{13}C NMR** (151 MHz, CDCl3): δ 158.0, 149.1, 143.7, 135.1, 134.2, 107.0, 101.9, 101.7, 101.6, 101.5, 73.6, 57.1, 56.6, 55.3, 53.4, 52.4, 44.8, 33.1.; **HRMS** (ESI): exact mass calculated for C$_{16}$H$_{20}$NO$_7$ [(M + H)$^+$], 338.1240; found 338.1238.
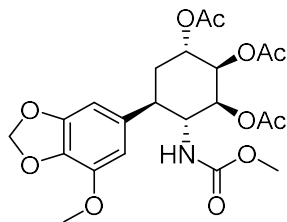
(1S,2R,3S,4R,5R)-5-(7-methoxybenzo [1,3]dioxol-5-yl)-4-((methoxycarbonyl) amino) cyclohexane-1,2,3-triyl triacetate 14. The epoxide **13** (0.010 g, 0.03 mmol) was suspended in water (2 mL) and sodium benzoate (0.0012 g, 0.014 mmol, 0.5 eq.) was added. The mixture was heated at 90-95 °C for 18 h. After the reaction was complete (TLC: Rf = 0.11 (CH_2Cl_2 / MeOH; 95:5; UV), solution was cooled to RT and the water was removed using a flow of nitrogen. The crude residue (light pink) was dissolved in CH_2Cl_2, to which was added acetic anhydride (0.01 mL, 0.112 mmol, 4.0 eq.) and pyridine (0.024 mL, 0.28 mmol, 10 eq.) at RT. The reaction mixture was stirred at RT for 12 h then it was poured into water and extracted with CH_2Cl_2 (2 × 5 mL). The combined organic layers were washed with brine (5 mL) then dried with anhydrous Na_2SO_4. The solvent was removed *in vacuo* and the residue was purified by silica gel column chromatography (CH_2Cl_2 / MeOH; 100:0 to 98:2) to afford the product **14** (0.010 g) as a colourless oil. This compound is known and matches the reported spectroscopic data.[5]

Yield: 75% (for 2 steps); **TLC**: Rf = 0.50 (EtOAc / Hexane; 50:50; UV); $[\alpha]^{20}_D$ = +53.9 (c = 1.0, $CHCl_3$, l = 1 dm) {$[a]D$ lit.= +63.7 (c = 0.95, $CHCl_3$)[6]}; **^{1}H NMR** (600 MHz, $CDCl_3$): δ 6.43 (d, J = 1.4 Hz, 1H), 6.39 (brs, 1H), 5.95 (q, J = 1.5 Hz, 2H), 5.34 (t, J = 3.0 Hz, 1H), 5.22 (dd, J = 10.1, 0.6 Hz, 1H), 5.05 (dd, J = 6.2, 2.9 Hz, 1H), 4.38 (d, J = 9.1 Hz, 1H), 4.22 – 4.13 (m, 1H), 3.91 (s, 3H), 3.51 (s, 3H), 2.89 (s, 1H), 2.21 (s, 3H), 2.16 (s, 3H), 2.06 – 2.03 (m, 1H), 2.01 (s, J = 4.0 Hz, 3H), 2.02-1.98 (m, 1H); **^{13}C NMR** (151 MHz, $CDCl_3$): δ 170.7, 169.4, 169.3, 156.5, 149.0, 143.5, 134.9, 134.22, 107.3, 101.5, 101.4, 71.1, 69.1, 68.8, 56.7, 53.2, 52.1, 43.4, 33.8, 21.1, 21.0, 20.7; **HRMS** (ESI): exact mass calculated for $C_{22}H_{27}NO_{11}Na$ [(M + Na)$^+$], 482.1584; found 504.1482.
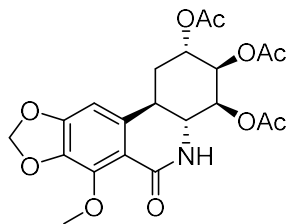
(2S,3R,4S,4aR,11bR)-7-methoxy-6-oxo-1,2,3,4,4a,5,6,11b-octahydro-[1,3]dioxolo[4,5-j]

phenanthridine-2,3,4-triyl triacetate 15. Into a 10 mL RBF, **14** (0.020 g, 0.04 mmol) and DMAP

(0.024 g, 0.2 mmol, 5.0 eq.) were dissolved in CH_2Cl_2 (2 mL) at 0 °C. A 1.0 M solution of Tf_2O in

CH_2Cl_2 (0.33 mL, 0.33 mmol, 8.0 eq.) was added dropwise to the reaction mixture over a period of 10

min. The reaction was stirred for 16 h at RT. The solvent was evaporated and the residue treated with

a mixture of THF (2 mL) and 1 M HCl (1 mL). After stirring for 1 h at RT, the mixture was partitioned

between a saturated aqueous solution of $NaHCO_3$ (1 mL) and CH_2Cl_2 (10 mL). The organic phases

were combined, dried with anhydrous Na_2SO_4 and concentrated. The brown product was purified by

flash column chromatography (CH_2Cl_2 / MeOH; 100:0 to 98:2) to afford 0.011 g of white solid. This

compound is known and matches the reported spectroscopic data.[5]

Yield: 61%; **TLC**: Rf = 0.30 (CH_2Cl_2 / MeOH; 95:5; UV); **[α]^{20}$_D$** = +119.2 (c = 0.45, $CHCl_3$, l = 1

dm) {[α]D lit.= +131.3 (c = 0.31, $CHCl_3$)[6] }; **^{1}H NMR** (600 MHz, $CDCl_3$): δ 6.47 (s, 1H), 6.02 (d, J

= 1.4 Hz, 1H), 6.00 (d, J = 1.4 Hz, 1H), 5.42 (t, J = 3.2 Hz, 1H), 5.21 – 5.13 (m, 2H), 4.07 (s, 3H),

3.72 – 3.60 (m, 1H), 3.08 (td, J = 12.5, 4.0 Hz, 1H), 2.40 (d, J = 14.4 Hz, 1H), 2.14 (s, 3H), 2.07 (s,

6H), 1.92 – 1.84 (m, 1H).; **^{13}C NMR** (151 MHz, $CDCl_3$): δ 170.4, 169.4, 169.1, 163.7, 152.1, 145.1,

137.4, 137.1, 115.5, 101.7, 99.0, 71.5, 68.5, 67.3, 60.8, 52.1, 35.9, 26.9, 21.0, 20.8, 20.7; **HRMS** (ESI):

exact mass calculated for $C_{21}H_{24}NO_{10}$ [(M + H)$^+$], 450.1395; found 450.1413.
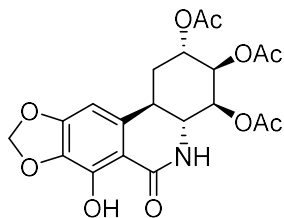
(2S,3R,4S,4aR,11bR)-7-hydroxy-6-oxo-1,2,3,4,4a,5,6,11b-octahydro-[1,3]dioxolo[4,5-j] phenanthridine-2,3,4-triyl triacetate 16. Boron tribromide (0.16 mL of 1.0 M in CH_2Cl_2, 0.156 mmol) was added to a solution of **15** (0.009 g, 0.02 mmol) in CH_2Cl_2 (2 mL) at -78 °C. The reaction mixture was allowed to warm to 0 °C and stirring was continued for 1 h. The reaction was then quenched by adding aqueous NH_4OH solution (2 mL) at 0 °C and the resulting mixture was stirred for 30 min at 0 °C. Then it was extracted with ethyl acetate (2 × 10 mL). The combined organic layers were washed with brine, dried with anhydrous Na_2SO_4 and concentrated. The crude product was purified by flash column chromatography (CH_2Cl_2 / MeOH; 100:0 to 98:2) to afford **16** (0.005 g, 57%) as a white amorphous solid.

KI (0.004 g, 0.022 mmol, 1.0 eq.) and TMSCl (0.06 mL of 0.5 M solution in CH_3CN, 1.3 eq.) were added to a stirred solution of **15** (0.010 g, 0.022 mmol, 1.0 eq.) in CH_3CN (1.5 mL). The reaction mixture was stirred for 1 h at 60 °C and quenched by the addition of H_2O (2 mL) at 0 °C. The organic layer was extracted with EtOAc (2 × 5 mL), washed with brine, dried over Na_2SO_4, filtered, and concentrated in vacuo. The crude residue was purified by silica gel column chromatography (CH_2Cl_2 / MeOH; 100:0 to 98:2) to obtain **16** (0.006 g, 63%) as a white solid. This compound is known and matches the reported spectroscopic data.[5]

TLC: Rf = 0.25 (CH_2Cl_2 / MeOH; 95:5; UV); **[α]^{20}$_D$** = +68.8 (c = 0.33, CHCl3, l = 1 dm) {[α]$_D$ lit.= +80.7 (c = 0.29, CHCl$_3$)[6] }; **^{1}H NMR** (600 MHz, CDCl$_3$): δ 12.32 (s, 1H), 6.33 (s, 1H), 6.05 (s, 1H), 6.04 (d, J = 0.6 Hz, 1H), 6.00 (s, 1H), 5.44 (t, J = 3.2 Hz, 1H), 5.19 (dd, J = 6.8, 4.2 Hz, S11 2H), 3.78 (dd, J = 12.6, 11.0 Hz, 1H), 3.14 (td, J = 12.7, 3.8 Hz, 1H), 2.44 (dt, J = 14.3, 2.8 Hz, 1H), 2.14 (s, 3H), 2.10 (s, 3H), 2.09 (s, 3H), 1.95 – 1.88 (m, 1H).; **^{13}C NMR** (151 MHz, CDCl$_3$): δ 170.2, 169.3, 169.1, 153.0, 146.5, 135.8, 133.2, 106.9, 102.3, 96.7, 71.6, 68.4, 67.3, 52.8, 34.5, 29.7, 26.7, 21.0, 20.8, 20.7.; **HRMS** (ESI): exact mass calculated for $C_{20}H_{22}NO_{10}$ [(M + H)$^+$], 436.1238; found 436.1236.
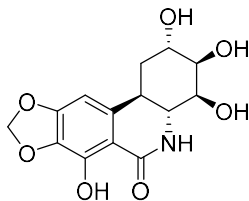
(+)-trans-Dihydronarciclasine 1. To a stirred solution of **16** (0.006 g, 0.014 mmol) in THF (1 mL) was added NaOMe (0.008 g, 0.14 mmol, 10.0 eq.) at RT, and the mixture was stirred at RT for 1 h. After completion of the reaction (TLC), it was quenched by the addition of saturated NH_4Cl solution and extracted with EtOAc (3 × 5 mL). The combined organic layers were washed with brine (5 mL), dried over Na_2SO_4, and concentrated in vacuo to give crude residue, which was purified by silica gel column chromatography (EtOAc/MeOH 10:1) furnished trans-dihydronarciclasine (**1**) (0.004 g, 95%) as a white solid. This compound is known and matches the reported spectroscopic data.[5]

TLC: Rf = 0.10 (CH2Cl2 / MeOH; 95:5; UV); **[α]$^{20}_D$** = +4.5 (c = 0.2, THF, l = 1 dm) {[α]$_D$ lit.= +4.7 (c = 0.27, THF)[6]}; **^{1}H NMR** (600 MHz, MeOD): δ 6.37 (s, 1H), 5.93 (d, *J* = 1.0 Hz, 1H), 5.92 (d, *J* = 1.0 Hz, 1H), 4.00 (dd, *J* = 5.9, 2.9 Hz, 1H), 3.83 (t, *J* = 3.2 Hz, 1H), 3.79 (dd, J = 10.2, 3.0 Hz, 1H), 3.39 (dd, *J* = 13.0, 10.2 Hz, 1H), 2.93 (td, *J* = 12.7, 3.8 Hz, 1H), 2.15 (dt, *J* = 13.8, 3.3 Hz, 1H), 1.75 (td, *J* = 13.6, 2.6 Hz, 1H).; **^{13}C NMR** (151 MHz, MeOD): δ 172.0, 154.4, 147.4, 139.8, 134.1, 108.4, 103.6, 97.8, 73.5, 71.7, 70.7, 56.5, 35.4, 29.8.; **HRMS** (ESI): exact mass calculated for $C_{14}H_{16}NO_7$ [(M + H)$^+$], 310.0927; found 310.0927.

Experimental References:

1) J. Sherma, B. Fried, *Handbook of Thin-Layer Chromatography*, Marcel Dekker, New York, **2003**.

2) W. C. Still, M. Kahn, A. Mitra, *J. Org. Chem.* **1978**, *43*, 2923–2925.

3) A. Gonzalez, J. Bermejo, E. Valencia, *Planta Med.* **1996**, *62*, 176–177.

4) F. Dallacker, J. Schubert, *Chem. Ber.* **1975**, *108*, 95–108.

5) I.-J. Shin, E.-S. Choi, C.-G. Cho, *Angew. Chem. Int. Ed.* **2007**, *46*, 2303 –2305.

6) C. Kumar Jana, A. Studer, *Chem. – Eur. J.* **2008**, *14*, 6326–6328.

5.8 References

1) M. He, C. Qu, O. Gao, X. Hu, X. Hong, *RSC Adv.* **2015**, *5*, 16562.

2) Z. Jin, G. Yao, *Nat. Prod. Rep.* **2019**, *Advance Article*.

3) Z. Jin, *Nat. Prod. Rep.* **2005**, *22*, 111.

4) Z. Jin, *Nat. Prod. Rep.* **2013**, *30*, 849.

5) A. W. Gerrard, *Pharm. J.* **1877**, *8*, 214.

6) L. J. Scott, K. L. Goa, *Drugs* **2000**, *60*, 1095.

7) J. Mcnulty, A. Thorat, N. Vurgun, J. J. Nair, E. Makaji, D. J. Crankshaw, A. C. Holloway, S. Pandey, *J. Nat. Prod* **2011**, *74*, 106.

8) D. Ma, P. Tremblay, K. Mahngar, P. Akbari-Asl, J. Collins, T. Hudlicky, J. McNulty, S. Pandey, *Invest. New Drugs* **2012**, *30*, 1012.

9) S. Pandey, J. McNulty, S. Pandey, *Int. J. Oncol.* **2011**, *38*, 1549.

10) C. Griffin, A. Karnik, J. McNulty, S. Pandey, *Mol. Cancer Ther.* **2011**, *10*, 57.

11) S. J. Chatterjee, J. McNulty, S. Pandey, *Melanoma Res.* **2011**, *21*, 1.

12) C. Griffin, C. Hamm, J. McNulty, S. Pandey, *Cancer Cell Int.* **2010**, *10*, 6.

13) J. McNulty, J. J. Nair, M. Singh, D. J. Crankshaw, A. C. Holloway, *Bioorg. Med. Chem. Lett.* **2010**, *20*, 2335.

14) J. McNulty, J. J. Nair, M. Singh, D. J. Crankshaw, A. C. Holloway, *Bioorg. Med. Chem. Lett.* **2009**, *19*, 5607.

15) J. McNulty, J. J. Nair, C. Griffin, S. Pandey, *J. Nat. Prod.* **2008**, *71*, 357.

16) P. Siedlakowski, A. McLachlan-Burgess, C. Griffin, S. S. Tirumalai, J. McNulty, S. Pandey, *Cancer Biol. Ther.* **2008**, *7*, 376.

17) C. Griffin, N. Sharda, D. Sood, J. Nair, J. Mcnulty, S. Pandey, *Cancer Cell Int.* **2007**, *7*.

18) J. McNulty, V. Larichev, S. Pandey, *Bioorg. Med. Chem. Lett.* **2005**, *15*, 5315.

19) A. McLachlan, N. Kekre, J. McNulty, S. Pandey, *Apoptosis* **2005**, *10*, 619.

20) S. Pandey, N. Kekre, J. Naderi, J. McNulty, *Artif. Cells. Blood Substit. Immobil. Biotechnol.* **2005**, *33*, 279.

21) N. Kekre, C. Griffin, J. McNulty, S. Pandey, *Cancer Chemother. Pharmacol.* **2005**, *56*, 29.

22) J. McNulty, J. Mao, R. Gibe, R. Mo, S. Wolf, G. R. Pettit, D. L. Herald, M. R. Boyd, *Bioorg. Med. Chem. Lett.* **2001**, *11*, 169.

23) J. McNulty, J. J. Nair, J. R. L. Little, J. D. Brennan, J. Bastida, *Bioorg. Med. Chem. Lett.* **2010**, *20*, 5290.

24) J. Mcnulty, J. J. Nair, M. Singh, D. J. Crankshaw, A. C. Holloway, J. Bastida, *Bioorg. Med. Chem. Lett.* **2009**, *19*, 3233.

25) J. McNulty, J. J. Nair, C. Codina, J. Bastida, S. Pandey, J. Gerasimoff, C. Griffin, *Phytochemistry* **2007**, *68*, 1068.

26) L. Ingrassia, F. Lefranc, V. Mathieu, F. Darro, R. Kiss, *Transl. Oncol.* **2008**, *1*, 1.

27) R. Fürst, *Planta Med.* **2016**, *82*, 1389.

28) F. Lefranc, S. Sauvage, G. Van Goietsenoven, V. Megalizzi, D. Lamoral-Theys, O. Debeir, S. Spiegl-Kreinecker, W. Berger, V. Mathieu, C. Decaestecker, R. Kiss, *Mol. Cancer Ther.* **2009**, *8*, 1739.

29) G. Van Goietsenoven, V. Mathieu, F. Lefranc, A. Kornienko, A. Evidente, R. Kiss, *Med. Res. Rev.* **2013**, *33*, 439.

30) D. Ma, C. Pignanelli, D. Tarade, T. Gilbert, M. Noel, F. Mansour, S. Adams, A. Dowhayko, K. Stokes, S. Vshyvenko, T. Hudlicky, J. McNulty, S. Pandey, S. Pandey, *Sci. Rep.* **2017**, *7*, 42957.

31) B. Gabrielsen, T. P. Monath, J. W. Huggins, D. F. Kefauver, G. R. Pettit, G. Groszek, M. Hollingshead, J. J. Kirsi, W. M. Shannon, E. M. Schubert, J. DaRe, B. Ugarkar, M. A. Ussery, M. J. Phelan, *J. Nat. Prod.* **1992**, *55*, 1569.

32) J. Mcnulty, C. Zepeda-Velazquez, *Angew. Chemie - Int. Ed.* **2014**, *53*, 8450.

33) J. Mcnulty, L. D'Aiuto, Y. Zhi, L. McClain, C. Zepeda-Velázquez, S. Ler, H. A. Jenkins, M. B. Yee, P. Piazza, R. H. Yolken, P. R. Kinchington, V. L. Nimgaonkar, *Med. Chem. Lett.* **2016**, *7*.

34) L. D'Aiuto, J. McNulty, C. Hartline, M. Demers, R. Kalkeri, J. Wood, L. McClain, A. Chattopadhyay, Y. Zhi, J. Naciri, A. Smith, R. Yolken, K. Chowdari, C. Zepeda-Velazquez, C. B. Dokuburra, E. Marques, R. Ptak, P. Kinchington, S. Watkins, M. Prichard, D. Bloom, V. Nimgaonkar, *Sci. Rep.* **2018**, *8*.

35) G. R. Pettit, G. M. Cragg, S. B. Singh, J. A. Duke, D. L. Doubek, *J. Nat. Prod.* **1990**, *53*, 176.

36) G. R. Pettit, S. Ducki, S. A. Eastham, N. Melody, *J. Nat. Prod* **2009**, *72*, 1279.

37) I.-J. Shin, E.-S. Choi, C.-G. Cho, *Angew. Chem. Int. Ed* **2007**, *46*, 2303.

38) T. Takeya, A. Ohguchi, T. Ikeya, S. Tobinaga, *Chem. Pharm. Bull.* **1994**, *42*, 677.

39) C.-G. Cho, Y.-W. Kim, Y.-K. Lim, J.-S. Park, H. Lee, S. Koo, *J. Org. Chem.* **2002**, *67*, 290.

40) H. Zhang, A. Padwa, *Org. Lett.* **2006**, *8*, 247.

41) H. Ko, E. Kim, J. E. Park, D. Kim, S. Kim, *J. Org. Chem.* **2004**, *69*, 112.

42) S. Kim, H. Ko, E. Kim, D. Kim, *Org. Lett.* **2002**, *4*, 1343.

43) T. Shioiri, K. Ninomiya, S. Yamada, *J. Am. Chem. Soc.* **1972**, *94*, 6203.

44) M. G. Banwell, B. D. Bissett, S. Busato, C. J. Cowden, D. C. R. Hockless, J. W. Holman, R. W. Read, A. W. Wub, *J. Chem. Soc. Chem. Commun* **1995**, *0*, 2551.

45) Y.-S. Cho, C.-G. Cho, *Tetrahedron* **2008**, *64*, 2172.

46) G. Varró, L. Heged, A. Simon, I. Kádas, *Tetrahedron Lett.* **2016**, *57*, 1544.

47) O. Mitsunobu, M. Yamada, *Bull. Chem. Soc. Jpn.* **1967**, *40*, 2380.

48) S. Hwang, D. Kim, S. Kim, *Chem. Eur. J.* **2012**, *18*, 9977.

49) C. K. Jana, A. Studer, *Chem. - A Eur. J.* **2008**, *14*, 6326.

50) P. Magnus, I. K. Sebhat, *Tetrahedron* **1998**, *54*, 15509.

51) T. Hudlicky, U. Rinner, D. Gonzalez, H. Akgun, S. Schilling, P. Siengalewicz, T. A. Martinot, G. R. Pettit, *J. Org. Chem.* **2002**, *67*, 8726.

52) S. T. Astley, G. R. Stephenson, *J. Chem. Soc., Perkin Trans. 1* **1993**, *0*, 1953.

53) G. R. Stephenson, I. M. Palotai, W. J. Ross, D. E. Tupper, *Synlett* **1991**, *1991*, 586.

54) T. Sturm, W. Weissensteiner, F. Spindler, *Adv. Synth. Catal.* **2003**, *345*, 160.

55) C. K. Jana, A. Studer, *Angew. Chemie Int. Ed.* **2007**, *46*, 6542.

56) T. Lee, S. Kim, *Tetrahedron: Asymmetry* **2003**, *14*, 1951.

57) M. Mohamed, M. A. Brook, *Helv. Chim. Acta* **2002**, *85*, 4165.

58) P. A. Bartlett, J. F. Barstow, *J. Org. Chem.* **1982**, *47*, 3933.

59) F. Cachoux, M. Ibrahim-Ouali, M. Santelli, *Synth. Commun.* **2002**, *32*, 3549.

60) D. G. Miller, D. D. M. Wayner, *J. Org. Chem.* **1990**, *55*, 2924.

61) K. Yamada, Y. Mogi, M. A. Mohamed, K. Takasu, K. Tomioka, *Org. Lett.* **2012**, *14*, 5868.

62) Y. Asano, A. Iida, K. Tomioka, *Tetrahedron Lett.* **1997**, *38*, 8973.

63) S. Harada, T. Sakai, K. Takasu, K. Yamada, Y. Yamamoto, K. Tomioka, *Tetrahedron* **2013**, *69*, 3264.

64) K. Tomioka, *Synthesis (Stuttg).* **1990**, *1990*, 541.

65) M. Shindo, K. Koga, K. Tomioka, *J. Org. Chem.* **1998**, *63*, 9351.

66) K. Tomioka, M. Shindo, K. Koga, *J. Am. Chem. Soc.* **1989**, *111*, 8266.

67) D. L. Comins, A. Dehghani, *Tetrahedron Lett.* **1992**, *33*, 6299.

68) G. Varró, L. Hegedűs, A. Simon, A. Balogh, A. Grün, I. Leveles, B. G. Vértessy, I. Kádas, *J. Nat. Prod.* **2017**, *80*, 1909.

69) S. J. Shaw, D. A. Goff, L. A. Boralsky, M. Irving, R. Singh, *J. Org. Chem.* **2013**, *78*, 8892.

70) R. B. Dehnel, G. H. Whitham, *J. Chem. Soc. Perkin Trans. 1* **1979**, *0*, 953.

71) T. Itoh, K. Jitsukawa, K. Kaneda, S. Teranishi, *J. Am. Chem. Soc.* **1979**, *101*, 159.

72) K. B. Sharpless, S. S. Woodard, M. G. Finn, *Pure Appl Chem* **1983**, *55*, 1823.

73) K. A. Jorgensen, *Chem. Rev.* **1989**, *89*, 431.

74) O. L. Chapman, M. R. Engel, J. P. Springer, J. C. Clardy, *J. Am. Chem. Soc.* **1971**, *93*, 6696.

75) D. Yang, G. Jiao, Y. Yip, M. Wong, *J. Org. Chem.* **1999**, *64*, 1635.

76) M. Ferrer, M. Gibert, F. Sanchez-Baeza, A. Messeguer, *Tetrahedron Lett.* **1996**, *37*, 3585.

77) S. E. Denmark, Z. Wu, C. M. Crudden, H. Matsuhashi, *J. Org. Chem.* **1997**, *62*, 8288.

78) M. Frohn, Z. Wang, Y. Shi, *J. Org. Chem.* **1998**, *63*, 6425.

79) D. Yang, W. Wong, Y. Yip, *J. Org. Chem.* **1995**, *60*, 3887.

80) V. K. Yadav, K. K. Kapoor, *Tetrahedron* **1995**, *51*, 8573.

81) A. Russo, G. Galdi, G. Croce, A. Lattanzi, *Chem. Eur. J.* **2012**, *18*, 6152.

82) K. M. Weiß, S. B. Tsogoeva, *Chem. Rec.* **2011**, *11*, 18.

83) A. Capobianco, A. Russo, A. Lattanzi, A. Peluso, *Adv. Synth. Catal.* **2012**, *354*, 2789.

6 Conclusions and Future Directions

This thesis has presented several novel, synthetically useful Wittig and organocatalytic methodologies. Perhaps more importantly, these have been used in the synthesis of a variety of potential chemotherapeutics with promising anti-viral and anti-cancer activities including triazole stilbenes, alkenyl phenols, cyclobutanes and the Amaryllidaceae alkaloid *trans*-dihydronarciclasine. Future efforts could focus on expanding the synthetic scope and applications of these reactions or could focus on the preparation of additional derivatives to improve the understanding of the SAR of the diverse compound classes mentioned above. In practice these goals are likely inseparable, and in some cases these research problems are already being explored by the McNulty group.

In Chapter 2, an aqueous Wittig methodology for the synthesis of α-methylstilbenes from novel phosphonium salts and the use of these stilbenes in the development of aromatase inhibitors with nanomolar potency was presented. Future work could explore the reactions of these salts with non-aromatic aldehydes, conjugated aldehydes, and ketones in order to expand the scope of the methodology. Current efforts in the McNulty group are already focused on the preparation of additional aromatase inhibitors that may be even more potent. As well, the exploration of these compounds in cell based or even mouse models may be warranted in the near future.

Chapter 3 focused on the development of a one-pot synthesis of various alkenyl phenols, including some natural product stilbenes. Interestingly, investigation of the biological activity of these compounds produced disparate results from several other reports in the literature. Thus, additional biological studies on these compounds are not current priorities. Instead, synthetic applications for these alkenyl phenols are being explored. Some have already proven to be useful, for example as substrates in the organocatalytic [2+2] cycloaddition discussed in Chapter 4. There are likely many other applications for these compounds due to their ability to readily form quinone methide

intermediates. Indeed, current work in the McNulty group is focused on the development of other organocatalytic cycloadditions with these alkenyl phenols.

As mentioned, a highly enantioselective synthesis of cyclobutanes was developed, detailed in Chapter 4. Notably, this method is one of few asymmetric organocatalytic [2+2] cycloadditions, and some of the product cyclobutanes displayed low micromolar anti-proliferative activity in several cancer cell lines. Future exploration of this biological activity is warranted and should be relatively straightforward. The cyclobutane derivatives prepared using this methodology are highly functionalized and contain several reactive handles that could be used to prepare compounds covering a broad chemical space. Thus, the establishment of SAR could be concurrent with the exploration of synthetic applications for these cyclobutanes.

Lastly, Chapter 5 describes the total synthesis of (+)-*trans*-dihydronarciclasine as part of the McNulty group's perennial focus on the synthesis of Amaryllidaceae alkaloids and the exploration of their biological activities. Although similar in principle to a prior synthesis of closely related *trans*-dihydrolycoricidine, this work highlights the fact that even small changes to the structure of a molecule can result in drastic, unpredictable changes to its reactivity and biological activity. Given the potent ant-Zika activity displayed by *trans*-dihydronarciclasine, future work should focus on further elaboration of the SAR for this molecule and the development of an improved synthetic strategy that avoids the troublesome late-stage epoxidation.

Overall, this thesis presents efforts to create synthetic methods that other chemists would find useful, with an emphasis on the Wittig reaction and its intersection with organocatalysis. As well, this work provides further evidence that unmet needs in organic chemistry are frequently discovered in the pursuit of high value compounds. Ultimately, this thesis offers multiple avenues for further research, with focuses on the discovery of novel reactions and the development of anti-viral and anti-cancer chemotherapeutics.

Appendices

Appendix A: NMR Spectra Pertaining to Chapter 2
8b ^{1}H NMR

8b ^{13}C NMR
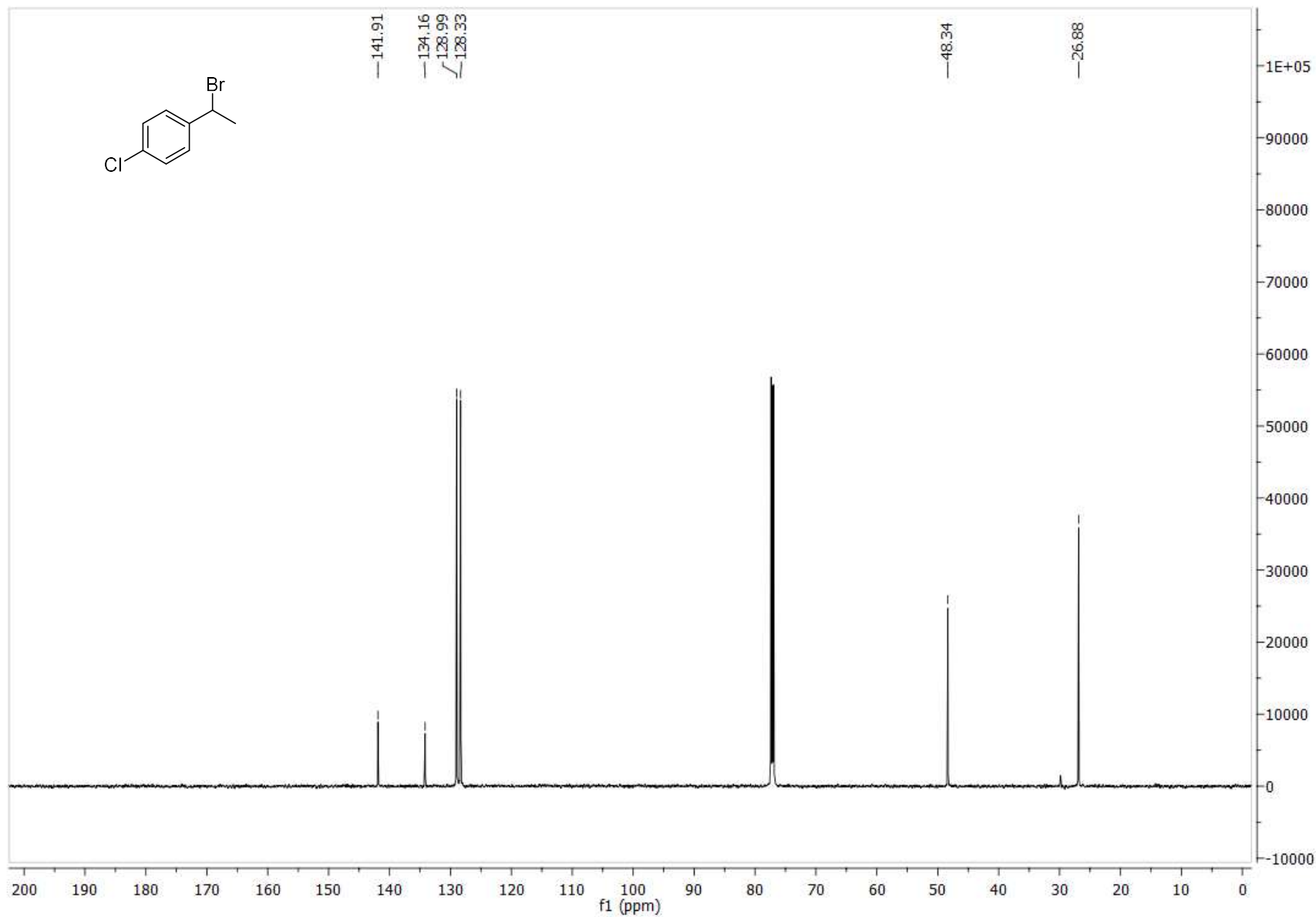
8c ^{1}H NMR
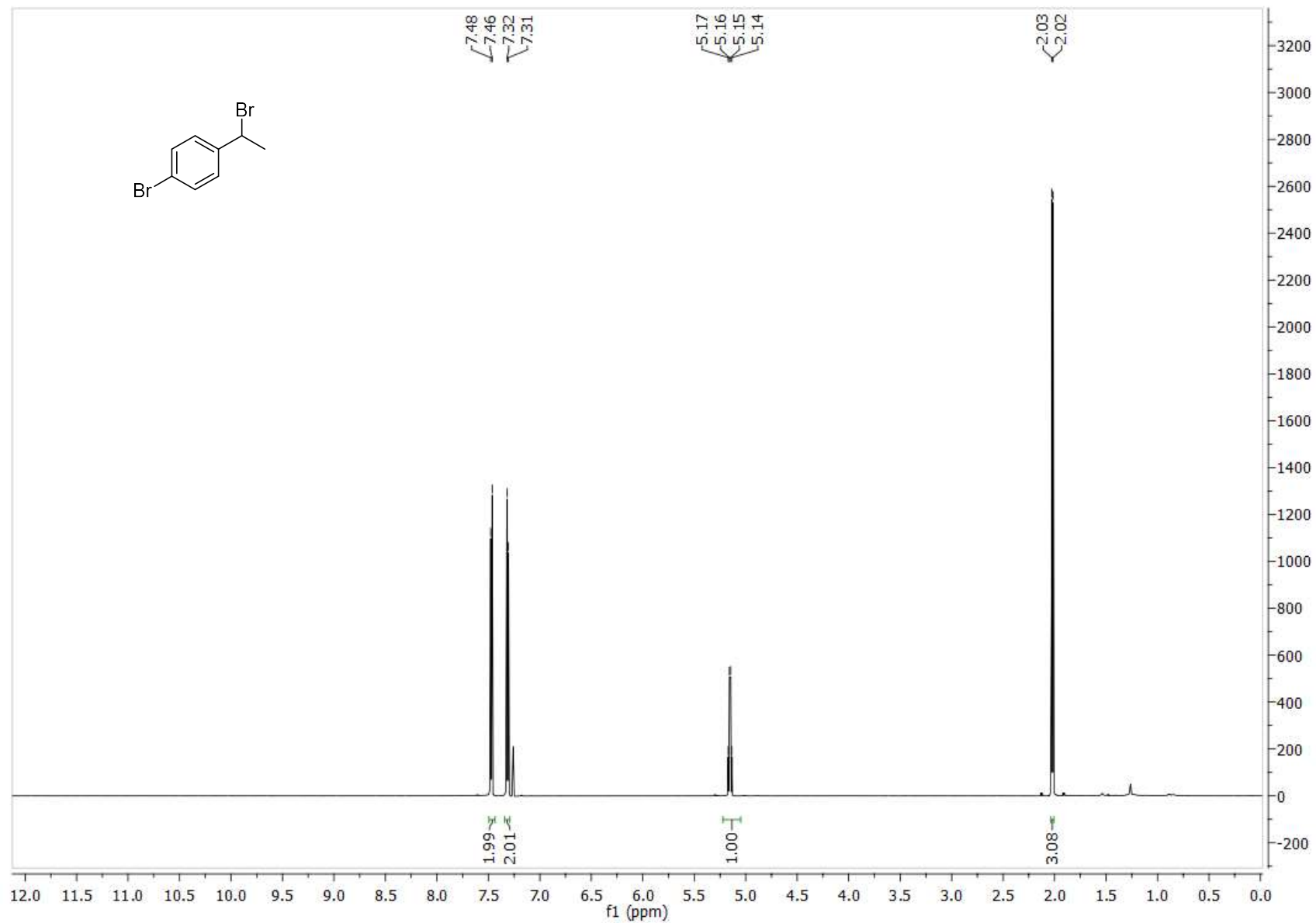
8c ^{13}C NMR
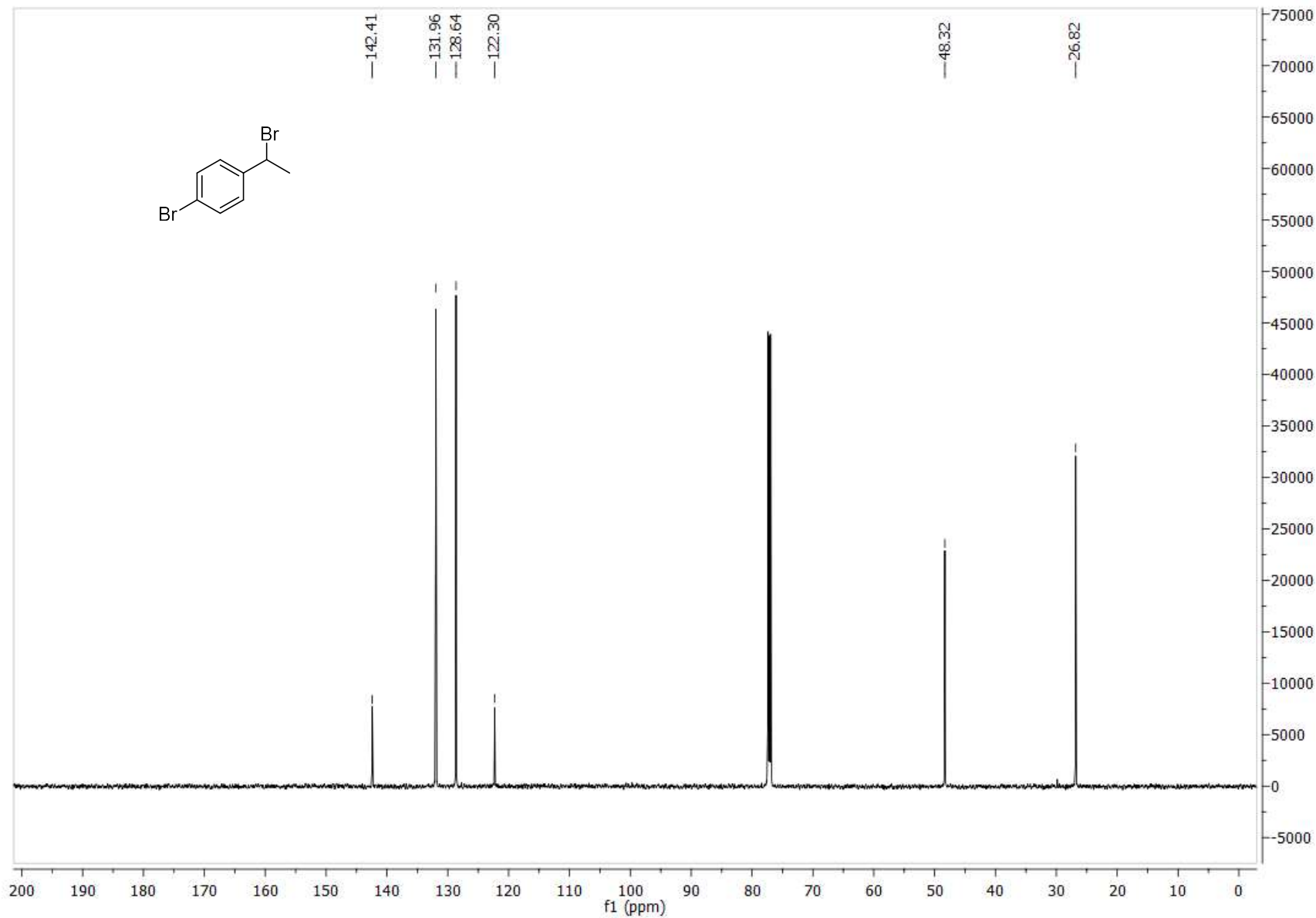
8d ¹H NMR
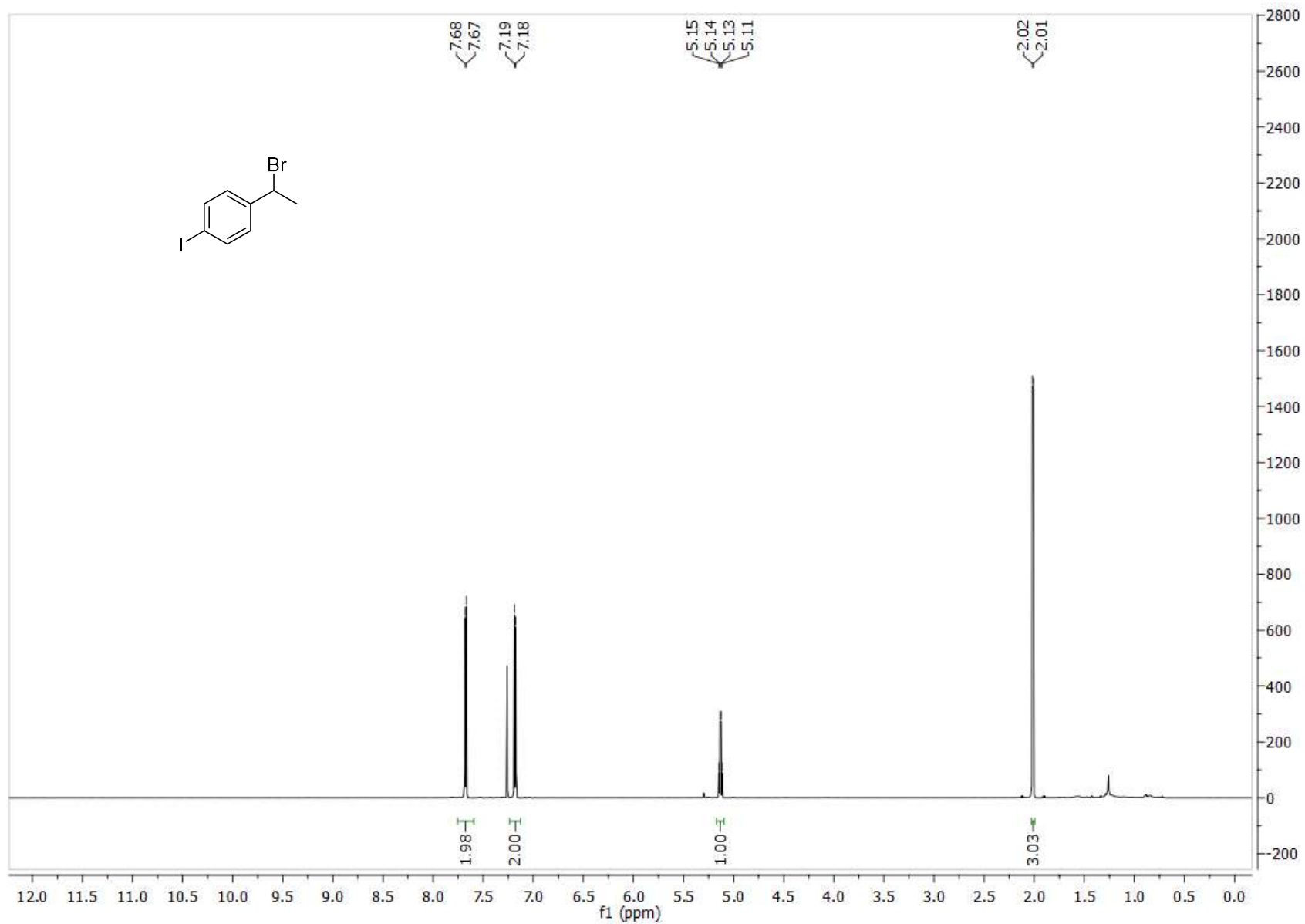
8d ^{13}C NMR
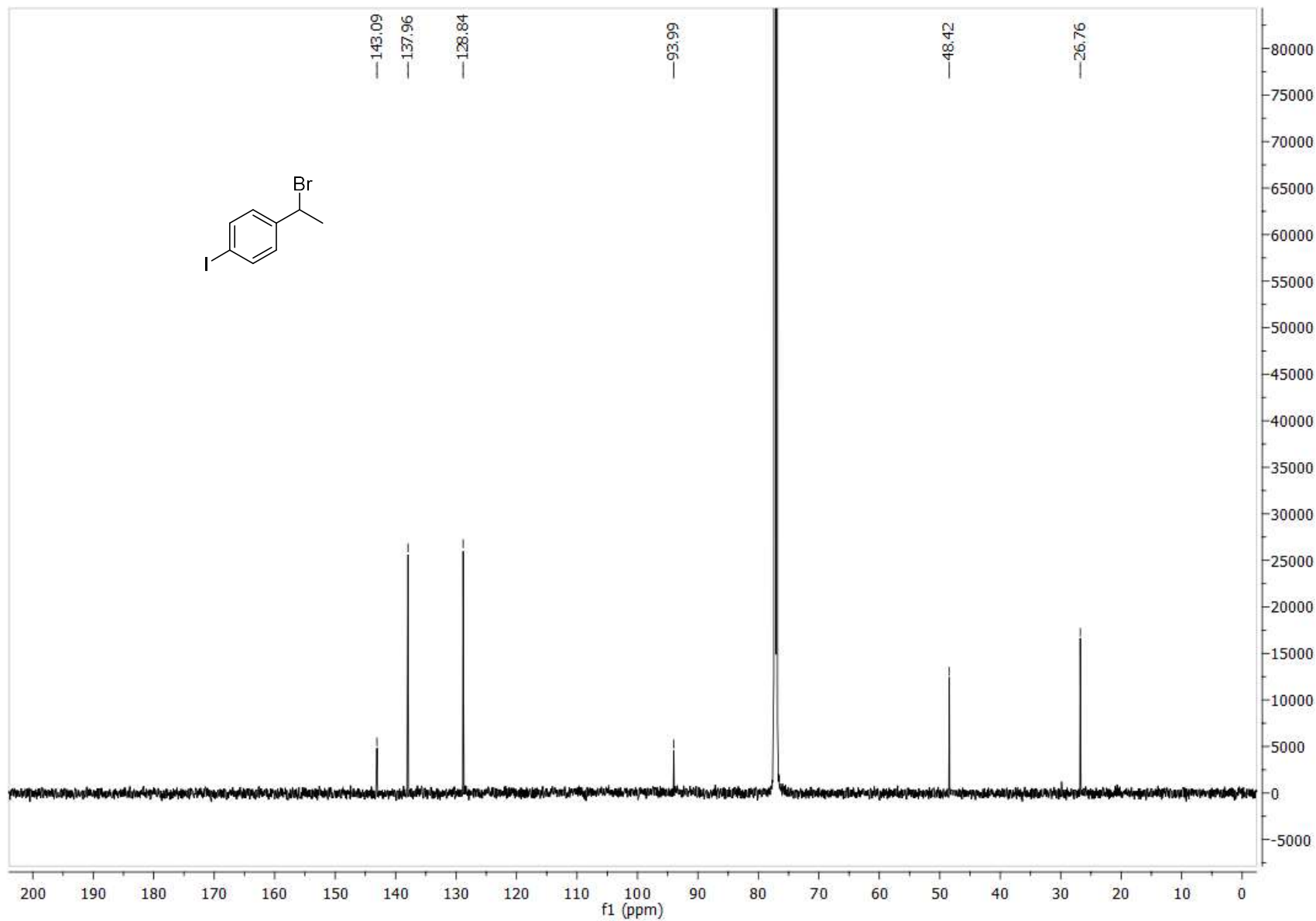
8e ^{1}H NMR
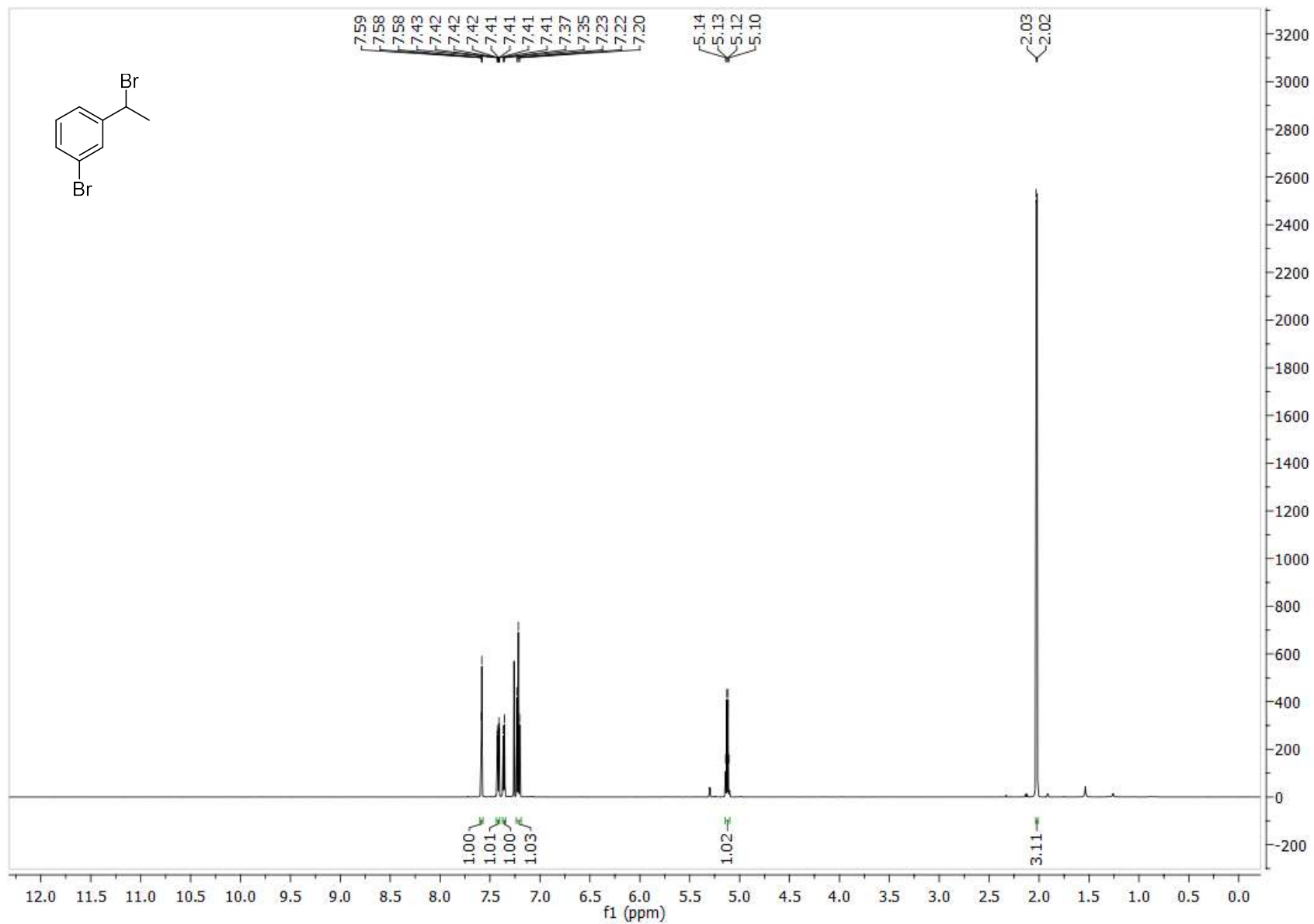
8e ^{13}C NMR
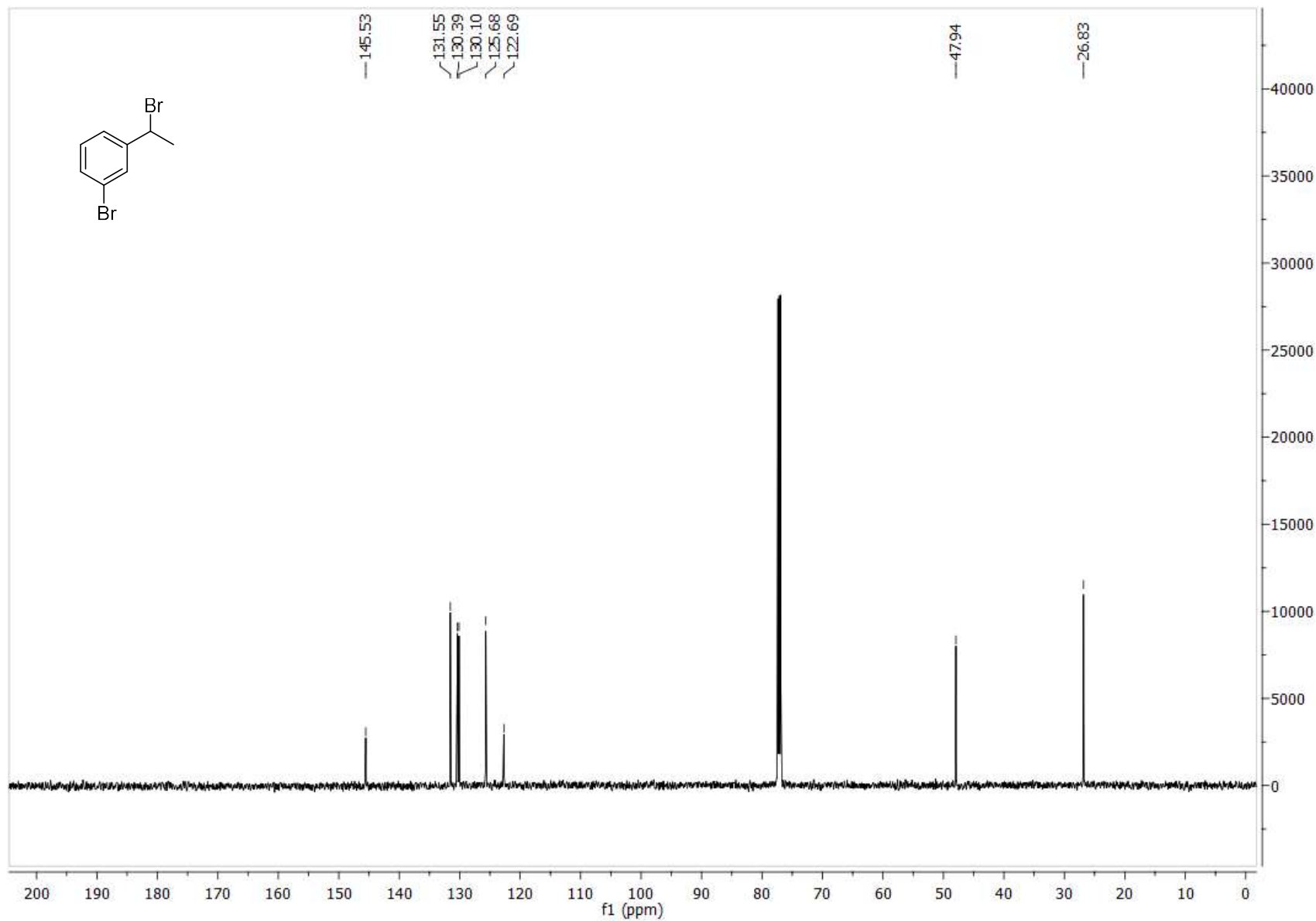
9a ^{1}H NMR
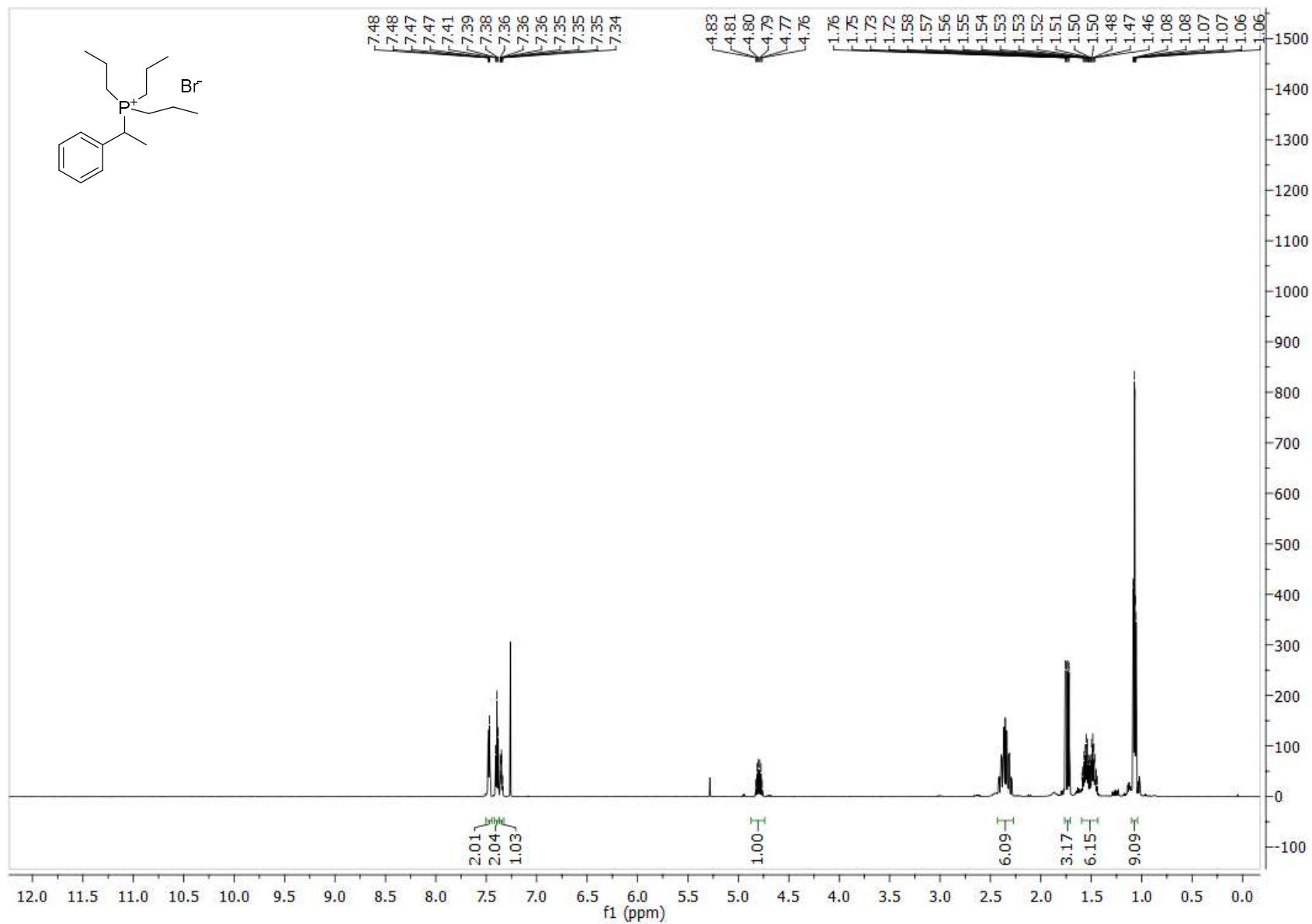
9a ^{13}C NMR
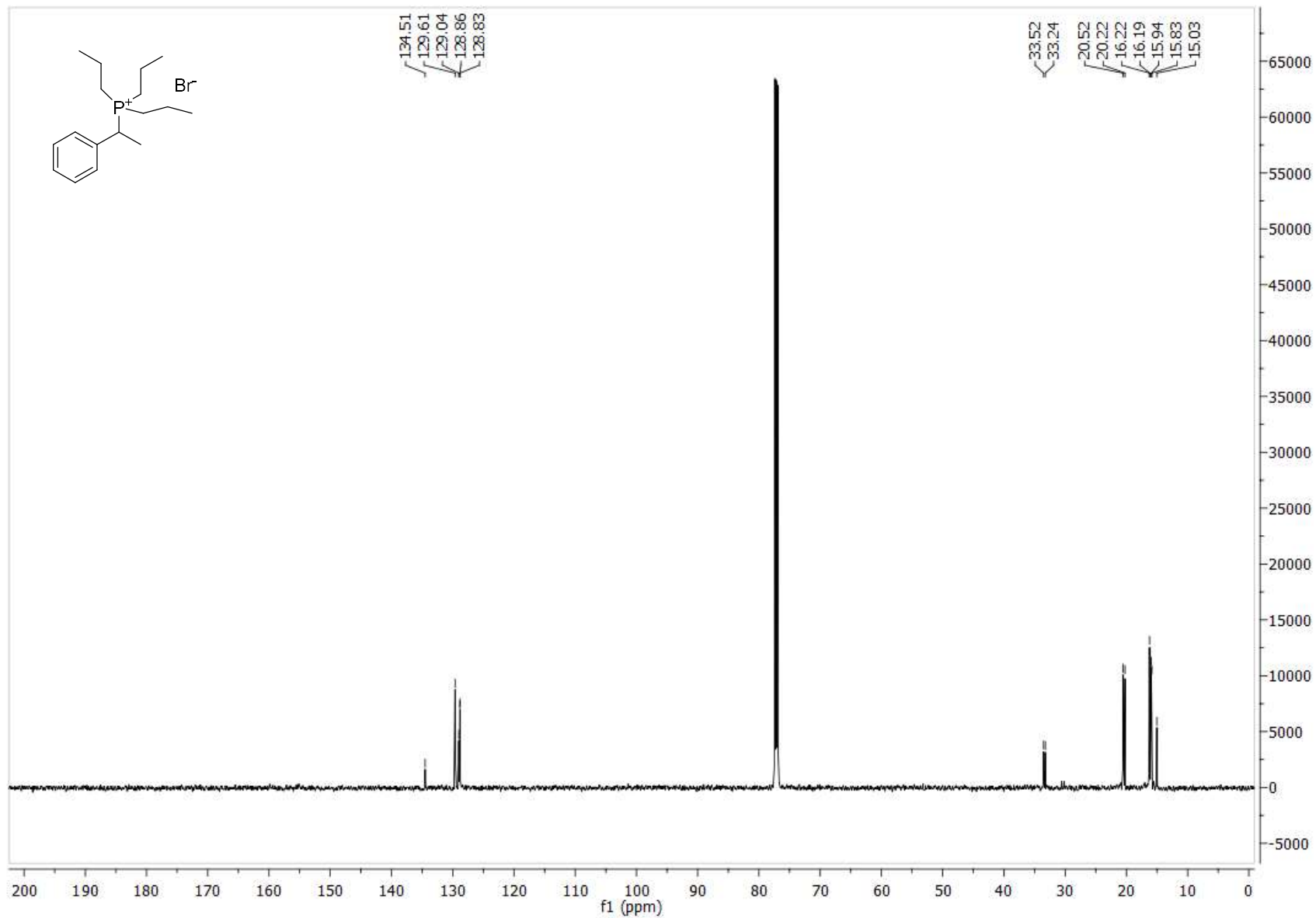
9b ¹H NMR
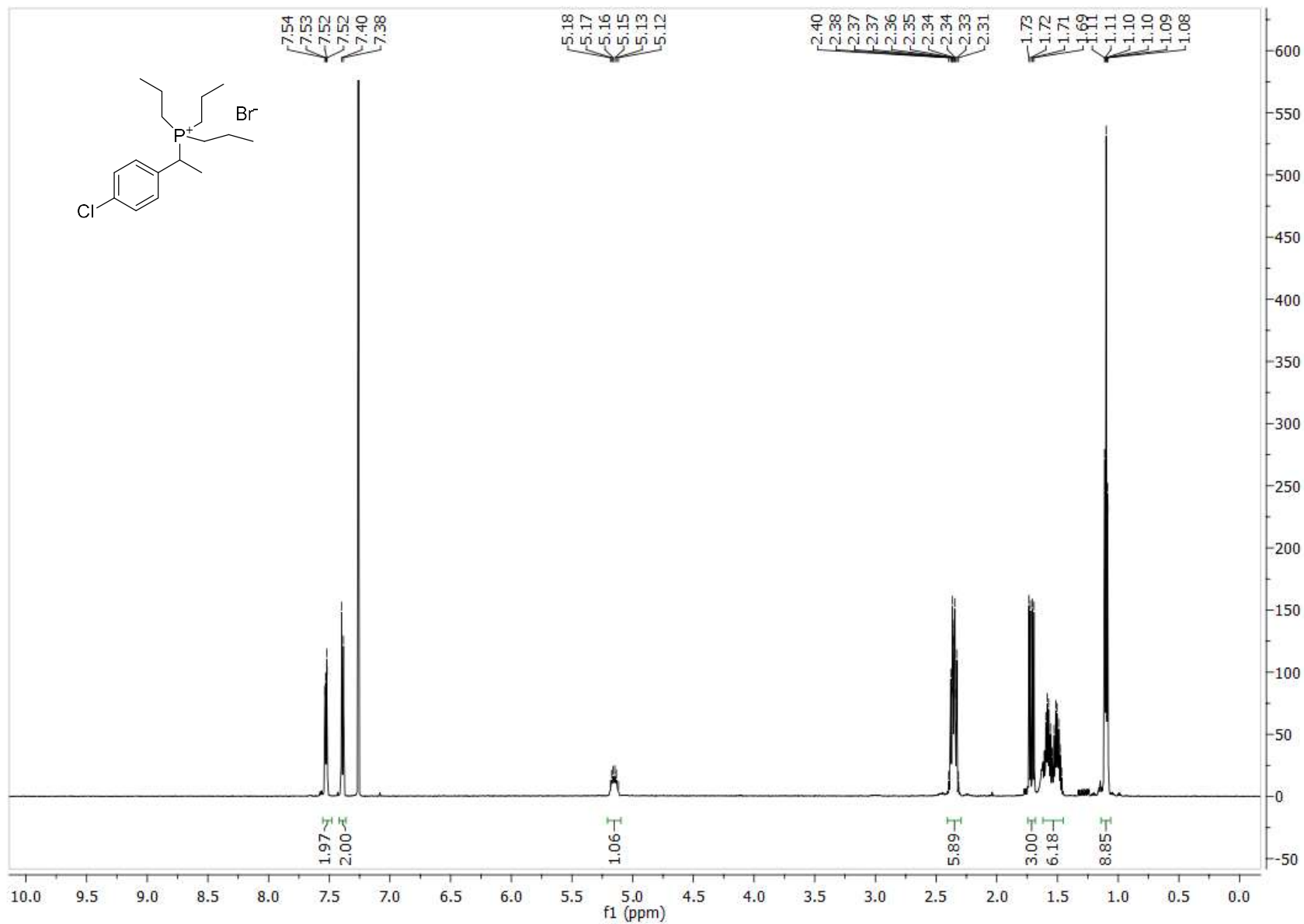
9b ^{13}C NMR
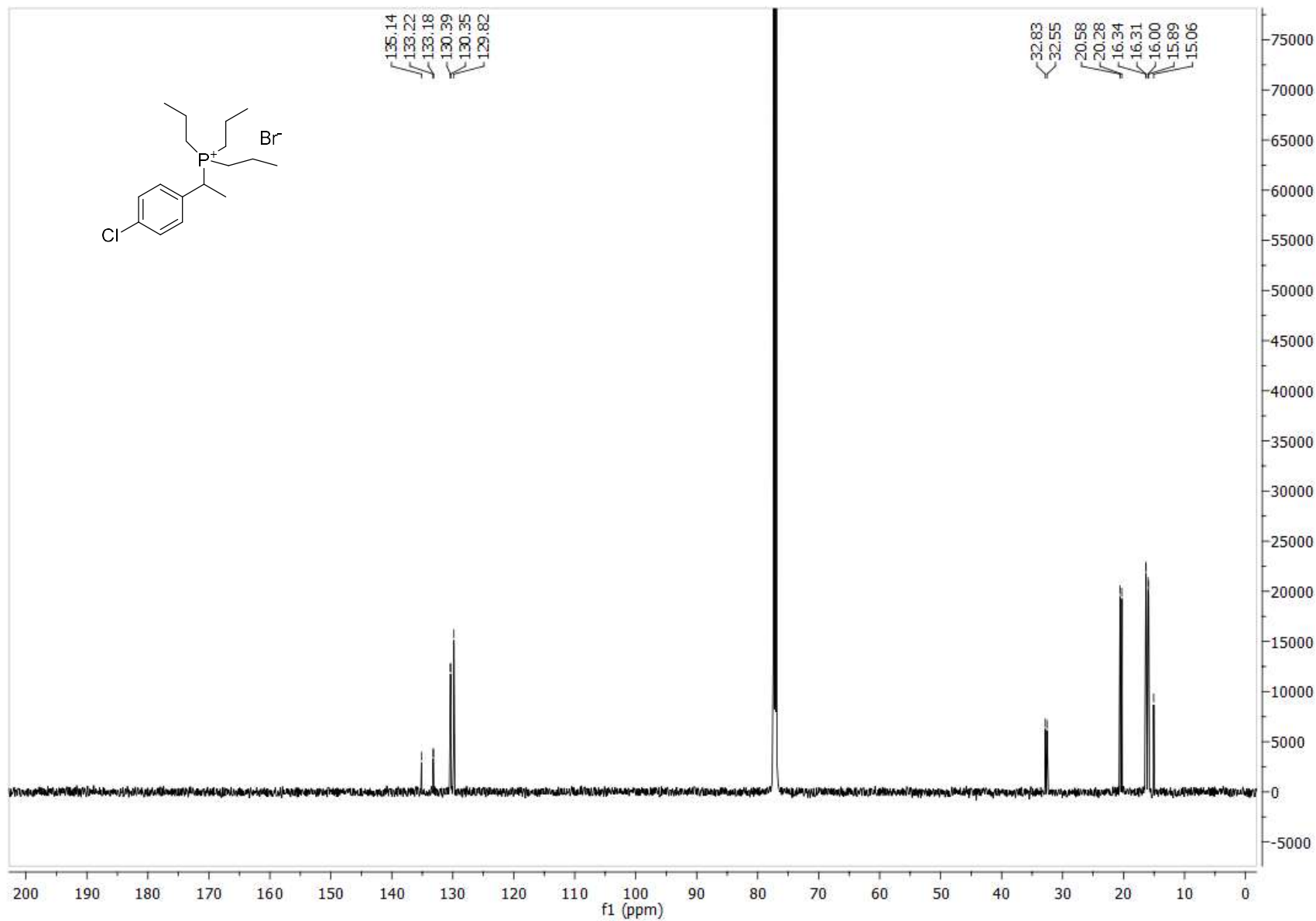
9c ¹H NMR
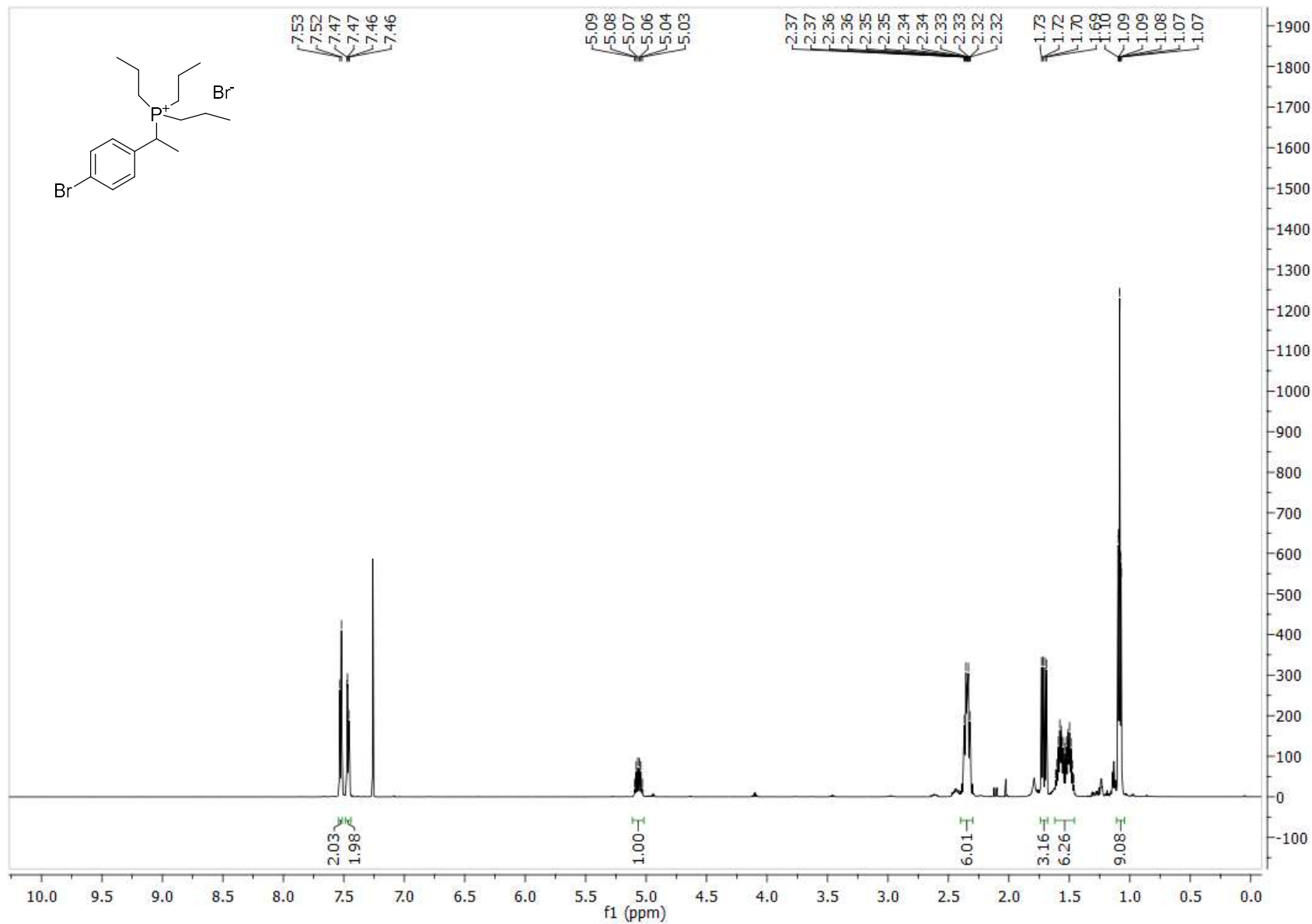
9c ^{13}C NMR
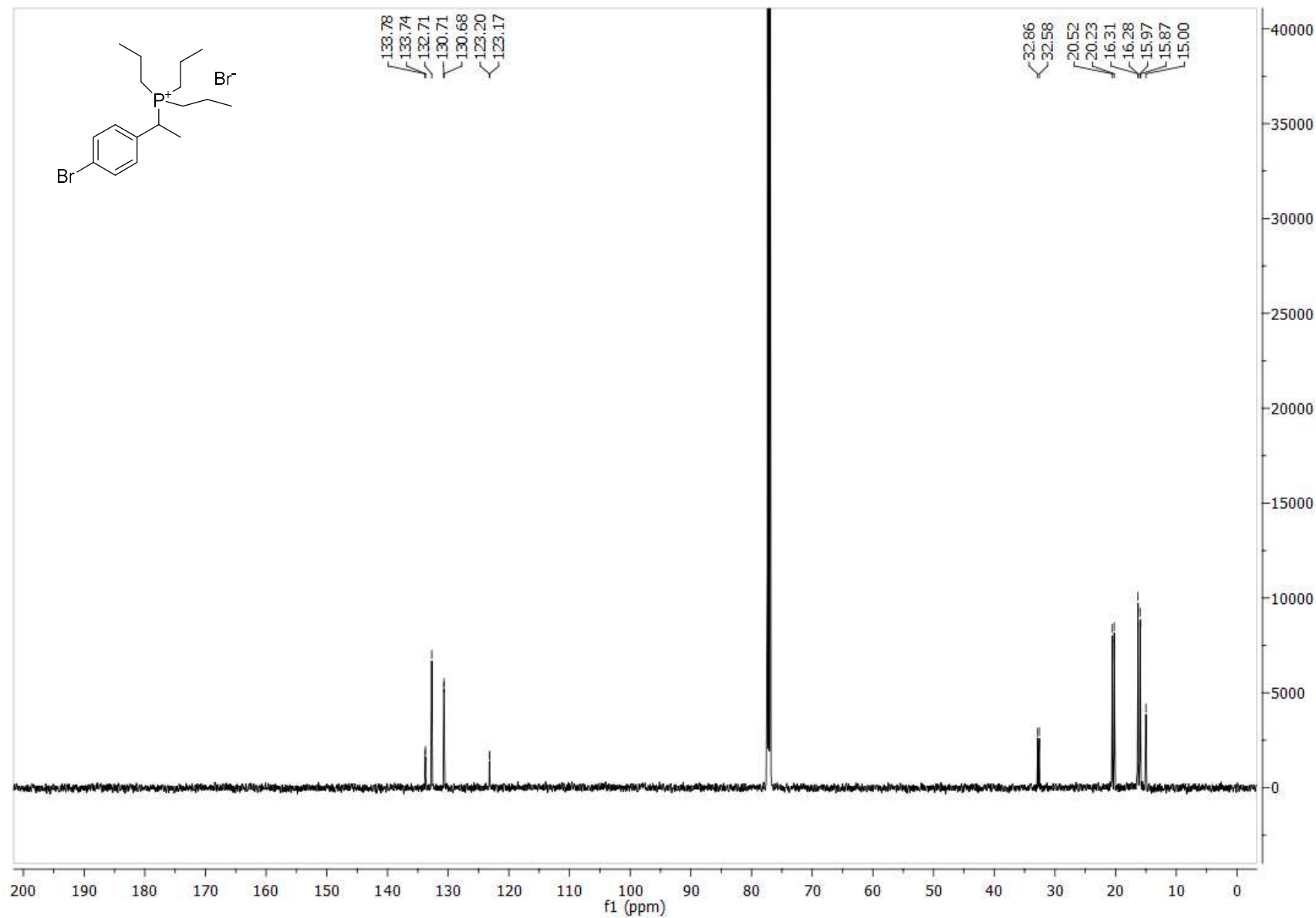
9d ¹H NMR
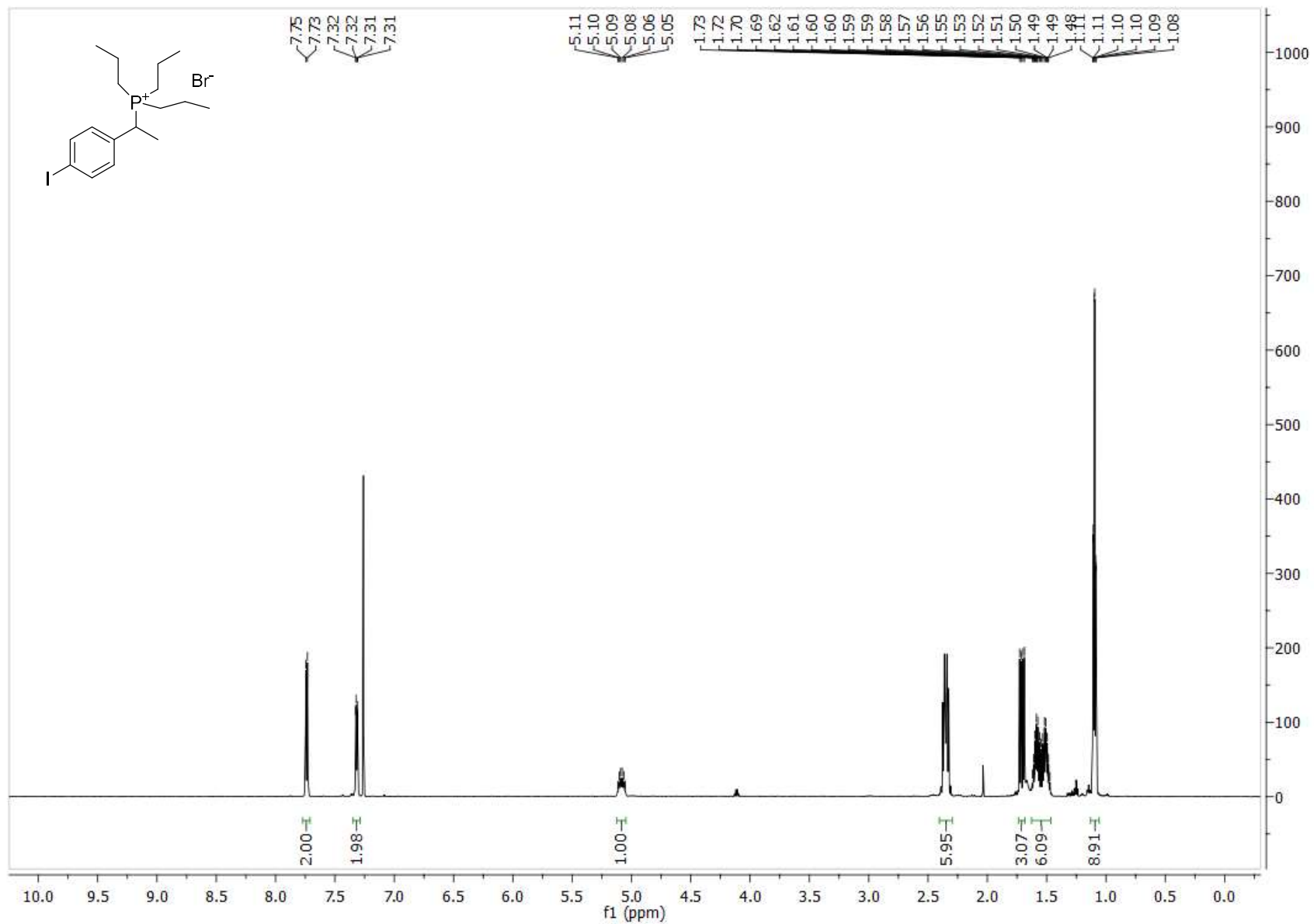
9d ^{13}C NMR
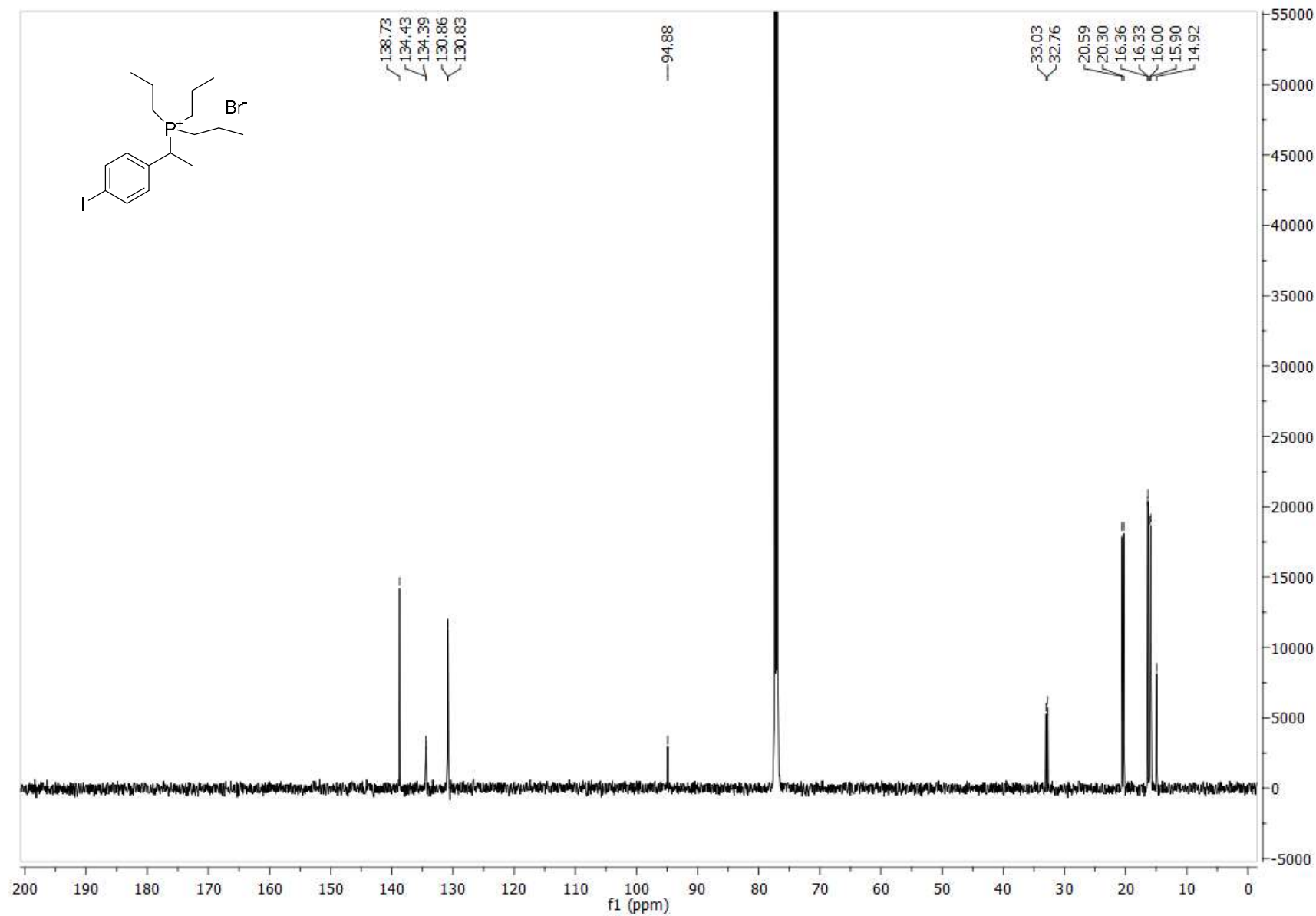
9e ¹H NMR
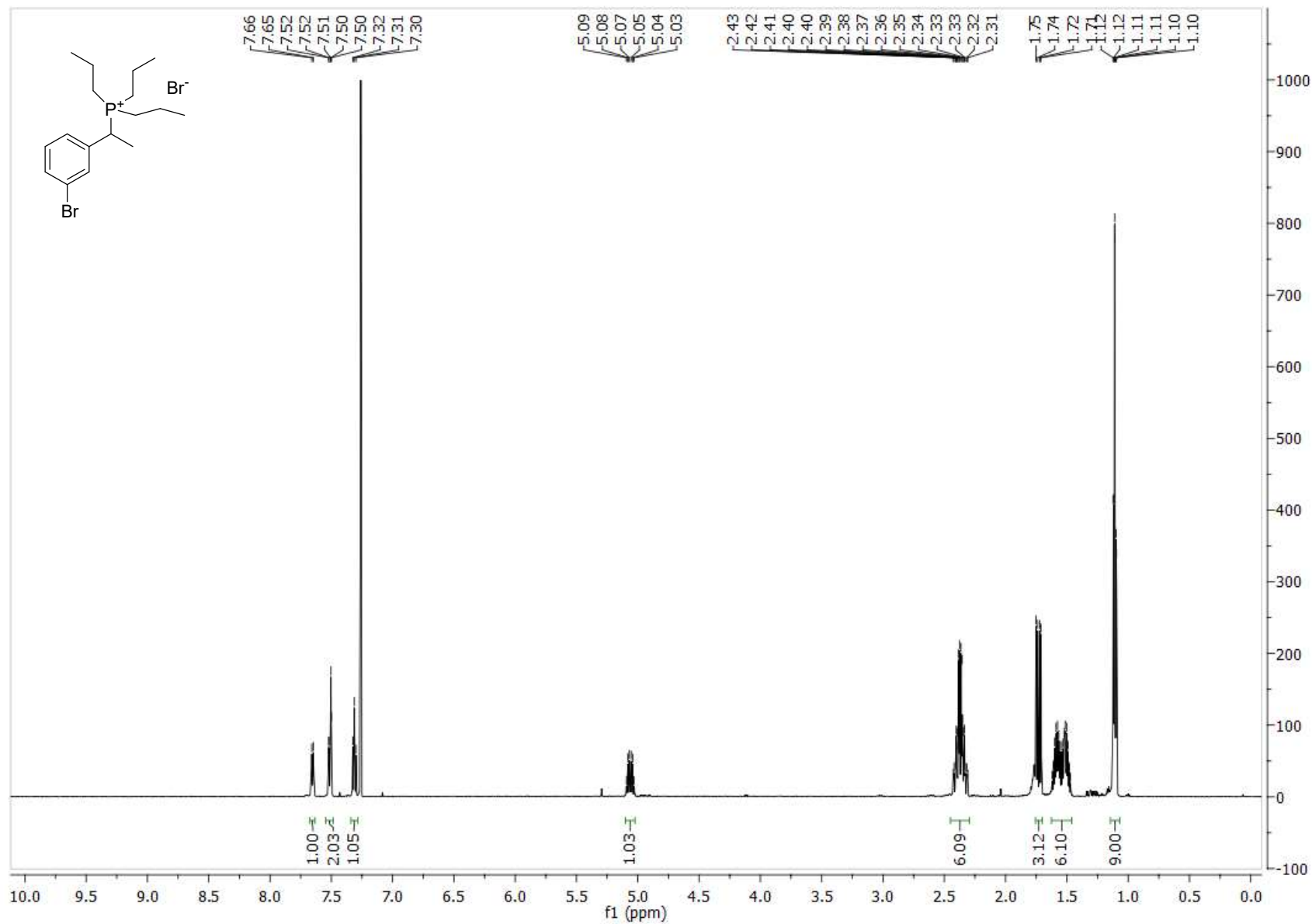
9e ¹³C NMR
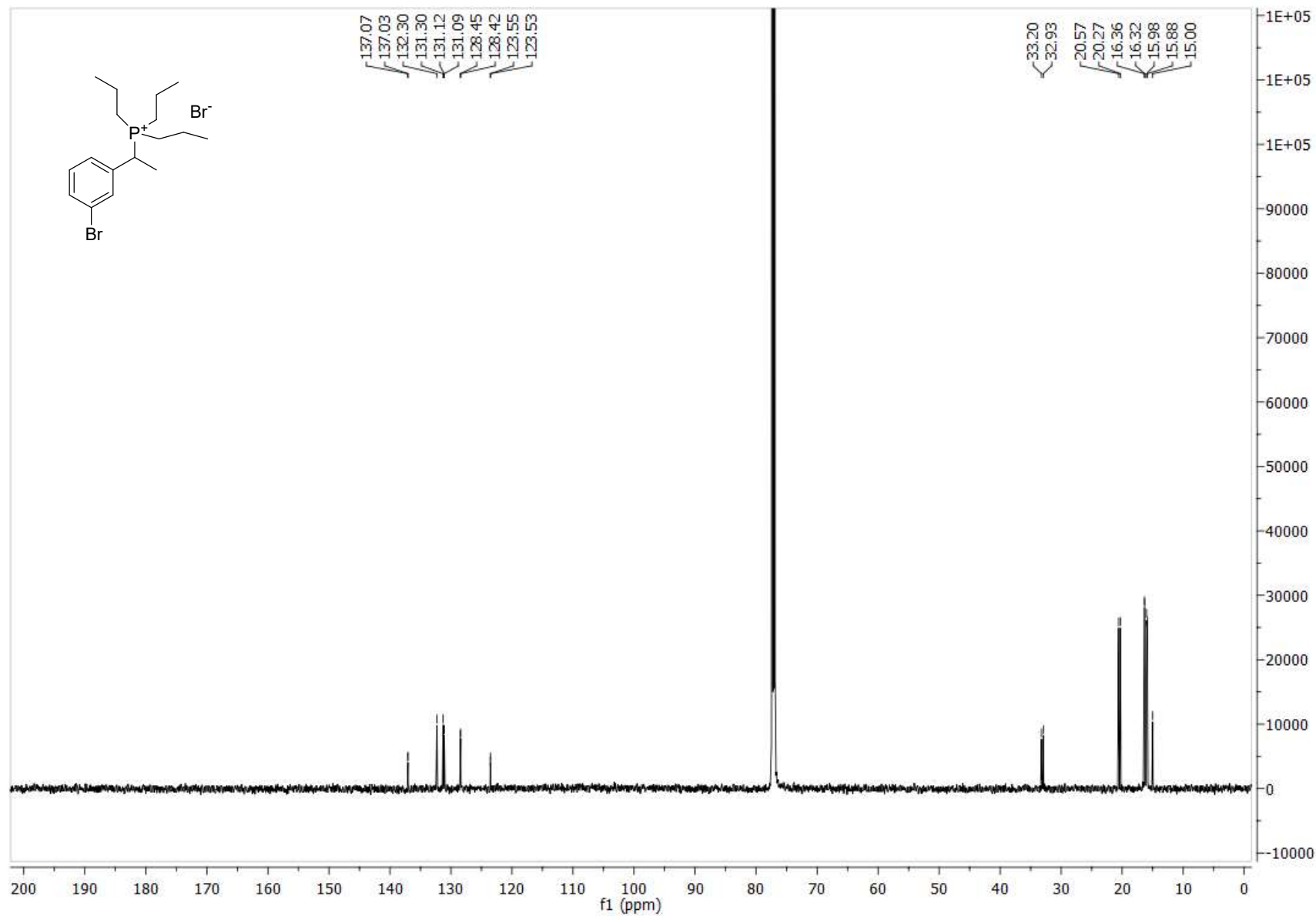
7a (*E*) ¹H NMR
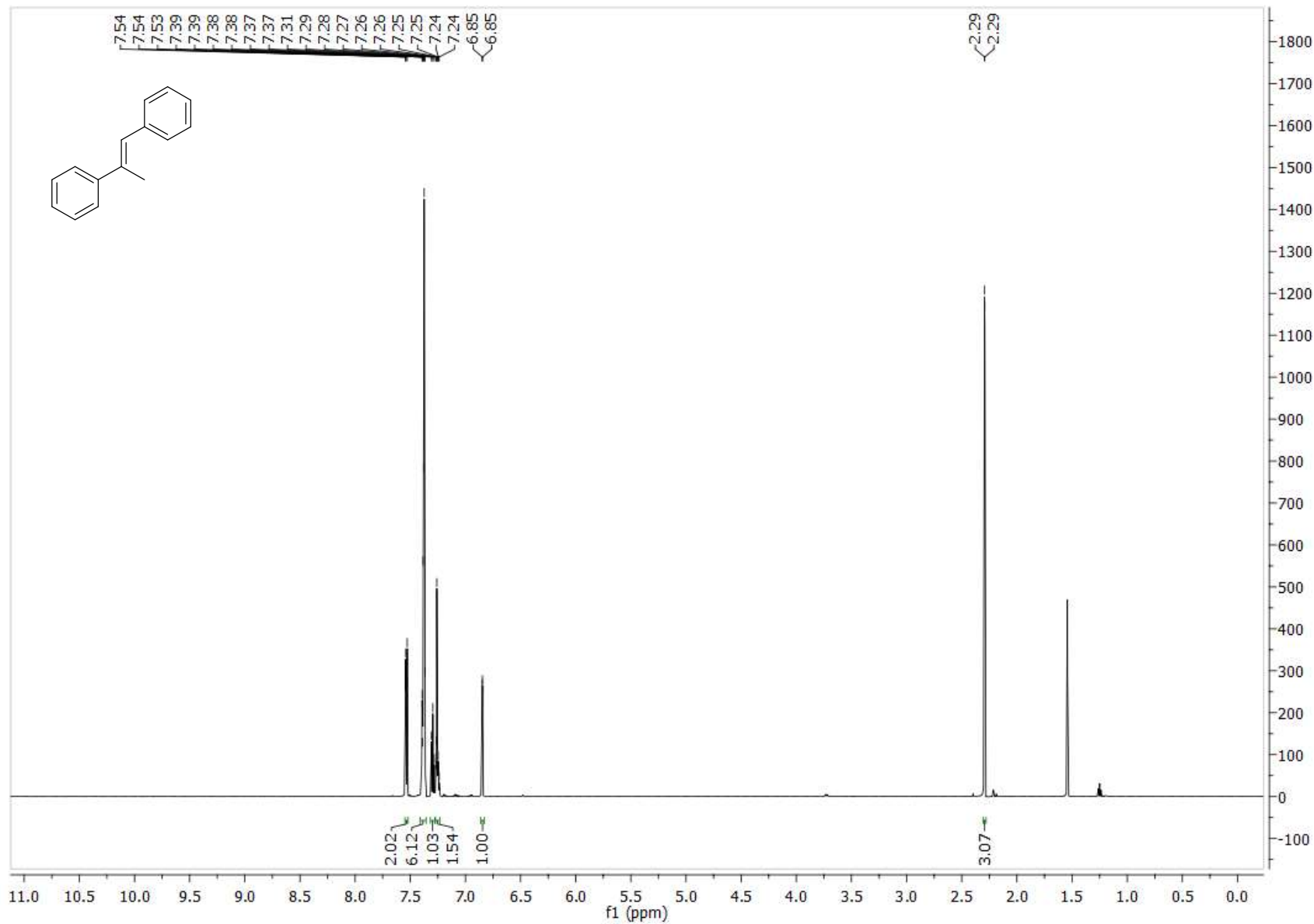
7a (*E*) ¹³C NMR
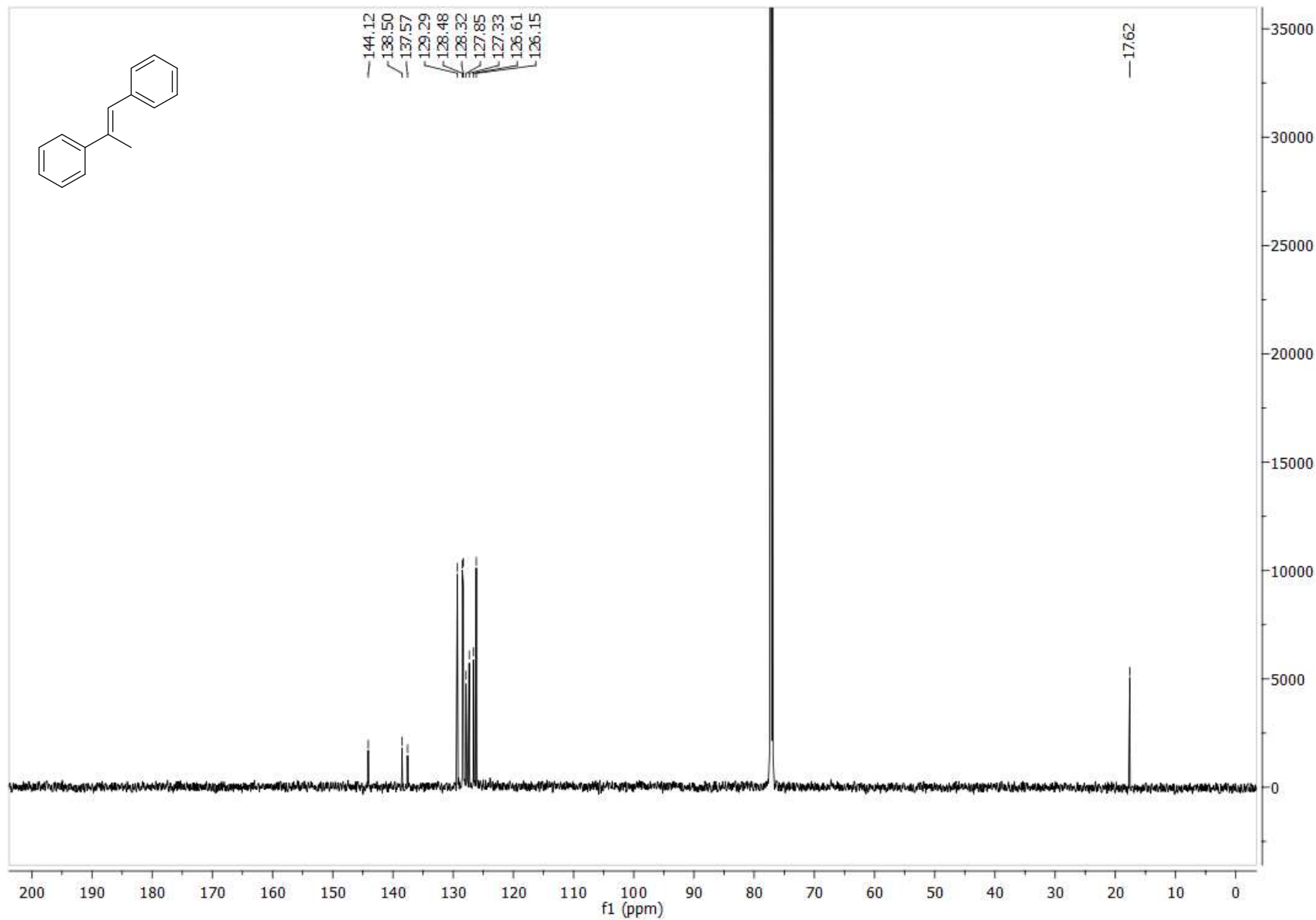
7b (*E*) ¹H NMR
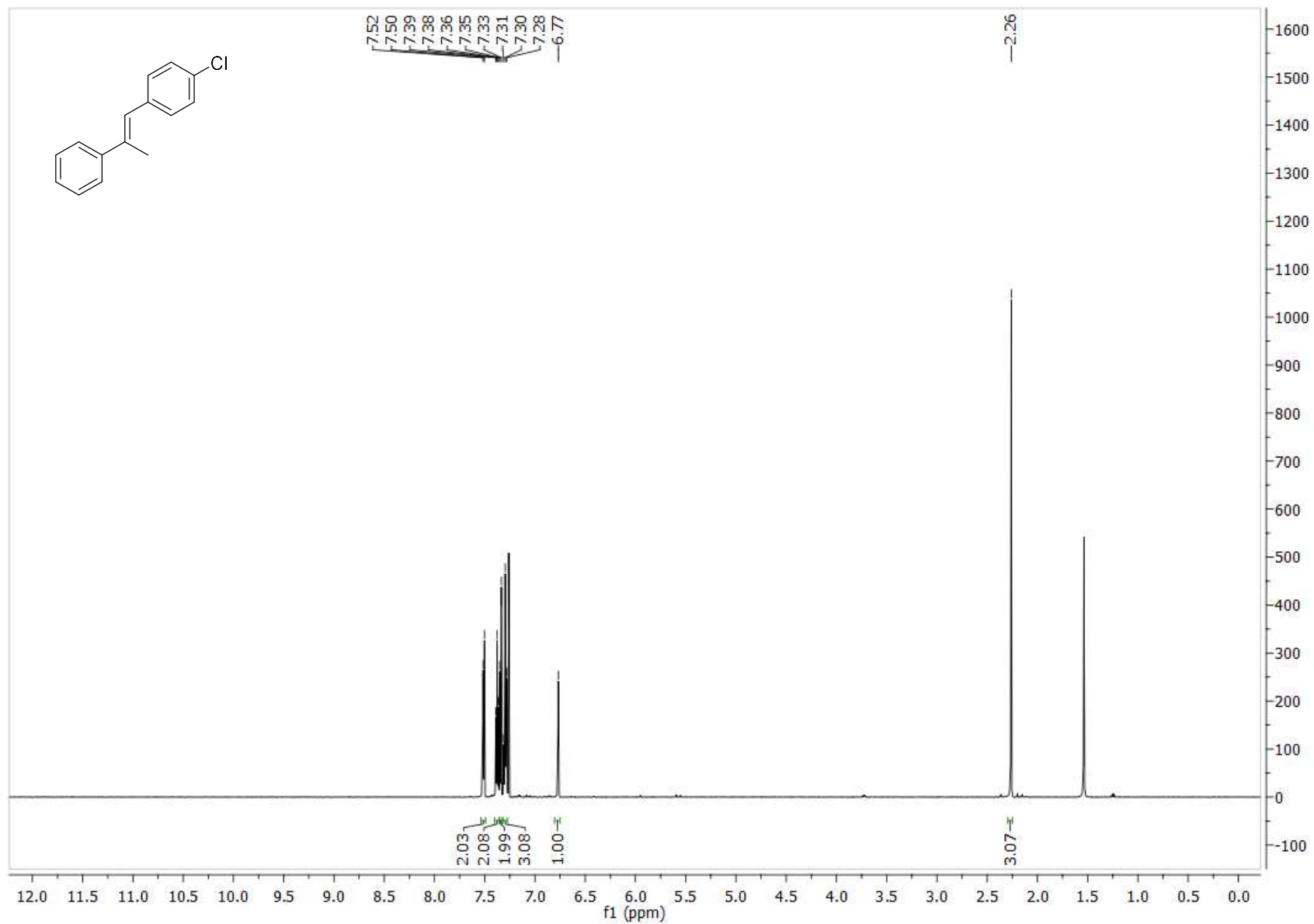
7b (*E*) ¹³C NMR
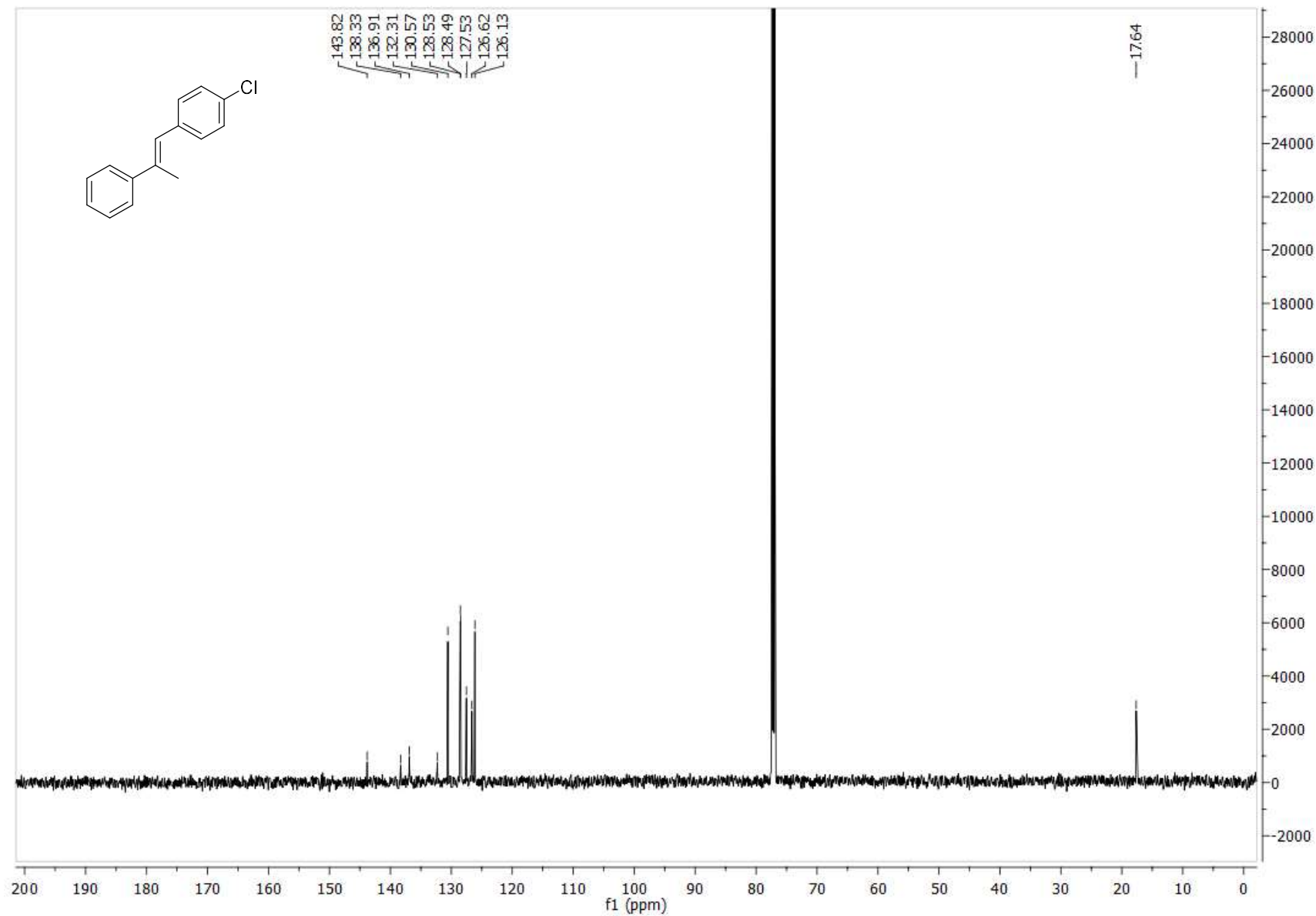
7c (*E*) ¹H NMR
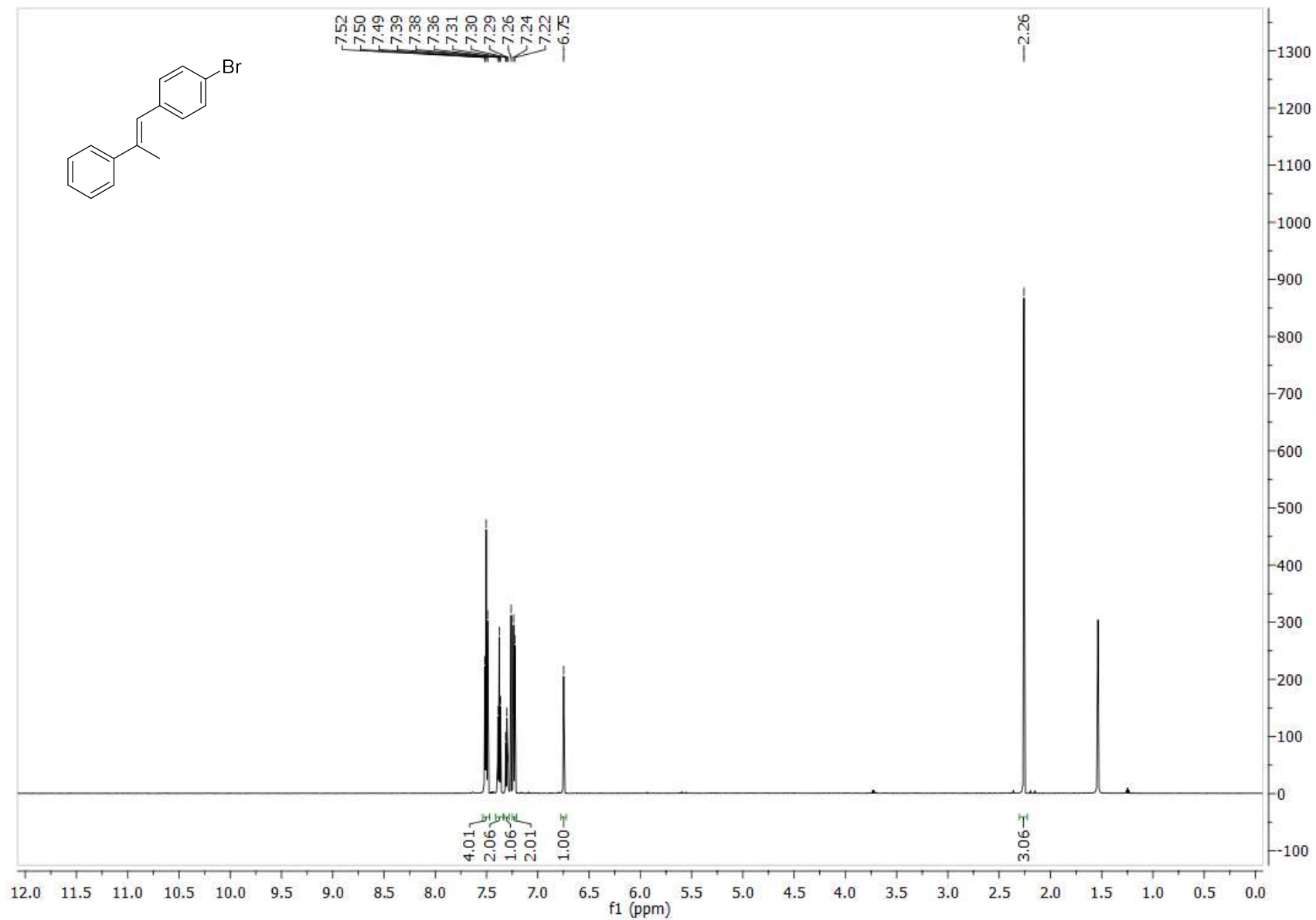
7c (*E*) ¹³C NMR
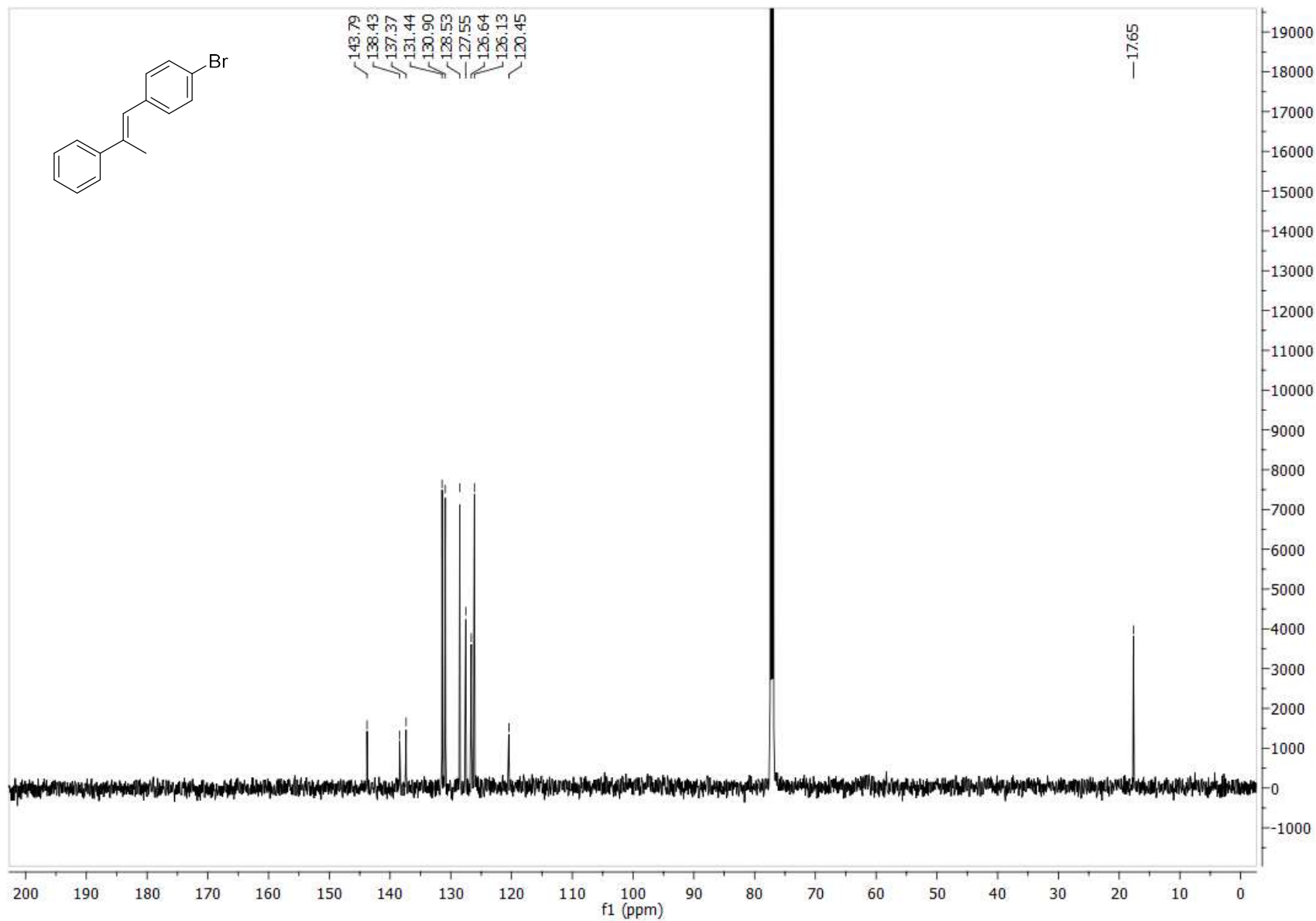
7d (*E*) ^{1}H NMR
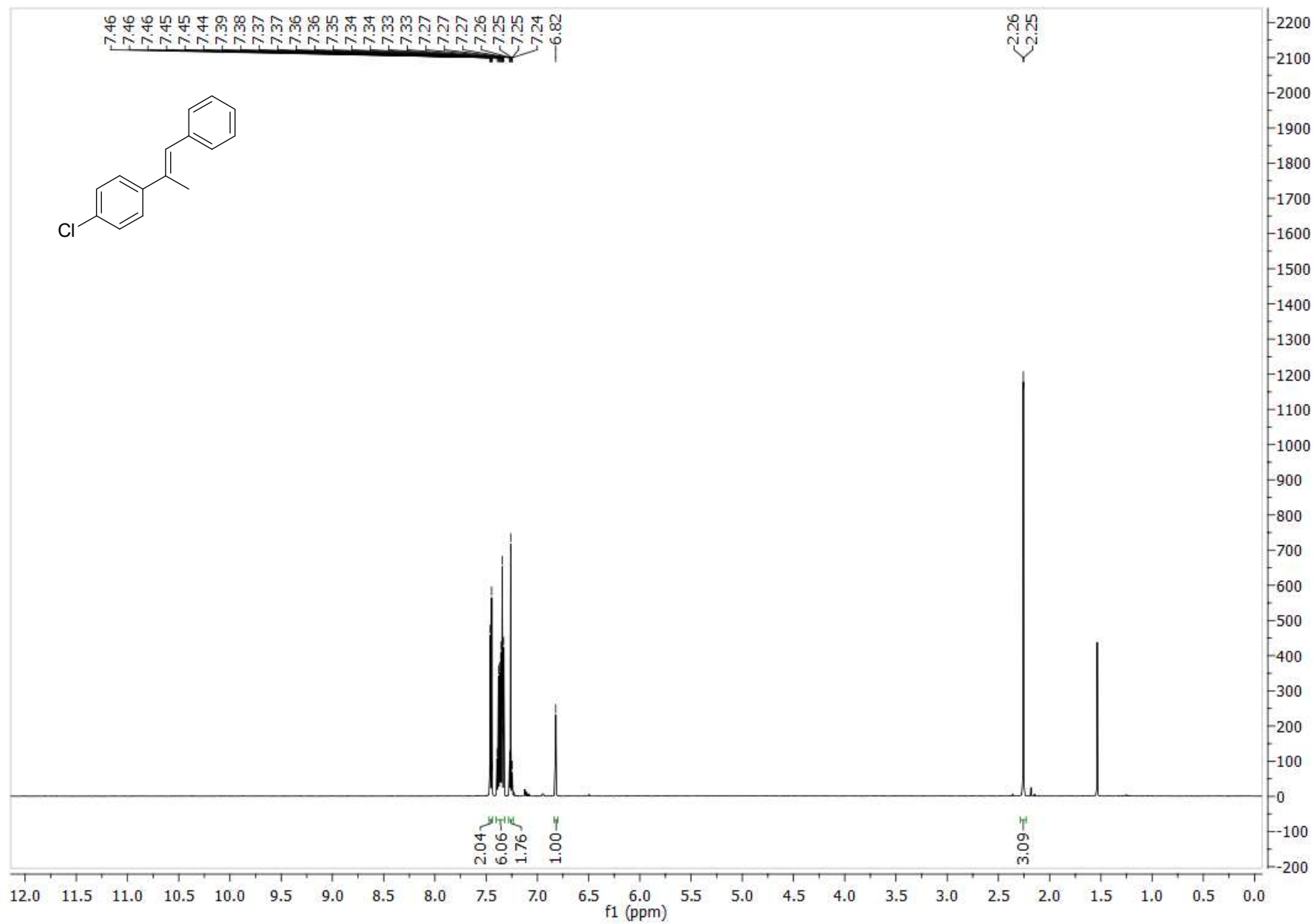
7d (*E*) ¹³C NMR
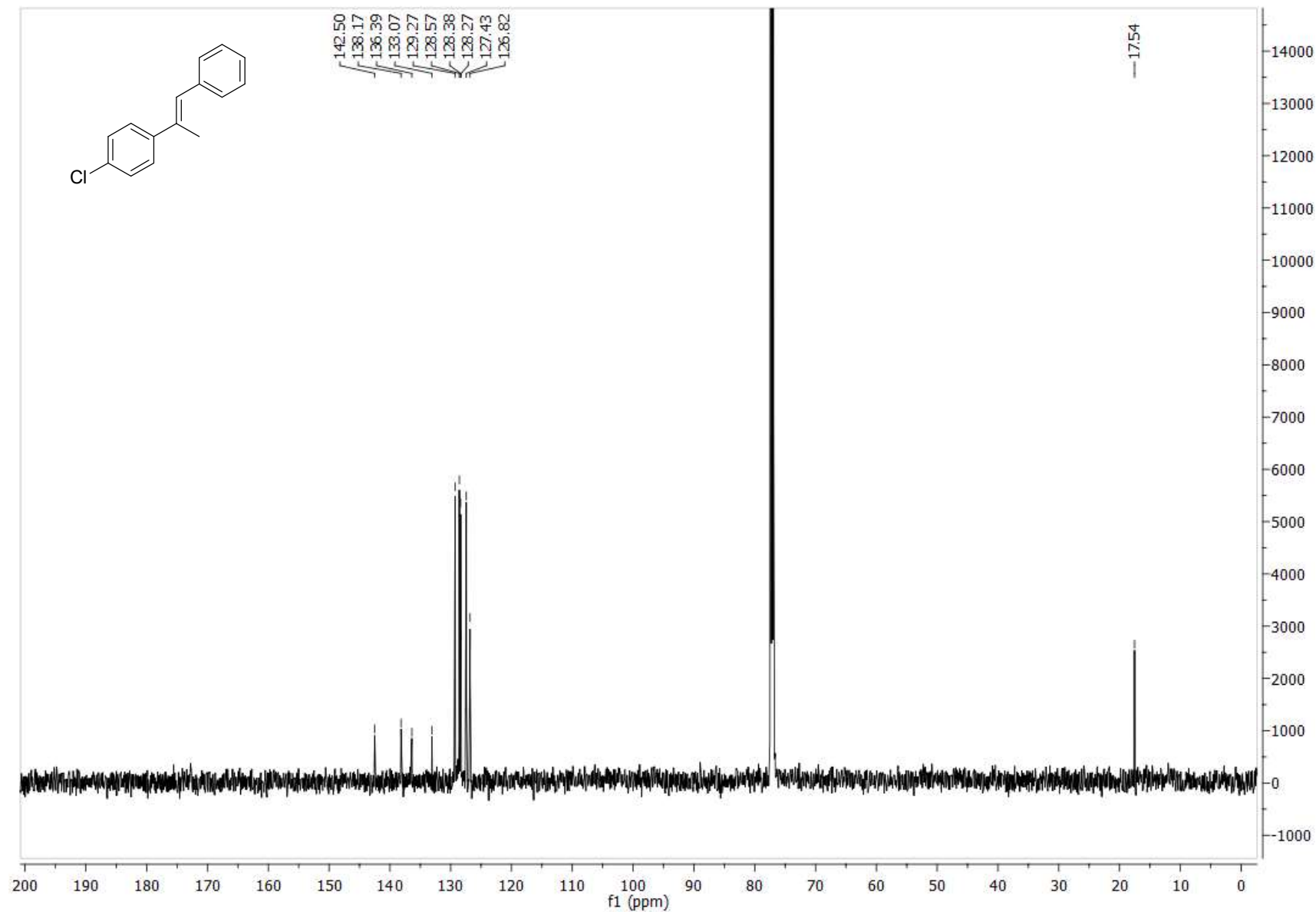
7e (*E*) ¹H NMR
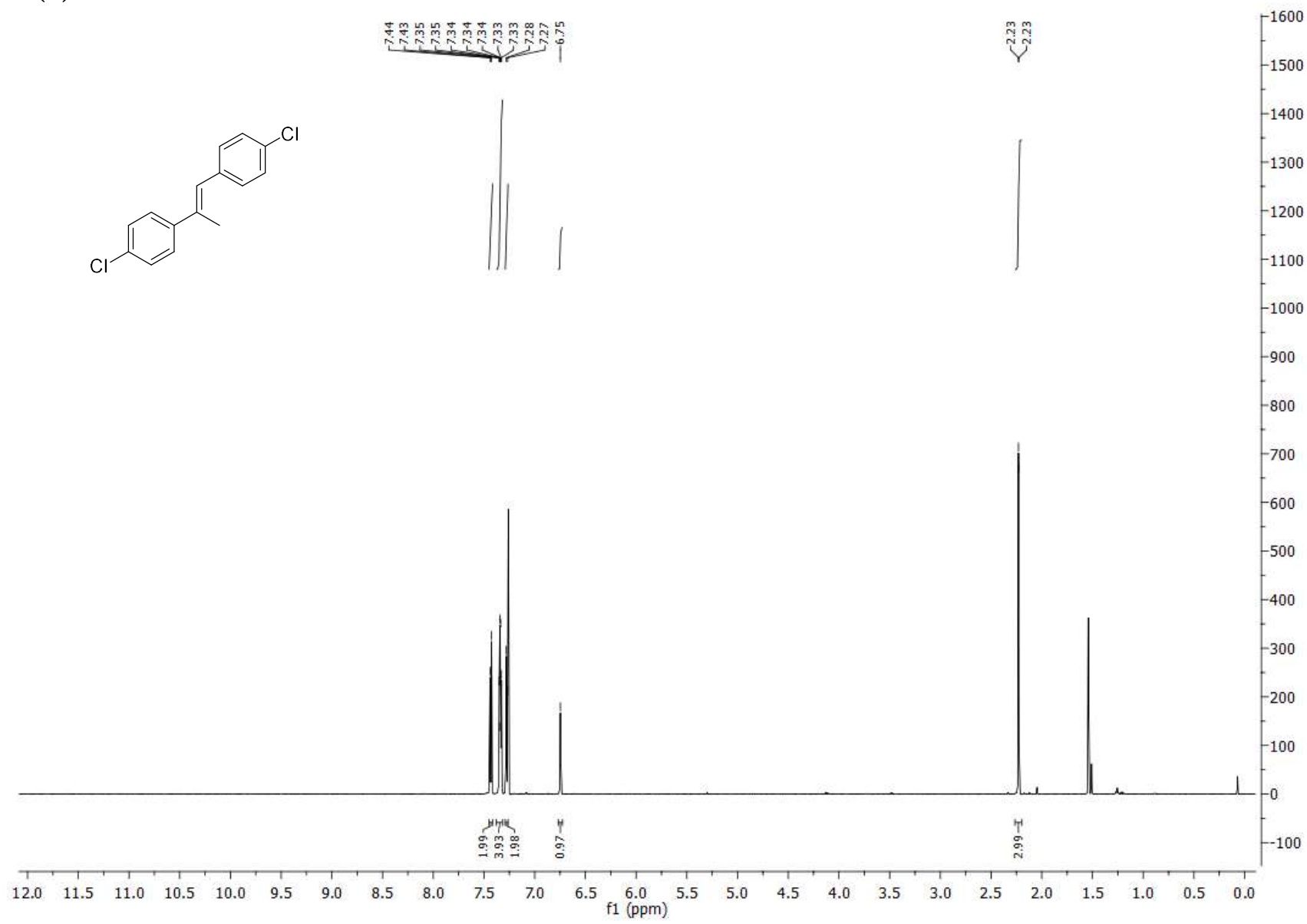
7e (*E*) ^{13}C NMR
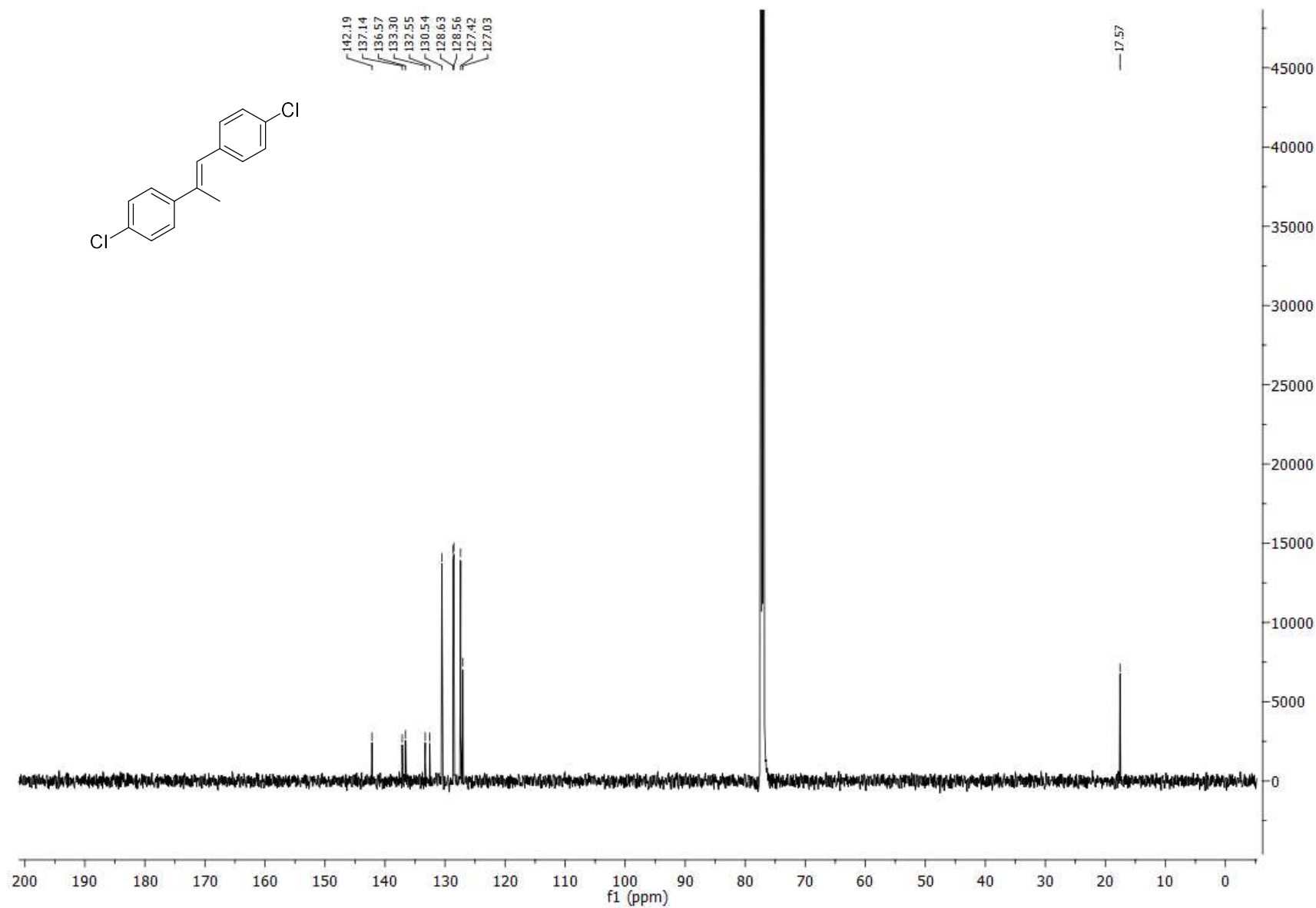
7f (*E*) ¹H NMR
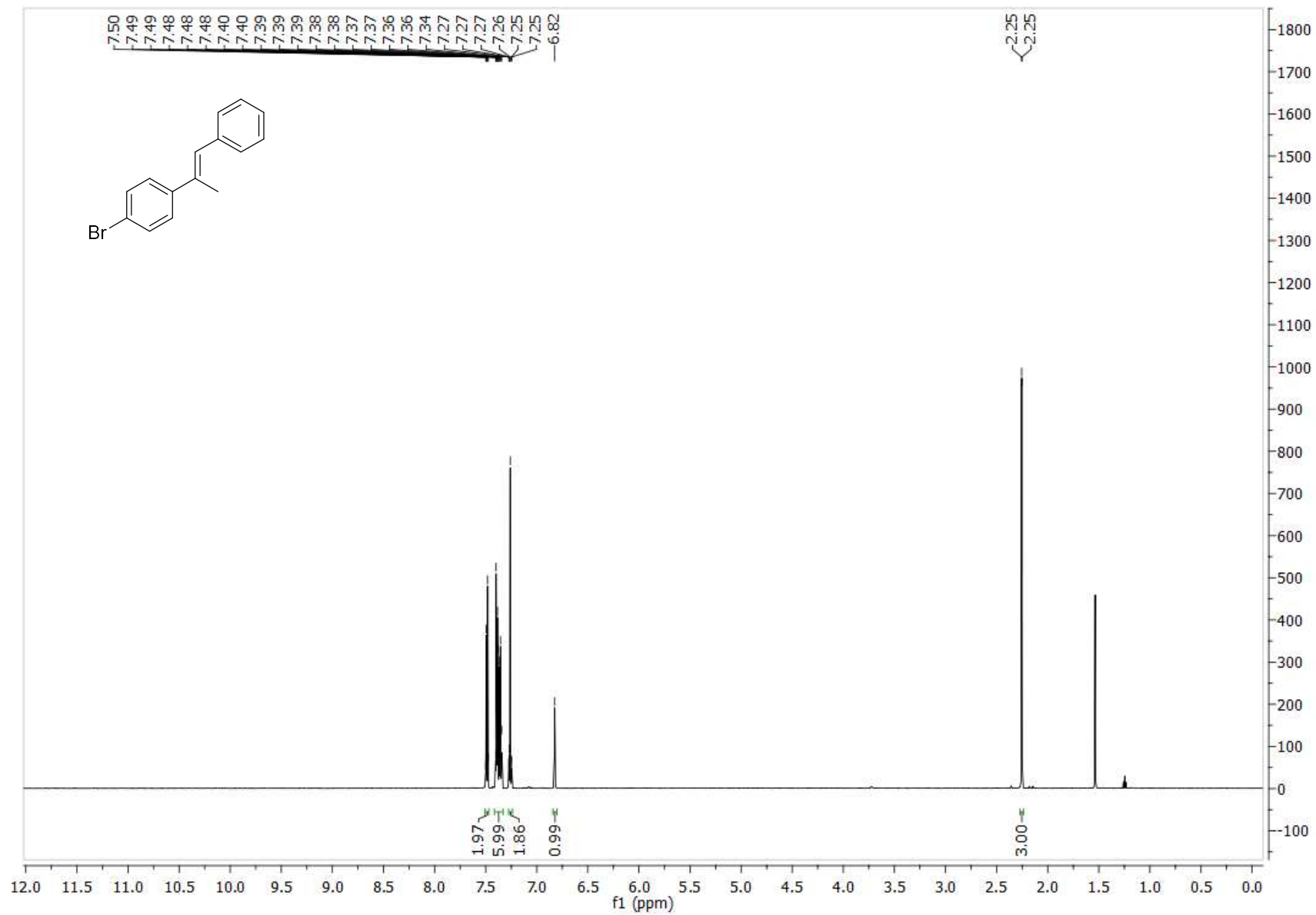
7f (*E*) ¹³C NMR
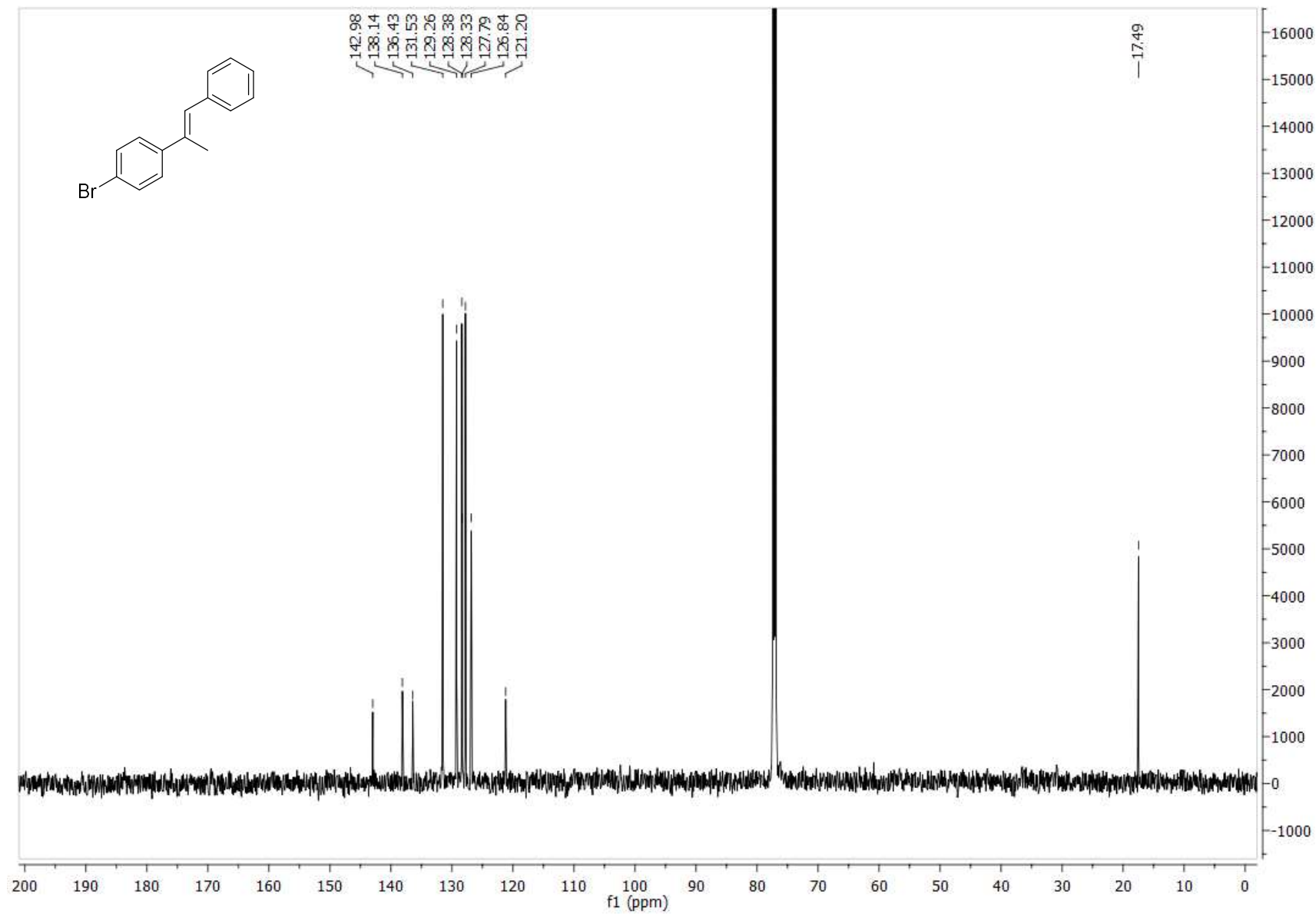
7g (*E*) ¹H NMR
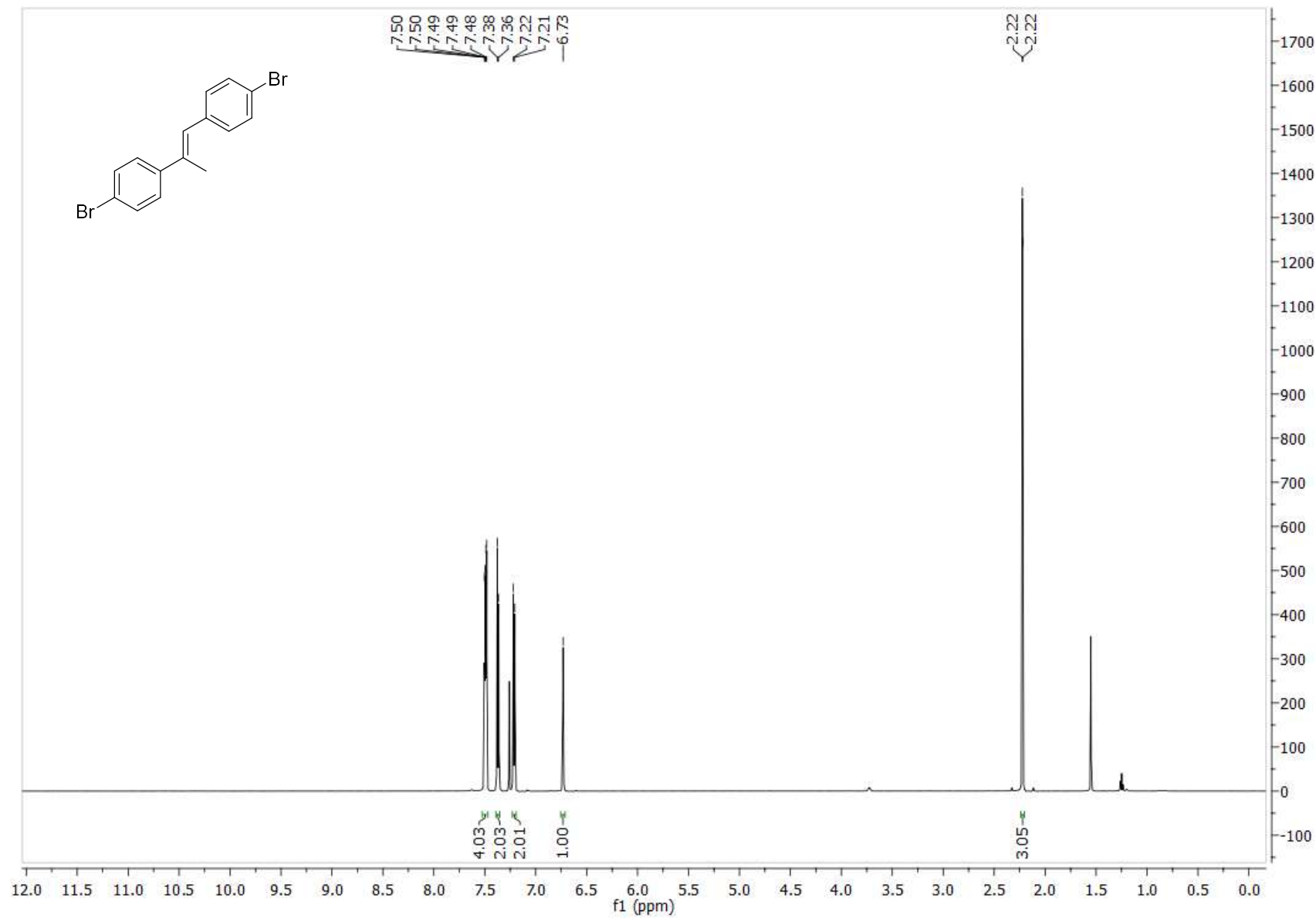
7g (*E*) ¹³C NMR
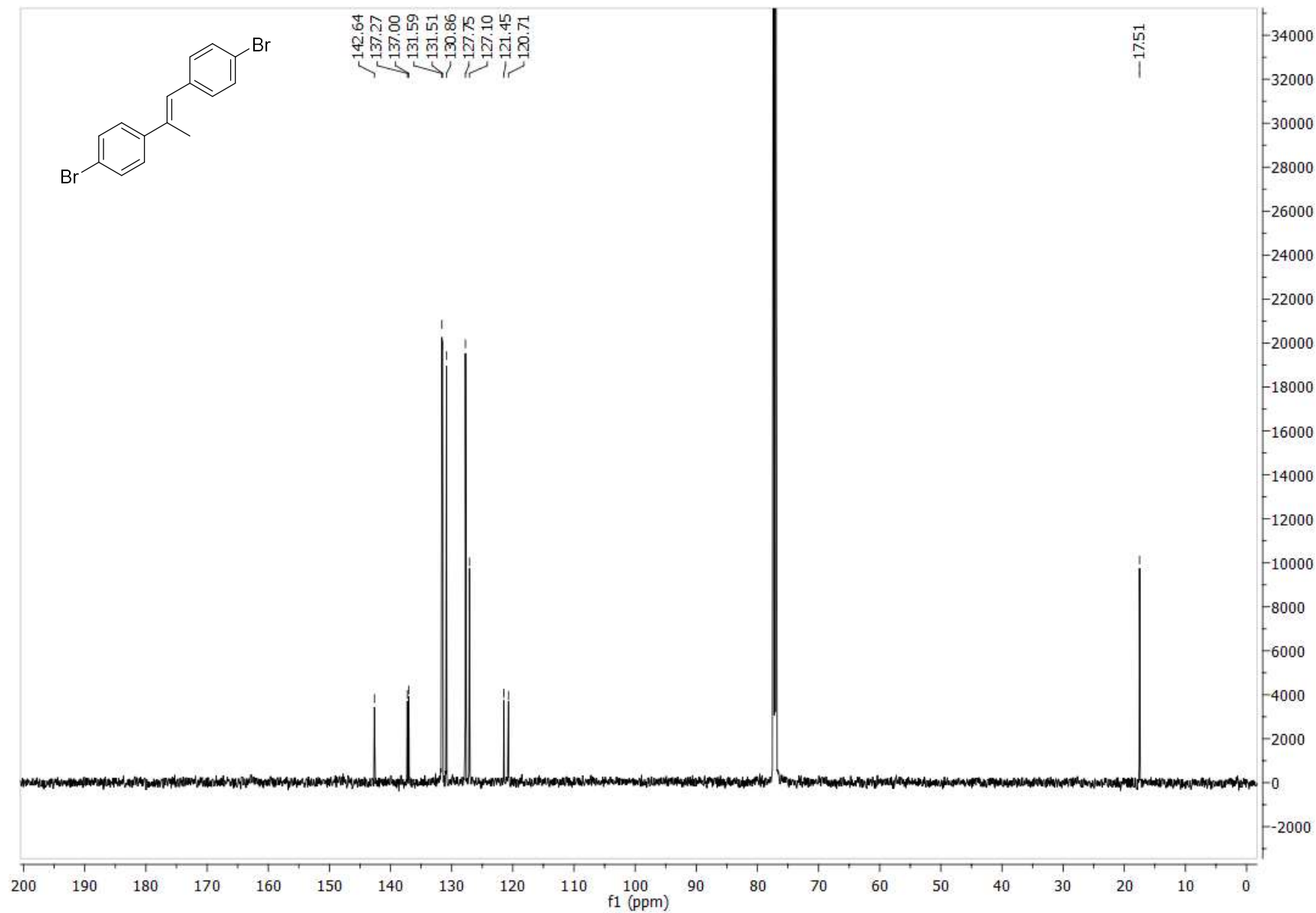
7h (*E*) ¹H NMR
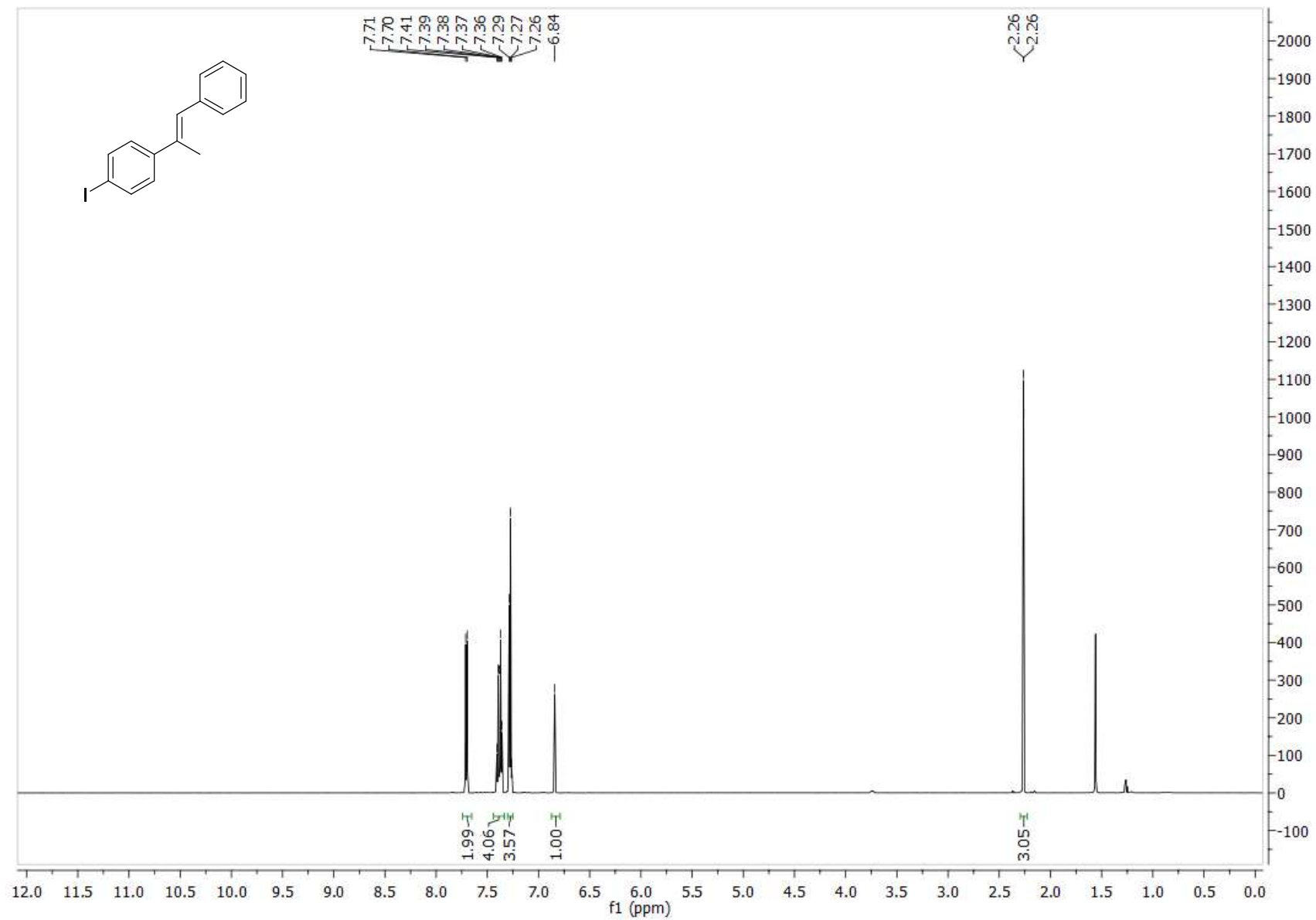
7h (*E*) ¹³C NMR
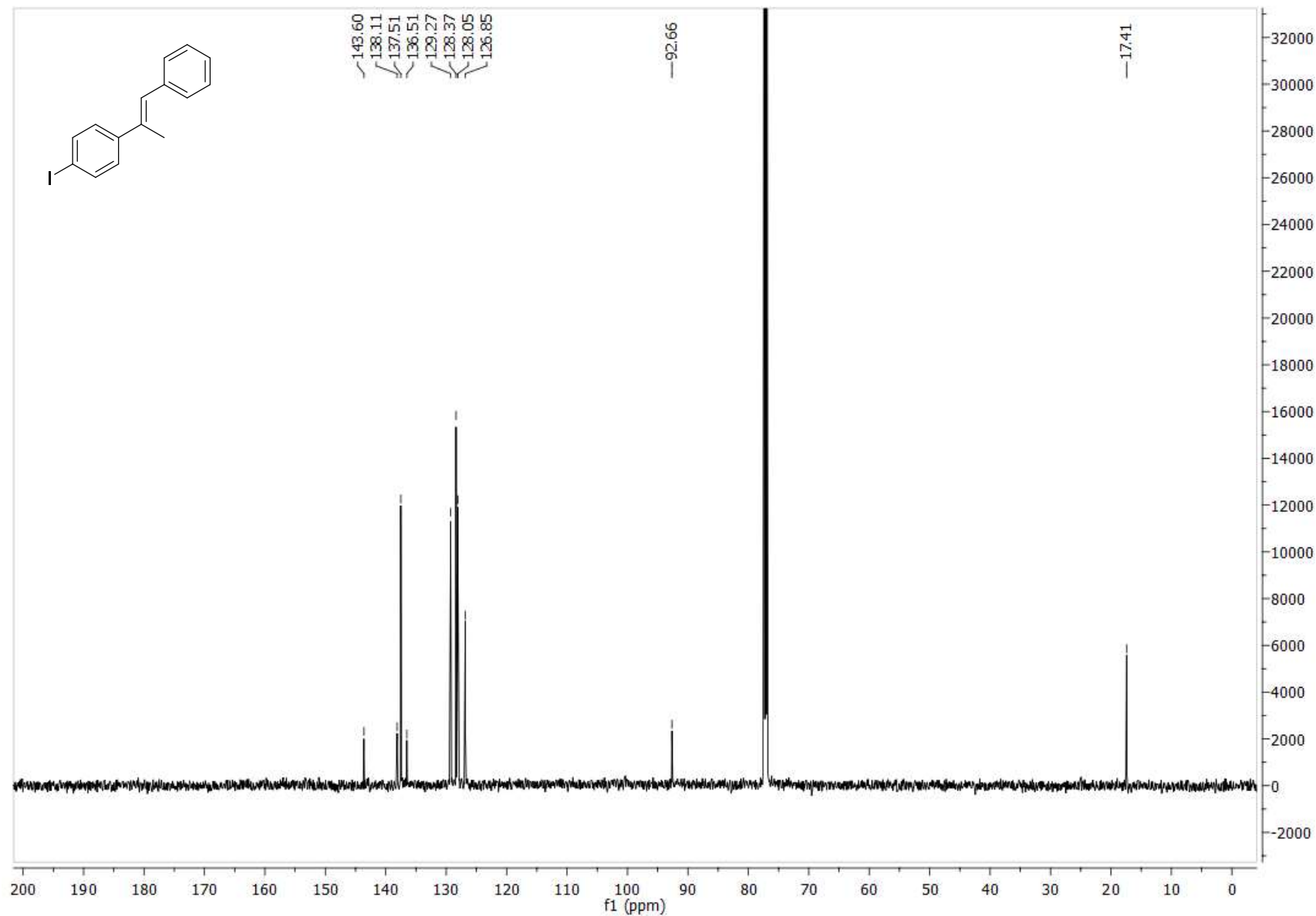
7i (*E*) ¹H NMR
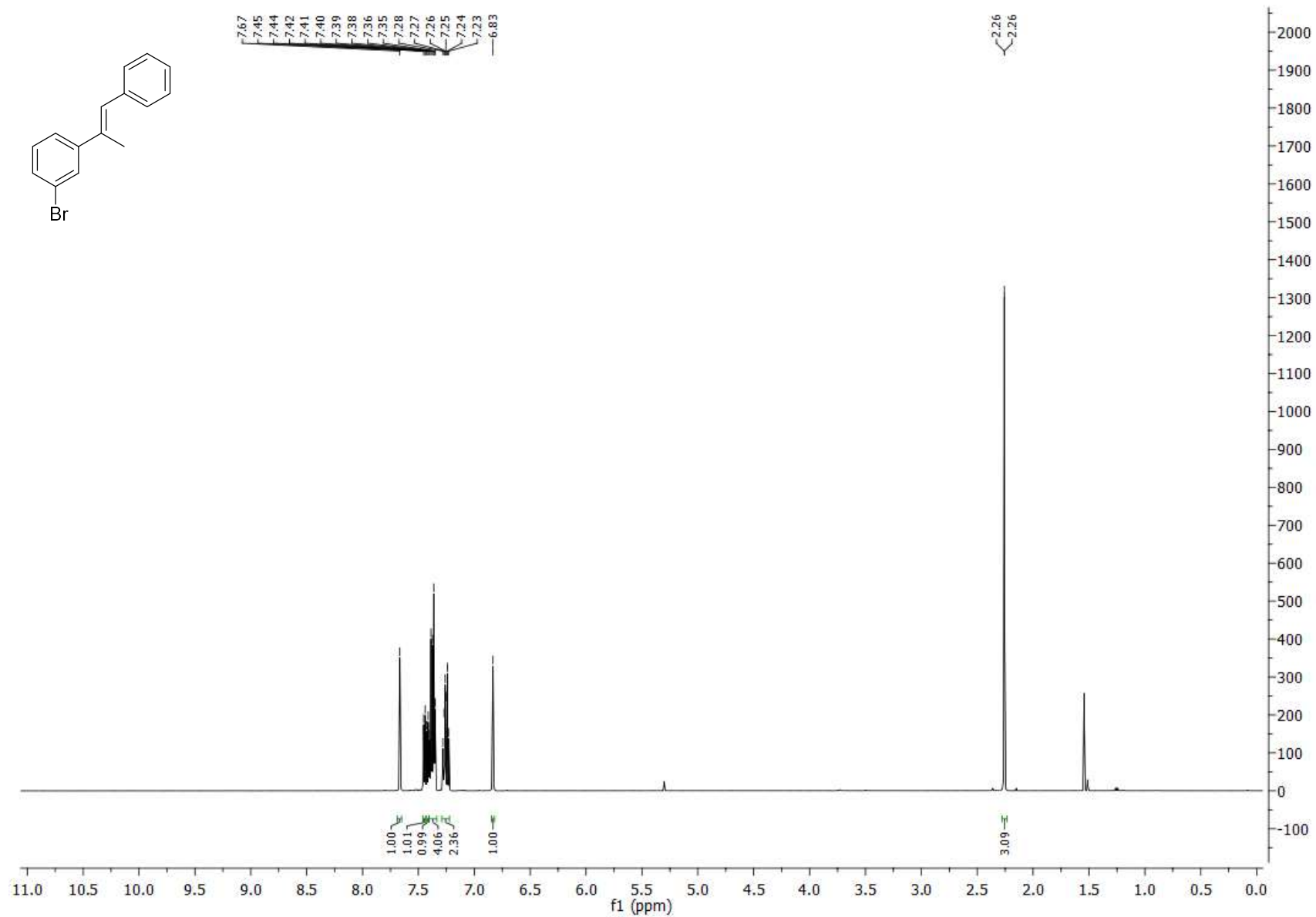
7i (*E*) ¹³C NMR
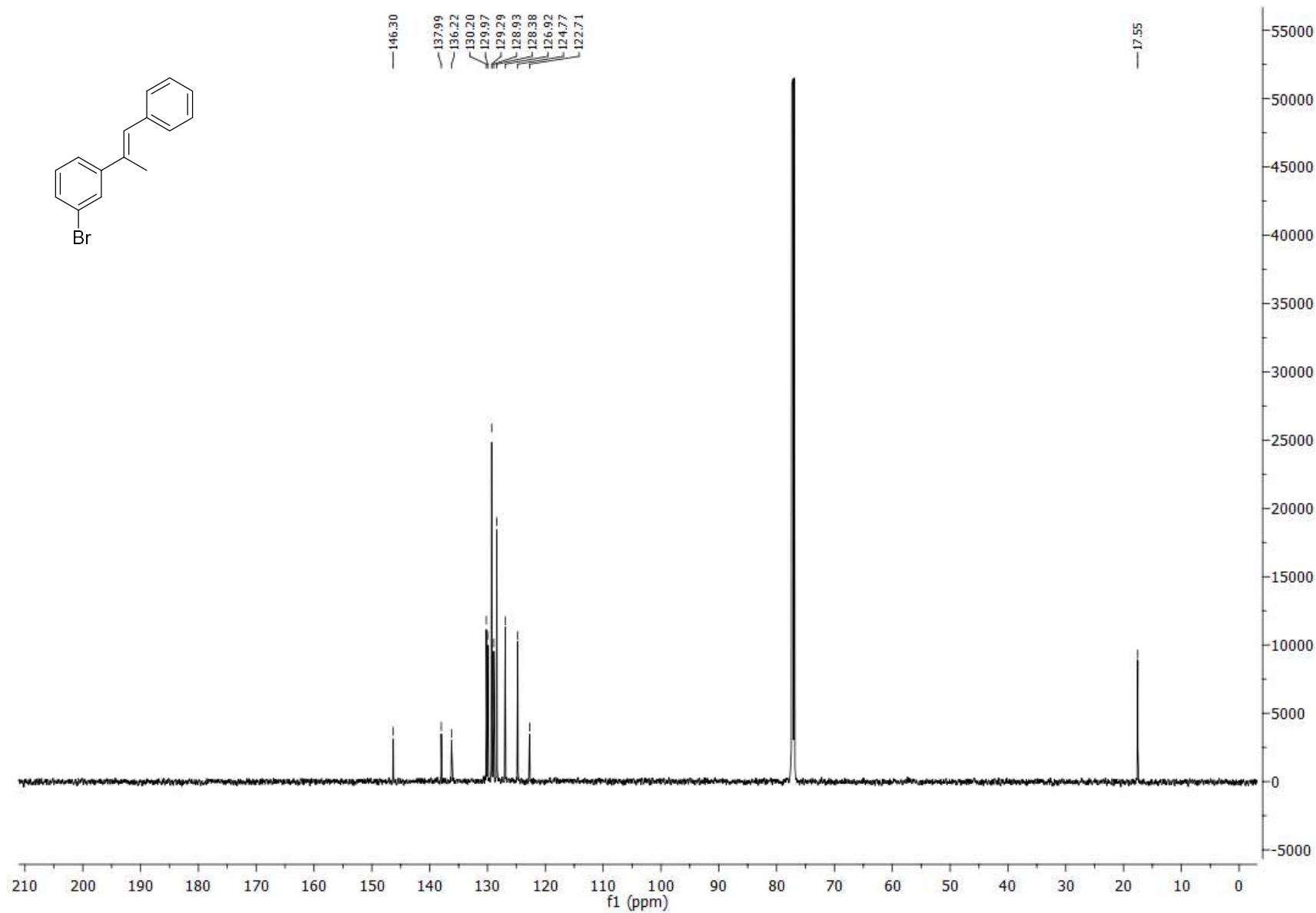
5a ¹H NMR
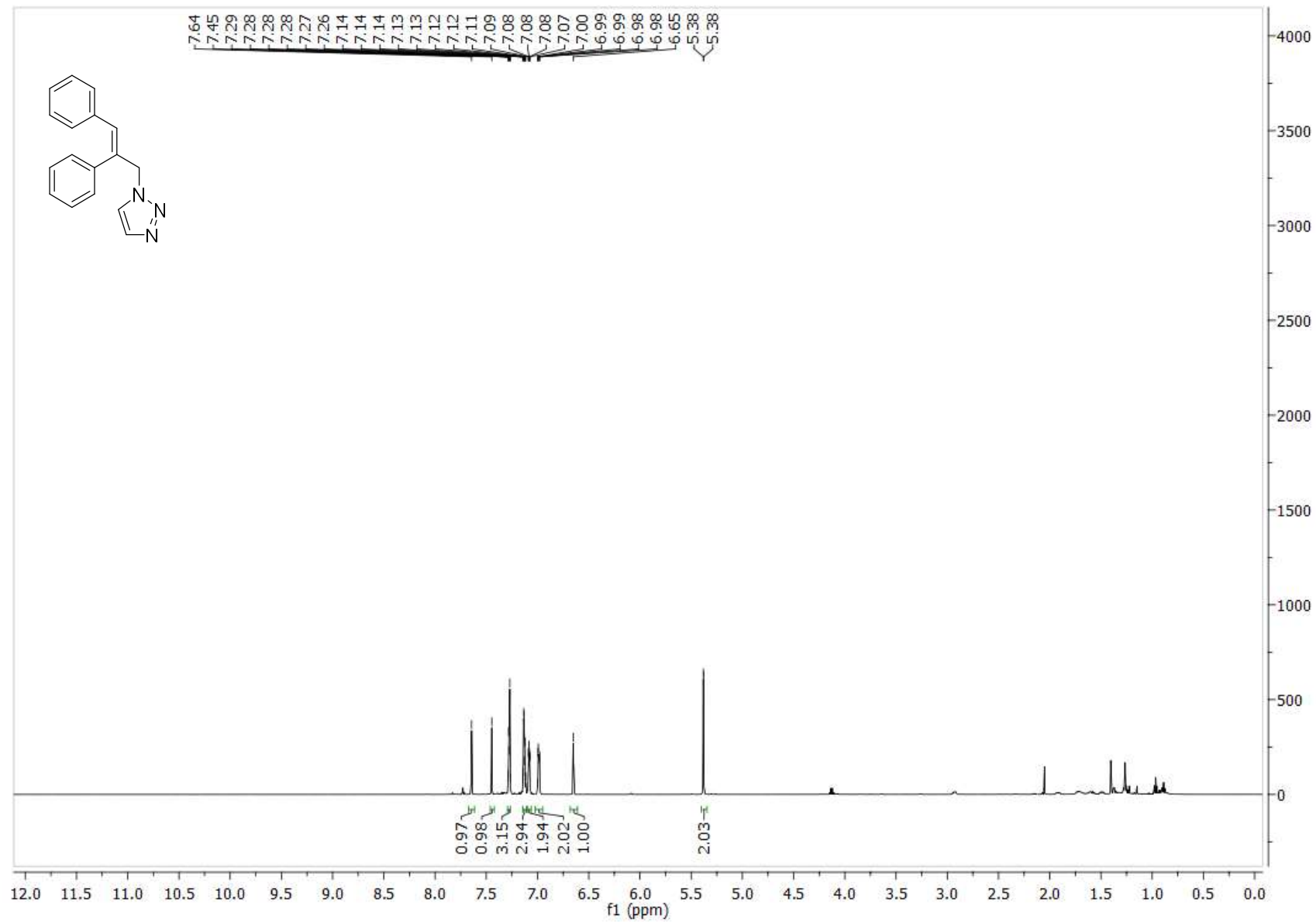
5a ^{13}C NMR
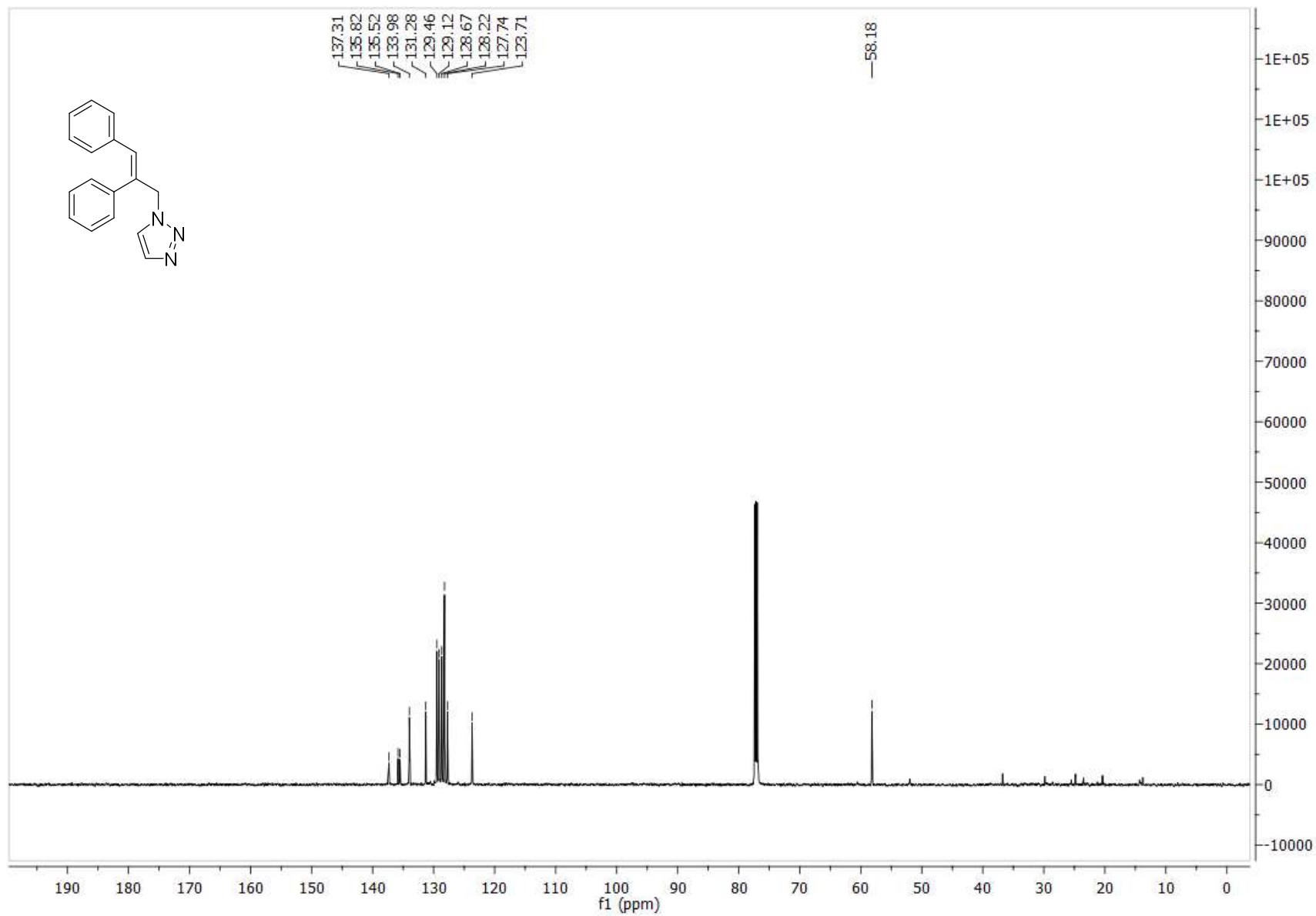
6a ¹H NMR
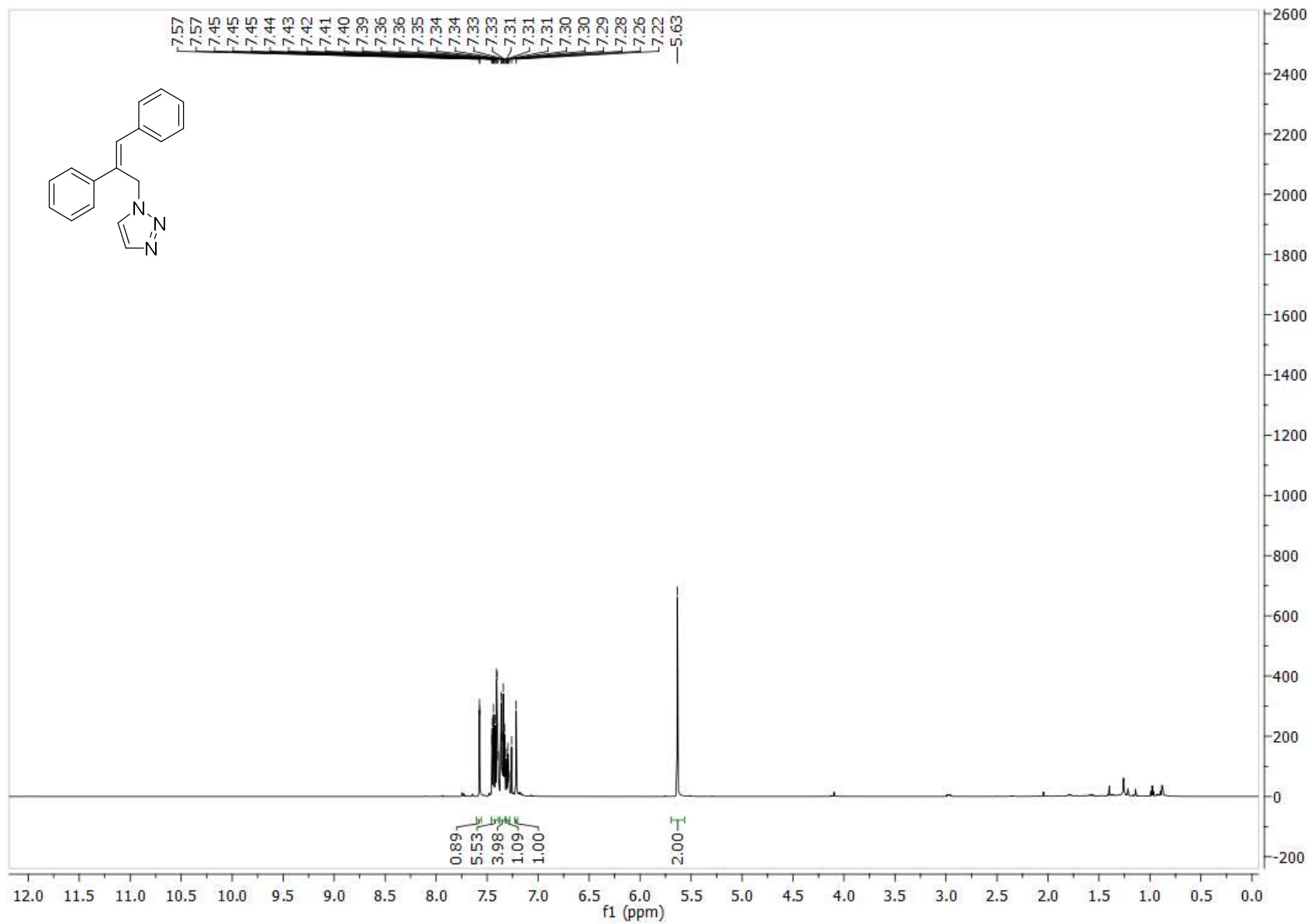
6a ^{13}C NMR
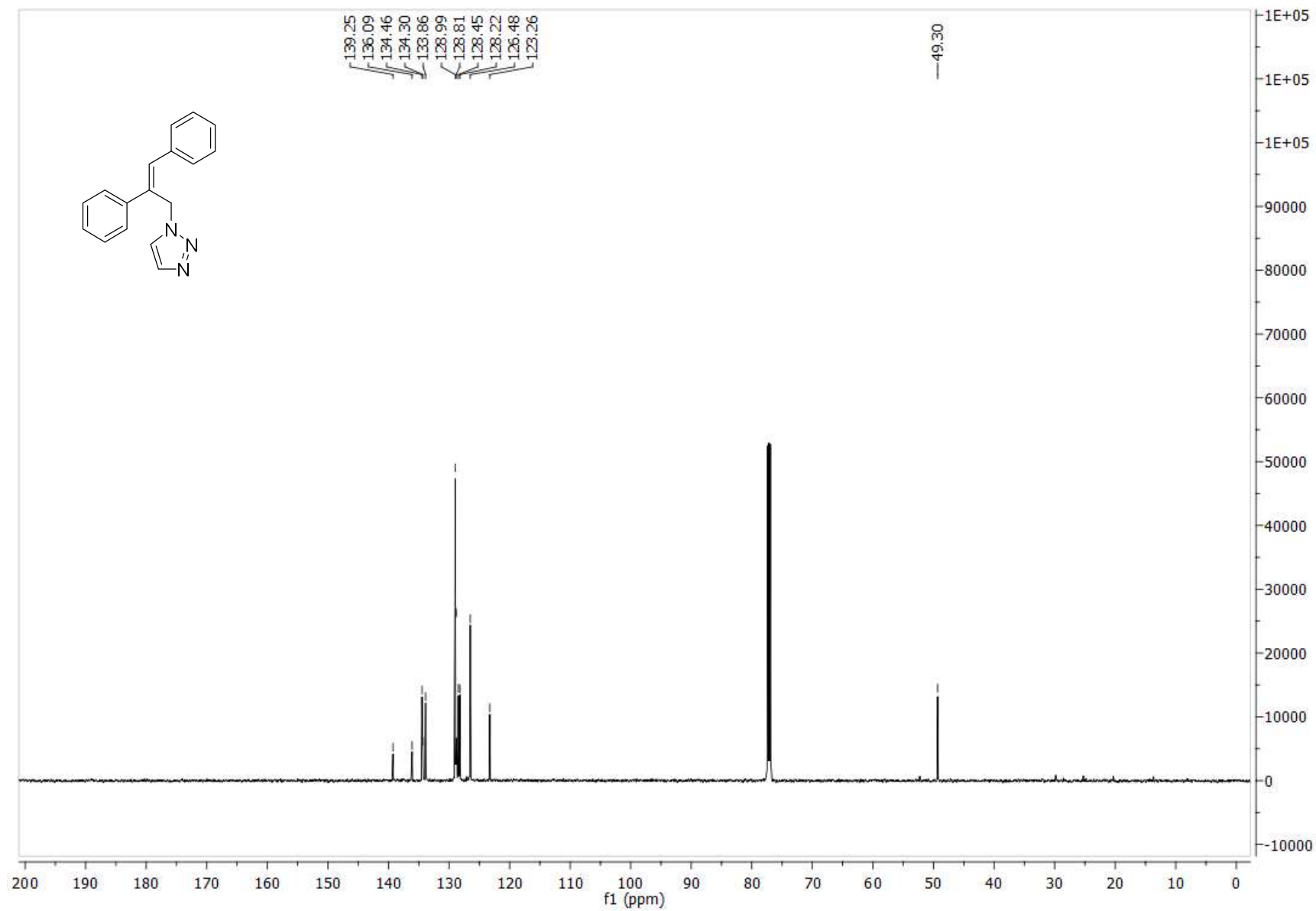
5b ¹H NMR
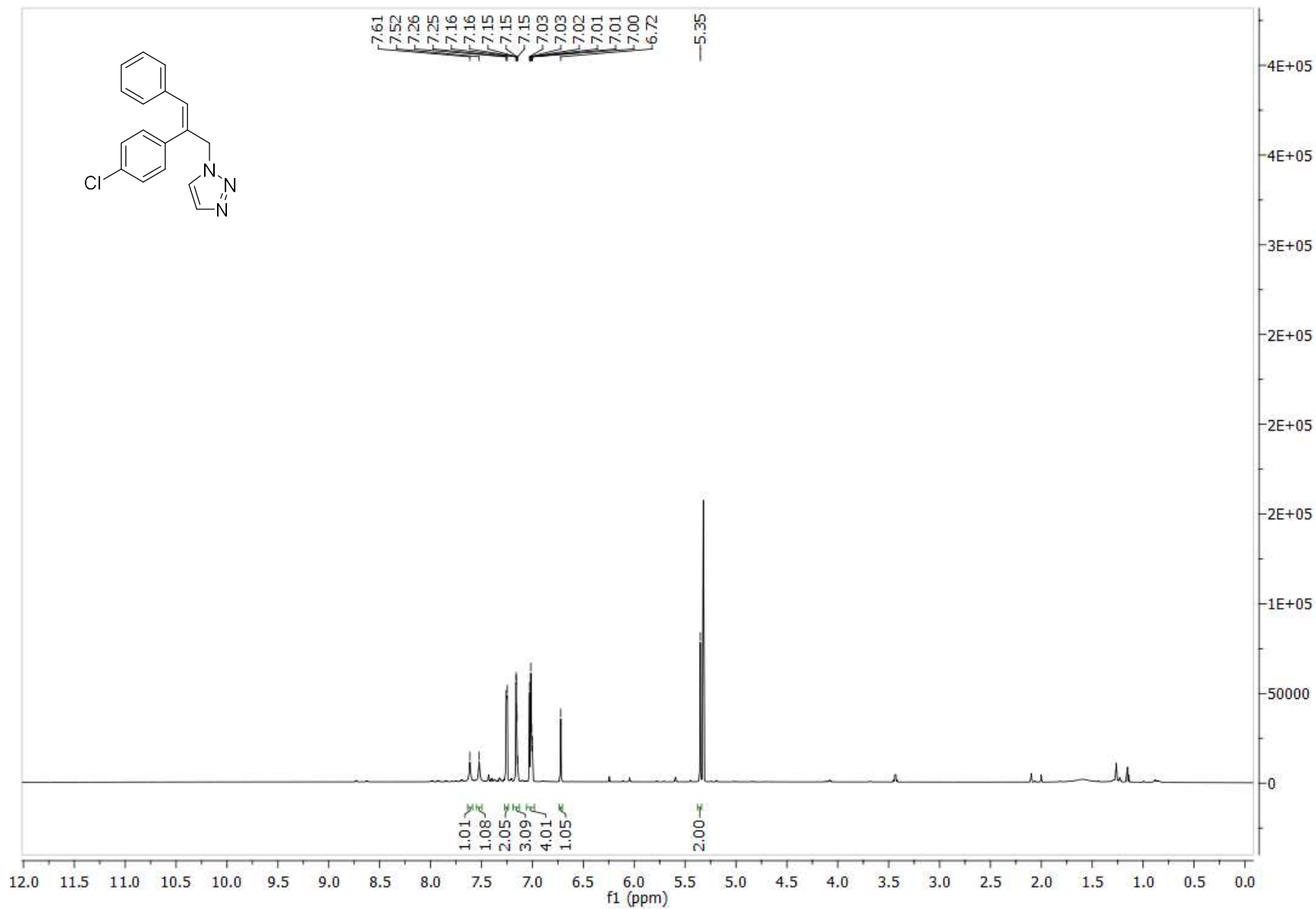
5b ¹³C NMR
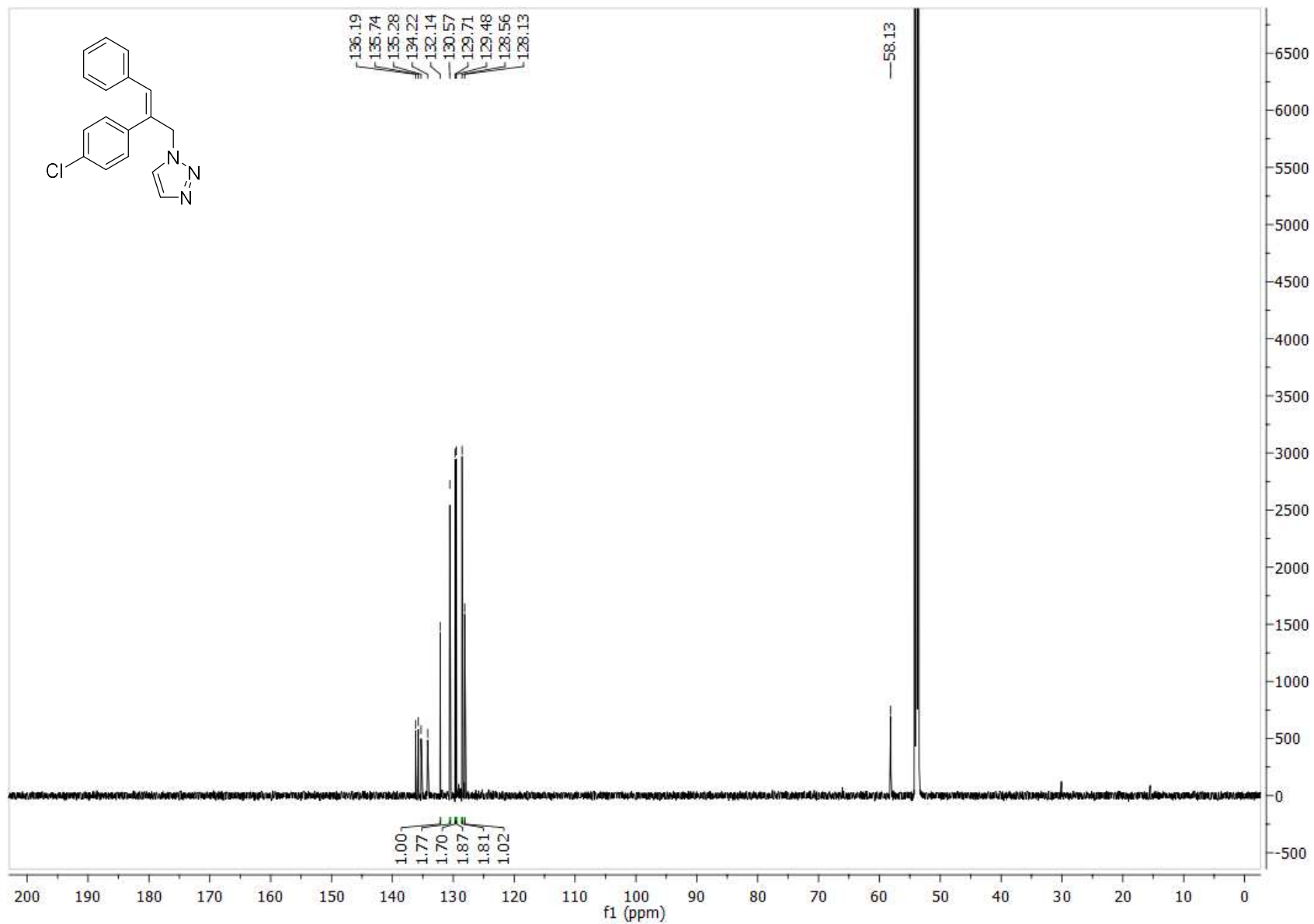
6b ^{1}H NMR
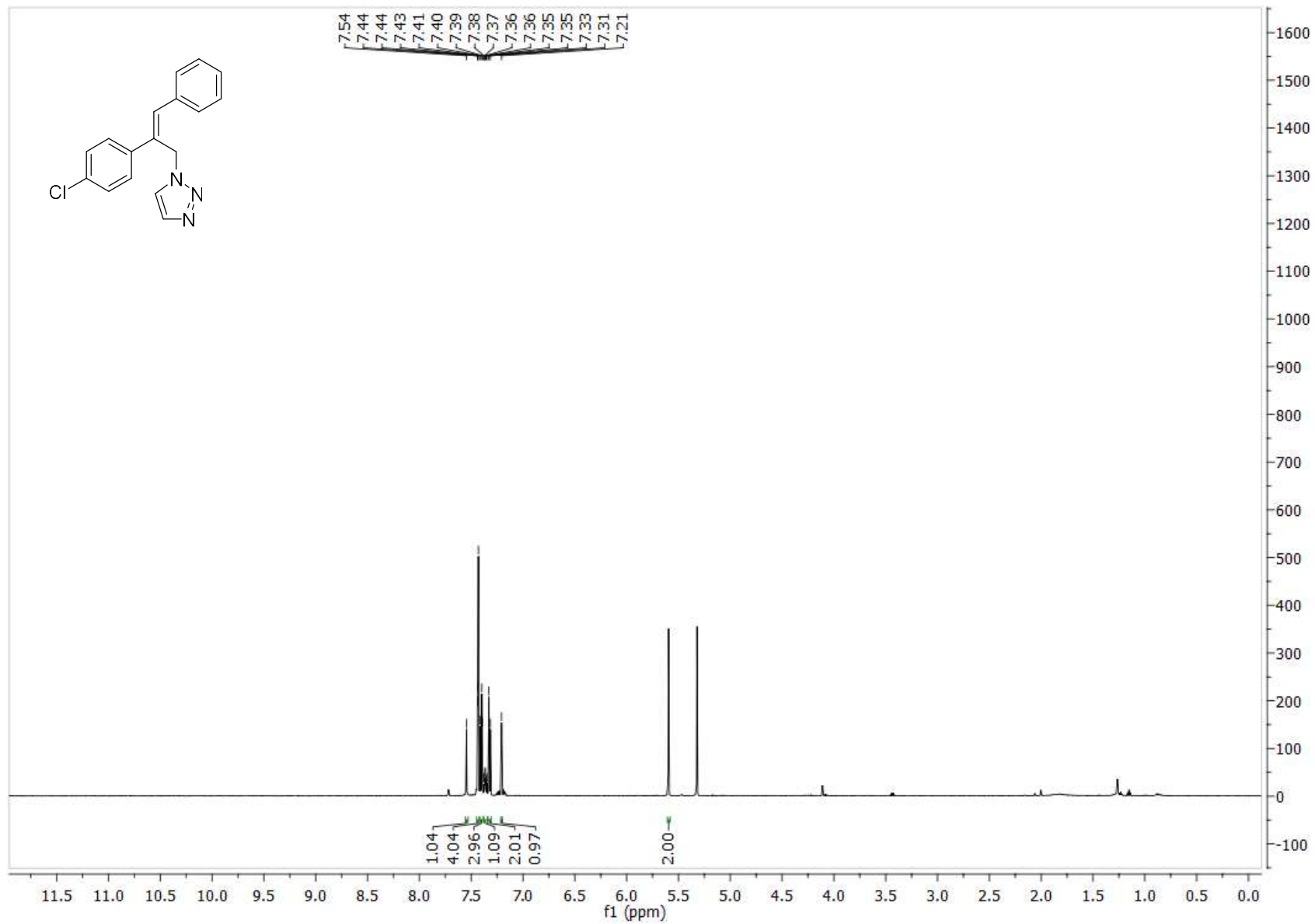
6b ^{13}C NMR
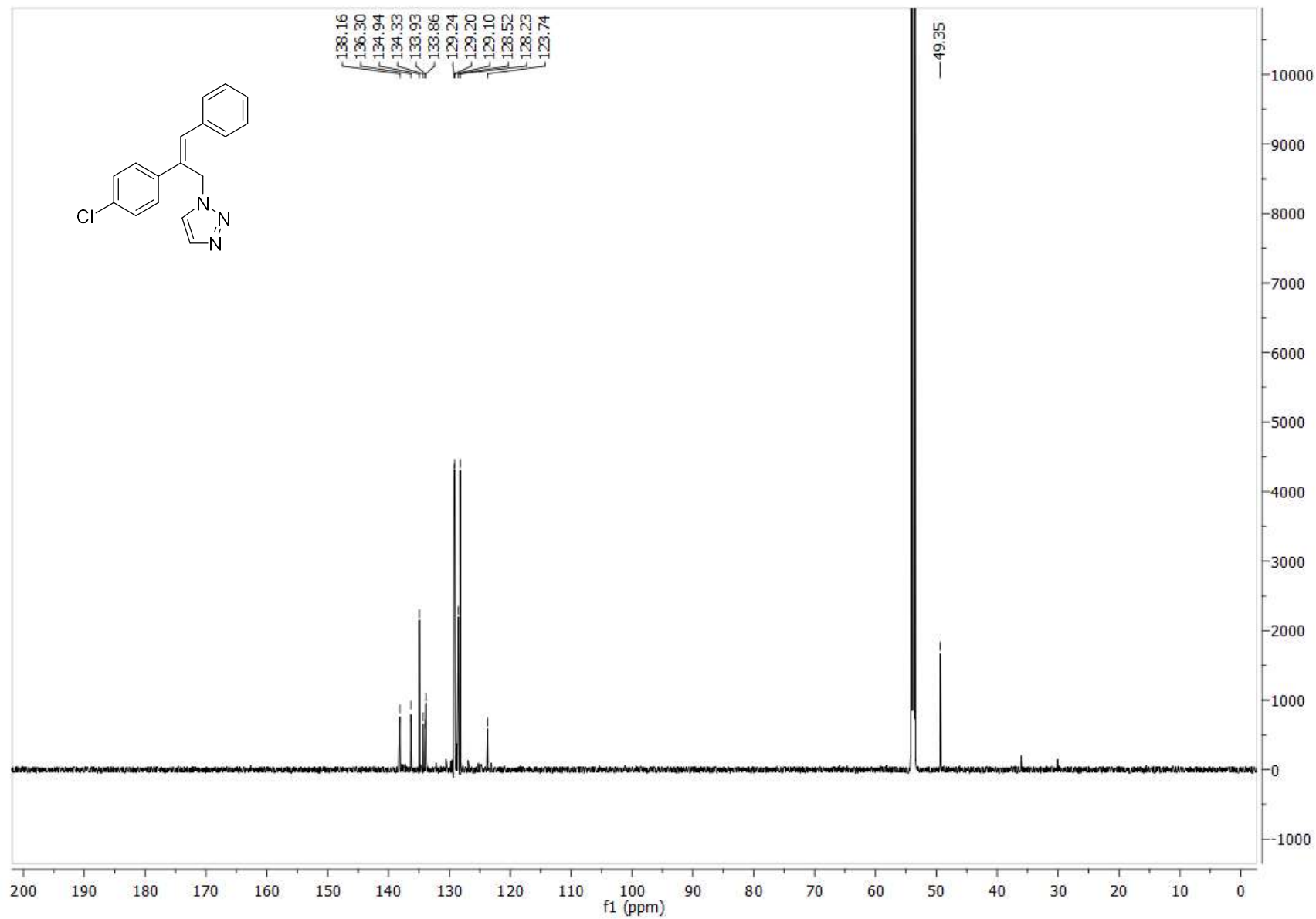
5c ¹H NMR
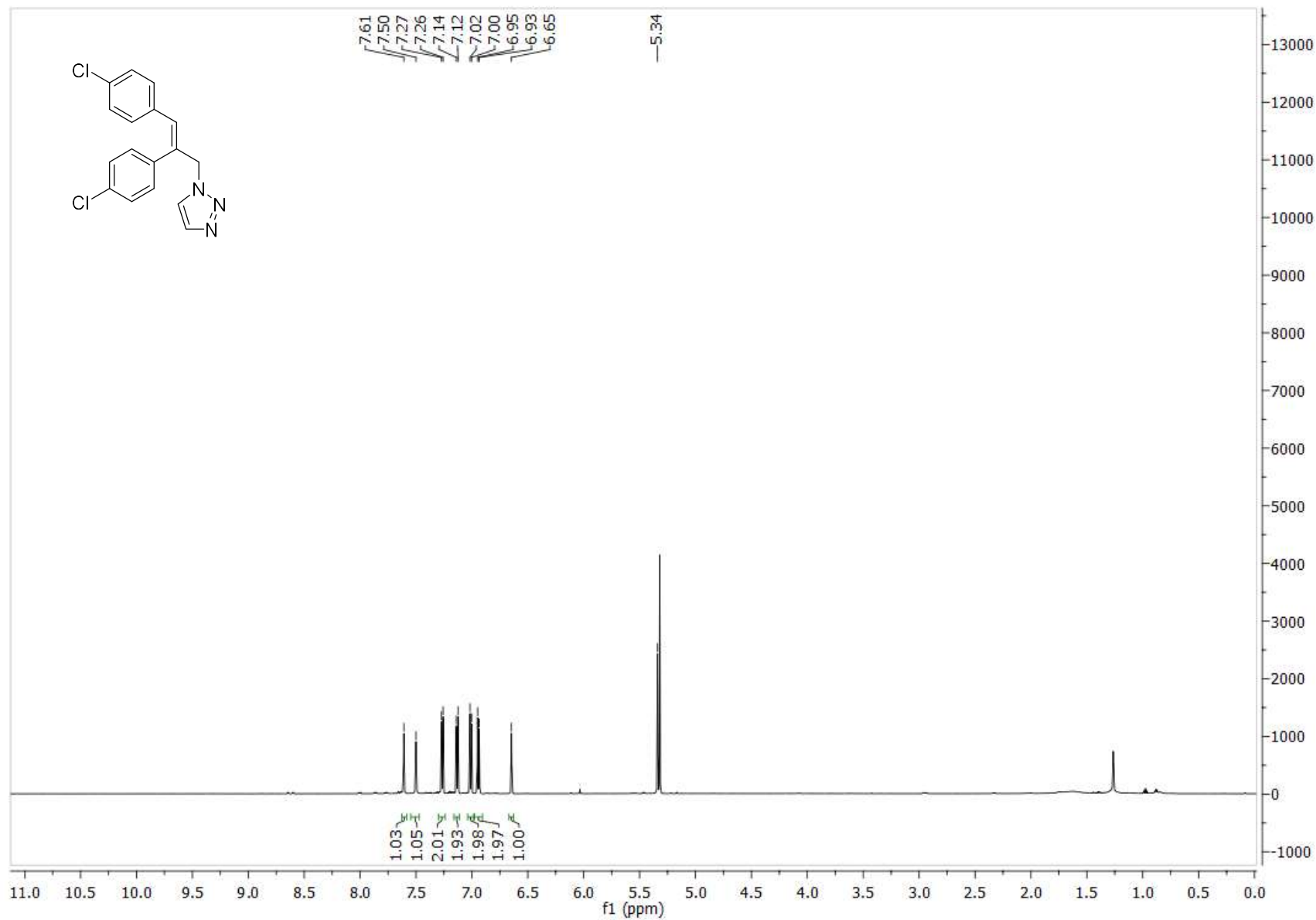
5c ^{13}C NMR
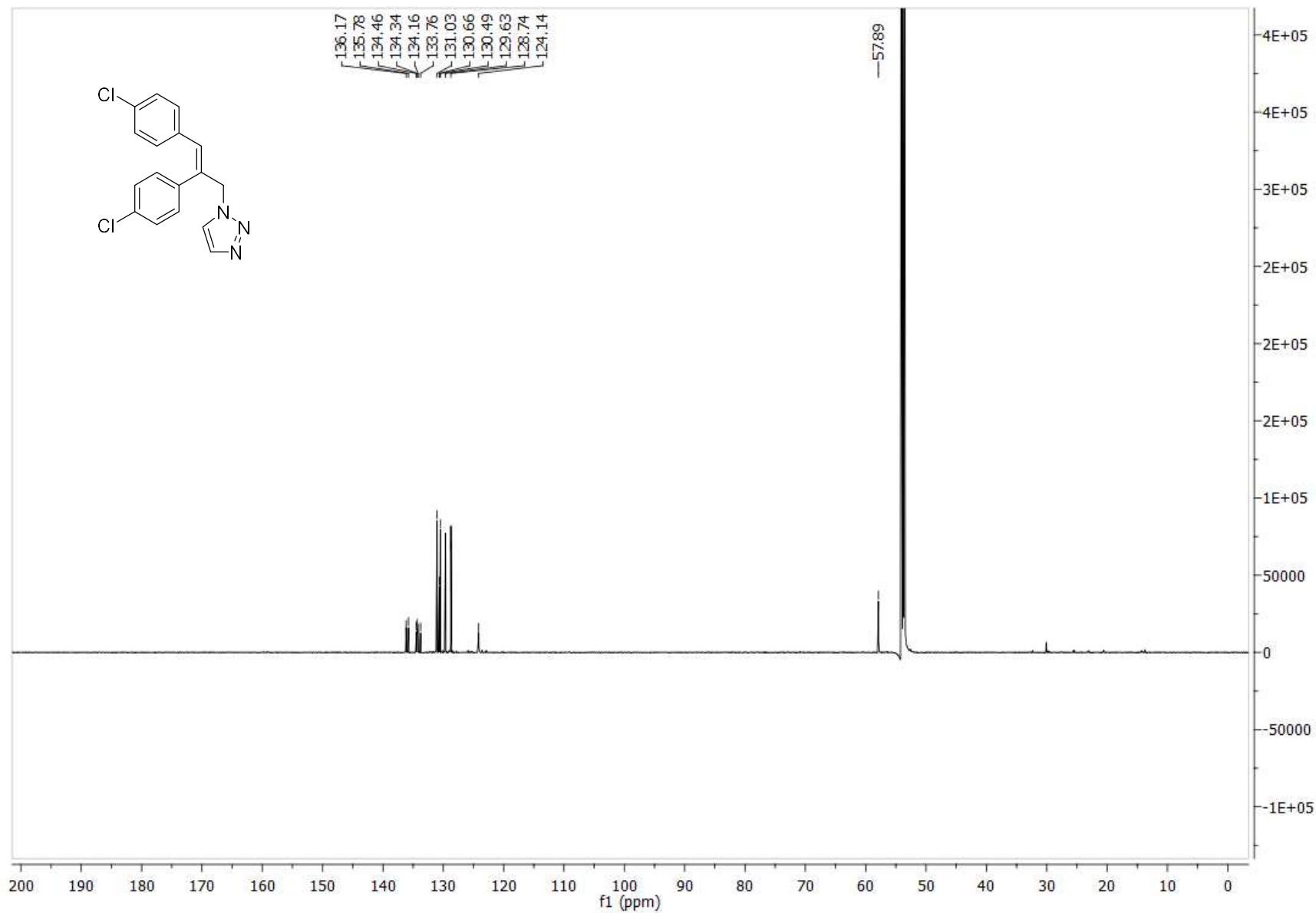
6c ^{1}H NMR
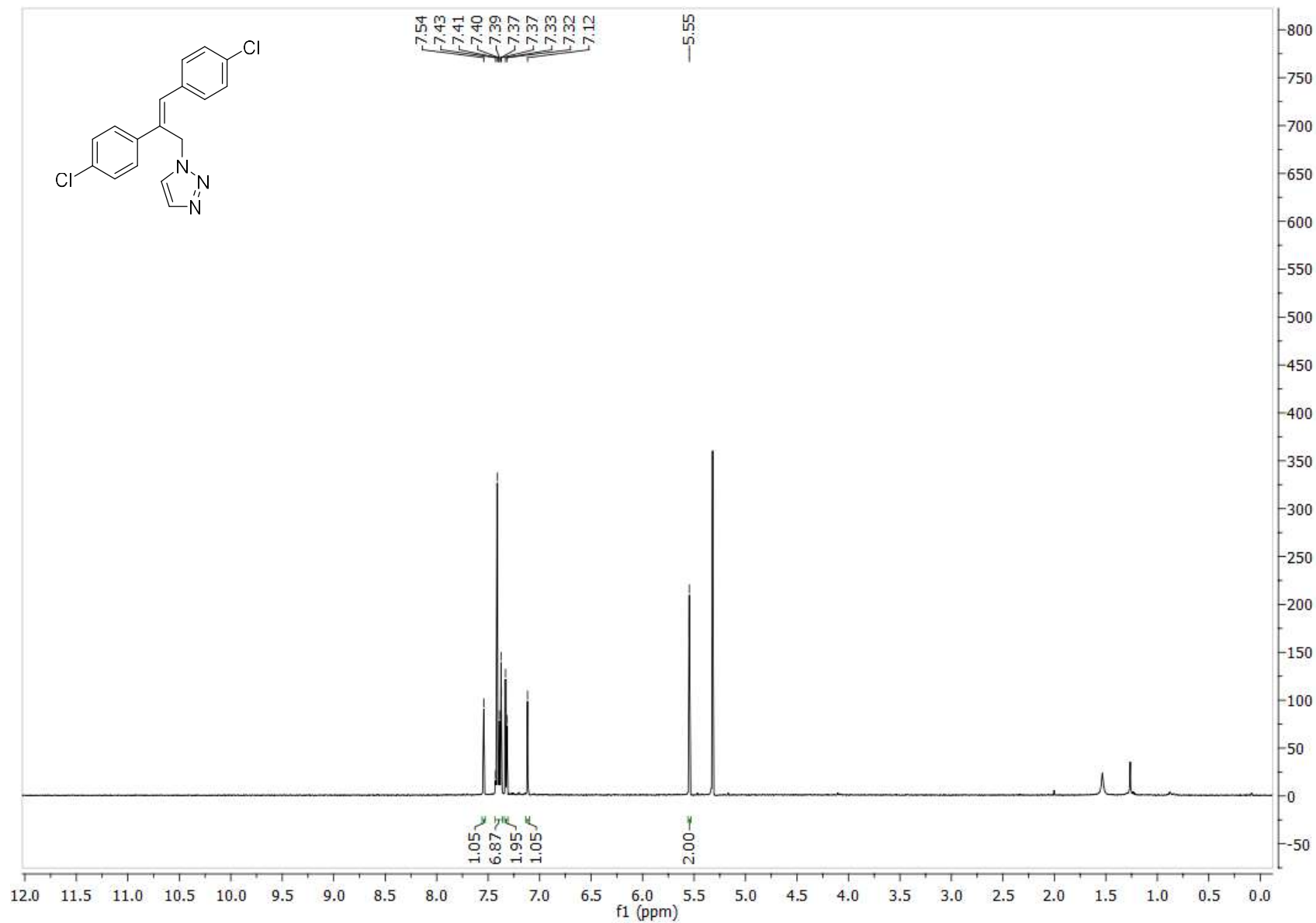
6c ^{13}C NMR
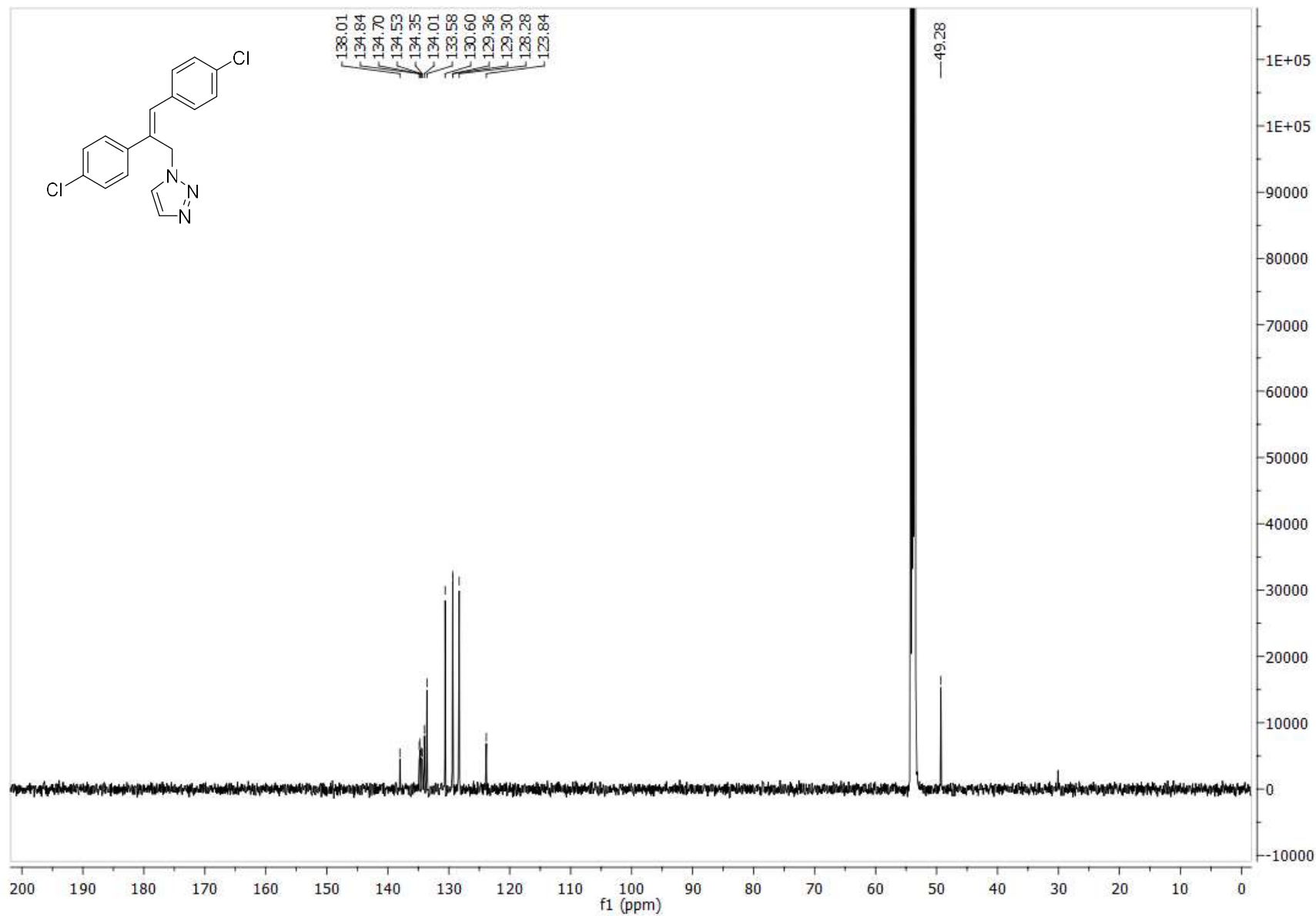
5d ^{1}H NMR
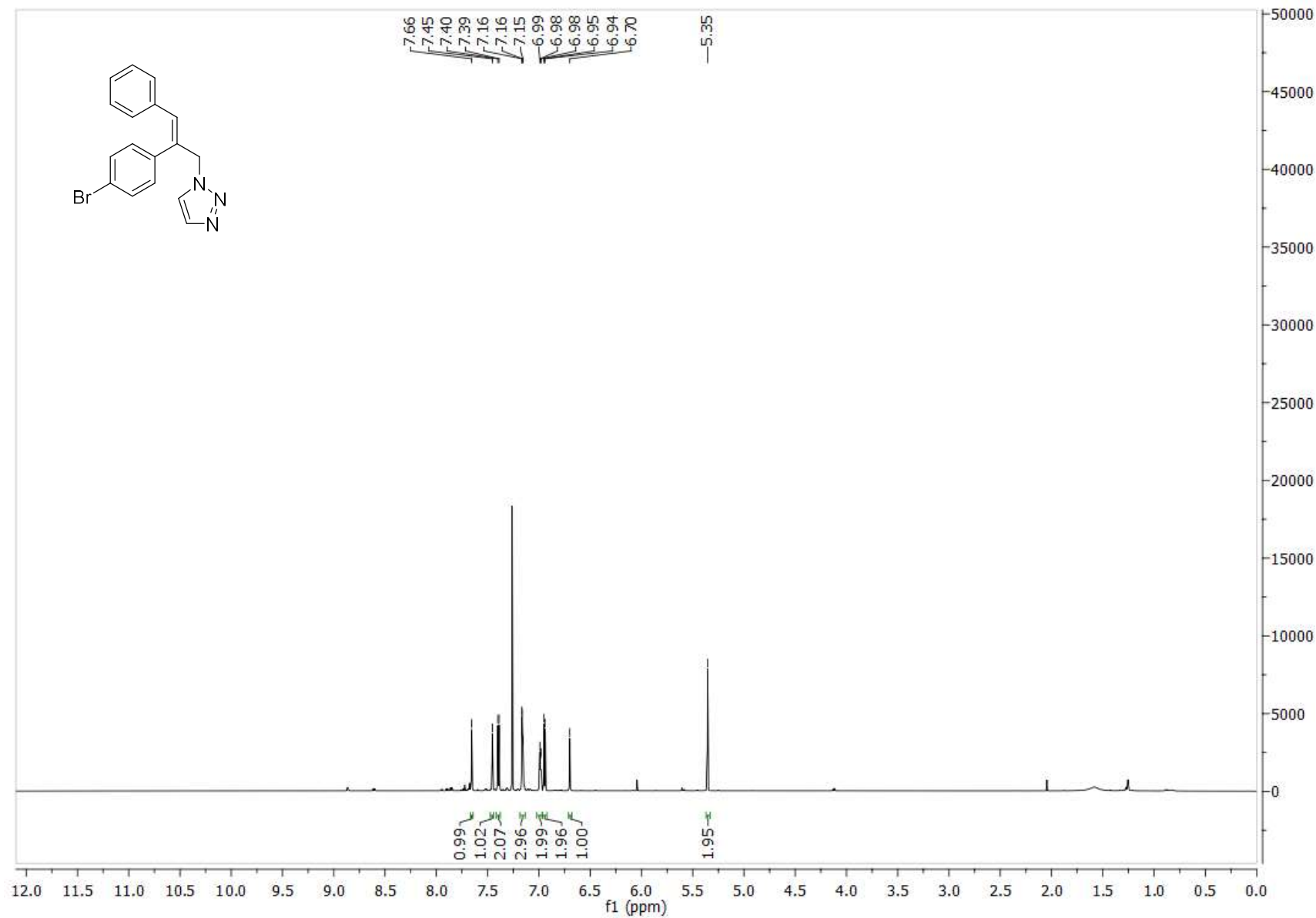
5d ^{13}C NMR
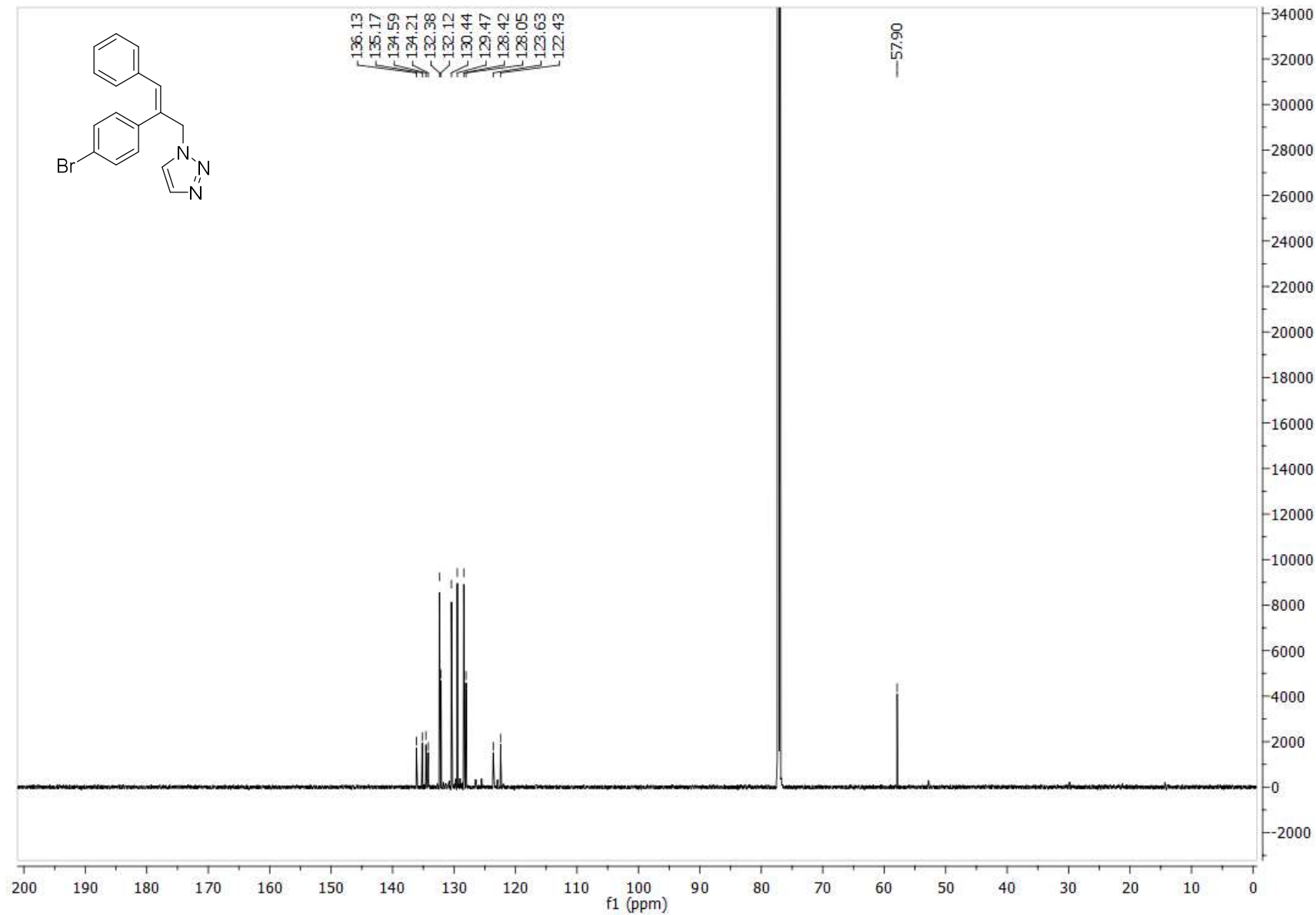
6d ¹H NMR
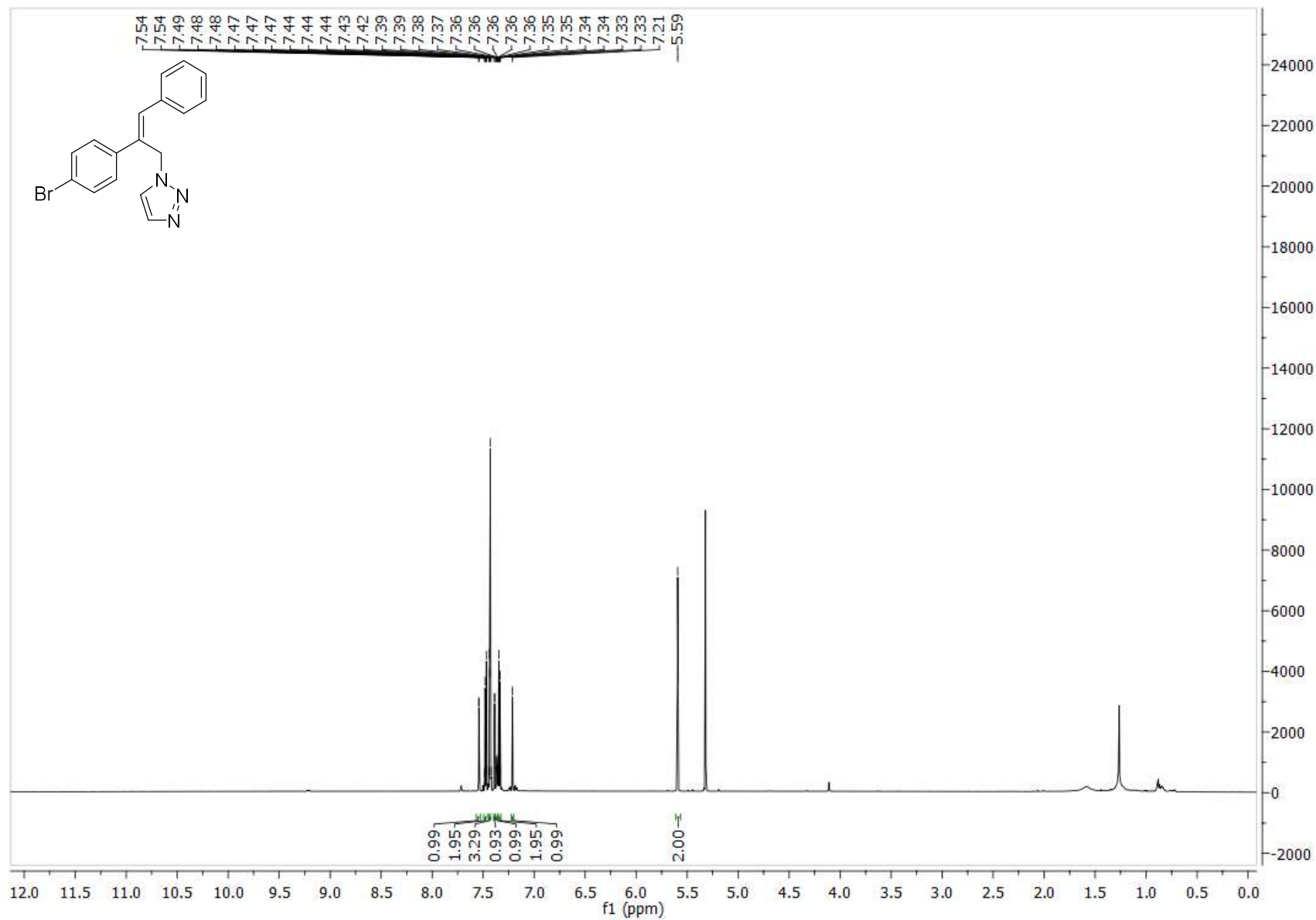
6d ^{13}C NMR
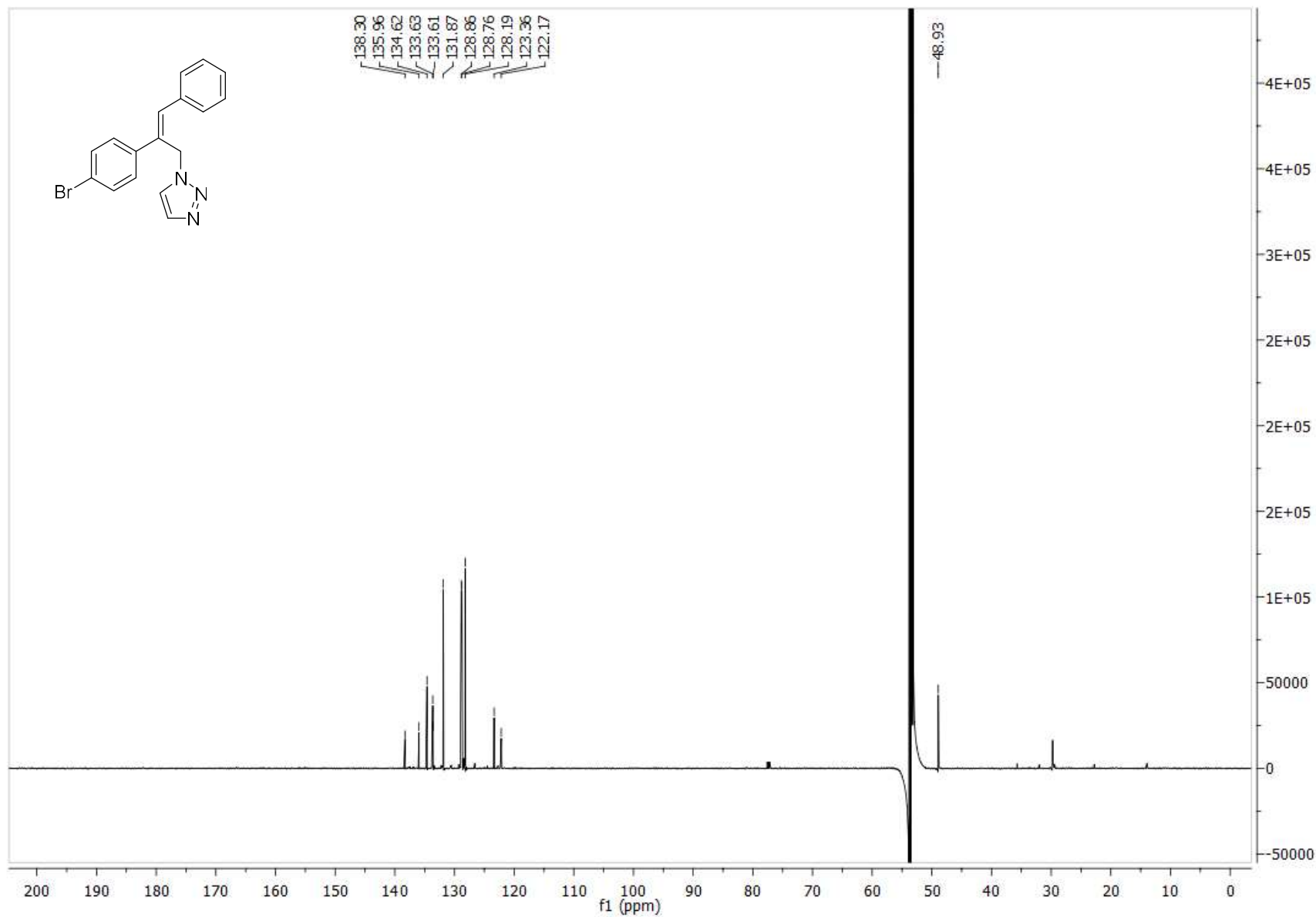
5e ¹H NMR
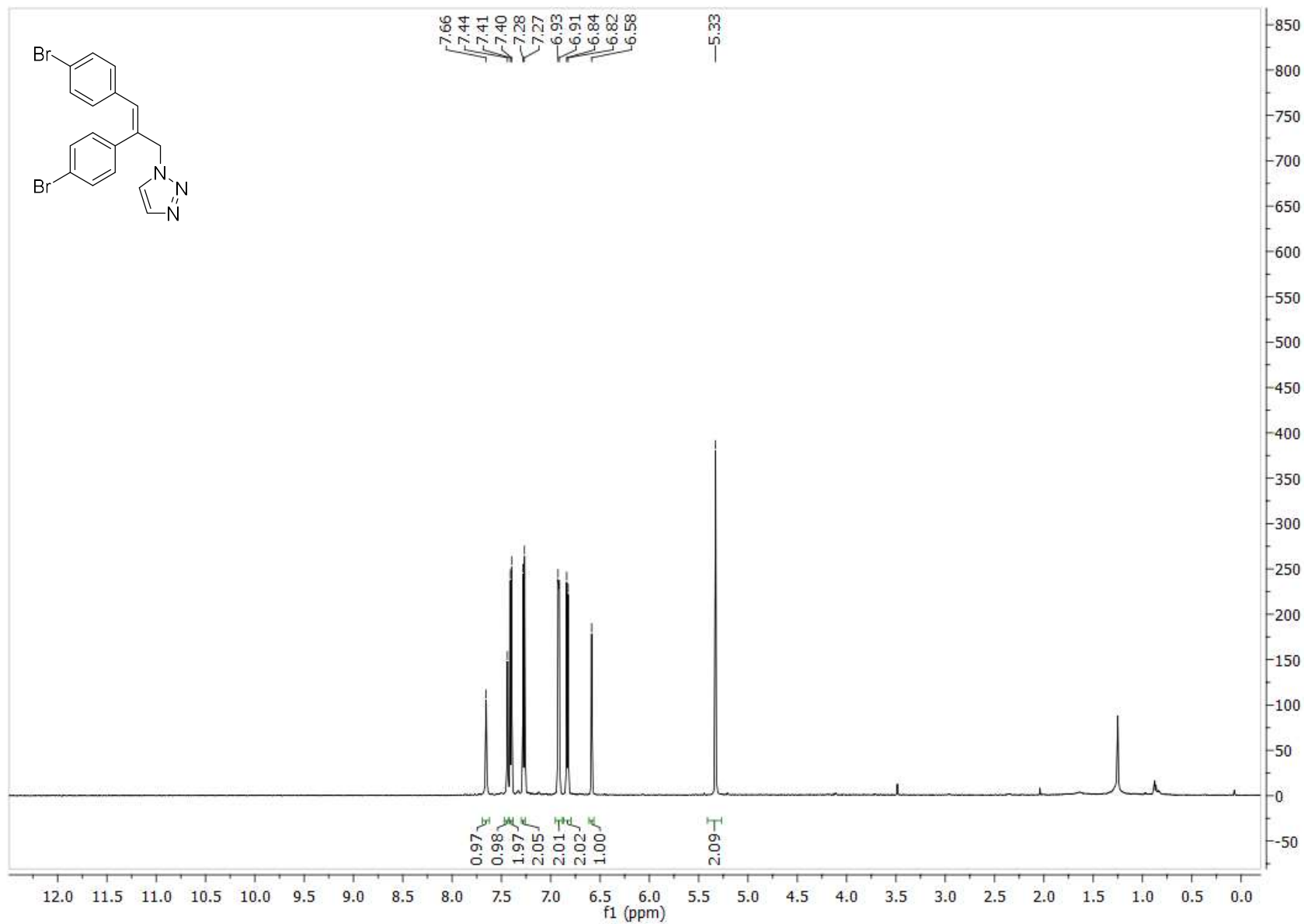
5e ^{13}C NMR
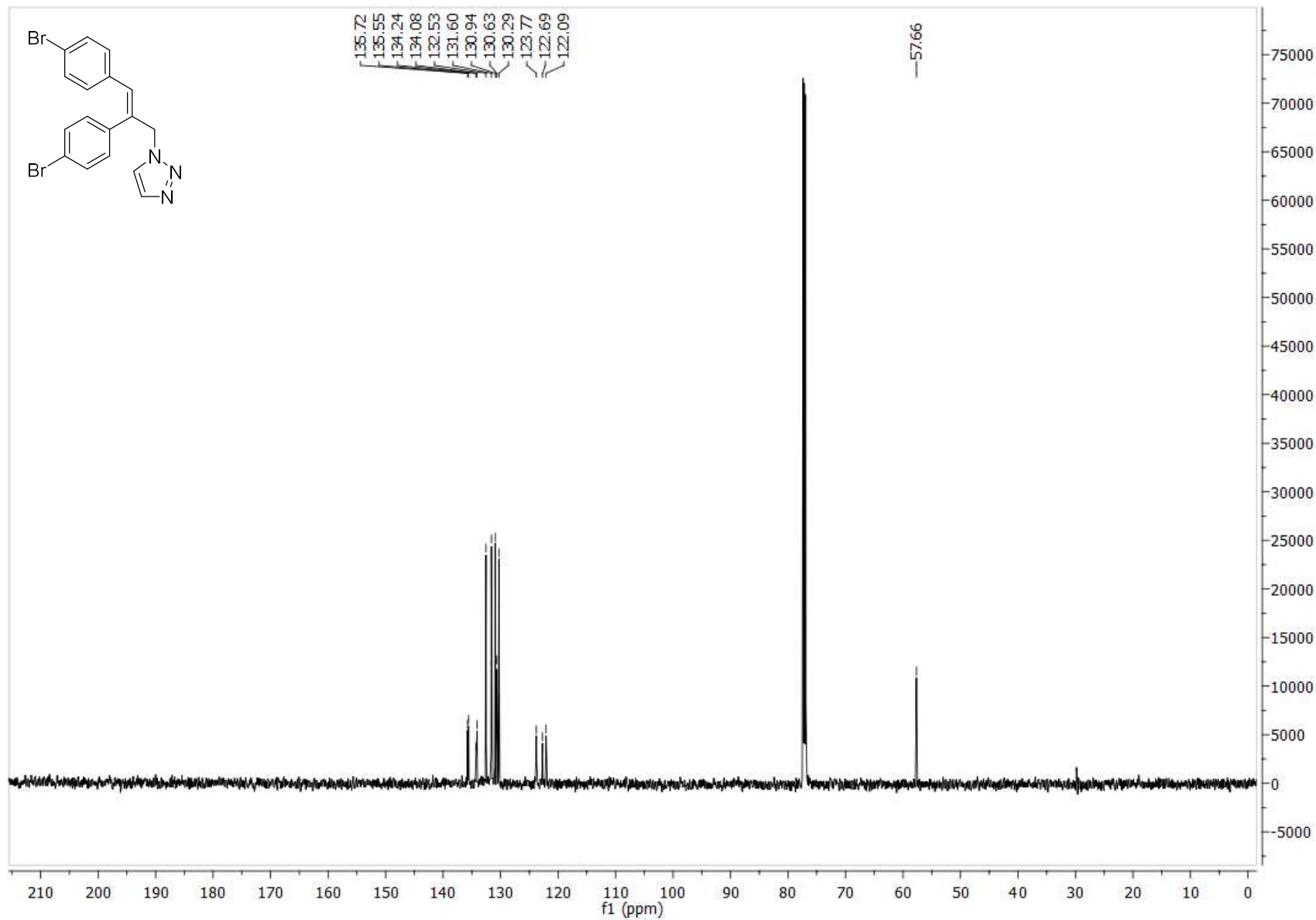
6e ¹H NMR

6e ^{13}C NMR

13 ¹H NMR
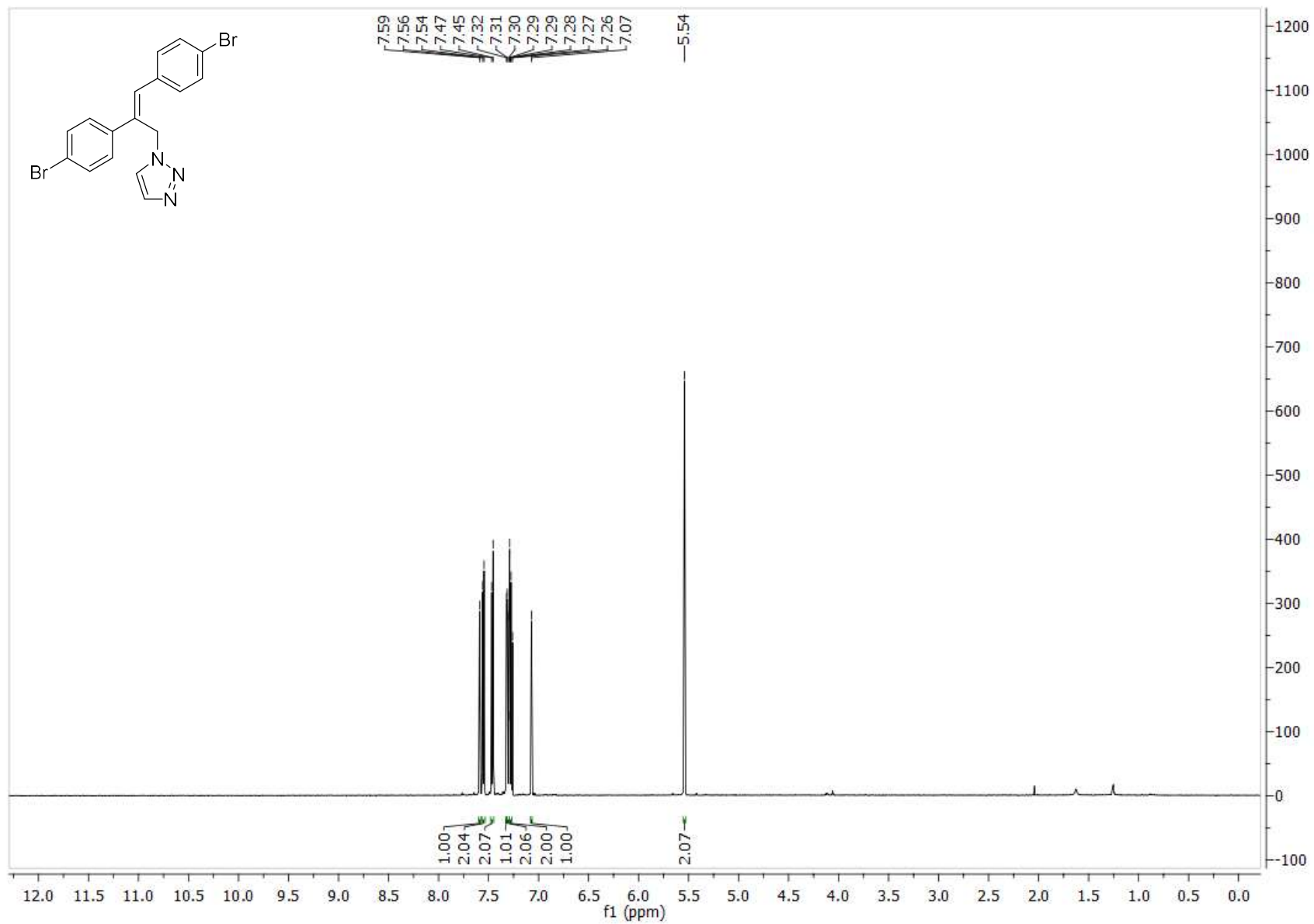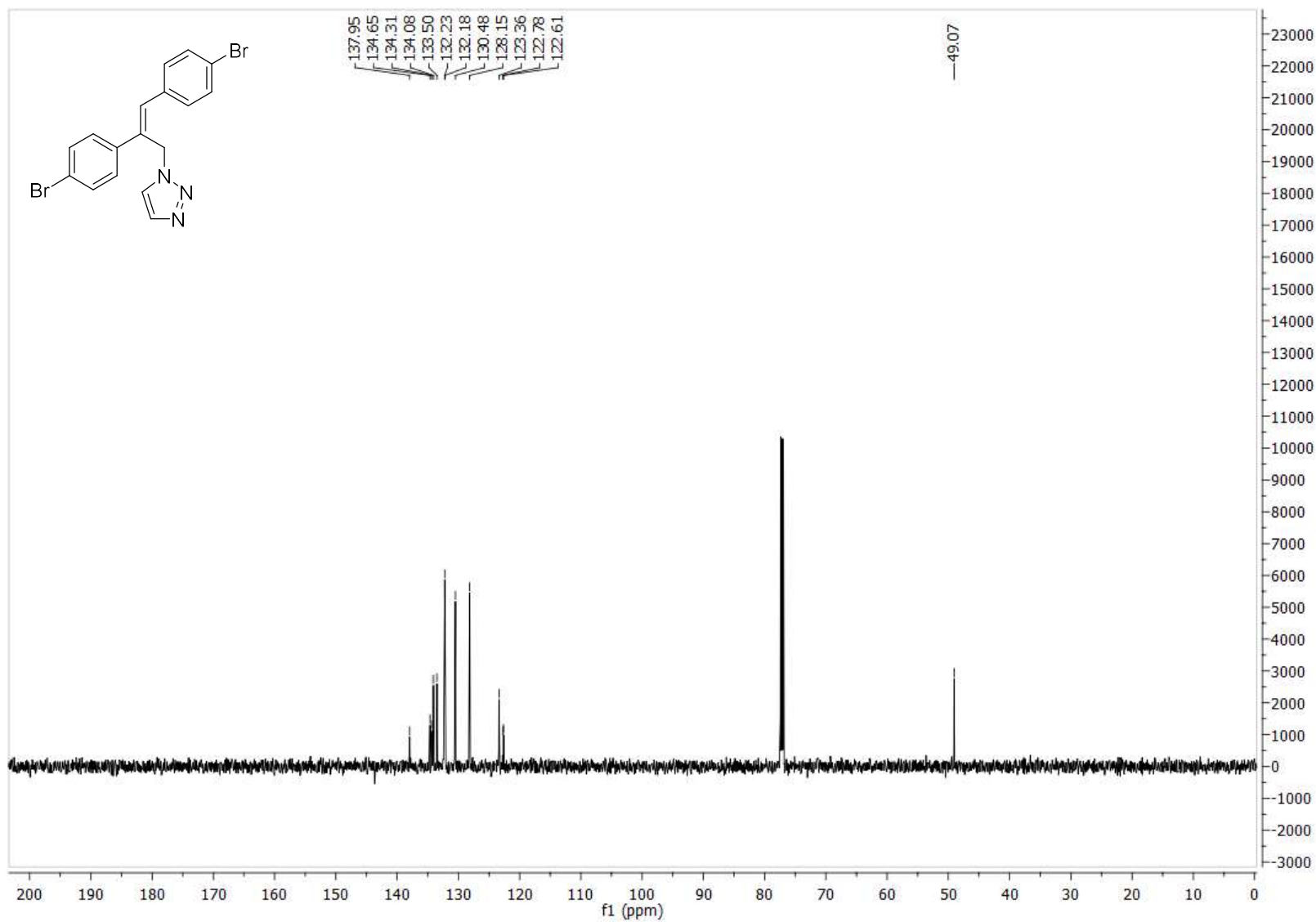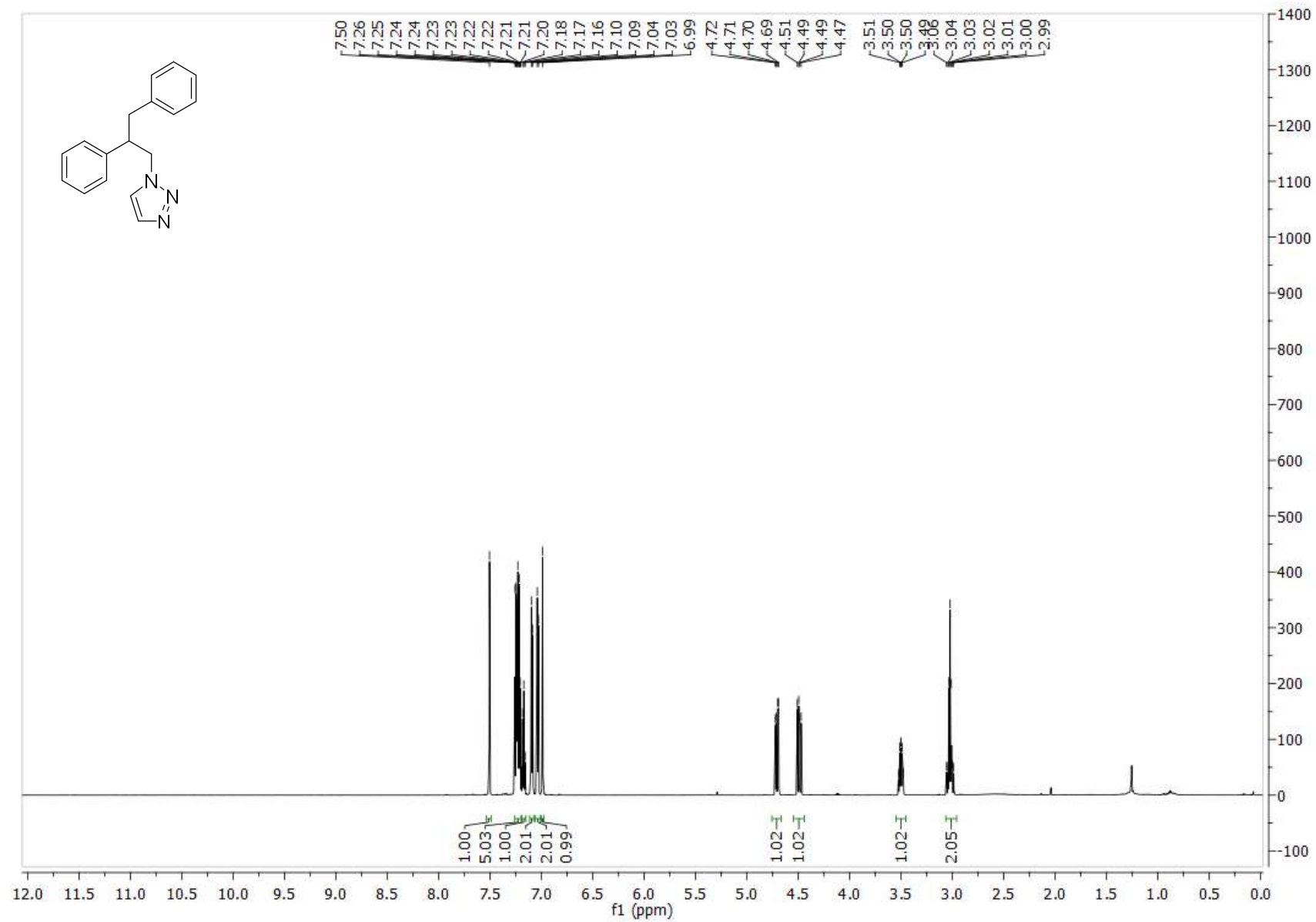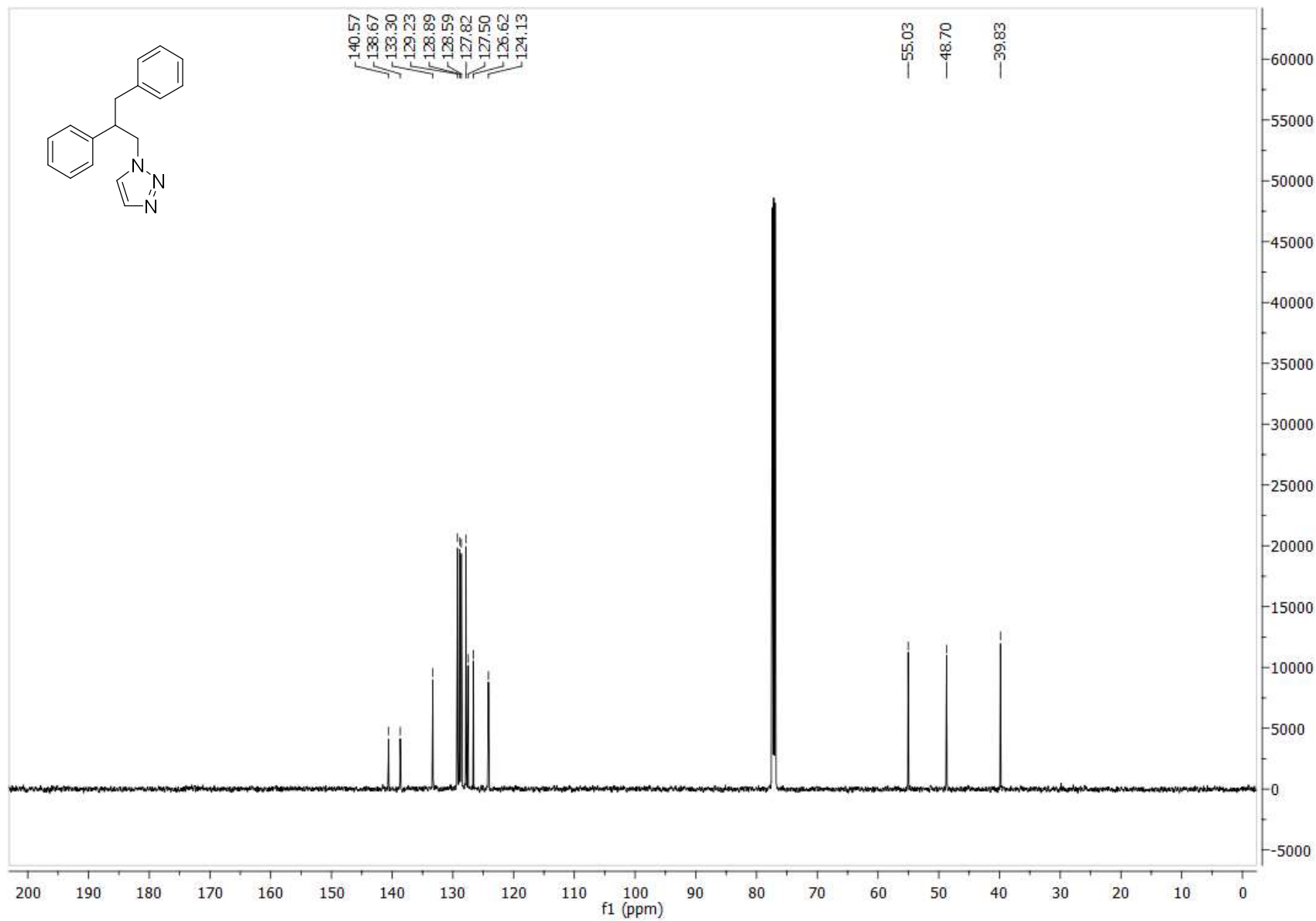
13 ^{13}C NMR

14 ^{1}H NMR
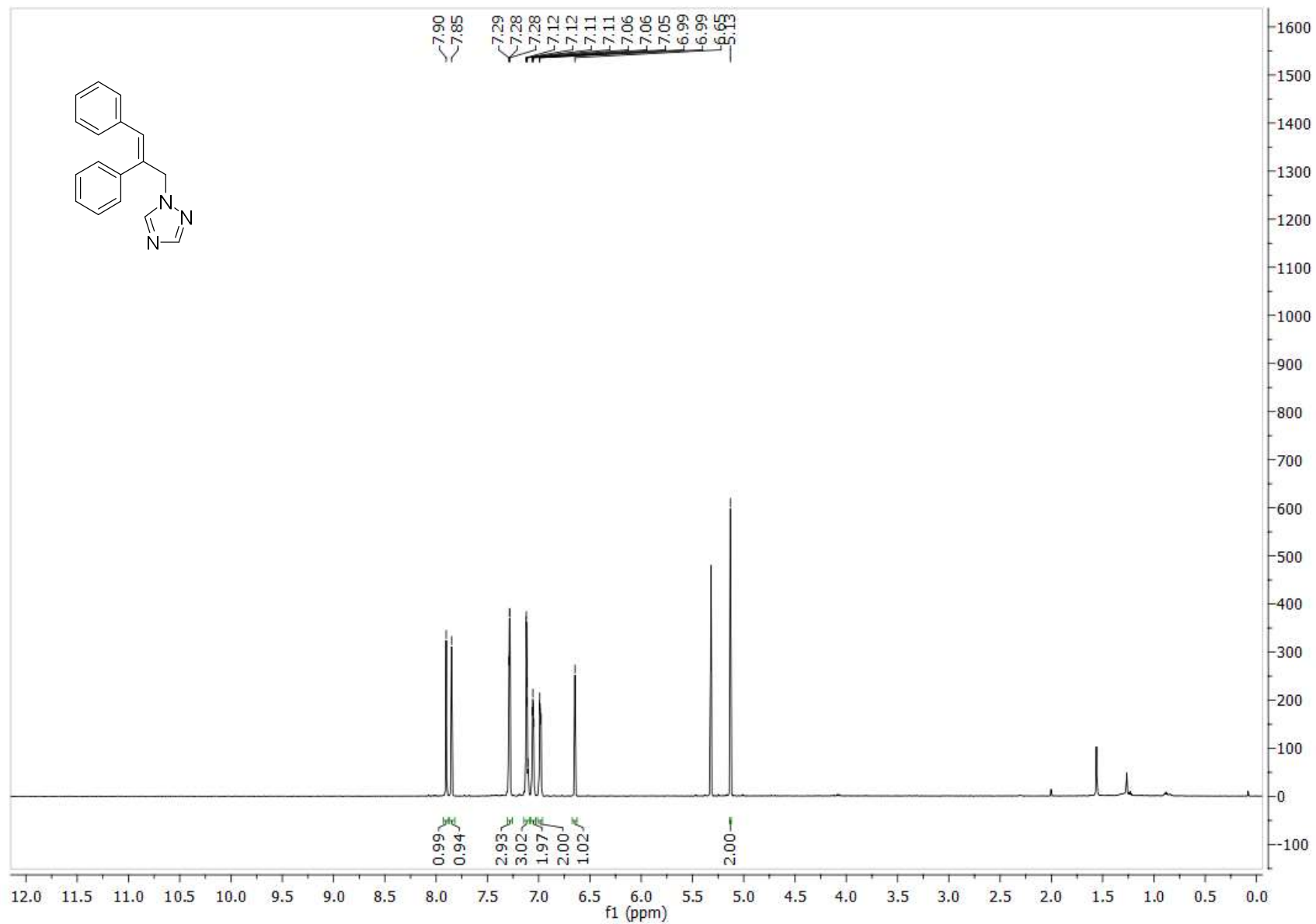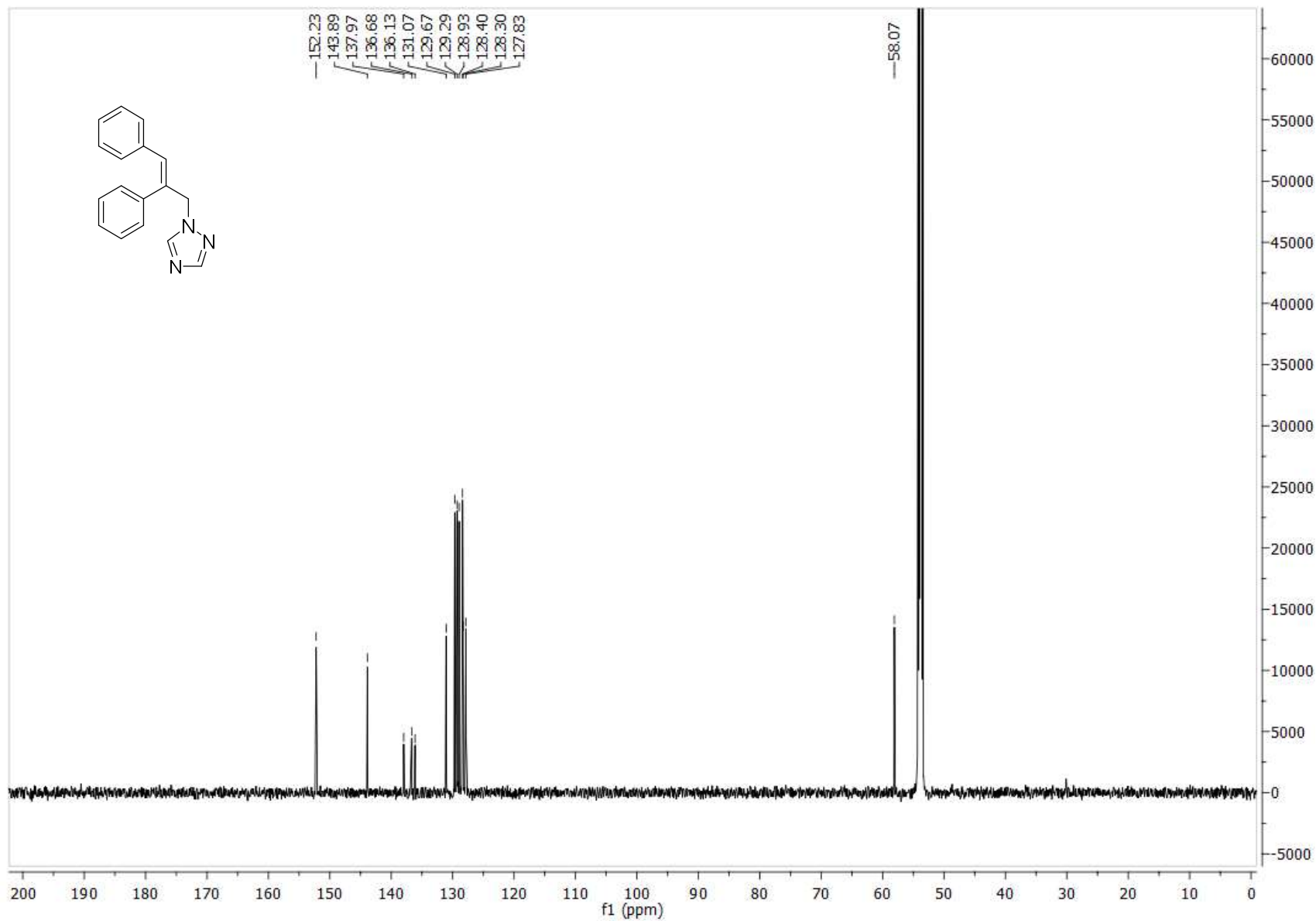
14 ^{13}C NMR

15 ^{1}H NMR
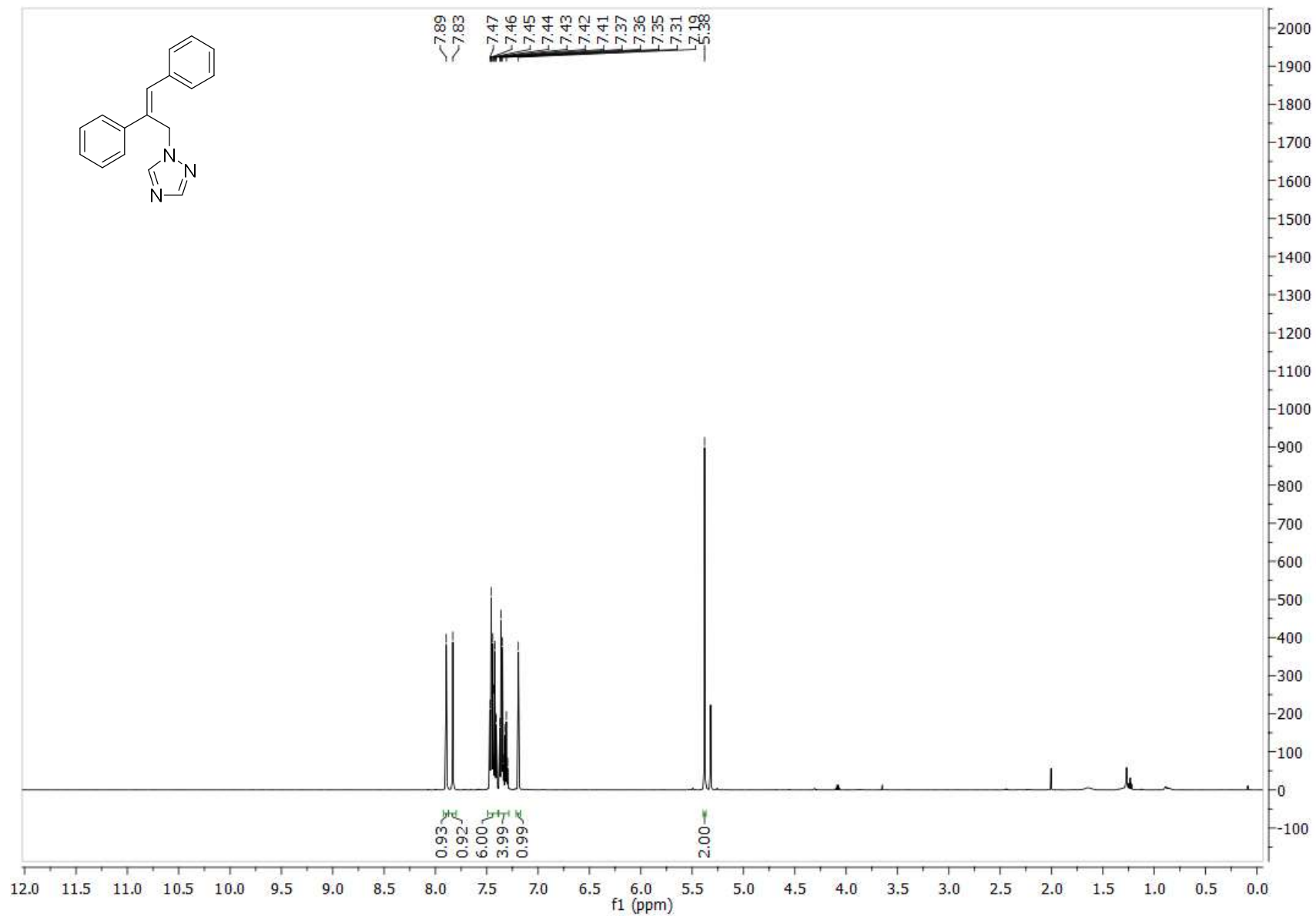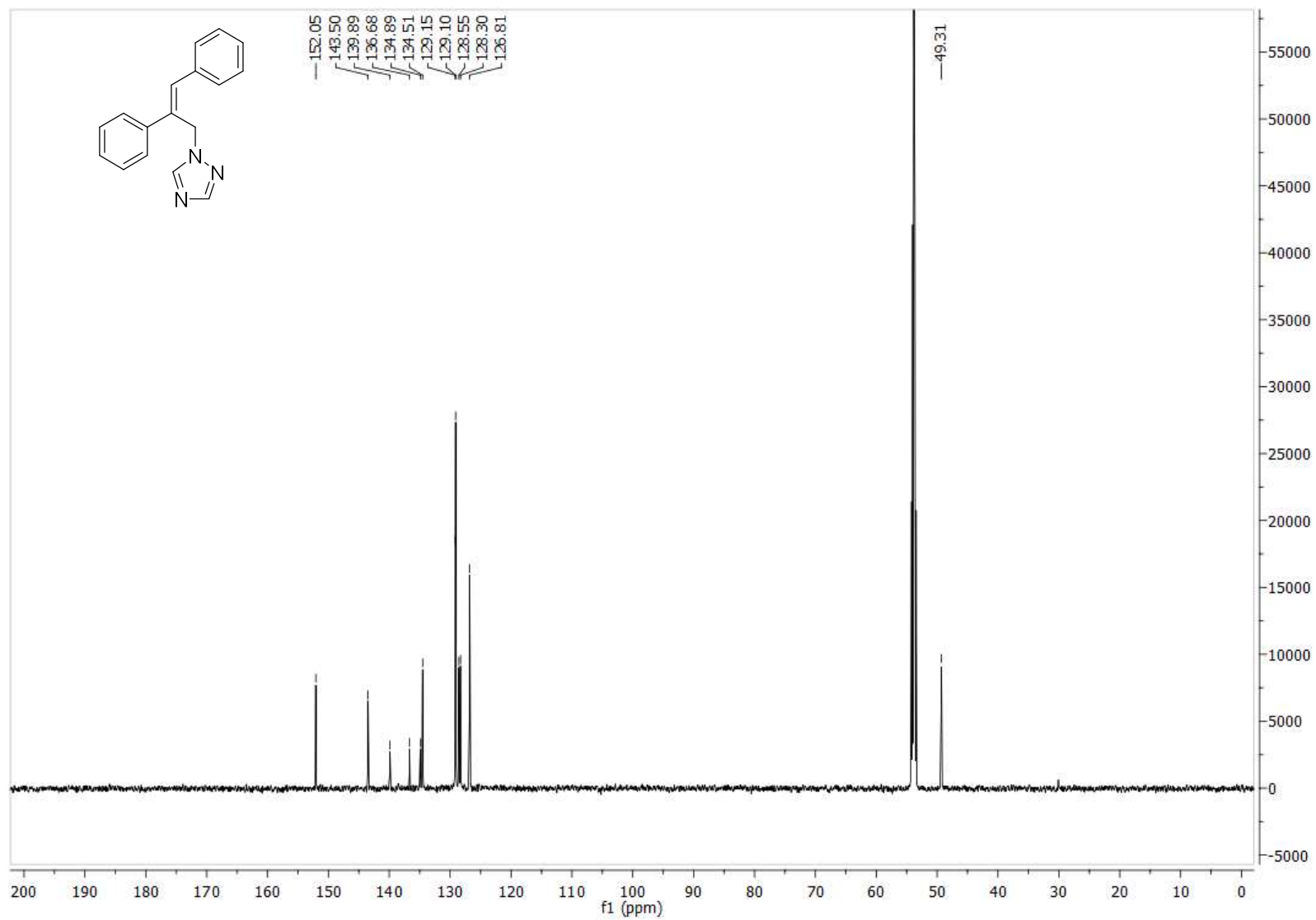
15 ^{13}C NMR

Appendix B: NMR Spectra Pertaining to Chapter 3

Tripropylphosphine hydrobromide ^{1}H NMR
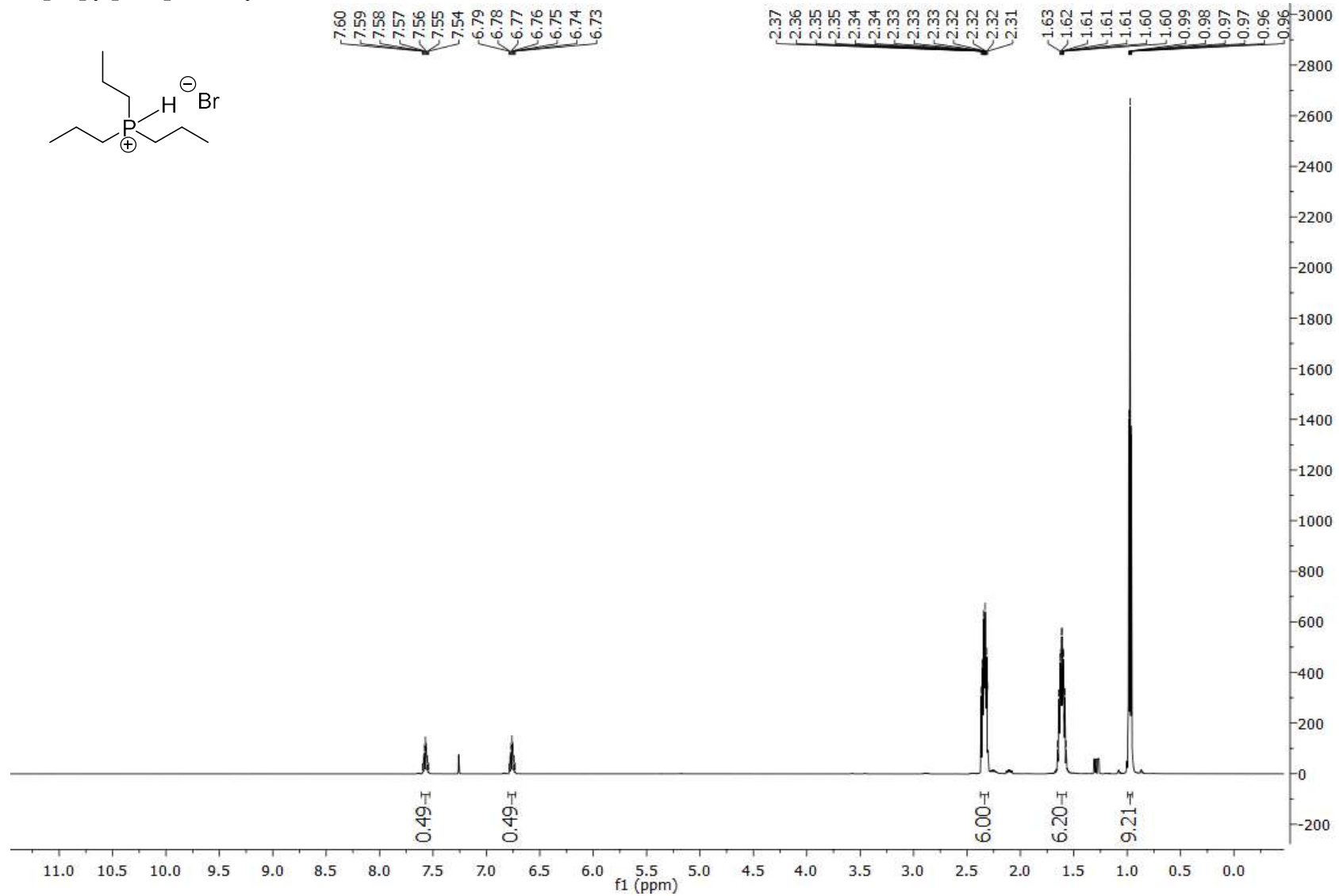
Tripropylphosphine hydrobromide ^{13}C NMR
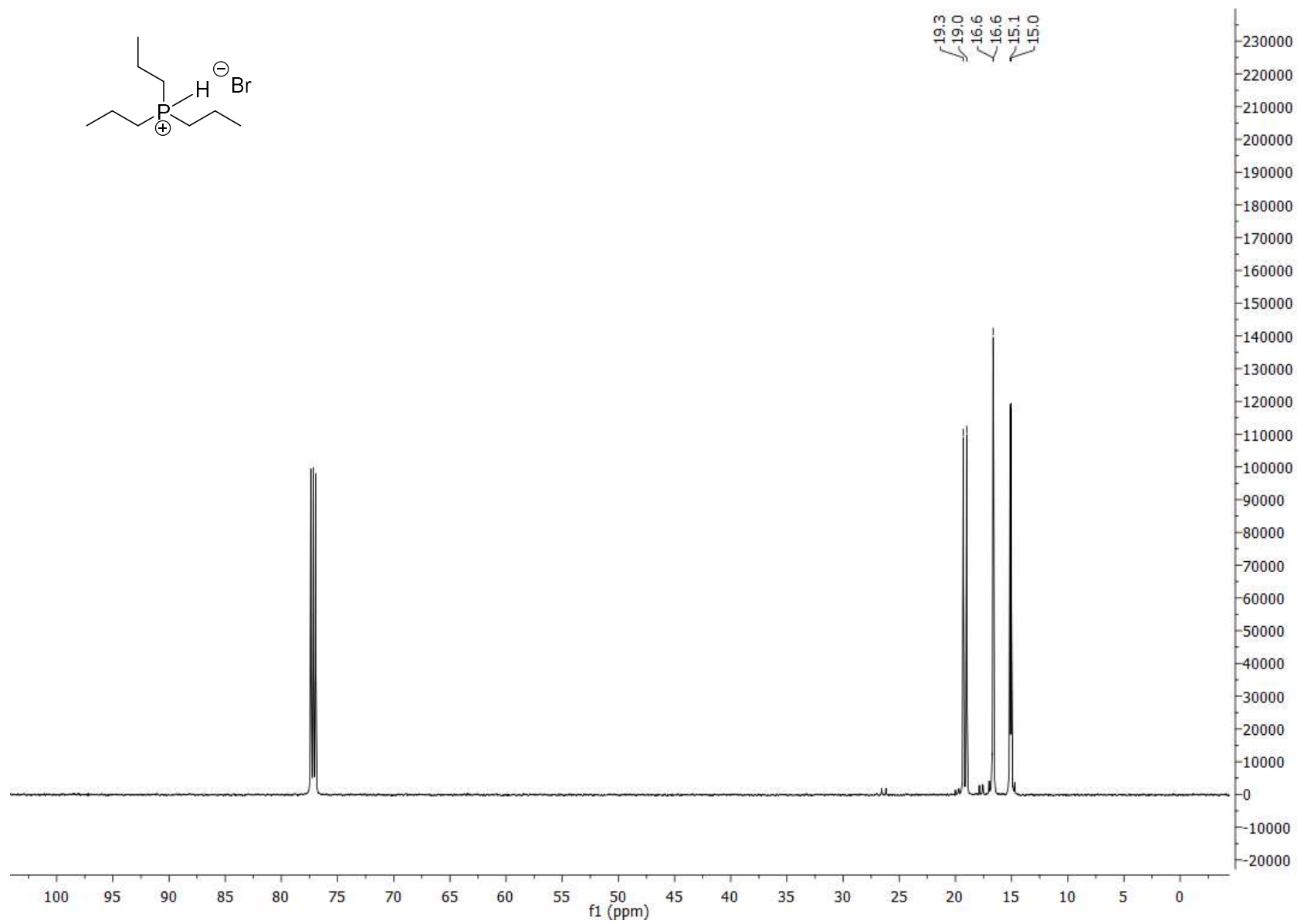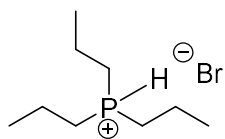
Tripropylphosphine hydrobromide ^{31}P NMR
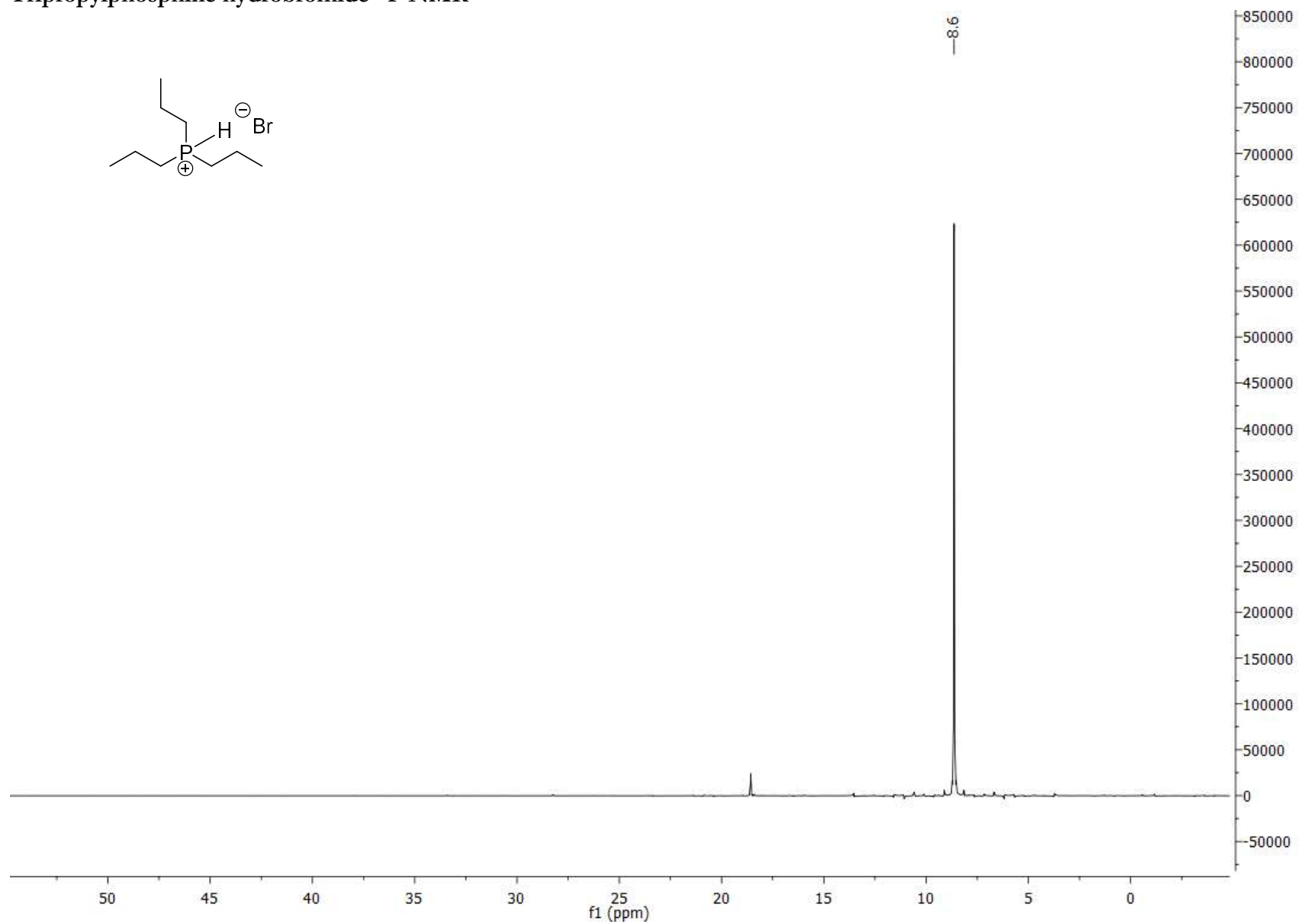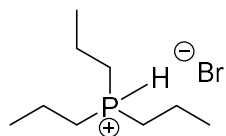
Salt 1a ^{1}H NMR
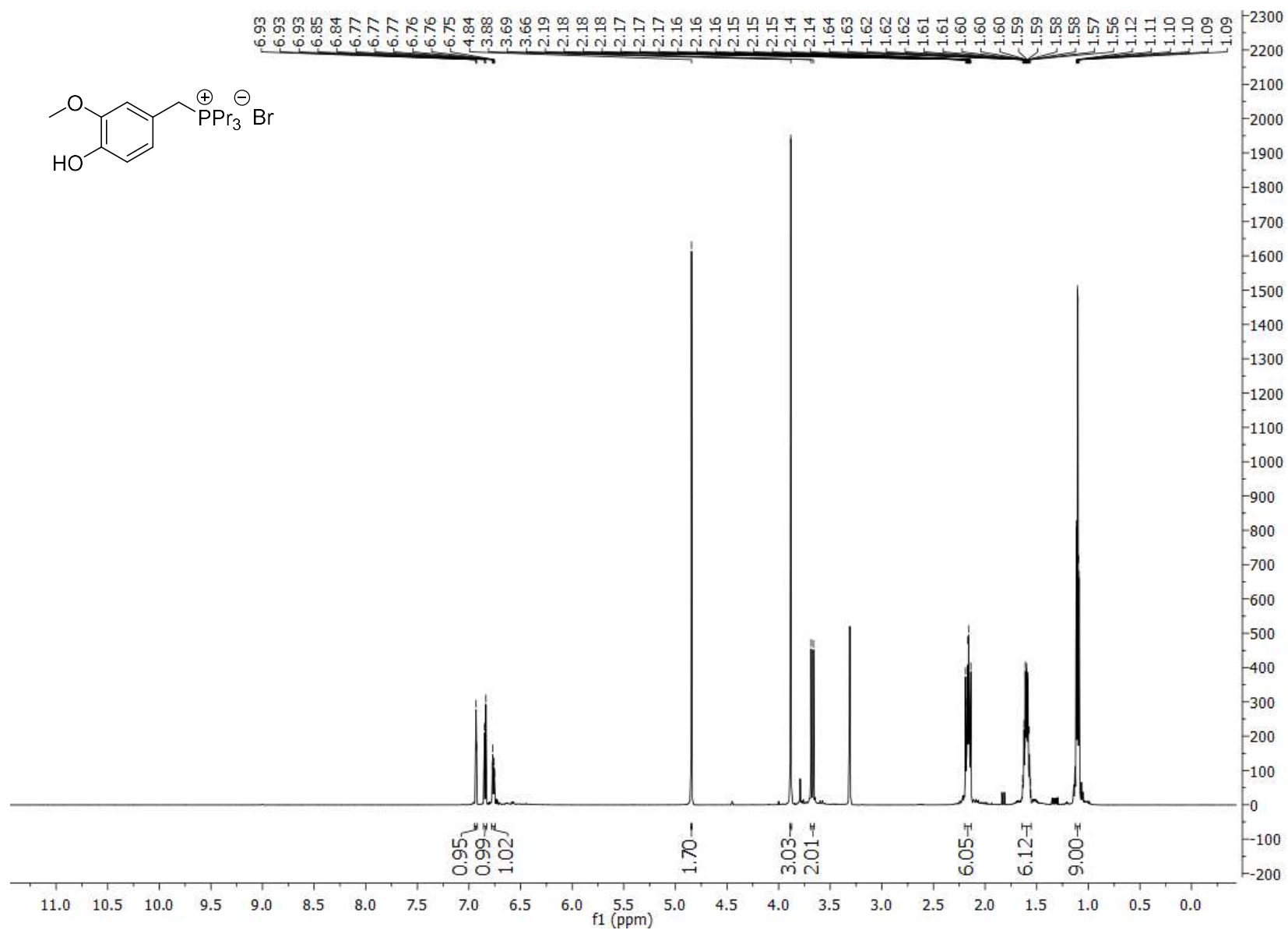
Salt 1a ¹³C NMR
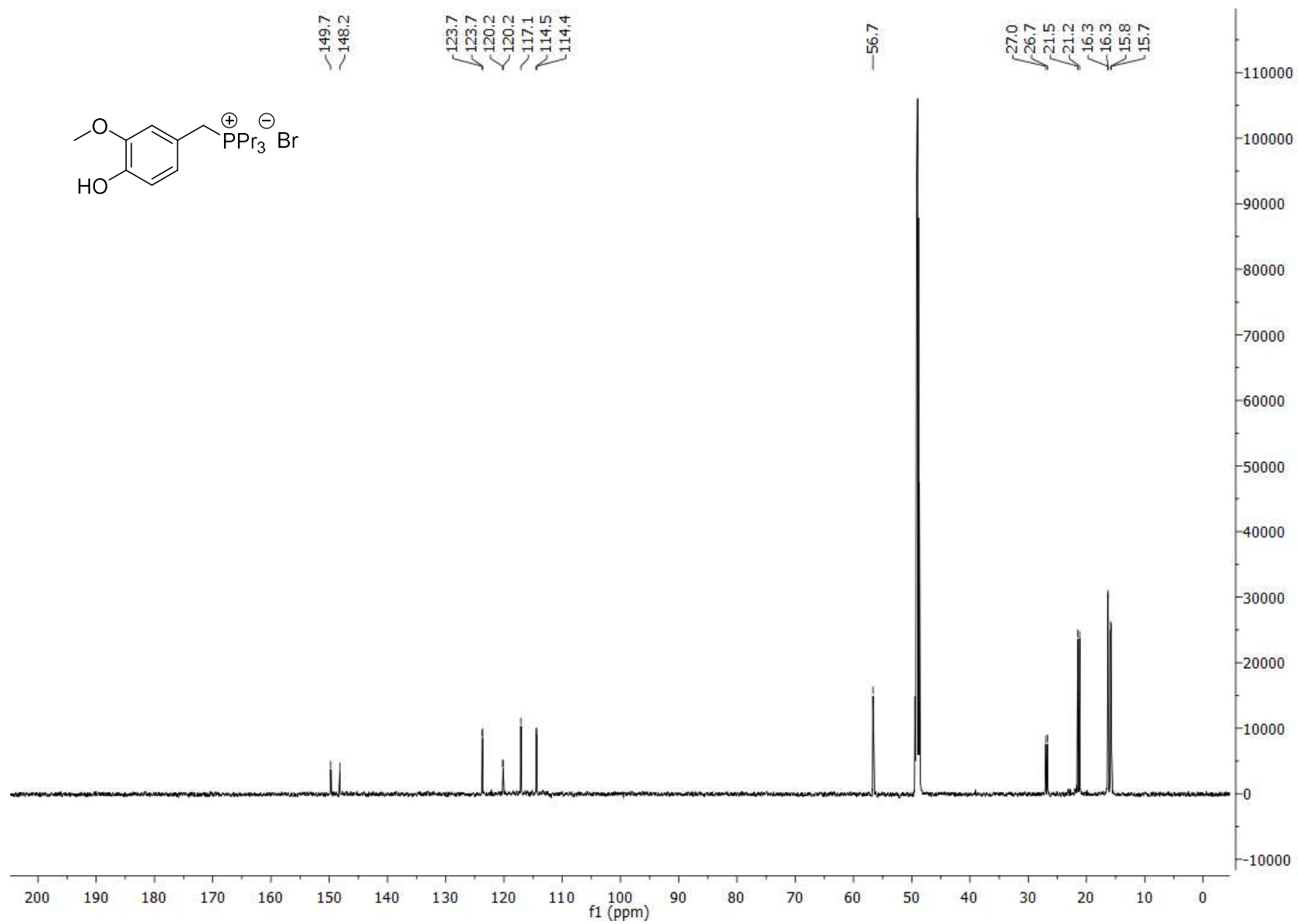
Salt 1a ³¹P NMR
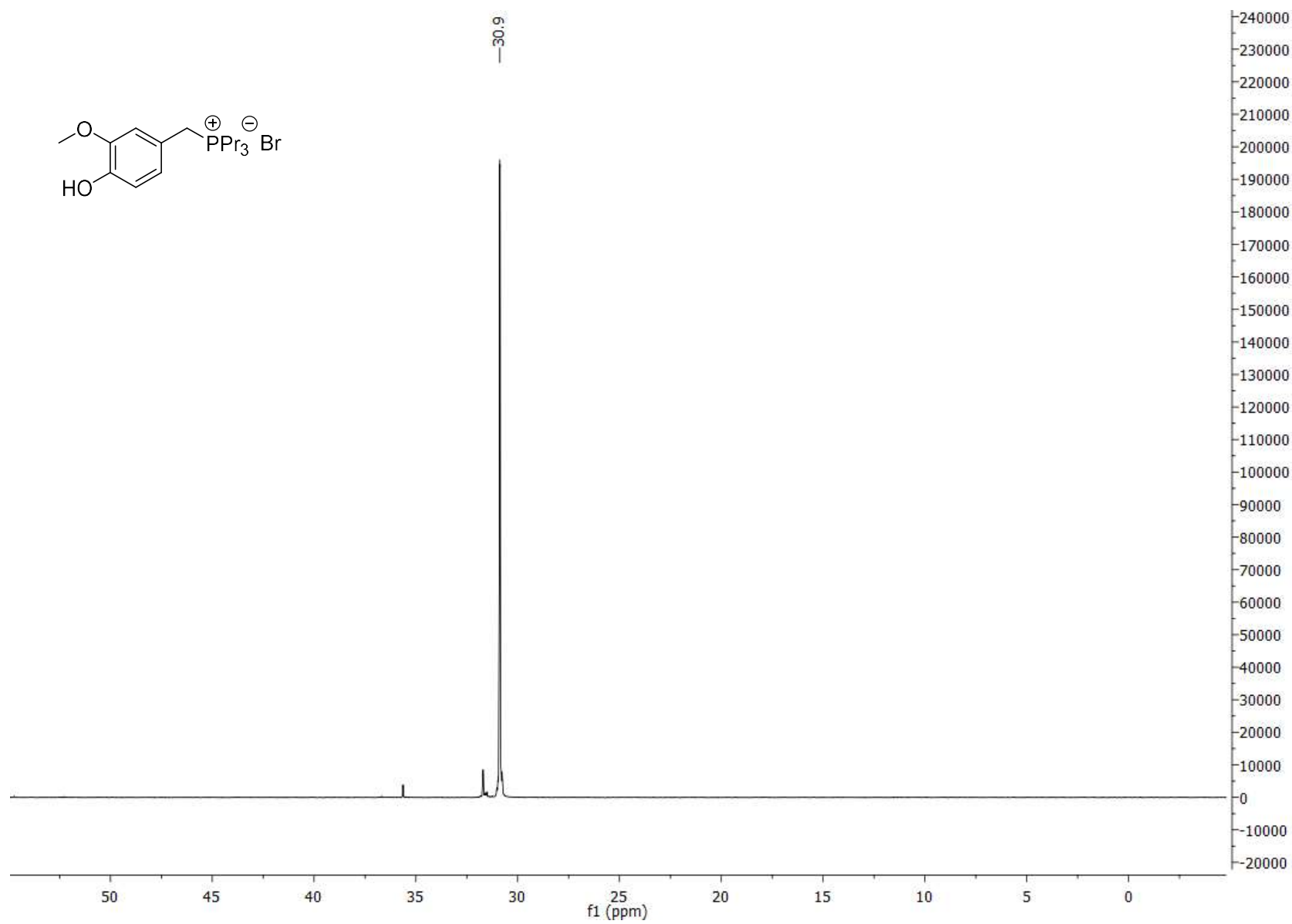
Salt 1b ¹H NMR
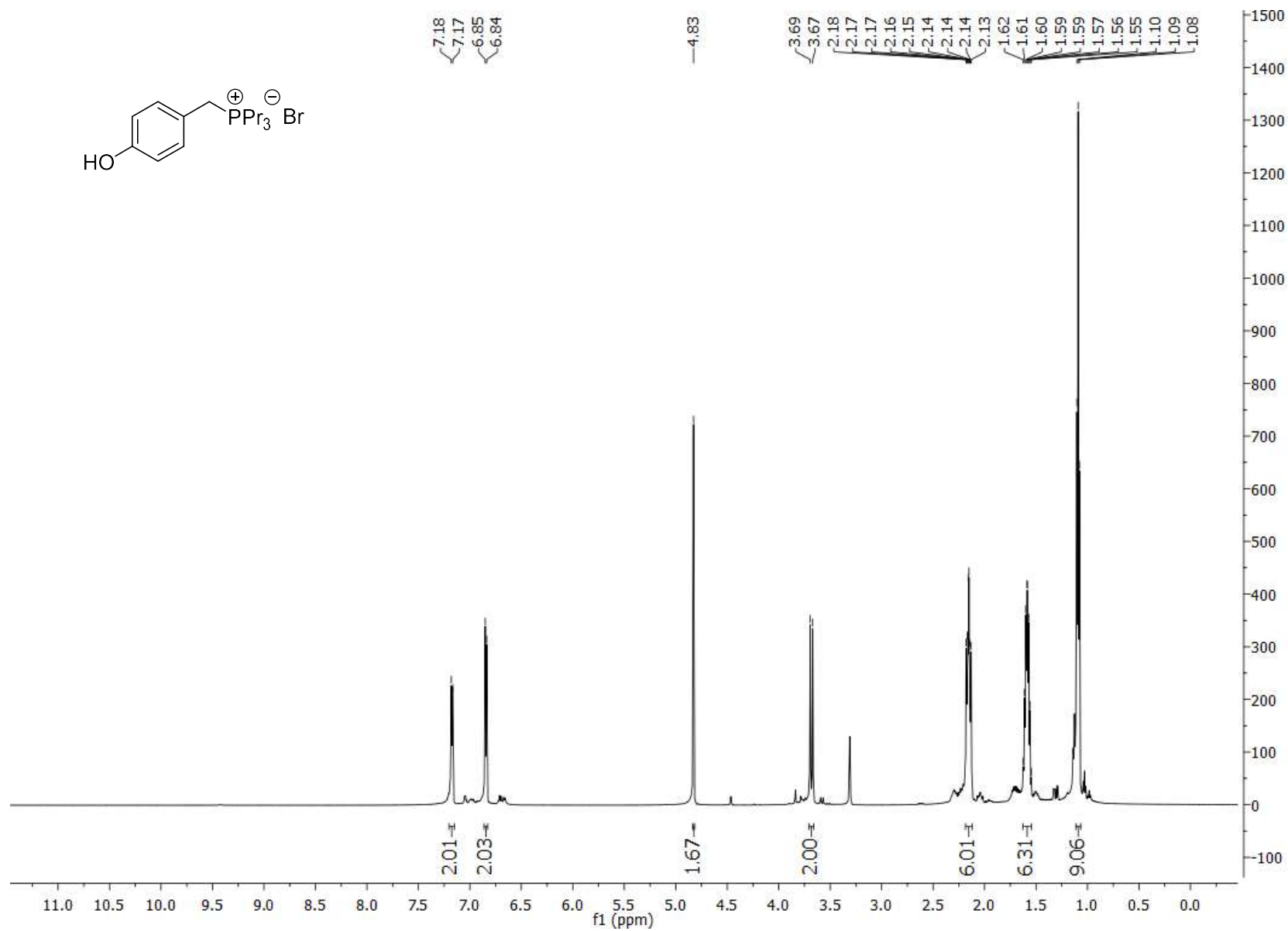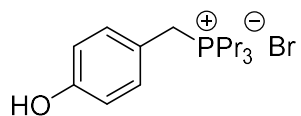
Salt 1b ^{13}C NMR
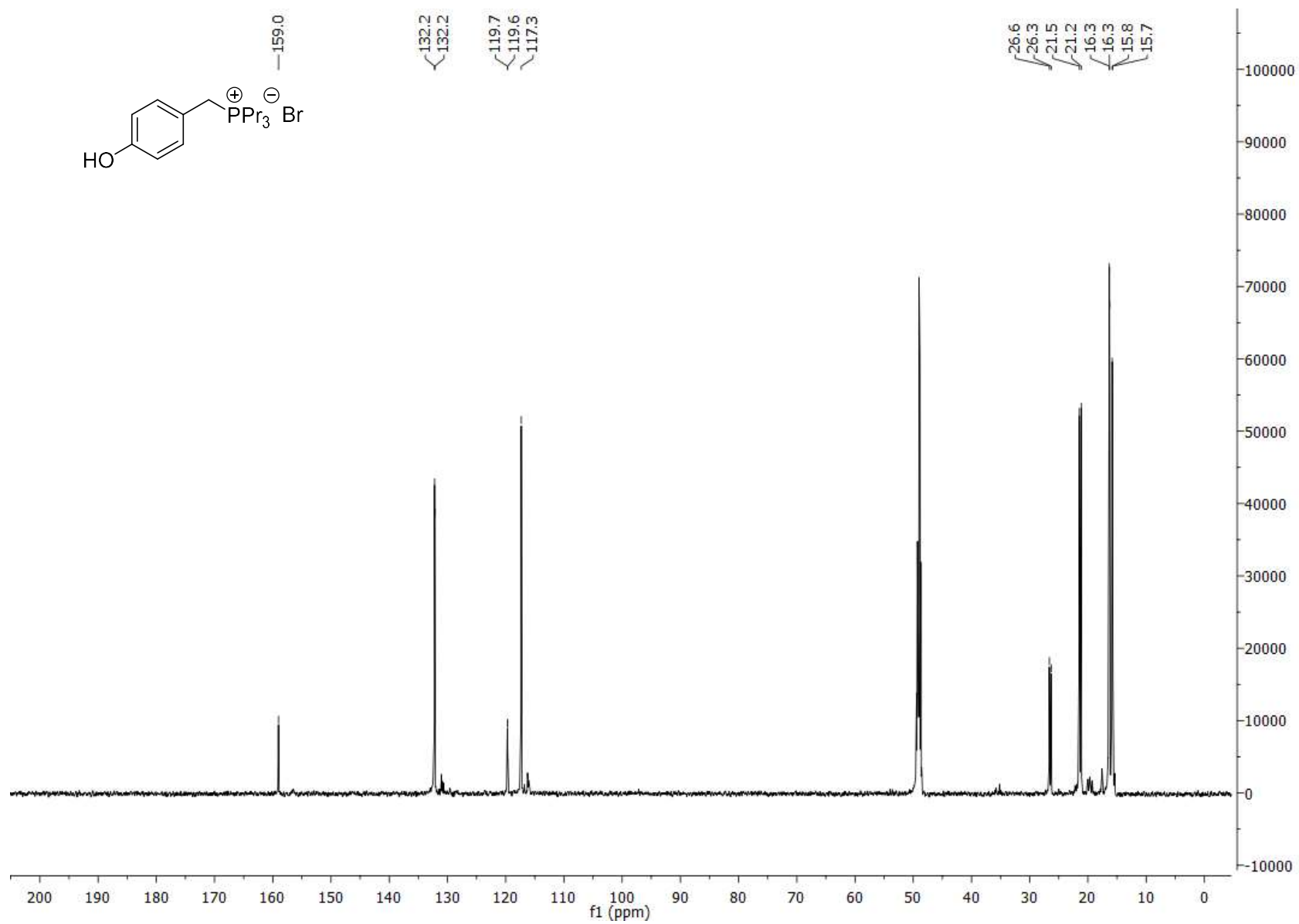
Salt 1b ^{31}P NMR
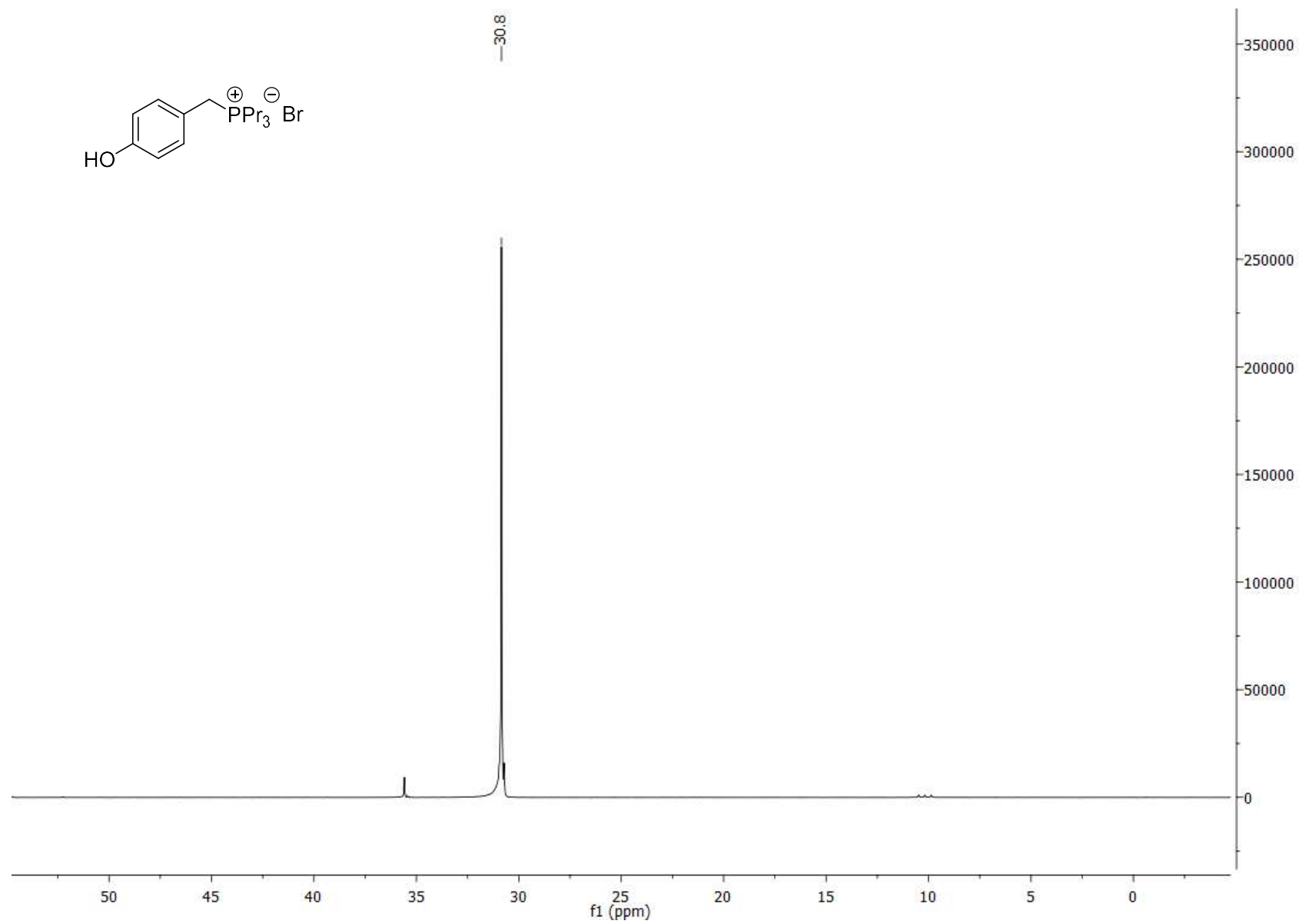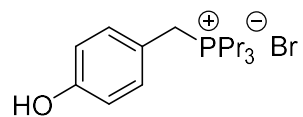
Salt 1c ^{1}H NMR
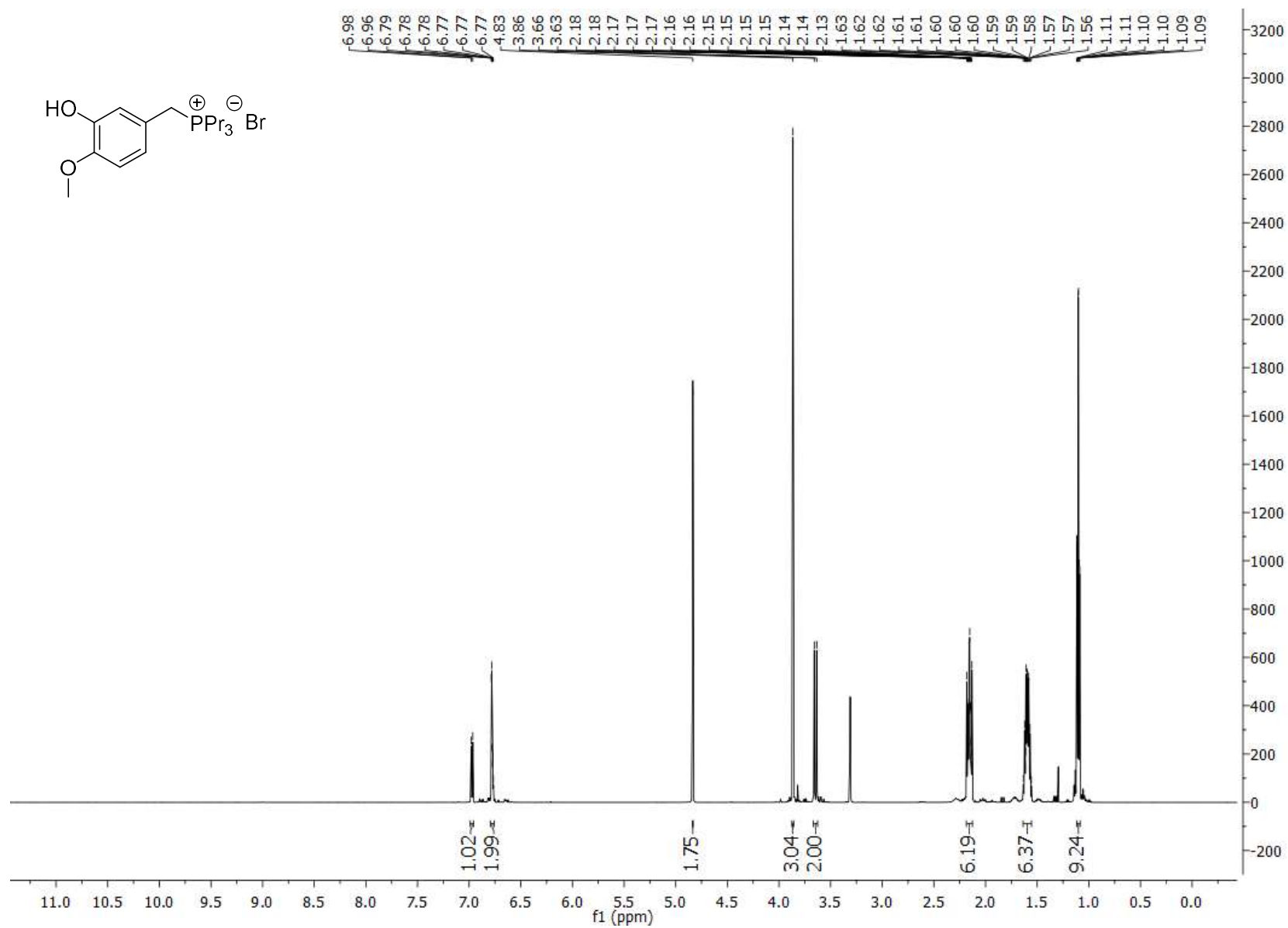
Salt 1c ^{13}C NMR
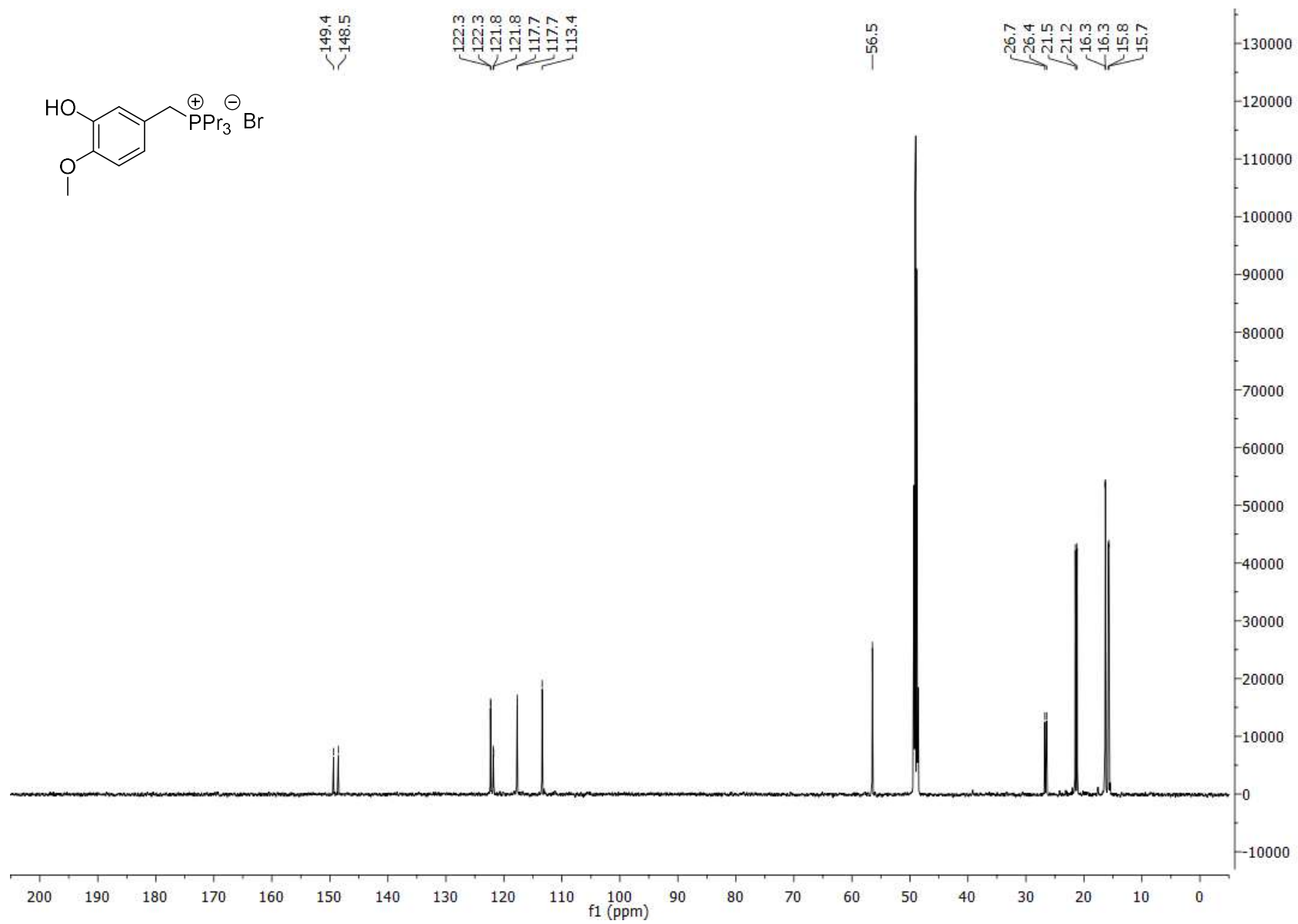
Salt 1c ³¹P NMR
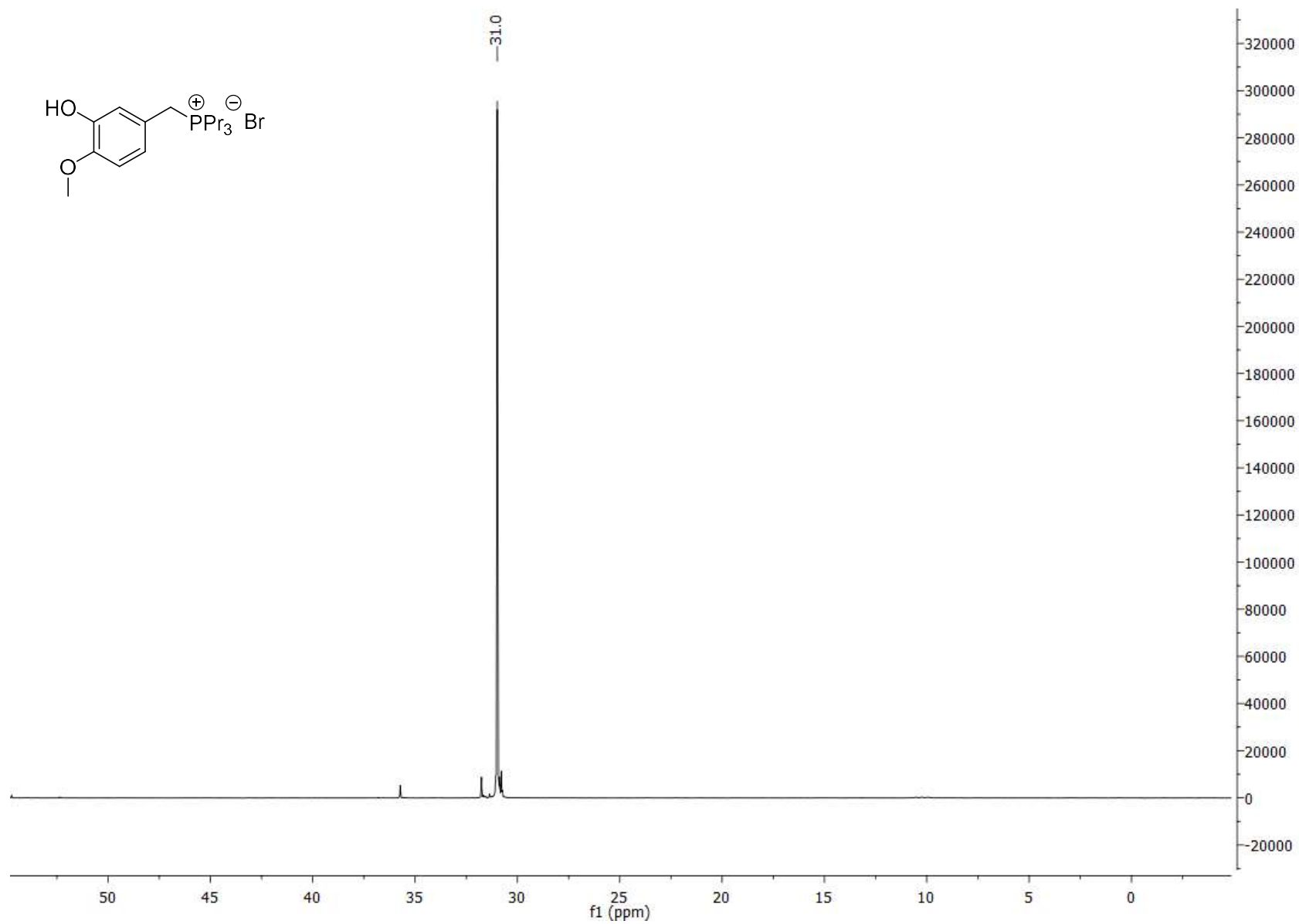
Salt 1d ^{1}H NMR
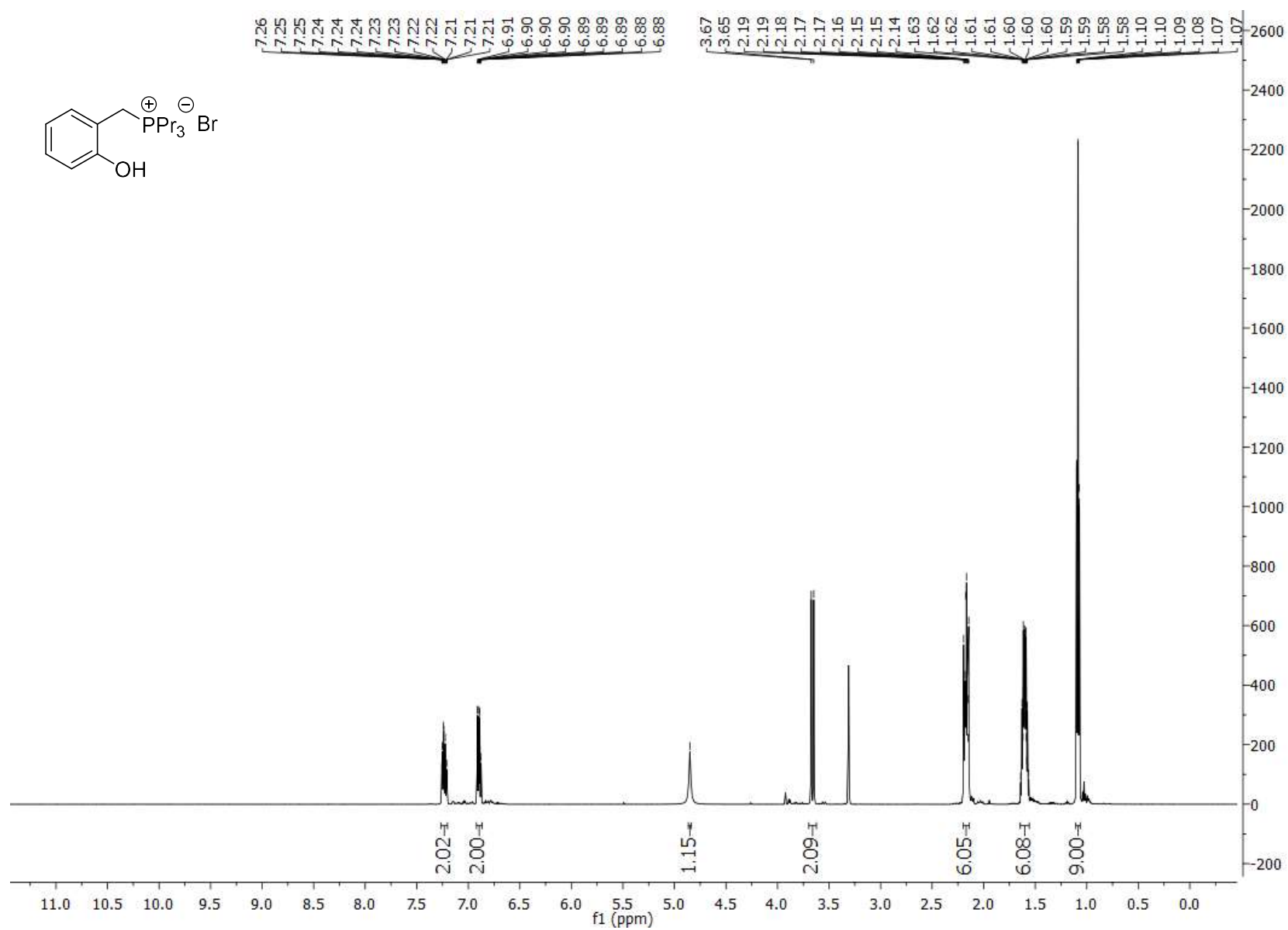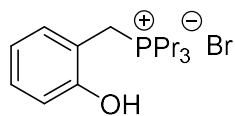
Salt 1d ^{13}C NMR
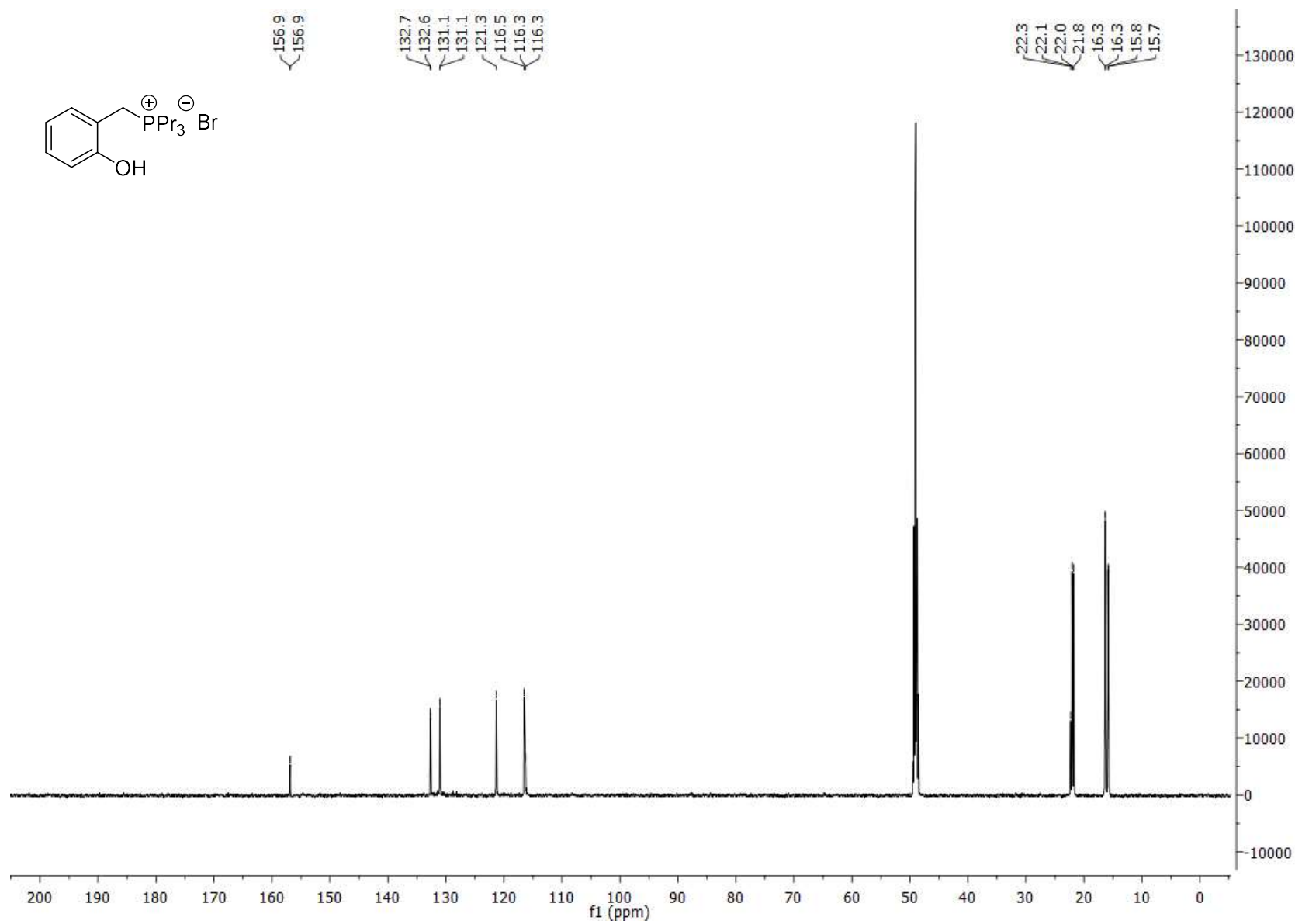
Salt 1d ^{31}P NMR
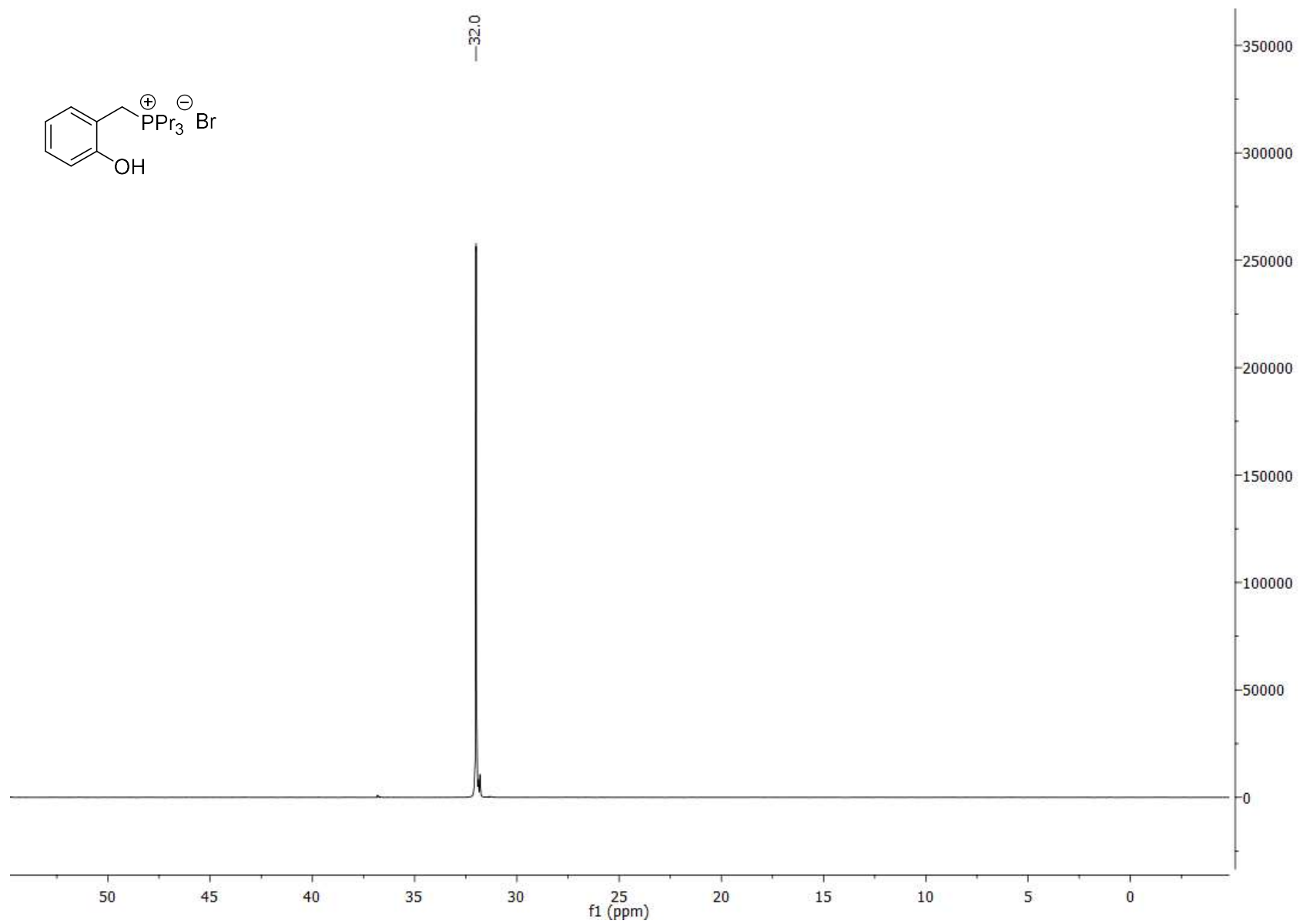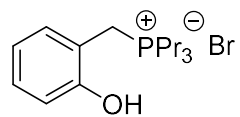
2a ¹H NMR
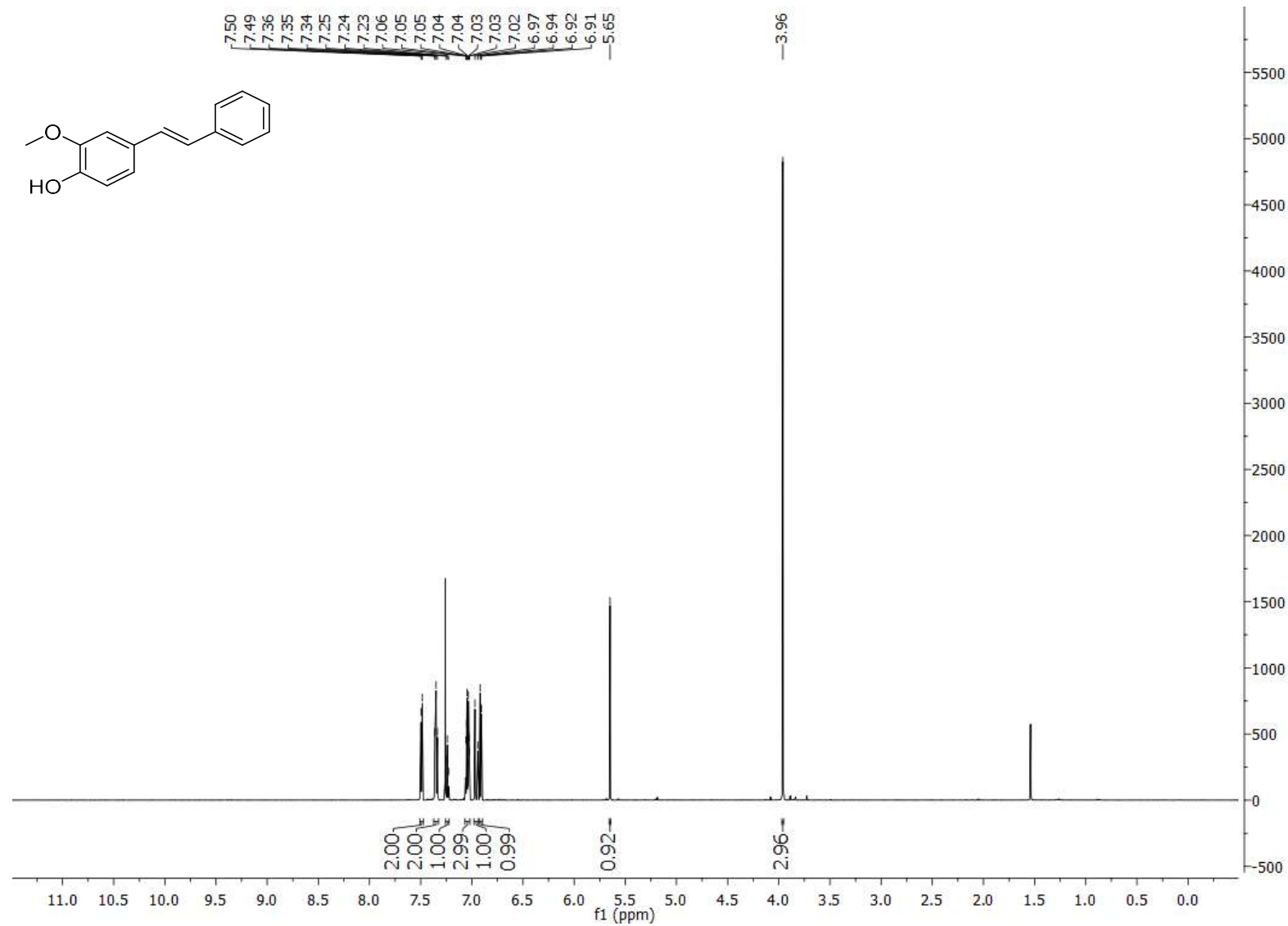
2a ^{13}C NMR
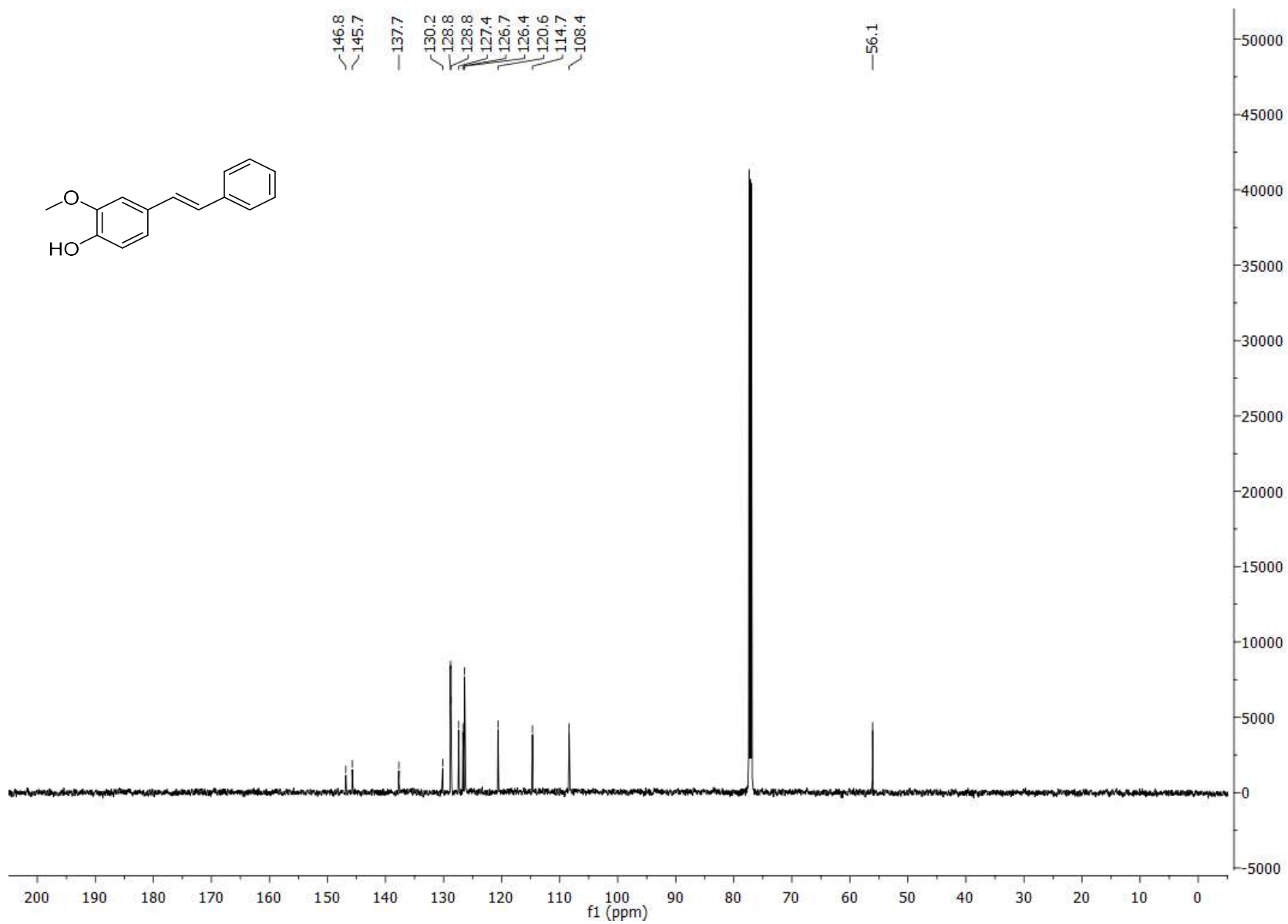
2b ¹H NMR
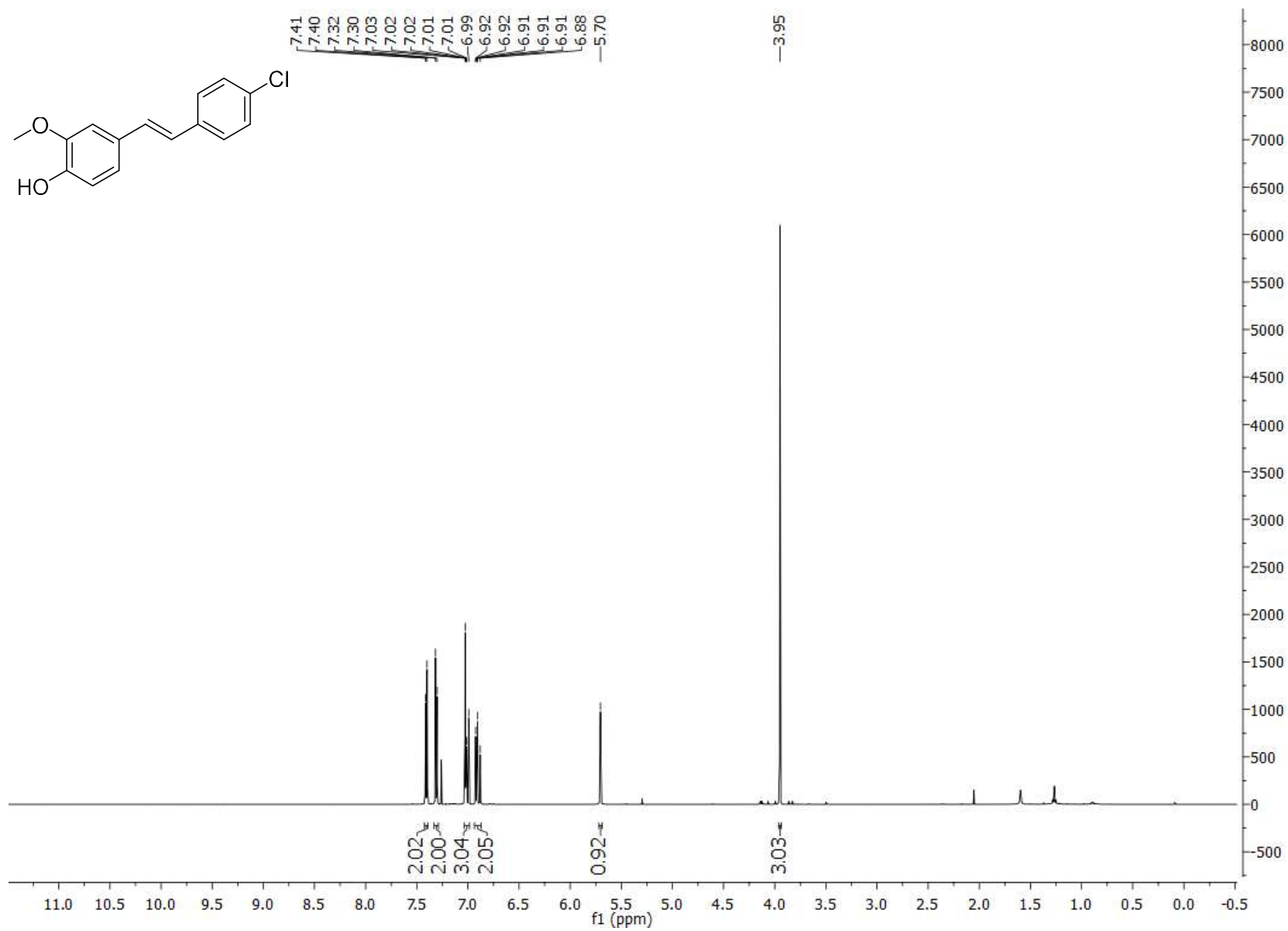
2b ¹³C NMR
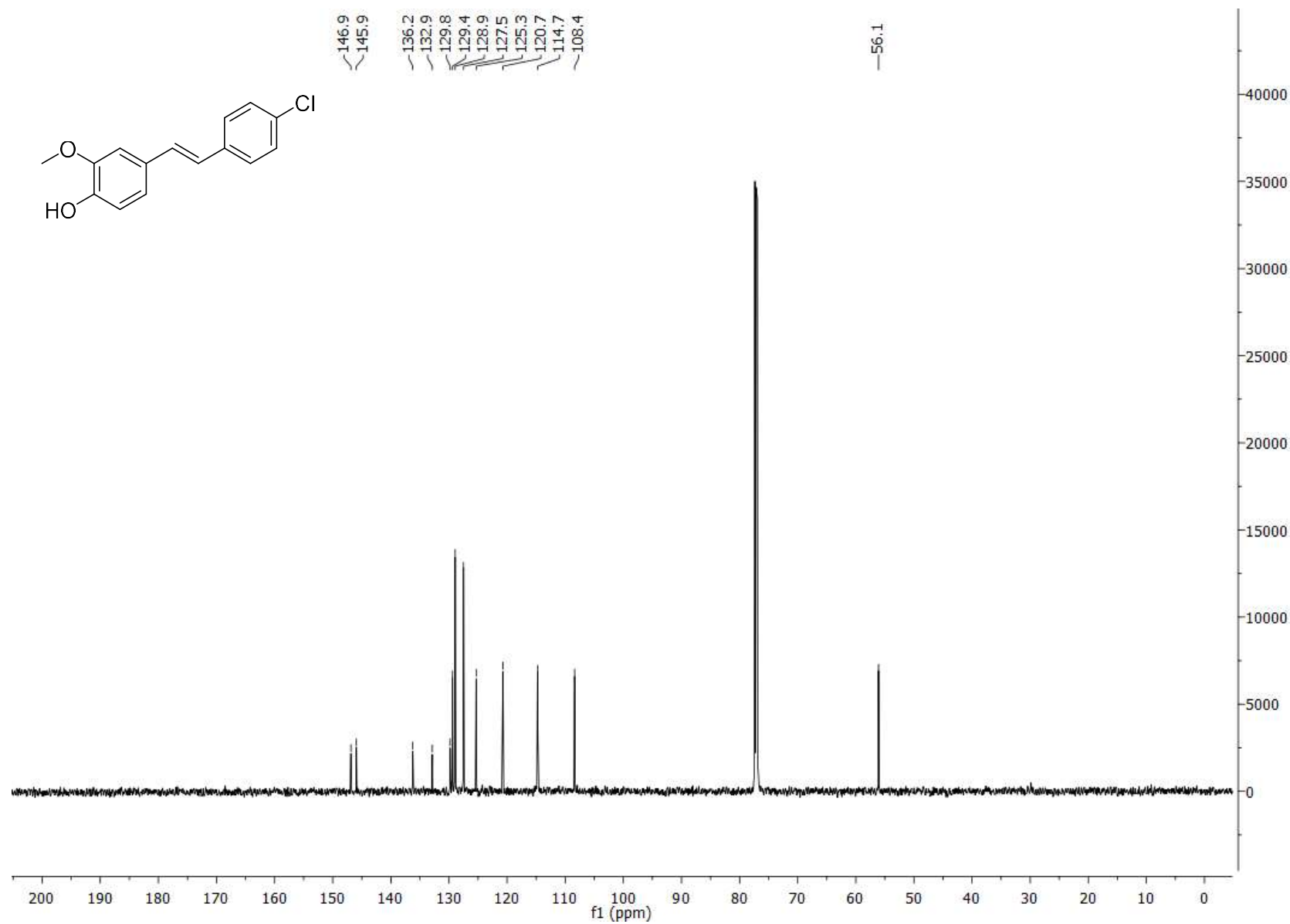
2c ^{1}H NMR
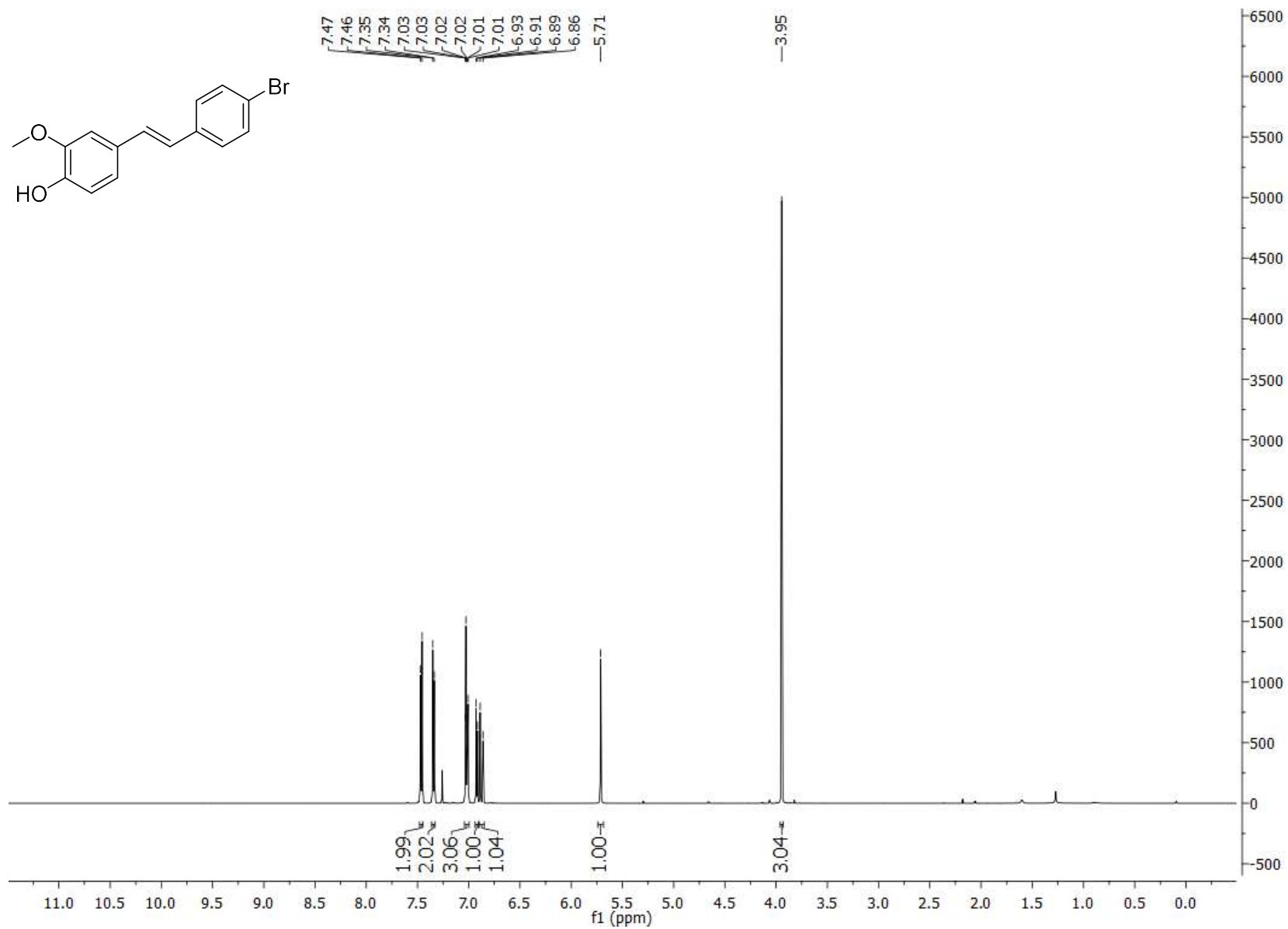
2c ¹³C NMR
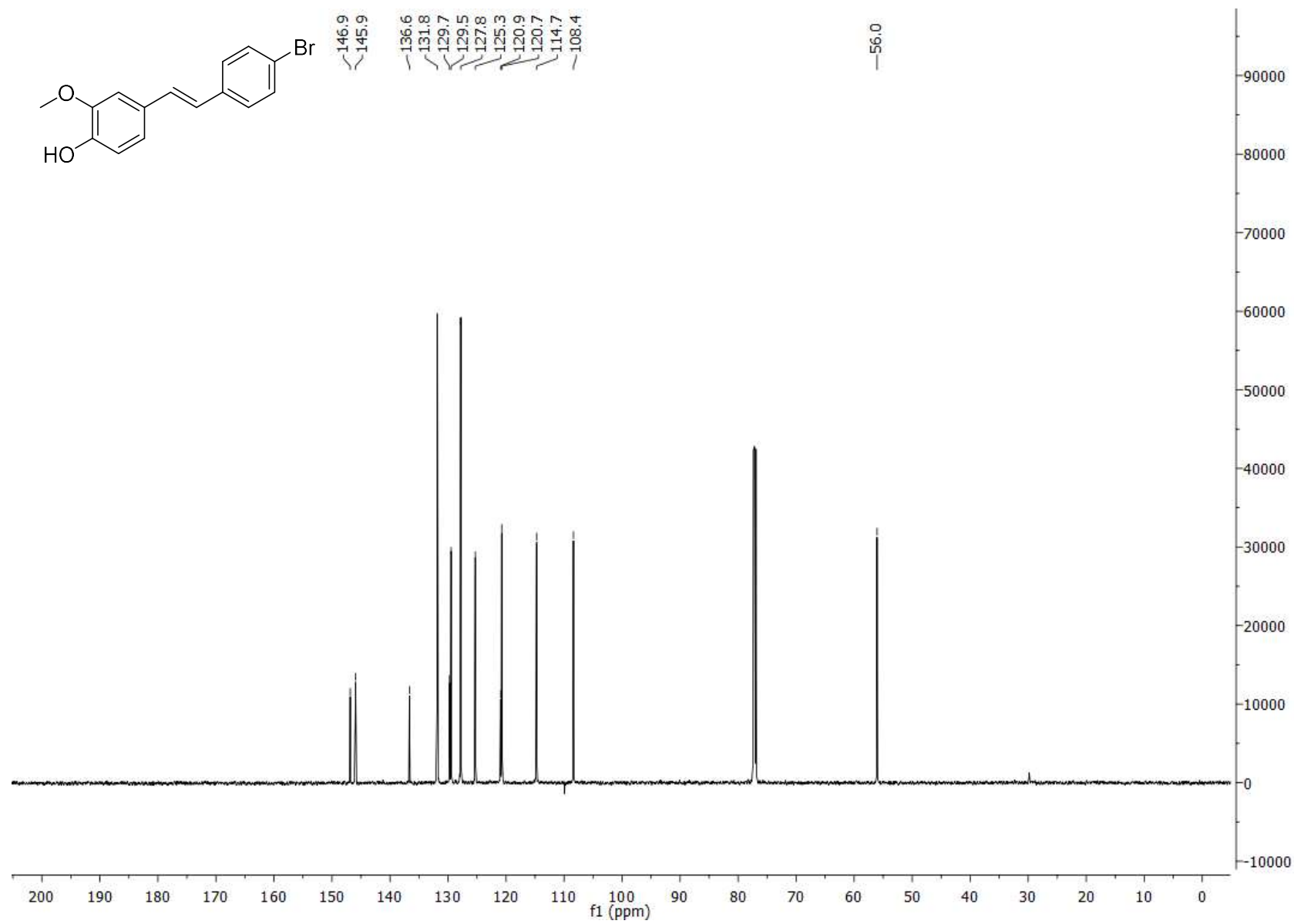
2d ^{1}H NMR
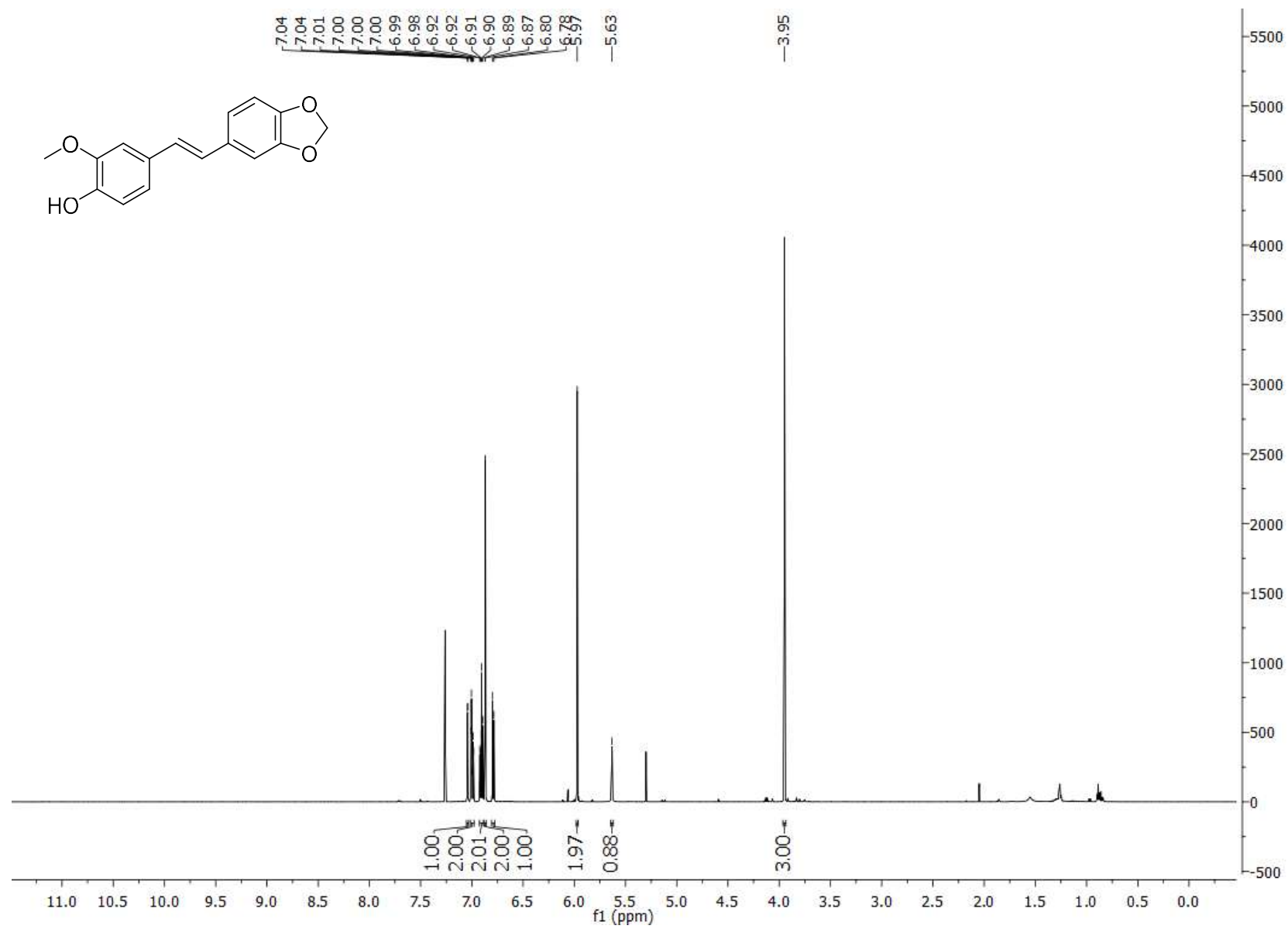
2d ^{13}C NMR
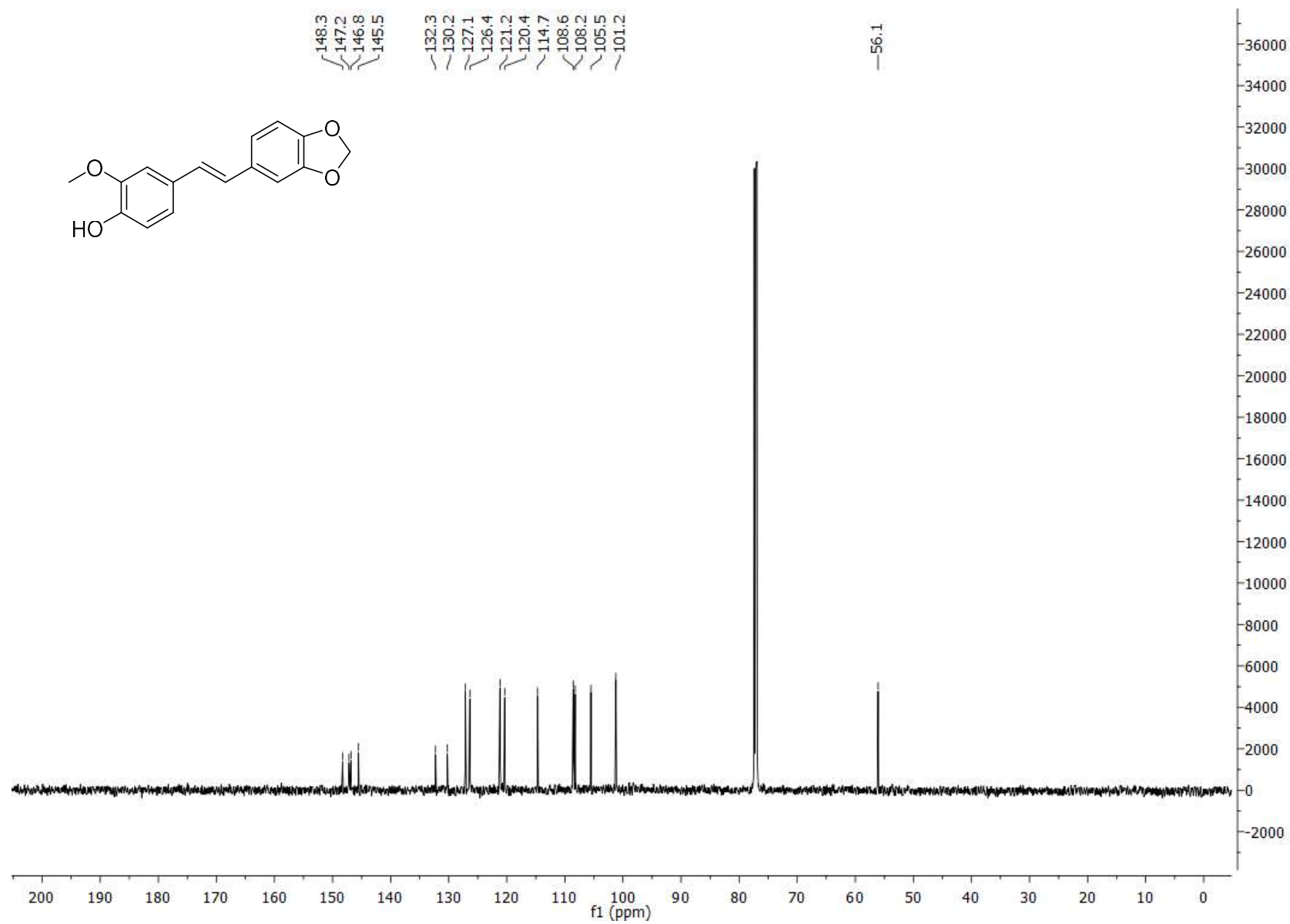
2e ^{1}H NMR
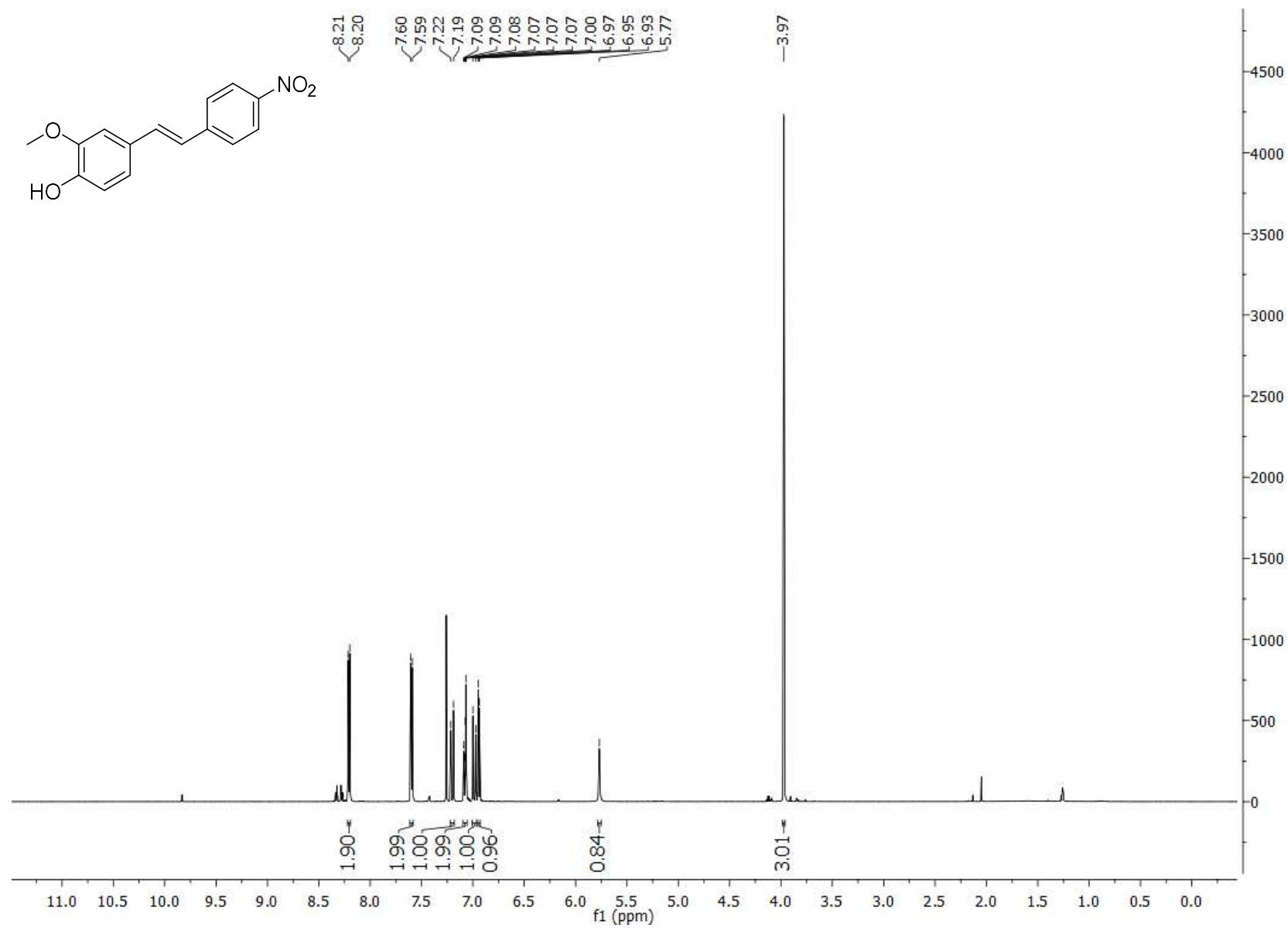
2e ^{13}C NMR
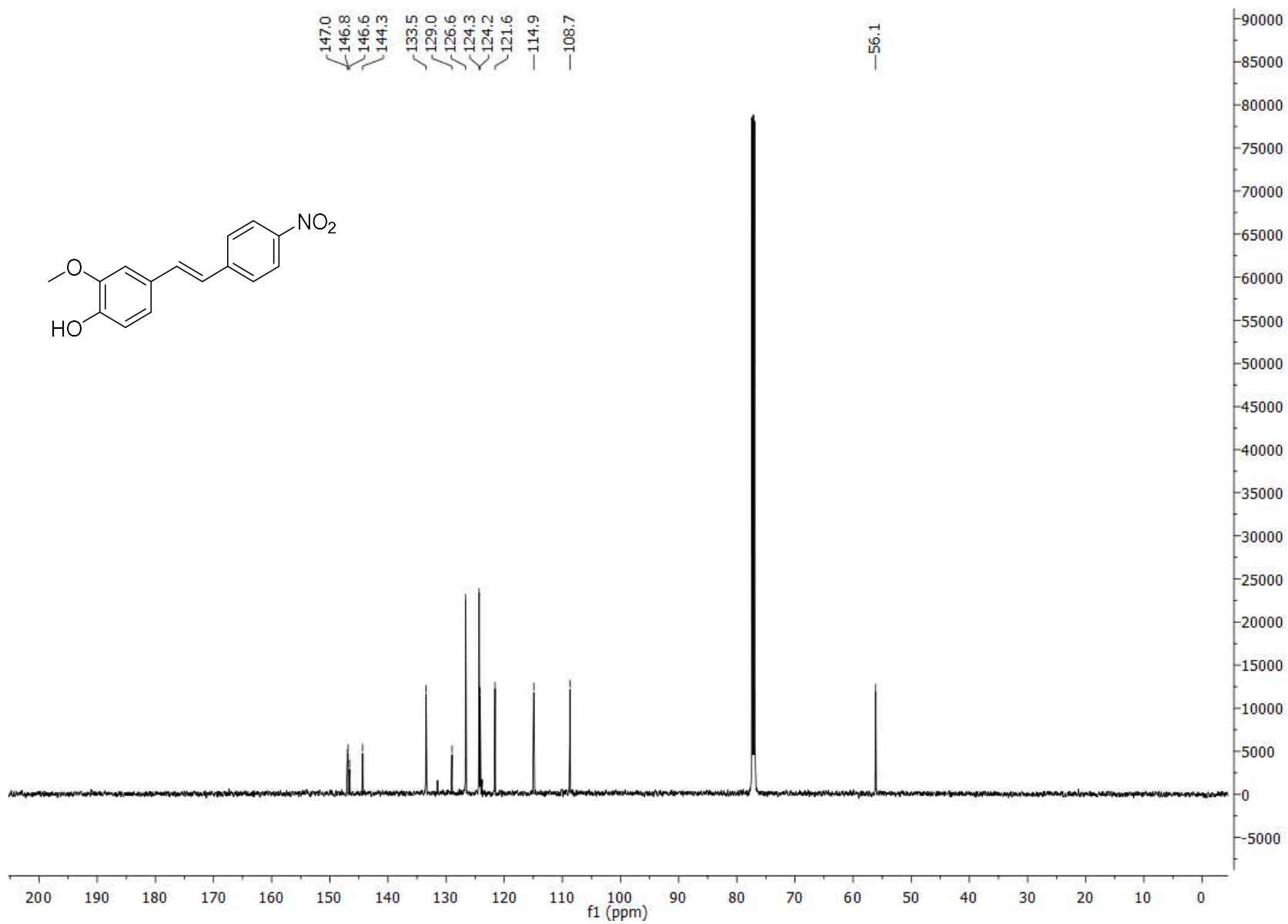
2f ¹H NMR
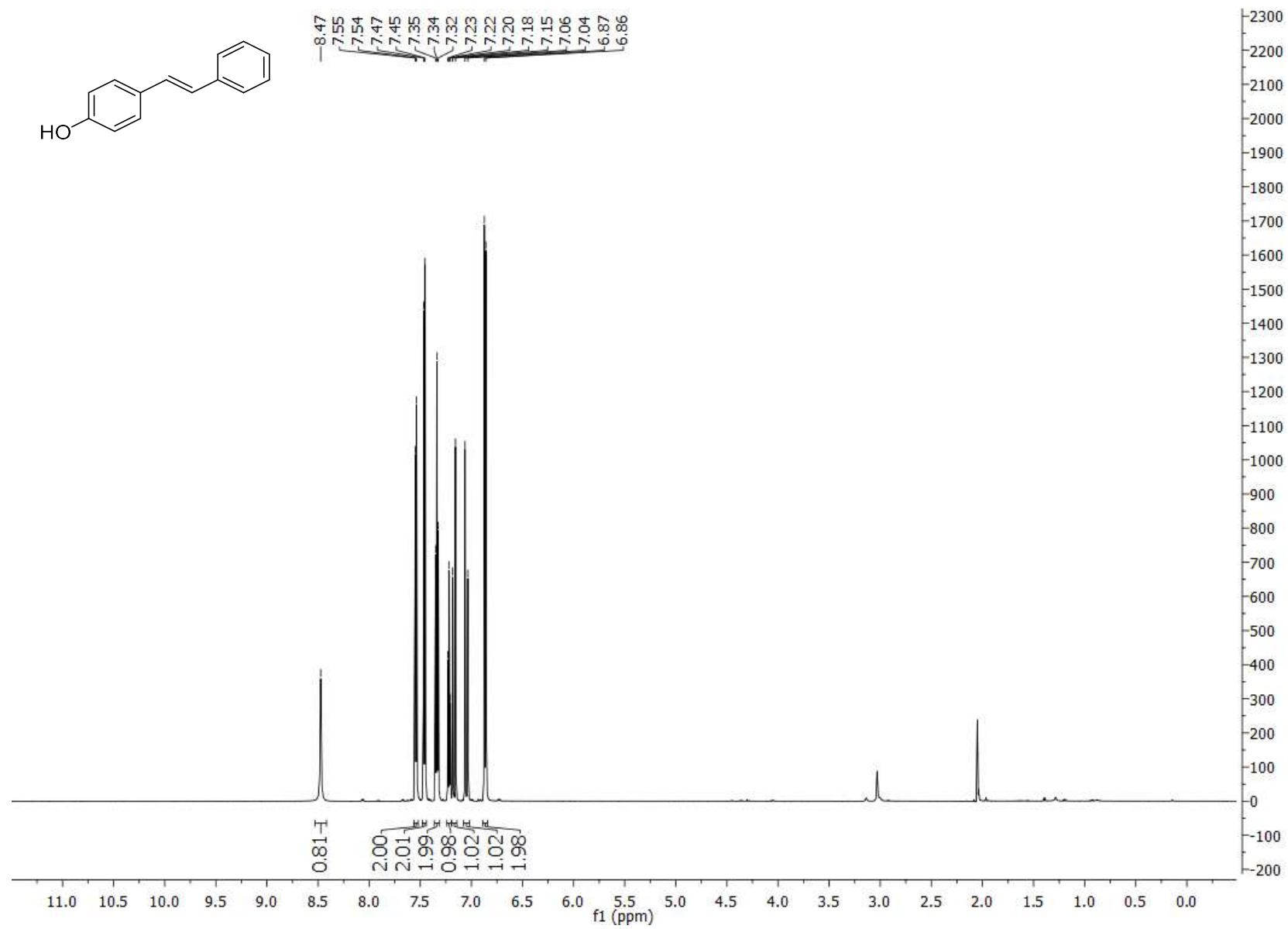
2f ^{13}C NMR
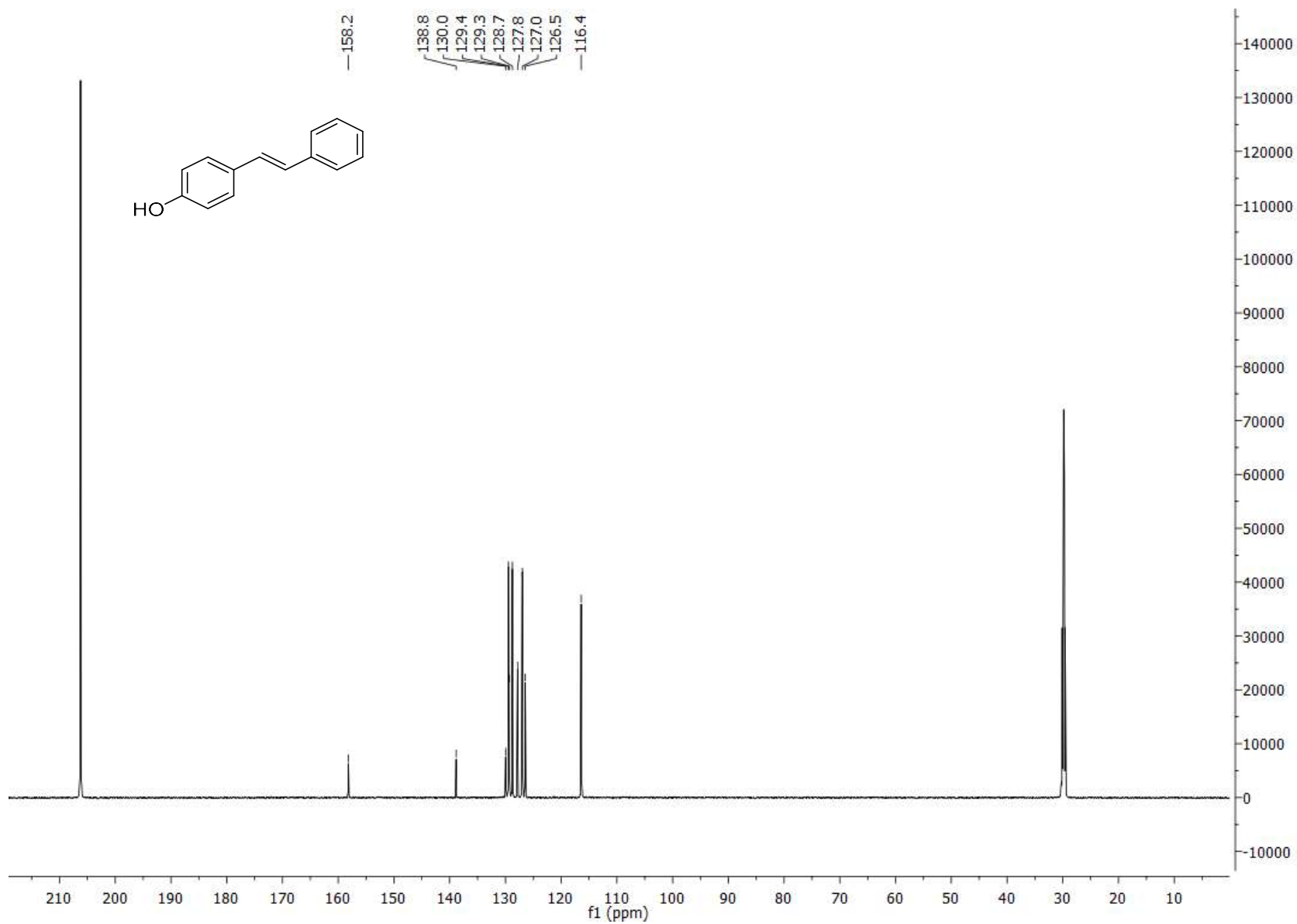
2g ^{1}H NMR
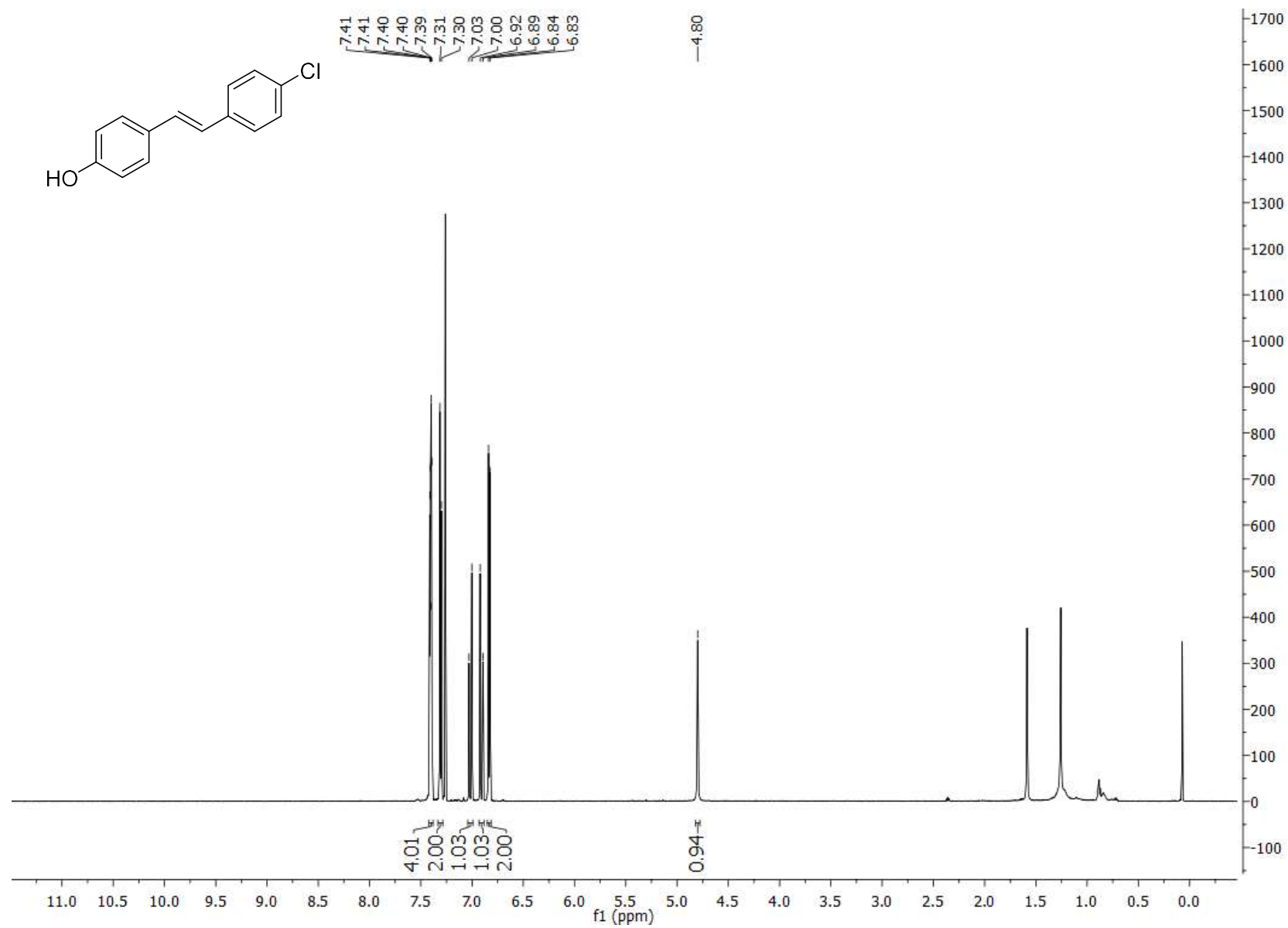
2g ^{13}C NMR
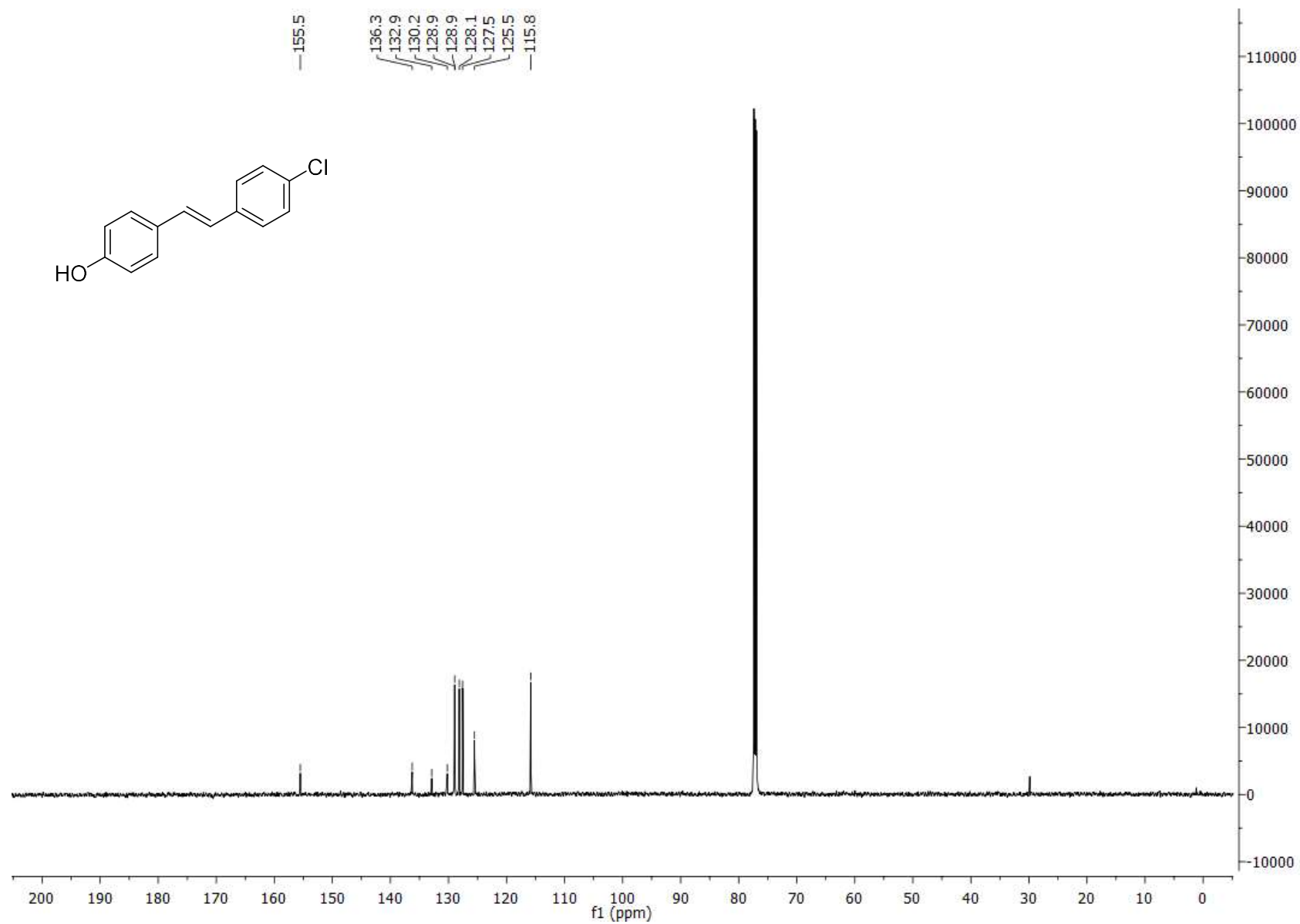
2h ¹H NMR
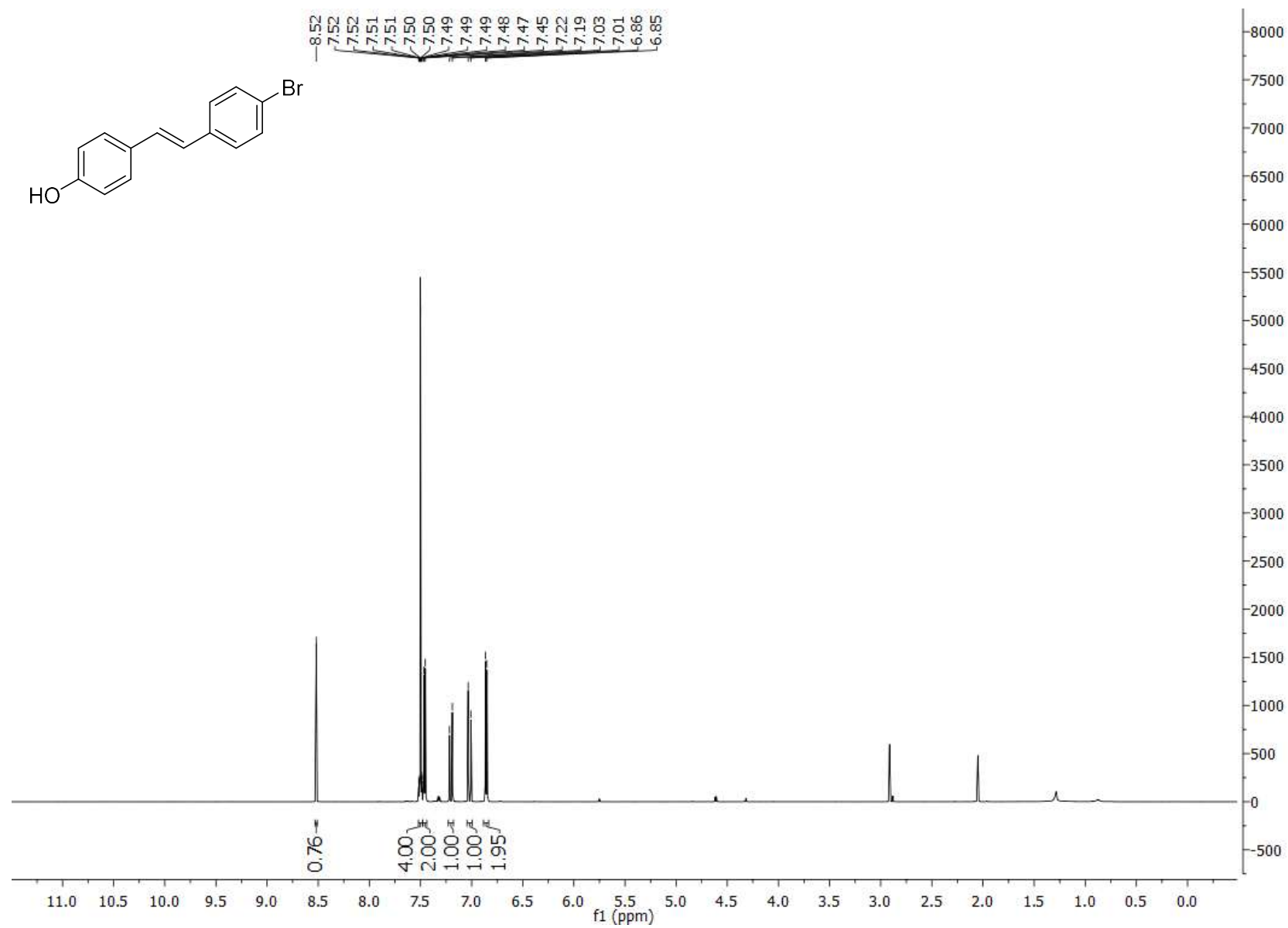
2h ^{13}C NMR
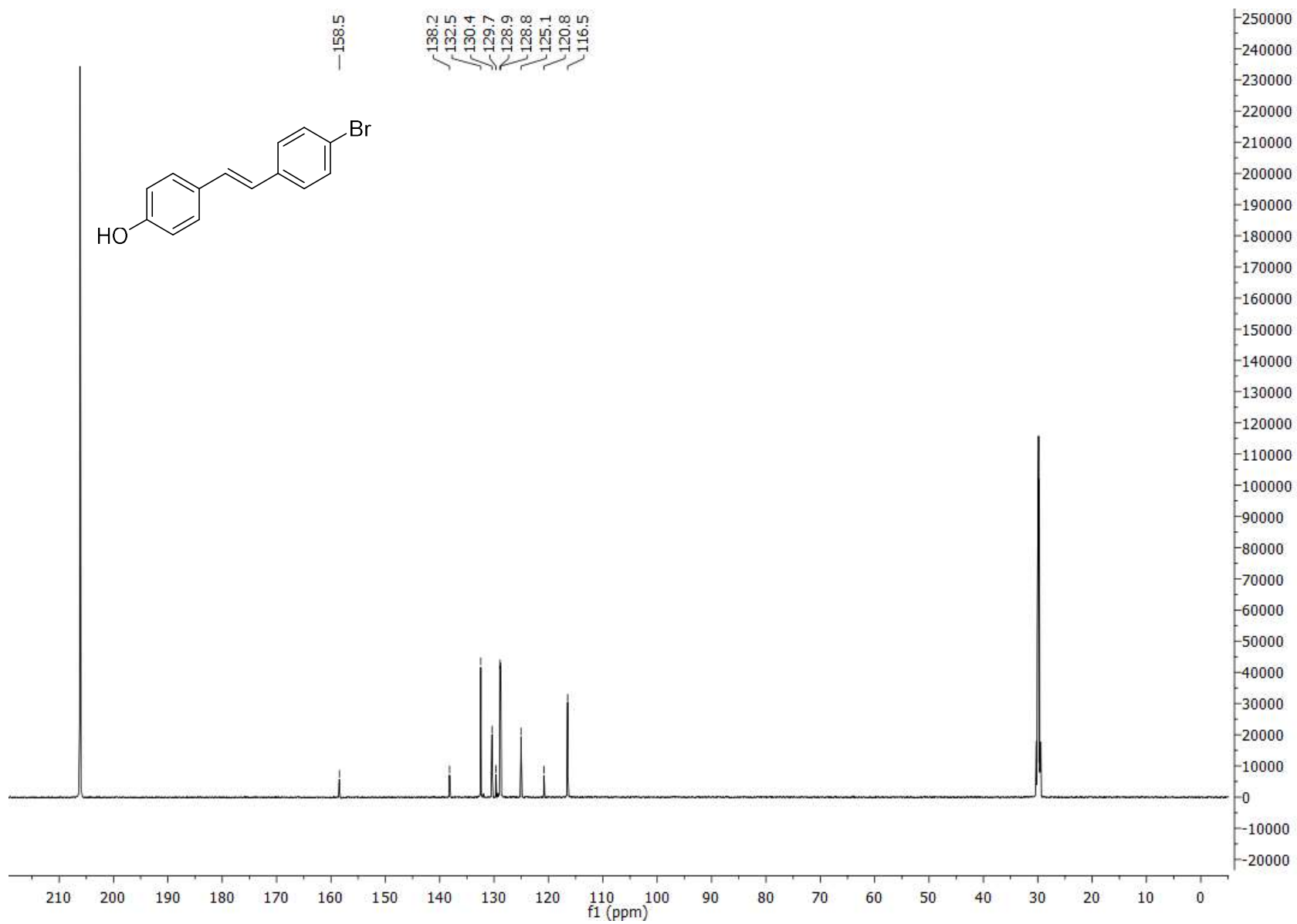
2i ¹H NMR
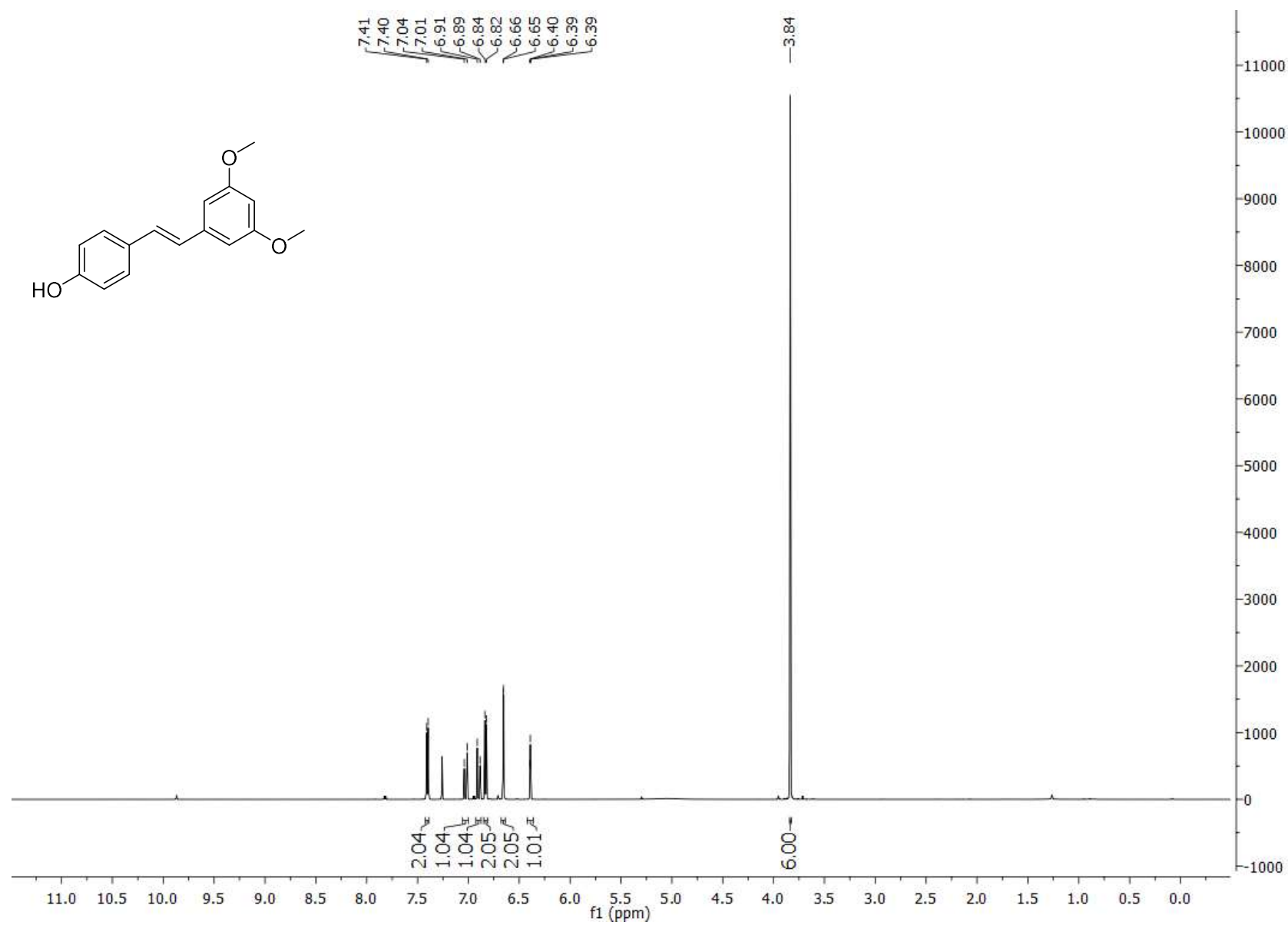
2j ^{1}H NMR
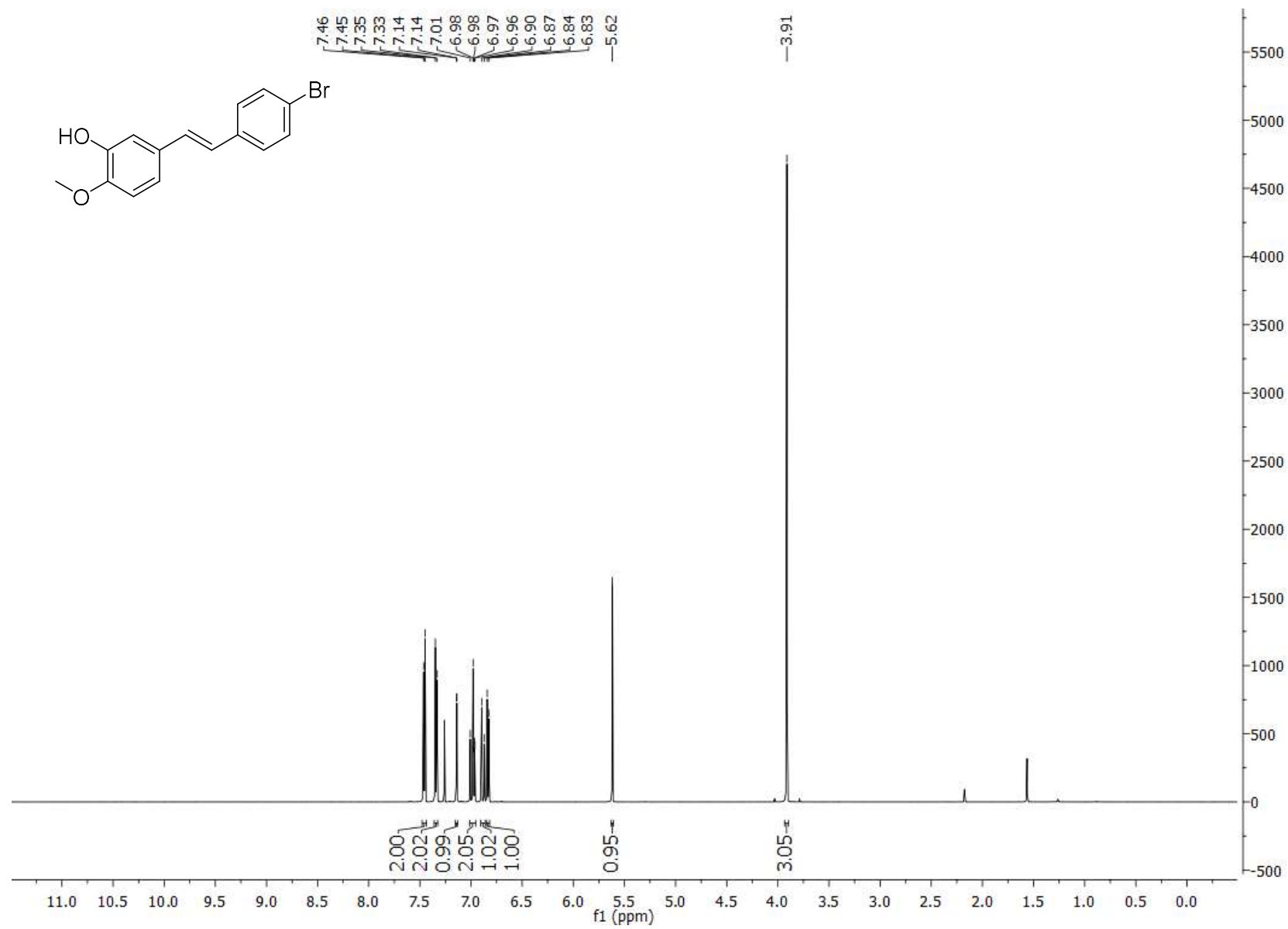
2j ¹³C NMR
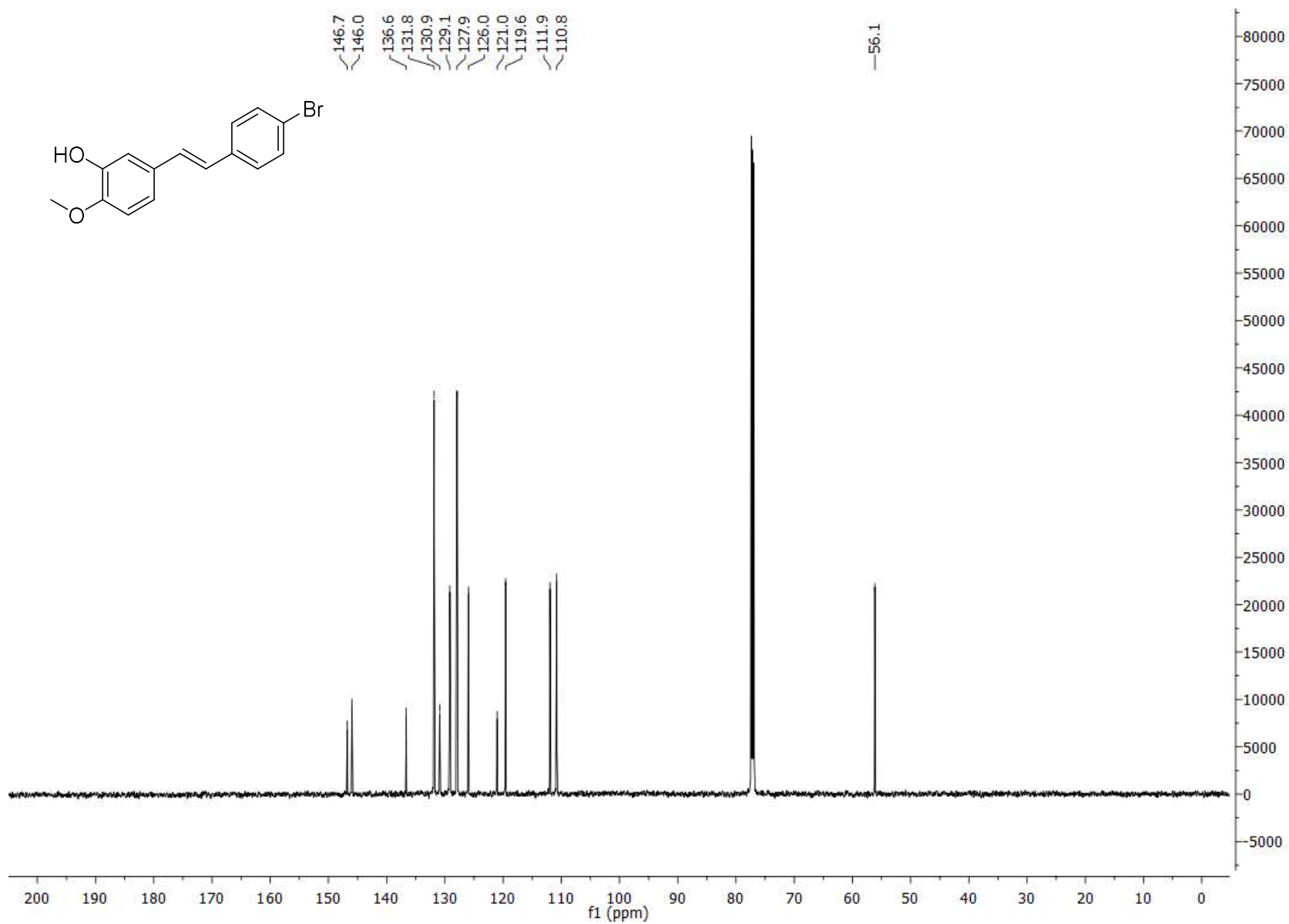
2k ^{1}H NMR

2k ^{13}C NMR

2l ¹H NMR
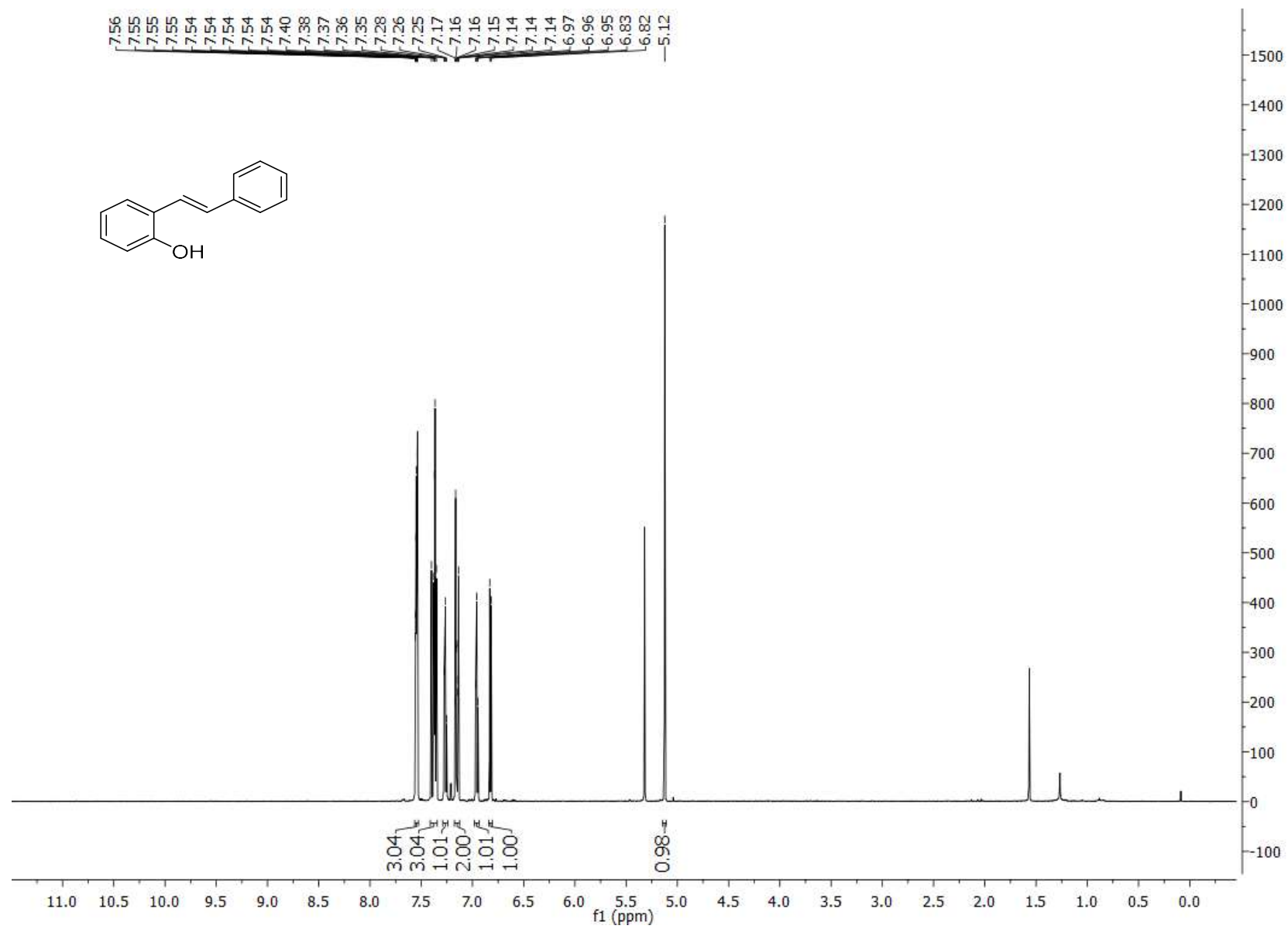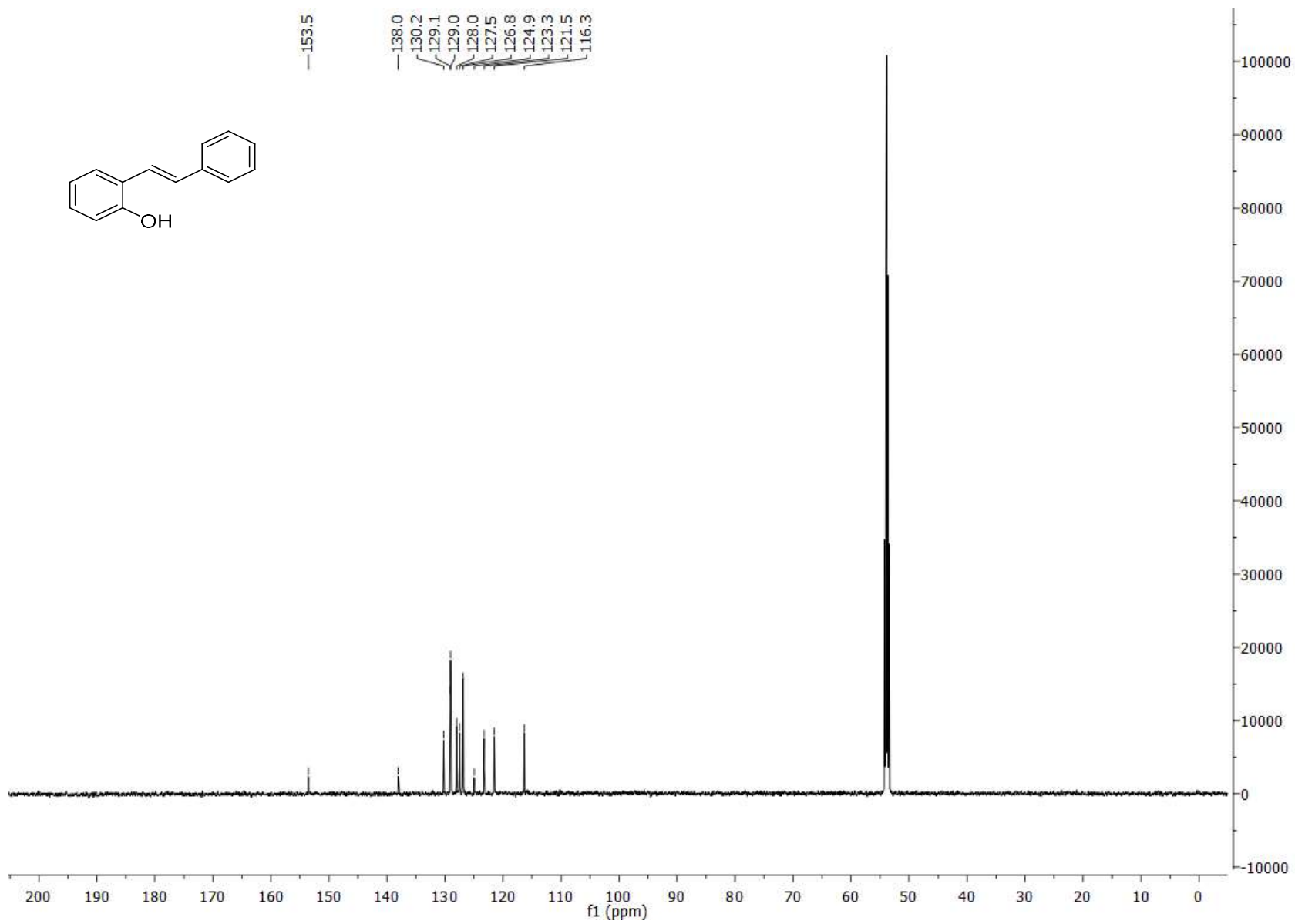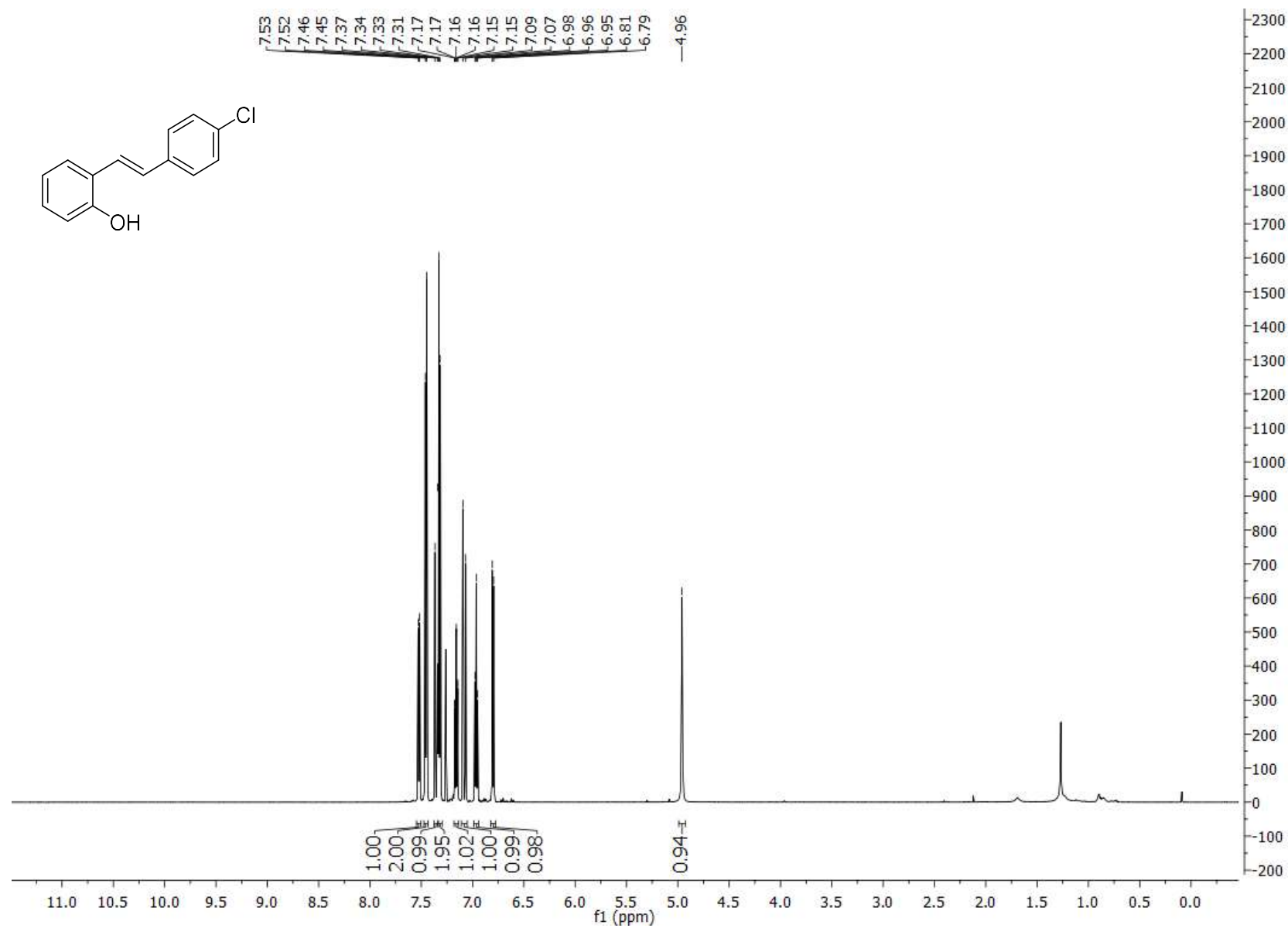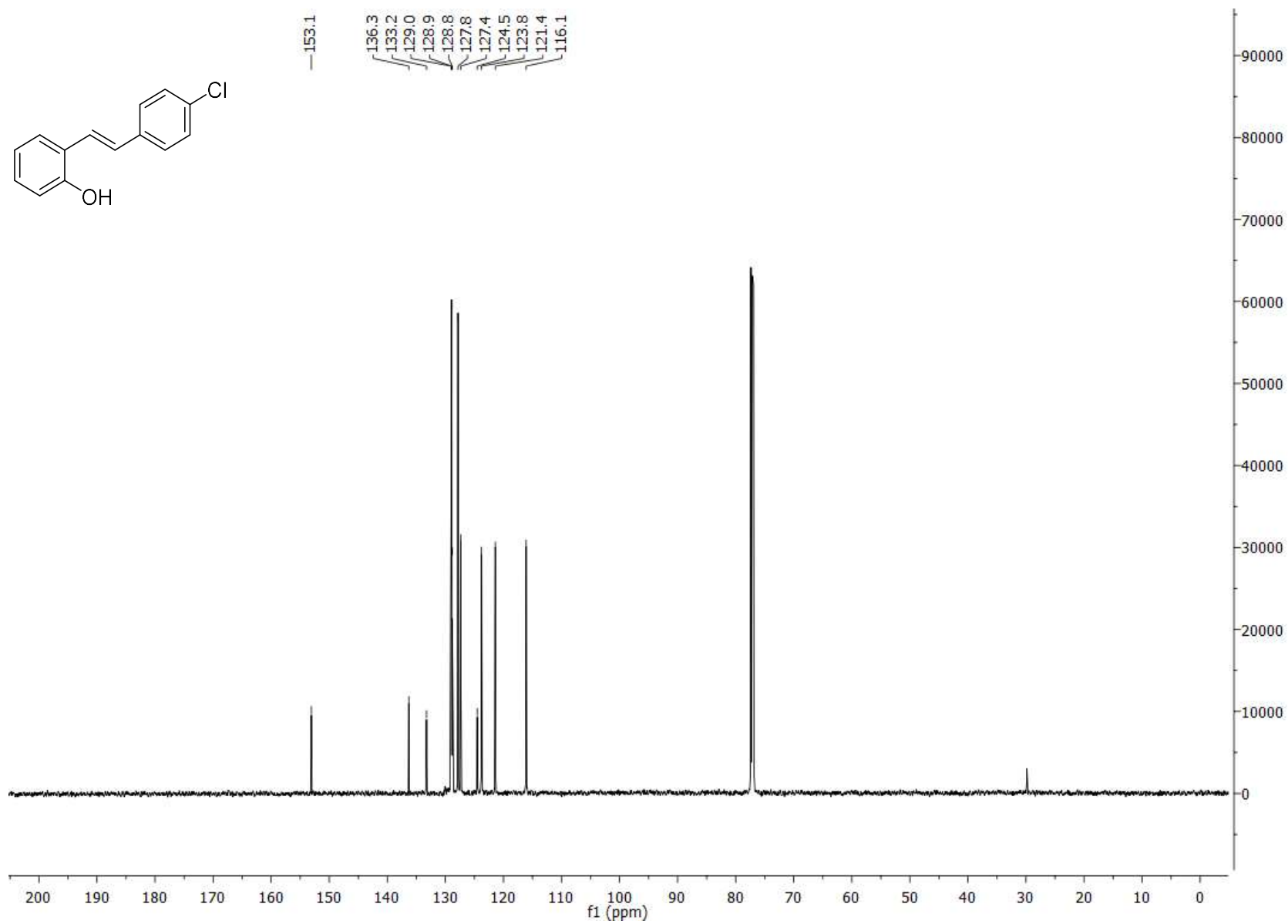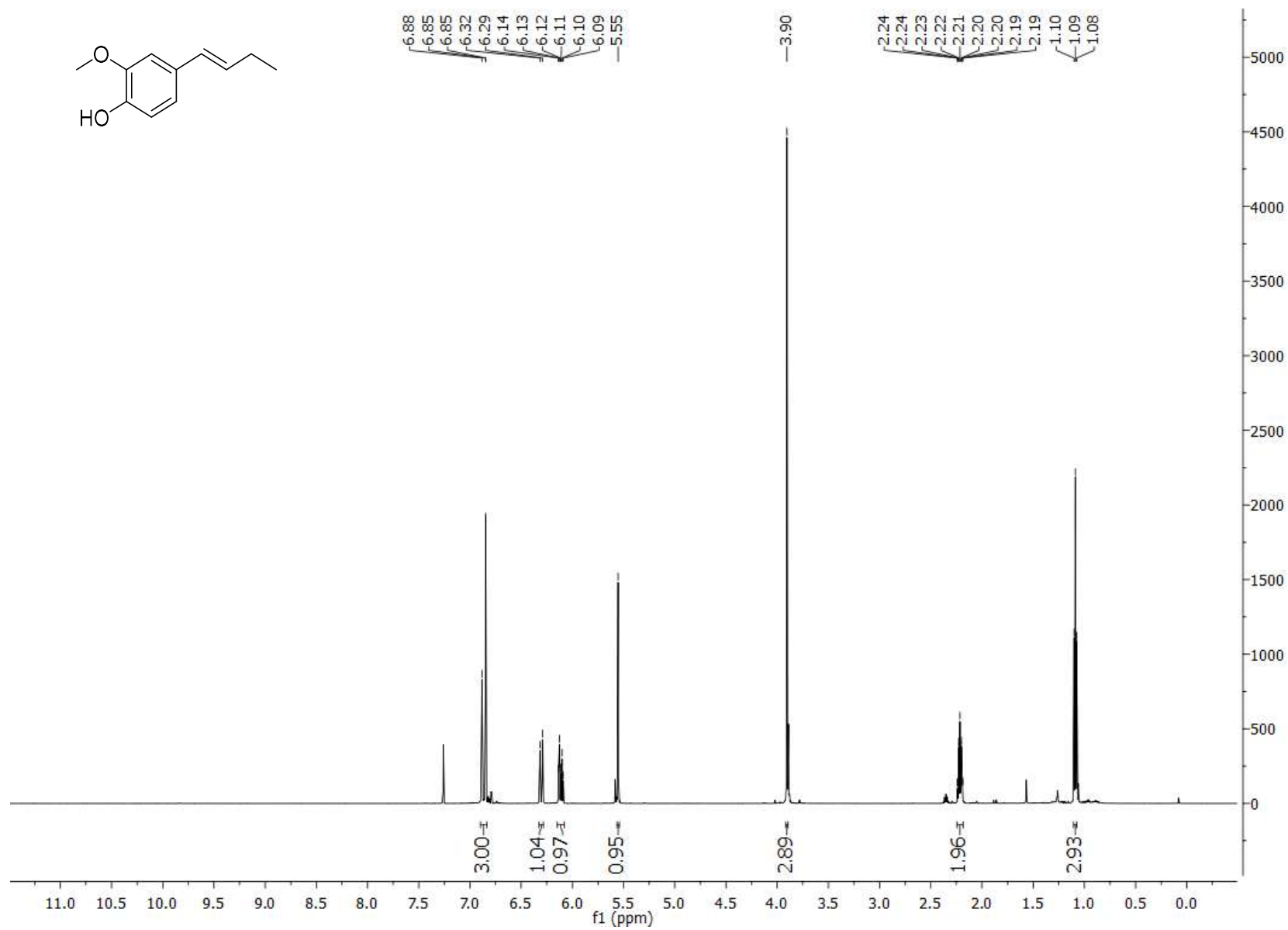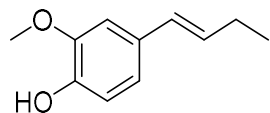
2l ^{13}C NMR

3a ^{1}H NMR

3a ^{13}C NMR
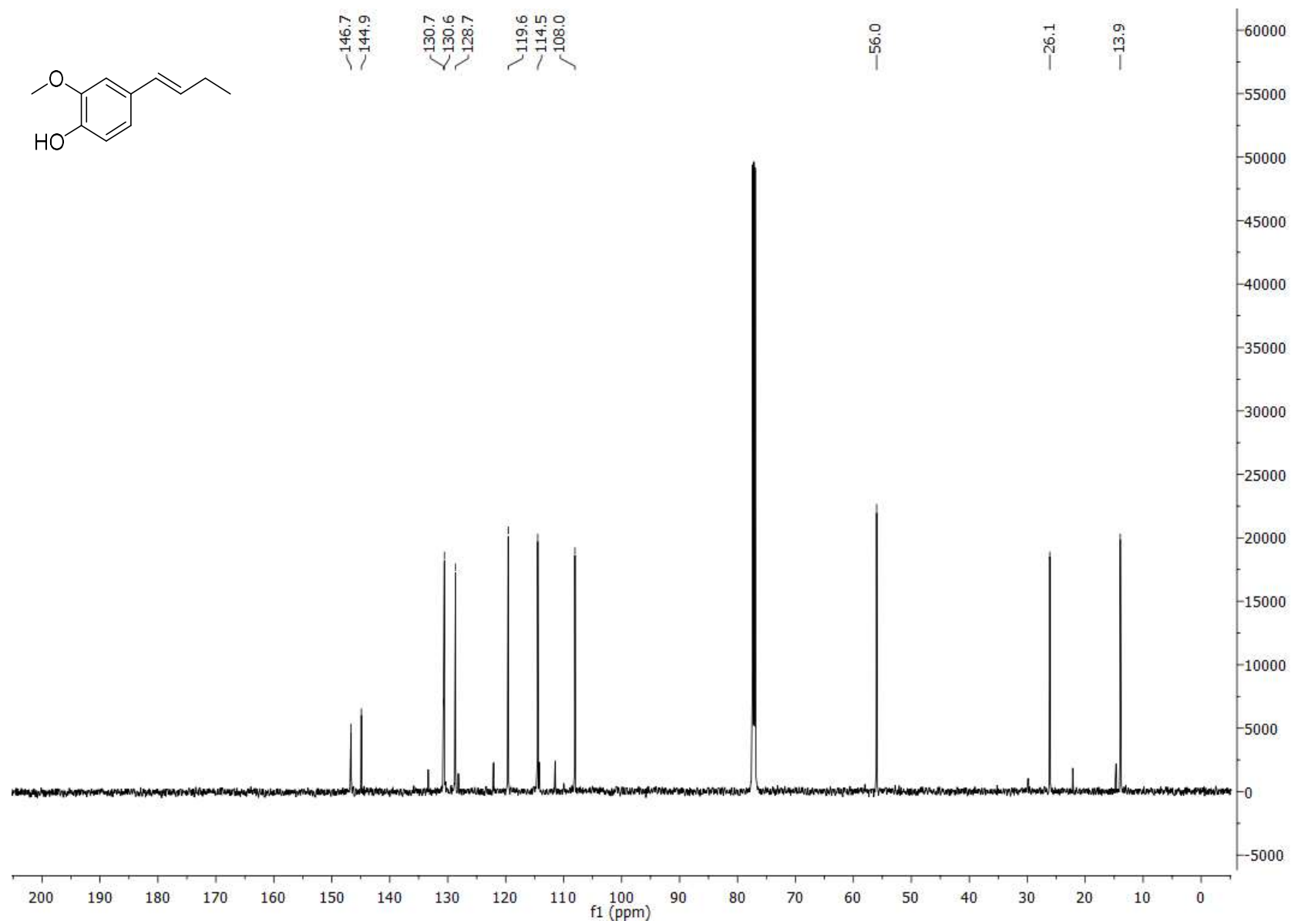
3b ¹H NMR
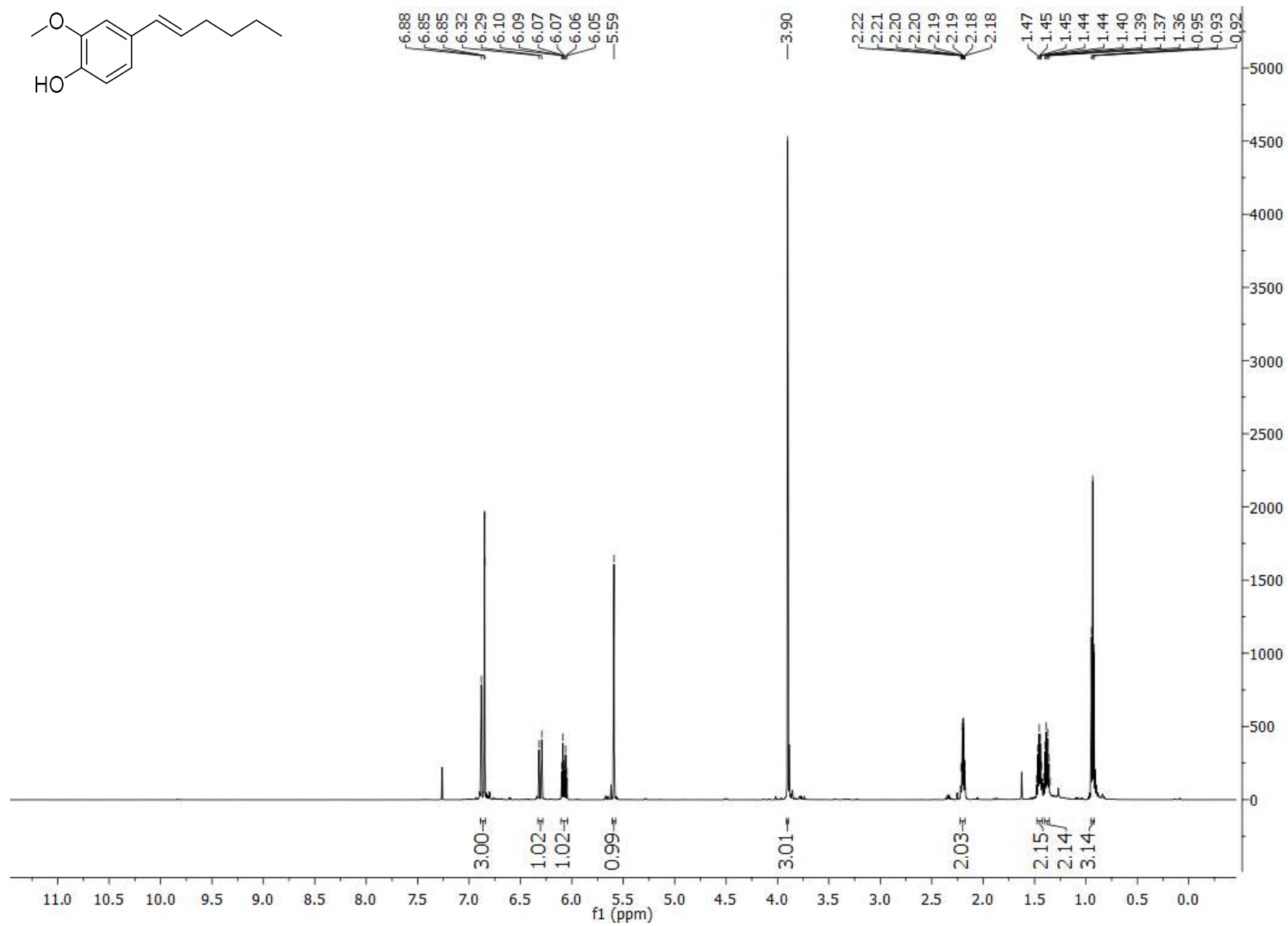
3b ^{13}C NMR
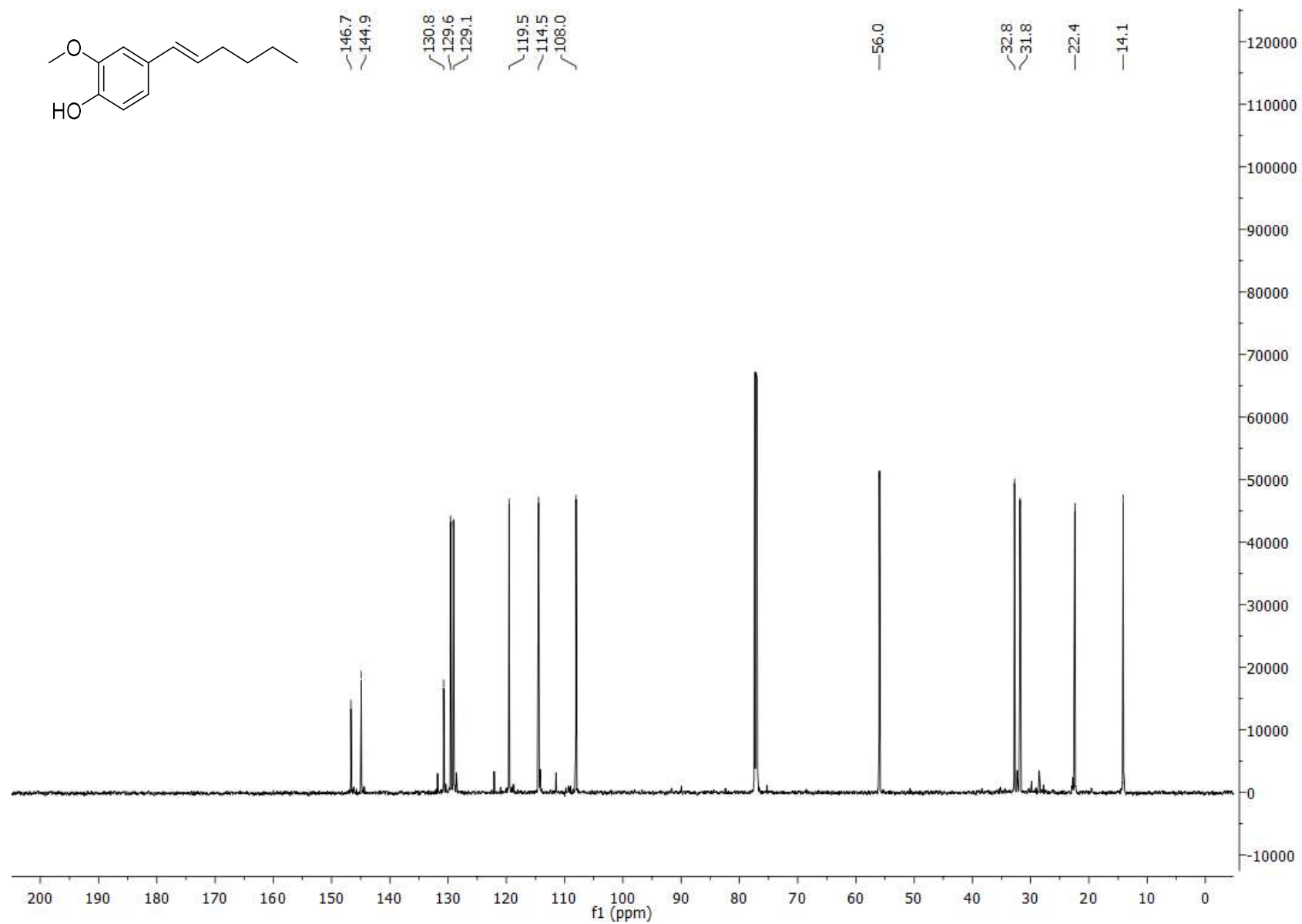
3c ¹H NMR
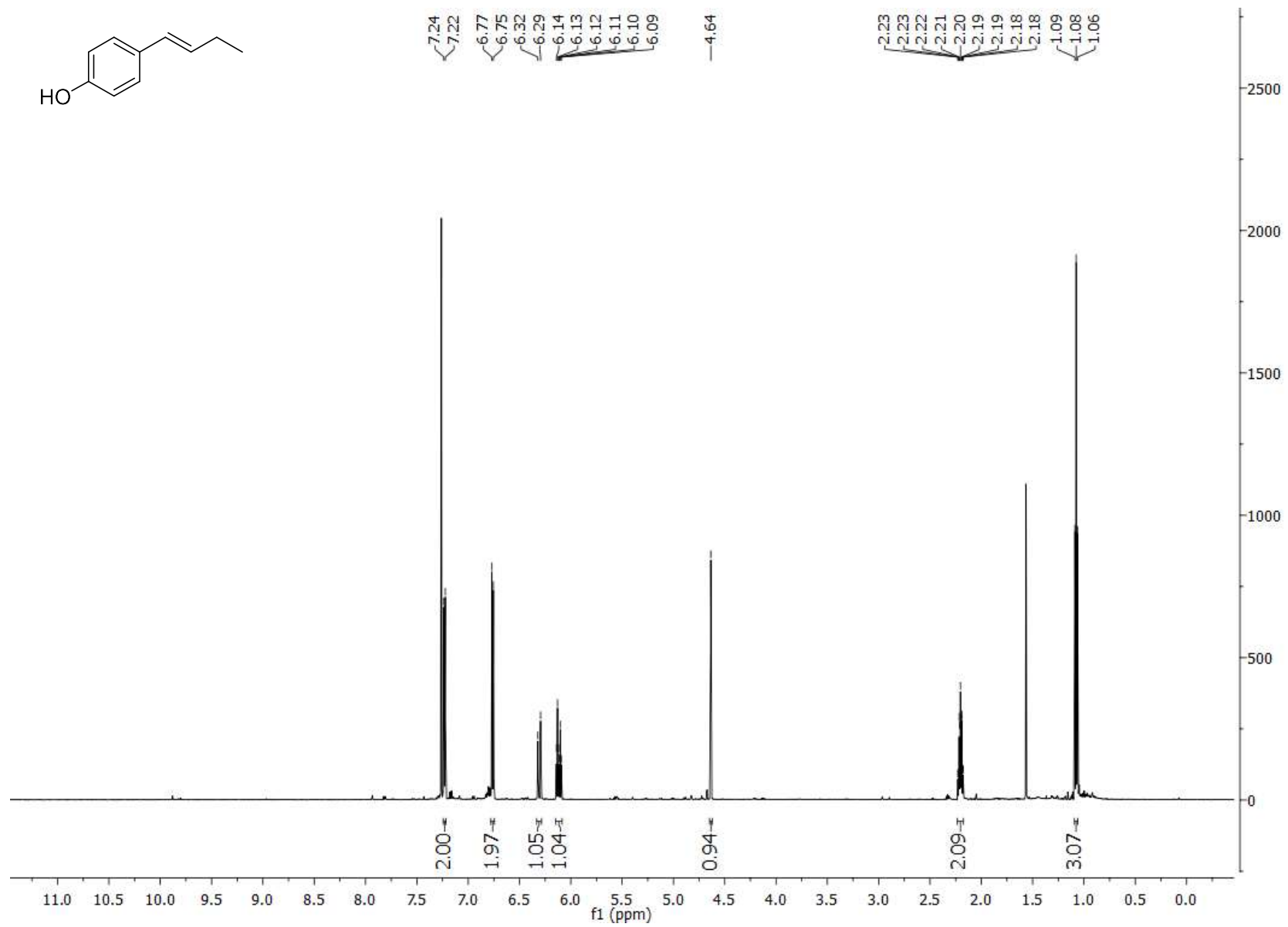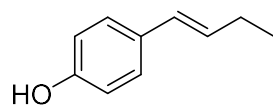
3c ¹³C NMR
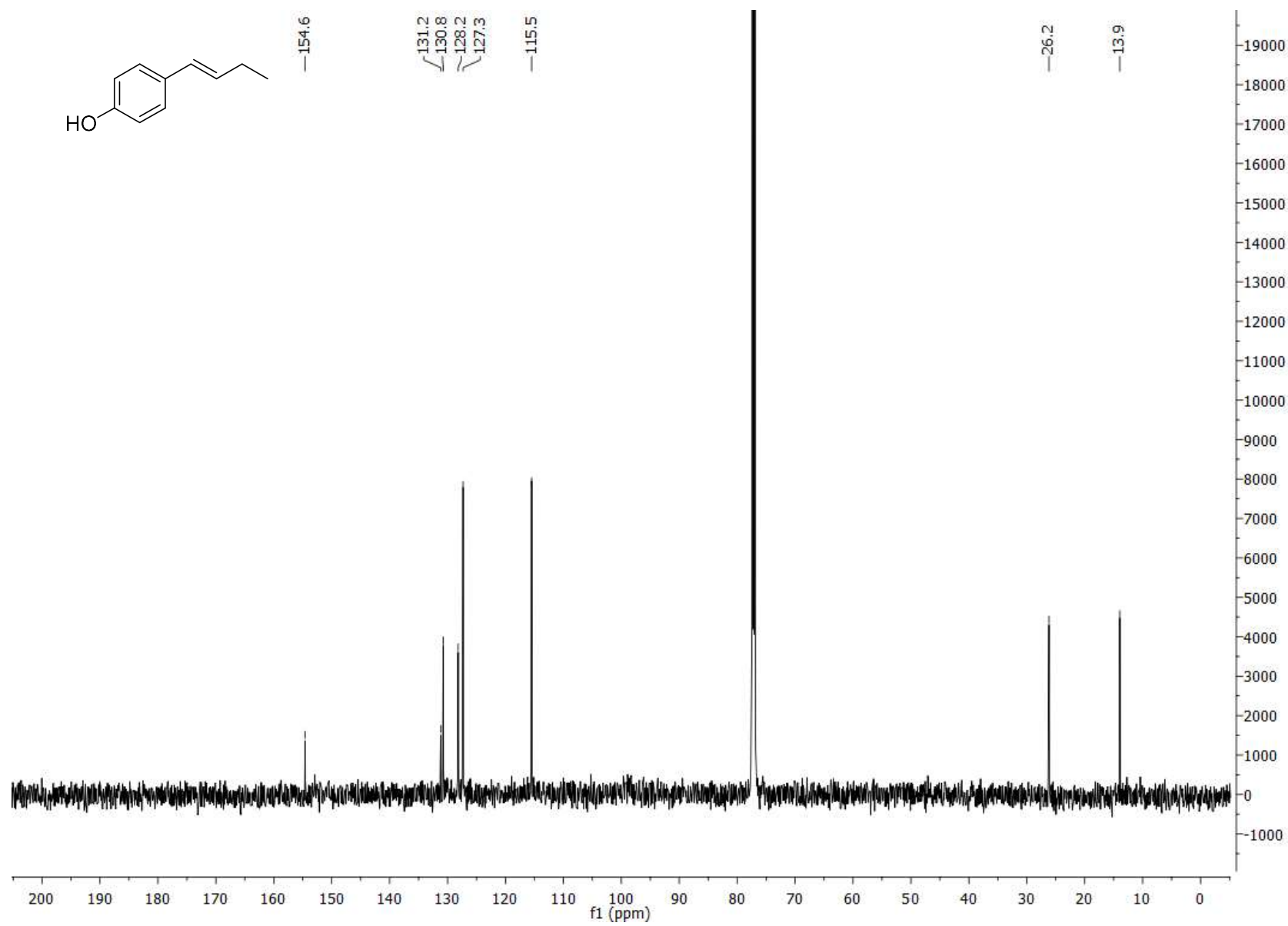
3d ^{1}H NMR
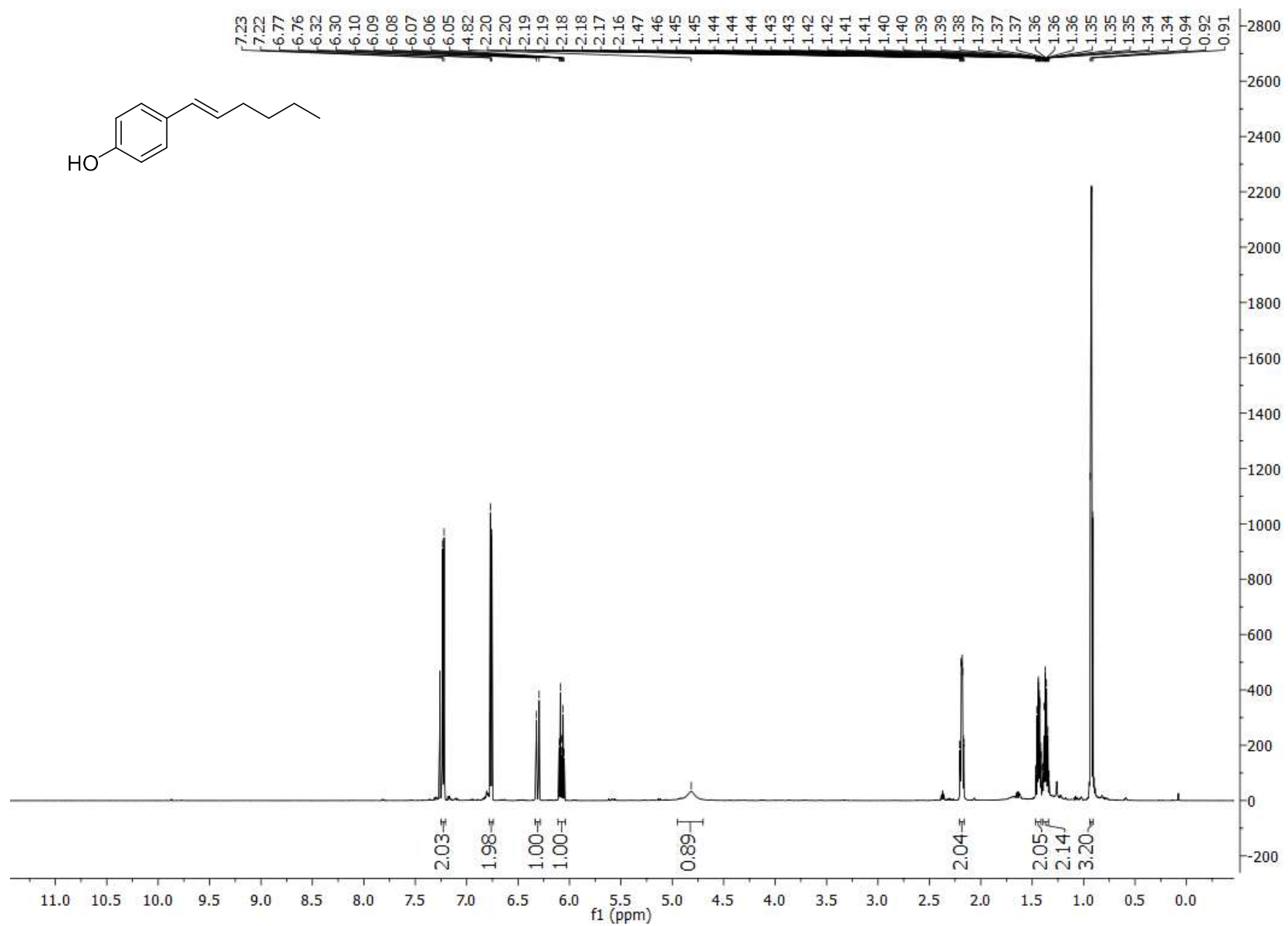
3d ^{13}C NMR
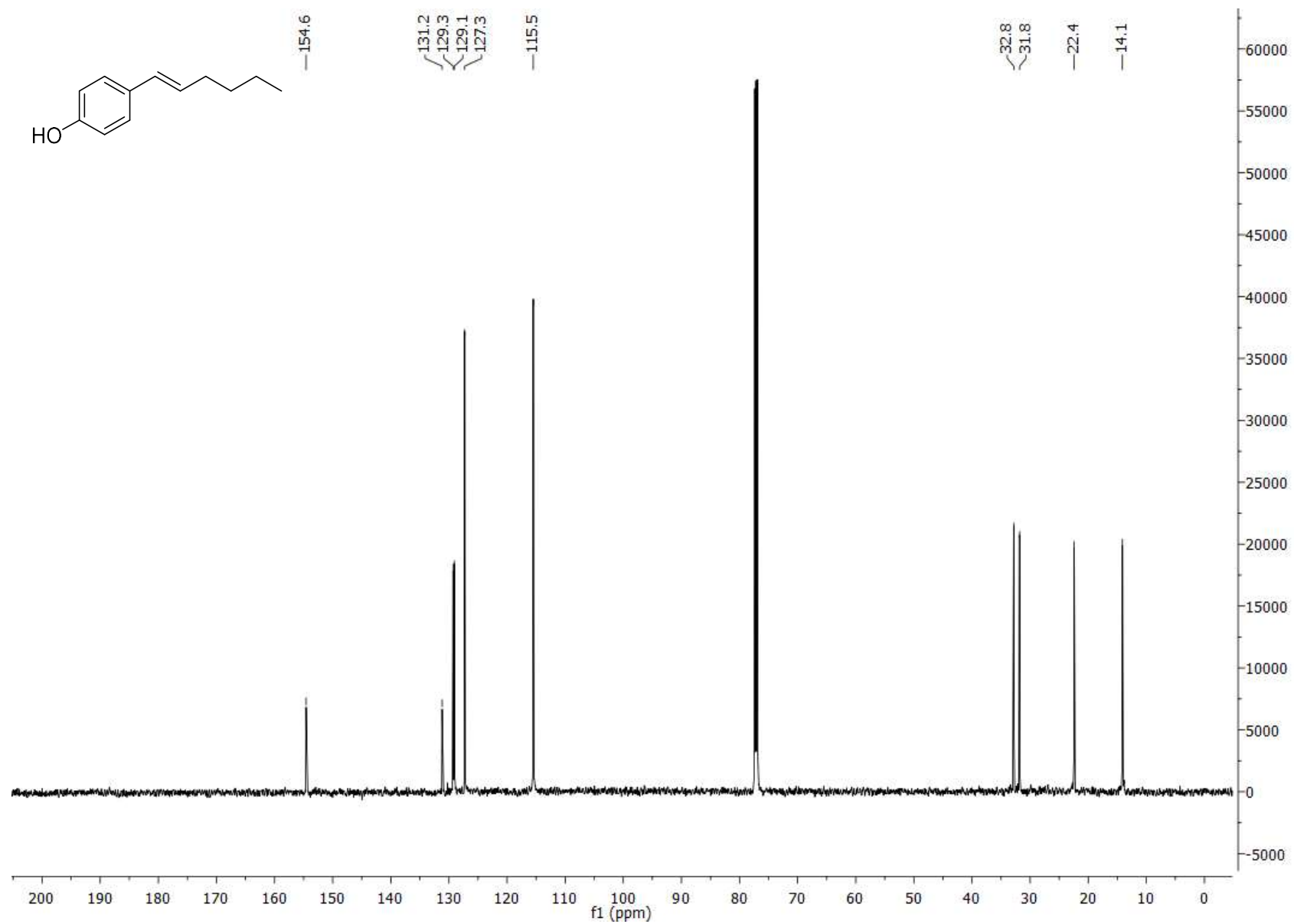
3e ^{1}H NMR
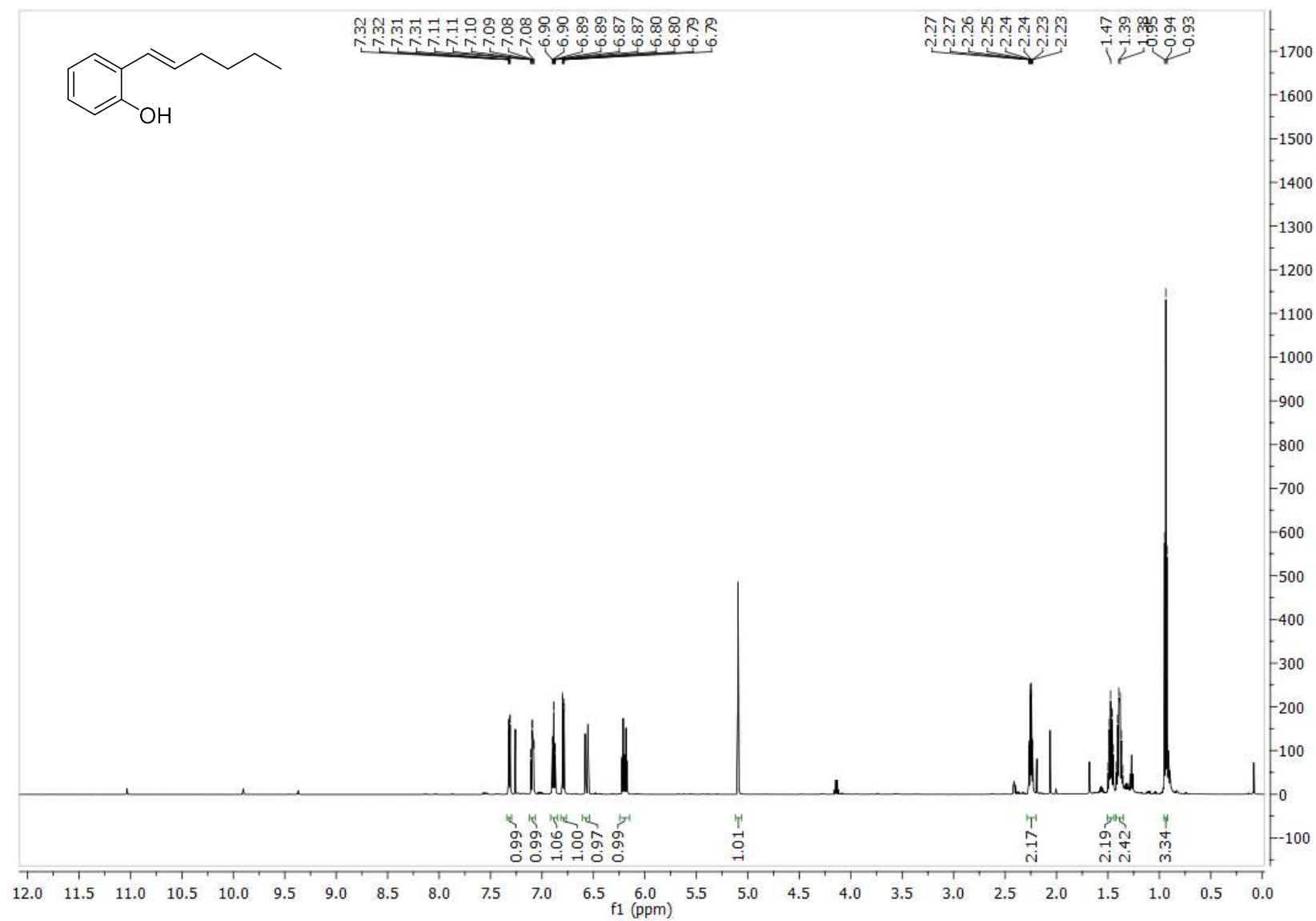
3e ^{13}C NMR
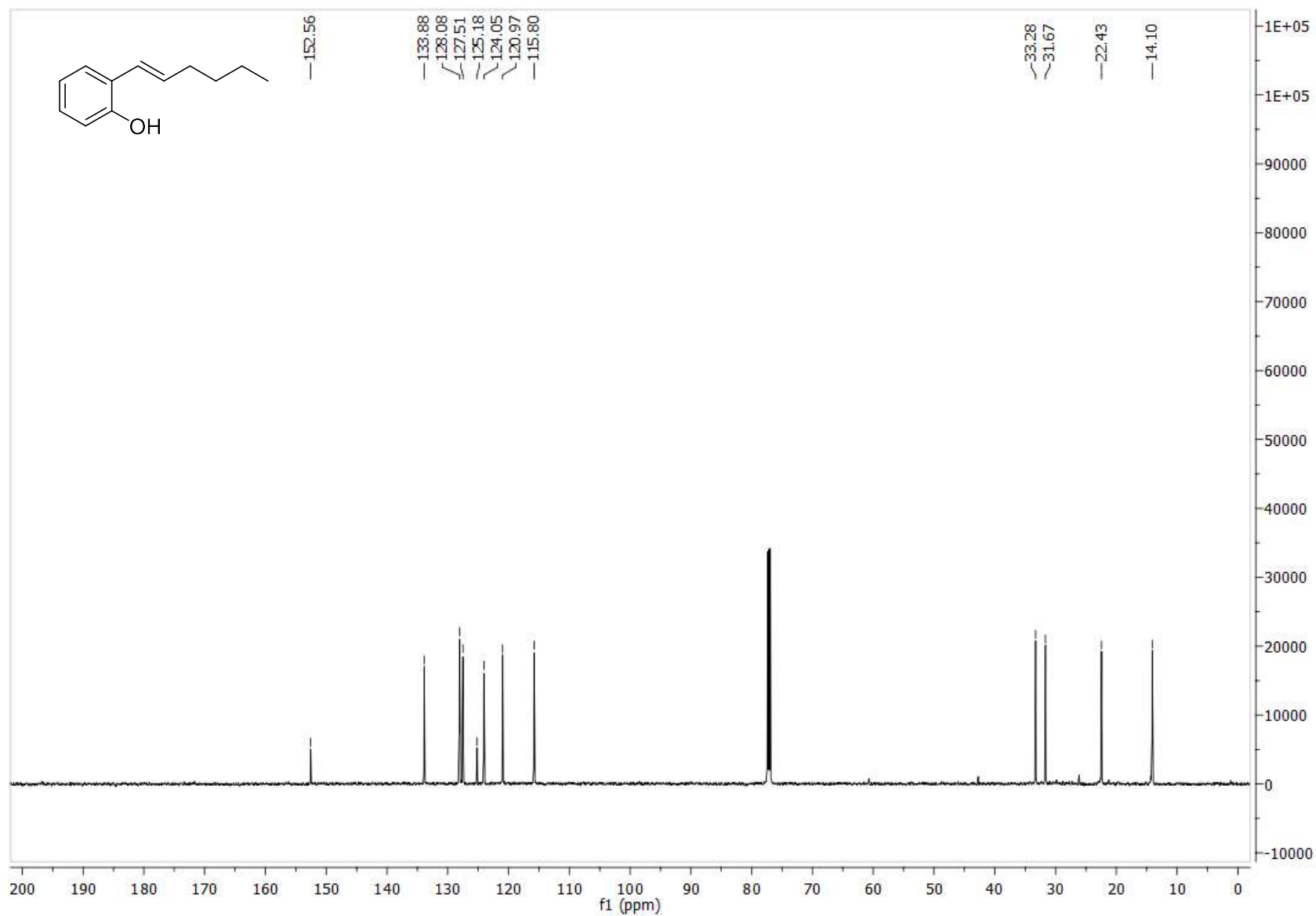
4a ¹H NMR
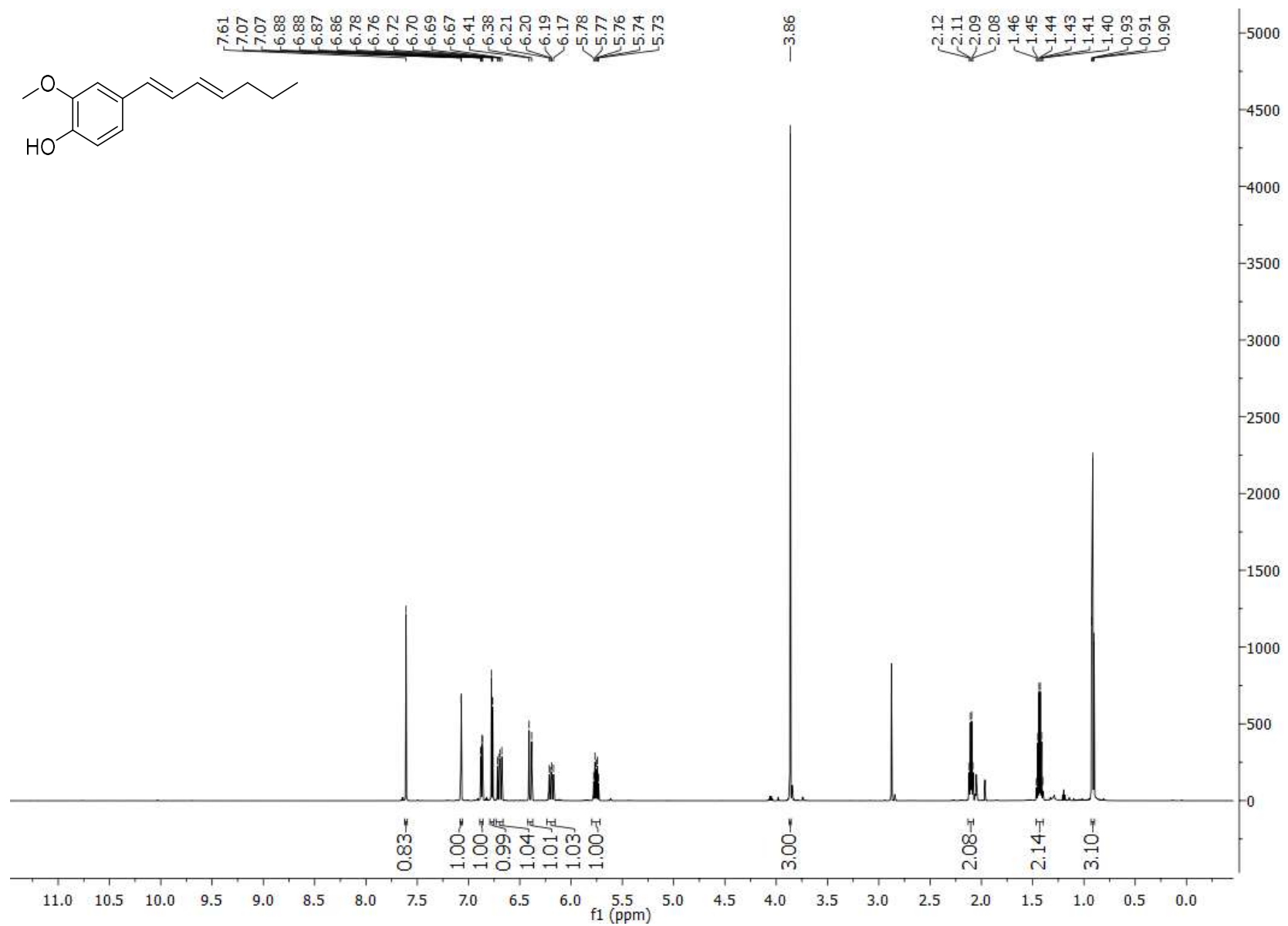
4a ^{13}C NMR
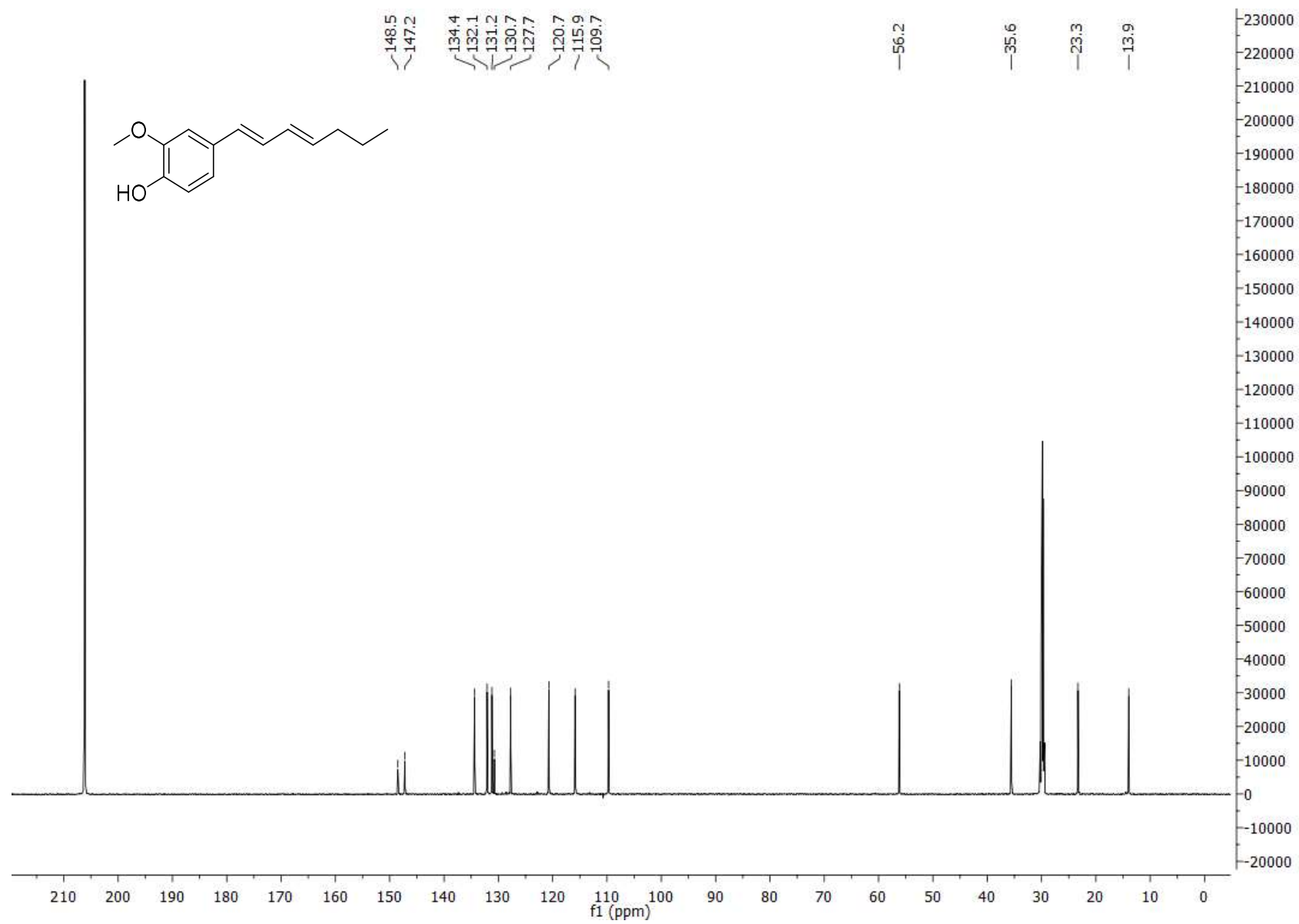
4b ¹H NMR
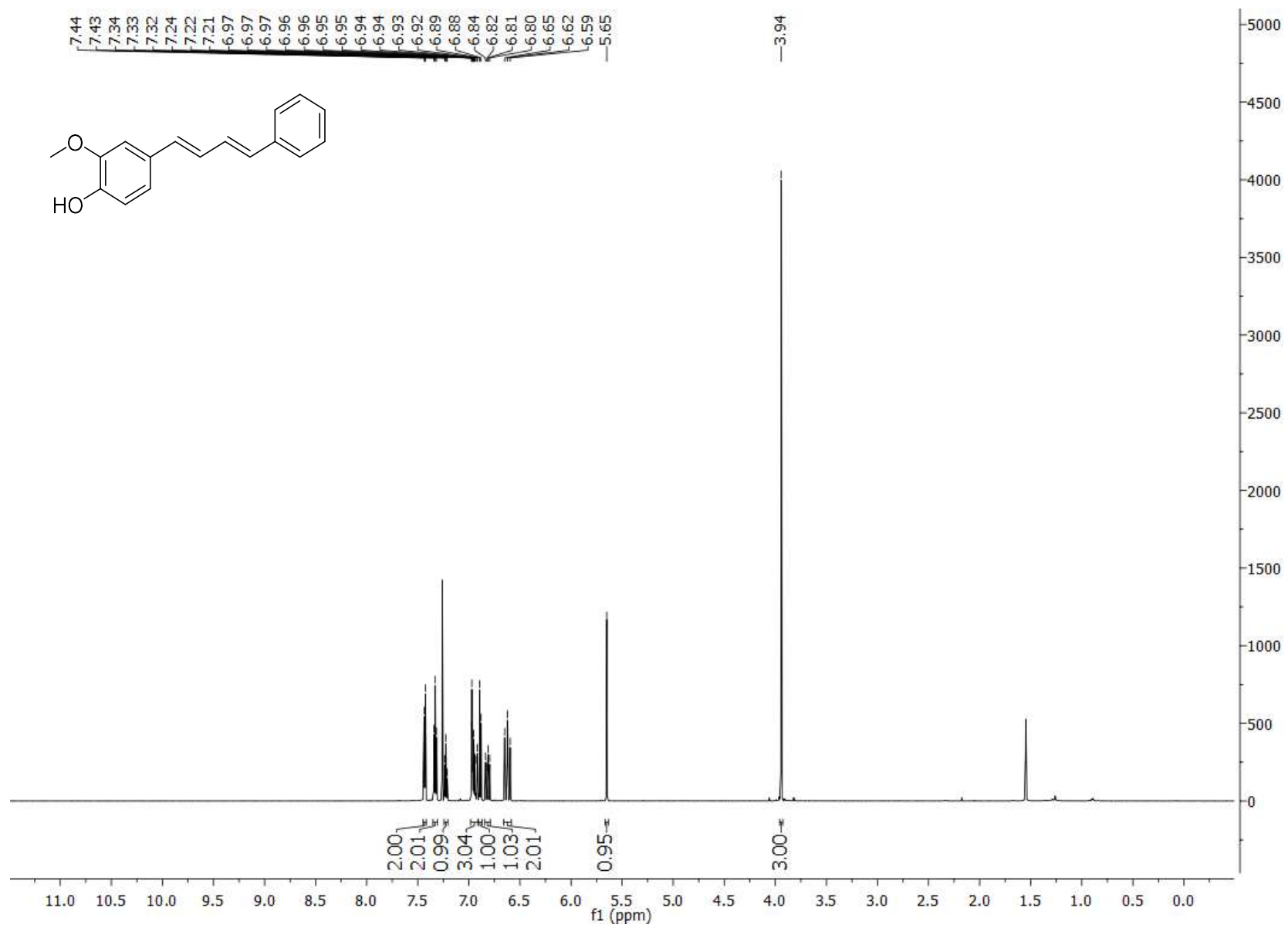
4b ^{13}C NMR
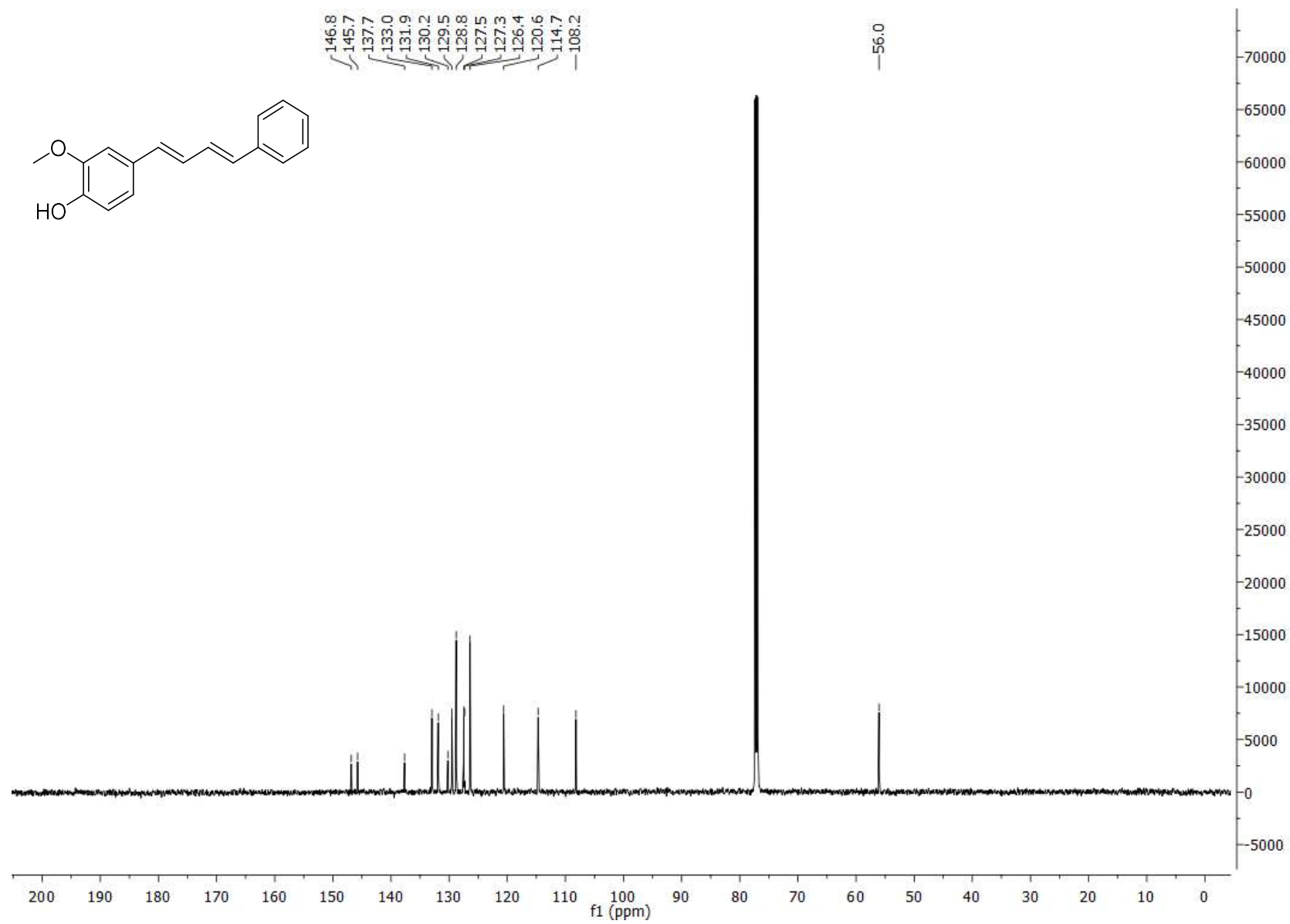
4c ^{1}H NMR
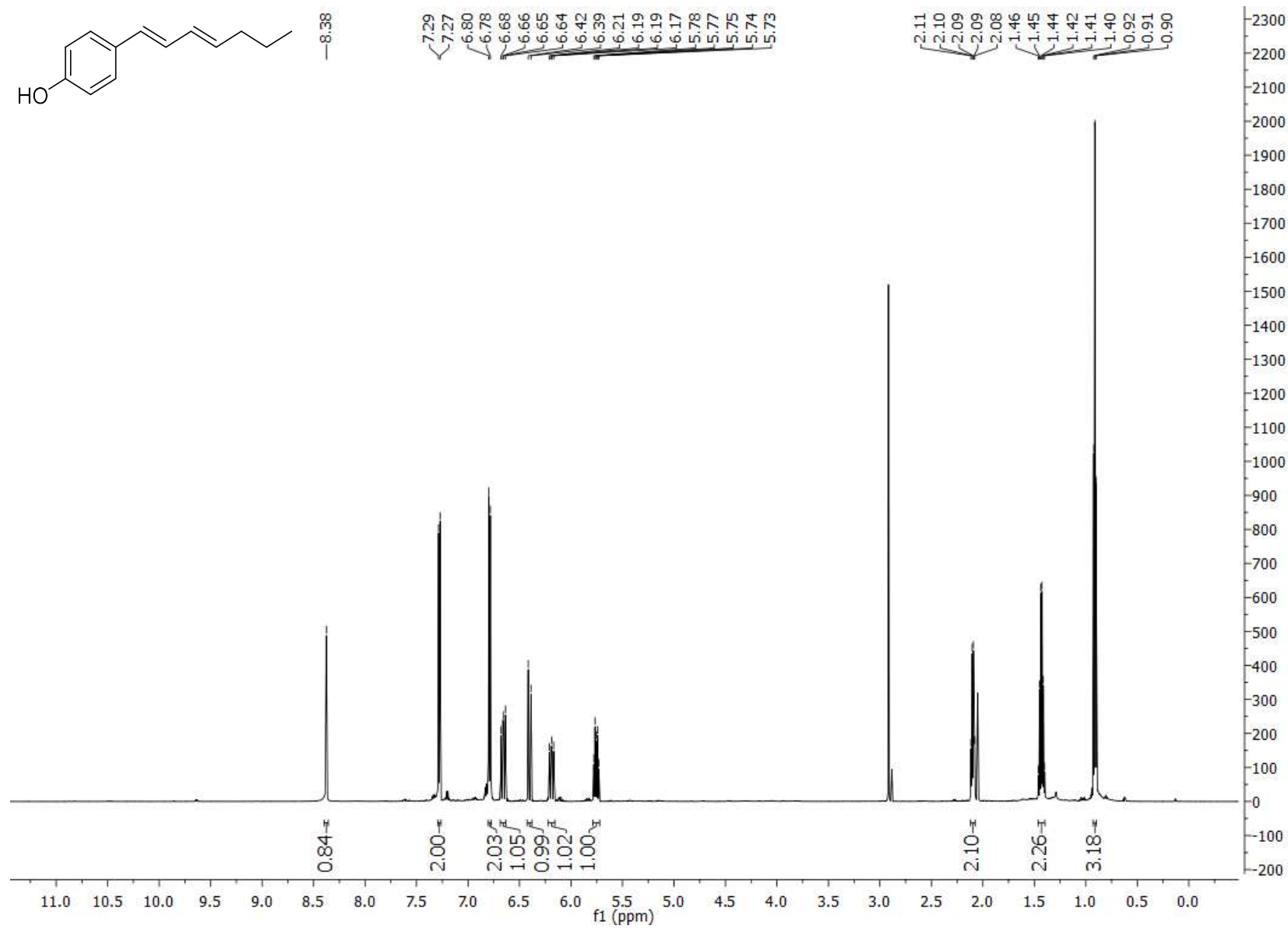
4c ^{13}C NMR
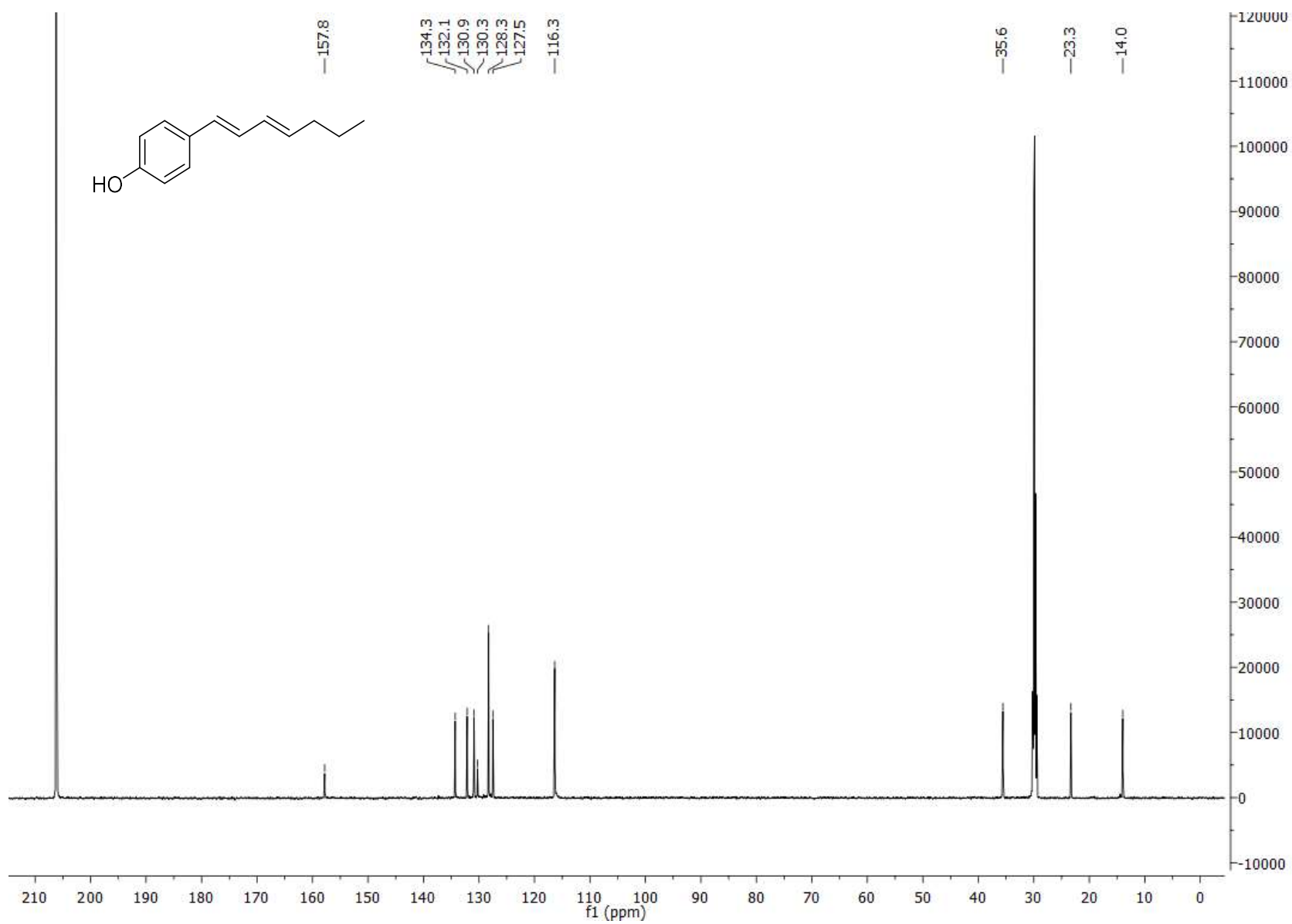
Appendix C: HPLC Chromatograms Pertaining to Chapter 4

5a Racemate

5a

Signal: VWD1 A, Wavelength=250 nm

RT [min]	Type	Width [min]	Area	Height	Area% Name
8.982	BB	0.4779	285.7023	9.4173	50.1422
11.103	BB	0.6094	284.0816	7.3429	49.8578
		Sum	569.7839		
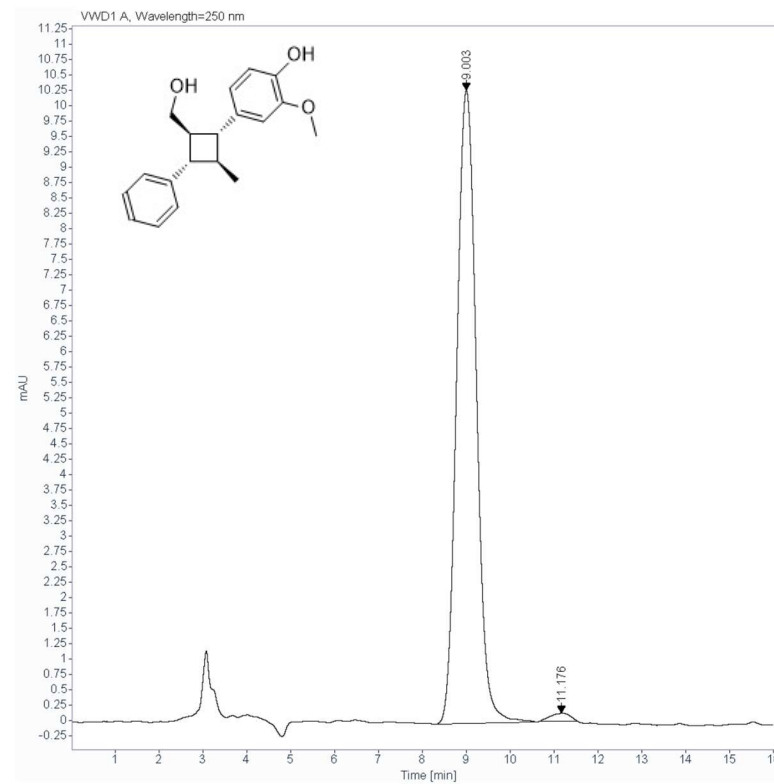
Signal: VWD1 A, Wavelength=250 nm

RT [min]	Type	Width [min]	Area	Height	Area% Name
9.003	BB	0.4884	319.2141	10.3052	98.7344
11.176	MM	0.5293	4.0918	0.1288	1.2656
		Sum	323.3059		

5a Racemate

ent - 5a

Signal: VWD1 A, Wavelength=250 nm

RT [min]	Type	Width [min]	Area	Height	Area% Name
8.982	BB	0.4779	285.7023	9.4173	50.1422
11.103	BB	0.6094	284.0816	7.3429	49.8578
		Sum	569.7839		
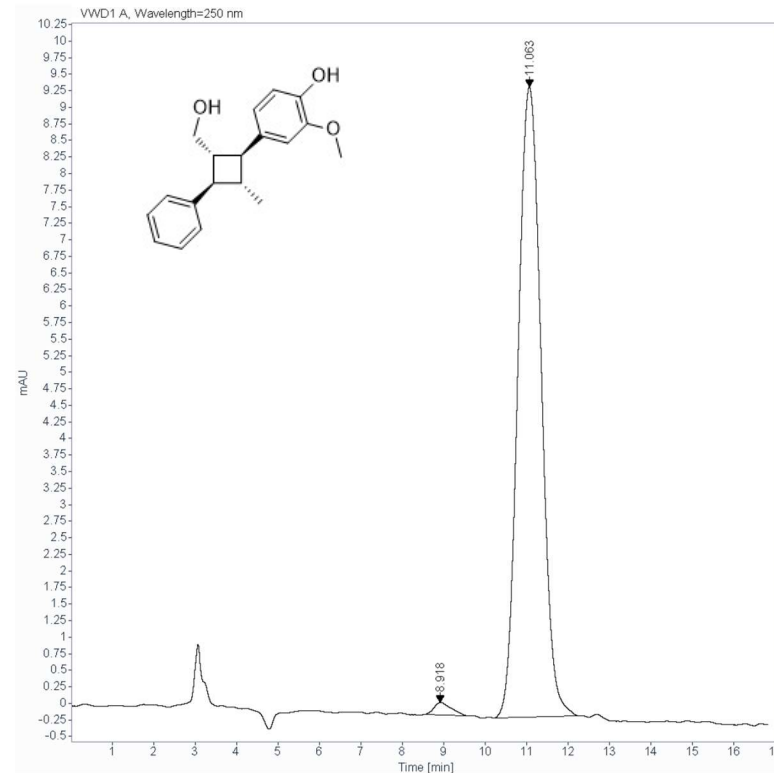
Signal: VWD1 A, Wavelength=250 nm

RT [min]	Type	Width [min]	Area	Height	Area% Name
9.003	BB	0.4884	319.2141	10.3052	98.7344
11.176	MM	0.5293	4.0918	0.1288	1.2656
		Sum	323.3059		

5b Racemate

5b
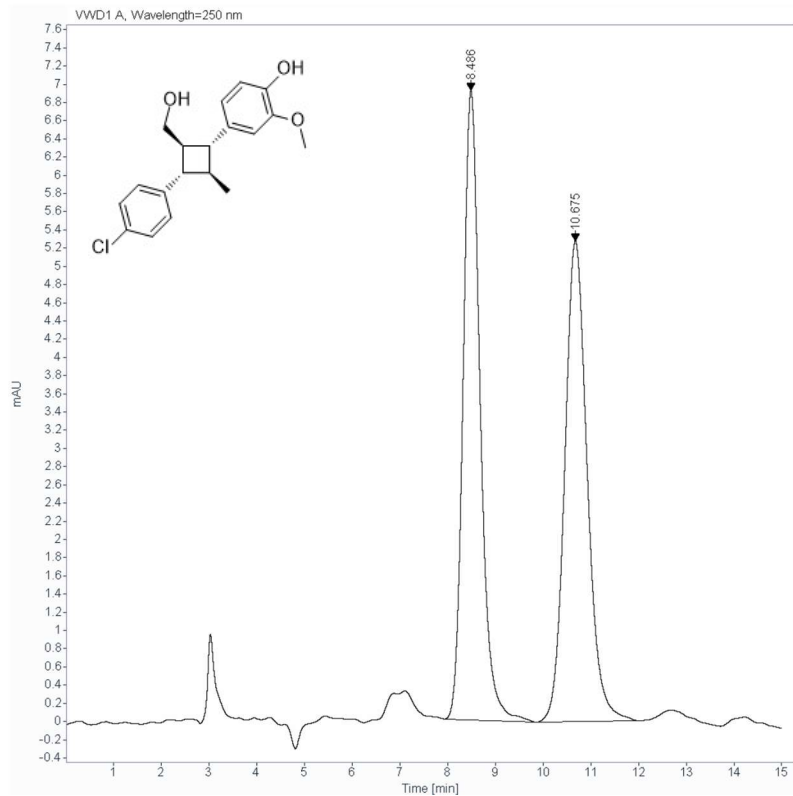
Signal: VWD1 A, Wavelength=250 nm

RT [min]	Type	Width [min]	Area	Height	Area% Name
8.486	BB	0.3794	172.1061	6.9153	49.9640
10.675	BB	0.4977	172.3543	5.2812	50.0360
		Sum	344.4604		
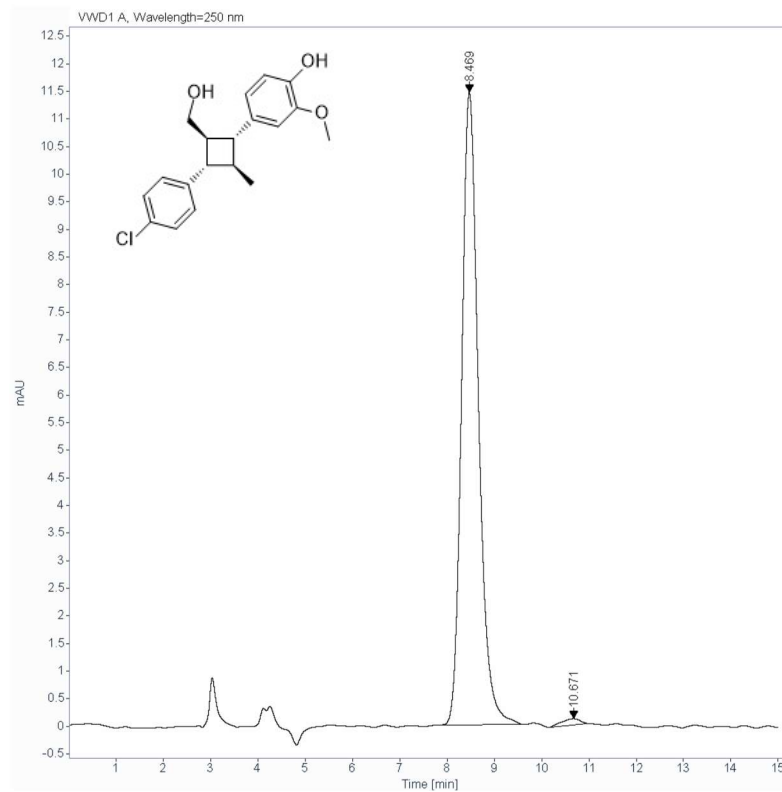
Signal: VWD1 A, Wavelength=250 nm

RT [min]	Type	Width [min]	Area	Height	Area% Name
8.469	BB	0.3753	282.2303	11.4622	98.9212
10.671	MM	0.4566	3.0780	0.1124	1.0788
		Sum	285.3084		

5c Racemate

5c
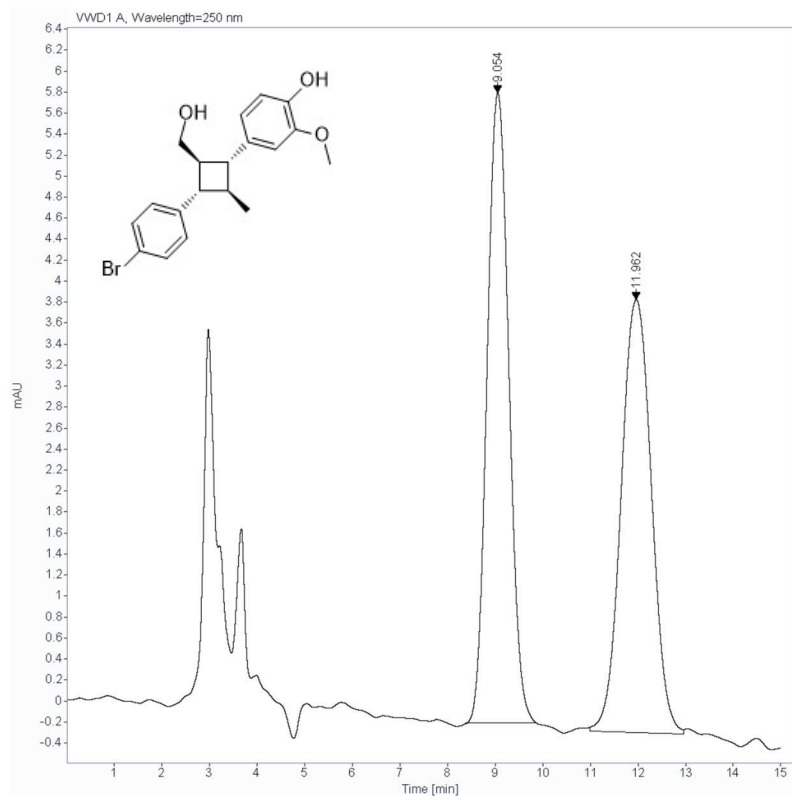
Signal: VWD1 A, Wavelength=250 nm

RT [min]	Type	Width [min]	Area	Height	Area% Name
9.054	MM	0.5278	190.0291	6.0005	51.0712
11.962	MM	0.7358	182.0572	4.1237	48.9288
		Sum	372.0863		
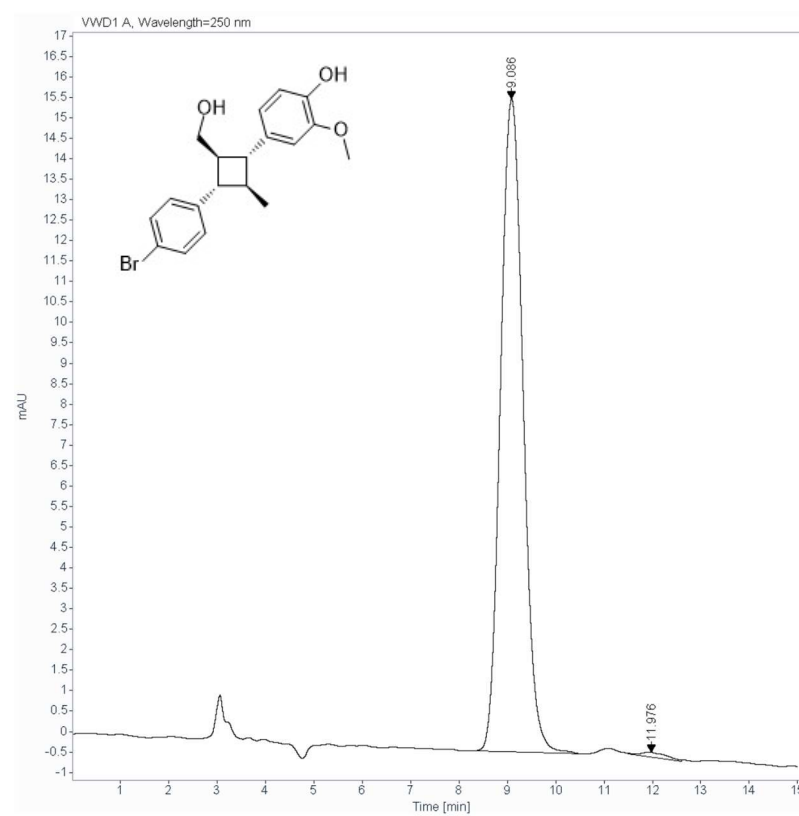
Signal: VWD1 A, Wavelength=250 nm

RT [min]	Type	Width [min]	Area	Height	Area% Name
9.086	BB	0.5137	516.5681	15.9578	99.1124
11.976	MM	0.6674	4.6261	0.1155	0.8876
		Sum	521.1942		

5d Racemate
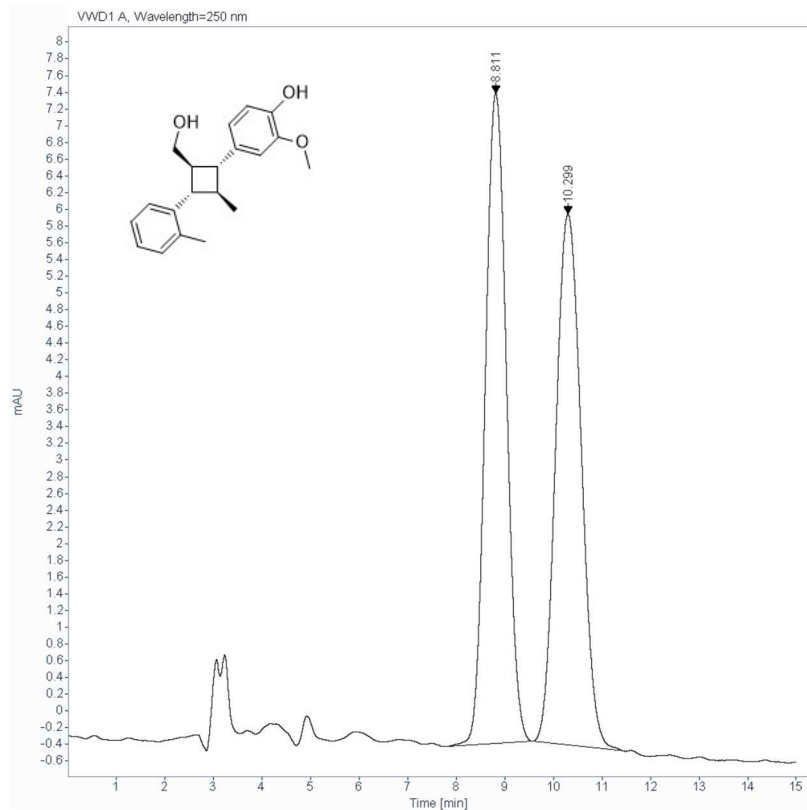
Signal: VWD1 A, Wavelength=250 nm

RT [min]	Type	Width [min]	Area	Height	Area% Name
8.811	BB	0.4783	234.9755	7.7808	50.3776
10.299	BB	0.5748	231.4530	6.3560	49.6224
		Sum	466.4285		

5d
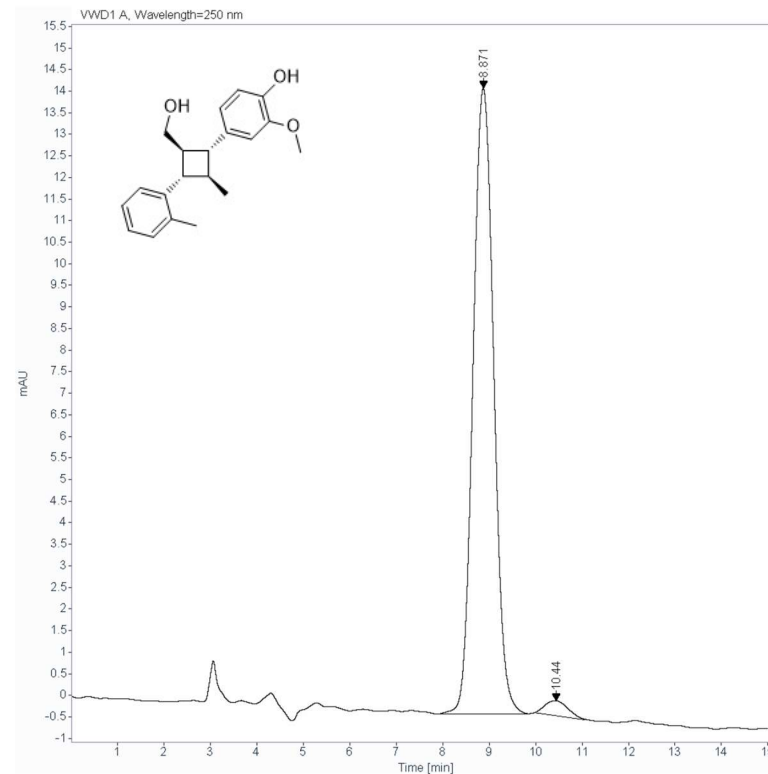
Signal: VWD1 A, Wavelength=250 nm

RT [min]	Type	Width [min]	Area	Height	Area% Name
8.871	BB	0.4877	447.1015	14.4996	97.3454
10.440	MM	0.5803	12.1922	0.3502	2.6546
		Sum	459.2937		

5e Racemate

5e
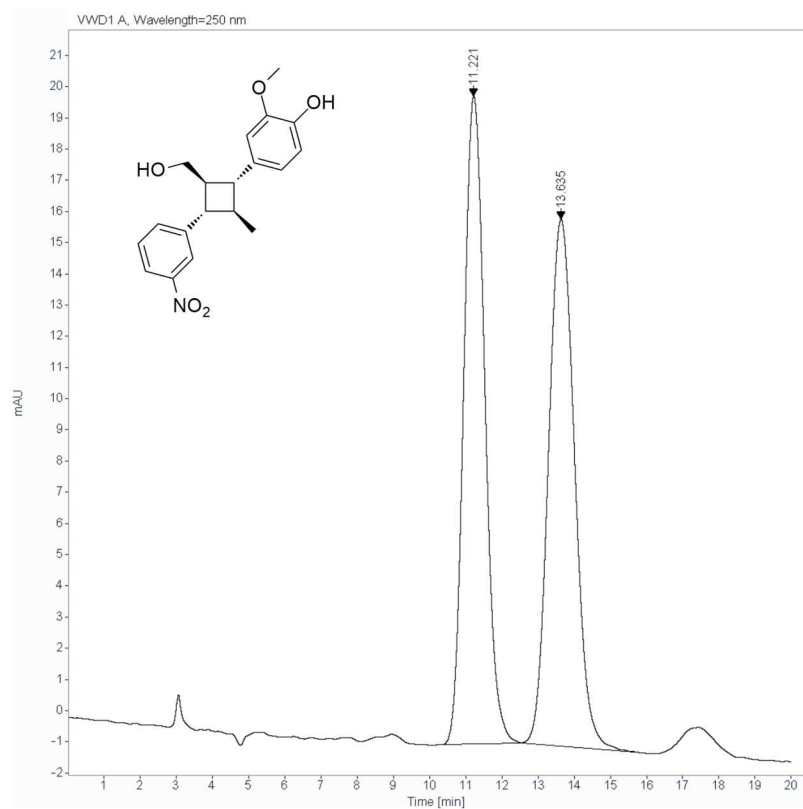
Signal: VWD1 A, Wavelength=250 nm

RT [min]	Type	Width [min]	Area	Height	Area% Name
11.221	BB	0.6383	838.8632	20.7663	49.8823
13.635	BB	0.7842	842.8210	16.8901	50.1177
		Sum	1681.6842		
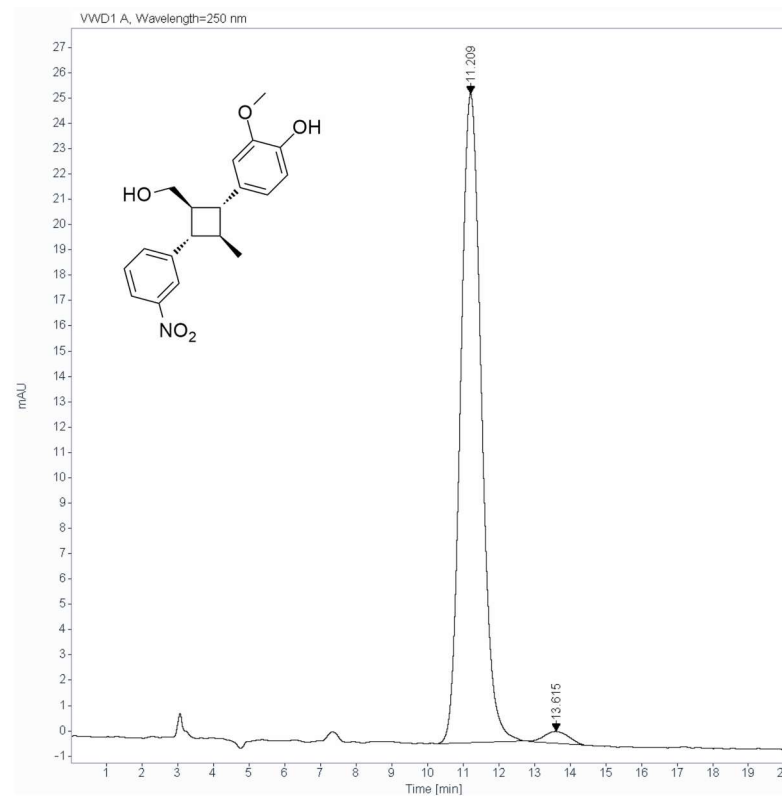
Signal: VWD1 A, Wavelength=250 nm

RT [min]	Type	Width [min]	Area	Height	Area% Name
11.209	BB	0.6314	1031.7932	25.6443	97.9468
13.615	MM	0.7856	21.6287	0.4589	2.0532
		Sum	1053.4219		

5f Racemate
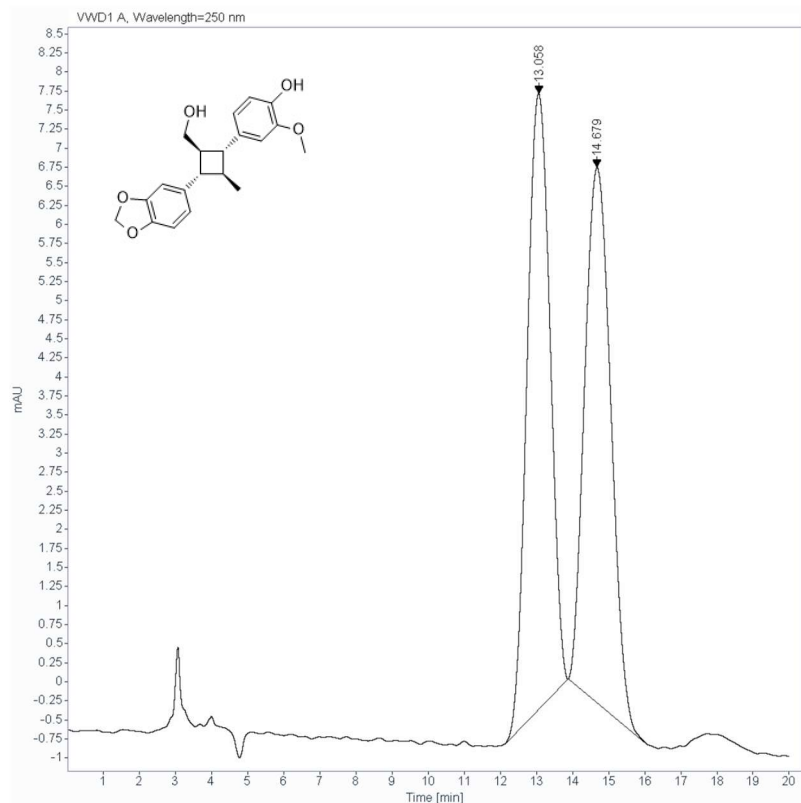
Signal: VWD1 A, Wavelength=250 nm

RT [min]	Type	Width [min]	Area	Height	Area%	Name
13.058	BB	0.6971	357.5092	8.0812	50.3273	
14.679	BB	0.8028	352.8591	7.0280	49.6727	
		Sum	710.3683			

5f
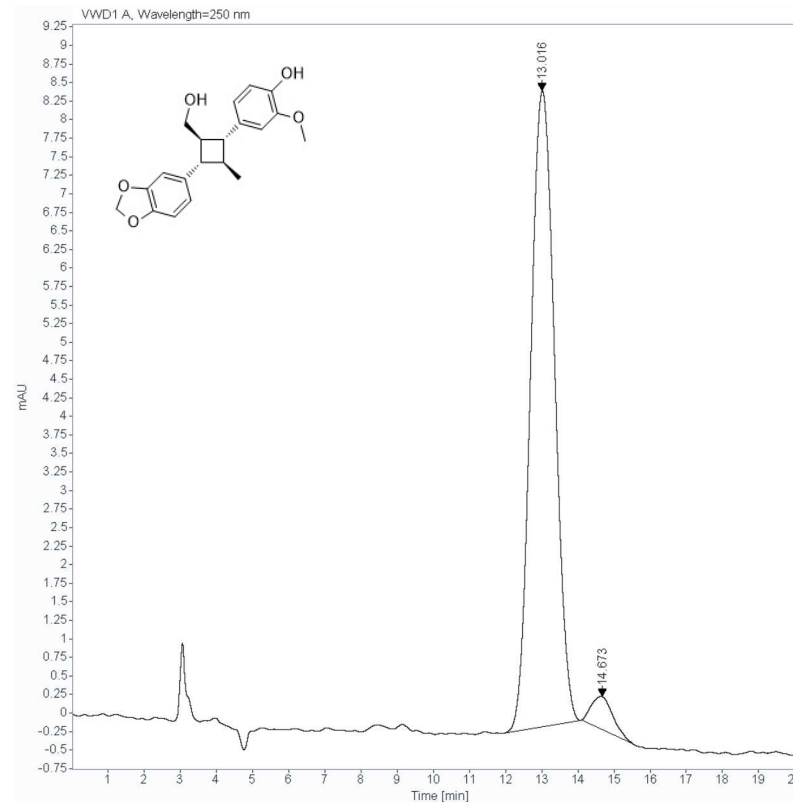
Signal: VWD1 A, Wavelength=250 nm

RT [min]	Type	Width [min]	Area	Height	Area%	Name
13.016	BB	0.7289	394.7533	8.5781	95.5151	
14.673	MM T	0.6917	18.5355	0.4466	4.4849	
		Sum	413.2889			

8 Racemate

8
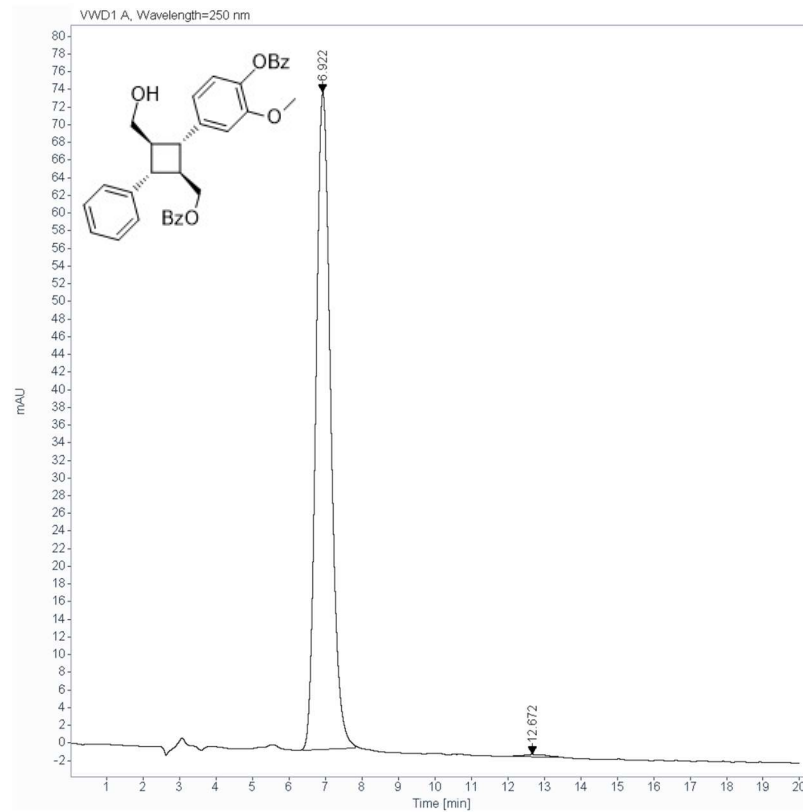
5h Racemate

VWD1 A, Wavelength=250 nm

Signal: VWD1 A, Wavelength=250 nm

RT [min]	Type	Width [min]	Area	Height	Area% Name
5.937	BB	0.3103	175.6711	8.8606	51.2261
8.332	BB	0.4541	167.2617	5.7892	48.7739
		Sum	342.9327		

5h
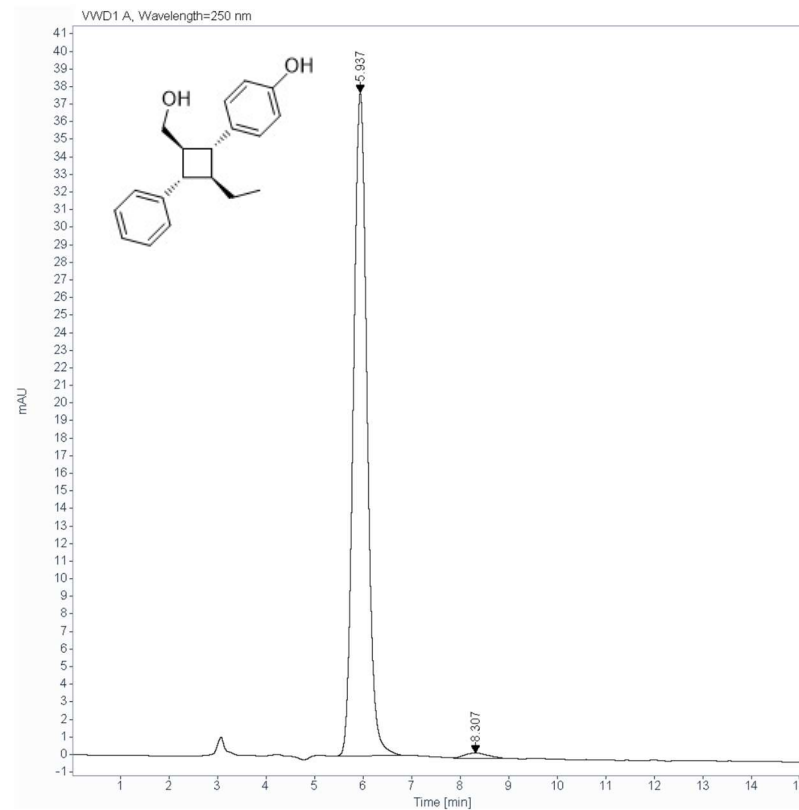
Signal: VWD1 A, Wavelength=250 nm

RT [min]	Type	Width [min]	Area	Height	Area% Name
5.937	BB	0.3059	737.1537	37.7358	98.6948
8.307	MM	0.5535	9.7485	0.2935	1.3052
		Sum	746.9022		

Appendix D: NMR Spectra Pertaining to Chapter 4

4a ^{1}H NMR
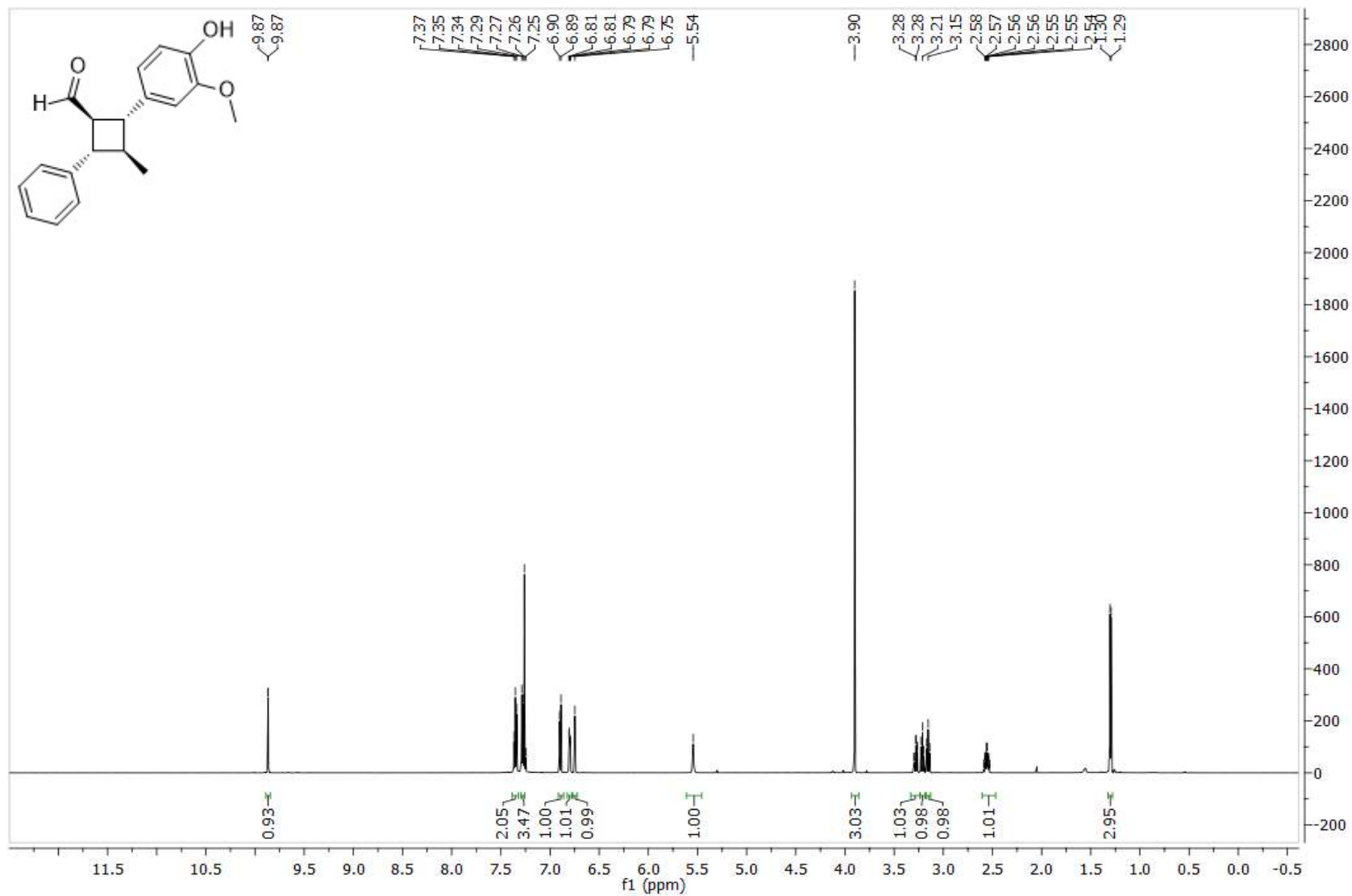
4a ^{13}C NMR
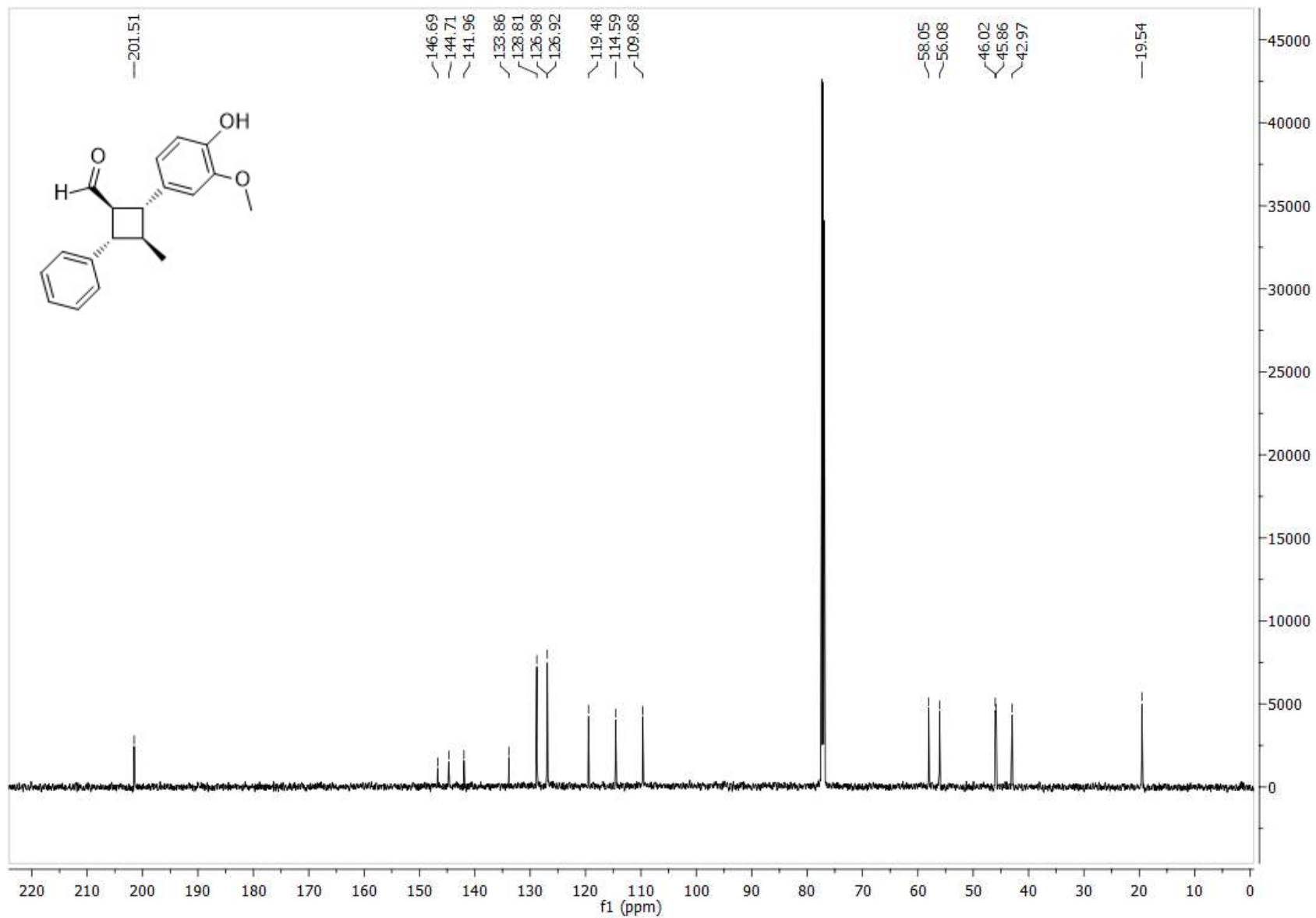
4a ^{1}H-^{1}H COSY – Full Spectra
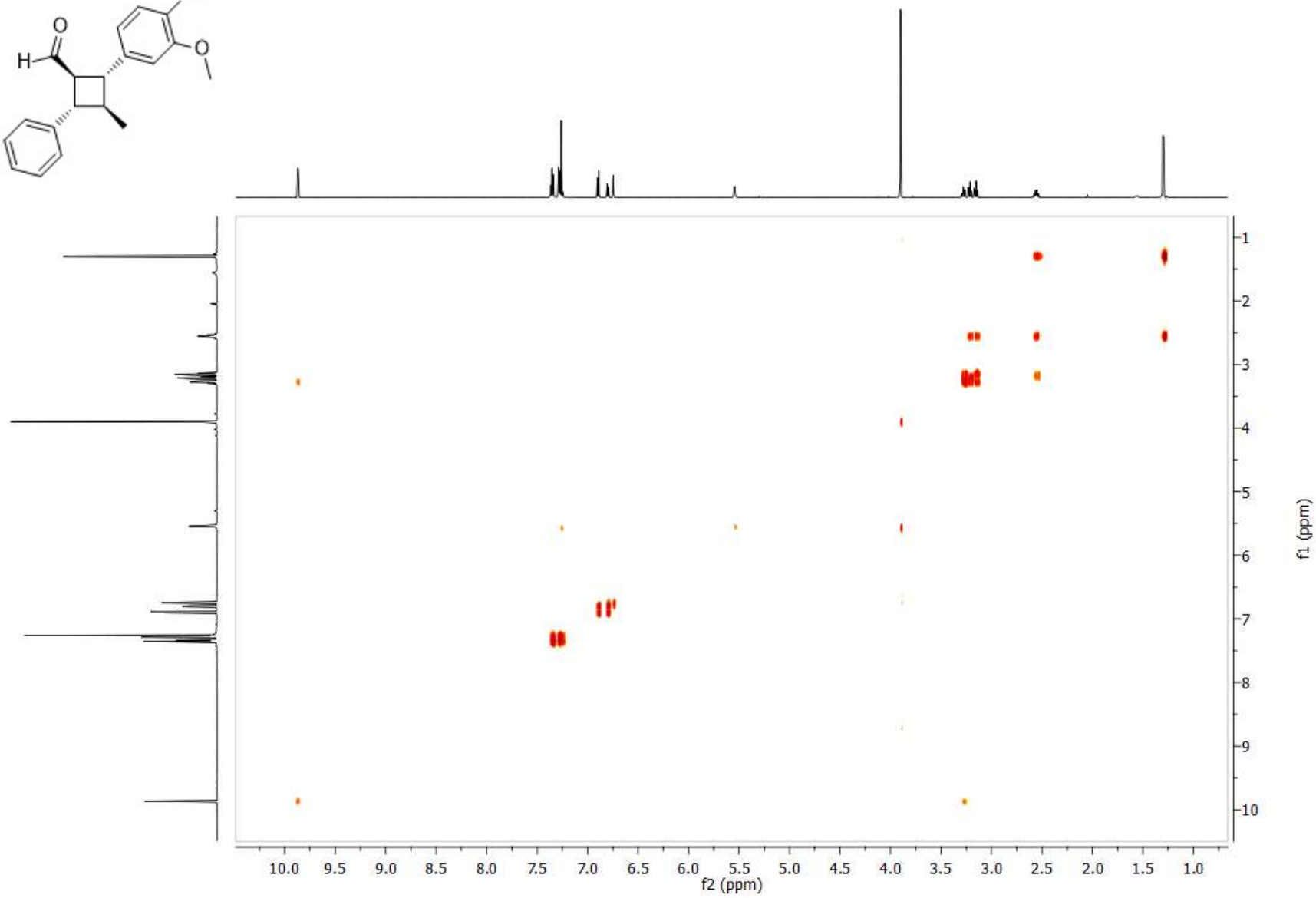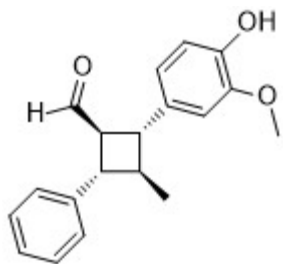
4a ^{1}H-^{1}H COSY – Aliphatic Region
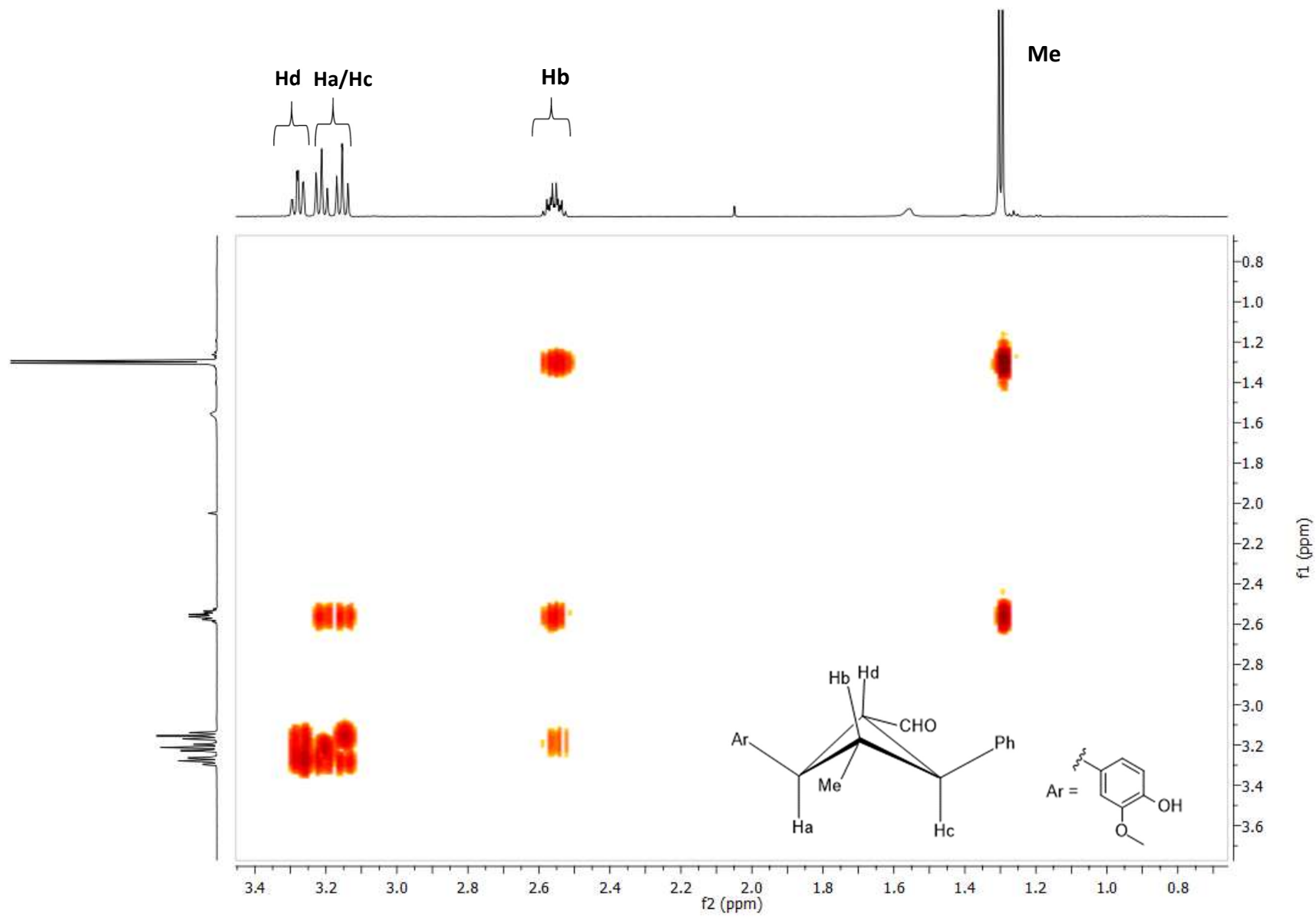
4a ¹H-¹³C HSQC – Full Spectra
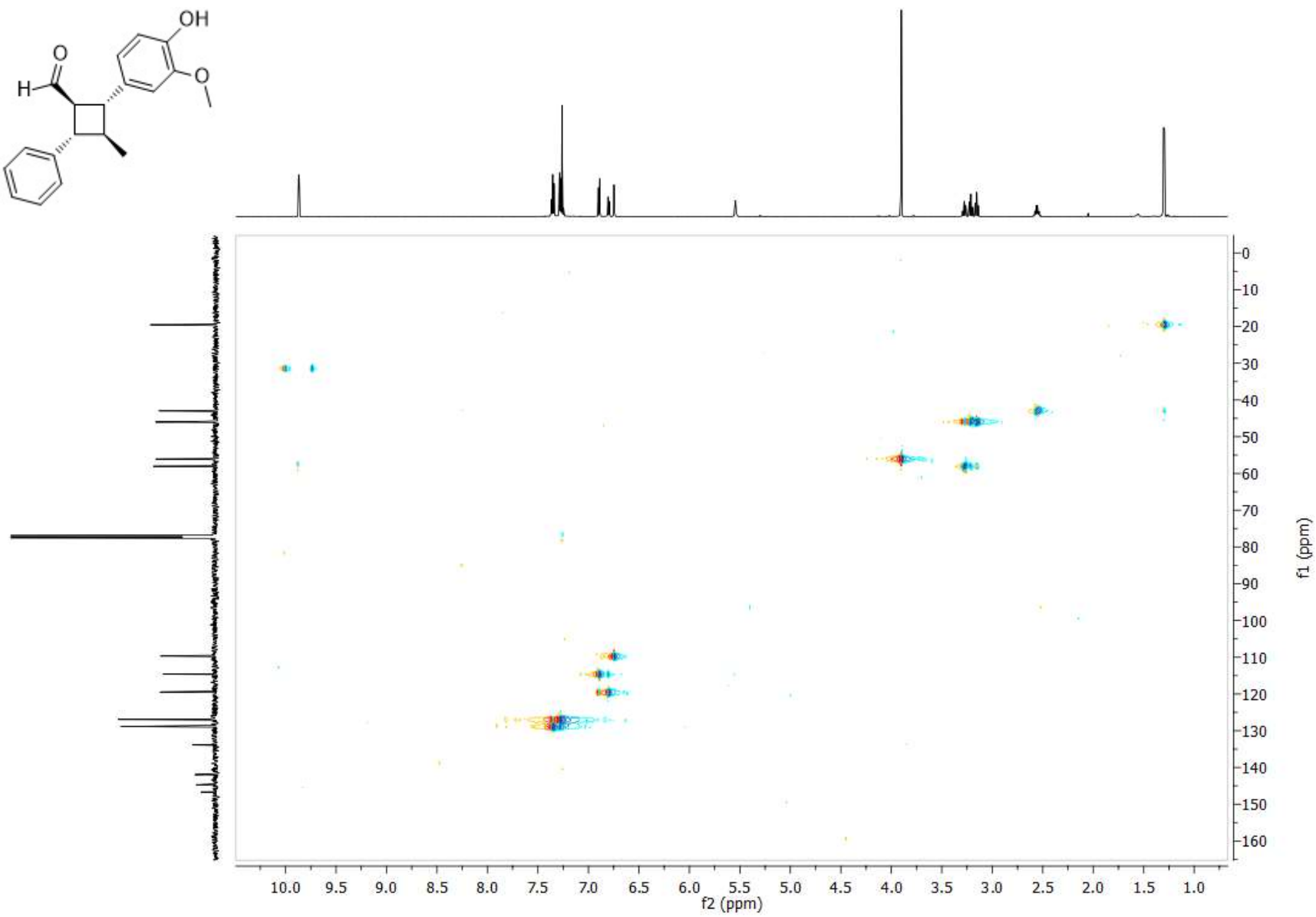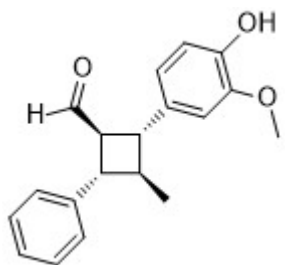
4a ^{1}H-^{13}C HSQC – Aliphatic Region
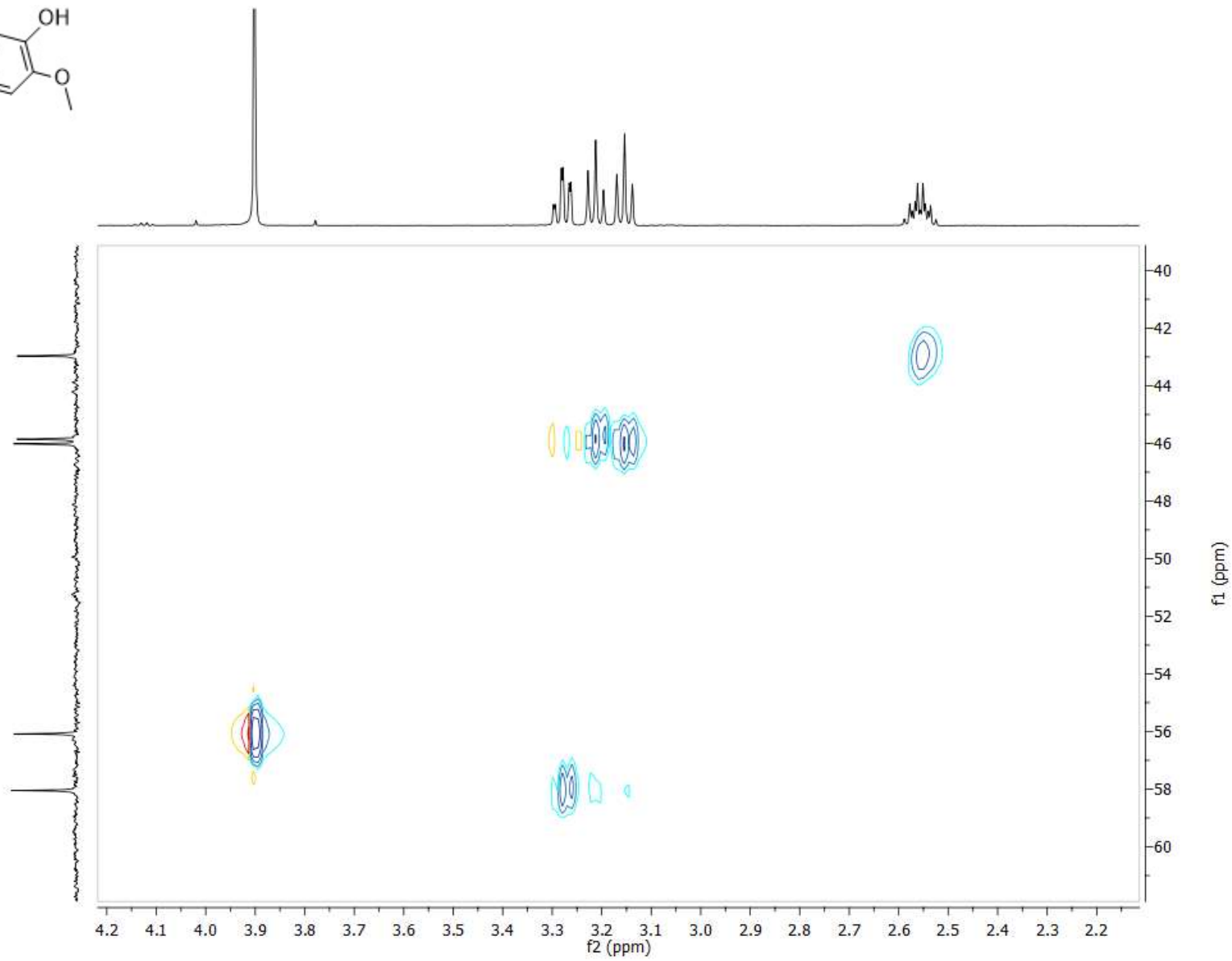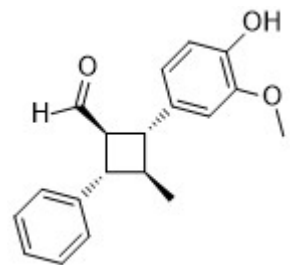
5a ¹H NMR
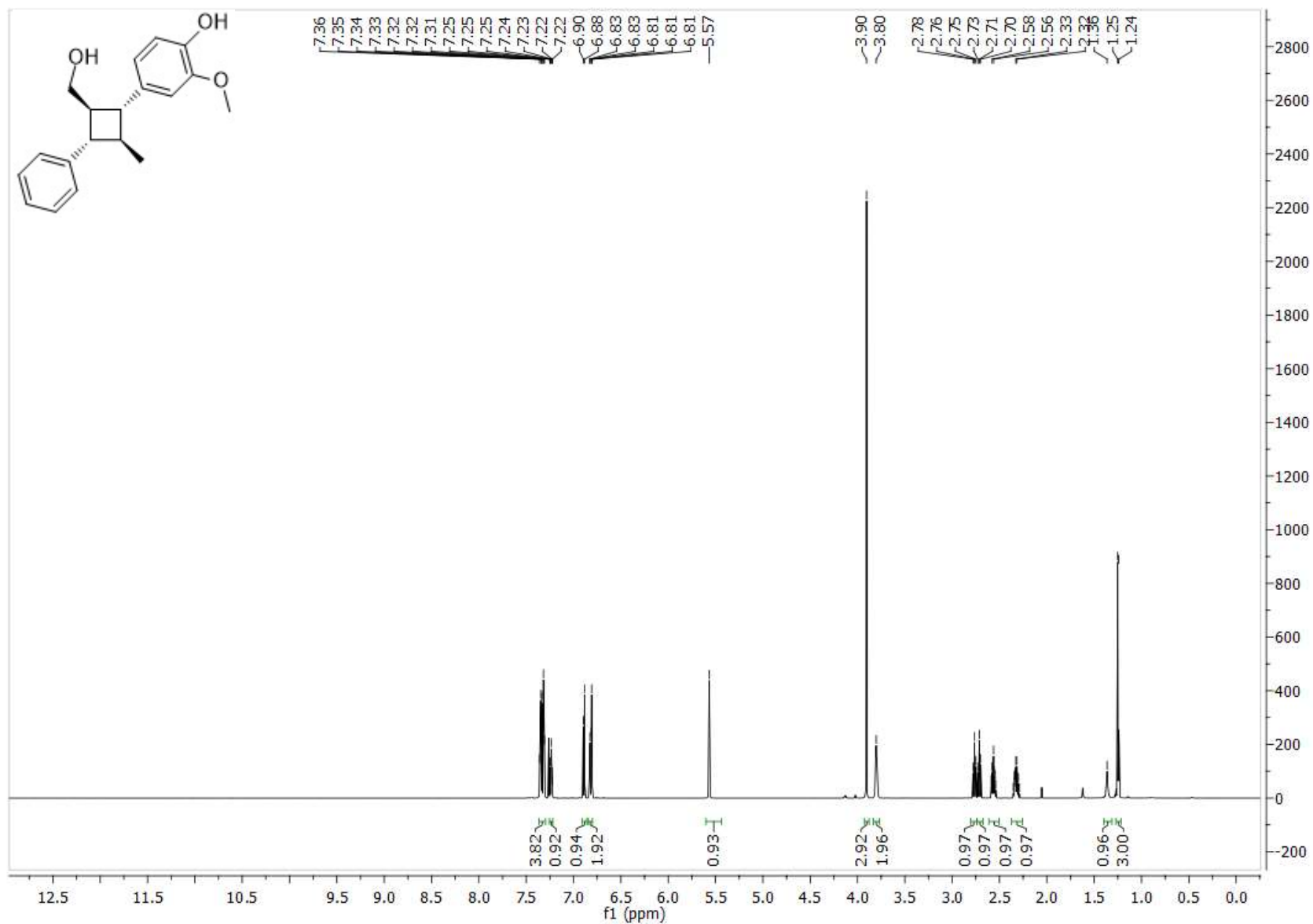
5a ^{13}C NMR
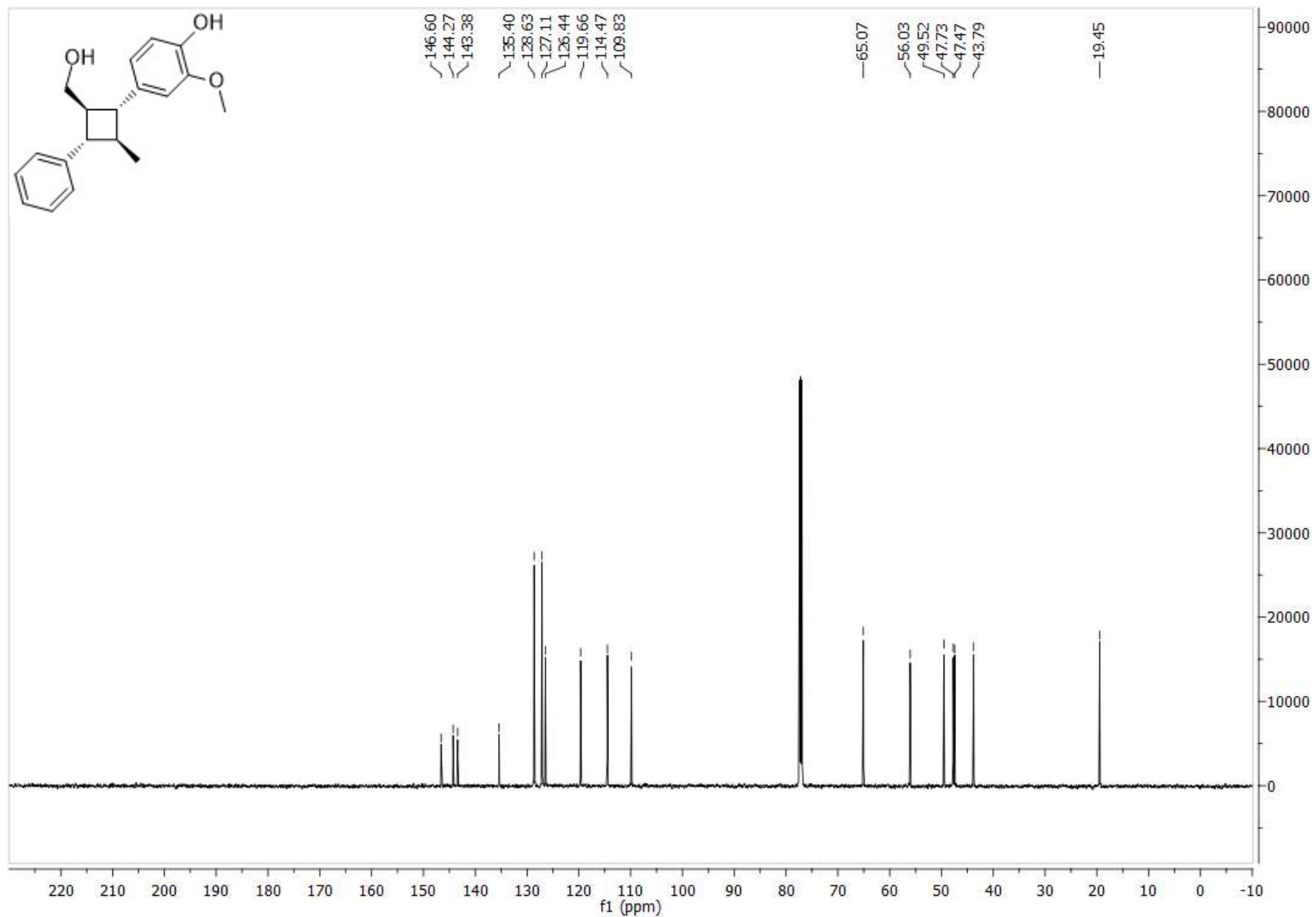
4b ¹H NMR
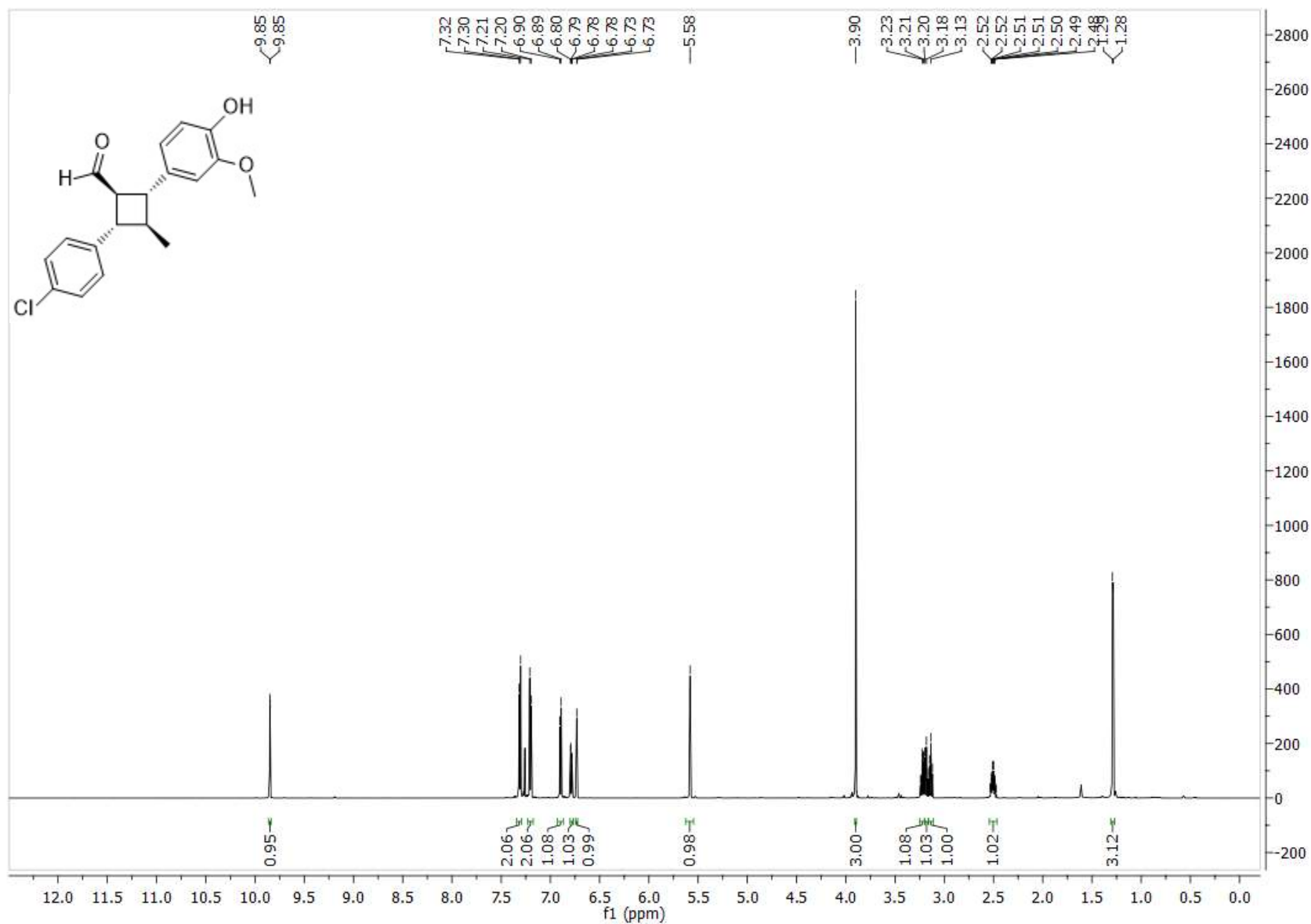
4b ^{13}C NMR
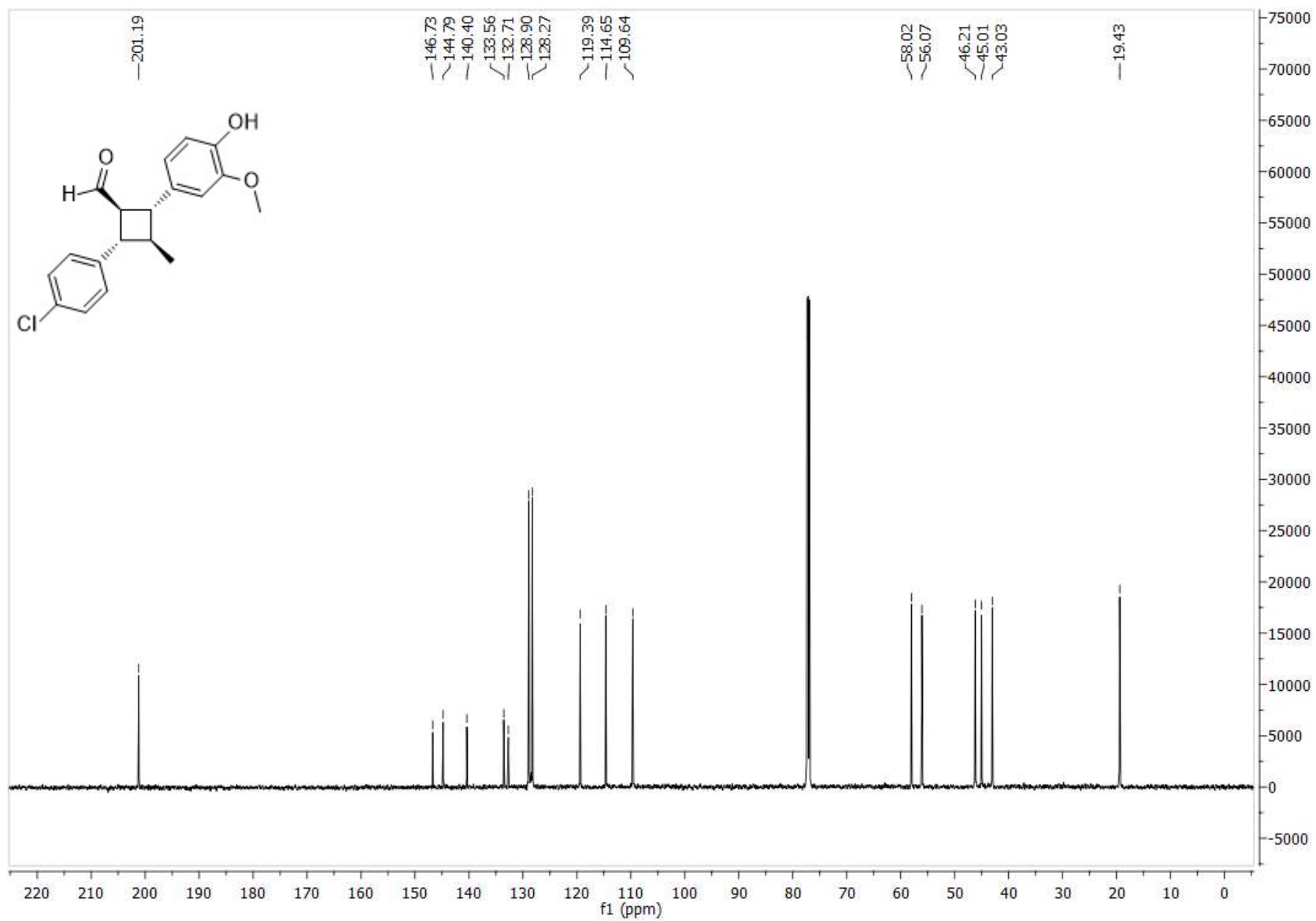
5b ¹H NMR
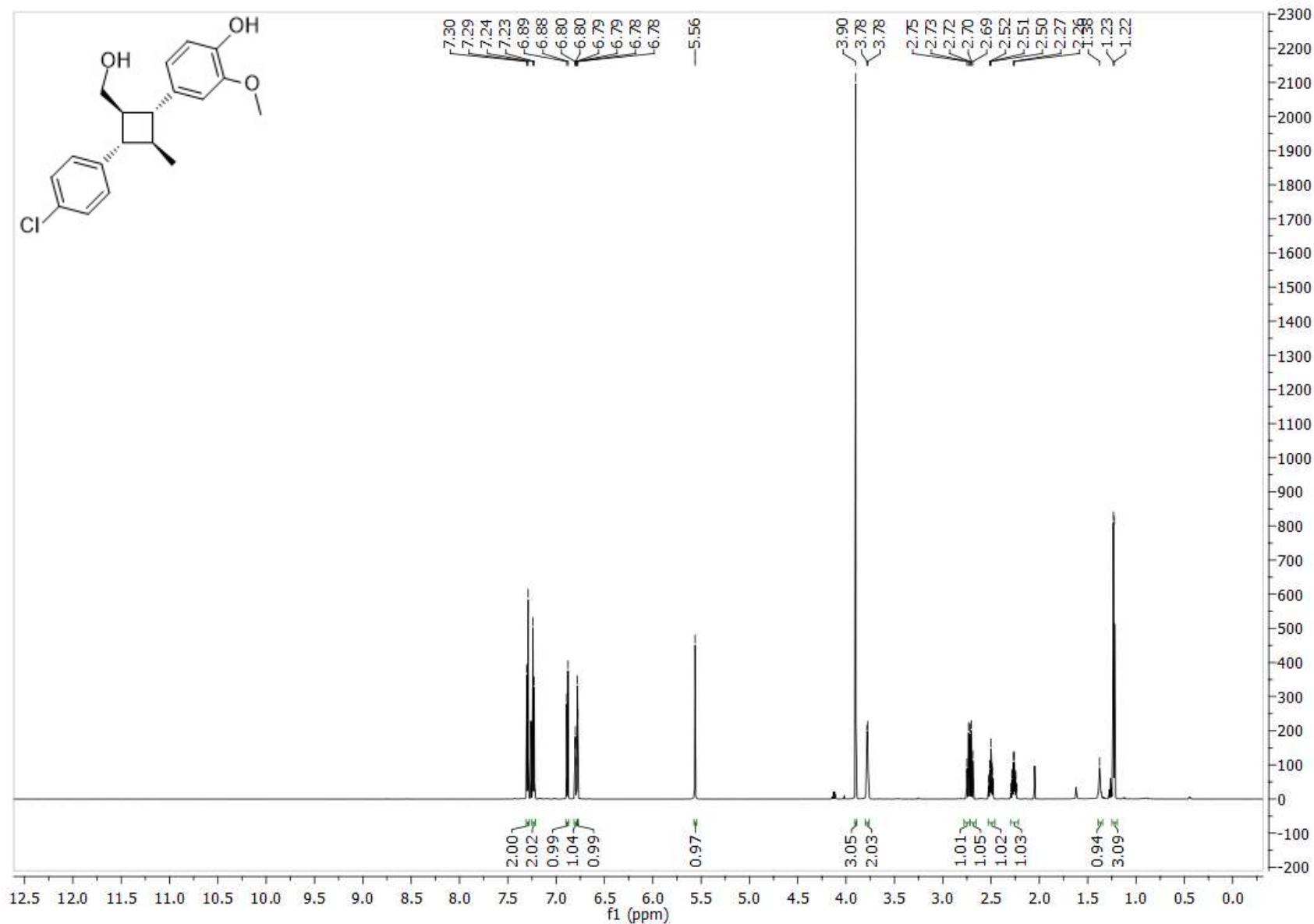
5b ¹³C NMR
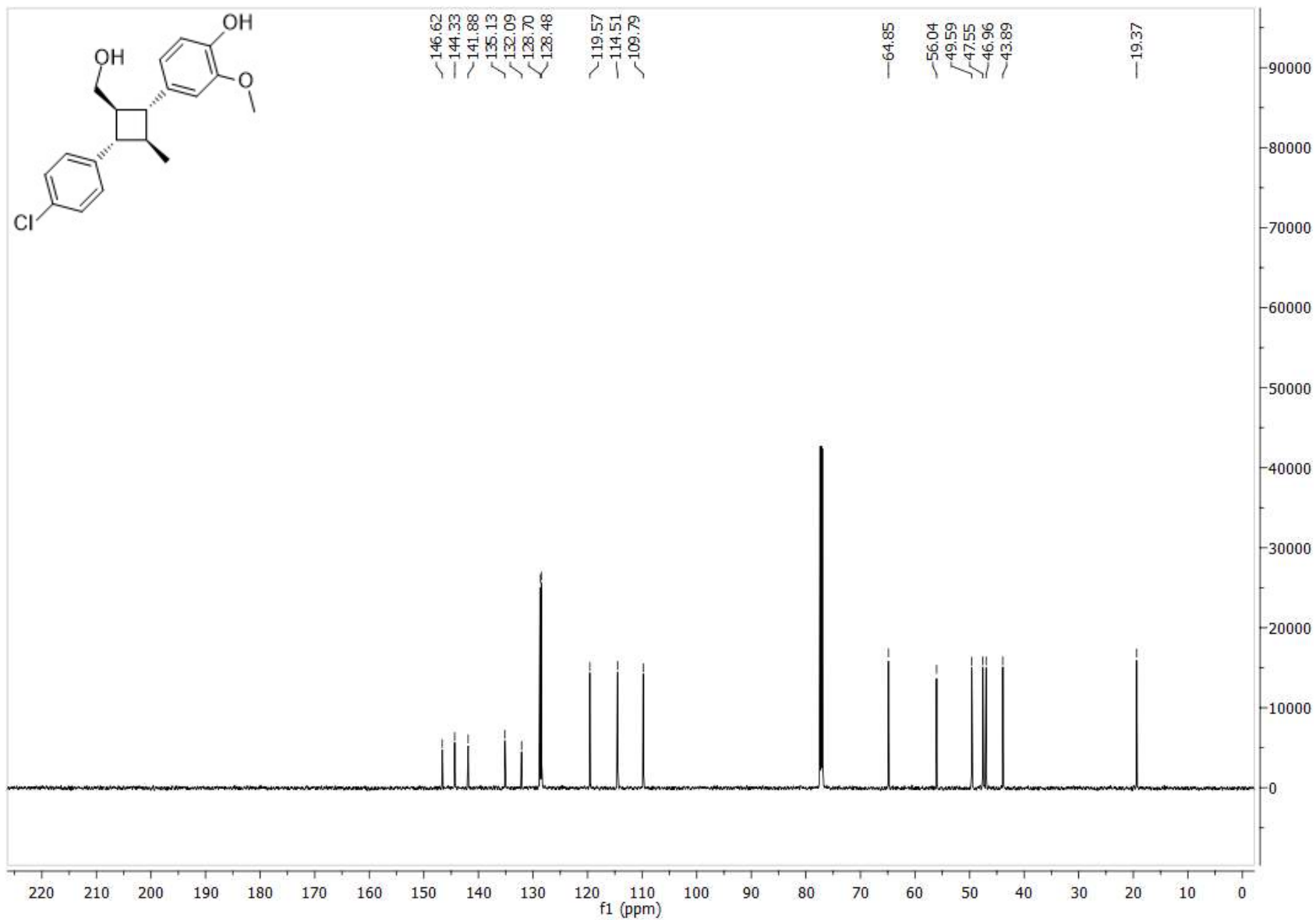
4c ^{1}H NMR
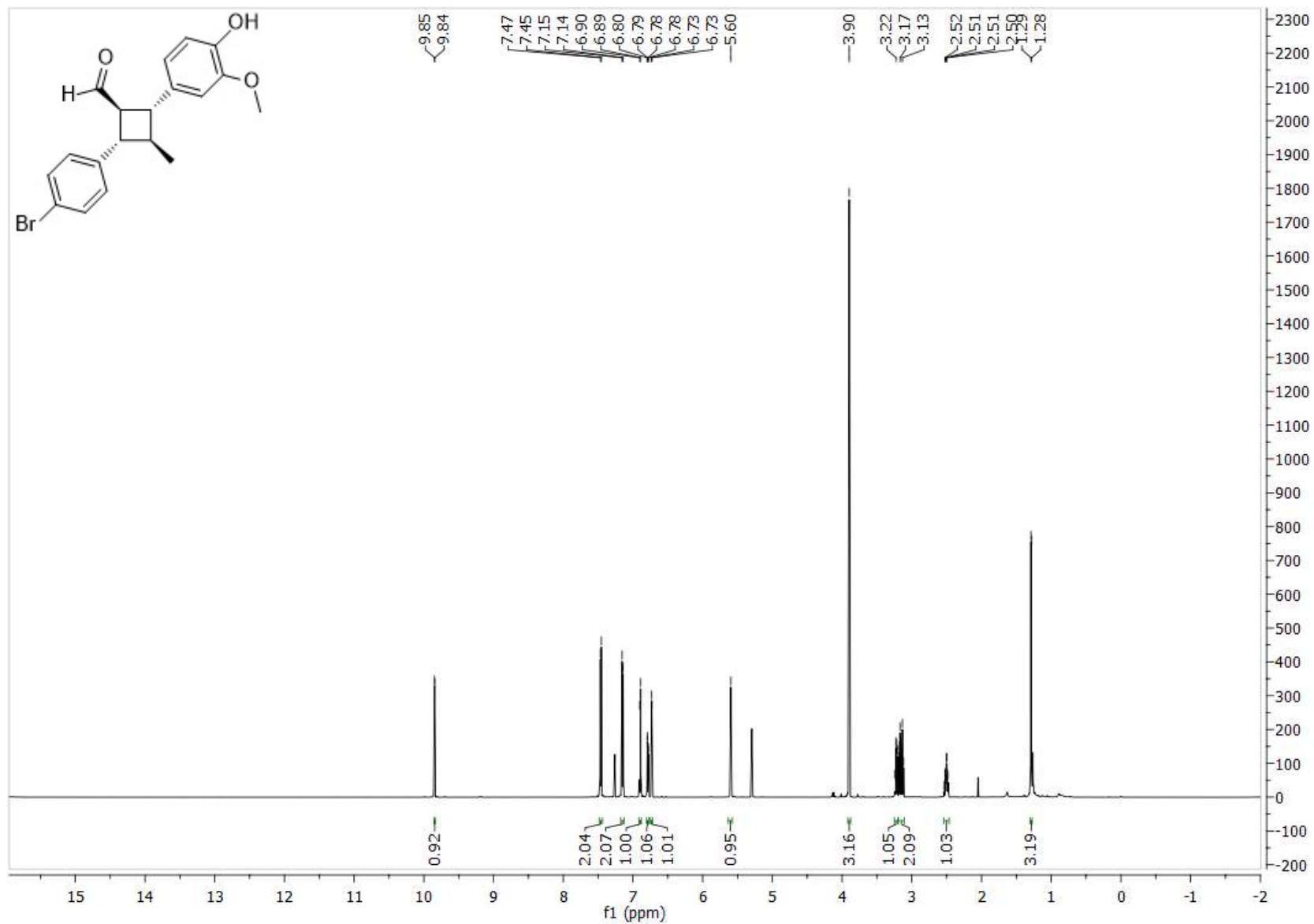
4c ^{13}C NMR
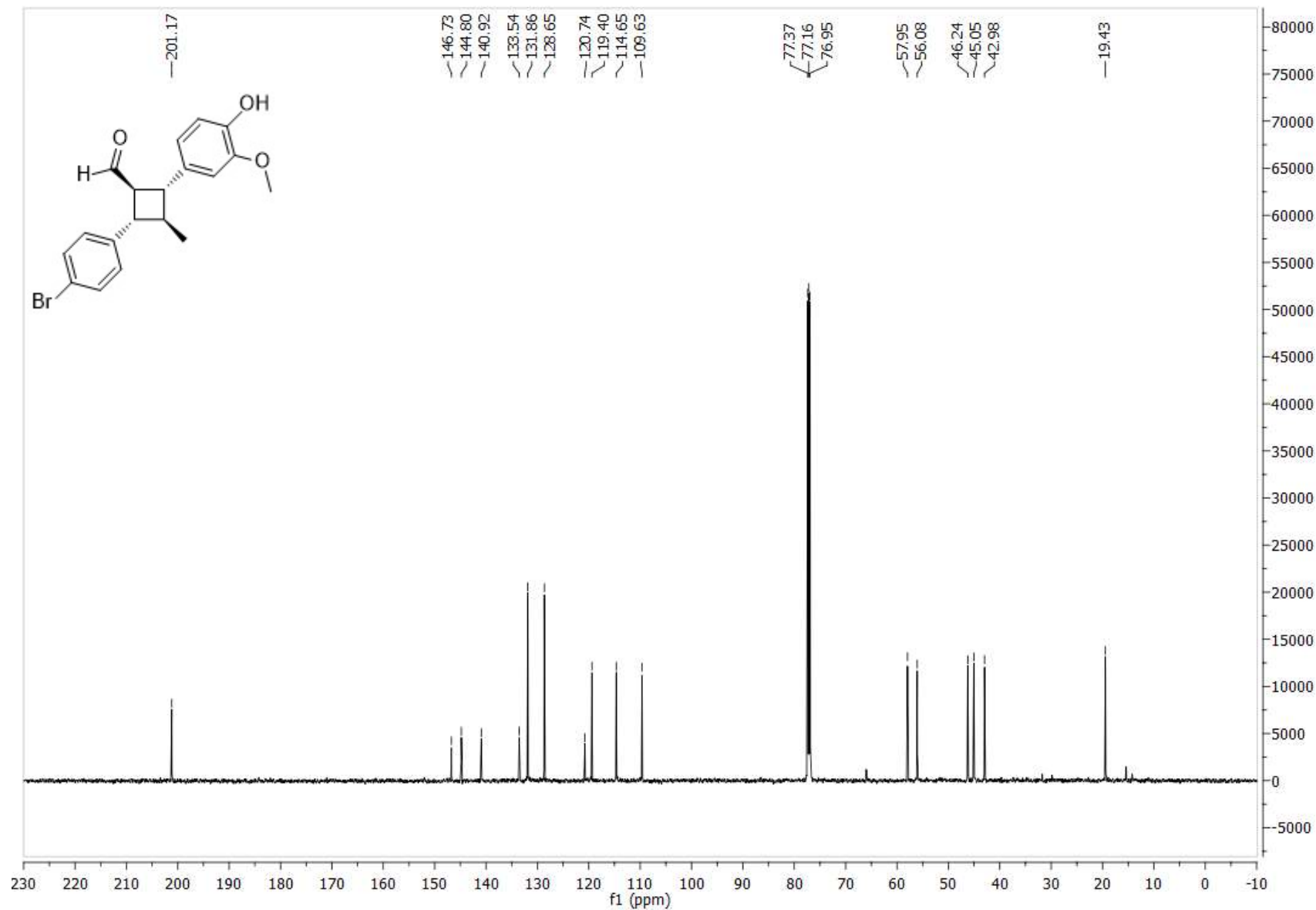
5c ^{1}H NMR
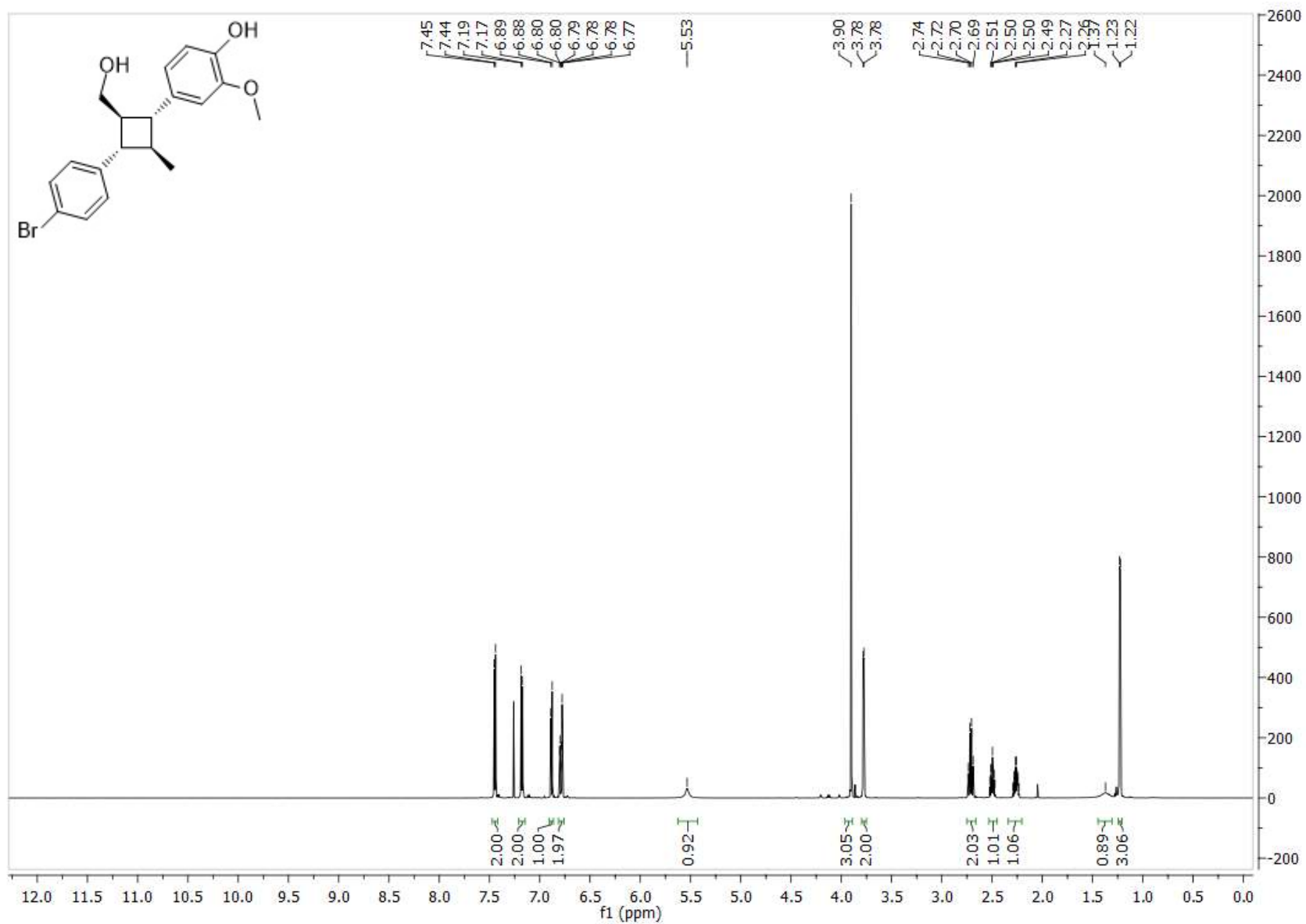
5c ^{13}C NMR
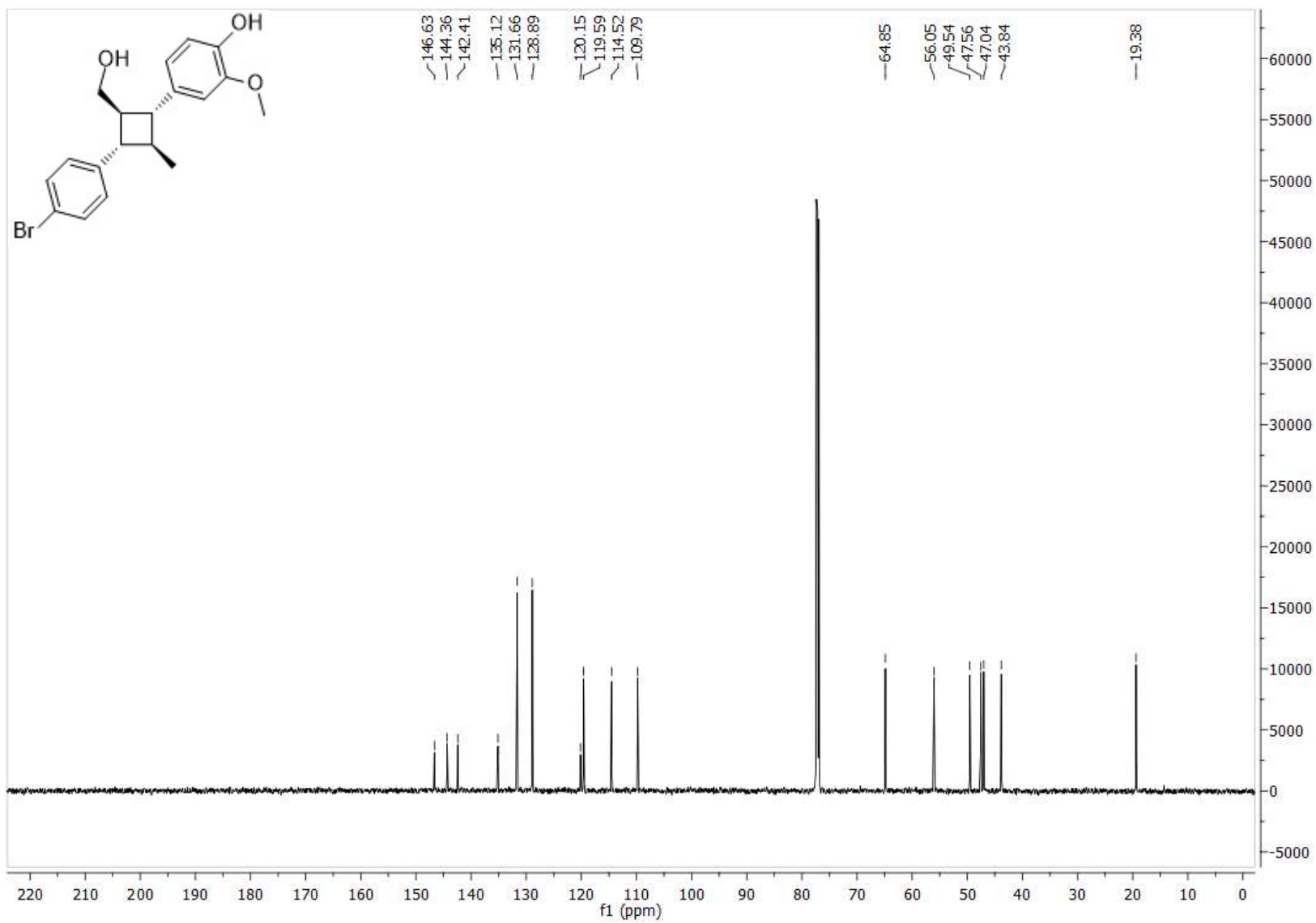
4d ¹H NMR
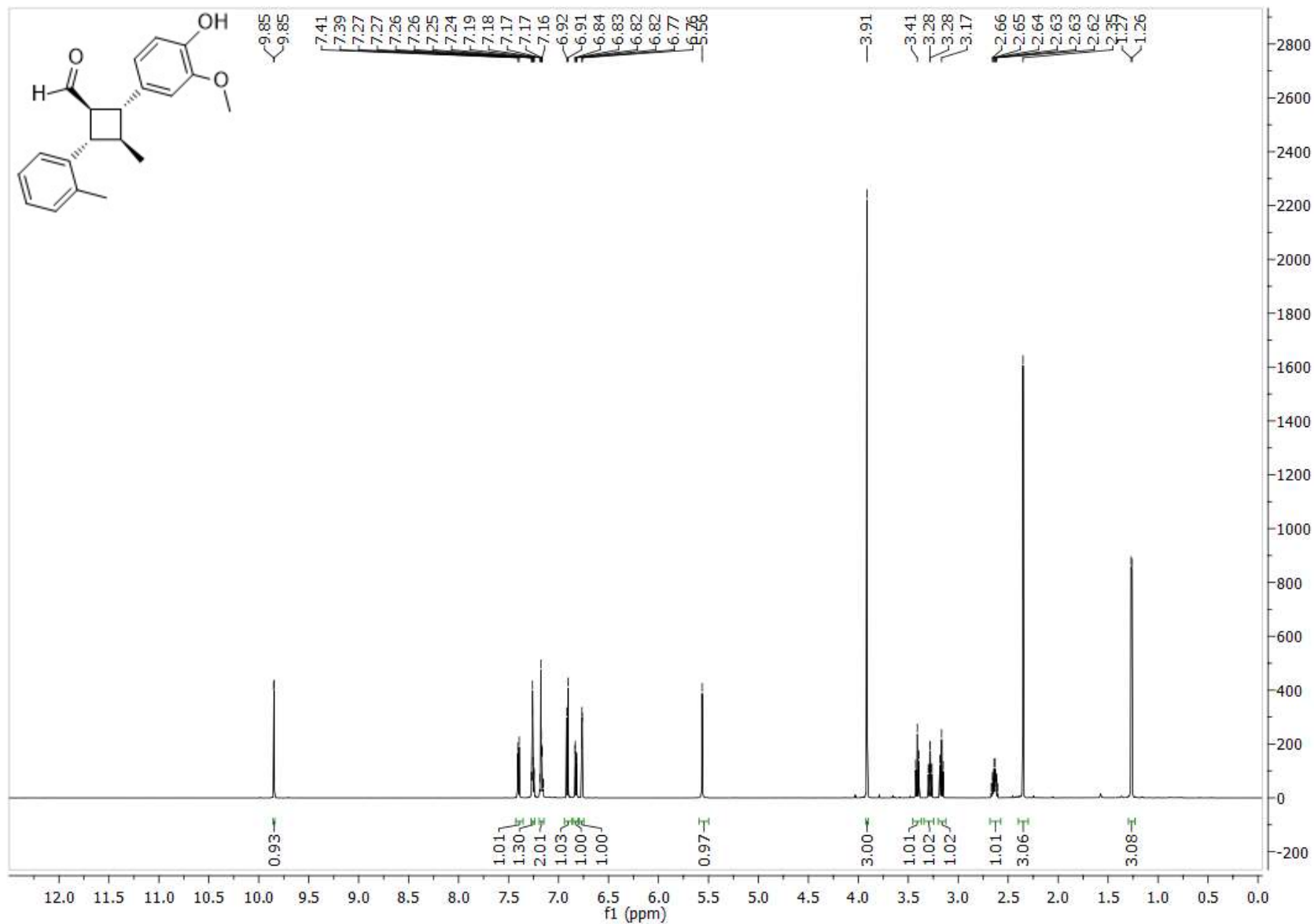
4d ¹³C NMR
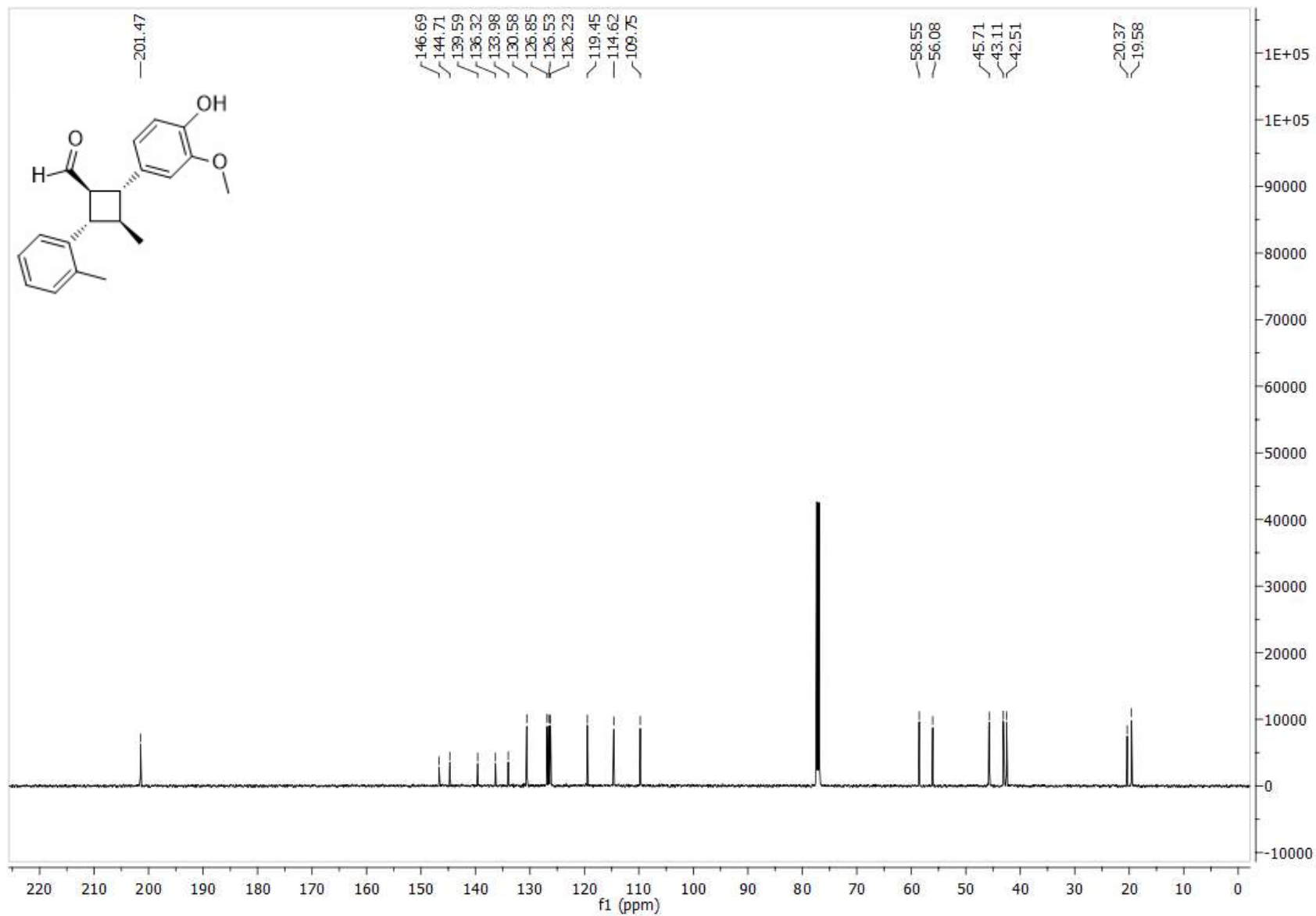
5d ^{1}H NMR
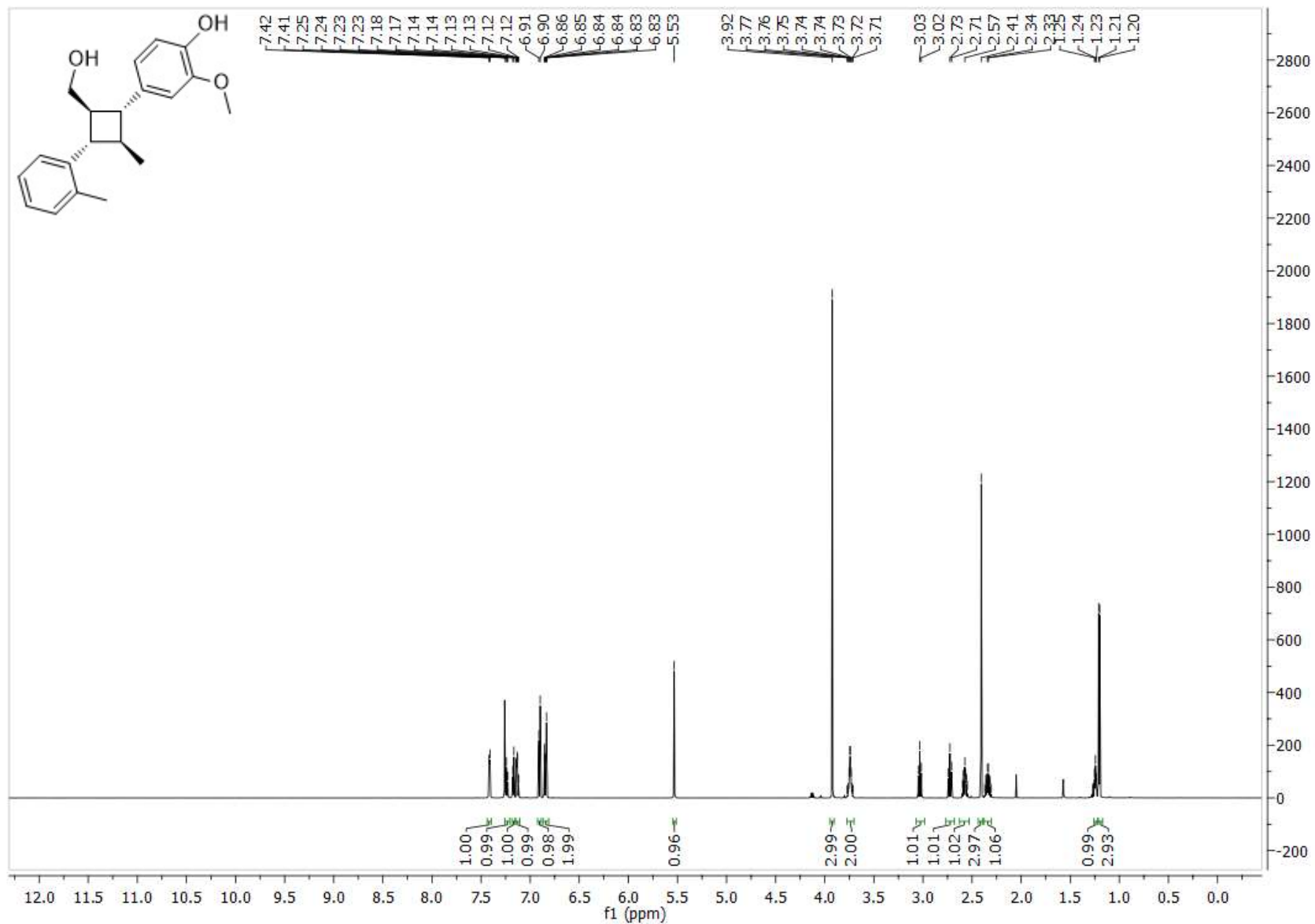
5d ¹³C NMR
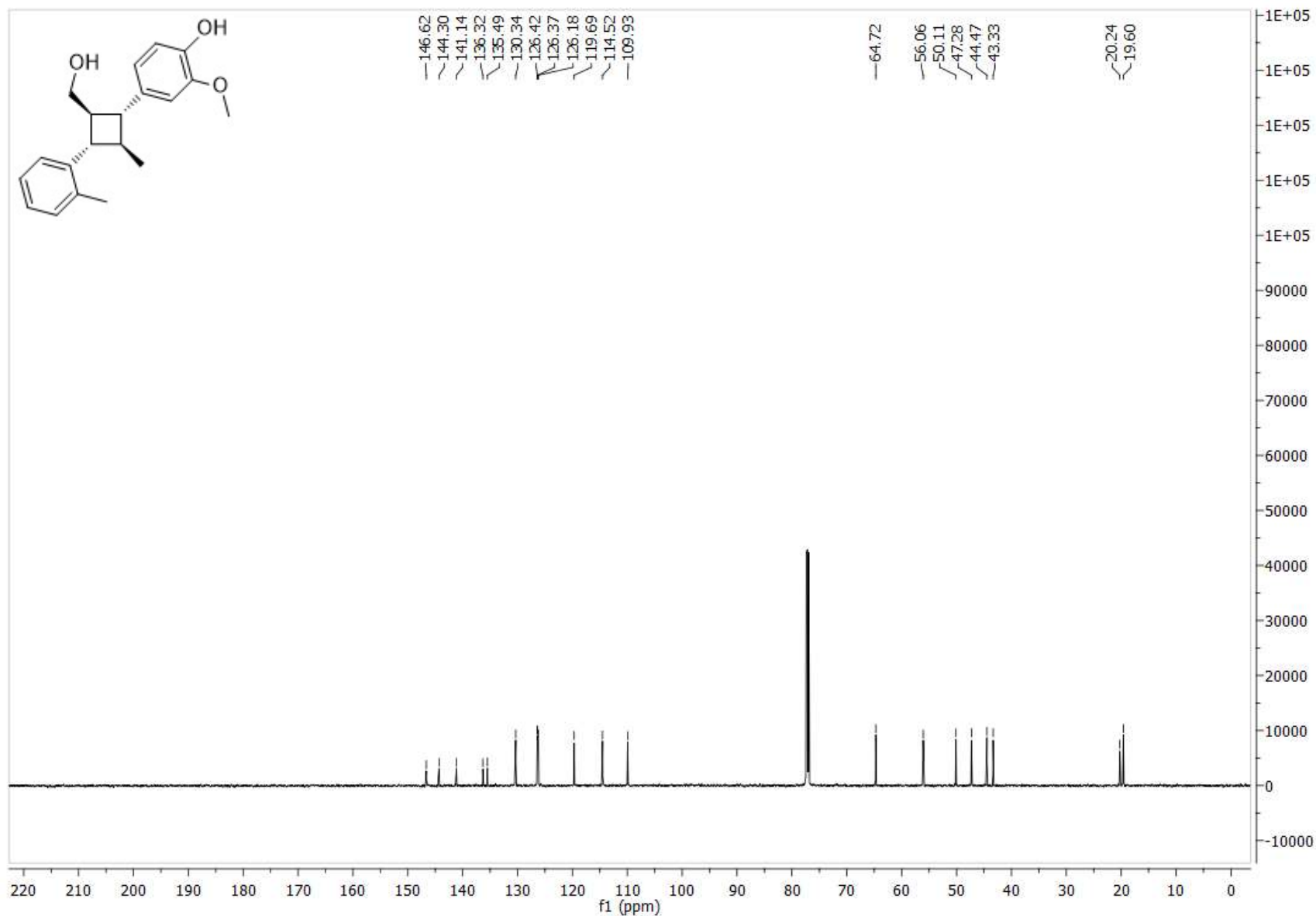
4e ¹H NMR
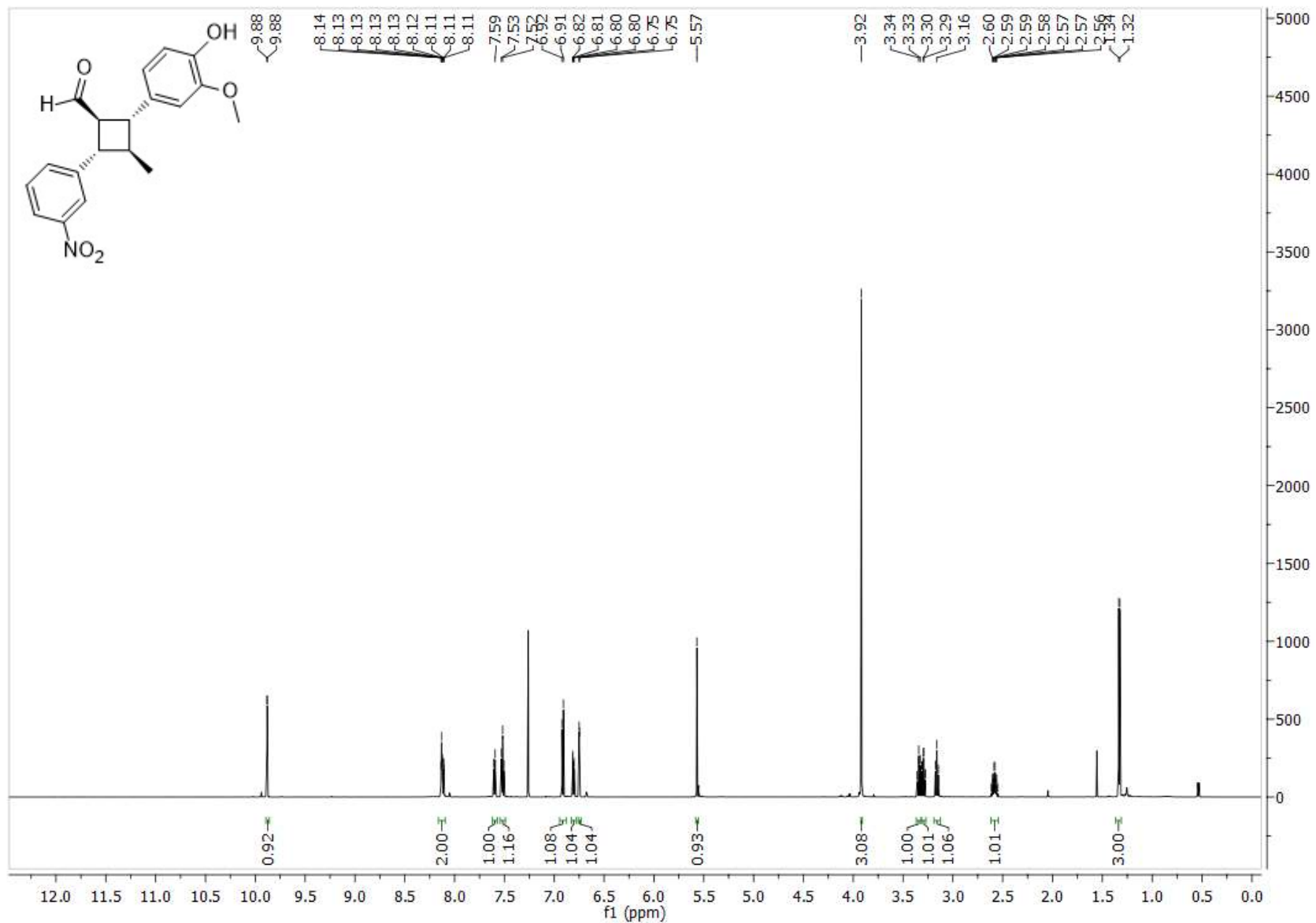
4e ¹³C NMR
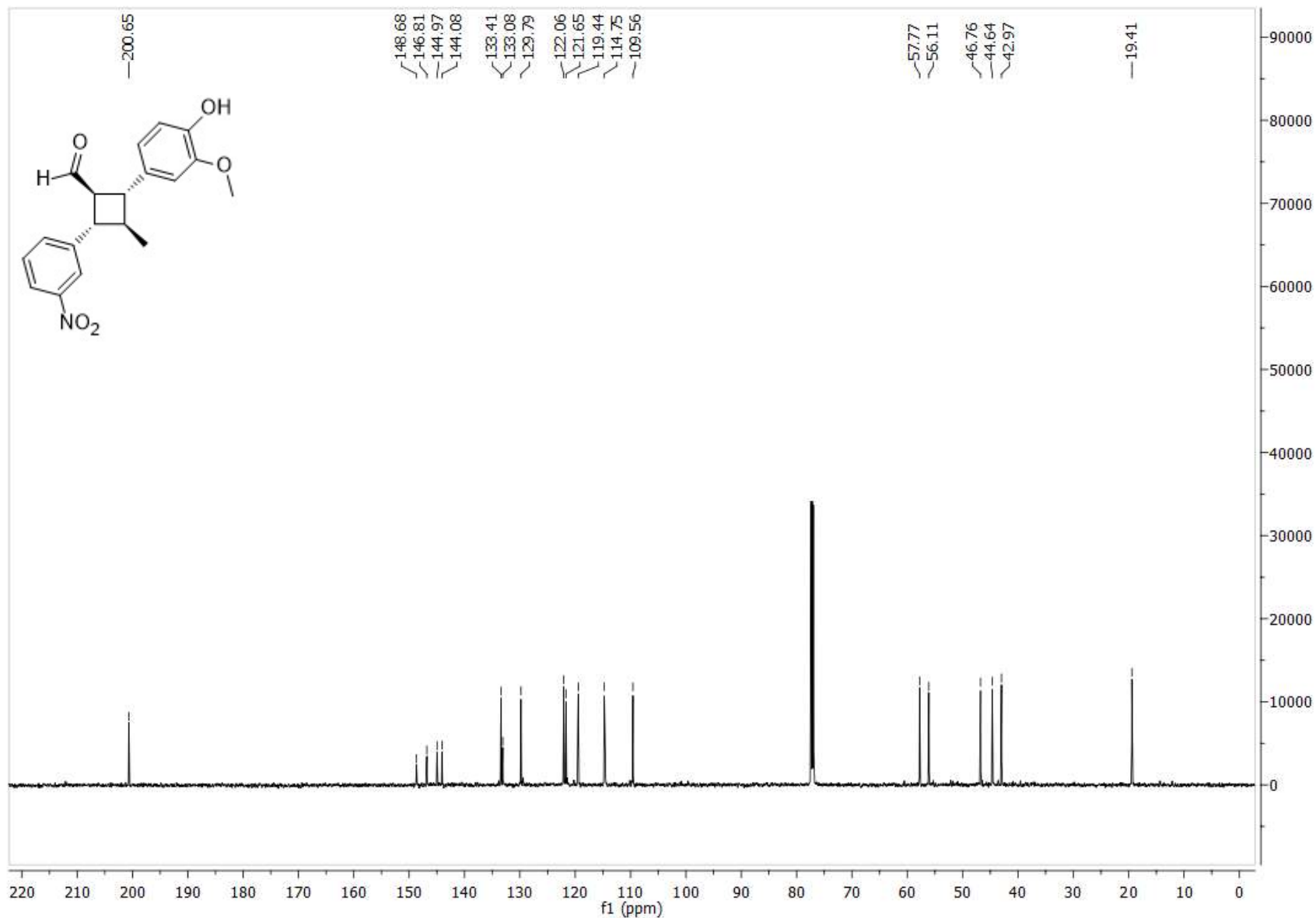
5e ^{1}H NMR
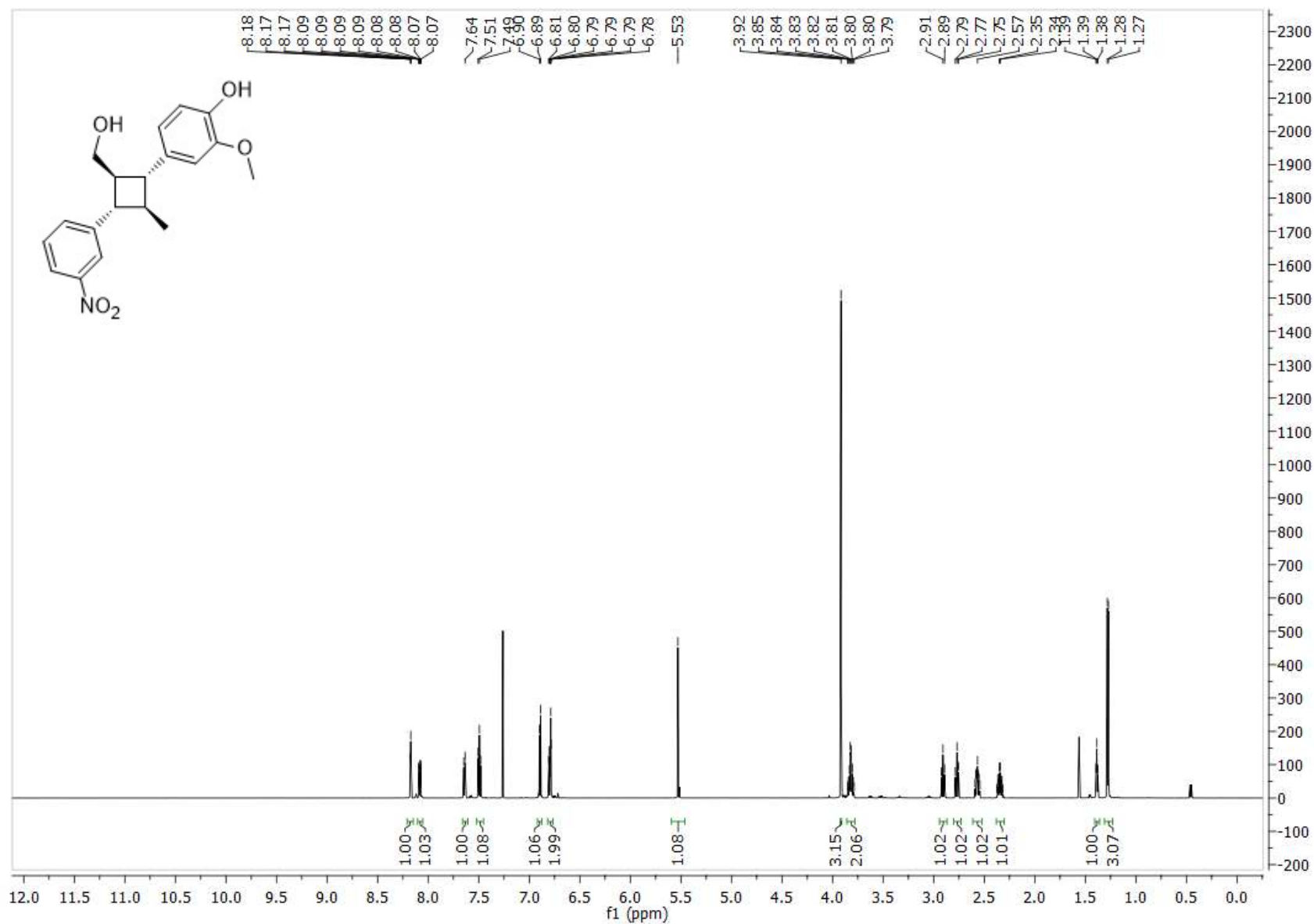
5e ^{13}C NMR
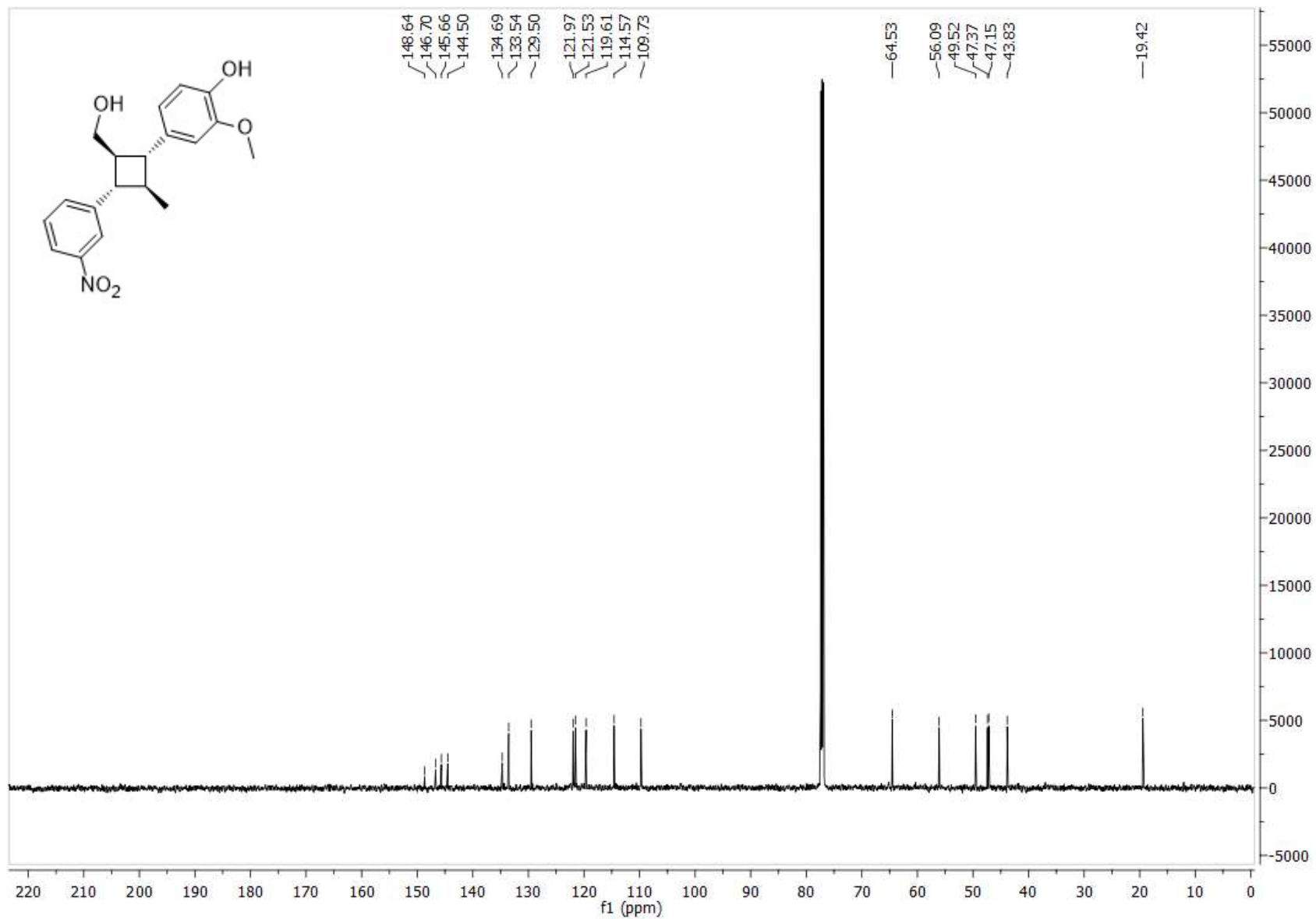
4f ¹H NMR
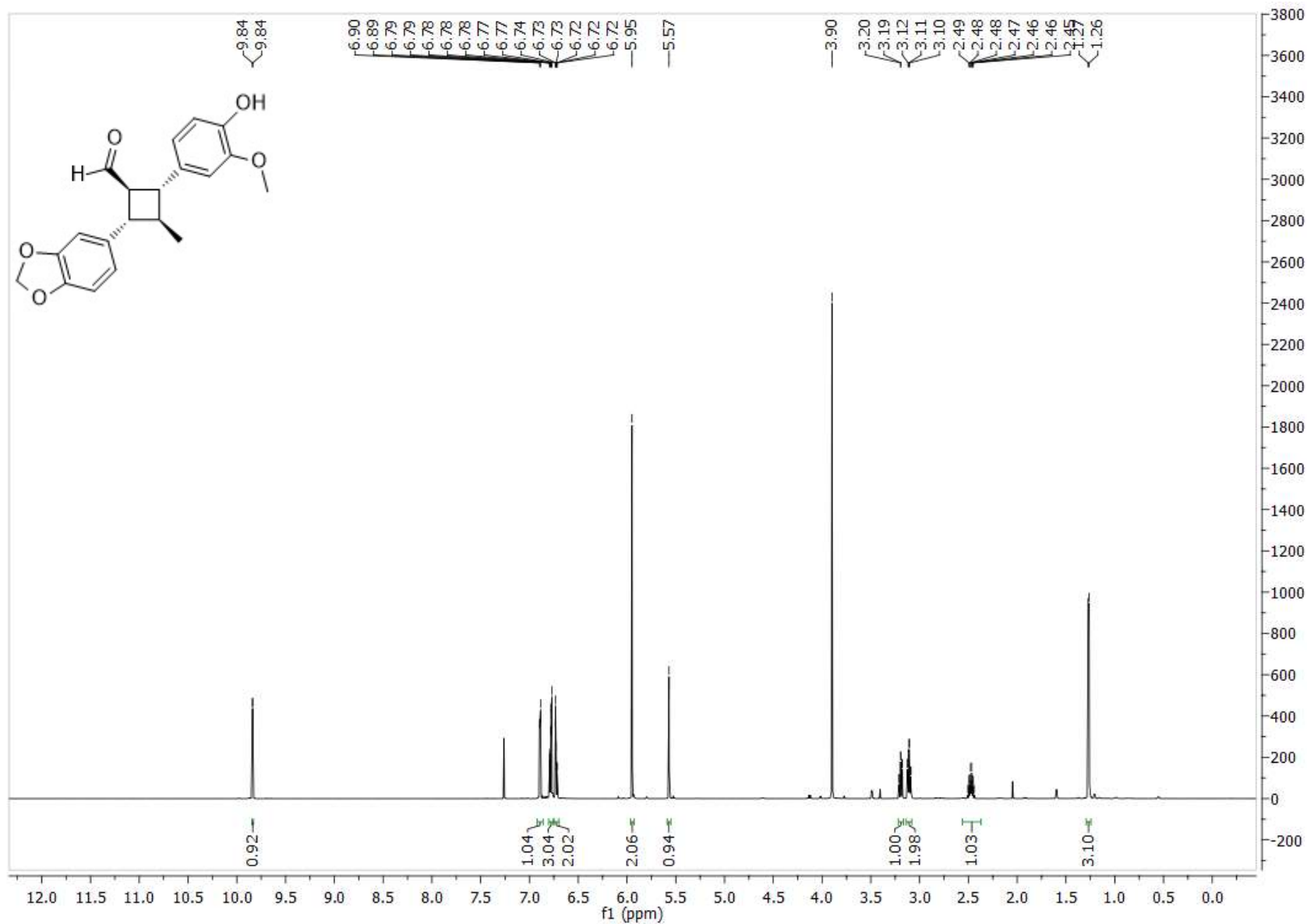
4f ^{13}C NMR
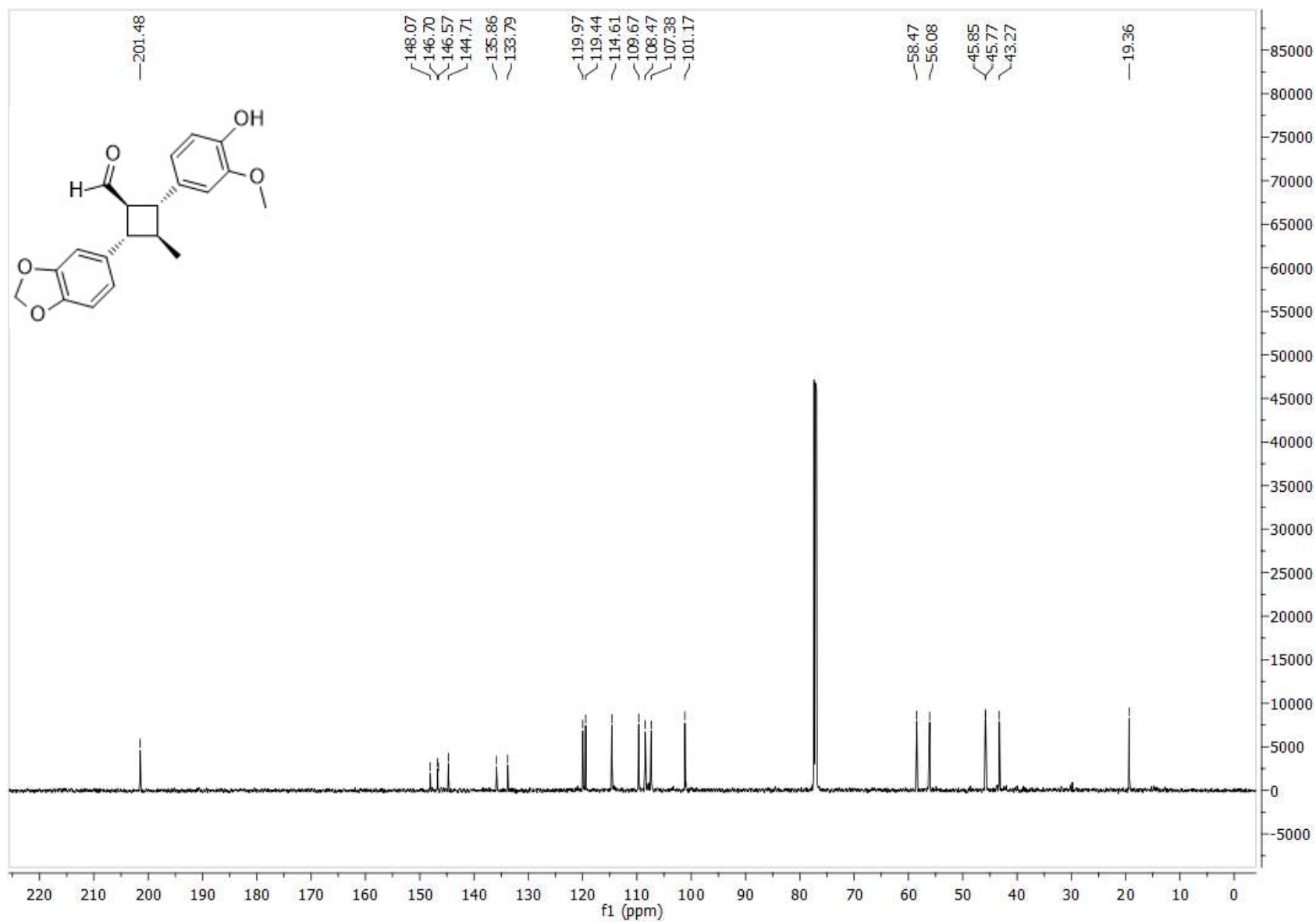
5f ¹H NMR
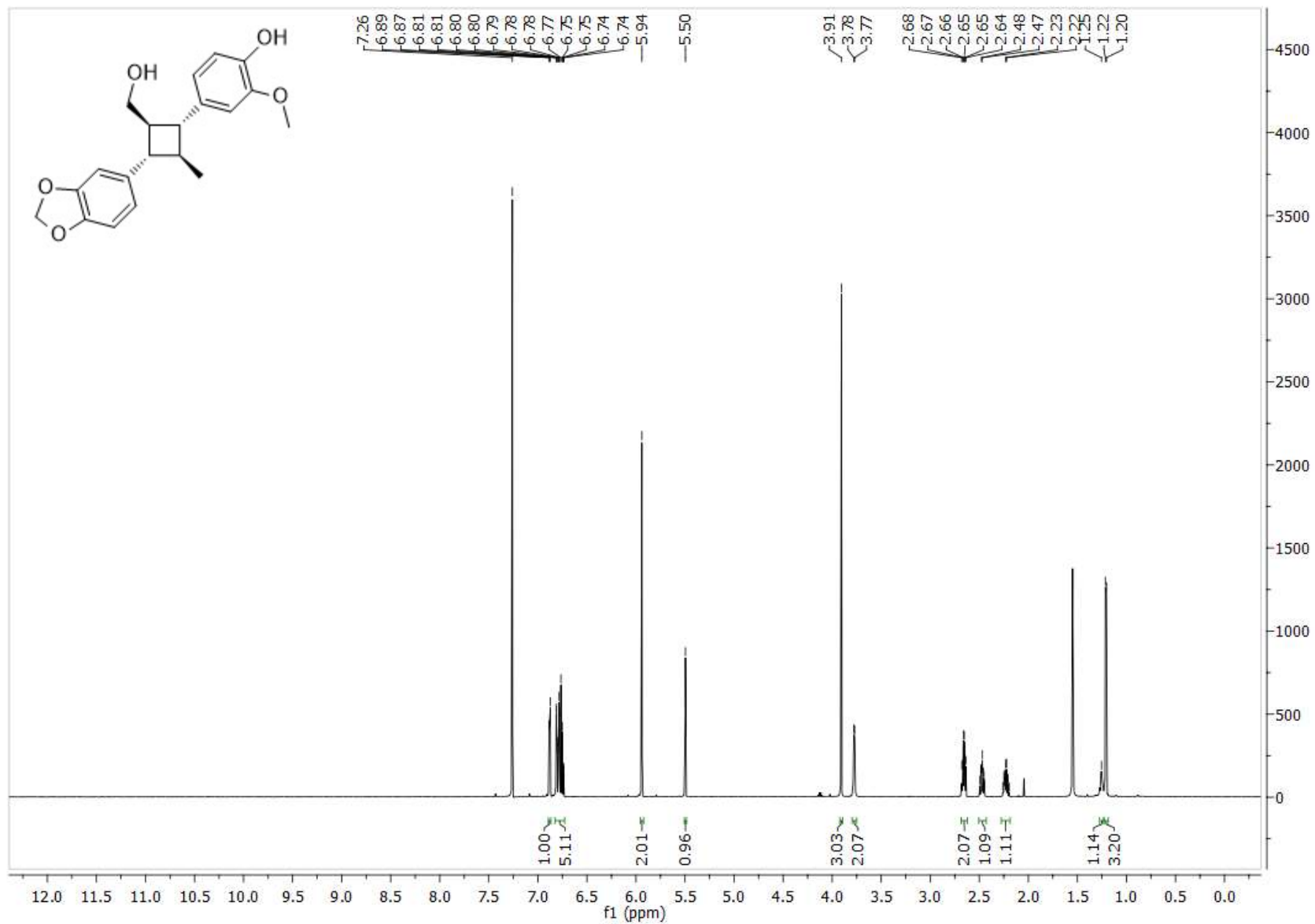
5f ^{13}C NMR
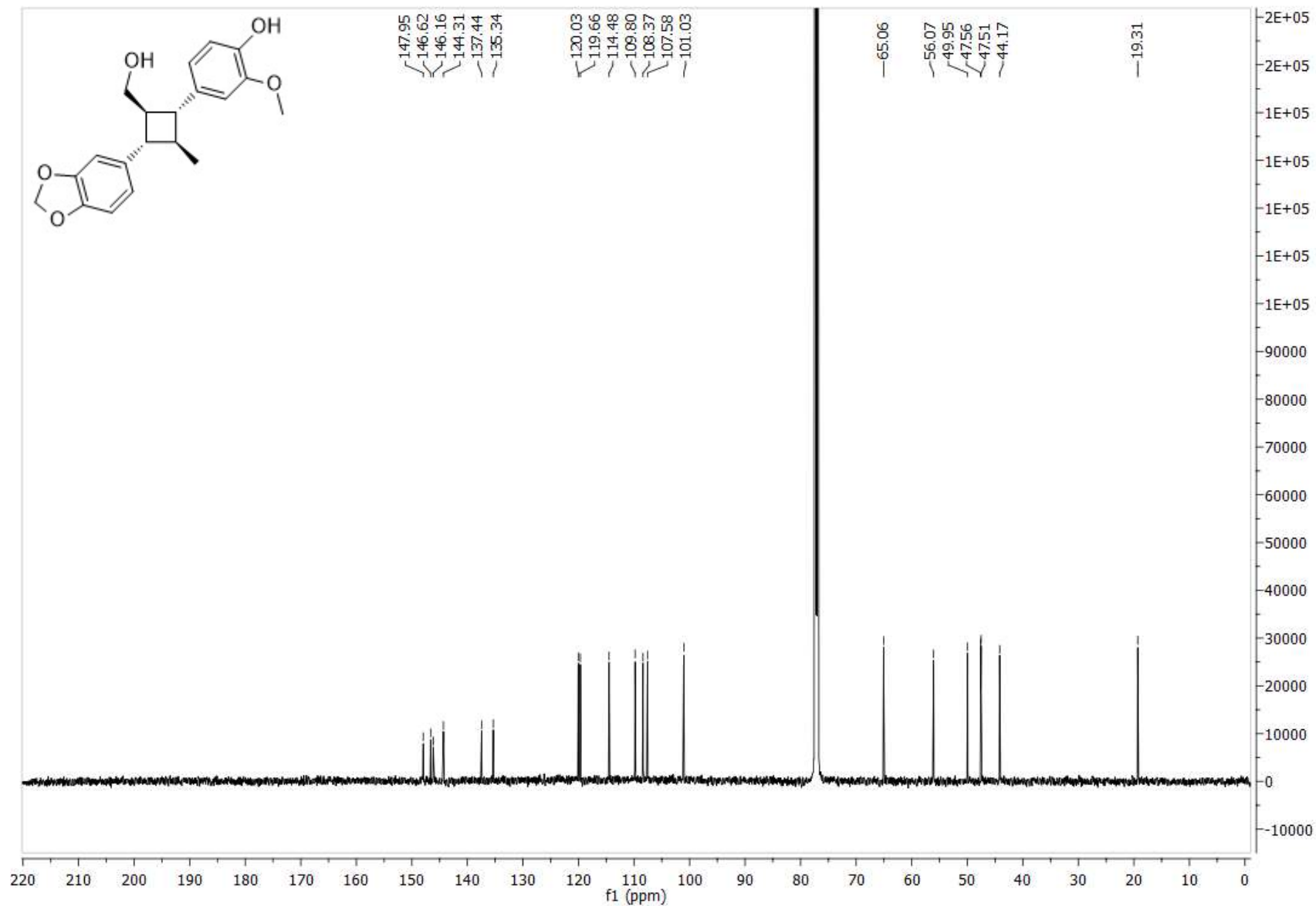
4g ¹H NMR
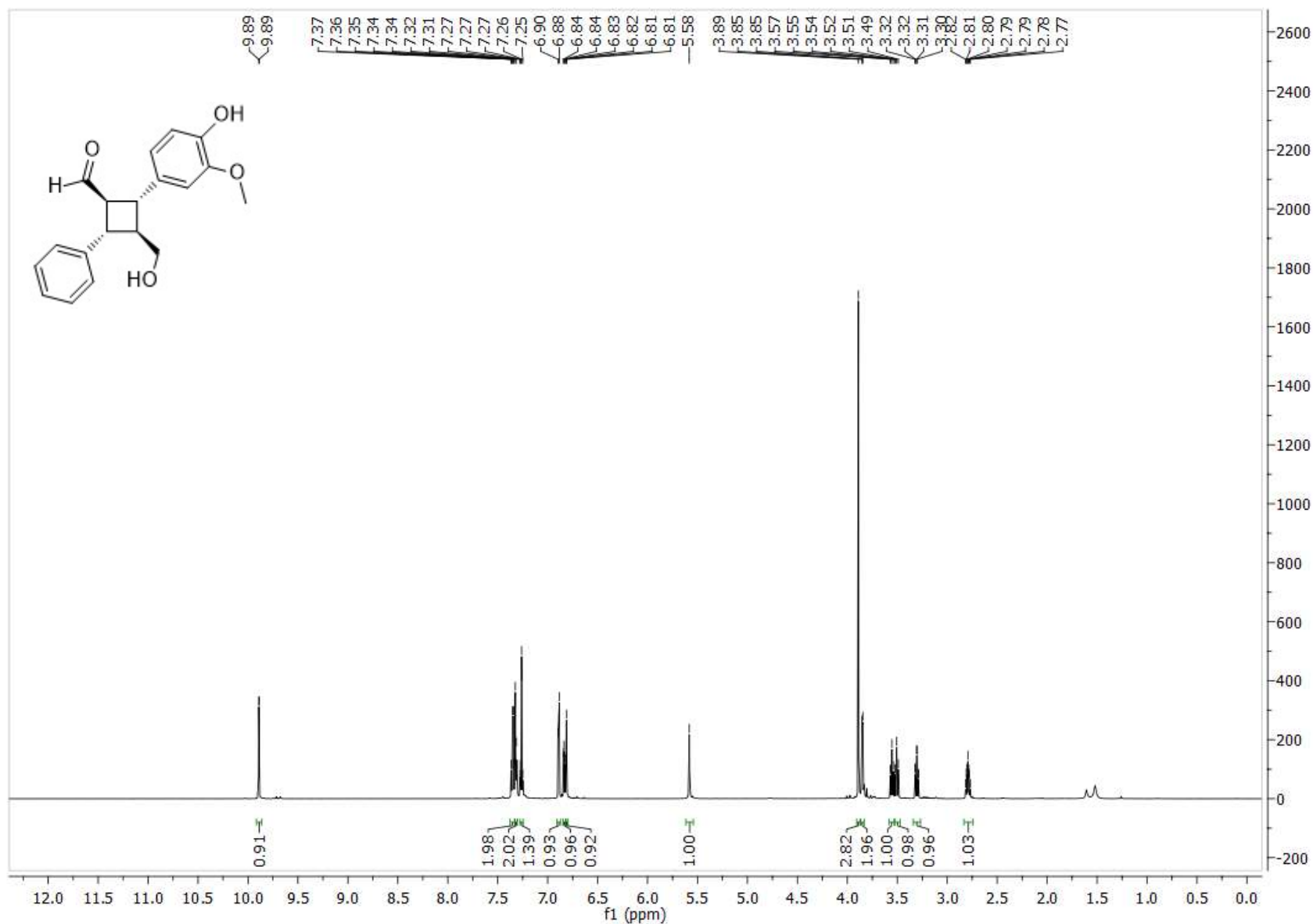
4g ^{13}C NMR
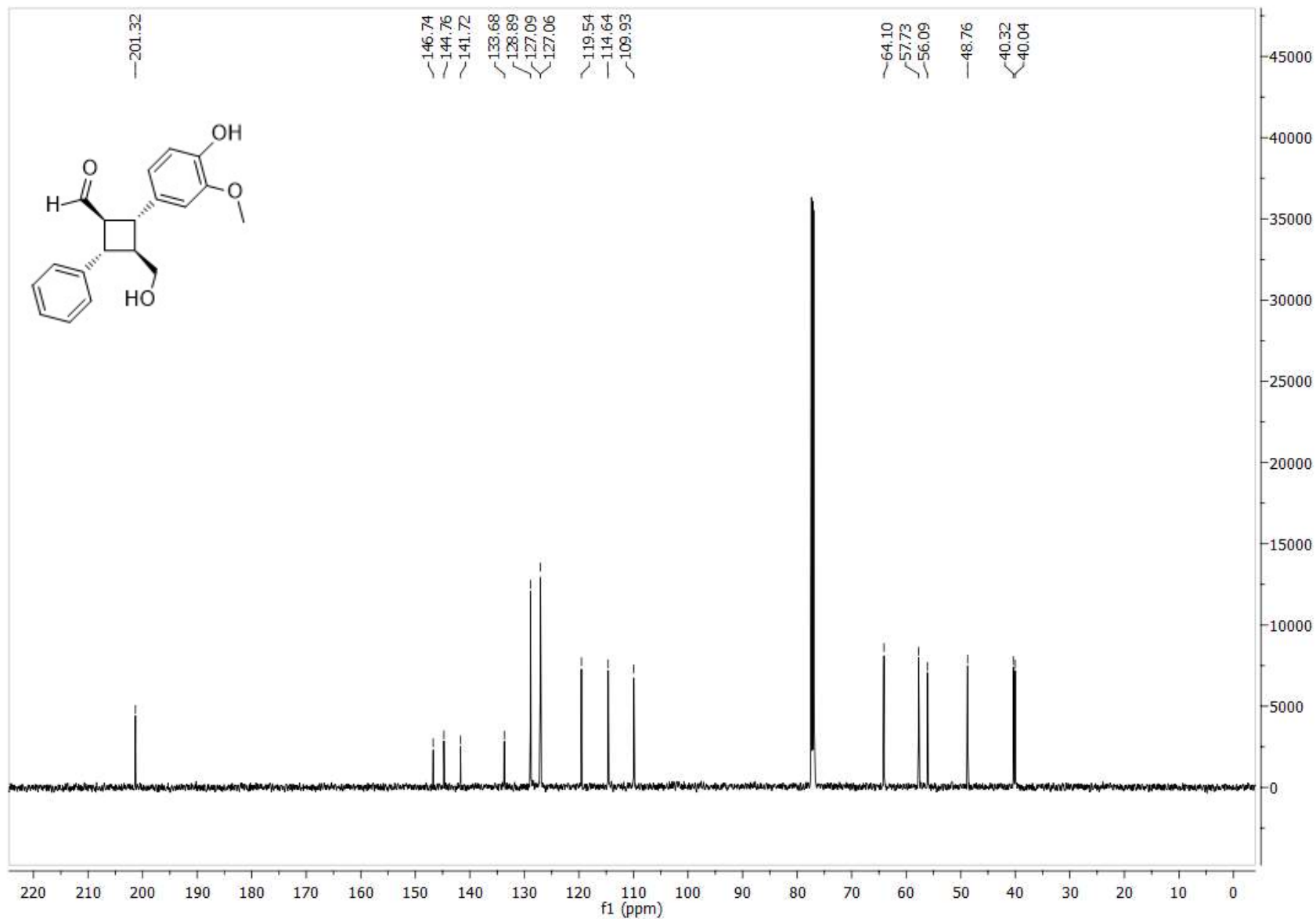
4h ¹H NMR
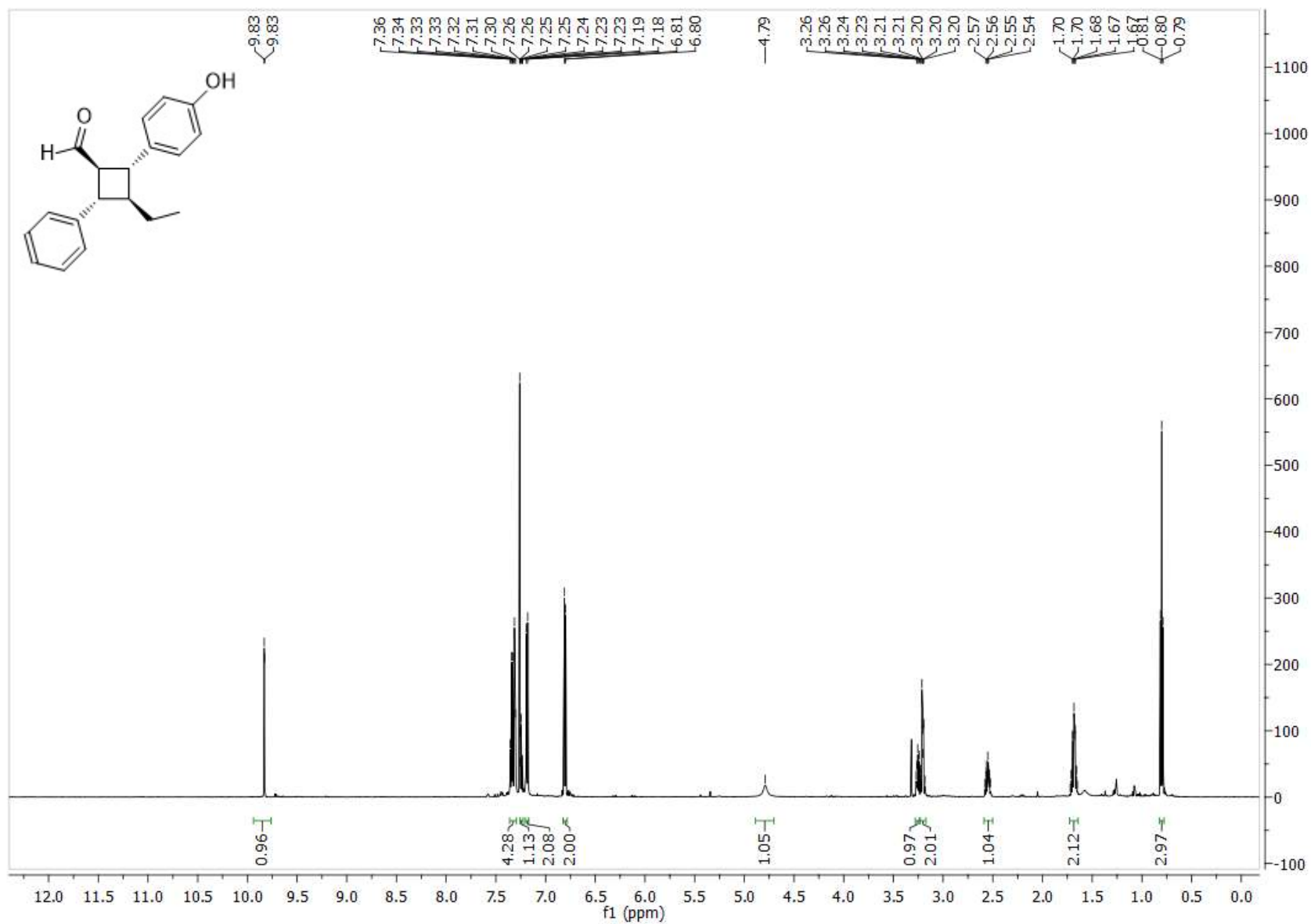
4h ^{13}C NMR
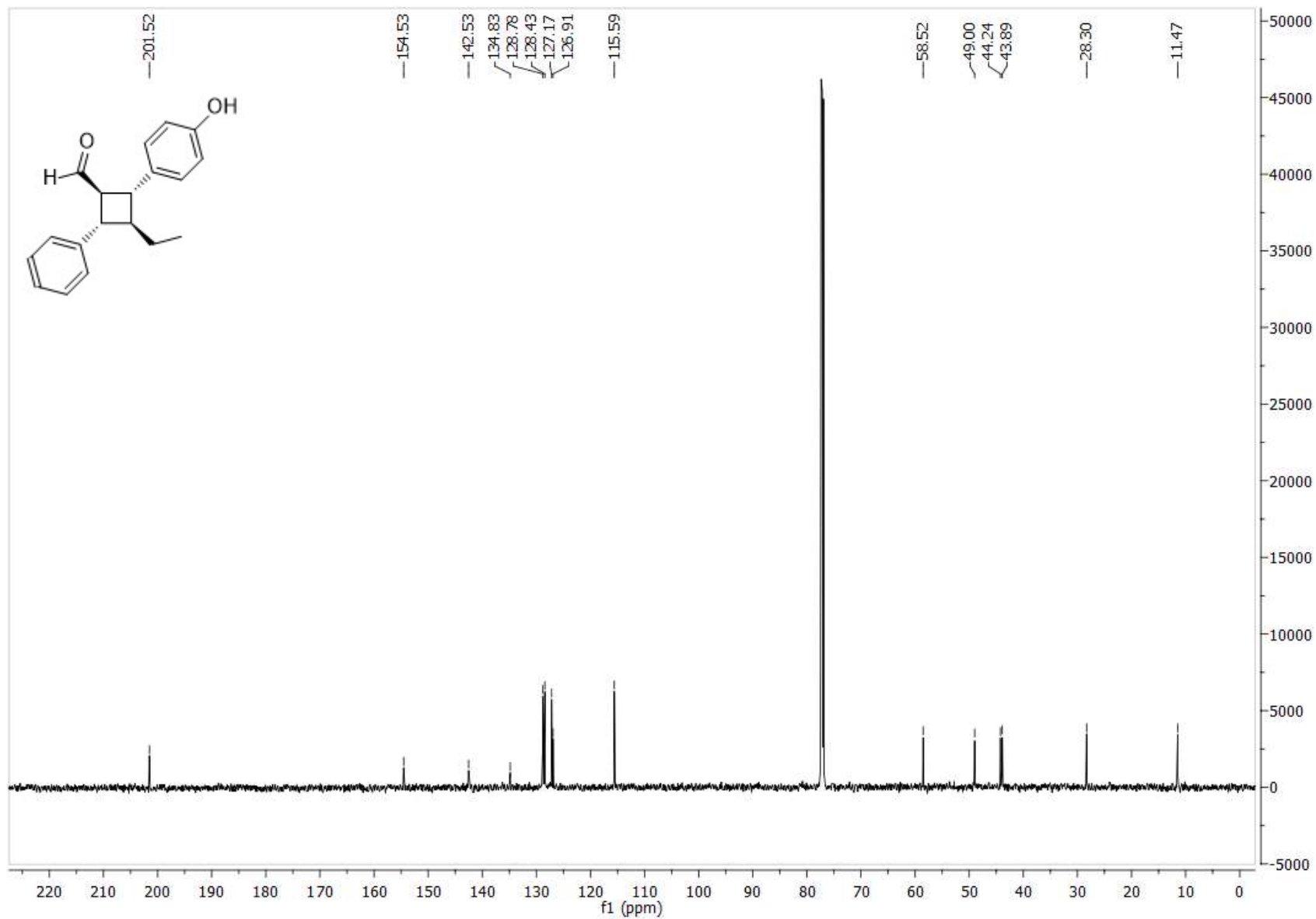
5h ¹H NMR
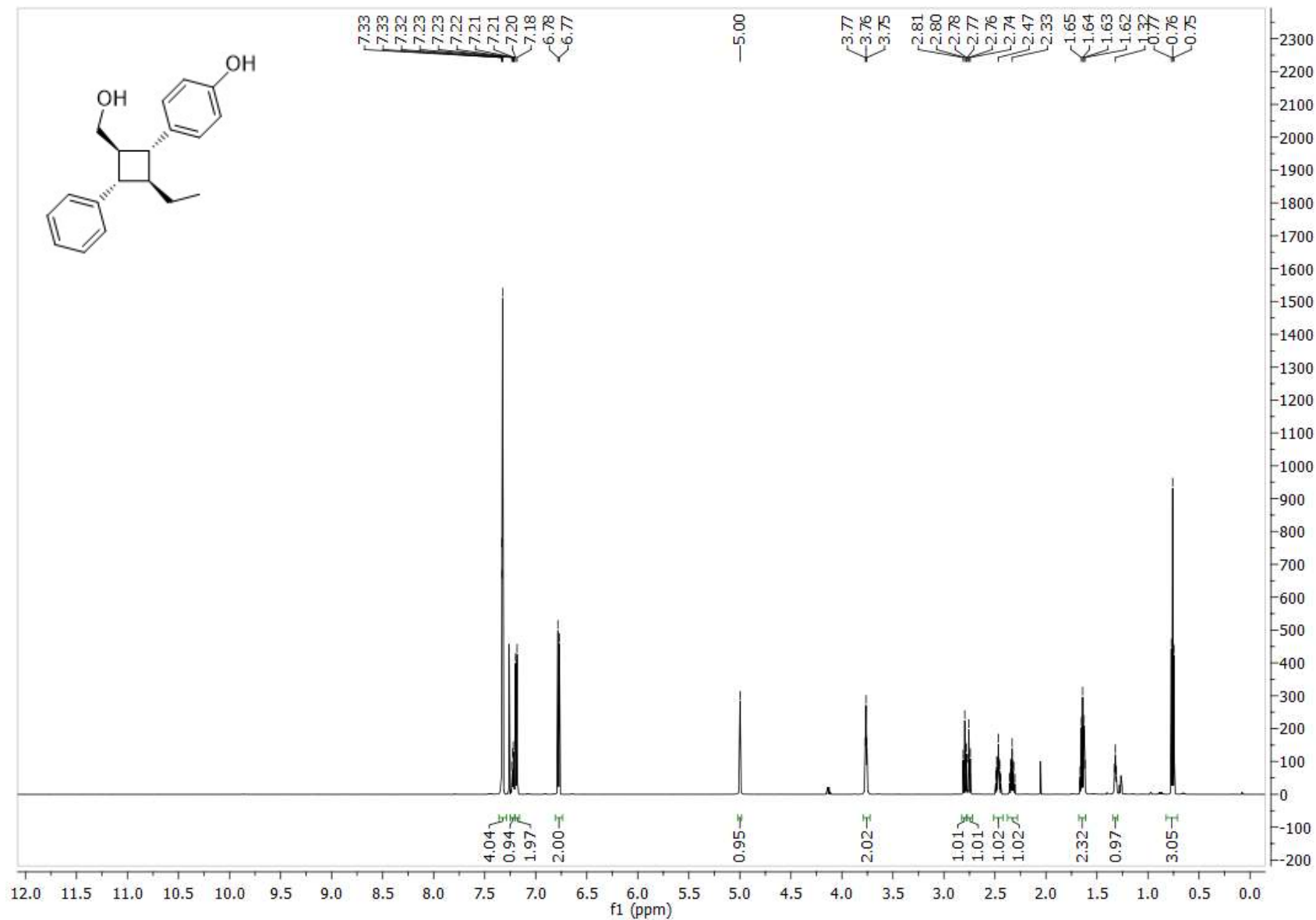
5h ^{13}C NMR
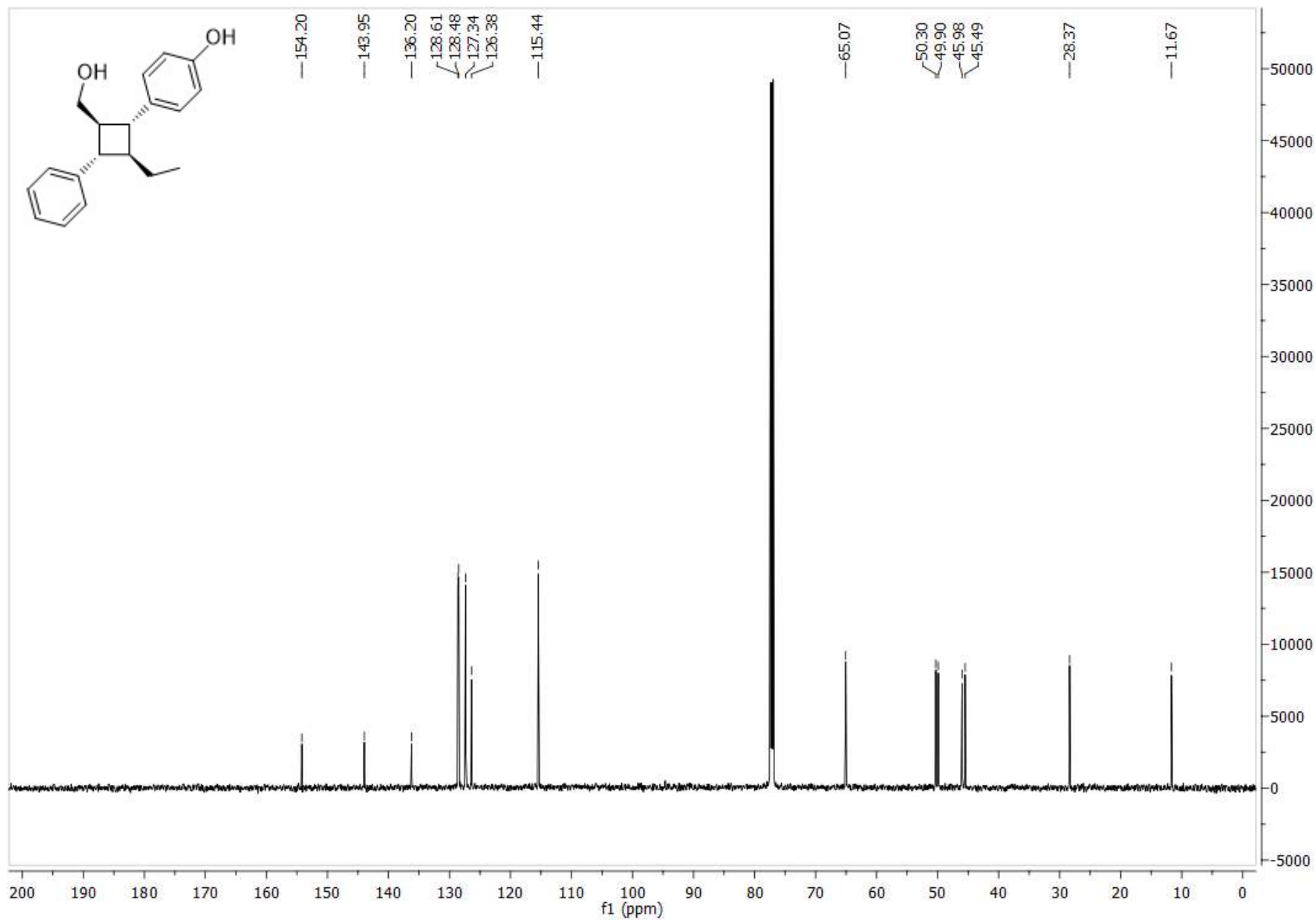
7 ¹H NMR

7 ^{13}C NMR

8 ¹H NMR

8 ^{13}C NMR

9 ¹H NMR

9 ¹³C NMR

10 ^{1}H NMR
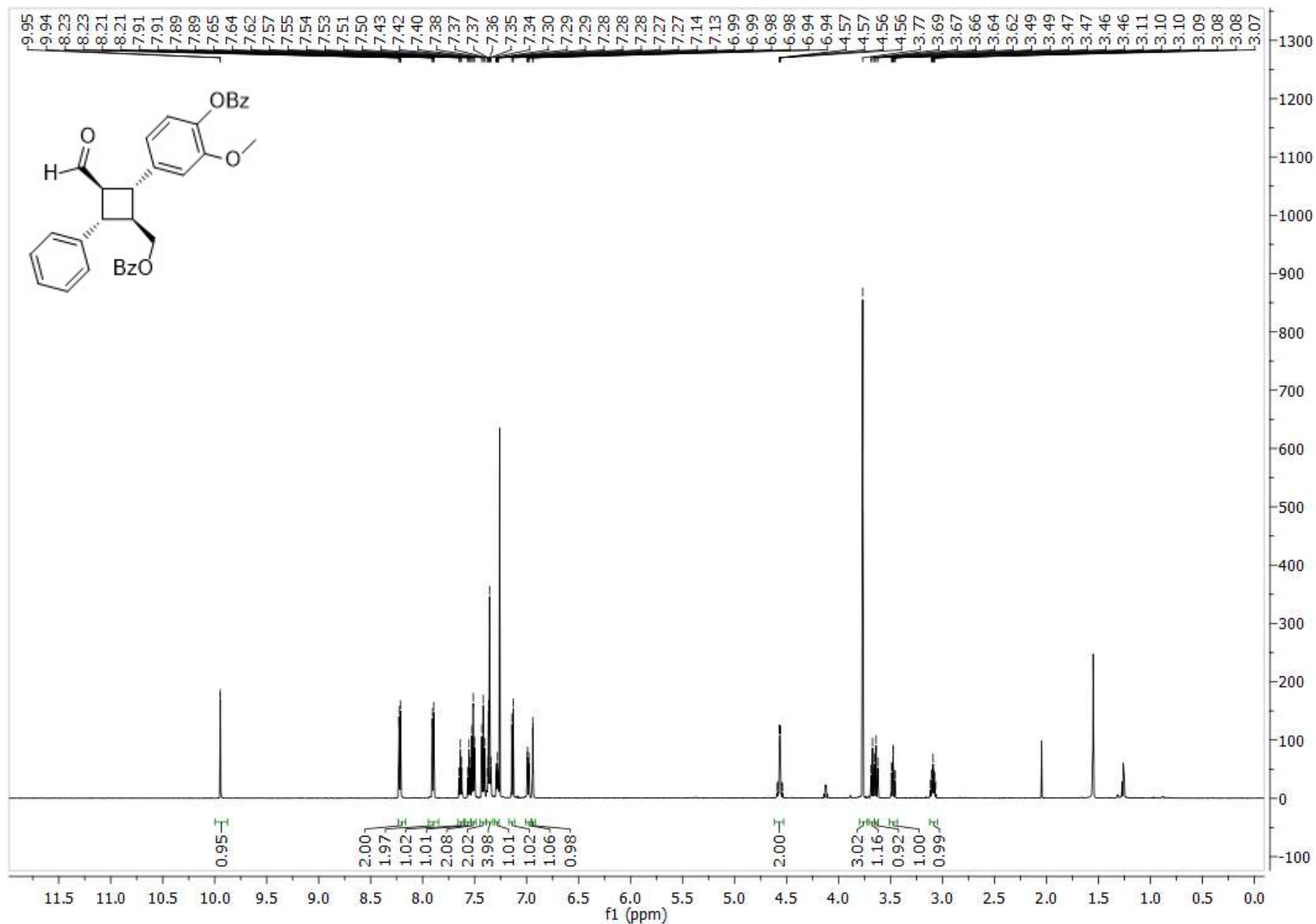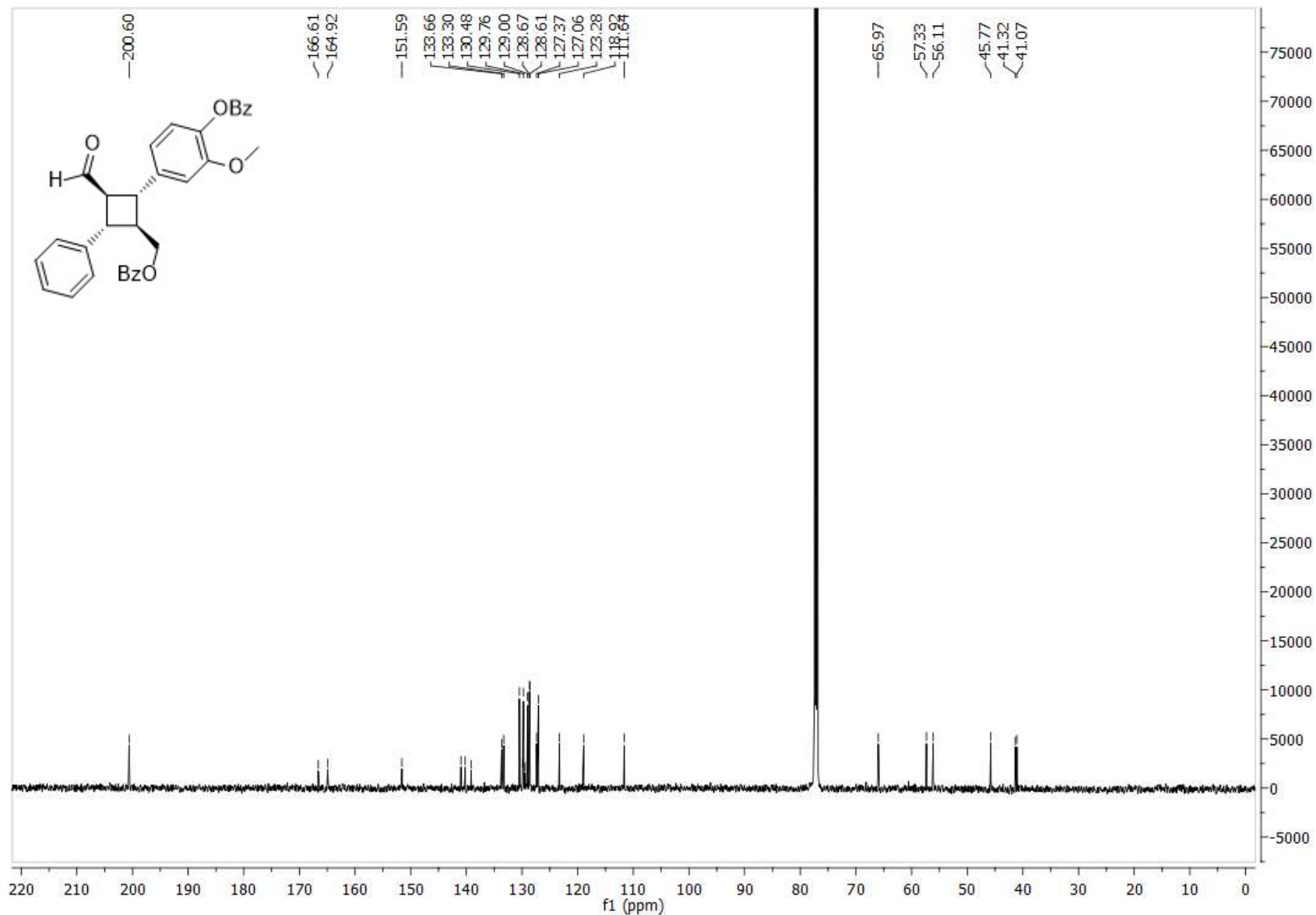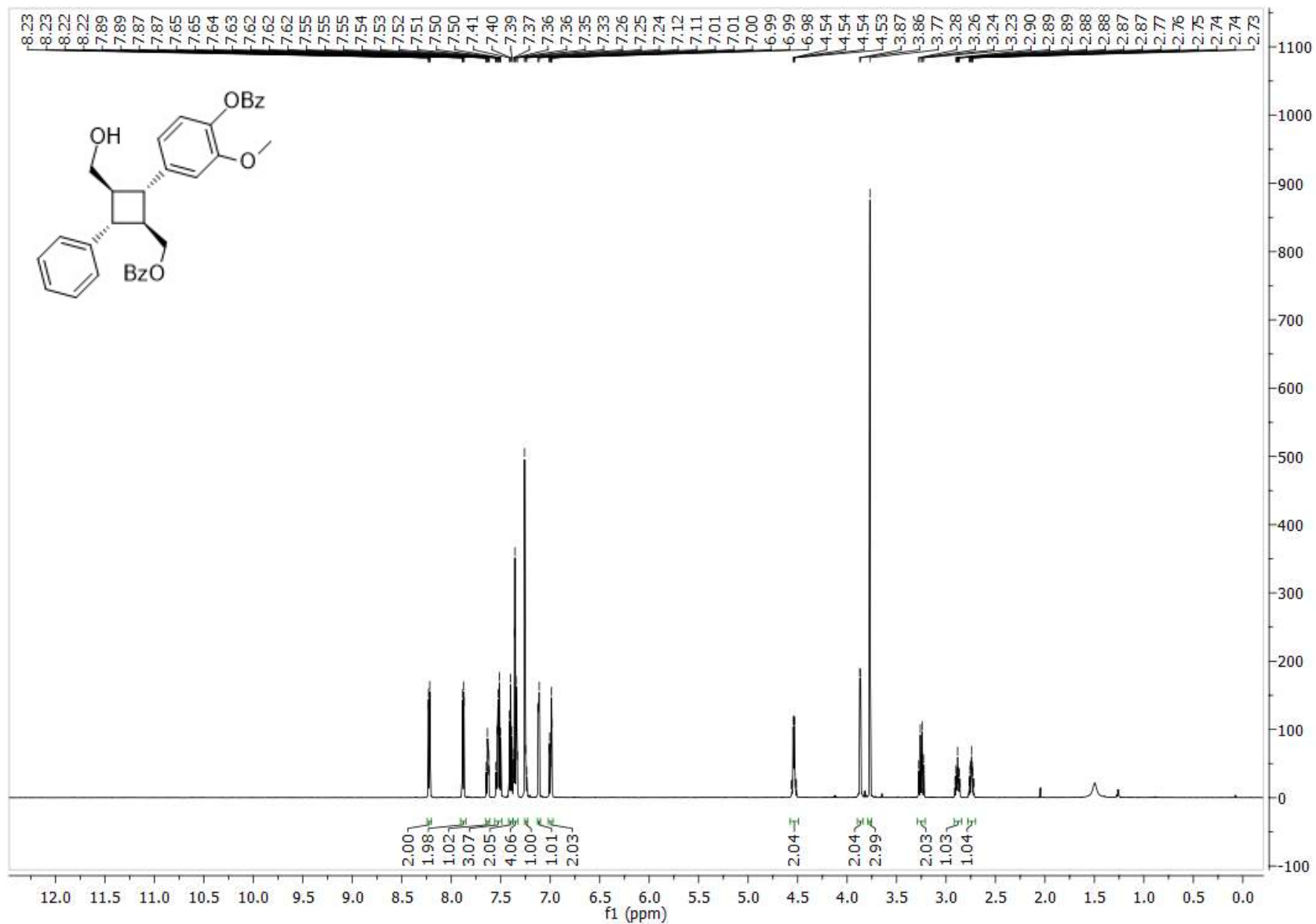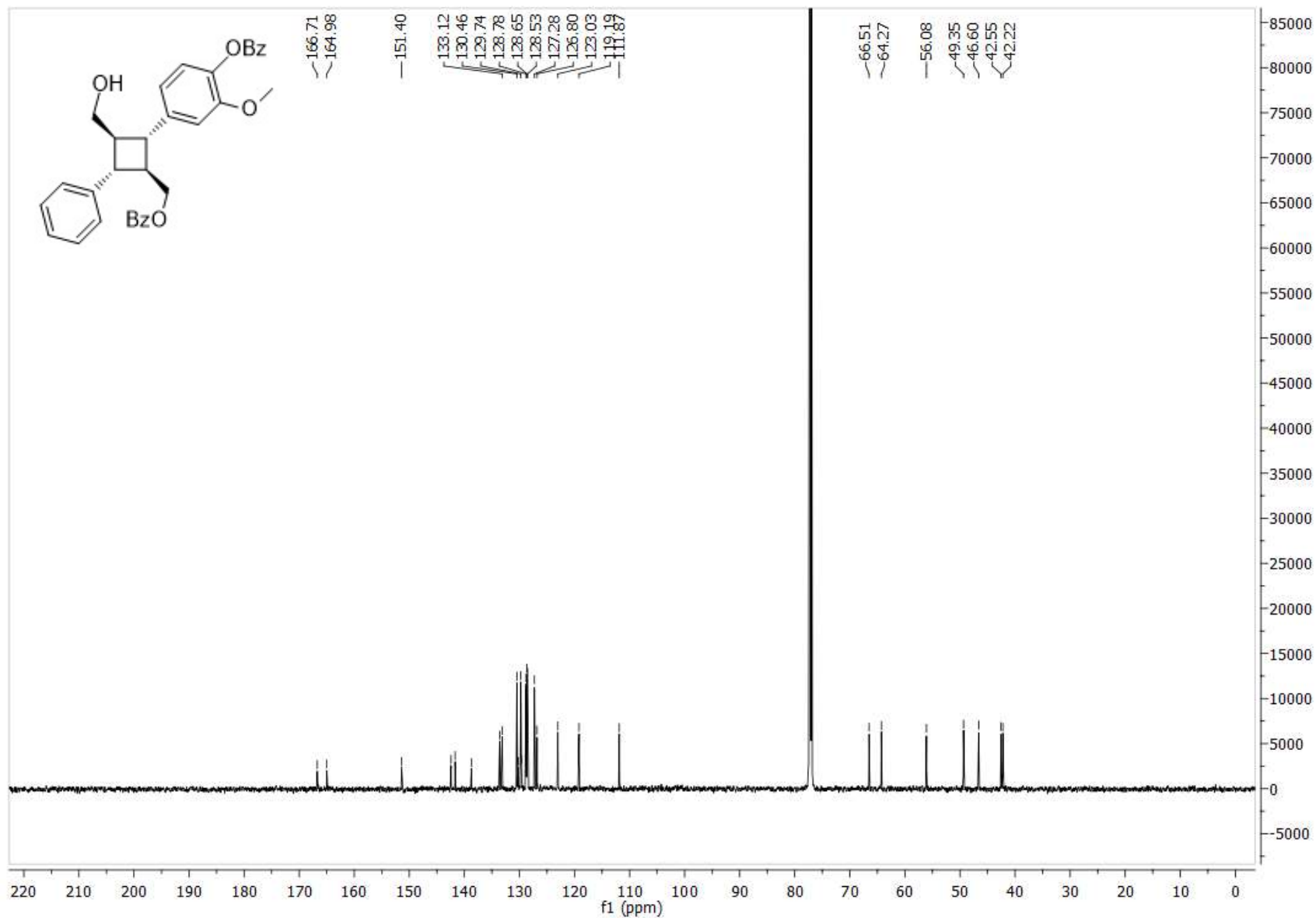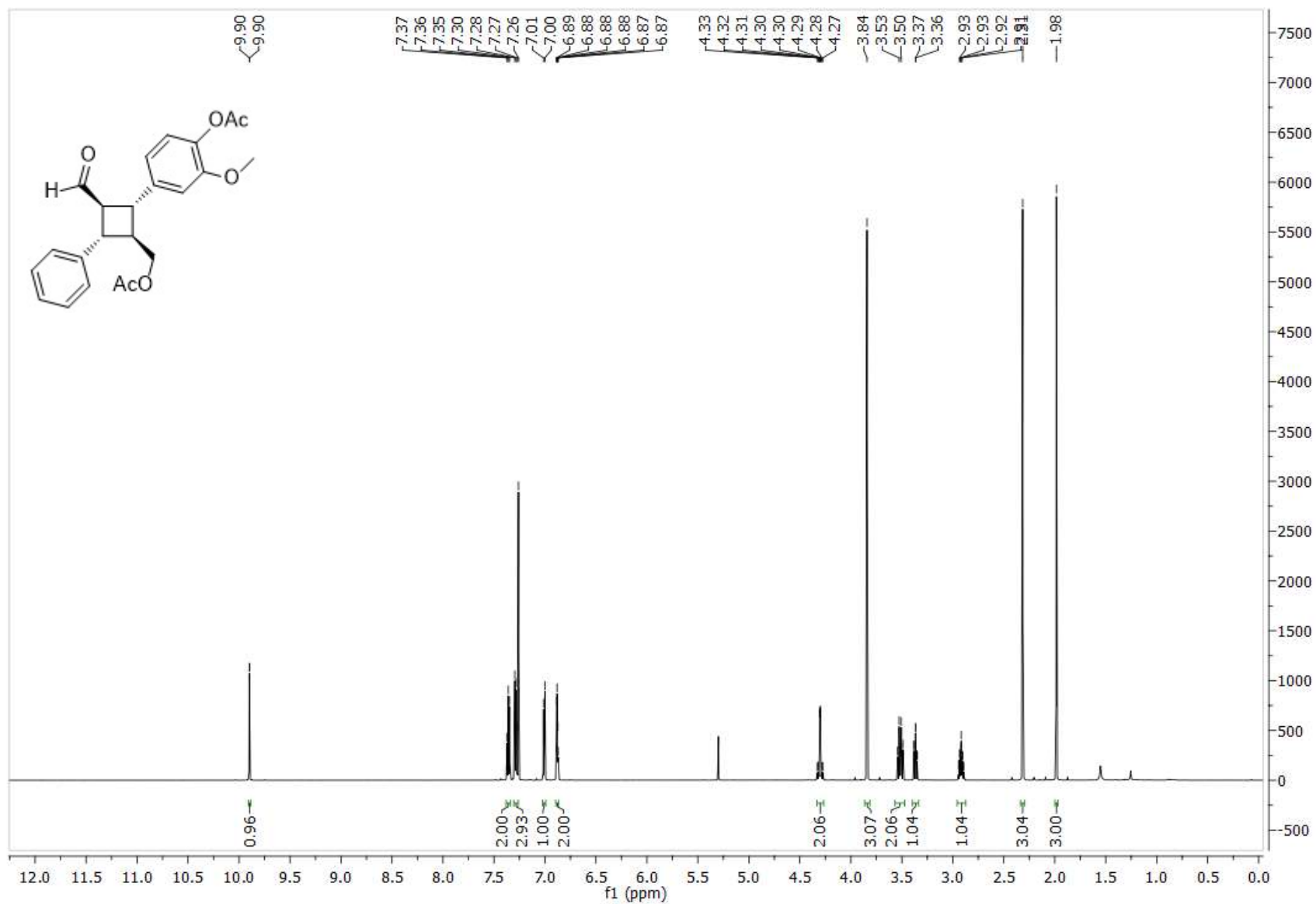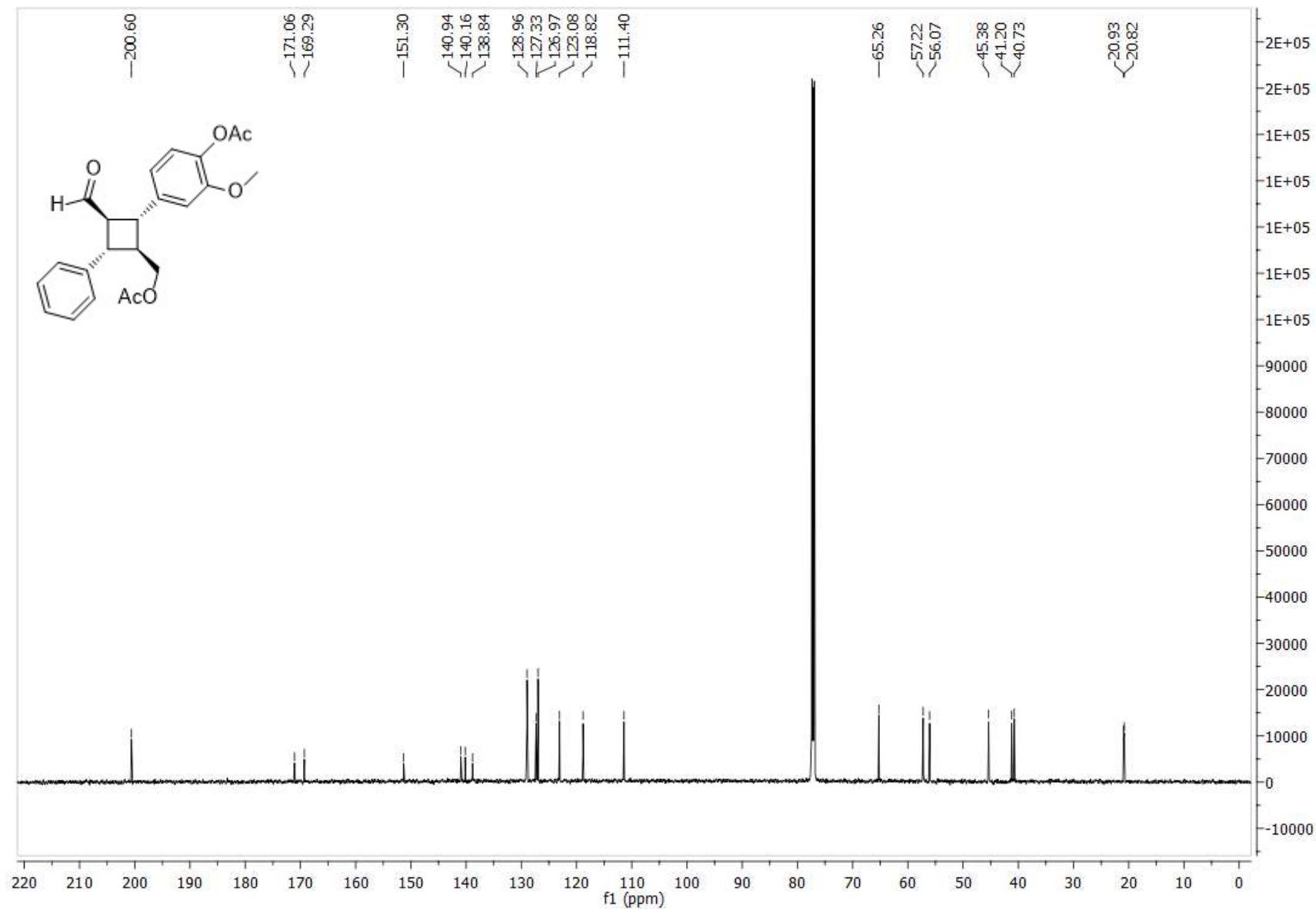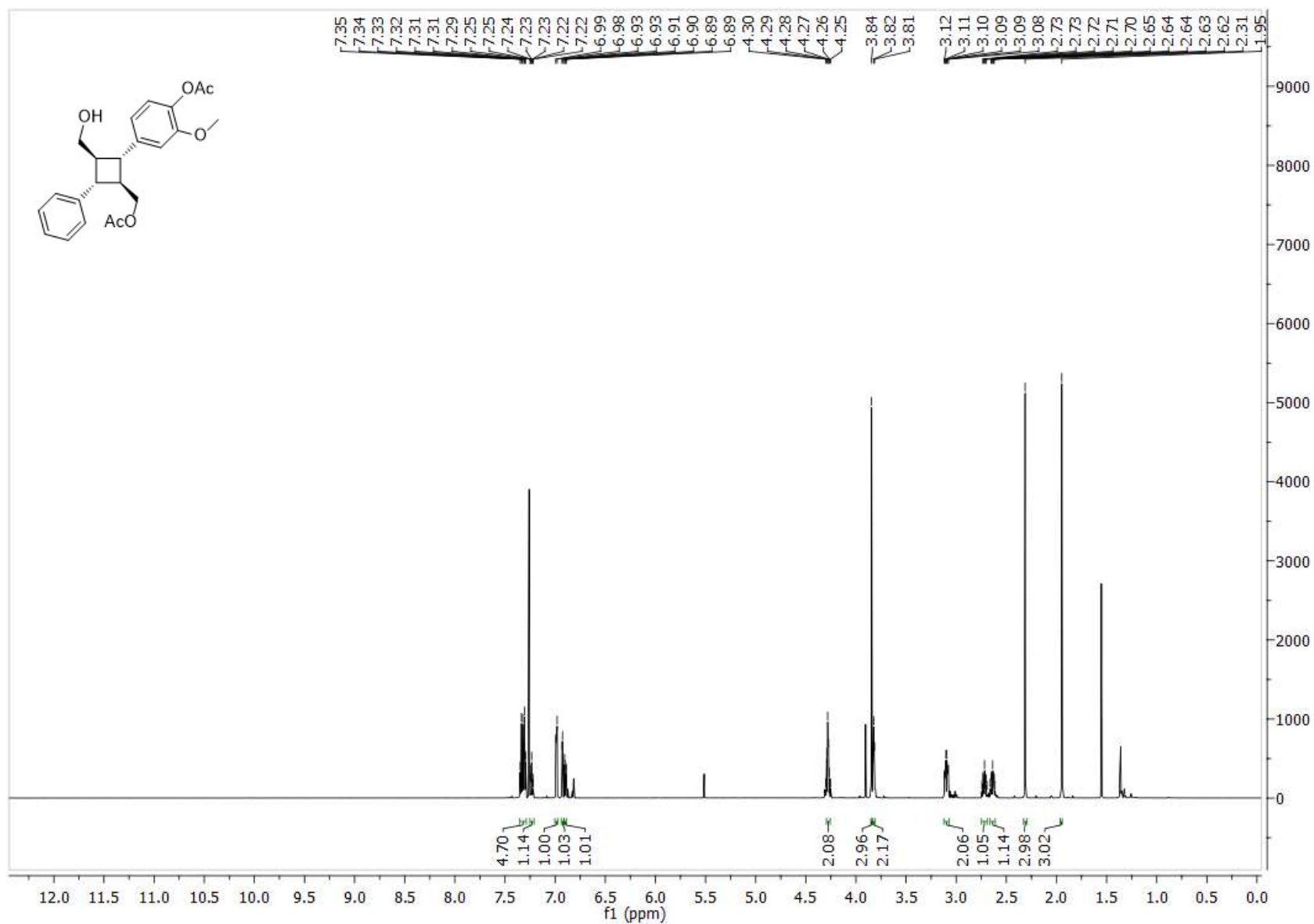
11 ^{1}H NMR
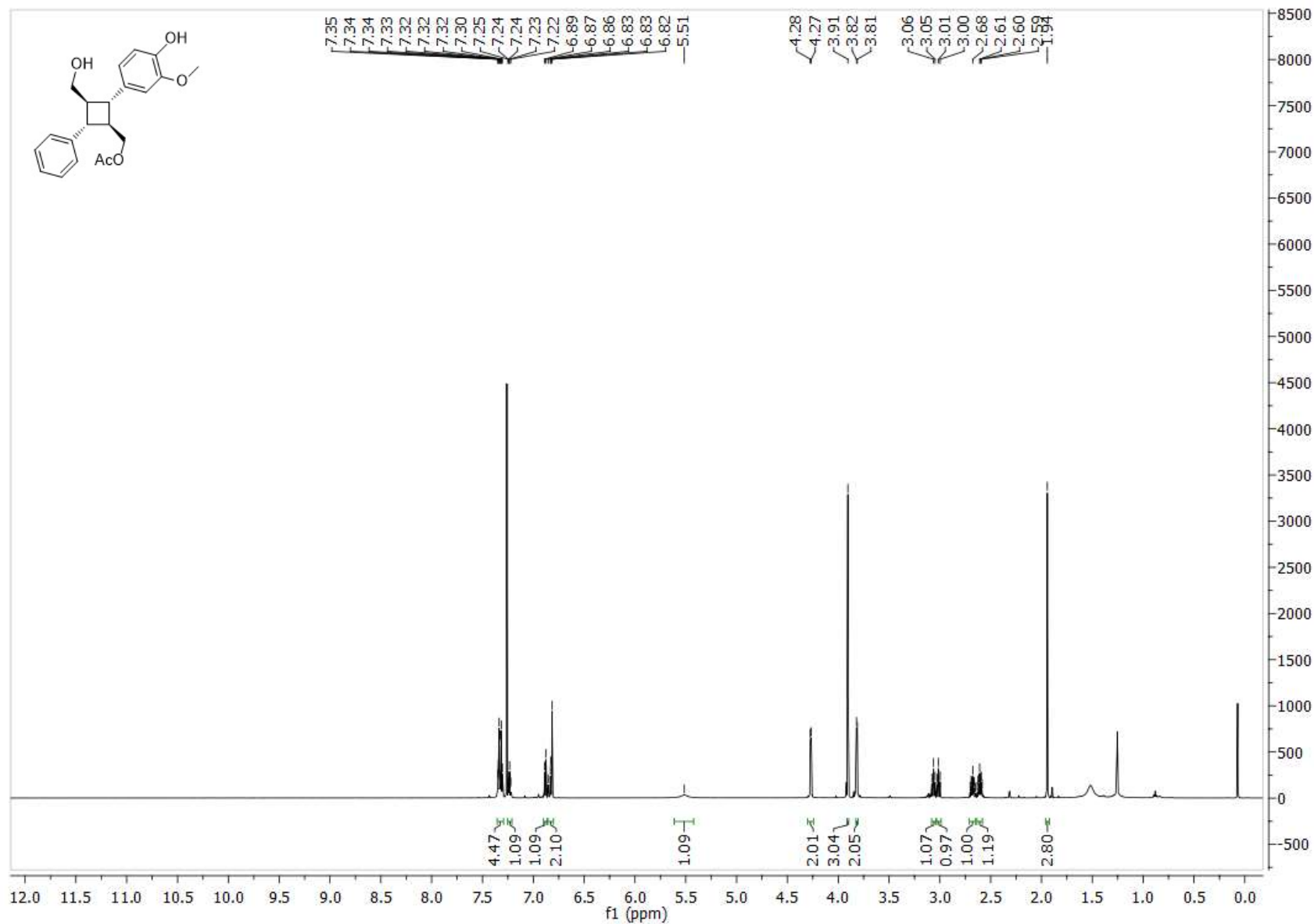
11 ¹³C NMR
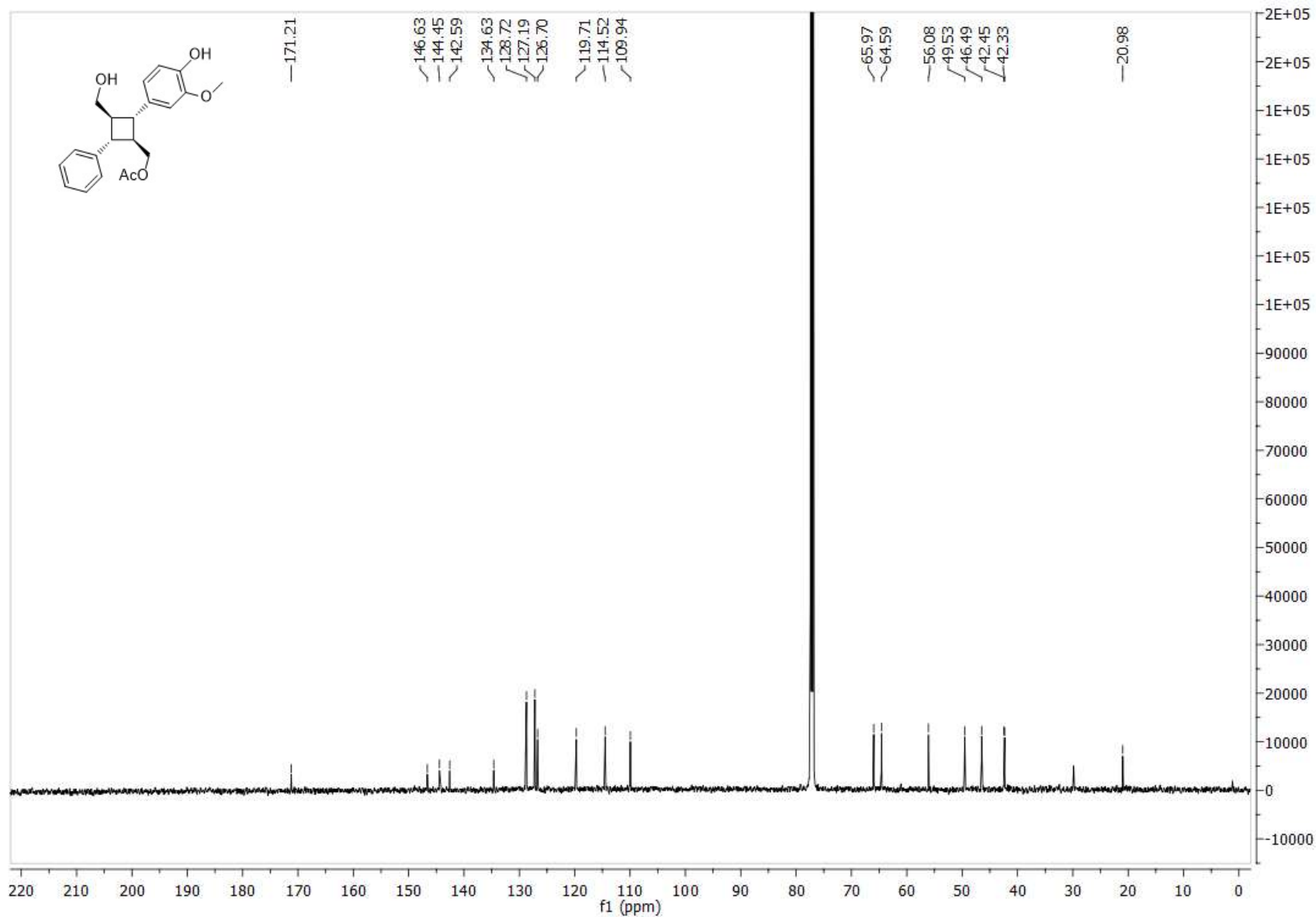
12 ¹H NMR
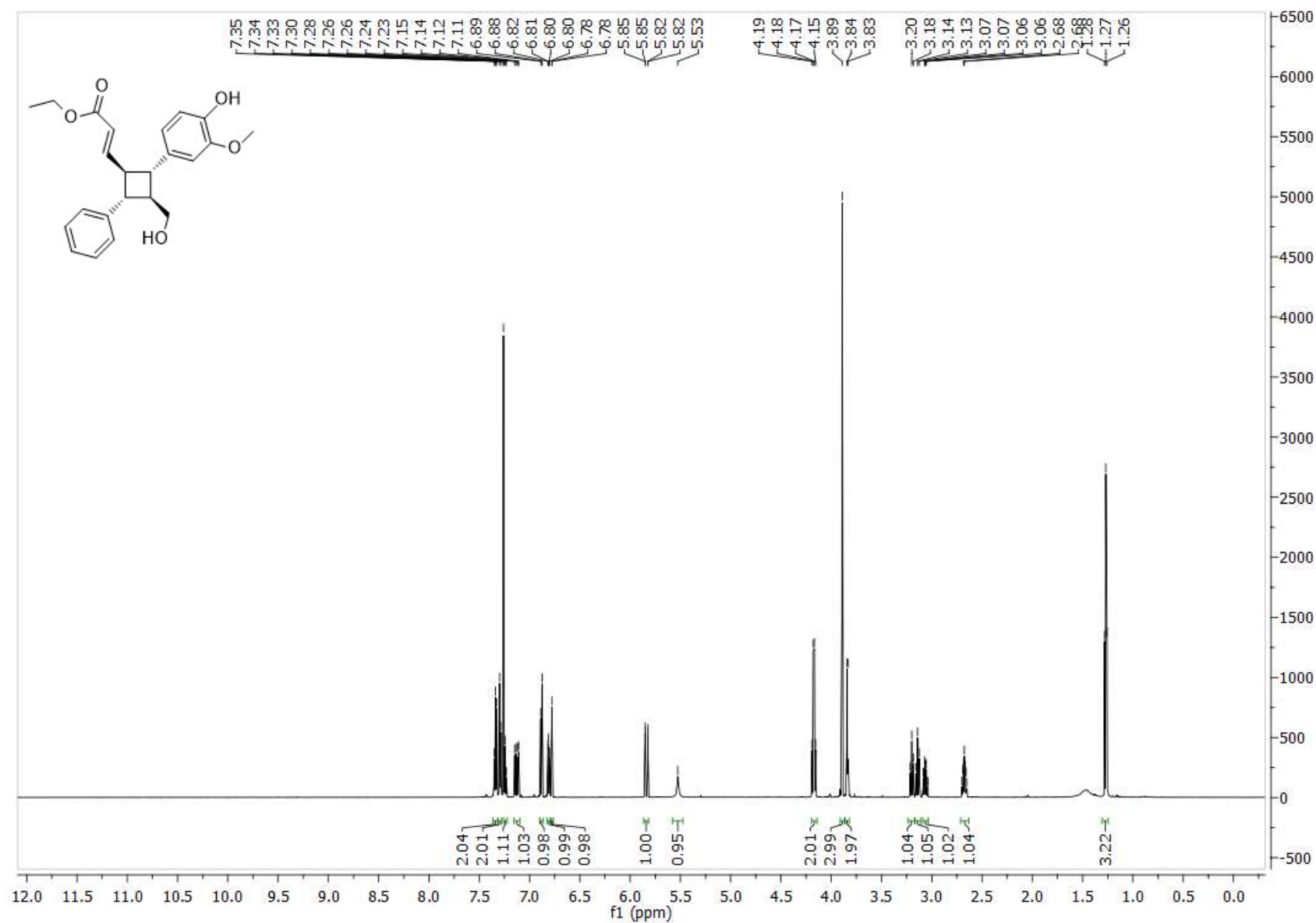
12 ^{1}C NMR
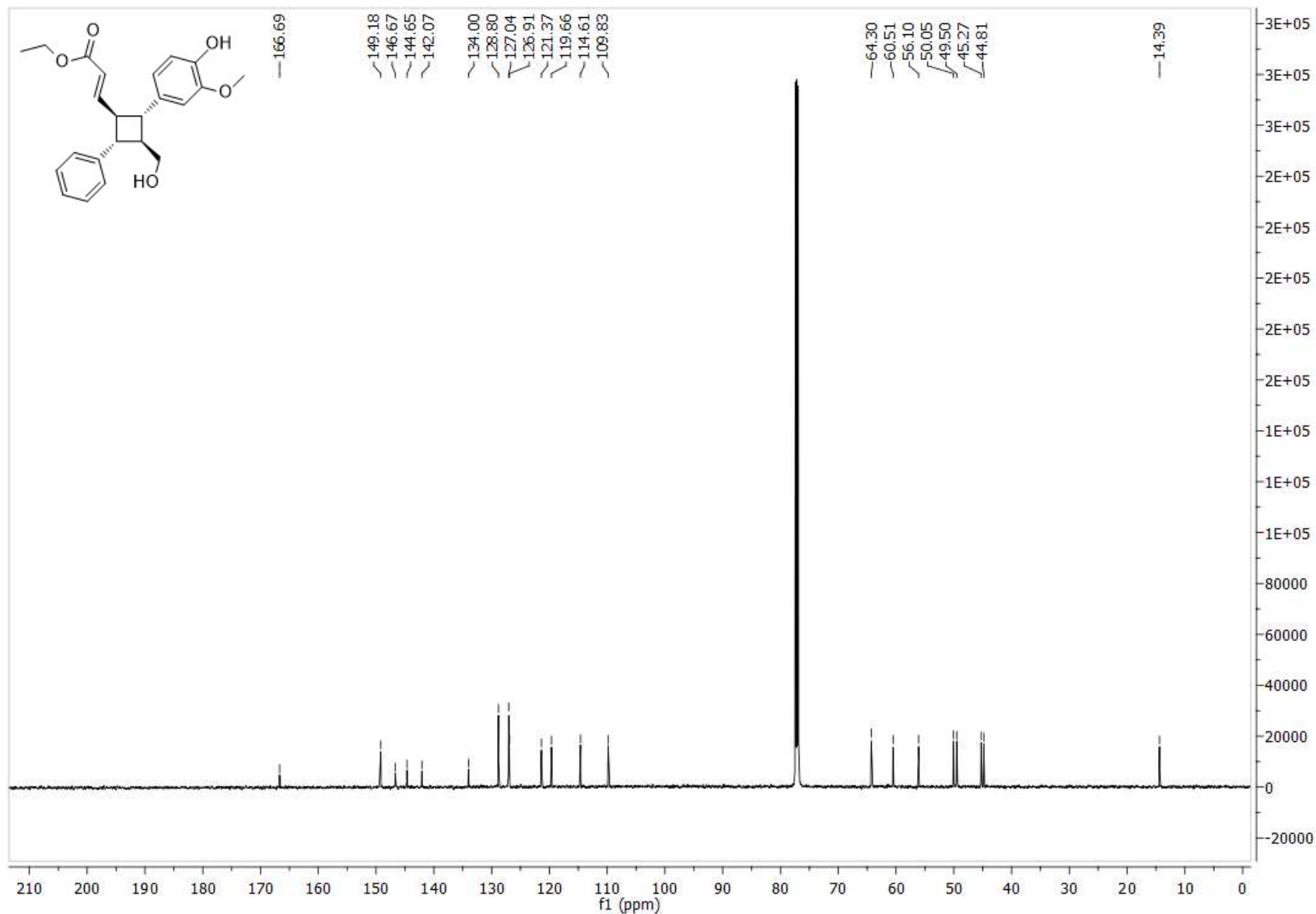
Appendix E: HPLC Chromatograms Pertaining to Chapter 5

File Information

LC-File	R521S5132014-03-3117-09-39SYSTEM.D
File Path	C:\CHEM32\1\DATA\AS-RH
Date	31-Mar-14, 17:09:58
Sample	R521S513
Sample Info	0.75 mL/min, 70:30 H2O:ACN, 20 min.
Barcode	
Operator	SYSTEM
Method	ORGANOCATALYSIS 2ND ART.M
Reference	
Analysis Time	19.997 min
Sampling Rate	0.0033 min (0.198 sec), 6000 datapoints

#	Time	Area	Height	Width	Area%	Symmetry
1	9.605	3228	150.2	0.3327	47.103	0.849
2	11.226	3625.1	143.8	0.3911	52.897	0.86

Agilent 1220 Infinity HPLC, AS-RH column (150 x 4.6 mm, 5µ), H$_2$O/MeCN (70:30) as a mobile phase; flow rate 0.75 mL/min, column temperature 20 °C, λ236, sample 0.2 mg/mL dissolved in the mobile phase.

	File Information
LC-File	R5212014-03-3117-35-51SYSTEM.D
File Path	C:\CHEM32\1\DATA\AS-RH
Date	31-Mar-14, 17:36:10
Sample	R521
Sample Info	0.75 mL/min, 70:30 H2O:ACN, 20 min.
Barcode	
Operator	SYSTEM
Method	ORGANOCATALYSIS 2ND ART.M
Reference	
Analysis Time	20 min
Sampling Rate	0.0033 min (0.198 sec), 6001 datapoints

#	Time	Area	Height	Width	Area%	Symmetry
1	9.514	36.9	1.8	0.3145	0.459	0.995
2	11.109	8004	310	0.3992	99.541	0.831

Agilent 1220 Infinity HPLC, AS-RH column (150 x 4.6 mm, 5μ), H₂O/MeCN (70:30) as a mobile phase; flow rate 0.75 mL/min, column temperature 20 °C, λ236, sample 0.2 mg/mL dissolved in the mobile phase.

File Information

LC-File	S5132014-03-3118-12-42SYSTEM.D
File Path	C:\CHEM32\1\DATA\AS-RH
Date	31-Mar-14, 18:13:05
Sample	S513
Sample Info	0.75 mL/min, 70:30 H2O:ACN, 20 min.
Barcode	
Operator	SYSTEM
Method	ORGANOCATALYSIS 2ND ART.M
Reference	
Analysis Time	19.997 min
Sampling Rate	0.0033 min (0.198 sec), 6000 datapoints

#	Time	Area	Height	Width	Area%	Symmetry
1	9.472	5622.8	252.7	0.3446	96.866	0.827
2	11.105	181.9	7.4	0.3842	3.134	0.875

Agilent 1220 Infinity HPLC, AS-RH column (150 x 4.6 mm, 5μ), H₂O/MeCN (70:30) as a mobile phase; flow rate 0.75 mL/min, column temperature 20 °C, λ236, sample 0.2 mg/mL dissolved in the mobile phase.

Appendix F: IR Spectra Pertaining to Chapter 5
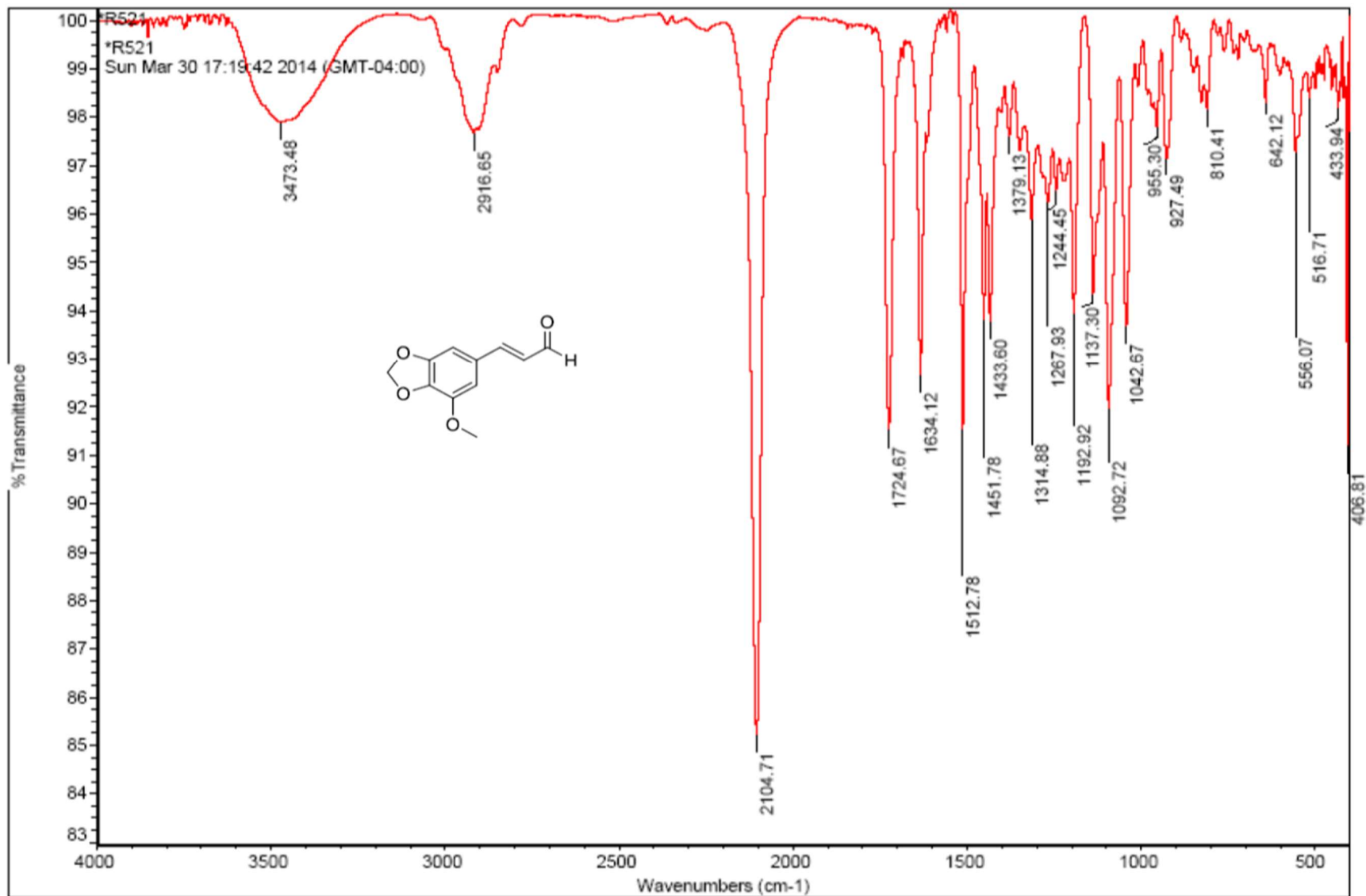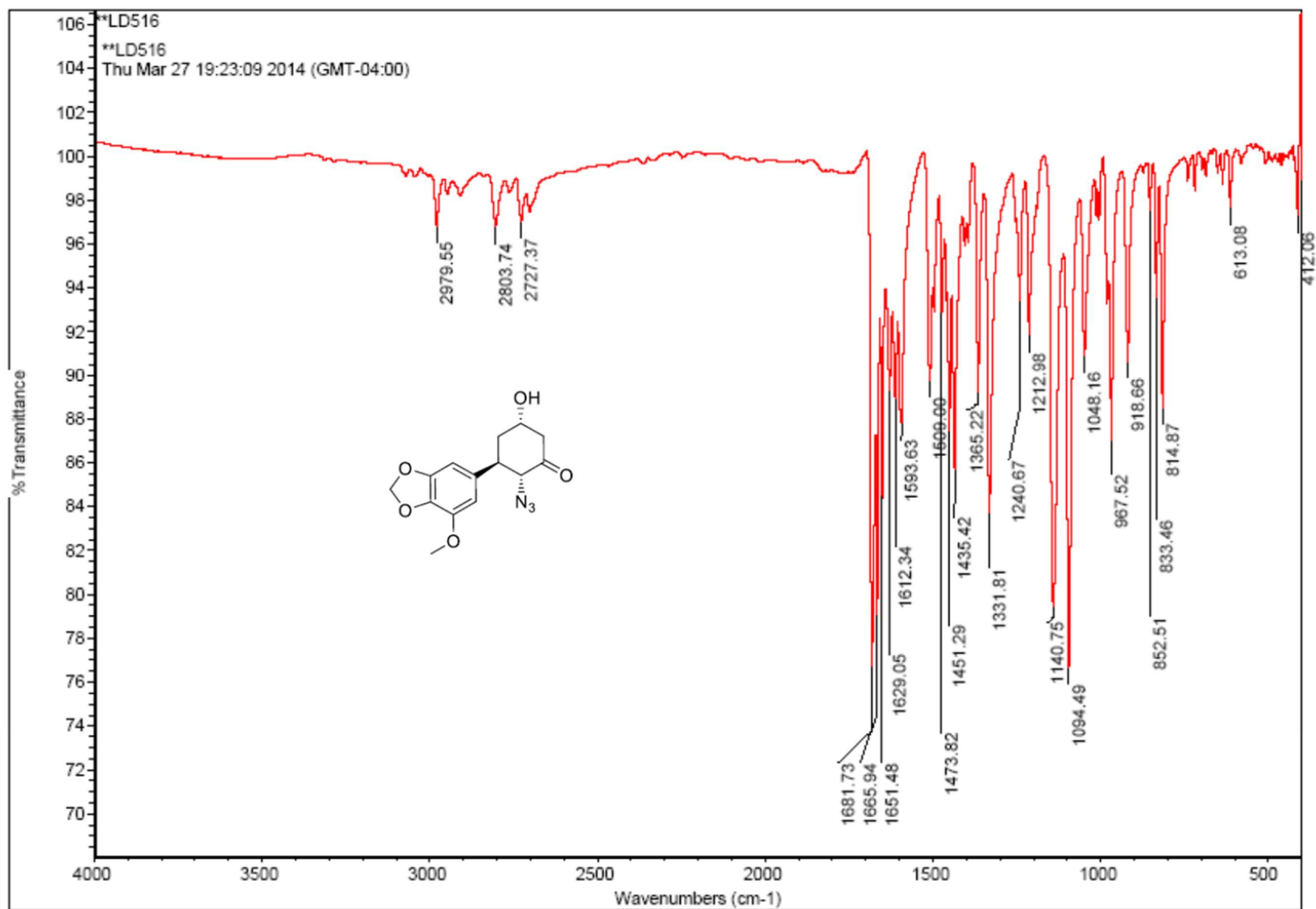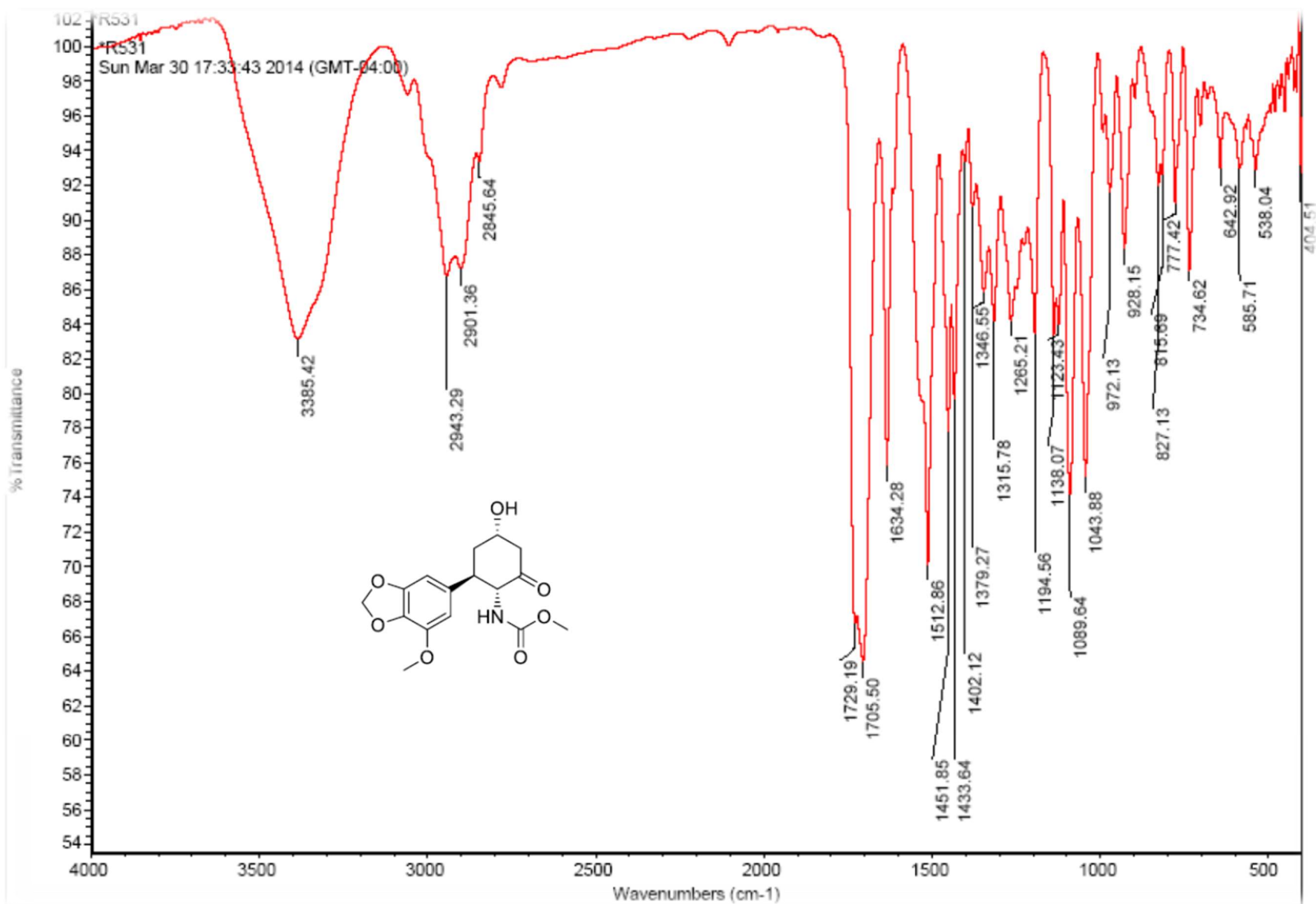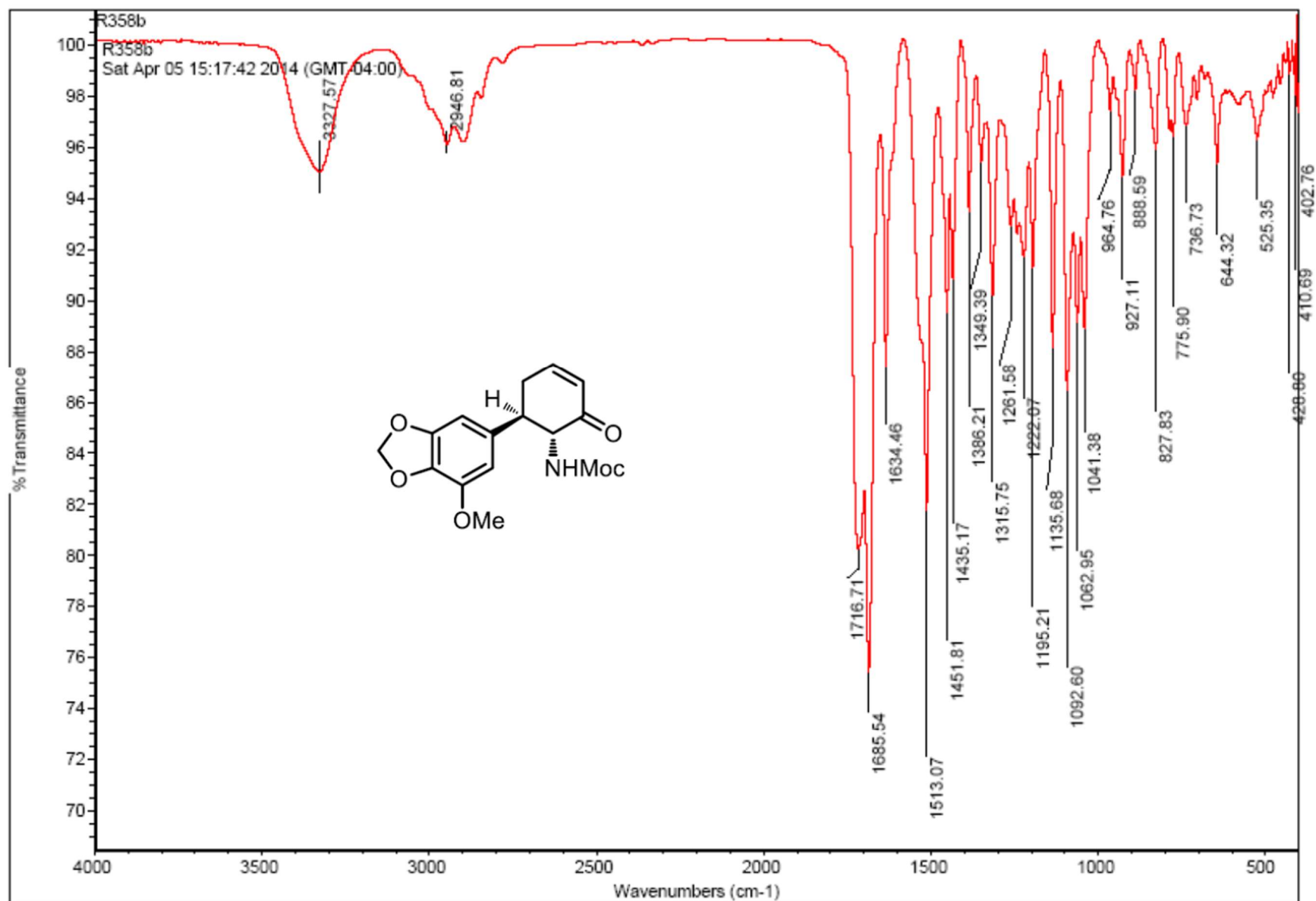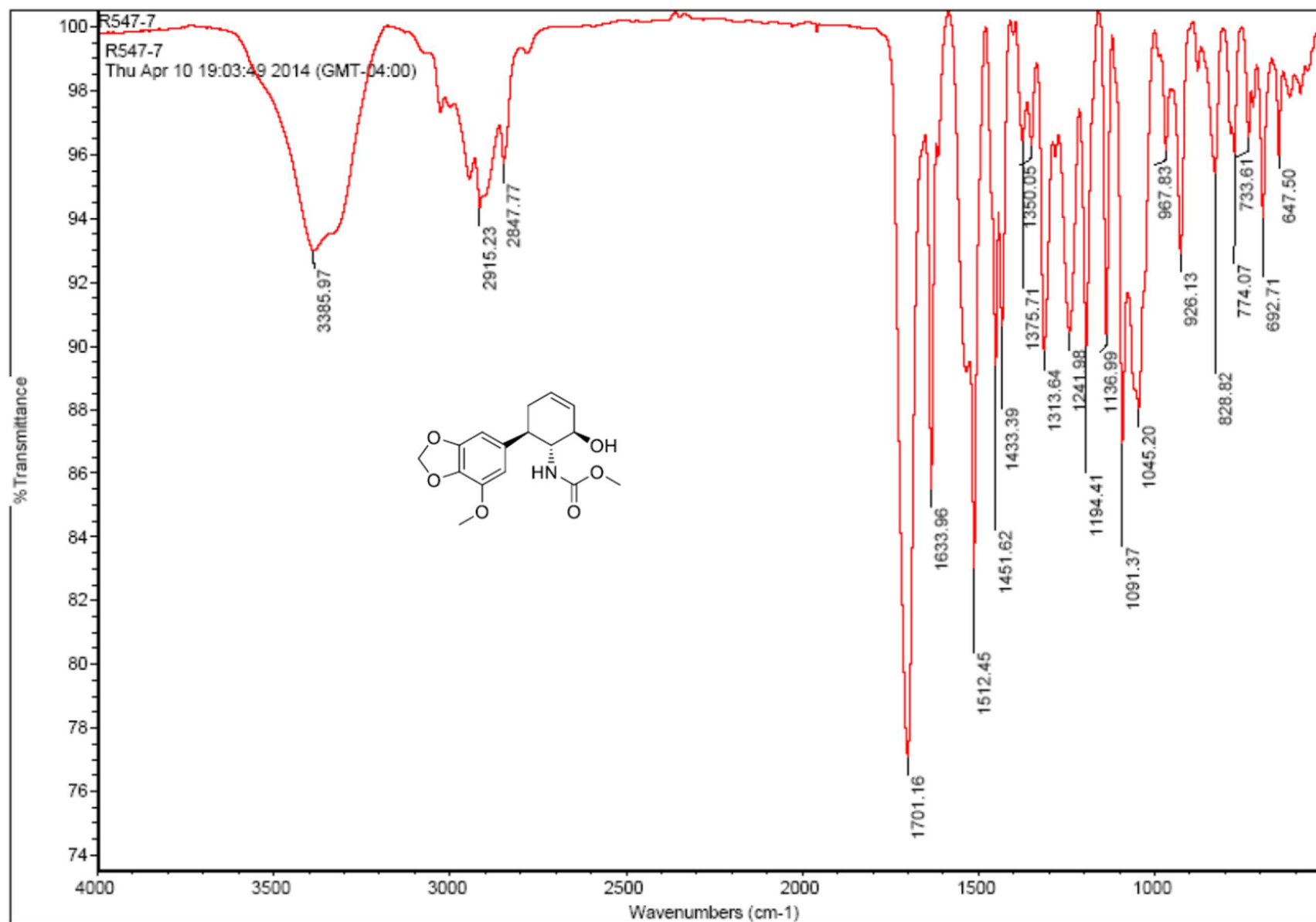
Appendix G: NMR Spectra Pertaining to Chapter 5
7 ¹H NMR
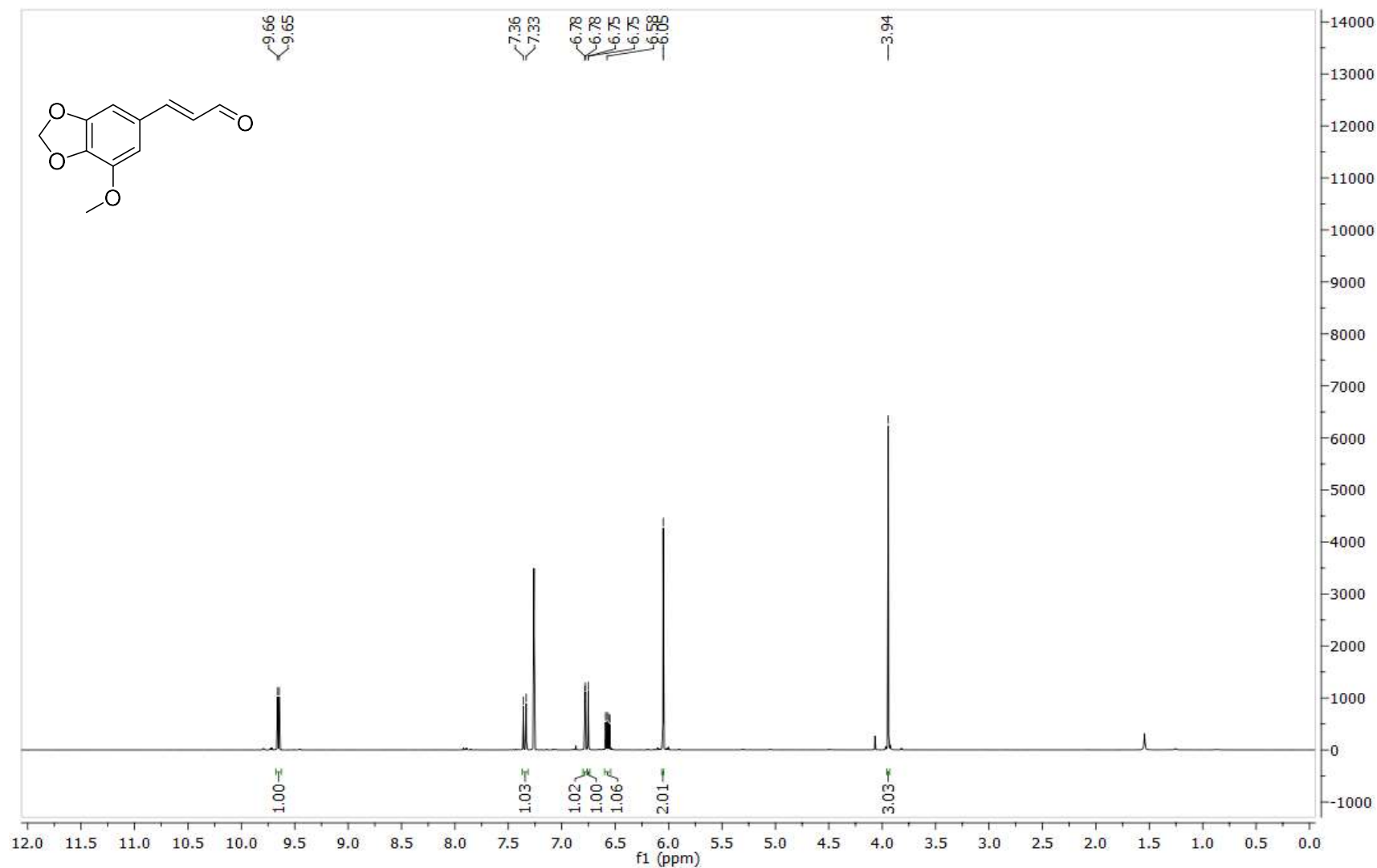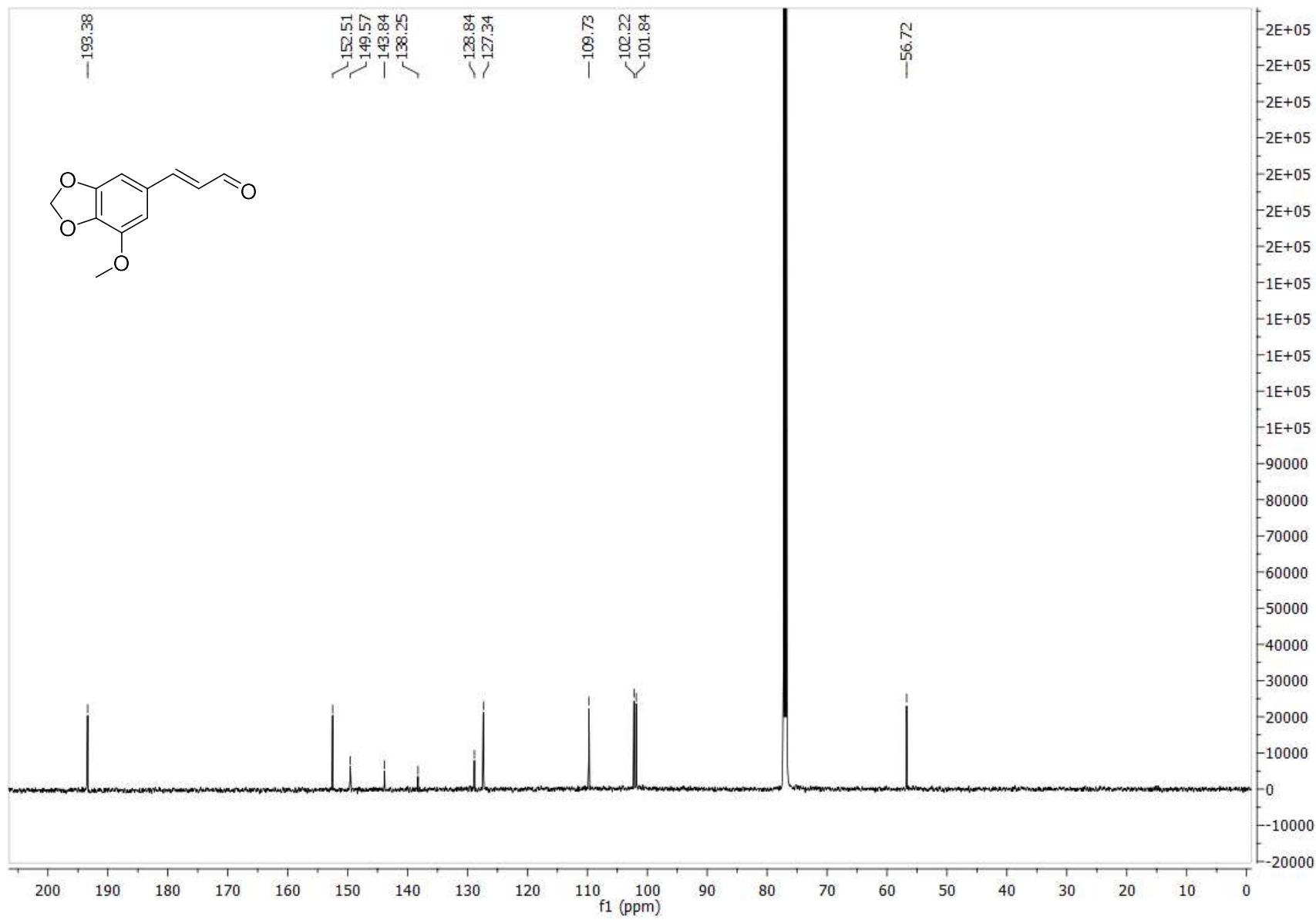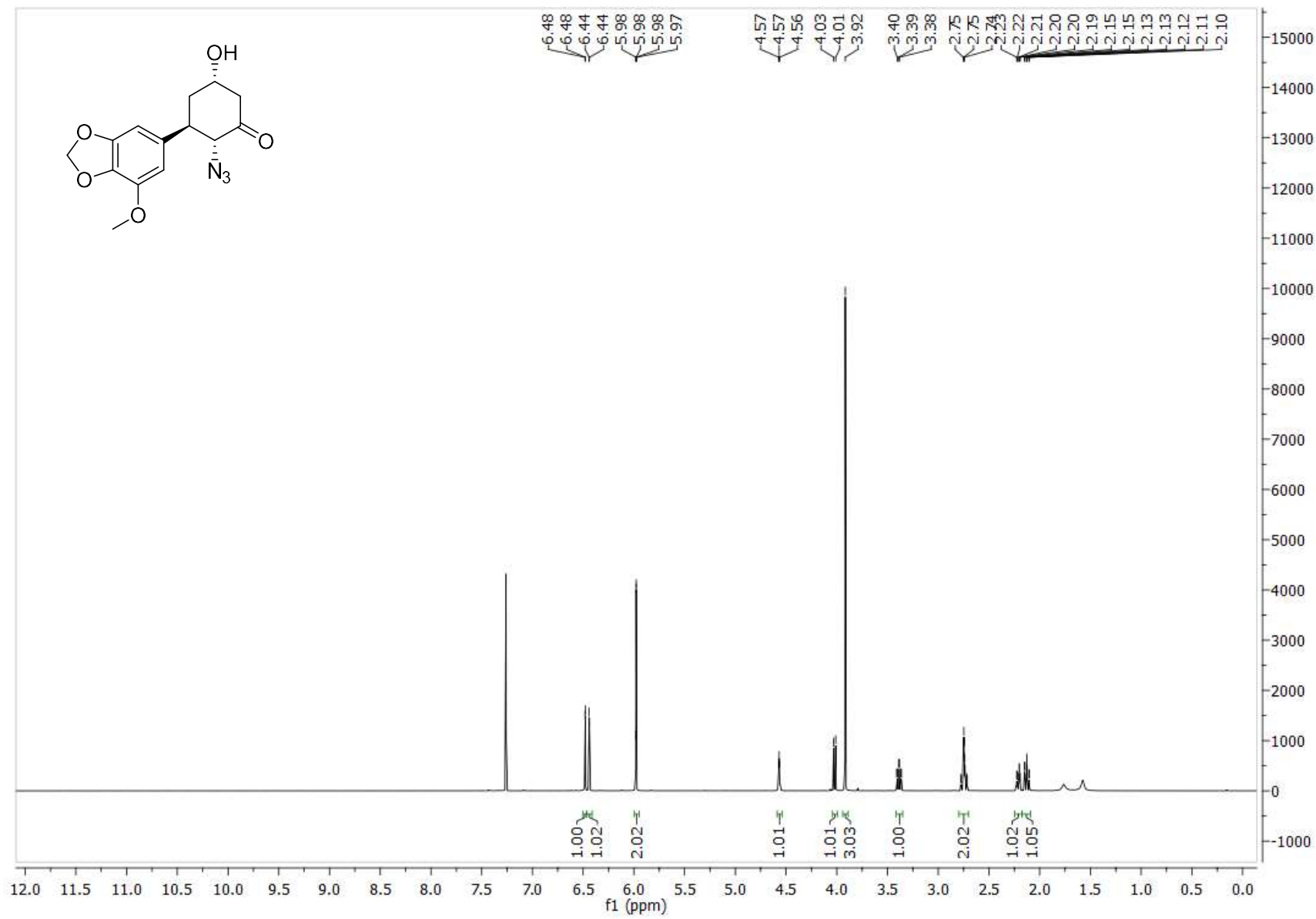
7 ¹³C NMR
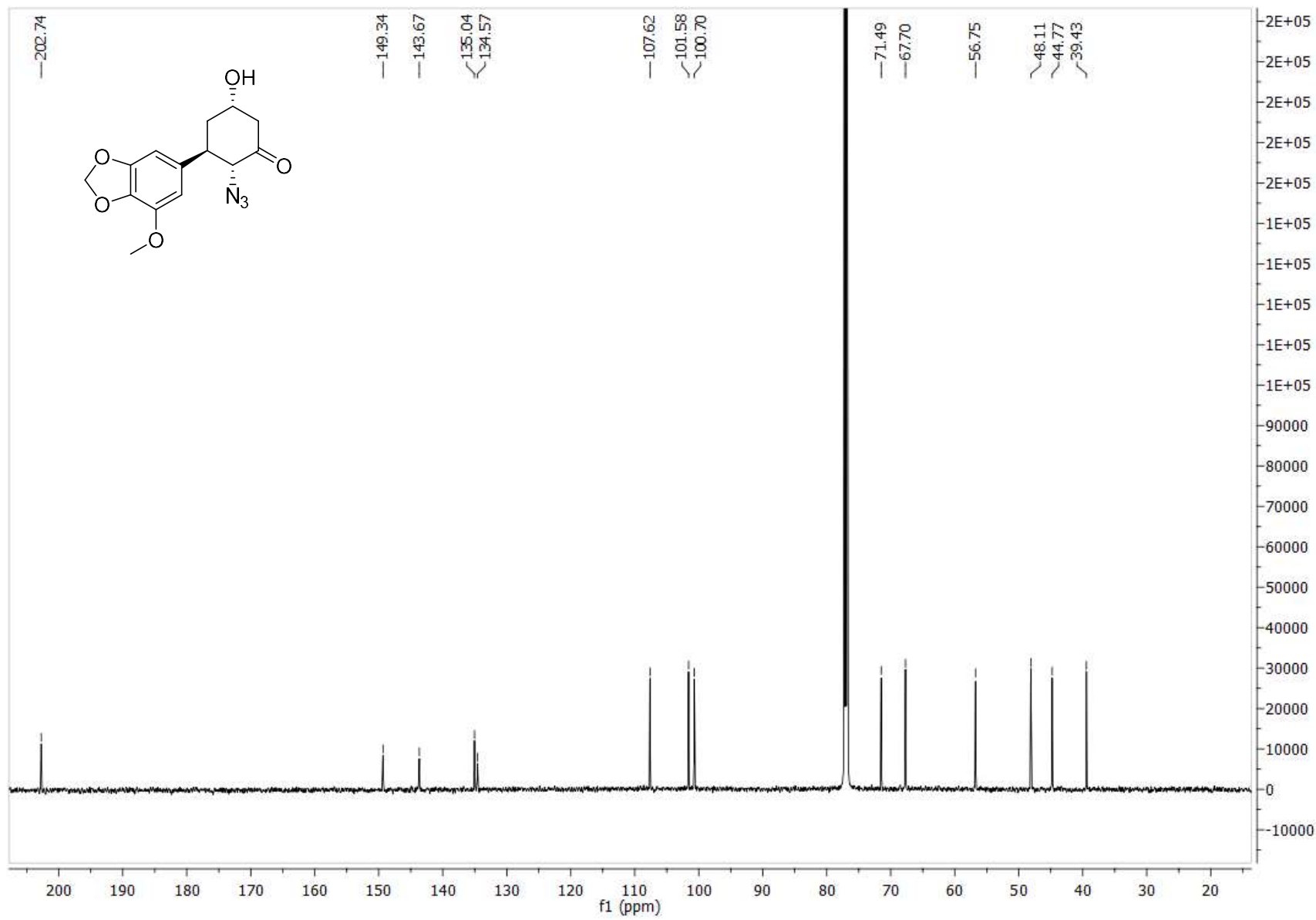
9 ^{1}H NMR

9 ^{13}C NMR

9 ^{1}H-^{1}H COSY
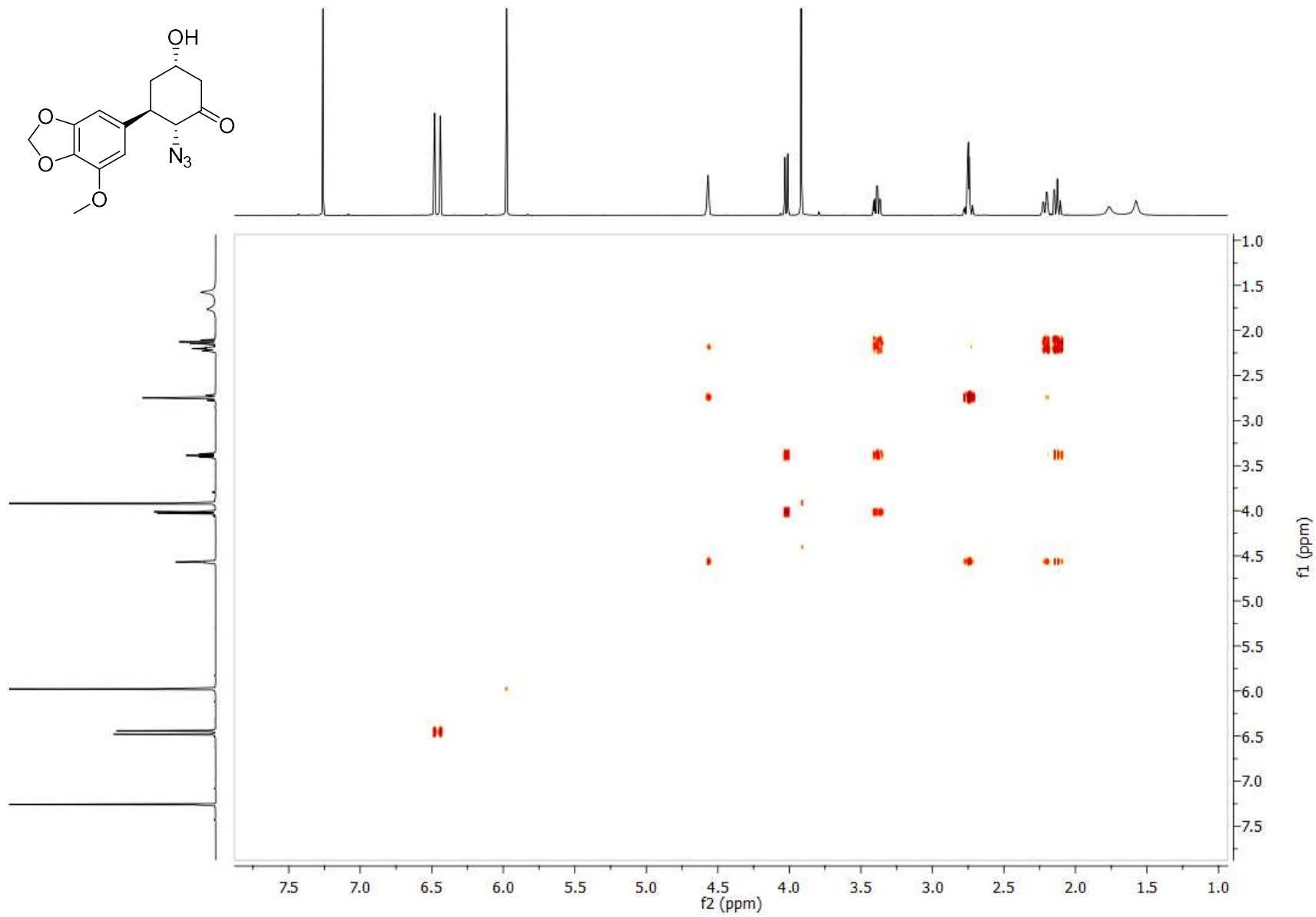
9 ¹H-¹³C HSQC
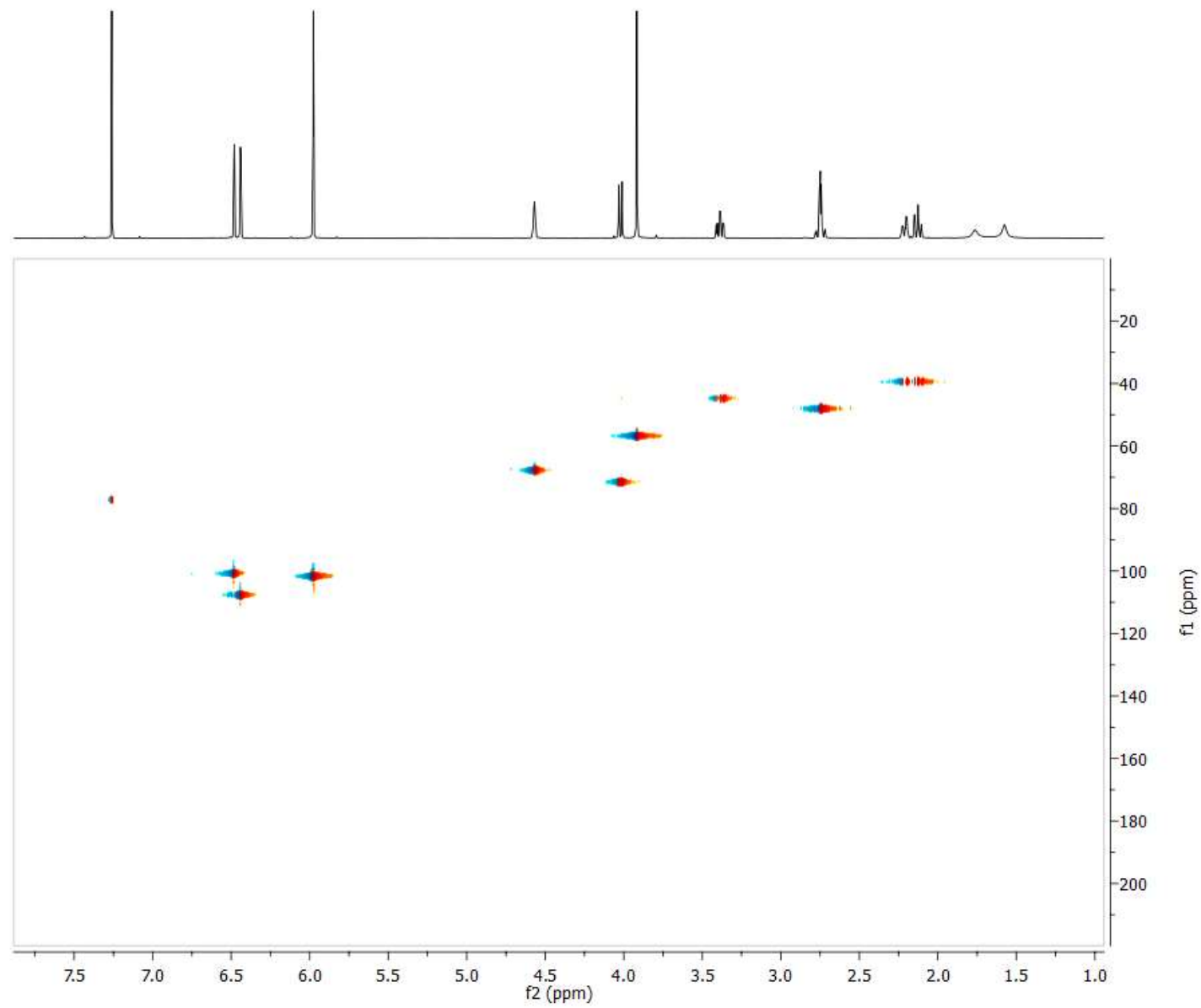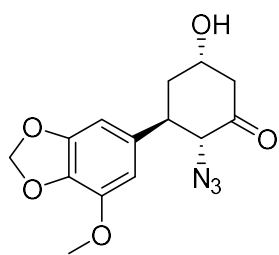
10 ¹H NMR
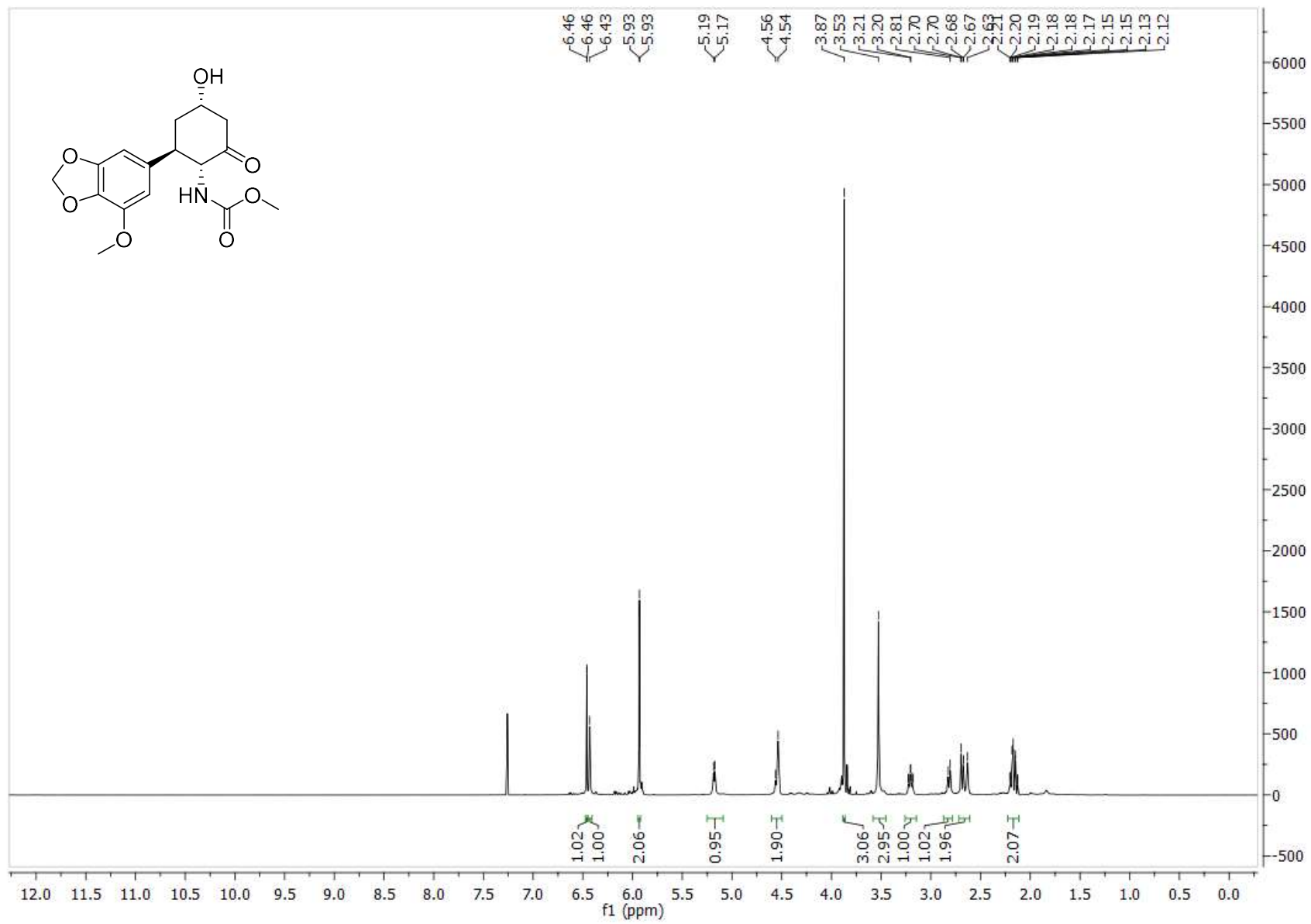
10 ^{13}C NMR
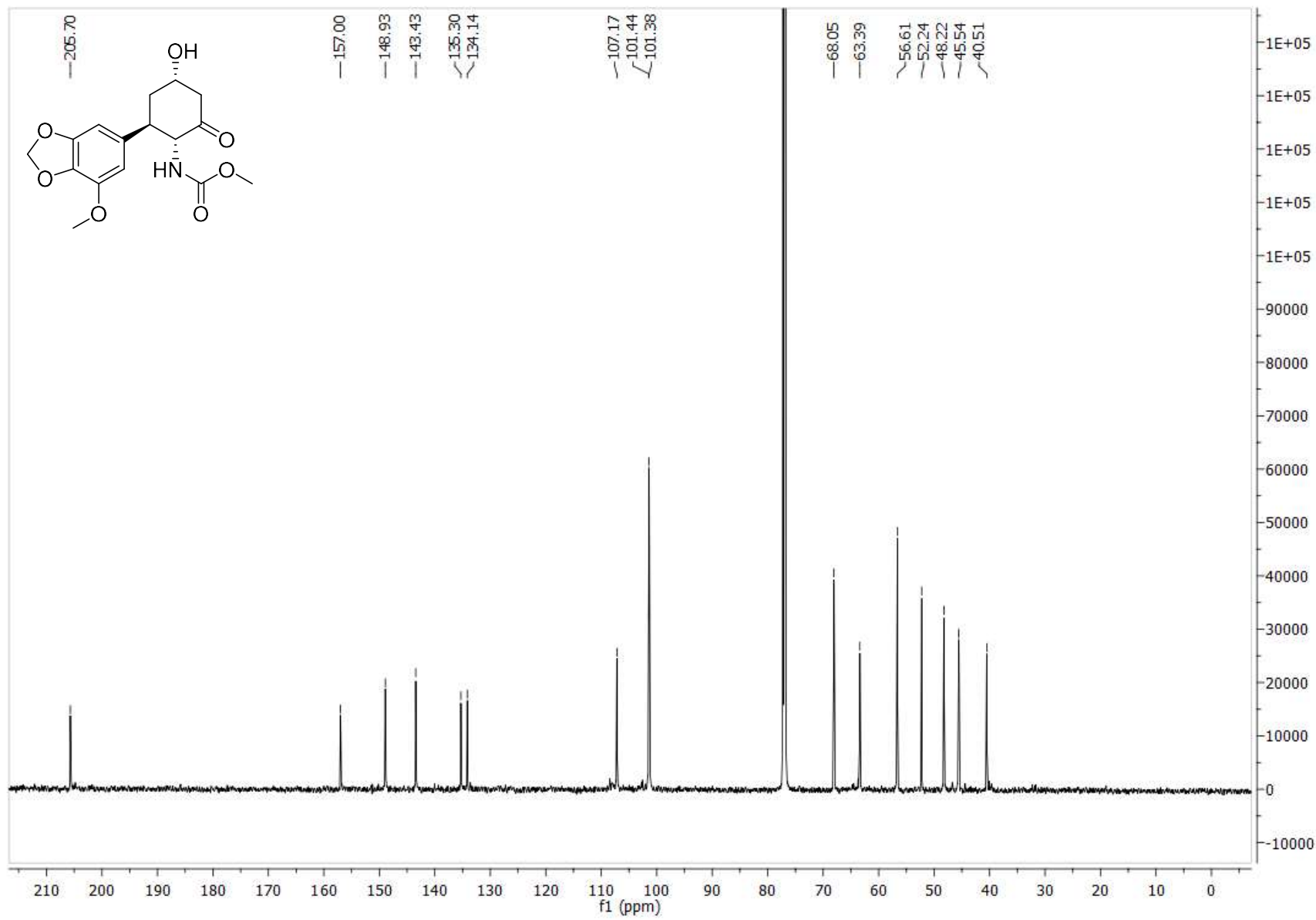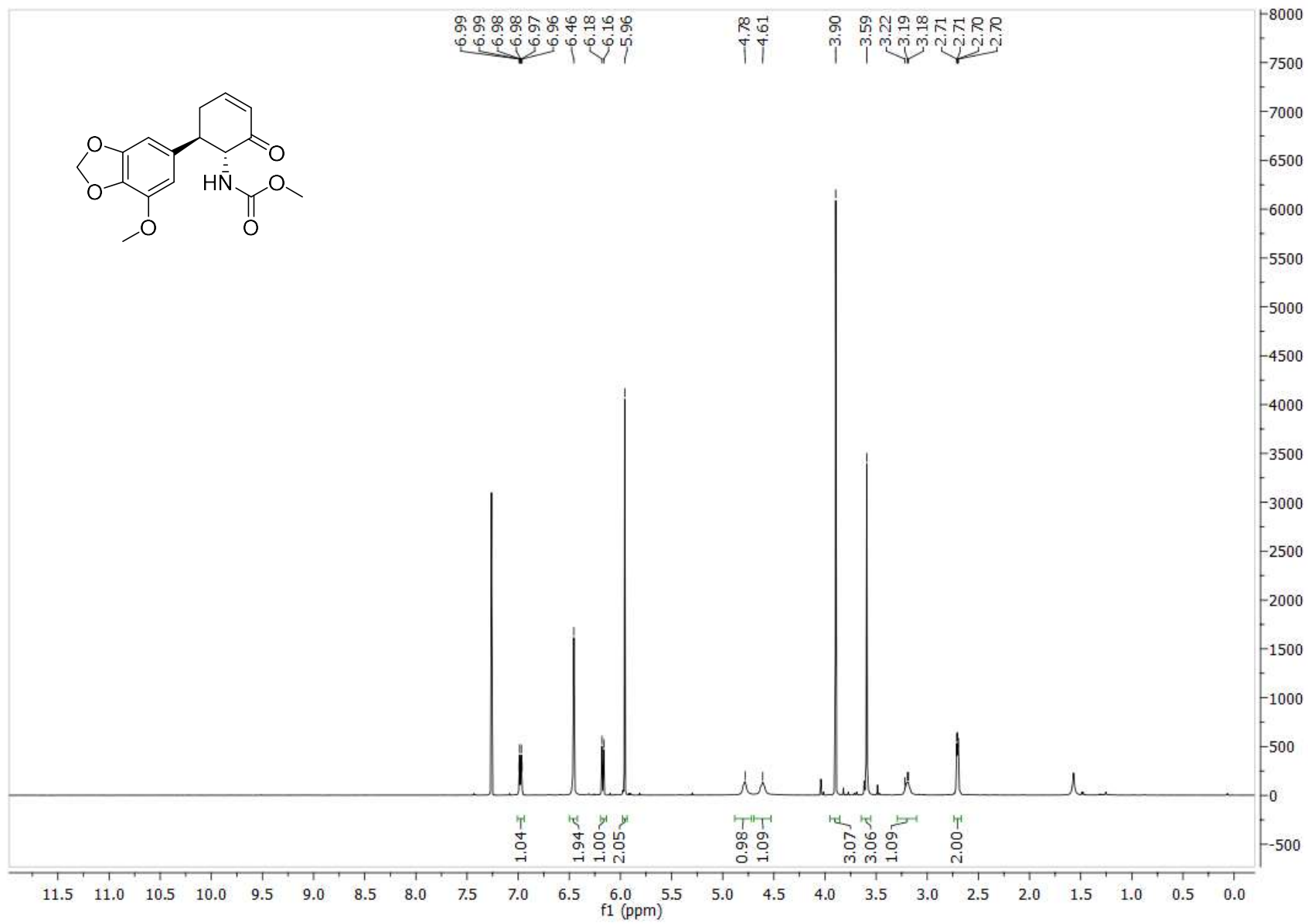
11 ¹H NMR

11 ¹³C NMR
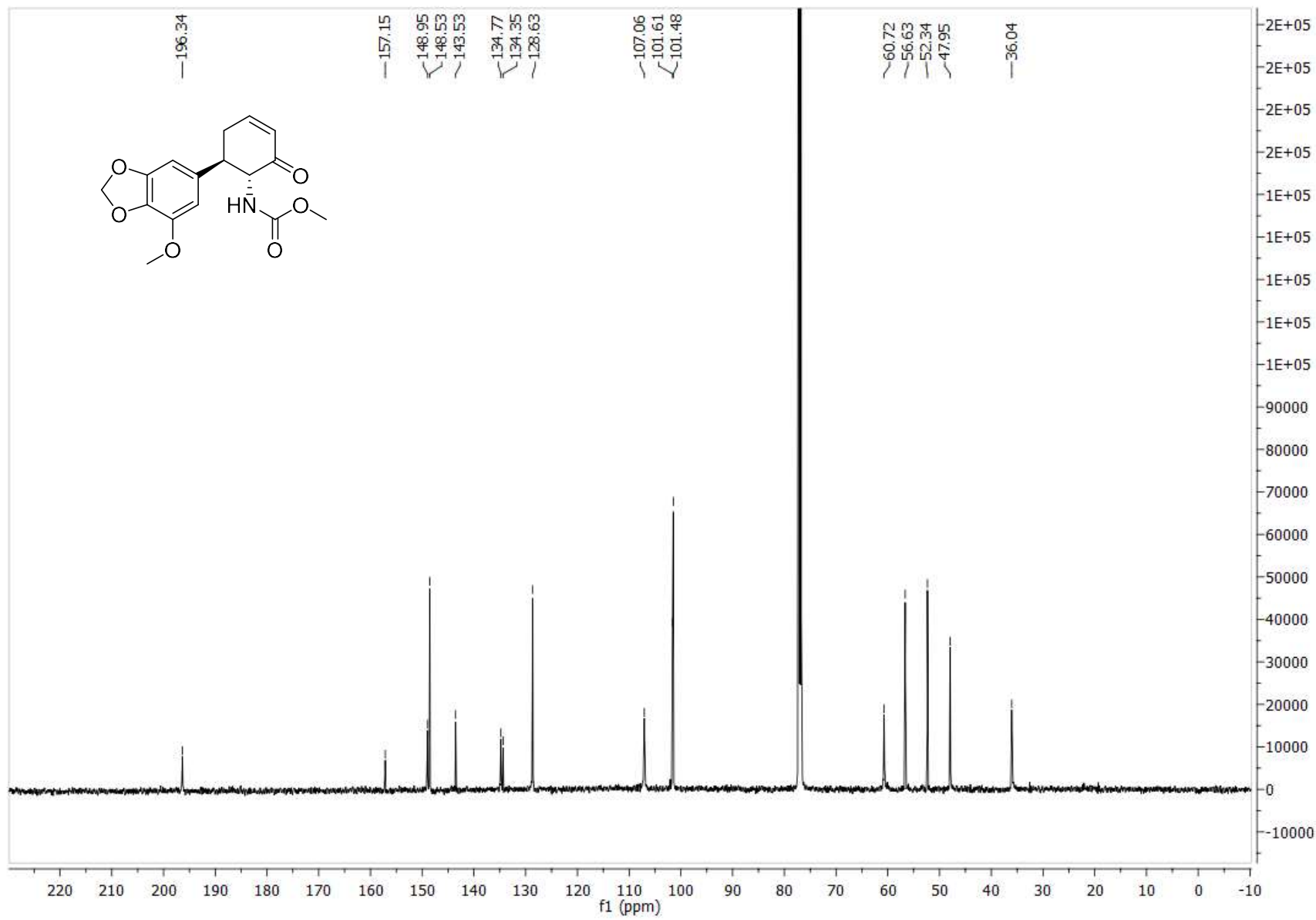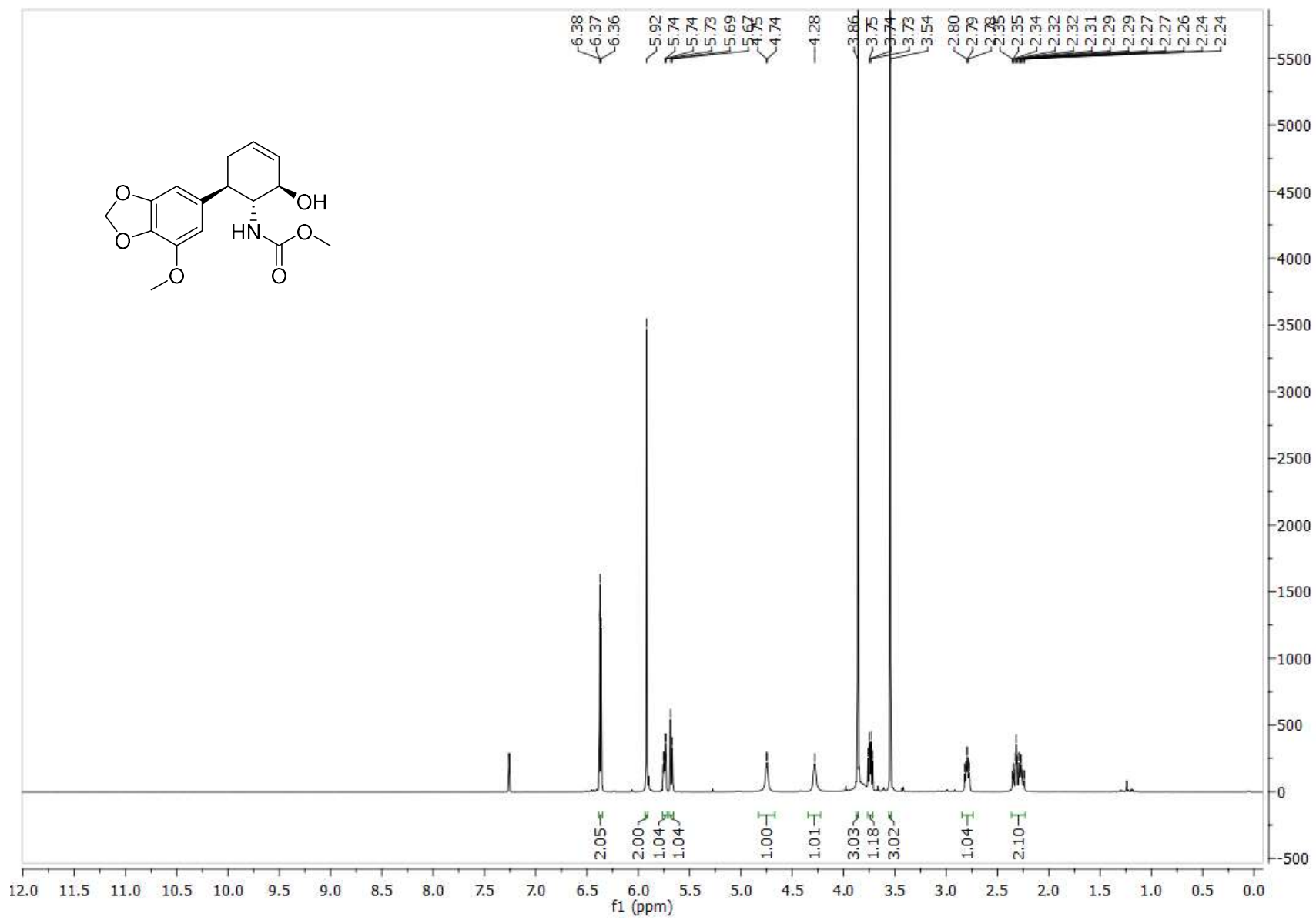
12 ^{1}H NMR

12 ^{13}C NMR

13 ^{1}H NMR

13 ^{13}C NMR

14 ^{1}H NMR

14 ^{13}C NMR

15 ^{1}H NMR
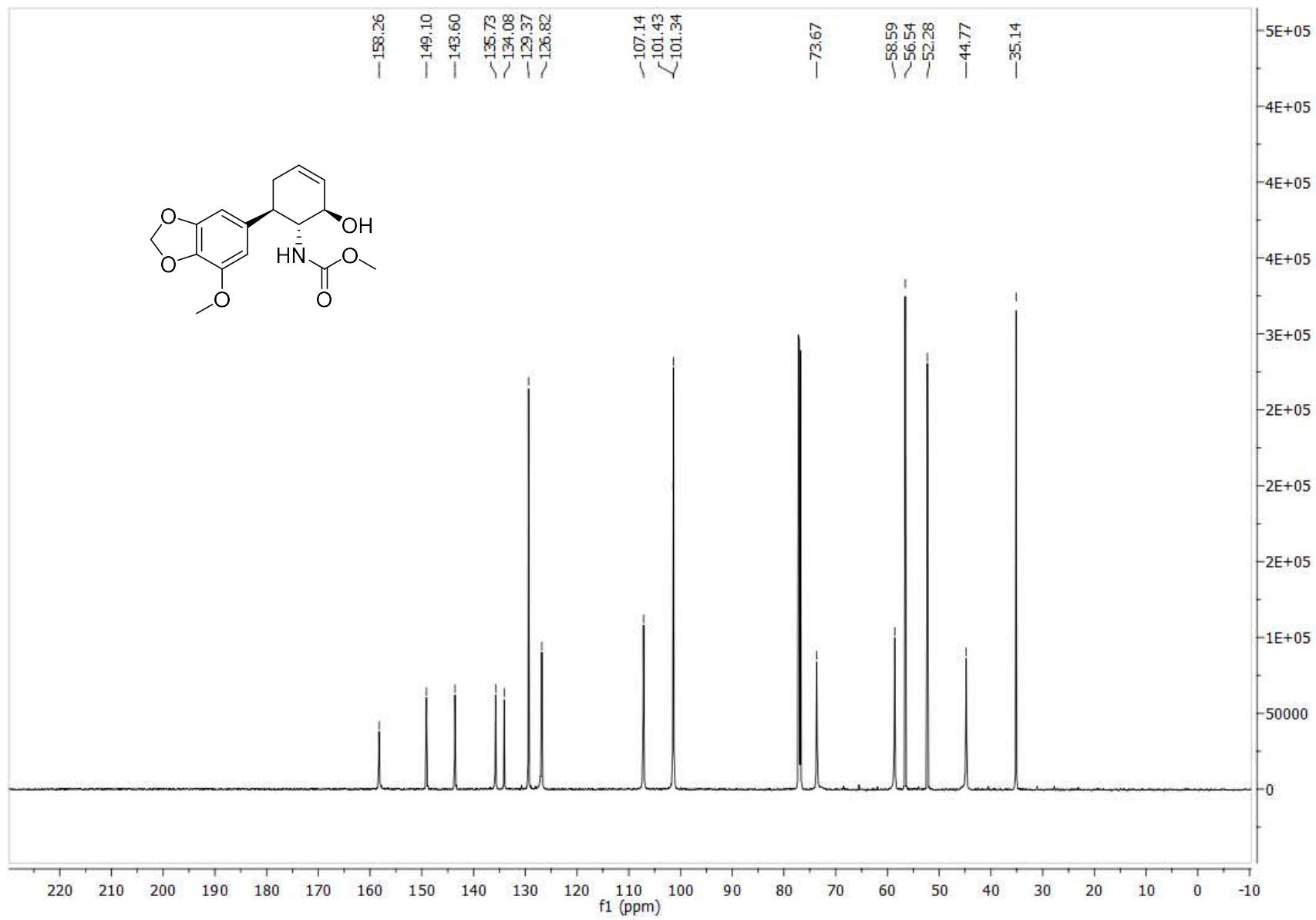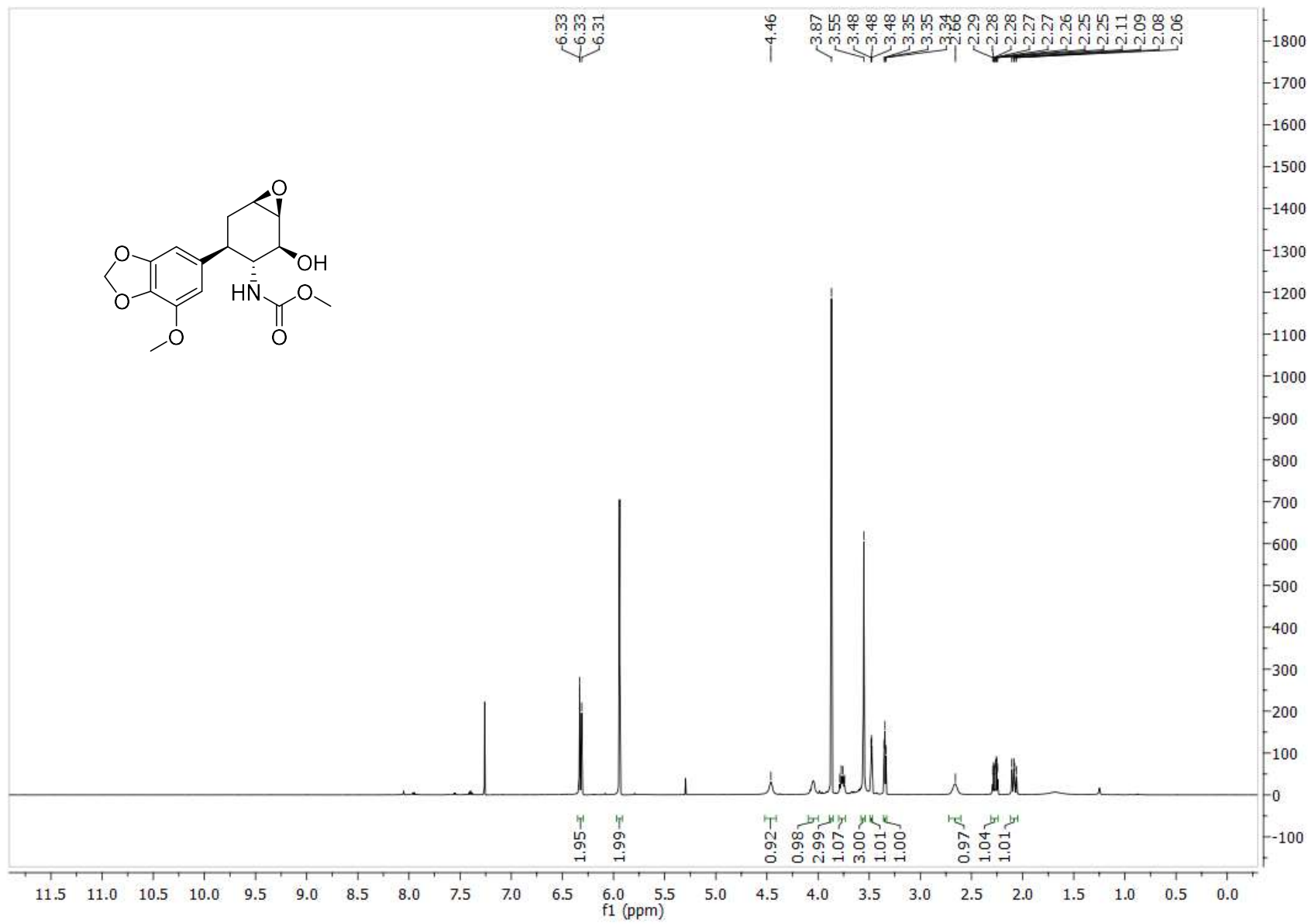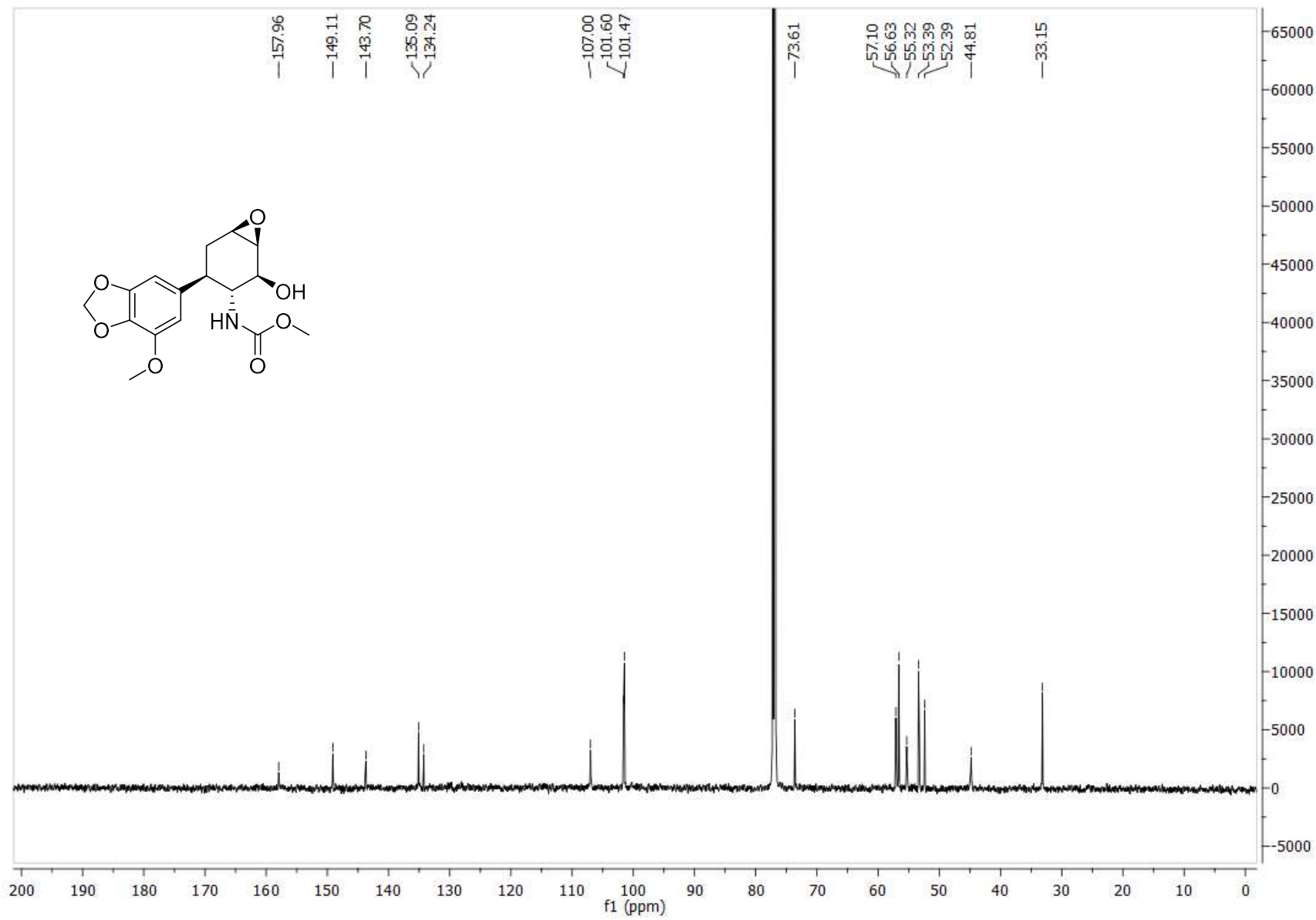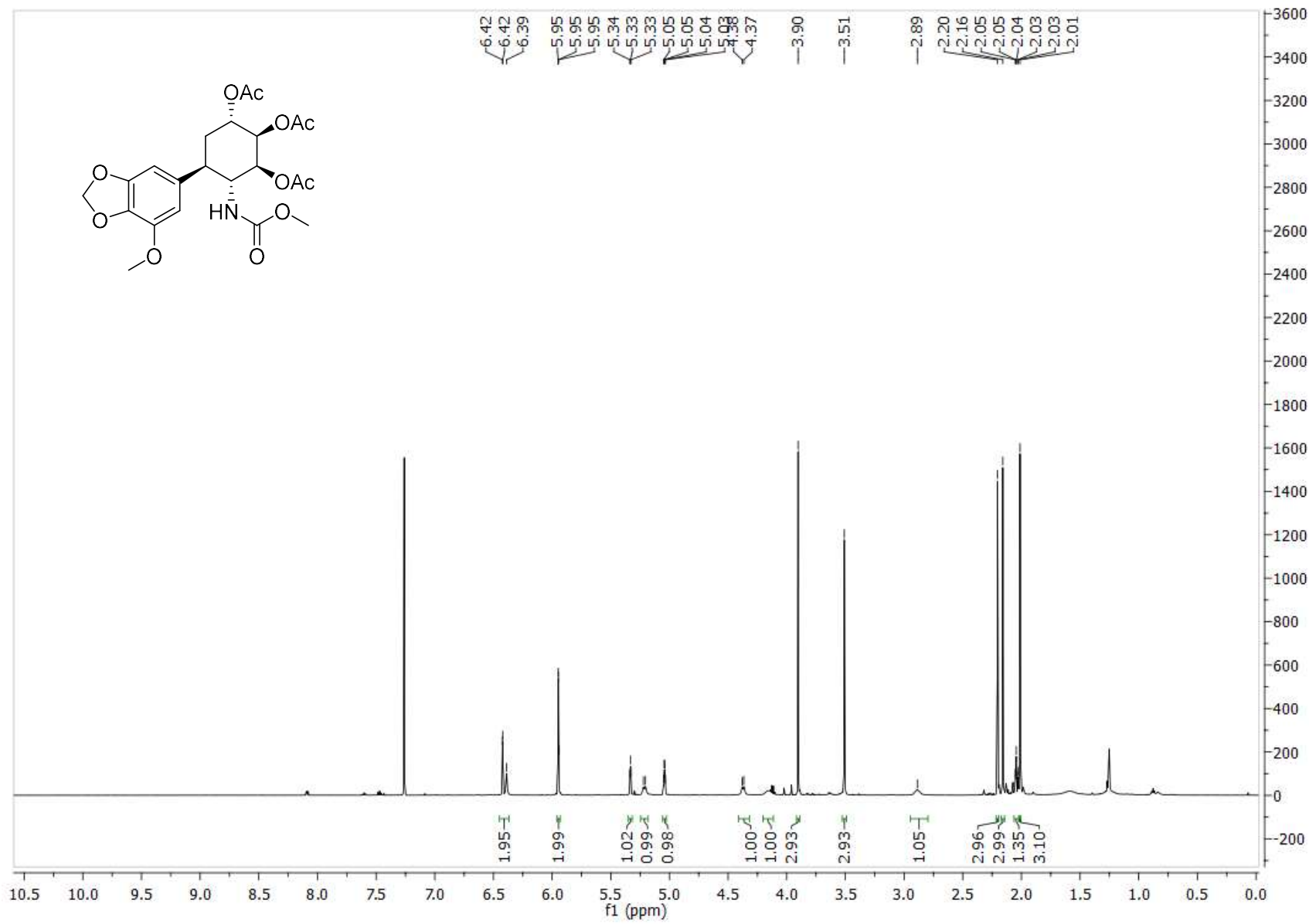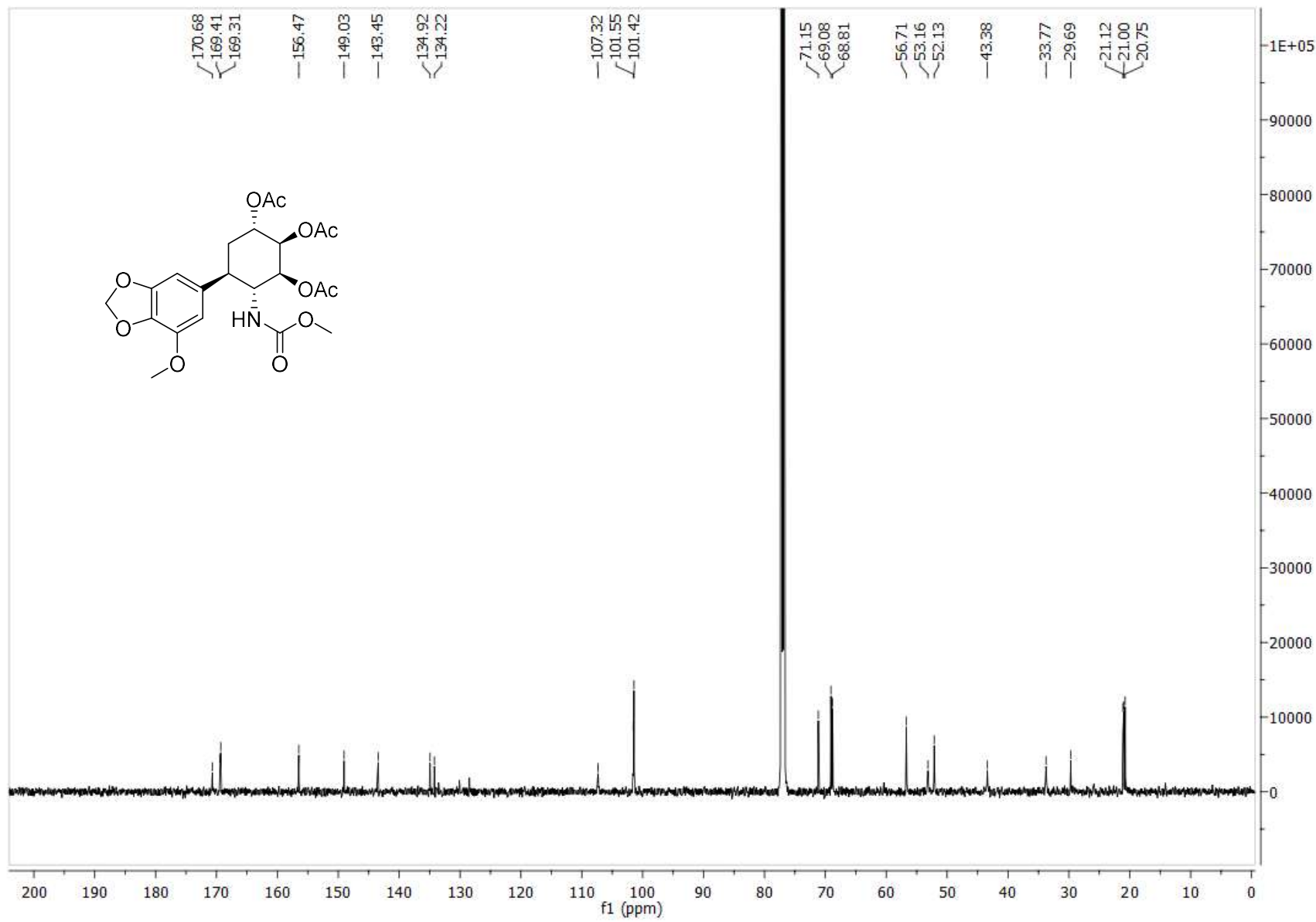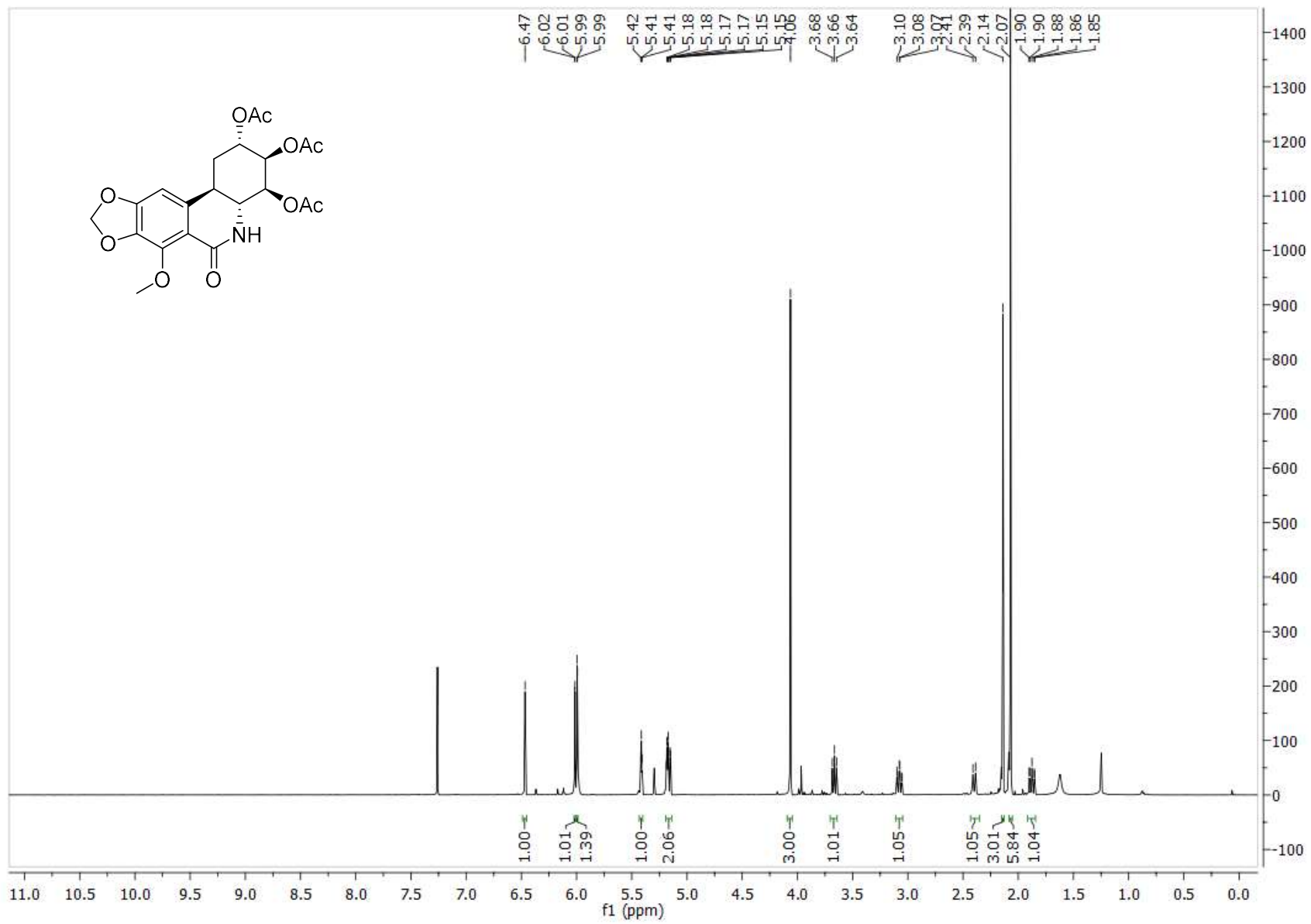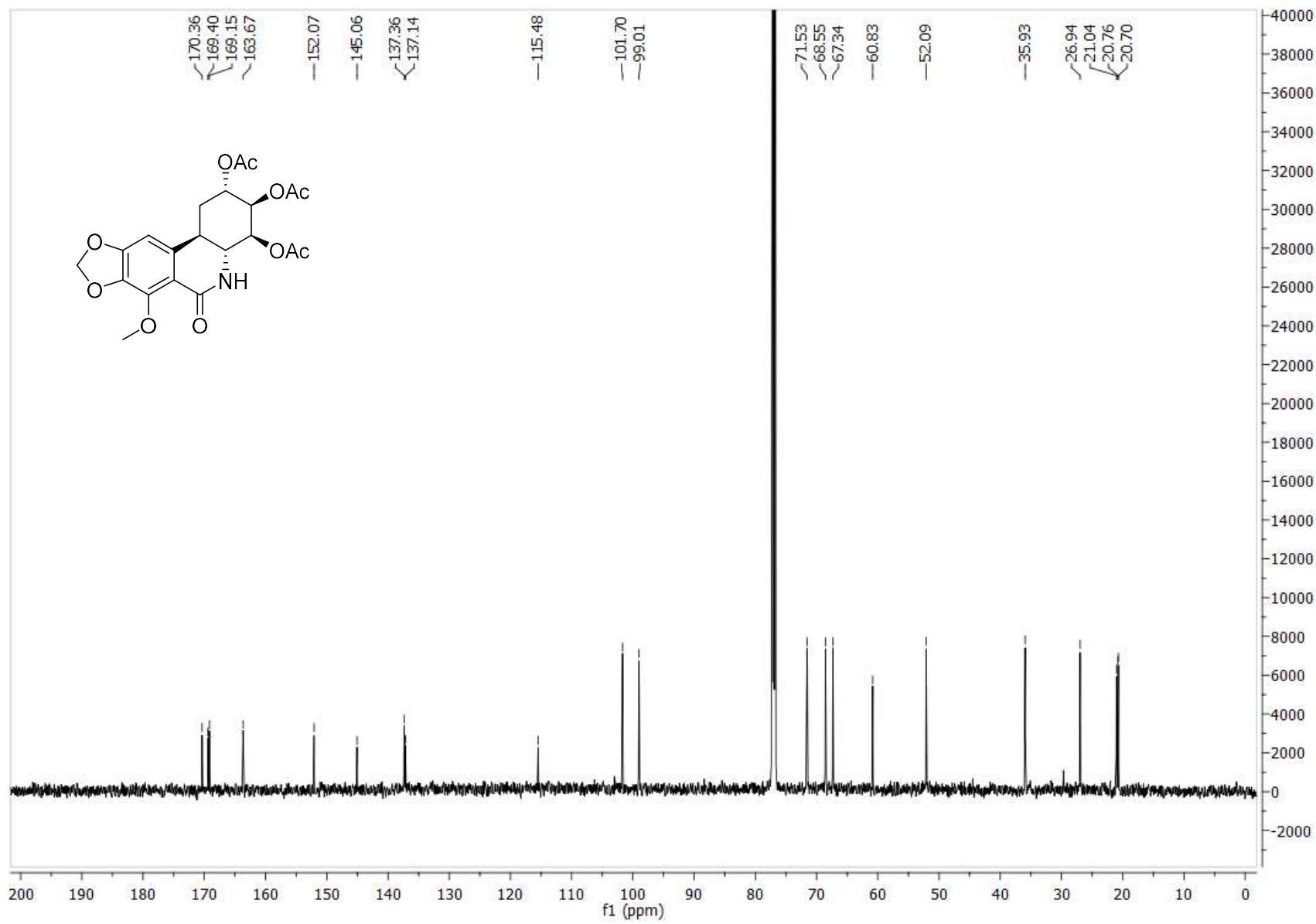
15 ¹³C NMR

16 ^{1}H NMR
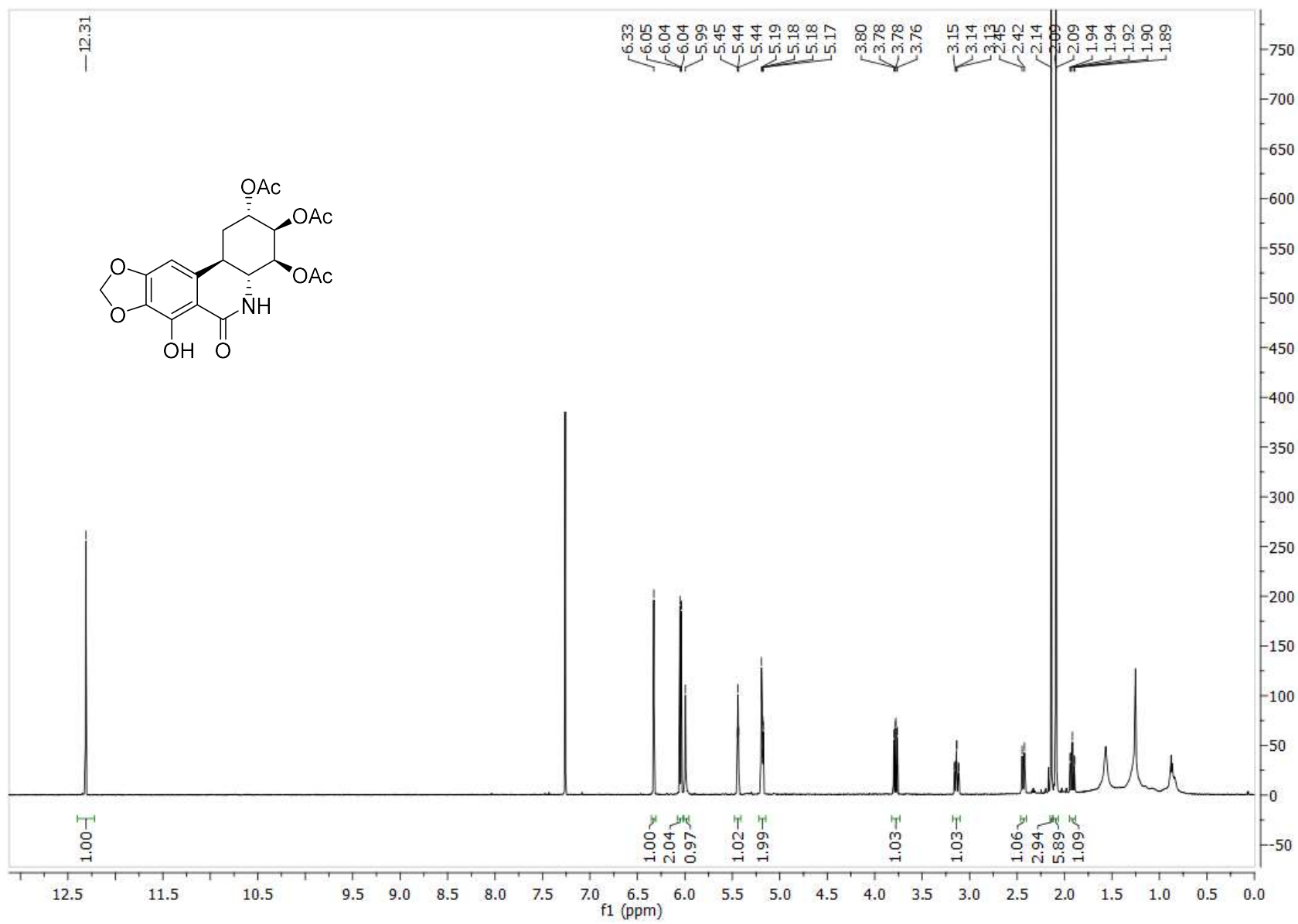
16 ^{13}C NMR
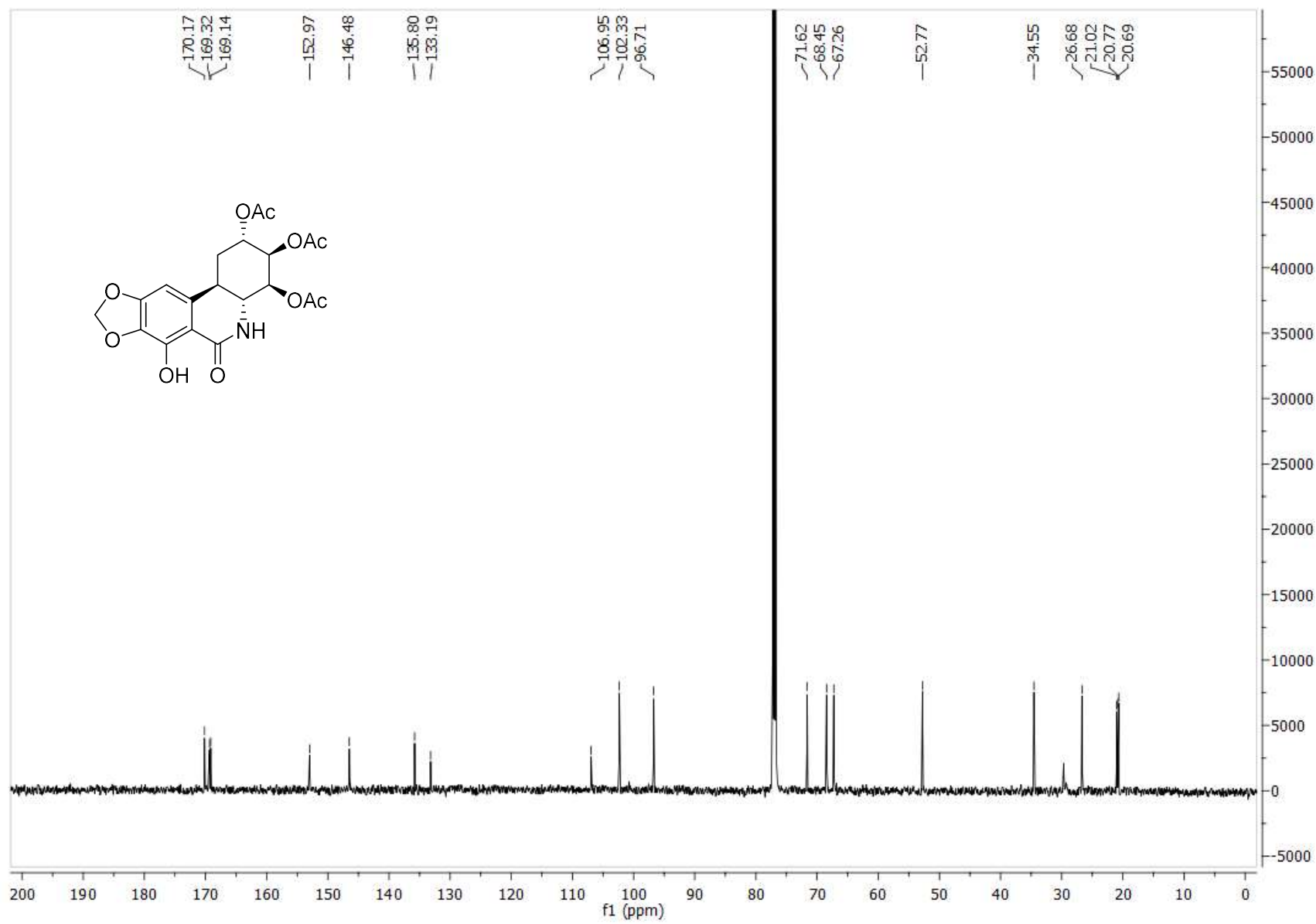
1 ¹H NMR
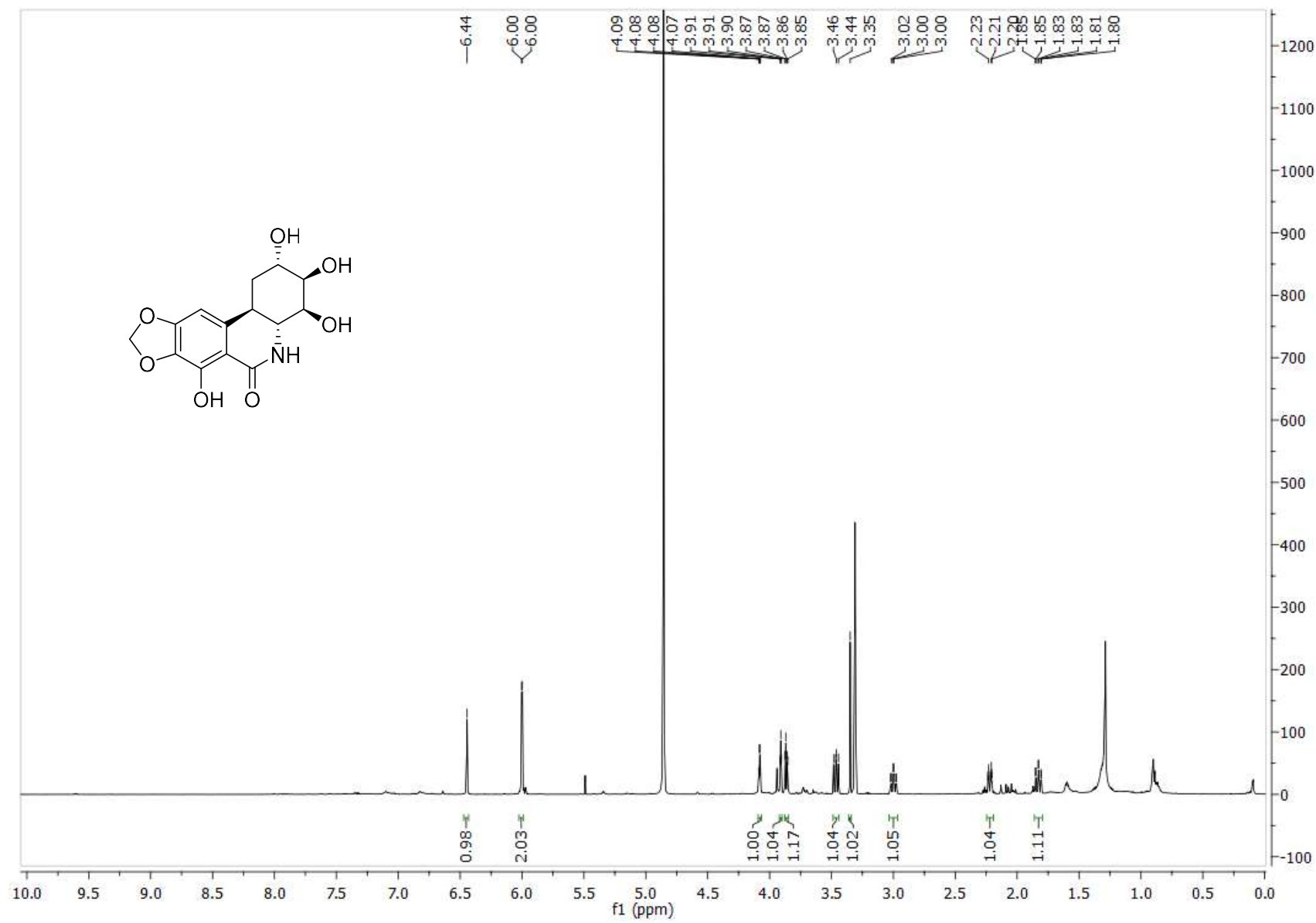
1 ^{13}C NMR
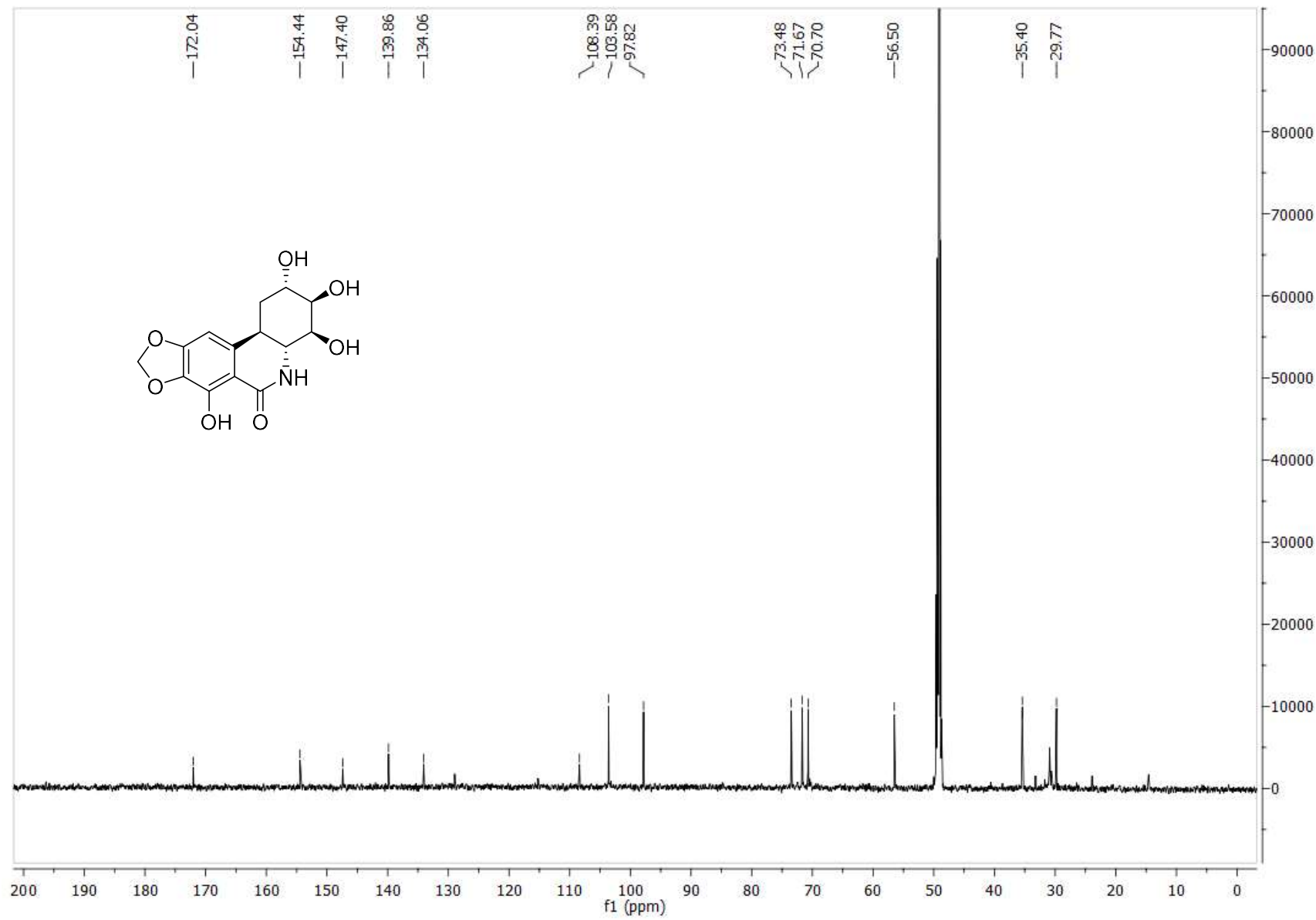
Appendix H: Copyright Statements

Copyright Statement Pertaining to Chapter 2.2

JOHN WILEY AND SONS LICENSE
TERMS AND CONDITIONS

Apr 25, 2019

This Agreement between Mr. Alexander Nielsen ("You") and John Wiley and Sons ("John Wiley and Sons") consists of your license details and the terms and conditions provided by John Wiley and Sons and Copyright Clearance Center.

License Number	4537240651915
License date	Feb 27, 2019
Licensed Content Publisher	John Wiley and Sons
Licensed Content Publication	Medicinal Research Reviews
Licensed Content Title	Polyphenolic natural products and natural product–inspired steroidal mimics as aromatase inhibitors
Licensed Content Author	Alexander J. Nielsen, James McNulty
Licensed Content Date	Sep 1, 2018
Licensed Content Volume	0
Licensed Content Issue	0
Licensed Content Pages	20
Type of use	Dissertation/Thesis
Requestor type	Author of this Wiley article
Format	Print and electronic
Portion	Full article
Will you be translating?	No
Title of your thesis / dissertation	Novel Wittig and Organocatalytic Methodologies for the Synthesis of Chemotherapeutic Compounds
Expected completion date	Mar 2019
Expected size (number of pages)	440

Copyright Statement Pertaining to Chapter 2.3

Title: Synthesis of α-methylstilbenes using an aqueous Wittig methodology and application toward the development of potent human aromatase inhibitors

Author: Alexander J. Nielsen,Sergio Raez-Villanueva,Denis J. Crankshaw,Alison C. Holloway,James McNulty

Publication: Bioorganic & Medicinal Chemistry Letters

Publisher: Elsevier

Date: 1 June 2019

Copyright Statement Pertaining to Chapter 4.4

Copyright Statement Pertaining to Chapter 5.4